# Novelty processing and smart delivery of Ganoderma lucidum spores

Anouska Riahi (née Bharath)

A thesis submitted for the degree of

**Doctor of Philosophy**

From

**University College London (UCL)**

*Department of Mechanical Engineering*
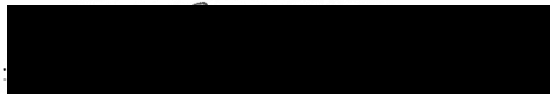
**Supervisors**

Dr Jie Huang
Dr William Suen

July 2022

# Declaration of Authorship and Originality

This thesis showcases research conducted in the department of Mechanical Engineering at University College London under the supervision of Dr Jie Huang and Dr William Suen. I, Anouska Bharath, confirm that the work presented in this thesis is my own. Where information has been derived from other sources, this has been indicated in the thesis.

Signature: ███████████████████████        Date: July 2022

*Novelty processing and smart delivery of Ganoderma Lucidum spores*

# Abstract

In recent decades the traditional Chinese medicinal mushroom Ganoderma lucidum (GL), a fungal specie widely consumed homoeopathically in the Eastern Hemisphere, has been studied particularly with respect to antitumour and immunoenhancing effects. Research into the various claims however remains limited owing to the lack of quality and consistency across investigations. As such, efficacy and feasibility of scale-up has not been evaluated in a way that allows widespread consumption or approved treatment. This project tackles three aspects of drug development from Ganoderma lucidum: *Biocompound extraction*, *healthcare evaluation via in-vitro testing*, and *encapsulation for smart delivery*. These avenues are brought together for the first time to evaluate the prospects of developing GL for effective and safe healthcare.

This research investigates the parameters that would influence the extractability of a biocompound from the spores of Ganoderma lucidum (GLS), via two conventional methods: Hot Water Extraction (HWE) and Ultrasound-Assisted Extraction (UAE). They are evaluated with respect to their crude water-soluble polysaccharide yield (GLPS). Solvent polarity and process duration were statistically significant factors affecting extract yield, with both extraction methods showing considerable gains over similar setups in literature, recovering over 6% crude GLPS using shorter durations and lower temperatures than other published investigations. This investigation highlighted the importance of solvent viscosity on specific *D-Glucan* extraction in the GLPS yield. Bioactive effects of the extract were evaluated via cytotoxicity toward Human Osteosarcoma (HOS) cells in-vitro, achieving over 40% cell growth inhibition. Cytotoxicity however was only achieved when water-*insoluble* fractions were administered – suggesting cytotoxicity was a result of the unextracted crude triterpenoids (GLTP) containing Ganoderic Acids. Therefore, HOS-inhibitory capabilities are then compared to a GLPS extract containing Ganoderic Acids (in this work termed "PSGA"), extracted using HWE subject to supervised machine learning optimisation. As well as determining that this yield was maximised at the longest HWE duration and smallest solvent volume, it was observed to inhibit HOS growth by nearly 58% after 24 hours. Low doses and shorter incubation were most effective - suggesting concepts such as resistance (clonal selectivity) and delayed apoptosis, but further work will verify the reported effects of PSGA dosage and exposure time on cancer proliferation. Lastly, research effort is devoted to creating an alginate matrix for the controllable delivery of GLS using Electrohydrodynamic Atomisation (EHDA). Significant effects of the system's process parameters on particle morphology are observed, in particular EHDA voltage. The carrier's size, shape and surface features are correlated with its release profile. Importantly, GLS content (something traditionally compromised to maintain particle integrity) was maximised at 50 wt% whilst maintaining a controlled and spherical shape and size – making this study novel and extremely important. It is established that GLS-Alginate particles could offer controlled release over a 2-week administration in pH-neutral conditions; an environment not yet established as "stable" for alginate, yet reflective of physiological passage. Thus, for the first time sodium alginate is proven to be a real contender in controlling the delivery of GLS biomolecules.

The reconciliation of these essential stages of drug development highlights some crucial points of focus as GL continues to undergo rigorous development in the realm of drug discovery.

*Novelty processing and smart delivery of Ganoderma Lucidum spores*

# Acknowledgements

I would like to express my deepest gratitude to my supervisors, Dr Jie Huang and Dr William Suen, without whom this study would have been impossible. In their unique ways, they showed me the difference between being a *researcher* and being a *research engineer*. Coming from a mathematical background where a right answer always existed, Dr Huang consistently stood by my side as I pursued wild and ambitious experimental paths. Your words of wisdom and reassuring voice were always appreciated when I would forget that the point of engineering isn't always to find the "correct solution", but also to formulate new ways of thinking when the solution may not yet exist. Being the expert that I aspire to be in your field, your input into this study's direction was invaluable; I cannot thank you enough for truly transforming me into an engineer. From you I learned that curiosity is one of the most essential and permanent characteristics of a successful intellect. Dr Suen I thank you for your guidance in becoming a respectable academic, always motivating me to reach above what I would expect of myself in this dynamically wonderful field. A special mention also goes to Dr Mohan Ederisinghe, providing unique and critical insight during primary parts of this research as well as its final stages as a successful thesis. Professor Lucy Di-Silvio, whose direction with in-vitro tissue studies was both riveting and vital, is also thanked enormously. Both at times of excitement and panic, you were ready to keenly contribute to my progress.

I would like to offer extraordinary appreciation to my best friend and now husband Daniel, who has been by my side through thick and thin. These years of study have been tough not just academically, but also emotionally. Your motivation invigorated me as I neared success. Thank you for making me excited to become the best version of myself. My brother Vidal, completing his PhD alongside the start of my own, showed me how to handle this journey with strength, pride, and passion. Your own journey inspired mine, and I would be lucky to achieve even close to what you have. To my parents Arvinder and Vasant, thank you for the support and sacrifices you make every single day to make sure I am living my best life; always showing me perspective and teaching me the lessons you know I will use to progress in life. Thank you for raising me with the values I flaunt today; I hope I have made you proud and that I forever continue to do so. Thank you to my sister Aurora, for offering that getaway I needed so much – you will forever by my grounded inspiration. And finally thank you to my parents-in-law, who provided comfort, support, love and happiness during this chapter of my life.

*Novelty processing and smart delivery of Ganoderma Lucidum spores*

# Table of Contents

*Novelty processing and smart delivery of Ganoderma Lucidum spores*

*Novelty processing and smart delivery of Ganoderma Lucidum spores*

*Novelty processing and smart delivery of Ganoderma Lucidum spores*

# List of Figures

## 2 Literature Review

*Novelty processing and smart delivery of Ganoderma Lucidum spores*

*Novelty processing and smart delivery of Ganoderma Lucidum spores*

## 3 Materials and Methods

## 4 Results and Discussion

*Novelty processing and smart delivery of Ganoderma Lucidum spores*

*Novelty processing and smart delivery of Ganoderma Lucidum spores*

*Novelty processing and smart delivery of Ganoderma Lucidum spores*

*Novelty processing and smart delivery of Ganoderma Lucidum spores*

## 5 Conclusions and Recommendations for Future Work

# List of Tables

## 2 Literature Review

*Novelty processing and smart delivery of Ganoderma Lucidum spores*

# 3 Materials and Methods

# 4 Results and Discussion

*Novelty processing and smart delivery of Ganoderma Lucidum spores*

*Novelty processing and smart delivery of Ganoderma Lucidum spores*

# List of Abbreviations (Nomenclature)

**AD** Air-Drying

**ANOVA** Analysis of Variance

**AR** Aspect Ratio

**CaCl$_2$** Calcium Chloride

**CaCO$_3$** Calcium Carbonate

**CO$_2$** Carbon Dioxide

**DDI** Distilled De-ionised (water)

**DDS** Drug Delivery System

**DG** D-Glucans

**DMEM** Dulbecco's Modified Eagle's Medium

**DMSO** Dimethysulfoxide

**EC** Electrical Conductivity

**EHDA** Electrohydrodynamic Atomisation

**FD** Freeze-Drying

**FTIR** Fourier Transform Infrared Spectroscopy

**GA** Ganoderic Acid

**GG** Guluronic Regions

**GL** Ganoderma lucidum

**GLS** Ganoderma lucidum Spores

**GLS-A** GLS-Alginate

**HOS** Human Osteosarcoma

**HPLC** High-performance liquid chromatography

**HWE** Hot Water Extraction

**ID** Internal Diameter

**LCMS** Liquid chromatography-mass spectrometry

**MEM** Minimal Essential Medium

**MTC** Maximum Tolerated Concentration

**MTT** 3-[4,5-dimethylthiazol-2-yl]-2,5 diphenyl tetrazolium bromide

**MW** Molecular Weight

**O/W** Oil-in-Water

**OD** Outer Diameter

**OM** Optical Microscopy

**PBS** Phosphate Buffered Saline

**PEG** Poly(ethylene glycol)

**PPM** Parts per Million

**PSGA** Polysaccharide-Ganoderic Acid complex

**PS** Polysaccharide

**RPM** Revolutions per Minute

**RSM** Response Surface Methodology

**SDR** Surface Defect Ratio

**SE** Standard Error

**SEM** Scanning Electron Microscopy

**TP** Triterpenoid

**UAE** Ultrasound-Assisted Extraction

**UV-Vis** Ultraviolet-Visible

**v/v (Liquids)** Working Volume

**W/O** Water-in-Oil

**w/v** Working Volume

**wt%** Weight %

*Novelty processing and smart delivery of Ganoderma Lucidum spores*

# Impact Statement

This work highlights some promising workflows and competencies of Ganoderma lucidum (GL) as a candidate for healthcare, particularly cancer treatment. The large scope covered by this project sparks further research into various aspects of GL development – from the engineering of extraction techniques to the engineering of effective and safe physiological drug delivery. By opening up some of the proposed future directions outlined in the last chapter, more specific feasibility studies can be carried out with an increasingly defined and understood GL treatment.

Cancer is the second leading cause of mortality worldwide, yet nearly 50% of all cases are preventable [World Health Organisation, 2019]. Of the preventative techniques that exist, those that were traditionally overlooked and labelled as "complementary" or "alternative" are now more sought than ever. In 2018, funding into global research into alternative treatments was over 50% higher than 2013, and the funding specifically granted to traditional Chinese medicine research surged by almost 500%. Nevertheless, as a result of the broad challenges presented by the development of novel pharmaceutical agents, the "problem" vs. "solution" template of its research is hard to define. The problem is a set of obstacles requiring clarification that would ultimately lead to a solution enabling the widespread use of traditional Chinese medicine *Ganoderma lucidum* (GL) for healthcare. The work presented here therefore bridges some crucial aspects of the development of GL for today's healthcare industry.

Many researchers have approached the exploitation of GL via target biocompound isolation and characterisation, particularly verifying astonishing potency toward cancer inhibition. These studies have shed light on the structures and pharmacokinetics of novel GL biocompounds, however there is no systematic study that targets the organism's overall feasibility in light of modern demands – in particular environmental and economic process efficiencies, human safety, and smart treatment. This is one of the first experimental studies that considers such crucial avenues in attempts to create foundations for larger more meaningful studies that will propel further development of GL.

A lack of understanding of the GL biocompound palette, concerning extraction protocol and physiochemical structure, is addressed to reveal the impact of certain process parameters on the yield of a valuable biocompound class. Subsequently, a novel complex containing both polysaccharides and Ganoderic Acids is isolated and compared cytotoxically in-vitro against cancer proliferation. Never before has this complex been evaluated, and so this work provides good insight into new bioactive extract from GL that should be further studied to fully characterise its pharmacokinetics. Its dual-role in cancer treatment is particularly exciting given the **cytotoxicity** of Ganoderic Acids and the **immunoenhancement** attributed to polysaccharides. A particular area of excitement in this section of study is the potential of applying a *machine learning approach* to investigations into the extraction and encapsulation of GLS. Machine learning tools are in fact increasingly used in pharmaceutical research and development when the experimental data contains many variables and resulting outcomes. Using just a sample of

experimental results, these multidimensional areas of research can be more extensively deciphered. This study is the first to date that suggests the prospect of machine learning approaches to the evaluation of GL extraction but only uses a basic form of supervised machine learning that sets a significant precedent for the development of an unsupervised approach.

The last leg of research concerns the aspect of drug development that would typically follow on from the discovery and evaluation of a novel drug compound – the encapsulation of GLS for physiological delivery. While this project acknowledges that this section of study is premature for the current stage of GL development, the investigation highlights some important evolvements in encapsulation materials that introduce greater biocompatibility to the field of drug delivery. Sodium Alginate uniquely demonstrated stability undergoing Electrohydrodynamic Atomization (EHDA) as a means for GL-Alginate microparticle formation. In a healthcare era whereby the importance of "smart" delivery introduces prospects of automated dosing and more effective tissue targeting, the proficiency of EHDA in controlling GLS-Alginate particle distributions with respect to size and shape is a major advancement. Uniform microparticles were achievable at sizes that undermine recent literature by up to 60% in similar setups. Where comparable or smaller sizes were obtained in literature, this research boasts the advantage of negating co-polymers typically employed to facilitate harsher fabrication, increasing the typical drug-loading capacity, and a subsequent controlled release in conditions typically unfavourable to alginate's stability (yet relevant to physiological delivery) [Brown et al., 1997; Feriberg et al., 2004; George et al., 2006; Raemdonck et al., 2009; Nagarwal et al., 2009; Koo et al., 2014]. It is particularly beneficial to have demonstrated a 1:1 drug:polymer ratio whilst maintaining particle morphology and integrity during processing, storage, and release [Singh et al., 2014; Zhu et al., 2019]. This study therefore engineered a unique workflow of creating a GLS-A microparticles that would release encapsulated GL in a sustained manner over 2 weeks with limited initial burst. This highlights significant potential for alginate as a foundation of drug delivery systems when processed using this setup, as this biopolymer is traditionally destabilised within hours in similar physiological conditions. Novel foundations have also been set for further improvements in particle distributions that could provide a more tailored solution for the smart delivery of a wide range of pharmaceuticals. Particularly these include particle surface topography and porosity; opening doors to enhancements in bioavailability, drug-loading, and more intricate release control.

Zion Market Research estimates the global medicinal mushroom market at USD 35.08 billion in 2015, with Ganoderma-related products representing USD 2.5 billion, or 2% [Zion Market Research, 2018]. As a result of considerable chemical differences between strains of the same species stemming from cultivation, the scale-up is a challenge. In western economies, there is little regulation of commercial fungal medicinal products like GL – further creating a "buyer beware" market in which manufacturers become liable for this enigmatic product [Raja et al., 2017]. In 2018, scientists tested the composition of manufactured GL marketed commercially and discovered that none were pure, containing a variety of mushroom species [Loyd et al., 2018]. These market habits further challenge scientific study of GL's palette.

# Impact of Research

## Publications

**(Research)** An Analysis of the Potential Global Impact of Dosing Regimen and Roll Out Options for the ChAdOx1 n-CoV-19 Vaccine (featuring machine learning techniques)

**Journal:** Nature Communications

## Publications Pending Publication

**(Research)** Modelling Plasmodium Falciparum Malaria Interventions in the Greater Mekong Subregion using machine-learning techniques

**Status:** Pending Peer Review

**Journal:** Lancet Global Health

## Publications Pending Submission

**(Review)** Ganoderma lucidum: A Review of its Composition, Pharmacology, and Administration

**Journal:** Elsevier Journal of Traditional Chinese Medical Sciences

**(Research)** The Encapsulation of Chinese traditional Medicine, Ganoderma lucidum, for Smarter Delivery Prospects

**Journal:** The Lancet Global Health

## Scientific Presentation

**Conference:** Poster Presentation at the United Kingdom Society for Biomaterials (UKSB) Annual Conference, and published proceeding

**Subject:** Electrospraying high-loaded GLS-loaded Alginate Microparticles for Drug Delivery

**Date:** 30 June - 1 July 2016, London

*Novelty processing and smart delivery of Ganoderma Lucidum spores*

# 1 Introduction

## 1.1 Background

The world's population is facing a rising prevalence of diseases that unfortunately implicate a declining quality of life even in the face of an increasingly developed world. Cancer for example, an uncontrolled mutated growth of normal body cells, will affect almost half of the current general population and is expected to increase by up to 50% by 2040 [World Health Organisation, 2019]. Unsurprisingly therefore, there are increasing questions surrounding the efficacy and safety of existing treatments.

### 1.1.1 Natural Medicines

Over 80% of the world's population rely on plant-derived medicines for healthcare, with the Eastern Hemisphere being their heaviest producer and consumer [Dias et al., 2012]. While treatments for progressive diseases are being researched and developed, there continues to be a high mortality rate and limited life expectancy following diagnosis of a multiplicative disease like cancer. Even at a time where the chance of survival is longer post-treatment, recovery patients endure low standards of living amidst the consequences of harsh treatments [Paraskevi, 2012]. This is attributed to the increasing complexities of new disease onset/progression and the physiological side-effects of conventional effective treatments. With the benefits of proactive and preventative healthcare showing more promise than ever today [Golubnitschaja, 2009; Sobradillo et al., 2011], combined with the fact that alternative treatments have potential to enhance existing treatments, a worldwide hunt has begun for safe and effective alternative treatments even in the face of their continued stigma and complexities. Consequently, this has instigated investigations into more sophisticated techniques to characterise them and their mechanisms of effect. In essence, modern science is revisiting the source of what we know as modern medicine: Nature [Phillipson et al., 1989].

Natural medicines are not a new phenomenon, existing for centuries before the man-made agents we consume today. While countrymen prescribed local victims of disease with these natural "backyard" remedies, scientists all over the world began the race to expose the mechanisms of the compounds responsible for these "miracle" substances in order to make them available for widespread use [Phillipson et al., 1989]. Among the benefits of naturally-sourced drugs, one of the most valuable is their possession of a privileged structure. This originates from the pressures of evolution, to which natural organisms were subject for many eras. As a result, their biological activity could not be "random". Thus, along with a therapeutically potent

bioactivity, these agents also pose a low risk of incompatibility with the body [Dias et al., 2012]. Particularly in a species-rich ecosystem where a competition culture implicates strong defence for survival, there is certainly an abundance of bioactive competencies waiting to be exploited by the human race.

Isolating bioactive compounds is the first step to understanding the mechanisms behind remedial effects, and this is especially important for primary sources of nutraceuticals which do not directly yield a "lead" compound or implicate a causal therapeutic effect [Mitra et al., 2009; Hughes et al., 2011]. Furthermore, there are numerous structural conformations within the biocompound classes, and coherent evidence of structural influence on bioactive capabilities – rendering structural elucidation somewhat essential for their development [Xie et al., 2016; Zeng et al., 2018; Cör et al., 2018]. Natural contraptions are indeed structurally and chemically complex laboratories of bioactivity, with molecules working synergistically to achieve a therapeutic effect. Popular commercial drugs such as Aspirin, Morphine, and Quinine were themselves the result of investigations into the bioactivity of natural organisms [Veeresham, 2012]. In the field of cancer alone in the last 40 years, 50% of all approved drugs were derived from natural products [Veeresham, 2012]. Of the remaining synthetic drugs approved, the majority were still *modelled from* natural compounds [Newman et al., 2007]. In fact the world has continued to witness "mimicked structures" of these chemically complex natural compounds using synthetic alternatives, however with today's technological advances permitting more advanced biochemical analyses natural compounds can now be more accurately identified and isolated as the foundation for increasingly effective and safe therapies. However, with ever-increasing varieties of organisms being cultivated, discovered, and even engineered, it has become difficult for scientists to establish a standard protocol for defining the compounds they yield [Cui et al., 2014]. This is because accurate characterisation would typically stem from the existence of a defined workflow of evaluative techniques that "fits all". Therefore, backbone methods have been established that require modifications in order to evaluate specific biocompounds during such a progressive and exploratory discovery process.

### 1.1.2 Traditional Chinese Medicines (TCM) and basidiomycota *Ganoderma lucidum*

TCMs encompass the bioactive agents from some natural sources, and a large focus has fallen on *basidiomycota*; a fungal class flaunting a plethora of unmatched and unrecorded healing properties. Basidiomycota were first utilised in East Asia, and the Polyporales family *Ganoderma* has proven particularly potent in targeting tumour onset and enhancing immunosuppression. Ganoderma lucidum (GL), also known as Reishi and Linghzi, is only one of many basidiomycota that have been used in TCM for centuries [Cheng et al., 2015]. GL boasts potency in a variety of

bioactivities, including immunoenhancement, cytotoxicity, hypertension, cardiovascular health, inflammation, diabetes, and hepatitis [Zeng et al., 2018]. However with such a diverse and unique bioconstituent palette, obstacles remain to the identification of its constituents and mechanisms; rendering their identification, isolation, and examination a challenge to its development.

### 1.1.2.1 Ganoderma lucidum as a Viable Candidate for Healthcare

In 1969, Ikekawa published the first study proving the anti-tumour potency of basidiomycota in mice implanted with Sarocoma-180 cancer [Cör et al., 2018; Zeng et al., 2018;]. Once it was revealed that the antitumour effects of basidiomycota could be attributed to certain biomolecules *polysaccharides* and *triterpenoids*, these studies became the inspiration for many commercial drugs; the most common being β-D-Glucan polysaccharides [Xie et al., 2016; Cör et al., 2018].

The development of an enigmatic material like GL, especially when intended for human consumption, is polygonal so that it offers consideration of many processes and materials that work together to achieve physiological safety and efficacy [Hughes et al., 2011; Eder et al., 2015]. While many techniques successfully extract and characterise GL biocompounds, they leave plenty room for efficiency gains [Zeng et al., 2018]. Recent investigations have developed more intuitive characterisation techniques to increase the accuracy of defining the structural conformities and physiochemical properties of GL polysaccharides and triterpenoids. These improvements have mainly been observed in the selectivity of spectroscopic techniques [Joana Gil-Chávez et al., 2013]. Unfortunately these findings have been inconsistently recorded, rendering the observed pharmacodynamics inaccurately associated with a biocompound structure – a good example being the antitumour effects of polysaccharides with numerously recorded structural variations [Zeng et al., 2018]. This has instigated investigation into processes that can selectively and effectively extract polysaccharides, triterpenoids, and certain complexes, so as to obtain a rich variety of structurally variable biomolecule configurations for a broader evaluation.

To date, the Ganoderma species has become a popular subject of study, boasting ongoing clinical trials for a variety of diseases. As yet, many of these remain as "failed" studies owing to significant inconsistencies.

### 1.1.3 Machine Learning Approaches

In such an underdeveloped field, established extraction methods are not consistent nor robust in the face of a varied GL physiochemical nature and a variable experimental workflow. As a result, multiple iterations of an experimental setup are beneficial to validate the method and

the GL sample. Statistical optimisation is at the heart of a concept known as machine learning, and is presented in this project as a foundation for more advanced artificial intelligence prospects. This approach allows relationships to be represented *and* predicted using just a sample of experimental results. It consists of variables (and their range or constraints), and objective (maximising GL yield). Machine learning tools are in fact increasingly used in pharmaceutical research and development when the experimental data contains many variables and resulting outcomes (biomarker studies traditionally, but also in multidimensional drug extraction and characterisation studies). Typically these studies, when carried out experimentally, are complex and expensive, generating a huge variety of data. Conventional statistical experimental designs, or supervised machine learning, are well-understood and frequently employed in drug R&D today. This project used a form of supervised machine learning, known as response surface methodology to optimise extraction.

### 1.1.4 Drug Development

Drug development is multidimensional, relying on efficiencies in the connections between compound recovery, bioactivity, and safe delivery [Katiyar et al, 2012]. To achieve desirable results at just one stage of drug development will not be sufficient to propel the drug through to clinical trials. Thus, a chain of processes must come together to demonstrate that the compounds can be feasibly and safely taken from raw material to an encapsulated delivery system whilst maintaining bioactivity [Eder et al., 2015]. Thus, the assessment of a drug delivery system expands beyond just "therapeutic effects". As mentioned previously, there is considerable significance placed on the techniques used to extract and characterise GL biocompounds. While this aspect is continuously studied to strengthen GL as a candidate for modern healthcare, what urgently requires focus in this field is the delivery system that could be used to target the body's complex and diverse biomolecules safely, effectively and sustainably [Zhao et al., 2016; Le et al., 2016; Shen et al., 2016].

### 1.1.4.1 Drug Delivery Systems for the Modern Era

Drug delivery systems effectively dictate how the body identifies and processes drug molecules, and this therefore determines the drug's biodistribution (through residence time and targeting), toxicity, release profile and ultimately efficacy [Kudgus et al., 2014]. Novel drug delivery systems are being developed to meet the needs of today's healthcare consumer. At its core, this refers to the formulations, technologies, and techniques that transport therapeutic agents in the body so that they efficiently achieve their intended effects. In particular the benefits of "smarter" treatment delivery systems that can delivery treatment controllably, effectively, and

safely, are widely explored. This is primarily because traditional drug delivery systems typically present undesirable side effects attributed to their seemingly "idealistic" material that withstands extremities in processing en-route to a "morphologically-perfect" system, but also attributed to non-targeted bio-availability, and uncontrolled release profiles [De Jong et al., 2008; Jahangirian et al., 2017] There is limited progress in the field of drug delivery using materials that work in harmony with the physiological environment, yet can provide effective targeted drug delivery, immune system evasion, and dosage manipulation [Soppimath et al., 2001]. With the added attractiveness of making a delivery system using natural materials that could enhance biocompatibility and avoid side effects associated with synthetic materials, the challenge of creating the current era's "ideal" drug delivery system increases [Huang et al., 2010 (a)]. "Smart" delivery introduces prospects of more controllable dosing and targeting using more desirable materials, rendering research into biopolymers to encapsulate pharmaceuticals a hot topic.

Along with system material, many challenges of traditional techniques can be overcome by controlling the features that influence the release profile; including surface topography, carrier morphology, and distribution uniformity [Rizvi et al., 2018]. As well as fostering efficient and effective bio-distribution, smarter systems also achieve efficacy by increasing patients' compliance; essentially alleviating the need to repeat doses through offering controlled release and more efficiently maintaining drug residence and concentration in target tissue. Resultantly, smart delivery systems present the revolutionary opportunity to regulate and control treatment course and minimise risks of toxicity.

## 1.1.4.2 Creating the "Ideal" Drug Delivery System

In the face of diseases like cancer, the physiological conditions presented in the body are particularly abnormal, with the efficacy of treatment becoming reliant upon changes to the vascular system, as well as an unusual extracellular matrix and gradient fluid pressures [Ariffin et al., 2014; Toy et al., 2014]. This renders innovative systems more essential so they can withstand extra "biobarriers" by enhancing flowability, increasing adhesion to tissue and subsequent residence time, and offer a biocompound shield until attaining the target site [Kshirsagar, 2000]. As such, a common theme in existing literature is the achievement of delivery using vehicles that are as small and uniform as possible [Nagayasu et al., 1999; Toy et al., 2014]. Typically, this fosters enhanced tissue targeting and adhesion, reduced risk of attack/clearance by the immune system, and greater dosage control [Rizvi et al., 2018; Singh et al., 2009]. In order to engineer a drug delivery system with these physicochemical qualities, extensive research has led to advances in the engineering of materials and process technologies to fabricate novel drug delivery systems. Particular interest has been directed toward processing polymers using powerfully mechanised systems like Electrohydrodynamic Atomisation (EHDA) [Mehta et al., 2017].

## Polymers to Encapsulate

Scientists have challenged the biocompatibility and biodegradability of the materials used in drug delivery systems, even when favourable to a desirable particle distribution [Jahangirian et al., 2017, Mehta et al., 2017]. Hence, many new polymers are being investigated and developed for drug delivery. In particular there has been extensive research into the biopolymer sodium alginate ("alginate"). Alginate systems have gained attention for their biodistribution - enhanced by tissue adhesion, reduced clearance by the immune system, and low coagulation [Soni et al. 2010; Hossen et al., 2019]. Traditionally difficult to process owing to fragile biopolymer chains, alginate is still a viable option for drug delivery systems as it is sustainably sourced, biodegradable, durable, and offers the prospect of a controllable release profile through responsiveness to basic stimuli pH and temperature [AbdelAllah et al., 2016; Rizvi et al., 2018]. Furthermore, alginate has been a significant aid in the delivery of drugs that are poorly water-soluble, as the biopolymer matrix can exhibit erosion-controlled drug delivery, but also provides control against compounds that would otherwise rapidly dissolve in water [Tønnesen et al., 2002]. Unfortunately to date, alginate-only particles fabricated using EHDA have been limited to sizes that are too large for many therapeutic applications as a result of the material's heat/pressure thresholds, or employ very little drug to achieve desirable physical characteristics] [Meng et al., 2009; Park et al., 2012; Sridhar et al., 2013; Ching et al., 2017]. To enhance the encapsulation properties of alginate during drug delivery, alginate is usually combined with other polymers like chitosan and gelatin to overcome these weaknesses and generate strong, small and uniform particles [Ranganath et al., 2009; Zhang et al., 2011; Huang et al., 2014; Wang et al., 2016]. Of course, however, a combined polymer matrix also modifies certain beneficial properties of alginate hydrogels and has been shown to reduce the controllability of particle features such as surface topography and size [Lucinda-Silva et al., 2005; Lu et al, 2010].

## Morphology and Surface

*Carrier Size*. A smaller vehicle *size* offers a simple route to injection to the tissue or intravenously, can increase local drug concentration, fosters greater dosage precision, is adaptable and flexible to be used as part of a wide range of treatment regimens like inhalation, can bypass the many bio-barriers presented by the body, and can increase flowability when compared to fibres, scaffolds, and beads [Kohane et al., 2007]. Thus, their candidacy for drug delivery is **promising** – particularly when positioned as a slightly more durable structure than nanosized carriers. Being larger than nanoparticles also implies slower release [Jamaati et al., 2014]. The size of delivery particles has a significant correlation with the rate of release from drug delivery systems, and thus its biodistribution [Soni et al. 2010; Sun et al., 2012; Chen et al., 2016]. Scientists are however now finding that *larger* particles have more efficient loading, and are

circulated for longer throughout the body– suggesting greater accumulation at target sites [Nagayasu et al., 1999; Owens 3rd et al., 2006; Toy et al., 2014]. Thus, a "one-size-fits-all" range of delivery vehicles is becoming less relevant. The ability to **control** aspects of a delivery system is instrumental in the governance of a treatment plan. In particular in the face of abnormal physiological conditions, "biobarriers" are overcome with features such morphology and surface topography which direct flowability, adhesion to tissue, and protection until attaining the target site [Kshirsagar, 2000]. Consequently, to date, the majority of drug delivery studies focus on developing small and spherical particles for their ability to bypass biobarriers, their free-flowability in the bloodstream, and their repeatability [Moghadam et al., 2008]. As a result, particular interest has been directed toward the processing of polymers using powerfully mechanised systems such as Electrohydrodynamic Atomisation (EHDA) [Mehta et al., 2017]. Even more prominently, alginate particles have demonstrated controllable particle shape and surface features – advantageous since it was discovered that this too can affect biodistribution via increased tissue uptake *and* faster drug release [Zheng et al., 2016; Chuang et al., 2017]

*Carrier Shape.* Shape has received limited attention in the drug delivery field, as its repeatability across studies is not straightforward and so their investigations are not consistently recorded. Diseased sites such as tumour cells typically receive a decreased blood flow resulting in an abnormally high interstitial pressure gradient. This creates an additional barrier to extravasation of particles toward the tissue site, especially for larger particles [Toy et al., 2013]. In the face of a decreasing concern of particle size, innovations in particle *shape* have been made to combat challenges faced in tissue attainment – for example during extravasation via adhesion to vessel walls at the target site (known as *margination*). Non-spherical particle transportation has been proven beneficial in these circumstances, creating unique anchorage and mucoadhesion sights [Gavze et al., 1997; Gentile et al., 2008; Le et al., 2009]. In addition, non-spherical particles exhibit greater resistance to macrophage clearance [Ghaghada et al., 2005; Decuzzi et al., 2006]. Overall, an enhanced biodistribution and efficacy could be achieved with non-spherical carriers like discs, rods, cones, and filaments [Liu et al., 2012; Toy et al., 2014; Chen et al., 2015]. There is however limited study into the control over particle shape in modern drug delivery systems, in particular shapes with geometrical extrusions. The main reason for this is the *lack of production reproducibility* of unique shapes.

## Fabrication Method

The fabrication of drug delivery systems has focused on achieving distribution uniformity in order to achieve the dosage (and fabrication) reproducibility required in clinical studies [Mathaes et al., 2015]. Highly mechanised methods like EHDA use electrical charge to create droplets for solidification into uniform particles [Kuang et al., 2005; Jeyhani et al., 2018]. This

technique has attracted a lot of interest owing to its control over particle morphological distribution, however mechanised processes like this are typically detrimental to the survival of the therapeutic biocompounds in the delivery matrix and even the encapsulation material itself (for example when this is a natural material like sodium alginate). Thus, the outlook of a system like this is not currently promising when used at its most efficient setup (boasting the highest level of control over system distribution), when employing biopolymers. The drug delivery development field has now found itself in an investigative dilemma balancing efficient production of a reproducible distribution, with the preservation of bioactive compounds [Moser et al., 2015].

### Drug Loading

Another relevant angle of study is the need to maximise the *drug-loading* of a delivery system in the face of the physical characteristics required for a strong and efficient carrier– high polymer content. This is typically evaluated via encapsulation efficiency with respect to specific fabrication techniques and material/surface features like porosity [Annabi et al., 2010]. In current DDSs based on *natural biopolymers*, there are challenges in creating a matrix that is not **primarily** loaded with a **polymer counterpart** (great concern is given to particle integrity during fabrication, storage, and physiological passage when concerning biopolymers [Baimark et al., 2014]).

Drug delivery continues to be an area of considerable uncertainty, simply because of the interrelations between exciting material innovations, carrier characteristics and fabrication techniques. There is limited study of a workflow that could create a delivery system meeting the requirements of controllable, biodegradable, biocompatible, efficient, and safe all at the same time [Rizvi et al., 2018]. It is particularly important to enhance the bioavailability of biocompounds that are susceptible to degradation such as proteins and lipids, typically a component of many compound structures isolated from GL.

## 1.2 Study Intent

With the development of Ganoderma lucidum taking place globally with a variety of strains and processing techniques, investigators have found difficulty in collating and reporting its therapeutic value in a way that is meaningful to designing and validating new studies. This introduction has outlined the current potential and challenges of developing GL within the alternative medicine space as well as within modern mainstream therapy. It has also highlighted the importance of a smart drug delivery system when maximising effectiveness, safety, and efficiency of bioactive compounds. After an extensive review of previous and current research

studies, the investigations that follow provide an evaluation of the stages in the process engineering of GL for healthcare: *Isolation*, *characterisation*, and *encapsulation* of this traditional Chinese medicine. The following project goals will be met:

• To extract specific biocompounds known for their bioactivity, from GL spores (GLS) using conventional methods modified to enhance efficiency with respect to biocompound yield. From reviewing literature, this suggests consideration for extraction conditions like extraction concentration (GL:Solvent), solvent, and extraction duration. Supervised machine learning will evaluate complex parameters, particularly as they interact during extraction.

• To define the cytotoxicity of the extracted compounds toward cancer cells (Human Osteosarcoma) with respect to extract formulation, dosage and exposure time.

• To develop a delivery vehicle using sodium alginate as the main carrier material, which would possess characteristics that render the delivery of GLS efficient, safe and effective. This delivery vehicle would improve on existing drug delivery systems with respect to material safety, drug loading capacity, distribution uniformity, tissue adhesion (via surface traits) and controlled release in a physiological environment. This new delivery system will also enhance the bioavailability of GL compounds and control its release over a sustained period of days. It will protect GL biomolecules and negate premature metabolic breakdown.

This project will contribute crucial findings to the foundation of GL development for healthcare. By evaluating aspects of three drug development stages (compound isolation, in-vitro testing, and compound delivery), the methodological approach and discussion will critically present an exciting candidate for today's medical needs. It is hypothesised that the most scalable extraction method will be revealed, and it is expected that cancer cells will be inhibited with the most triterpenoid-rich compounds from GL, in-vitro. Voltage will be a significant factor affecting the drug delivery system achieved with EHDA, and using sustainable and non-toxic polymer alginate, a competitive size and shape range will be achievable along with a sustained release – something not yet achieved with this biopolymer.

## 1.3 Project Structure

The investigations presented in this thesis aim to contribute to the development of Ganoderma lucidum (GL) for healthcare by tackling the current limitations outlined in the literature review of this project. In light of this, this project will propose and evaluate solutions to the challenges faced so far in the development of Ganoderma lucidum for healthcare. The studies

target the evaluation of an effective extraction process for GL spores (GLS), the bioactivity achieved by the GLS yield, and the feasibility of using an established mechanical process to encapsulate GLS with respect to controlled, smart delivery.

**Chapter 1** introduces GL as a major player in the Chinese Traditional Medicine (CTM) field. A background of the field creates context for the experimental framework outlined, and the subsequent developments.

**Chapter 2** presents an extensive literature review of the field at the current time. This survey is an in-depth summary of the progress made to date, with particular focus on GLS biomolecule extraction, and yield bioactivity, and potential delivery channels. The existing literature provides a good foundation for the engineering of investigations presented in this thesis.

**Chapter 3** details all experimental materials and methods. **3.1** describes the methodologies engineered to manipulate the extraction of crude GL polysaccharides (GLPS) from GLS using two conventional methods. This allows an evaluation of each process with respect to its yield efficiency and scalability. **3.2** employs supervised machine learning to evaluate HWE with respect to the yield of a polysaccharide-Ganoderic Acid complex. This analysis provides a representative model for this yield across a larger parameter range. This chapter subsequently examines the in-vitro cancer inhibition activity of both the PSGA extract and GLPS extract. **3.3** presents a process to generate polymer-based micro-vehicles for drug delivery, demonstrating crucial roles played by certain process variables with respect to vehicle physical characteristics and release kinetics.

**Chapter 4** puts forward a critical discussion led by the results obtained from the investigations in Chapter 3. The biomolecule extraction and bioactivity results are reviewed with respect to their implications on the prospects of developing GL for healthcare today, and the encapsulation findings are discussed in light of "smart" GL delivery.

**Chapter 5** concludes the findings of the experimental work, and its current standing in a wider context of developing a pharmaceutical drug in today's healthcare market.

**Chapter 6** describes the potential for future work, implicated by the findings in this project. Limitations of the investigations are raised and discussed with regard to their methods and conclusions. It puts forward experimental recommendations with respect to GL development, but also with respect to a wide range of natural organisms in the food and drug sector.

**Chapter 7** finally provides details of the referred work cited throughout this project.

# 2 Literature Review

The aim of this literature review is to collate and discuss work done so far in the development of Ganoderma lucidum (GL) for healthcare. A comprehensive overview of the healthcare benefits of GL is provided and current achievements in, along with prospects for the development and delivery of its biomolecules. Through the understanding and evaluation of published work surrounding the crucial stages of development, solid foundations can be set for areas of further investigation.

## 2.1 Medicinal Basidiomycota and Ganoderma lucidum (GL)

For centuries the health benefits of basidiomycota have been known, and their use has been documented in records across Eastern Asia. The earliest extracts of basidiomycota were obtained from boiling to produce a *tincture* in which the compound was available for consumption [McKee, 1988]. In 1969 Ikekawa's study on hot water extracts of basidiomycota propelled studies into the anti-tumour activity of basidiomycota, and parallel studies highlighted potential areas of development in immunoenhancement [Ikekawa et al., 1969; Shibata et al., 1968]. Investigations revealed that much of the bioactivity could be attributed to monosaccharides linked glycosidically (*polysaccharides*), and steroid-synthesising organic compounds (*triterpenoids*). To date, scientists have striven to elucidate the biocompounds and their structural discrepancies that are known to lead to distinct mechanisms of therapeutic action.

GL is a strain of the Ganoderma polyporaceae. It has been employed in the Far East as a remedy for many ailments including cancer, diabetes, cardiovascular disease, and general immunosuppression [Shibata et al., 1968]. Compounds from GL have also been effective against allergies, arthritis, bronchitis, hyperglycaemia, hypertension, hepatitis, inflammation and ulceration [Boh et al., 2007]. These bioactivities have been shown to stem from its chemical molecules include phenols, terpenoids, steroids, nucleotides, as well as their derivatives—glycoproteins and polysaccharides [Yuen et al., 2005]. Polysaccharides (mostly in the form of glucans with different types of glycosidic linkages) and terpenoids are particularly important potent components, and recent studies also recognize the importance of phenolic compounds [Ferreira et al. 2009]. Many crude extracts have a synergistic effect, achieving an increase in biological activity [Zhu et al., 2000; Liu et al. 2002].

The GL biomass encompasses a pool of bioactive constituents; its main elements being a variable composition of polysaccharides, triterpenoids, proteins, peptides, and amino acids [Yue et al., 2008]. Generally, studies have observed that crude carbohydrates typically compose between 35 and 50% of GL, and across literature the triterpenoid and polysaccharide content has been reported between 0.5-8%, and 1-20%, respectively [Chang et al., 2008; Nhi et al., 2012; Sharif et al., 2017] – with compositional discrepancies between arising from strain, origin, and cultivation conditions (substrate typically includes Sawdust, Woodlog, or Grain) [Yue et al., 2008; Erkel, 2009; Zhou et al., 2012]. Recent research however has shown a tremendous dependence of composition and bioactivity on the extraction process used to isolate bioactive compounds, which exposes the constituents to various physicochemical conditions to facilitate their extraction [Zhou et al., 2012].

Physical structures known as the Fruiting Body (GLFB), Mycelium (GLM) and Spores (GLS) form the main body of GL. The GLFB consists of the pileus (cap) and a basidia porous layer that produces GLS during reproduction. GLM refers to the thread-like features of the fungus, present in the substrate in which growth takes place. Once spores germinate, they produce a mass of single-celled structures known as hyphae, collectively termed mycelia. Figure 2.1 is a simple representation of the GL physical structure.
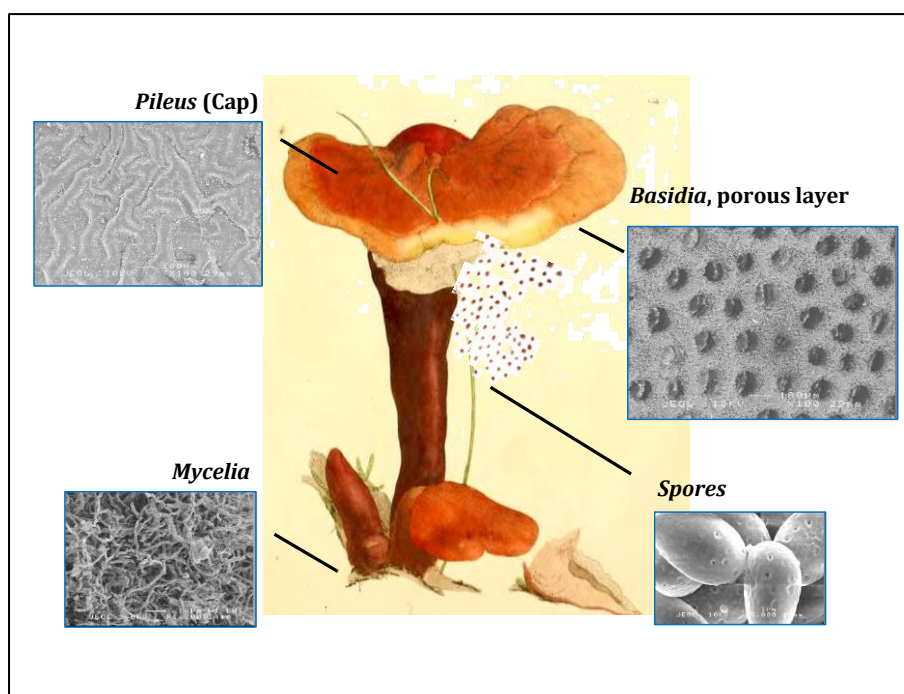


**Figure 2.1:** Schematic of Ganoderma Lucidum's physical structure [Sowerby 1797] and scanning electron microscopic images of the main structural elements. GL provided by the Longquan province of China and imaged using a JEOL 8600 Superprobe Field Emission Gun Scanning Electron Microscopy

*Novelty processing and smart delivery of Ganoderma Lucidum spores*

Mizuno reported the composition of a crude GL extract to be mainly D-Glucose [Mizuno et al., 1984], and this was verified by a 2002 study on a commercially-available crude GL extract (table 2.1) [Wang et al., 2002]. This study also observed that 15.6% of the extract could be attributed to proteins. It is the D-Glucan (and its crude forms) that have most often demonstrated immunomodulating and anticancer effects [Miyazaki et al., 1981; Kim et al., 2017]. Hence, most studies on GL have focused on this polysaccharide.

| Sugar Components | Percentage (%) |
|---|---|
| d-Glucose | 58.0 |
| d-Mannose | 15.5 |
| l-Fucose | 9.7 |
| d-Galactose | 9.3 |
| d-Xylose | 5.4 |
| d-GlcNAc | 1.0 |
| l-Rhamnose | 0.5 |

**Table 2.1:** Carbohydrate composition of a commercially available crude GL extract [Wang et al., 2002]. D-Glucose is a principal constituent

Another bioactive protein isolated from GL, a protein named *Ling Zhi-8 (LZ-8)*, portrays a structure similar to antibodies, presenting scope as an immunoenhancing agent with proven mitogenic capacity in vitro. Established antitumour effects of this protein via suppression of pro-inflammatory mediator expressions was documented, presenting it as a potential anti-inflammatory agent for modulating in vitro immune responses involving inflammation [Chen et al., 2017]. A study in 2011 found that this protein activated p53 and p21 expressions and demonstrated apoptosis of Lewis lung carcinoma in mice in-vivo – effects that appear consistent across literature [Wu et al., 2011; Lin et al., 2014]. This protein is typically isolated via gel filtration and ion-exchange chromatography.

*Novelty processing and smart delivery of Ganoderma Lucidum spores*

## 2.1.1 Ganoderma lucidum Spores (GLS)

Despite ancient records of GL Fruiting Body studies, the investigation into spores can only be traced to 1988 in a study carried out by Hou et al [Hou et al., 1988]. GLS have been reported to have higher bioactive yields than other GL fractions and its antitumor effects have been observed at 80–90% tumour inhibition, with studies suggesting a variety of distinct yet inconsistent chemical characteristics responsible for the bioactivity [Yue et al., 2008]. GLS extracts were also shown more effective in the inhibition of cervical cancer cell line, HeLa, in-vitro when *broken* spores were used. The authors observed greater apoptotic activity of the broken spore extract via cell cycle arrest, inhibited DNA synthesis, and reduced intracellular calcium in particular [Müller et al, 2006, Cao et al., 2003]. While other GL structures have been observed rich in specific phenolic compounds typically associated with antioxidation and immunoenhancement, GLS have additionally been observed to contain cytotoxic compounds *as well* [Cao et al., 2003, Na et al., 2017]. Increasing studies are focusing on the attribution of spore extract bioactivity to Ganoderic Acid triterpenoids in the spores [Min et al., 2000; Zhang et al., 2011]. Combined with the spores' polysaccharide content, GLS extracts can indeed be a remarkable candidate for disease prevention; possessing both cytotoxic *and* immunoenhancing biocompounds [Yue et al., 2008; Jin et al., 2015]. While studies comparing the bioactivity of different GL fractions are rare in literature, the assertion that spores are a more promising source of bioactive agents has nevertheless been consistent owing to chemical profiling. A study by Sliva in 2003 demonstrated that human breast cancer cells as well as human prostate cancer cells were most effectively inhibited when the aqueous extract from spores was administered, via its effect on cell migration [Sliva et al., 2003]. Broken spores were particularly effective in inhibiting human prostate cancer cells, as figure 2.2 shows, however overall the study found little correlation between sample composition and cell inhibition.
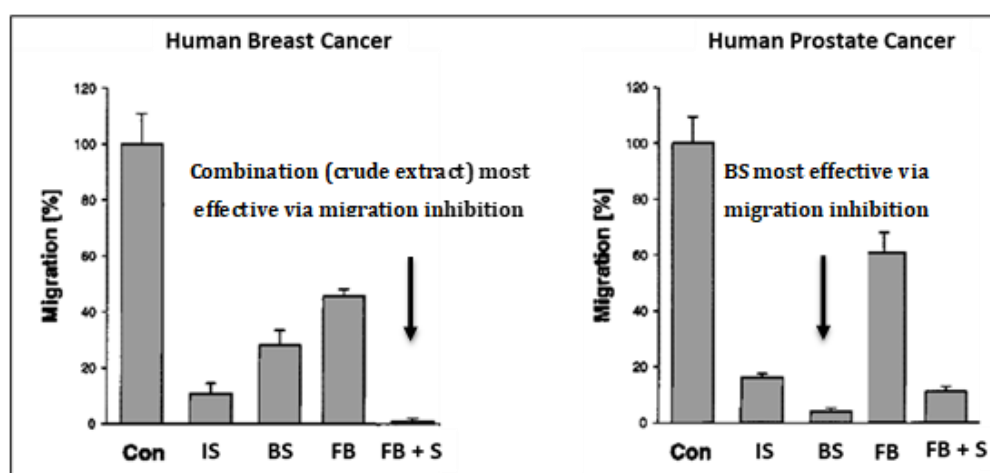


**Figure 2.2:** Effect of GL fractions on the migration (indicating growth) of two cancer cell lines. Spore extracts were most effective, along with the fruiting body/spore mix. IS = Intact Spores, BS = Broken Spores, FB = Fruiting Body , FB+S = Fruiting Body and Spores [adapted from Sliva et al., 2003]

Interestingly however, this study found that the mixture of fruiting body and spores was most effective at preventing cancer growth. The authors attributed the differences to chemical composition previously discussed. Of course there will be differences in treatment potency depending on the cell line as they express different genes. In the study by Sliva for example, breast cancer cells express estrogen receptor b (ERb), whereas prostate cells express ERa as well as ERb.

### 2.1.1.1 Extracting Bioactive Compounds from GLS

A wall composed of chitin and chitosan, known as the sporoderm, protects GLS bioactive compounds residing in the spores. Despite the bioactive wealth of spores, the extraction from these tough structures is therefore more energy-demanding than the nutraceutical isolation from other parts of the typical plant structure; potentially depleting bioactivity and exhausting economic scalability through exposure to extreme heat, pressure, force, and chemicals [Ma et al., 2007]. An example of this is shown in figure 2.3 via the scanning electron microscopy (SEM) images of intact (A) and broken (B) GLS from physical grinding. However with today's rate of advancement in technological developments, over 90% sporoderm breakage can be achieved whilst retaining bioactivity of the extracted yield [Fu et al., 2009; Li et al., 2017].
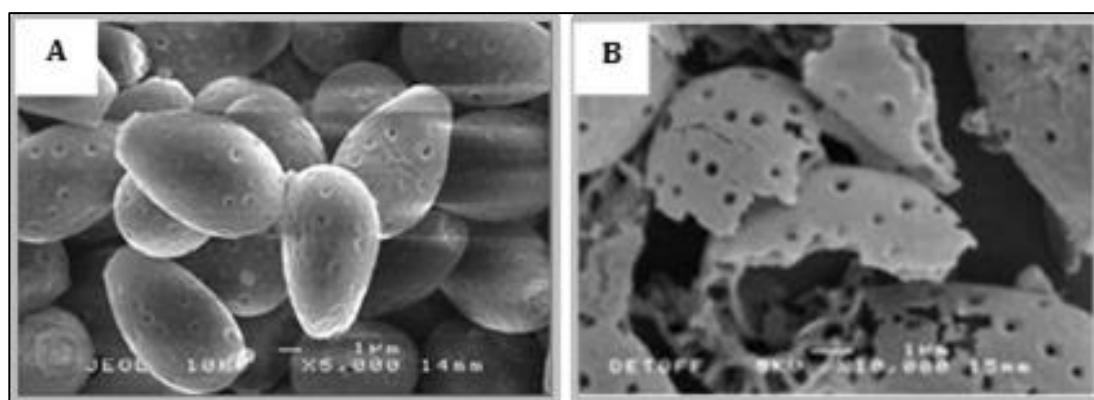


**Figure 2.3:** Scanning Electron Microscopy of A) Intact and B) Mechanically-broken GLS obtained from Longquan, China and imaged using a JEOL 8600 Superprobe Field Emission Gun Scanning Electron Microscopy. Intact spores typically range from 7-12µm diameter and once broken they can yield broken spore pieces with a diameter below 2-3 µm (while intact/broken spore diameter is typically measured using the Feret's diameter, irregular fractions are often not recorded as a diameter – rather for a sporoderm breakage rate)

### 2.1.2 Bioactive Compounds: Polysaccharides

The focus on **polysaccharides** stems from increasing evidence of their ability to combat and prevent certain diseases via immunoenhancement. Specific focus has fallen on the Glucan

polysaccharide configuration known as the D-Glucan [Bao et al., 2001]. Unfortunately the structural complexity and diversity implicated by their degree of branching and conformation results in difficulty streamlining its processing. Often the extraction of Glucans from basidiomycota results in a complex involving other monomer compounds like xylose, mannose and galactose [Raher et al., 2011, Descroix et al., 2014]. In addition, many conjugations are formed with proteins to form proteoglycans and glycopeptides, which fortunately show significant antiviral and immunoenhancement activities via processes such as macrophage production and cytokine modulation [Ji et al., 2007; Li et al., 2005; Ho et al. 2007].

Polysaccharides, also known as *Glycans*, are composed of monomer carbohydrates linked by glycosidic covalent bonds and are structural components of all living organisms. They are involved in vital cell mechanisms such as recognition, signalling and proliferation. Contrary to other biopolymer structures such as amino acids, monosaccharide units of polysaccharides link at various points, creating branched as well as linear structures [Sone et al., 1985]. In 2001 Reshetnikov's infamous study on 651 basidiomycota containing pharmacologically active polysaccharides revealed unique polysaccharides that induced tumour regression in mice; of which Ganoderma lucidum possessed a particularly high amount [Reshetnikov et al., 2001]. These water-soluble compounds display significant bioactivity in immunoenhancement assays [Bao et al., 2001]. The most prevalent polysaccharide has been found to be Glucan, and studies have indicated its immunopotency when isolated from a variety of organisms including barley, yeast and oat [Johansson et al. 2006; Chan et al., 2009]. Importantly, polysaccharides are often isolated whilst attached to proteins and peptides/amino acids to form complexes such as glycoproteins, glycopeptides, and other *unidentified* forms which have become the subject of many investigations surrounding GL [Cao et al., 2006, Zhong et al., 2015].

### 2.1.2.1 Structure of Polysaccharides

Polysaccharides exist in a variety of forms and typically follow an organized arrangement, however they are consistently undefined in shape, differing in the location and configuration of glycosidic bonds between the monosaccharides, and also differing in their degree of attachment to other biomolecules [Sone et al., 1985]. GL polysaccharides like β-D-Glucans, heteropolysaccharides and glycoprotein have been isolated and characterized and are considered the major contributors of bioactivity of the mushroom.

Recent analytical techniques have allowed elucidation of specific structures of these complex molecules, with popular methods employing liquid chromatography and mass spectroscopy [Ma et al., 2018]. High costs and analytical complexities however have instilled a considerably rigid

"norm" of feasible polysaccharide analytical methods, including the Phenol-Sulphuric Acid assay and Enzyme Hydrolysis. These methods however are not conclusive enough, owing to their limited selectivity and thus incomparability with other studies' findings. For example the Phenol-Sulphuric Acid assay involves analysing the extract in the UV-Visible spectrum at a wavelength, and elucidates the presence of numerous hexose polysaccharides. It is however quick and reproducible [Dubois et al., 1956]. Fortunately, most medicinal mushroom polysaccharides have been confirmed as *D*-Glucans consisting of glycosidically-linked D-Glucose; where "D" refers to the specific configuration of a chiral carbon in its structure. Spectroscopic analyses have endeavoured to elucidate the structural configurations D-Glucans from medicinal mushrooms, including Nuclear Magnetic Resonance (NMR), Gel Chromatography (GC), High Performance Liquid Chromatography (HPLC), Ultraviolet-Visible (UV-Vis) Spectroscopy and Fourier Transform Infrared (FTIR) Spectroscopy among others [Bao et al., 2001; Li et al., 2008, Rahar et al., 2011].

### 2.1.2.2 D-Glucan Polysaccharides

D-Glucose, the monomers comprising D-Glucans, contains an aldehyde carbonyl group with five hydroxyl groups, forming C1-5 in a cyclic form. An alpha- (α, axial) or beta- (β, equatorial) configuration results depending on the position of the hydroxyl on first carbon (C1) of the monosaccharide units. In fungal species, the presence of both (1→3) -β and -α configuration linked D-Glucans suggests that the hydroxyl group on C1 of one D-Glucose monosaccharide is bound to the hydroxyl group on C3 of another. These species typically display branches at (1→6) where C1 is linked glycosidically to C6 [Li et al., 2018]. Figure 2.4 shows this. It shows the structure of a β-D-Glucan consisting of a linear backbone of β-(1-3)-linked D-glucose groups with varying branching degrees at the C6 position. D-Glucans also exist with heteropolysaccharide chains of monomers that typically include xylose, mannose, galactose, and uronic acid glucan–protein complexes that often represents 10–50% of dry crude GL. In medicinal mushrooms, studies have drawn focus to the therapeutic value of the β-D-Glucan; a structure composed of linear unbranched β-D-glucose. The linear units can differ by branching and length, yielding many species, but also influencing the polysaccharides' extractability and bioactivity [Sone et al., 1985, Rahar et al., 2011]. For example, one of the first studies investigating the structure of GL extracts by Miyazaki in 1981 reported a correlation between the structural branching of fruiting body compounds, and tumour inhibition [Miyazaki et al., 1981; Bao et al., 2001; Yanaki et al., 1983]. Similarly, when the structure of the lentinan, a β-(1-3)-D-Glucan from Lentinus Elodes, was denatured its ability to inhibit tumour growth was compromised. Lentinan has a high molecular weight and contains mostly β-(1→3)-glucose linkages in its backbone and β-(1→6)-glucose side-branches. Studies typically attribute lost bioactivity to lentinan's transition from triple-helical to

single random-coil chains in certain organic solvents like NaOH and DMSO or at high temperatures [Nandi et al., 2013; Zhang et al., 2004]. This conformity shown in figure 2.5. Studies endeavour to investigate methods that extract varying forms of the molecules to verify bioactive discrepancies.  This will be discussed in 2.1.5 in detail, but effective isolation is often a function of extraction conditions like temperature, solvent, and duration [Sone et al., 1985; Zhang et al., 2011]. Characterisation methods are also briefly talked about in 2.1.6.2.1, and most commonly include chemical degradation like Smith degradation and methylation analysis [Sone et al., 1985; He et al., 2010]. Infrared-based spectroscopic techniques such as Fourier Transform (FTIR), Nuclear Magnetic Resonance (NMR) and Exchange-ion Chromatography (EIC) are often employed, alongside microscopic techniques such as Scanning Electron Microscopy (SEM) and X-Ray Diffraction (XRD), but typically are complementary to chemical techniques [Bao et al., 2001].
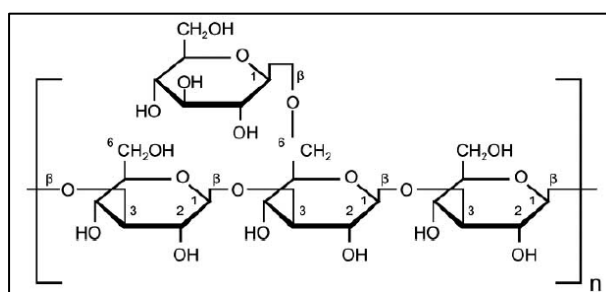


**Figure 2.4:**  Linear backbone of β-(1-3)-linked D-glucose groups with varying degrees of branching from the C6 position [Sanodiya et al., 2009]. Each monosaccharide is an aldehyde with hydroxyl groups added onto carbon atoms
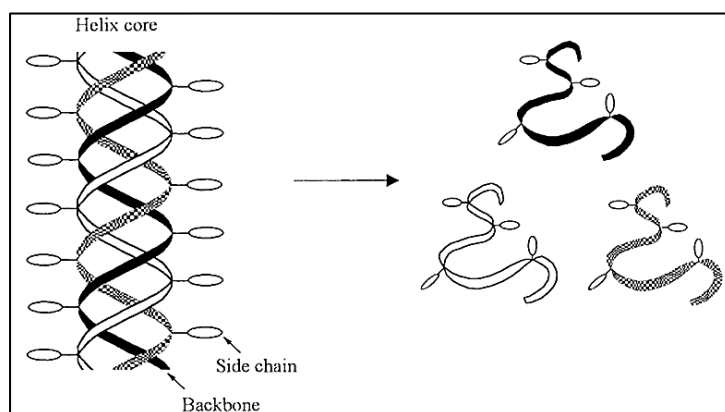


**Figure 2.5:** Schematic of the transition of β-D-Glucan triple-helical structure to single-helical, usually in response to degradation. Adapted from [Zhang et al., 2002].

## 2.1.3 Bioactive Compounds: Triterpenoids

Triterpenoids have recently gained attention owing to their considerable tumour cytotoxicity when isolated from many plant species. Triterpenoids are organic hydrocarbons

*Novelty processing and smart delivery of Ganoderma Lucidum spores*

(terpenes) possessing functional groups, and compose the other principal compound in Ganoderma lucidum [Ma et al., 2011; Fukuzawa et al., 2008]. They traditionally represent the most popular products derived from plants. Based on the number of building blocks (isoprenes, C5H8)n, terpenes are classified as either monoterpenes, sequiterpenes, diterpenes, sesterterpenes, triterpenes, tetraterpenes, or polyterpenes. β-carotene is a well-known example of a triterpene. *Triterpenes*, comprised of isoprene blocks, are increasingly studied for their antitumour mechanisms, including apoptotic mediation and anti-inflammation [Haralampidis et al., 2002]. Terpenes can be modified chemically, such as by oxidation or rearrangement of the carbon skeleton, giving rise to compounds generally identified as terpenoids. Naturally-occurring triterpenoids from GL have a structure based on lanostane, a metabolite of lanosterol. The vast majority are Ganoderic and Lucidenic acids [Chen et al., 2010; Jiang et al., 2008; Ma et al., 2002]. Their purified forms are quickly creating inspiration for novel effective drugs – especially as a treatment for cancer, allergies, HIV-1, and angiostenosis [Müller et al., 2006; Radwan et al., 2011]. At a molecular level, triterpenoids have indicated bioactivity via the reduction of oxidative stress, regulation of cell cycle (for example via apoptosis) and the modulation of signal transduction pathways in the tumour environment.

It has been estimated that more than 20,000 triterpenoids exist in nature, being predominantly found in various plants including sea-weeds as well as in wax-like coatings of various fruits and medicinal herbs [Bishayee et al., 2011]. Over 150 triterpenoid structures have been identified from GL alone, with many studies observing the greatest quantity in the spores [Radwan et al., 2011]. Among them, more than 50 were found unique to this GL – with particular importance given to the oxygenated triterpenoid acid *Ganoderic Acid* (GA). These compounds have typically been extracted using organic solvents like ethanol, methanol, chloroform and ethyl acetate, which raises concerns over toxicity. Figure 2.6 shows the structure of a GA (GA-F specifically) [Teekachunhatean et al., 2012]. Red circles denote the points of variation between the GA structures where functional groups typically represent carboxyl, carbonyl, or methyl moieties.
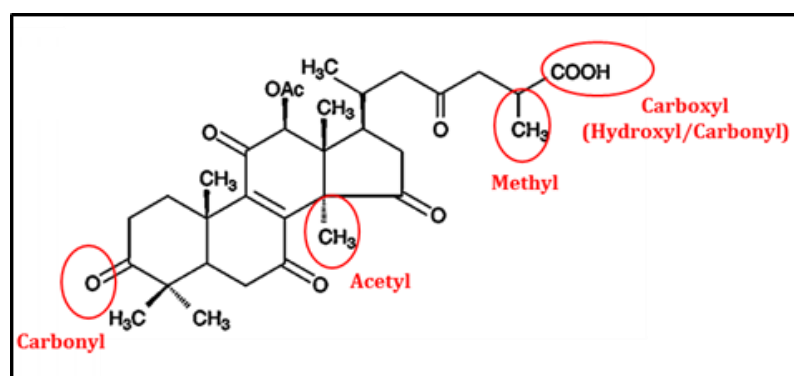


**Figure 2.6:** Basic skeleton of Ganoderic Acids, where the red indicates points of variation between isomers [Teekachunhatean et al., 2012]

*Novelty processing and smart delivery of Ganoderma Lucidum spores*

Even amidst technological advancements in evaluative spectroscopic techniques, GA triterpenoid characterisation is severely underdeveloped. As a result, correlations between structure and bioactivity are not yet defined, yet the lanostane structure is known to play a significant role in biological function – so much so, that the hydroxylation of this structure was found to influence inhibition potency toward breast cancer cells when administering ganoderic acid isomers GA-A, GA-H and GA-F [Jiang et al., 2008].

Different types of GAs are hydroxylated at different positions, determining the isomer classification. Typically, GA isomers are defined using fragmentation behaviour following repeated spectroscopic steps at a UV wavelength between 252nm and 257nm [Sun et al., 2012]. In particular liquid chromatography – mass spectroscopy (LCMS) can indicate the loss of functional groups in GA isomers, indicating fragments that uniquely identify these isomers. Figure 2.7 below shows fragmentation behaviour during LCMS. The loss of 130 Da represents the characteristic cleavage of the αβ bond (C20–C22) from the C=O in the side chain [Sun et al., 2012].
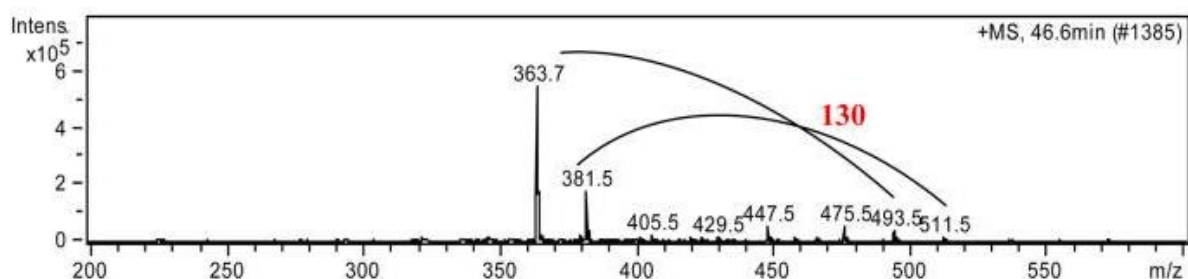


**Figure 2.7:** Example of the loss of fragments (130 Da) in the cleavage of Ganoderic Acid F (GA-F) during LCMS [Sun et al., 2012]

Still, to date very little consistency remains across the isolation of specific GA isomers. This limitation in reference standards has diminished efforts dedicated to the development of this invaluable biocompound. Figure 2.8 shows the LCMS mass distribution of GA-D, a GA isomer, indicating again how the spectrum can portray the isomers via their stage of fragmentation [Cheng et al., 2012].

*Novelty processing and smart delivery of Ganoderma Lucidum spores*
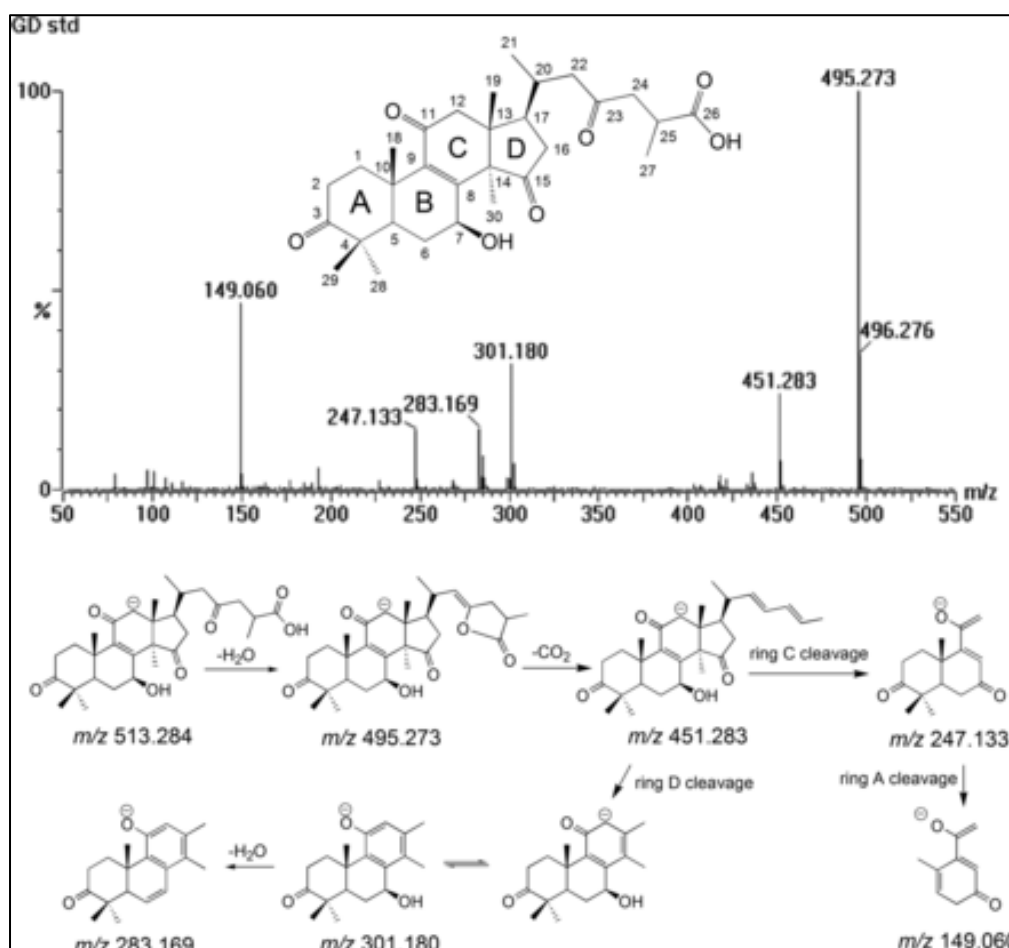
**Figure 2.8:** Mass spectrum of Ganoderic acid D (obtained on a Q-TOF mass spectrometer) and the proposed fragmentation pathways of Ganoderic acid D [Cheng et al., 2012]

Structural importance has been given to two particular moieties in the GA structure: a carbonyl group at C-3 and a carboxyl/methyl group at C-26 [Sone et al., 1985]. The former has been shown to elicit apoptotic effects, whereas the latter has fostered permeation of the cancer cell membrane; rendering both structures essential to tumour inhibition via apoptosis [Zhou et al., 2011; Wu et al., 2012]. For example in 2012 Liu observed that structural modification at these structural points changed inhibitory action toward human prostate cancer cells. These factions of the GA isomer were found instrumental to the binding to tubulin, a building-block cell protein often targeted for growth suppression in tumours. The binding affinity of GA to tubulin was observed to be similar to that of an established chemotherapy drug, however GA was also found to have a separate tubulin-stimulating effect that could inhibit tumour cells via a second mechanism that essentially "stunts" growth through tubulin stability and subsequent cell cycle disruption [Liu et al., 2012].

*Novelty processing and smart delivery of Ganoderma Lucidum spores*

## 2.1.4 Pharmacological function of GL Biocompounds

Table 2.2 details the published effects of commonly extracted from GL. It is clear that the effects are a function of health purpose, extract type, and administration. Their undefined structures have led to undefined bioactivities that continue to be studied. In nearly all investigations listed in table 2.2, the focus is on polysaccharides and triterpenoids and their complexes and derivatives. Generally, polysaccharides (and "water extracts") demonstrate immunoenhancing effects, whereas triterpenes (and "ethanol extracts") are potent against cancer growth. GL extracts are purified to yield either various degrees of purity – typically referred to as a "crude" or "neutral" extract. The former typically does not undergo chemical purification that removes proteins, fats and amino acids; leading to the debate as to whether these crud extracts are in fact more potent against certain illnesses.

| Extract | Cell/mice | Optimum Dose | Time | Pharmacological Effects | Reference |
|---|---|---|---|---|---|
| Crude Water Extract | γ-ray-irradiated mice | 400 mg/kg | 35 days | Enhanced recovery of immuncompetence from γ-ray-irradiation. | Chen et al., 1995 |
| | RAW 264.7 | 100 µg/ml | 24h | Inhibited LPS-induced NO production | Song et al., 2004 |
| | NK92, pNK, K562 | 5% drug/tissue | 24h | Induced NK cell cytotoxicity against cancer cell lines by activating NKG2D/NC receptors and MAPK signalling pathways. | Chang et al., 2014 |
| Ethanolic Extract | MDA-M8 231, B16-F10 | 250 µg/ml | 48 h | Decreased viability in time/dose dependent manner | Barbieri et al., 2017 |
| Polysaccharide | HL-60 and U937 | 100 µg/ml | 5 days | Increased IL-1 and IL-6 and might play indirect role in potentiating anti- tumor immunity in vitro | Wang et al., 1997 |
| | C57BU6j, BALB/c mice | 12.8 mg/L | 5 days | Promoted the cytotoxicity of specific T-lymphocytes induced by dendritic cells (DC), which were pulsed with P815 tumor antigen during antigen presentation | Cao et al., 2003 |
| | L929, P815, YAC-1, C57BU6 mice | 400 or 100 mg/L | 15 days | Promoted cytokine-induced killer (CIK) cell proliferation and cytotoxicity relevant to enhancing IL-2, TNF production | Zhu et al., 2006 |
| | S180, Heps, EAC, ICR species mice | 300 mg/kg | 8 days | Inhibited the growth of inoculated S180, Heps, and EAC tumor cells | Pang et al., 2007 |

*Novelty processing and smart delivery of Ganoderma Lucidum spores*

| | | | | | |
|---|---|---|---|---|---|
| | S180, BALB/c mice | 200 mg/kg | 14 days | Activated the immune response by stimulating NK cells, T cells and macrophages | Wang et al., 2012 |
| | Wistar rats | 2.6 mg/mL | 48h | Enhanced the antioxidant enzyme activities, and reduced levels of IL-1b, IL-6, and TNF-ci in rats with cervical cancer. | XiaoPing et al., 2009 |
| | B16F10, C57BU6 and BABUc mice | 12.8 p.g/mL | 72 h | Antagonistic effects on the immunosuppression induced by B16F10 | Sun et al., 2011 (a) |
| | B16F10, BALB/c mice | 400 µg/mL | 5 days | Suppressed lymphocyte proliferation and perforin and granzyme B production in lymphocytes after induction with phytohemagglutinin | Sun et al., 2011 (b) |
| | B16F10 | 400 µg/mL | 48 h or 21 days | Enhanced major histocompatibility complex (MHC) class I, more efficient immune cell-mediated cytotoxicity against these B16F10 cells might be induced | Sun et al., 2011 (c) |
| | B16, A375, 057131/6J | 400 µg/mL | 21 days | Inhibited the adhesion of fibrinogen to melanoma cells and reversed the blocking effect of the fibrin coat on NK cytotoxicity against melanoma cells | Zheng et al., 2012 |
| β-Glucan | Neutrophils | 100 µg/mL | 24 h | Induced anti-apoptofic effects on neutrophils relying on activation of Akt-regulated signaling pathways | Hsu et al., 2002 |
| | | 10 µg/mL | 24 h | Promoted the activation and maturation of immature DC | Lin et al., 2005 |
| | THP-1, U937 | 100 µg/mL | 72 h | Induced selected monocytic leukemic cell differentiation into DCs with immuno-stimulatory function | Chen et al., 2007 |
| Proteoglycan | Lymphocytes from BALB/c mice spleens | 500 p.g/mL | 72 h | Activated B cells and expressed CD71 and CD25 on the cell surface. Enhanced the expression of protein kinase Cα and protein kinase Cγ in 13 cells. | Zhang et al., 2002 |
| Triterpenes | A549, C57BU6 mice | 120 mg/kg | 14 days | Anti-lung cancer activity *in vitro* and *in vivo* via immunornodulation and cell apoptosis. | Feng et al., 2013 |

*Novelty processing and smart delivery of Ganoderma Lucidum spores*

| | | | | Up-regulated expression of Nuclear Factor-KB which might be involved in the production of IL-2 | Wang et al., 2007 |
|---|---|---|---|---|---|
| Ganoderic Acid | YAC-1, LLC, C57BU6 mice | 28 mg/kg | 20 days | | |
| | 2LL, C57BU6 mice | 10 | 48h | Induced the apoptosis of competent T cells and increased the proportion of T-reg cells | Que et al., 2014 |

**Table 2.2:** Summary of the therapeutic effects of some extracts from GL. It is evident that most isolated compounds in literature express antitumour effects via effects on the immune system

The effects achieved by GL extracts vary both in potency and mechanism, where discrepancies are attributed to differences in the lead compound and general structure. As previously asserted, the effects of GL biocompounds are typically either associated with direct cytotoxicity or immunoenhancement. Indeed it has been shown by many investigators that large-scale therapeutic effects have often stemmed from cellular-level biological functions. Furthermore, while a variety of tumour cell lines have exhibited inhibition when exposed to these compounds from GL (in-vitro *and* in-vivo), the application of the extracts to more stubborn (resistant) aggressive tumour cell lines has not yet been studied, suggesting a treatment that is not yet robust. This includes rapidly-reproducing cells like human Osteosarcoma (HOS) [Endo-Munoz et al., 2010]. The effects of the two main GL biocompounds of study (polysaccharides and triterpenoids) are detailed in the following sections. More cytotoxic findings are often attributed to *crude* forms of GL extracts, containing a variety of polysaccharide and triterpenoid complexes, often resulting from one-step solvent extraction that maintains important biomolecules [Liu et al. 2002]. For example the anti-migration effects of GL were investigated in a 2019 in-vitro study on the inhibition of Triple-negative breast cell motility, with focus on protein involvement. The extract was a crude concoction containing 13.5% polysaccharides, 6% triterpenes, and 1% cracked spores. Triple-negative breast cell occurs in the absence of estrogen and progesterone receptors and there are currently very limited treatment options besides chemotherapy. 24h GL treatment could inhibit the cancer with no cell recovery after a 72h period of withdrawal. A significant finding was the impact of GL cell invasion and migration and regulated proteins that contribute to the cells' viability.

### 2.1.4.1 Bioactivity Attributed to GL Polysaccharides

Disease progression is driven by various mechanisms, which are either fuelled or inhibited by the body's natural processes. Studies typically identify polysaccharides as immunoenhancers; an elite group of compounds displaying the capabilities of a Biological

Response Modifier (BRM); possessing the ability to generate disease-fighting mechanisms in the body non-invasively and with non-specific mechanisms.

Literature continues to elucidate a vast array of evidence suggesting considerable potency of GL polysaccharides, with most of observing tumour inhibition via an enhanced immune system [Sone et al., 1985; Yue et al., 2008]. For example, in 1989 Nishijima and Miyazaki carried out a study investigating the effects of β-D-Glucan polysaccharides from GL on S-180 cancer cells in mice. Antitumor activity was found to be attributed to $(1\rightarrow3)$-, $(1\rightarrow4)$- and $(1\rightarrow6)$-linked β-D-Glucans, and while several polysaccharides were isolated from other Ganoderma species, those isolated from Ganoderma lucidum inhibited the cancer by 98.5%; unattainable by the other species [Miyazaki et al., 1981].

The therapeutic effects of β-D-Glucan polysaccharides in particular have been successfully elucidated via immunoenhancing effects both in-vitro and in-vivo [Yoshida et al., 2012]. The consistently positive impact observed on the body's immune system and resulting disease inhibition have therefore indicated that the "anticancer" effect of β-D-Glucan polysaccharides is principally attributed to immunoenhancement. It should be noted however that some studies do still claim a direct cytotoxic effect of these polysaccharides, likely because of *cruder* polysaccharide forms that contain a variety of complexes including proteins and triterpenoids that may open up additional synergistic pathways [Zhu et al., 2000; Liu et al. 2002]. Generally, studies report a polysaccharide-induced immune response reflected by enhanced phagocytosis, dendritic cell maturation, boosted cytokine production and improved lymphocyte cytotoxicity/generation [Ji et al., 2007; Li et al., 2005; Ho et al. 2007]. Polysaccharides have shown evidence of effectively binding to immune cell receptors, including the Dectin-1 protein receptor and Complement Receptor-3 (CR-3) in-vitro, in the activation of a more efficient immune response through increased molecular pathways. Many of the effects displayed by polysaccharides are potent tumour-suppressing effects such as anti-inflammation, regulating the pro-inflammation cytokines involved in tumour survival (including TNF-α and Nitric Oxide). Some of these effects are more recently attributed to Ganoderic Acid triterpenoids [Liu et al., 2015].

As natural compounds are typically substrate-specific, they work synergistically with the compounds naturally found in their host organism. This renders their extracted forms arguably less effective unless in the presence of similar environments to that in which they are found. *In-vitro* studies have therefore been criticised for their lack of an accurate physiological environment. A good example of the importance of basic bodily functions (such as immunity and cell signalling) was demonstrated in 2003, when Cao observed that polysaccharides in an immune conditioned media suppressed leukemic cell lines; yet without media no activity was observed

owing to the lack of metabolites, growth factors, and extracellular matrix proteins [Cao et al., 2003]. Similarly, in a study investigating the effect of Lentinan polysaccharides on immune systems in mice, a compromised immune system (instigated by either T-cell suppression, Neonatal Thymectomy, or anti-lymphocyte chemicals prior to administration) exhibited no antitumour effect following the polysaccharide treatment [Maeda et al., 1971 (a)(b)]. Numerous in-vivo studies using murine models have verified significant bioactive properties of basidiomycota Glucans that contribute to immunoenhancement, and typically indirectly have impacts on tumour inhibition [Awadasseid et al., 2017; Moreno-Mondieta et al., 2017; Sargowo et al., 2018; Chan et al., 2009]. A number of human trials have revealed clinical promise of specific D-Glucans in phase II and phase III trials in East Asia, with human subjects increasingly being employed for in-vivo assays [Stier et al., 2014; Volman et al. 2011]. These will be discussed later in the review.

### 2.1.4.1.1 Immunotherapeutic Action of GL Polysaccharides

#### *"Immunotherapy"*

The idea of using the body's immune system to navigate treatment is known as immunotherapy. In the late 1990s, studies on the interaction between immune cells and tumour cells showed that lymphocytes (T-cells and B-cells) use surface receptor proteins to detect cancerous cells by latching onto their surface proteins. Further studies found that T-cells also carry co-receptors, which are activated by certain cancer cell proteins [Brown et al., 2001]. Thus, through introducing the patient to their own tumour cells, their immune system can detect and destroy the cancer [Yuan et al., 2012]. Many obstacles are still present in this technique of tumour treatment, one being the discovery of the B7 protein (PD-L1), found on the surface of immune cells, revealing that they can be manipulated. Generally immune cells are "instructed" to either *activate* or *stand down* from attacking normal cells, avoiding autoimmune inflammation. Cancer cells can however overexpress these instructive proteins and thus avoid immune system recognition, mimicking an adaptive immune resistance [Chen et al., 2013]. The proteins bind to the co-receptors on T-cells and deter attack, avoiding autoimmune inflammation. The T-cells subsequently remain suppressed in the tumour environment. Figure 2.9 depicts the interaction between an activated T-cell and the tumour entity. Thus, even in the face of an active and efficient immune response to disease, each strain of disease evolves uniquely and progressively develops a growing resistance to conventional therapies and the body's immune system [Chen et al., 2013]. By better understanding the immune system response and its interaction with cancer cells, scientists have engineered ways to boost disease response efficiency.

*Novelty processing and smart delivery of Ganoderma Lucidum spores*
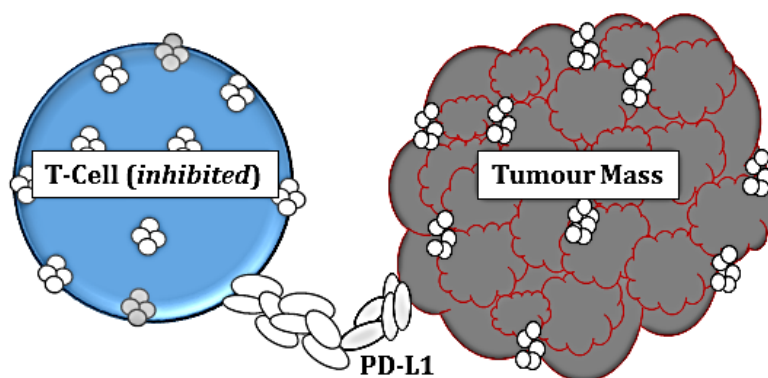
**Figure 2.9:** Current believed mechanism shown by cancer cells when evading immune system detection using Programmed death-ligand-1 protein

The late 20<sup>th</sup> century saw various strategies to prevent the ability of cancer to evade immune cells, and recently antibody therapies have shown promising results such as commercially-available *Nivolumab* and *Pembrolizumab* [Postow et al., 2015]. Recent research is devoted to further understanding the elements of the cancer that allow it to manipulate the immune system, but that may also promisingly act as a marker for their detection [Chen et al., 2013].

### The Role Played by GL Polysaccharides in Immunotherapy

Until recently, the interactions between polysaccharides and the immune system were not mapped out in a way that allowed investigators to draw accurate causal associations between *biocompound* and *therapeutic effect*; let alone the relationship between structural conformation, processing technique, and therapeutic effect. While these relationships are still unclear, the discovery of specific receptor-binding mechanisms displayed by β-D-Glucans when interacting with immune cells indicate definite relationships between molecular physiochemical structure and therapeutic effect [Fan et al., 2014].

Detailed studies on the immunoenhancing mechanisms of polysaccharides involved arose in the late 20<sup>th</sup> century, elucidating the particular importance of D-Glucans from a variety of natural organisms. β-Glucan polysaccharides from yeast were able to stimulate phagocytosis (cell engulfment) and cytotoxicity by binding onto phagocytic cell receptors and NK cells [Wang et al., 199]. Binding to immune cells initiates the body's *innate* defence through an enhanced expression of certain signalling cytokines (including *Interleukin* (IL)-1β, IL-6, *Interferon* (INF)-γ and *Tumour Necrosis Factor* (TNF)-α). These cytokines create cytotoxicity pathways that can induce

*Novelty processing and smart delivery of Ganoderma Lucidum spores*

apoptosis of target tumour cells. A study on polysaccharides from red algae *Sarcodia Ceylonensis* demonstrated a significant increase in the thymus and spleen indices (significant measures of the body's immune system functionality), and elevated expressions of the signalling cytokines involved in immune response when administered to Sarcoma 180 (S-180) induced in mice. There was subsequently a stimulation of T-cells (a white blood cell in the adaptive immune response system) and overall an improved immune response [Fan et al., 2014].

Studies increasingly emphasise that GL polysaccharides (in particular D-Glucans) have effects on the body's macrophage activity, boosting phagocytosis function, enhancing the immune system's cytokine production, and deterring the migration of cancer cells to prevent metastasis. In this way, cytotoxicity is often observed. Hsu, et al. for example reported that GL polysaccharides enhanced the expression of cytokines via the activation of ERK, JNK, and p38 Mitogen-activated protein kinases (MAPKs) [Hsu et al., 2004]. Li et al. reported similar findings, additionally attributing breast cancer cytotoxicity to enhanced macrophage activity and altered gut microbial that could well be associated with the tumour shrinkage in this study [Li et al., 2018]. Wang's study on the production of cytokines by both macrophages and T-lymphocytes observed significant results with a 29-fold increase in IL-6 and considerable increases in interferon (IFN)-ɣ. The resulting enhanced cytokine media were subsequently observed to suppress the proliferation of leukemic cell lines via apoptosis and differentiation into monocytic cells carrying crucial expressions [Wang et al., 1997]. As expected, all effects of polysaccharide administration required cell-conditioned media containing the cytokine expressions.

In a study investigating the effects of GL polysaccharides on immunosuppressed mice, the authors observed enhanced expressions of cytokines on dendritic cell (DC) surfaces; namely expressions of IL-12p40 and 70 which suggested a greater propensity to take-up antigens. In the same study GL polysaccharides also promoted the maturation of the bone marrow-derived DCs that specifically facilitate the cytotoxicity of t-cells [Zhu et al., 2007]. The study emphasised the need for functional lymphocytes in disease eradication. It is not uncommon in literature to make this inference about polysaccharide treatment. Macrophages, lymphocytes that digest and destroy debris that could present a threat to the body and stimulate lymphocyte toxicity, experienced a 30-fold increase in expression when treated with GL polysaccharides alongside chemotherapy in a study. Leukemic cells were also triggered to differentiate into non-threatening cells [Müller et al., 2006]. A similar study found that human macrophage cytokine expressions IL-1β, TNF-α, and IL-6 were enhanced along with T-cell IFN-γ expressions by up to 30-fold in the presence of GL polysaccharides. The polysaccharide-enhanced cytokine media subsequently suppressed the proliferation of human leukemic cell lines through apoptosis [Wang et al., 1997; Chan et al., 2008]. Maturation of cancer cells subsequently occurred, inducing the tumour to express specific

surface antigens to be detected by the immune system. Polysaccharides administered to the cancer cells in the absence of the cytokine media were not inhibitory; reinstating GL polysaccharides induced antitumour action via enhanced cytokine expression of the immune cells. The polysaccharides in the study were reported to be protein-bound branched β-(1-3)-D-Glucans. This study is well-supported by other studies observing that polysaccharide administration is ineffective against tumour proliferation in the absence of functional immune system elements, and thus in-vitro antitumour experiments necessitate immune system elements to observe polysaccharide antitumour effects. Another study investigated the polysaccharide extract of three species from the Ganoderma family for insulinotrophic and hypoglycaemic activities on rat pancreatic β-cell lines, observing a 4-fold increase in insulin secretion from the cell lines subject to Ganoderma lucidum treatment in particular. Cytotoxic assays showed that all Ganoderma species attained at least 50% cancer inhibition [Bastami et al., 2007].

Nishikawa and Ikekawa both observed a host-mediated antitumour effect of the aqueous polysaccharide extract from a variety of fungi on mice implanted with S-180, and the Ganoderma species extract was the highest inhibitor at 77% inhibition [Nishikawa et al., 1969; Ikekawa et al., 1968]. Ikekawa's study also elucidated that *polysaccharides* and *polysaccharide-protein complexes* were responsible for bioactivity via immunoenhancement and antioxidation, and many were in the form of β-(1–3)-Glucans. In particular, these polysaccharide complexes were particularly effective against tumours when administered *in parallel to* conventional chemotherapeutic agents – likely owing to the effects on the body's ability to utilise and recover from the treatment [Ikekawa, 2001]. The polysaccharide extracts identified in these studies are the foundations for many recognised antitumour medicines today; Lentanin (from *Lentinus Elodes*), Proflamin (from *Flammulina Velutipes*), Krestin (from *Trametes Versicolor*), and Schizophyllan (from *Schizophyllum Commune*). It should be mentioned that many of these early studies were based on even earlier investigations performed by the National Cancer Research Institute in Japan in the early sixties, on the polysaccharide complexes extracted from basidiomycota *Trametes Versicolor*, *Phellinus Linteus* and *Flammulina Velutipes*. A 15-year follow-up demonstrated a life-lengthening effect of the polysaccharides on mice injected with Lewis Lung Cancer, and the findings also showed a reduced cancer rate of the famers in close proximity with the organisms [Ikekawa, 2001].

"Ganopoly" was the first commercially available form of a GL polysaccharides, and was employed in many studies during the late 20th century. It was a formulation of low-temperature extracted polysaccharide complexes from GL Fruiting Body (GLFB), and studies proved that it inhibited over 80% of cancer proliferation in mouse models [Gao et al., 2005]. Immunoenhancement was

demonstrated via splenocyte proliferation, macrophage performance, and splenocyte-specific cytokine expressions. T-cells and Natural Killer (NK) cells exhibited enhanced cytotoxicity, and the extract further displayed cytotoxicity against some cancer cell lines in-vitro with marked apoptotic effects.

Aside from immune system pathways, polysaccharides from GL have been observed potent in the suppression of *angiogenesis.* This is the process whereby tumour cells embed themselves into a nourished extracellular matrix. Polysaccharides from GL had anti-angiogenic properties when administered to Human Umbilical Vein Endothelial Cell (HUVEC) models (shown in figure 2.10). The figure shows the reduction in microvessels during PS treatment; indicating an effect on the angiogenesis required to advance the tumour. The authors attributed the effect to pro-apoptotic enhancement, anti-apoptotic suppression, and downregulation of growth factor cytokine secretion from angiogenic tumour cells [Cao et al., 2004]. The study also observed anti-angiogenic behaviour of GL polysaccharides on prostate cancer, stimulated by an enhanced Activator Protein 1 (*AP-1*) transcription factor to down-regulate the cancer gene expression.
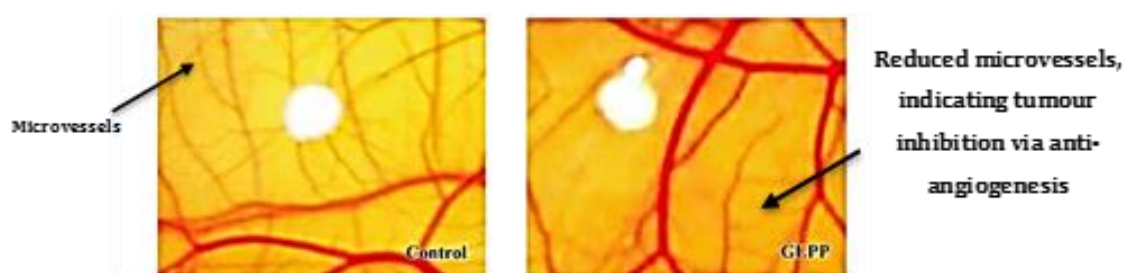


**Figure 2.10:** Anti-angiogenic effect GL polysaccharides: The extract reduced the microvessels created during tumour progression [Cao et al., 2004]

In a study investigating the difference in bioactivity between the physical fractions of GL, broken spores were shown to have a greater effect in-vitro on the proliferation rate of splenocytes, attaining more than 6000% growth when administered without further processing [Yue et al., 2008]. While GL spores actually contained significantly less D-Hexose compounds (glucose, mannose, and fructose) than other fractions, their D-Glucan content was significantly higher, and thus the enhanced splenocyte proliferation in mice was attributed by the authors to D-Glucans. Nonetheless, an enhanced cytokine response, splenocyte proliferation, and tumour inhibition was observed upon administration of *all fractions* (spores, whole fruiting body, pileus and stipe).

*Novelty processing and smart delivery of Ganoderma Lucidum spores*

The rate of splenocyte proliferation using GL spores was significantly greater in tumour-bearing mice than healthy mice, in agreement with studies that frequently observe increased polysaccharide efficacy on *compromised* immune systems.

Immunoenhancing agents are frequently employed alongside conventional therapies for increased treatment efficacy stemming from a more potent defence system, avoiding physiologically-degrading side-effects. Polysaccharides thus present the opportunity to exert their own tumour-fighting mechanisms, alongside facilitating better host-competence in the face of harsh treatment. Collectively, the outcome is a better result from treatment owing to a stronger immune system. Studies today therefore continue to reiterate the importance of a sufficiently active immune system in facilitating the bioactivity of GL polysaccharides, however mechanisms observed are not consistent between studies. This is a direct result of study protocol which fosters discrepancies between polysaccharide extracts, as well as the administration conditions.

## 2.1.4.2 Bioactivity Attributed to GL Ganoderic Acid Triterpenoids

Ganoderic Acids (GAs) have a significantly shorter history of development. In fact, studies on the triterpenoic compounds in the Ganoderma species only kicked off after a study by Striginia et al. in 1971 [Strigina et al., 1971]. GAs are a promising treatment for the inhibition of tumour progression, with apoptotic pathways being the most reported anticancer mechanism. These biomolecules are cytotoxic in nature but continue to present obstacles to characterisation owing to small and near-analogous structures [Keypour et al., 2010]. The bioactive mechanism exerted by Ganoderic Acids is typically reported as cell death via apoptosis and the regulation of cytokines that control tumour growth [Chi et al., 2018]. They have further shown capability in preventing DNA synthesis and intracellular calcium that are involved in cancer proliferation. More recently, they have shown potency delaying Alzheimer's by down-regulating the expression of certain intracellular markers that contribute to changes to DNA methylation [Lai et al., 2019]. As with polysaccharides extracted from GL, the mechanisms exerted by this biomolecule are however not fully mapped out even though their potency has been widely recorded. Combined with the immunoenhancing properties of GL polysaccharides, the biocompounds yields from GL now present a multidimensional approach to disease treatment.

Interestingly, many GAs are extracted in conjunction with polysaccharide structures, yet traditionally this fraction is "washed off" in attempts to evaluate just polysaccharides – hence the term "ethanol-washing". GA characterisation is usually analysed via spectroscopic techniques as its isomers are very small and typically only identifiable chemically. Despite this however, the

*Novelty processing and smart delivery of Ganoderma Lucidum spores*

uniqueness of extraction processes often renders these analytical references inconsistent amongst each other (the case with many biocompounds) [Jin et al., 2015]

Ganoderic Acids (GAs) have become increasingly popular for their considerable antitumour activity. These compounds are unique to the Ganoderma family, and have shown particular prevalence and bioactivity when isolated from Ganoderma *lucidum*. GAs can exert very specific mechanisms towards tumour progression in the body via their effects on cytokine production, apoptotic pathways and androgens (in the case of androgen-responsive tumours such as breast cancer). The lanostane terpene structure of GAs has been shown significantly influential on their bioactivity – in particular hydroxylation [Thyagarajan et al., 2006].

### 2.1.4.2.1 Apoptotic Action of Ganoderic Acid Triterpenoids

Apoptosis is a physiological process that controls crucial biological functions. Cells in all living organisms are programmed to self-destruct usually via apoptosis to modulate normal cell renewal and development, and further regulate the functionality to vital physiological processes such as defence (immune system) and hormonal control [Norbury et al. 2001]. Many degenerative diseases such as cancer and neurological disorders stem from too much or too little apoptosis [Elmore et al., 2007]. Thus, being able to control the life cycle of a cell presents a considerable opportunity for disease treatment and prevention. In light of this, research into the mechanisms and facilitators of apoptosis is extremely fast-paced. The two main pathways observed during apoptosis are intrinsic and extrinsic. Intrinsic pathways are not mediated by receptor stimuli, but are mitochondrial-initiated intracellular signals towards locations within the cell. The extrinsic signalling pathways involve membrane receptor-mediated interactions stemming from death receptors [Locksley et al., 2001]. Unfortunately, even though many key apoptotic mechanisms and proteins are now known, many pathways remain unclear. Although there are a wide variety of stimuli and environments under which apoptosis will cause cell death, the resistance of different cells to certain apoptotic mechanisms can vary. This would imply that treatments like chemotherapy can be effective on some cells, and no others.

Apoptotic events can typically be observed visually via cell shrinkage indicated by a dense cytoplasm, and pyknosis from chromatin condensation [Häcker et al., 2000]. Eventually, membrane blebbing occurs and nuclei burst in a process called karyorrhexis prior to the separation of cell fragments into distinct apoptotic bodies ("budding"). Plasma membrane of the apoptotic bodies remains intact and are subsequently phagocytosed and degraded by the body. Biochemically, apoptotic cells display protein cleavage and crosslinking, DNA breakdown, and the cell surface expressions that induce phagocytic recognition quickly and thus avoid effects on

surrounding tissue [Hengartner et al., 2000]. Events are typically interlinked and dependent, creating a cascade-like chain of apoptotic cell death.

Typically in literature, the anticancer action of GL has been linked to cytokine activity. Cytokines determine the antigen-specific T-cell response by indicating the specific T-helper pathway, and thus have generated a lot of importance in the field of immunoenhancement. GA has induced apoptosis via the upregulation of apoptotic expression Bax and protein p53, the suppression of mitochondria transmembrane potential in the destruction of the cell mitochondrial membrane pathway, and the discharge of cytochrome c into cell cytosol (thereby upregulating specific protease enzymes that play essential roles in mitochondrial dysfunction and programmed cell death) [Zhou et al., 2011; Wu et al., 2012]. The apoptotic mechanisms expressed by GA implicate very little risk of damage to surrounding tissue, as these classic apoptotic pathways can selectively attack tumour cells using selective protein expressions as previously mentioned. Commonly observed pathways exerted by GA treatment both in-vivo and in-vitro are schematized in figure 2.11.
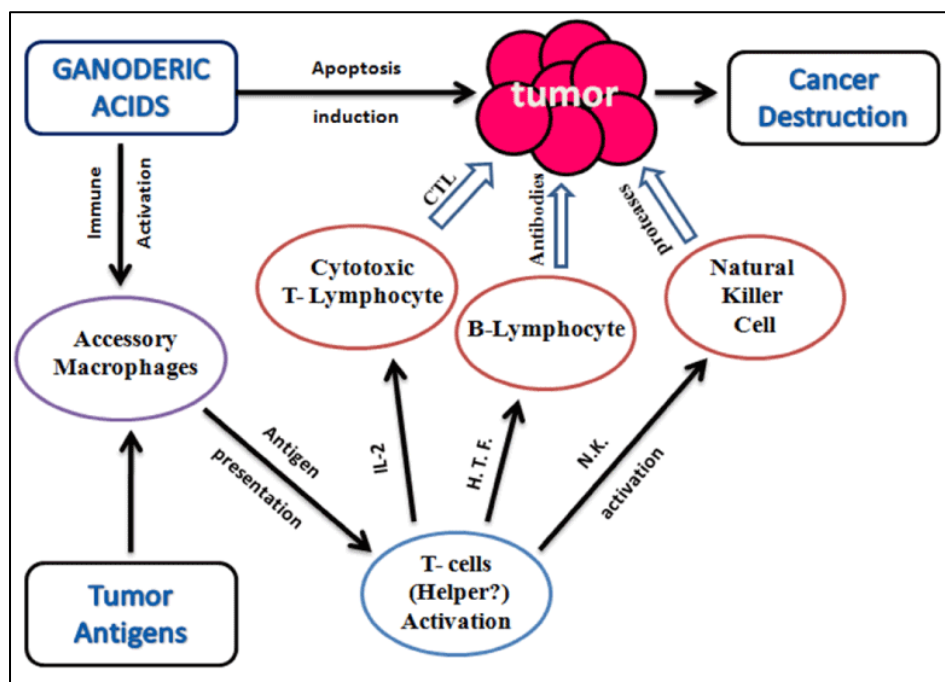


**Figure 2.11:** The mechanisms of tumour inhibition attributed to Ganoderic Acid administration [Radwan et al., 2011]. T-cells are typically activated upon recognition of tumour antigens, and this process is often enhanced with GA administration – typically via apoptosis along with immunoenhancement

*Novelty processing and smart delivery of Ganoderma Lucidum spores*

The observed molecular events in the inhibition of human hepatoma HuH-7 cells' DNA synthesis, ERK/JNK activation, and induction of apoptosis were recorded as the degradation of chromosomal DNA, decreased levels of BclxL, disruption of mitochondrial membrane potential, cytosolic release of cytochrome c and activation of caspase-3. The involvement of mitochondrial dysfunction is indeed something frequently reported upon GA administration, as its apoptotic pathway continues to be studied. In-vivo studies have also demonstrated that GA isomers can suppress the growth of human solid tumours in athymic mice. A particularly renowned study by Tang et al. in 2006 demonstrated in-vivo effects of GA-T on lung cancer cells by apoptosis and cell cycle arrest at the G1 phase; supported by other studies [Liu et al., 2011; Tang et al., 2006]. Apoptotic effects were characterised as a reduction of mitochondria membrane potential and cytochrome c release. The cancer cell proteins p53 and Bax exhibited boosted expressions resulting in a reduced Bcl-2/Bax ratio and successful tumour inhibition. A GA isomer also promoted inhibited adhesion of colon and lung cancer cells to the extracellular matrix (ECM), impairing its migration and stunting growth. Similarly, a GA mixture (containing isomers GA-C2, GA-G, GA-C6, GA-B, GA-A, GA-D, GA-C and lucideric acid A) inhibited human lung adenocarcinoma via apoptosis dose-dependently (7.5 µg/mL induced 6.30%; 15 µg/mL induced 31.74%; 30 µg/mL induced 34.35%). In-vivo, the GA mixture inhibited the tumour weight by 63.38% in mice when treated with 120 mg/kg, owing to increases in the immune response induced by up-regulated expression of IL-6 and TNF-α][Feng et al., 2013].

The potential use of GAs as a *complementary* anticancer therapy has been sparked in similar ways to the complementary use of GL polysaccharides. Isomer GA-Me reversed the resistance of typically resistant colon cancer cells by inducing apoptosis via upregulation of apoptotic cytokines p-p53, p53, Bax, caspase-3, and caspase-9 – typically reflective of mitochondrial dysfunction. Ultimately, GA-Me reduced mitochondrial membrane potential and induced the release of cytochrome c into the cytosolic compartment [Jiang et al., 2011]. GA-Me has also demonstrated immunoenhancing activities whilst inhibiting lung cancer cells in mice via increases in NK cell activity and the production of IL-2 and IFN-γ Wang et al., 2007(b)]. IL-2, IFN-γ and IL-12 cytokines are primary indicators of a T-helper response and thus overall immunological reactions. This activation of the innate and adaptive immune response typically further boosts the immune system response via T-cell development, maturation, and proliferation.

Very few studies have been performed in-vivo using human patients, owing to the primary stage of development of Ganoderic Acids. Nonetheless, murine models have consistently demonstrated in-vivo cancer inhibition via the mechanisms discussed above. One study using GLFB extracts observed that Ganoderic Acid F inhibited spleen-specific tumour growth in Lewis lung carcinoma (LLC)-implanted mice. There was additional evidence of inhibited metastasis to

the liver, and also reduced angiogenesis via downregulation of the *Vascular Endothelial Growth Factor* signalling protein (VEGF) [Kimura et al., 2002]. In another study, in-vitro treatment of human hepatoma cells with Ganoderic Acid T (GA-T) from GL mycelia inhibited DNA synthesis, halted the activation of mitogen-activated protein kinases (MAPKs) that usually foster tumour cell division, and induced apoptosis. In fact the MAPK pathway has been shown to play a vital role in apoptotic response. Mitochondrial dysfunction played a large role in tumour inhibition in this study, via a decreased level of tumour-stimulating protein Bcl-2, and apoptotic behaviour via the release of cytochrome C and activation of apoptosis-driving pathways such as Caspase-3 [Li et al., 2005]. GA-induced mitochondrial dysfunction and apoptotic activity was also documented by investigators who found that GA-T disrupted the growth cycle of metastatic lung tumour cells in-vitro and in-vivo in mouse models. In addition, tumour-suppressing protein p53 was enhanced. This study also detected the exposure of p53, however the tumour-stimulating protein Bcl-2 was not changed [Tang et al., 2006]. GA-T was also observed effective in promoting cell aggregation and subsequent inhibition of cell adhesion to the extracellular matrix (ECM) enough to hinder the migration of colon and lung cancer cells, in addition to inducing a variety of mechanisms inhibiting protein-coding genes and ultimately halting cell growth in-vitro [Chen et al., 2010]. In-vivo tests in the same study using the same extract observed suppressed lung tumour growth via the mechanisms observed in-vitro [Chen et al., 2010]. GA isomers GA-Mf and GA-S also induce apoptosis of human HeLa cells through a mitochondrial disruption via activated apoptosis-driving pathways and tumour-suppressing proteins, as well as Cytochrome C release and cell growth cycle disruption as observed in previous GA studies [Liu et al., 2011].

Typically, the bioactivity demonstrated by GL triterpenoids suggests that the antitumour effects via enhancing the body's immune response as well as cytotoxic tumour targeting. Fully understanding the mechanisms of GAs is crucial to their attainment of clinical use, and as of yet this has not been sufficiently achieved. Cytotoxicity in combination with an enriched immune system is invaluable in achieving disease recovery as well as long-term wellbeing. *Combination therapy* is therefore widely employed in the medical industry as a way of capitalising on the therapeutic effects of more than one pharmaceutical administration or technique [Zhao et al., 2012]. Table 2.3 details some findings on bioactive potencies of ganoderic acids, including those in crude GL extracts. In many of these studies, cruder forms showed more potent bioactivity; both with respect to immunomodulation and cancer cytotoxicity.

| Ganoderma lucidum Extract | Applications | Observed Activities | Suggested Mechanism(s) | Refs |
|---|---|---|---|---|
| Dried powder GL (aqueous) | Highly invasive breast cancer (MDA- MB-231) and prostate cancer (PC-3) cell lines. | Downregulates transcription factors AP-1 and NF-κB in breast and prostate cancer cells. | Inhibition of uPA and uPAR reduces cell motility. | [Jiang et al., 2004] |
| Dried powder GL (13.5% polysaccharides & 6% triterpenes) | Human prostate cancer cells (PC-3), and human aortic endothelial cells (HAECs) | Inhibits early events in angiogenesis & capillary morphogenesis of HAECs, and modulates the phosphorylation of Erk1/2 & Akt kinases in PC-3 cells, potentially decreasing the activity of AP-1. | Inhibition of AP-1 down-regulates the secretion of VEGF and TGF-β1 from PC-3 cells. Suppression of angiogenesis by modulating MAPK and Akt signaling. | [Stanley et al., 2005] |
| Ethanol and water GL extract | Human urothelial cells (HUC, bladder cancer ) consisting of two cell lines (HUC-PC cells and MTC-11 cells). | Ethanol extracts show a stronger growth inhibition than those of water extracts. Induces growth arrest and reduces cell migration in vitro. | Increased actin polymerisation inhibits carcinogen 4-aminobiphenyl-induced cellular migration. | [Lu et al., 2004] |
| Methanolic GL extract | 26 types of human cancer cell lines including16 hematological cell lines (lymphomas & multiple myelomas), and 10 other solid tumor cell lines. | Exhibits cytotoxicity to HL-60 (ED50 ≥26 µg/ml), U937 (ED50 ≥63µg/ml), K562 (ED50 ≥50µg/ml), Blin-1 (ED50 ≥38µg/ml), Nalm-6 (ED50 ≥30 µg/ml) and RPMI8226 (ED50 ≥40 µg/ml) | Induction of cell cycle arrest, mitochondrial dysfunction, and upregulation of p21/p27. | [Müller et al., 2006] |
| Methanolic GL extract | Human leukemic cells NB4. | Induces apoptosis | Reduction and modulation of Bcl2/Bax, p53, Akt, Erk; Inhibition of NF-κB. | [Calviño et al., 2010] |
| Ethanol GL extract | Pre-cancerous human uroepithelial cells (HUC-PC) | Induces apoptosis and upregulates IL-2, IL-6, and IL-8 in HUC-PC cells | Enhancement of cytokine expression by p50/p65 NF-κB activity. Migration of neutrophils via upregulation of IL-8. | [Yuen et al., 2011] |
| Isolated Ganoderic Acid isomers | | | | |
| Ganoderic acid X (GA-X) | Hepatoma cells (HuH-7), colorectal carcinoma (HCT-116), Burkitt's lymphoma (Raji cells), acute promyelocyte leukemia (HL-60). | Inhibits topoisomerases I and IIa in vitro, resulting in immediate inhibition of DNA synthesis as well as activation of ERK and JNK mitogen-activated protein kinases. | Induction of apoptosis with degradation of chromosomal DNA; decreased levels of Bcl-xL, disruption of mitochondrial membrane, release of cytochrome c and | [Yuen et al., 2011] |

| | | | |
|---|---|---|---|
| | | activation of caspase-3. | |
| Ganoderic acid T (GA-T) | Human metastatic lung tumor (95-D), liver tumor (SMMC7721), epidermal cancer (KB-A-1&KB-3-1), cervical cancer (HeLa), melanoma (A375), normal lung (HLF), embryonic liver (L-02), kidney (HEK293), and colon carcinoma (Ls174t) cell lines. | Induces cytotoxicity to cancer cells, but less toxic to normal cells. Induces cell cycle arrest at G1 phase. Suppresses MMP-2 and MMP-9 gene expression through the inhibition of NF-κB activation | Reduction of mitochondrial membrane potential (Δψm), release of cytochrome c and apoptotic activity in lung cancer cells. Induction of p53 and Bax, which stimulates the activity of caspase-3 but not caspase-8. | [Tang et al., 2006] |
| Ganoderic acid ME (GA-Me) | In vivo Lewis lung carcinoma in C57BL/6 mice, human colon carcinoma cells (HCT-116), MDR human colorectal carcinoma cell lines, and metastatic lung carcinoma (95-D), p53-null lung cancer (H1299),HCT-116 p53+/+ and HCT-116 p53 -/- colon cancer cells. | Inhibits tumor growth and lung metastasis in rodents (28 mg/kg i.p.), increases NK activity with upregulation of NF-κB. Kills cancer cells via p53 and mitochondria-mediated apoptosis. Reverses multidrug resistance of HCT-116 cells enhancing chemosensitivity to anticancer agents. | Induction of cell cycle arrest. Induction of apoptosis in MDR cells via upregulation of p-p53, p53, Bax, caspases-3/9 with downregulation of Bcl-2. Upregulation of IL-2 and IFN-γ in vivo. | [Tang et al., 2006; Zhou et al., 2011] |

**Table 2.3** Recent applications and observed activities of GL extracts – Ganoderic Acids specifically

## 2.1.5 Extraction of GL Biocompounds

While medicinal basidiomycota have shown efficacy against cancer in Eastern Asia for centuries, the development of the technologies to best utilize their bioactivity has taken place only in the last 50-60 years. Particularly, the field has seen marked advances in the *extraction*, *isolation* and *identification* of their biocompounds. As the antitumour and immunoenhancing compounds of GL have largely been attributed to Ganoderic Acids and β-D-Glucan polysaccharides, the majority of research has focused on extracting these compounds, along with their complexes/derivatives for characterisation [Jiang et al., 2004]. Nutraceutical extraction is traditionally carried out using techniques that foster mass transfer of compounds out of the solid raw material. As such, this typically requires a source of kinetic energy and a surrounding liquid medium into which the compounds can dissolve and thus be isolated. The same concept has been

*Novelty processing and smart delivery of Ganoderma Lucidum spores*

applied to Ganoderma lucidum extraction. The effect of extraction conditions on the bioactivity retained by the biomolecules is of particular interest, and the extraction procedure needs to be economically and environmentally scalable.

### 2.1.5.1 Current Status of GL Extraction

Conventionally, *polysaccharide* extraction from GL comprises defatting the raw materials to remove lower molecular weight compounds such as lipids/triterpenoids. Subsequently, the water-soluble polysaccharides are extracted using water at high temperatures [Huang et al., 2010 (c)]. *Triterpenoid* fractions are principally water-insoluble and thus are usually extracted in organic solvents like ethanol. Changes to conventional practices however have been demanded in light of the need for better characterisation of biocompounds and also new findings on human toxicity and drug efficacy. For example, GL polysaccharide extracts are purified to yield either various degrees of purity – typically referred to as a "crude" or "neutral" extract. The former typically does not undergo chemical purification that removes proteins, fats and amino acids; leading to the debate as to whether these crude extracts are in fact more potent against certain illnesses. Neutral extracts are preferred when quantifying specific biocompounds. The considerable difference in this protocol however renders the extract yield unique each time – with respect to structure and thus bioactivity [Sone et al., 1985; Zhang et al., 2011].

### 2.1.5.2 The "Efficiency" of an Extraction System

The extraction of GL compounds has traditionally been built on the concept that kinetic energy, typically provided by mechanical pressure and heat, can enhance the disruption of organism cell walls and facilitate the mass transfer of compounds into the extraction medium. The efficiency of extraction however is not yet sufficiently defined for the setup used, the variety of biocompounds in GL, nor the biocompounds' structural variants. This is partly a result of the limited understanding of the bioconstituents' physiochemical nature, but also due to the limited selectivity of existing techniques in the face of such a complex bioconsituent palette. The efficiency and selectivity of dissolution thus plays an important role in GL compound extraction by facilitating mass transfer kinetics. This mechanism has thus been the foundation of most extraction methods and as such, the parameters affecting extraction are typically conducive of high dissolution rates of the biocompounds - *temperature, dilution factor, solvent, duration* in particular [Sood et al., 2013; Sao Mai et al., 2015]. While established relationships do generally exist for these variables in the extraction of many biocompounds, there remains inconsistency in

*Novelty processing and smart delivery of Ganoderma Lucidum spores*

their widespread findings when targeting GL bioconstituents. This is largely owing to the confounding effects of each variable.

"Efficient" extraction has traditionally referred to a *high yield of the bioconstituent*, *low energy consumption,* and *retained bioactivity*. However a greater process intensity that fosters greater mass transfer rates, such high temperatures, could affect the structure and thus bioactivity of compounds [Zhang et al., 2011]. This has been particularly investigated in the case of polysaccharides, which have shown a structural dependence of its bioactivity. For example, in 2006 a study by Chang et al reported that the yield of bioactive polysaccharides from Aloe Vera was stable only at temperatures below 70°C, however many extraction processes employ temperatures considerably higher with the aim of maximising physical yield rather than bioactivity [Chang et al., 2006]. A similar study on specific acemannan polysaccharides from Aloe Vera also found that when testing the effects of heat treatment on the polysaccharide at temperatures 30–80°C, its physicochemical properties were modified from 60°C onwards. The study observed that acemannan was stable up to around 70°C [Femenia et al., 2003].

### 2.1.5.3 Biomolecule Extraction Techniques

The sections that follow describe the mechanisms behind some commonly employed GL extraction techniques. Hot Water Extraction (HWE), Ultrasound-Assisted Extraction (UAE), Microwave-Assisted Extraction (MAE), Supercritical Fluid Extraction (SCFE), and Enzyme-Assisted Extraction (EAE) are among the most common extraction techniques employed to isolate biocompounds from GL. Some of these techniques are also often used to pre-treat GL fractions that require rupturing prior to extraction, as is the case with spores. Each parameter will have similar effects across different techniques, owing to their effects on dissolution. However in some extraction techniques, the impact of physical rupture can affect extraction efficiency.

#### *Impact of Time*

Increasing time will increase the length of exposure between the solvent/solute, thus increasing the likelihood of successful interactions and therefore extraction. However, many studies demonstrate a maximum time, after which the compound yield *stagnates* or *declines*. This is typically a result of saturation in the extraction medium and/or thermal degradation [Kan et al., 2015]. For example ultrasonic-microwave assisted extraction (UMAE) of Trametes orientalis polysaccharides was optimized by response surface methodology. The optimal ratio of water to raw material 28 mL/g, microwave power 114 W, extraction time 11 minutes. Figure 2.12 shows the impact of extraction time [Zheng et al., 2019].

*Novelty processing and smart delivery of Ganoderma Lucidum spores*
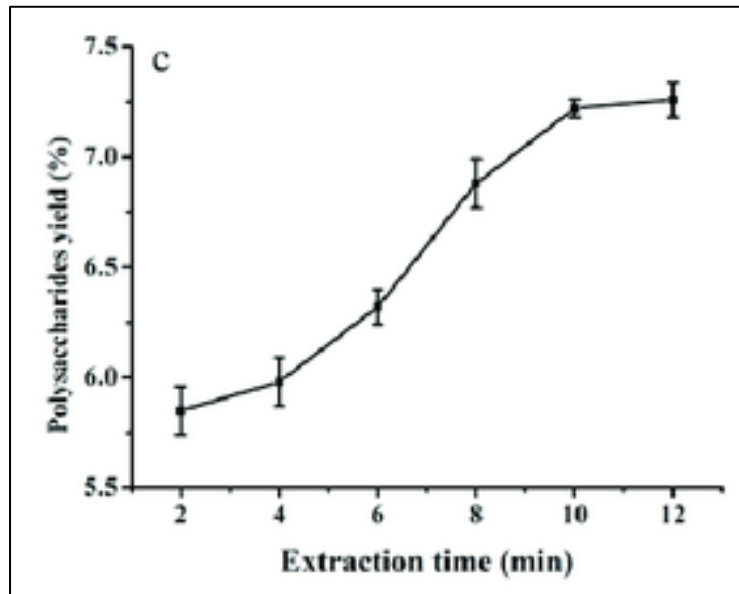
**Figure 2.12:** Effect of extraction time on yield of crude GL polysaccharides using UMAE [Zheng et al., 2019]. Ratio of water to raw material and microwave power were fixed at 20 mL/g and 100 W

In a study investigating the yield of polysaccharides from star anise, at 100°C and solvent proportion 11:1, 4 hours of UAE yielded 10.5% polysaccharides that contained principally Glucans. The yield declined after 4 hours, and the polysaccharides subsequently inhibited the growth of Sarcoma-180 cancer in vivo [Shu et al., 2010]. A similar study recorded that a solvent proportion of 26:1 at 70.5°C yielded the most polysaccharides from Pleurotus Ostreatus fruiting bodies of after just 62 minutes (5.32%). A good scavenging ability was observed, along with cytotoxicity against Ehrlich ascites carcinoma in-vitro [Uddin PK et al., 2019]. An hour was also deemed optimal when in UAE of polysaccharides from GL when UA power was 590 W at 81°C. Extraction from GL further implicates the need for additional kinetic energy when its *spores* are the subject of extraction owing to the tough protective chitin wall. When polysaccharides from GL fruiting bodies were extracted using HWE at 30:1 solvent:solute and 60°C for example, another study reported an optimal time of 120 min, before yield slowly declined [Kan et al., 2015]. At 100°C however, a longer HWE time of 8 hours yielded polysaccharides of 25.1%, but the solvent proportion in this investigation was approximately 1.5-fold literature averages (40:1) [Cheng et al., 2013]. The same study showed capacity to efficiently extract Ganoderic Acids, and the total crude extract showed effective antioxidant activity in rats. This could indicate that a longer time was required to extract the polysaccharides which were more degraded at this higher temperature. Increasing studies actually point to the ability to extract polysaccharides at boiling point for up to 9-10 hours yet maintain bioactivities like antioxidation at solvent proportions as low as 20:1. This is an ongoing debate in literature today. Many studies have continued to advocate that that if duration exceeds 2-3 hours at mild room temperatures, yield typically

*Novelty processing and smart delivery of Ganoderma Lucidum spores*

declines owing to degradation of compounds [Kan et al., 2015; Basanta et al., 2012; Gross et al., 1979].

Extraction time can also affect the selectivity of the solvent, often via the effect of temperature on polarity, with some studies reporting that longer extraction times favour the yield of non-polar compounds, or of specific low-molecular weight polysaccharides [Dent et al., 2013]. It was reported that a long extraction time (10 hours) could for example increase the extraction of polysaccharides from BaChu mushroom [XueJie et al., 2008].

### Impact of Solvent:Solute Ratio

The solvent:solute ratio is an important parameter in the extraction of biomolecules; especially in techniques that rely heavily on molecule collision. In any system, a larger quantity of analytes can usually be extracted using a greater volume [Kan et al., 2015; Huang et al., 2010 (b)]. This is attributed to a greater surface area upon which interactions can take place. Ratios between 20:1 and 40:1 have been shown optimal for biomolecule yield from GL as well as from other organisms [Kan et al., 2015]. A study recorded that a solvent proportion of 25:1 at 60°C yielded the most polysaccharides from Pleurotus Ostreatus fruiting bodies. If extraction time increased, the optimal yield required a greater "optimal" solvent proportion [Uddin PK et al., 2019]. In the same way, more solvent calls for more kinetic energy to achieve the same system efficiency; leading to potential losses of efficiency if there is insufficient energy input or too little time. A study employing HWE to extract polysaccharides from GL observed that at 50°C and for 2.5 hours, the most yielding water proportion was 50:1. The authors further reported that if temperature decreased at these conditions, yield declined but that increasing time had a less detrimental effect [Sao Mai et al., 2015]. Another found that 75:1 was most yielding of polysaccharides, however at 100°C and for 30 minutes [Vũ Kim et al., 2017]. Many studies however exhibit the dilution threshold to be between 20:1 and 30:1 when extraction biocompounds from GL [Oludemi et al., 2018; Chen et al., 2012It is also asserted in literature that additional solvent can introduce the need to employ more extensive drying and concentration steps (introducing greater risk of biocompound degradation) [Rezaei et al., 2013; Plaza et al., 2015]. A similar study using UAE to extract polysaccharides from GL fruiting body required 25:1 solvent:solute in order to extract maximum polysaccharides at 590 W for an hour at a temperature of 81°C [Alzorqi et al., 2017].

### Impact of Solvent

The solvent employed is instrumental to both extraction efficiency and yield type. Polar solvents are required for the extraction of polar compounds like polysaccharides, and non-polar solvents are more efficient for non-polar organic compounds like triterpenoids and other lipids [Sun et al.,

2016]. Thus, the impact of solvent on the yield is of great interest. While GL polysaccharides have been extracted most frequently using water due to the polarity of traditionally sought-after compounds (i.e. polysaccharides), researchers are increasingly enhancing the efficiency of solvents that target specific structural complexities of a wider range of biocompounds [Fang et al., 2018; Sone et al., 1985]. For example, yields are often reported larger and higher-quality using acid-based HWE owing to the solvent's ability to hydrolyse the complex polysaccharide structure and increase its dissolution into the medium [Ziping et al., 2011]. This also facilitates greater dissolution of typically complex polar molecules into less polar solvents like ethanol [Sun et al., 2013]. When extracting from plant cells, while kinetic energy via heat and mechanical energy is effective, acidic solvents can also aid the chemical hydrolysis of the cell walls. This is particularly important when extracting from GL spores. This is why increasing solvent:solute ratio in an extraction system can enhance extraction. For example, UMAE polysaccharide extraction from the fruiting bodies of GL was optimally yielding at power 114 W, for 11 minutes at water:GL 28:1 - after which yield declined (figure 2.13) [Zheng et al., 2019].
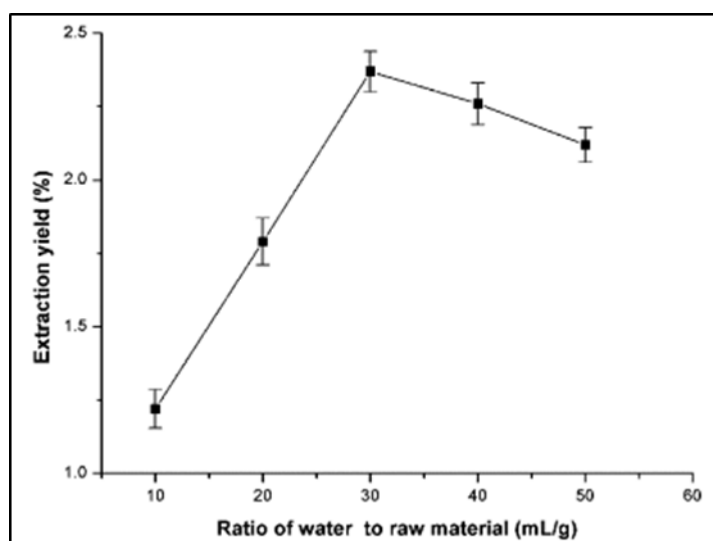


**Figure 2.13:** Effect of extraction solvent:solute on yield of crude GL polysaccharides using UMAE [Zheng et al., 2019]. Microwave power and extraction time were fixed at 100 W and 20 min, respectively

Investigations into the effect of different solvents on GL are rare in literature, however it is common ground that most studies observe the extraction of polysaccharides with polar water and the extraction of triterpenoids with less polar alcohols [Sun et al., 2016]. As such, when extracting triterpenoids, there is greater focus on the strength of the alcohol employed. Many find this to be between 60-90% ethanol.

*Novelty processing and smart delivery of Ganoderma Lucidum spores*

*Impact of temperature*

Increased temperature of a solvent usually fosters enhanced "wetting" of the sample matrix, and encourages a higher rate of diffusivity and increased mass-transfer kinetics by disrupting analyte-matrix interaction, thus driving desorption of analytes from the sample matrix [Kan et al., 2015; Greve et al., 1994]. Most studies typically therefore observe higher yields at higher temperatures. High temperatures have however been shown to degrade valuable structures into less bioactive forms, and of course also reduce yield when quantifying the large polysaccharides – skewing the merit of the method [Cai et al., 2018; Alvarez et al., 2014; Sereewatthanawut et al., 2008; Plaza et al., 2010]. For example the yield of specific Glucans from golden oyster mushroom was affected by extraction temperature and time in subcritical HWE, where 200°C for 60 minutes was most yielding. As temperatures were increased above this however, the Glucan structures degraded [Jo et al., 2013]. Similarly the yield of polysaccharides from a cactus specie was negatively correlated with temperatures above 80°C for 3 hours [Cai et al., 2018]. Polysaccharides from the fruiting bodies of GL were extracted at 137 min and 66°C, using a 35:1 water proportion, attaining 2.4% yield [Kan et al., 2015]. While the interaction rate between the raw components and water molecules increases with increasing extraction temperature, literature commonly cautions that a high yield could be reflective of the presence of a broad range of constituents (and impurities) at these conditions. Therefore, when combined with the requirement for "bioactive" polysaccharides, it is popular to maintain temperatures below boiling point. While heat-induced structural degradation can enhance solubility and thus extraction, this will not necessarily satisfy investigations that require a yield that is to be subsequently tested as the most effective therapeutic agent. Precautions need to be taken for scalability of a technique that in energy efficient, environmentally friendly, and of course non-degenerative of the biocompounds. As well as the degree of hydrolysis, interestingly the extraction temperature can also affect the polarity of solvents. Polarity of course can influence which compounds are actually extracted [Kan et al., 2015]. When water is employed, investigators usually observe changing solubility, therefore creating the possibility to extract a large range of compounds (polar *and* non-polar). This is because of reducing electrostatic interactions between water molecules, and with its surrounding ions and molecules at higher temperatures. The resulting increased rotation of water molecules is therefore conducive of dissolving less polar compounds, since intermolecular interactions are weaker [Plaza et al., 2015].

While the extraction of biocompounds from GL is typically carried out at temperatures between 60-100°C, solvent extraction yields are usually reported highest when extraction is carried out at boiling point [Kan et al., 2015; Choong et al., 2018]. Studies increasingly suggest the ability to

*Novelty processing and smart delivery of Ganoderma Lucidum spores*

extract efficiently (at high temperatures in particular) yet maintain bioactivities such as antitumour and antioxidant capacities.

### *Ganoderic Acid Extraction*

Unfortunately to date, the extraction of Ganoderic Acids has not been well-documented owing to a lack of interest, their low concentrations in GL, and the challenging and costly detection techniques (leaving behind little reference for new studies). When extracted, these compounds are not measured by dry weight, but instead via spectroscopy [Cheng et al., 2013]. In a HWE study, ethanol at 60°C for 6 hours yielding 0.2% GA. In this particular investigation, 7 GA isomers were identified as GA-A, B, D, G, H and I. Cytotoxity was observed with IC50 values up to 0.14 mg/mL against colon cancer cells in-vitro [Ruan et al., 2014]. Another study obtained a GA yield of 1.74% and 1.56% using ethanol and water respectively when extracted using hot solvent extraction for 1 hour at a solvent:solute ratio of 32:1. This extract was termed GA-Σ [Murata et al., 2016]. HWE was used to extract GA-T, Me and H in a study employing a sonic waterbath employing chloroform. A solvent:solute ratio of 20:1 for 40 minutes. While the yield was not reported in this study, the investigation was informative in its suggestion that, unlike the polysaccharide content of GL, GA composition can vary wildly between strains [Keypour et al., 2010].

## 2.1.5.3.1 Interrelated Effects of Extraction Variables: Supervised Machine Learning via Response Surface Methodology (RSM) Statistical Optimisation

The interrelated nature of extraction parameters complicates the ability to model and predict an extraction yield, as certain parameters typically affect the influence had by others on extraction yield. These "confounding relationships" have exhibited only very limited study, and no clear interrelationships have robustly been defined for application to different species and extraction techniques. Recent studies have employed supervised machine learning in the form of statistical optimisation to optimise the variable range in the presence of other variables. Regression, also known as supervised machine learning, is the basic building block of more advanced machine learning and models the effect of input variables on an output variable using an algorithm based on supervised learning using a few experimental data. Using just a fraction of the possible experiments, a model is created that will account for the effects of multiple parameter combinations in the absence of many experiments. This allows the compound yield to be accurately modelled as a function of all process variables at the testable values [Yin et al., 2008].

RSM in particular has been a popular approach to nutraceutical extraction, including GL. This technique controls (and explains) confounding effects using training (experimental) data as the

basis for the "optimal" result determined by the model. For example one study was able to use RSM to show that an increase in hot water extraction (HWE) temperature had a negative impact on GL polysaccharide yield only when the extraction time and solvent dilution were high enough [Sood et al., 2013]. Similarly in a study of GL polysaccharide extraction via ultrasound (UAE), ultrasound power only had a positive effect on yield when extraction time was lower [Shi et al., 2014]. This design depicts the interactions between variables but also with themselves ("quadratic effects"). Quadratic effects imply that the variable influences the extraction yield non-linearly, typically reaching a maximum effect before declining [Sood et al., 2013]. It is common for extraction variables to exhibit this "maxima" effect on biocompounds, after which their change can negatively affect yield but also bioactivity [Gil-Chávez et al., 2013; Soquetta et al., 2018].

### 2.1.5.3.2 Enzyme-Assisted Extraction (EAE)

Enzyme-Assisted Extraction uses enzymes to disrupt the cell wall of plant material to improve its extraction yield. In the case of GL spores particularly, sporoderm walls can be disrupted using EAE and enzymes can further lyse polysaccharides into smaller extractable structures [Rodrigues et al., 2015]. Figure 2.14 shows the setup. This method has been used to extract essential oils, proteins, and polysaccharides from many natural species as it is highly selective and employs a low extraction temperature in order to maintain enzyme activity (thus also preserving bioactive compounds' activities) [Mai et al., 2015]. There are many studies on EAE extraction of GL biocompounds, however yields are typically below 10%, and the effect of enzyme concentration is limited as a result of low kinetic energy in the extraction system [Chunhua et al., 2014]. For example, one study employed cellulase to achieve a 4.4% GL polysaccharide yield, and suggested that the maximum time needed was 2.5 hours with very little cellulase and low temperature (50°C). This yield was higher than the yield obtained using other extraction methods: HWE (2.1%), UAE (2.2%), and MAE (2.2%), all of which required near-boiling temperatures. However other methods required significantly less extraction time to achieve similar yields. The study went on to combine UAE, MAE and EAE using a statistical model, and found that 5.24% crude polysaccharides could be attained at a low power for just 9 minutes using that setup [Mai et al., 2015].

Ganoderic Acids have rarely been extracted using EAE, simply because these compounds are not complex enough to require lysis. More recently, laccase has been tested in combination with ultrasound to verify effects on yield. At a solvent:solute ratio of 60:1, enzyme concentration, 0.04 g/mL and extraction time 9 hours; 1.69% GA was obtained. The extracts subsequently demonstrated antioxidative capacity in rats [Liu et al., 2015].

*Novelty processing and smart delivery of Ganoderma Lucidum spores*
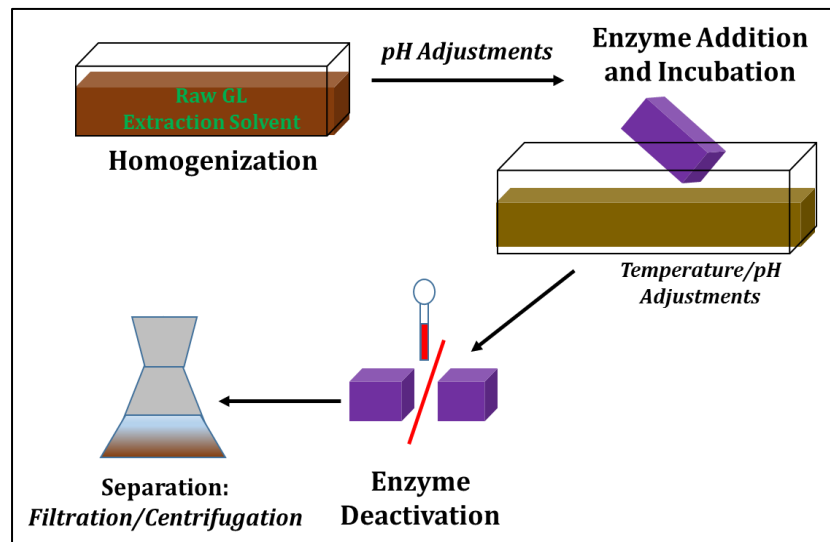
**Figure 2.14:** EAE process using cellulase to extract GL polysaccharides

Enzymes are often employed to pre-treat spore walls for extraction of many biocompounds from GL and other plant organisms – and in particular more recently triterpenoids from spores. However even amidst reported high extraction efficiency, EAE is complex and its resources are typically non-recyclable; rendering it insufficiently economical for process scaling [Rodrigues et al., 2015].

### 2.1.5.3.3 Supercritical Fluid Extraction (SCFE)

SCFE employs a liquid or gas solvent possessing characteristics such as high density, low viscosity and diffusivity to facilitate effective material dissolution and solid penetration [Fu et al., 2009]. Carbon dioxide, water, and ethanol are popular solvents for supercritical fluid extraction, possessing excellent dissolution capabilities and experimental safety. Supercritical carbon dioxide in particular is environmentally friendly and nontoxic, being used for many years in the extraction of hops, caffeine, and flavour compounds. At moderate pressure supercritical carbon dioxide is relatively non-polar, and thus while polar polysaccharides are not soluble, non-polar triterpenoids are. In the case of $CO_2$ as the fluid, by modifying the extraction solvent with polar solvents (like ethanol) the range of extractable compounds increases. In the case of water, at high enough temperatures a change in polarity is typically observed. SCFE, even when modified, can reduce the extraction temperature when compared to conventional hot solvent extraction like HWE [Oliveira et al., 2013; Hsu et al., 2001]. The high pressure involved in this technique enhances the extraction of triterpenoids like Ganoderma lucidum, and in fact Ganoderic Acid yields from SCFE

have surpassed those of UAE [Zhang et al. 2016]. Figure 2.15 shows a basic schematic of the process employing $CO_2$.
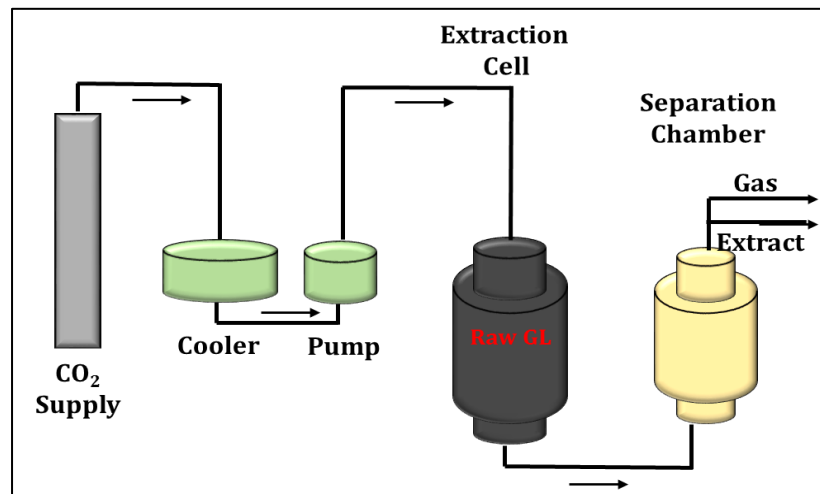


**Figure 2.15:** Schematic of supercritical fluid extraction setup

The fluid density, flow rate, solvent nature, pressure, extraction time and temperature have been shown significantly influential on the efficiency of SCFE for both GL extraction and sporoderm breakage [Rodrigues et al., 2015; Askin et al., 2007]. The constant flow creates favourable mass transfer kinetics for effective dissolution and compound extraction, and the process has been shown more yielding than traditional solvent extraction. D-Glucans specifically have been effectively extracted from GL using SCFE employing both carbon dioxide as well as water, with carbon dioxide normally generating yields with larger molecular weights and thus an acclaimed unique bioactivity [Askin et al., 2007]. One particular study observed that extraction with SCFE using water can achieve up to 78% crude extract recovery at 200°C (figure 2.16), however only 1% yield could be achieved using carbon dioxide due to the reduced efficiency of carbon dioxide's lower extraction temperature of 50°C [Askin et al., 2007]. The extraction was strongly influenced by solvent nature and flow rate; a common finding [Hsu et al., 2001]. The study observed that extraction time had a positive correlation with yield only at lower tested temperatures (373K and 423K). Another study investigating the effects of SCFE variables on the yield of water-soluble *organic* compounds (WSOCs) from GL reported that at a pressure of 10 MPa and solvent:solute 80:1, a longer extraction time was favourable only if the temperature was below 250°C. At this pressure, the effect of extraction time was positive on WSOC yield efficiency. The effect of temperature on polysaccharide yield was positive. At this temperature, water demonstrated the

*Novelty processing and smart delivery of Ganoderma Lucidum spores*

ability to extract organic compounds owing to the reduction in solvent polarity. As long as the fluid was in liquid state, the study reported no additional effects of pressure [Askin et al., 2007].
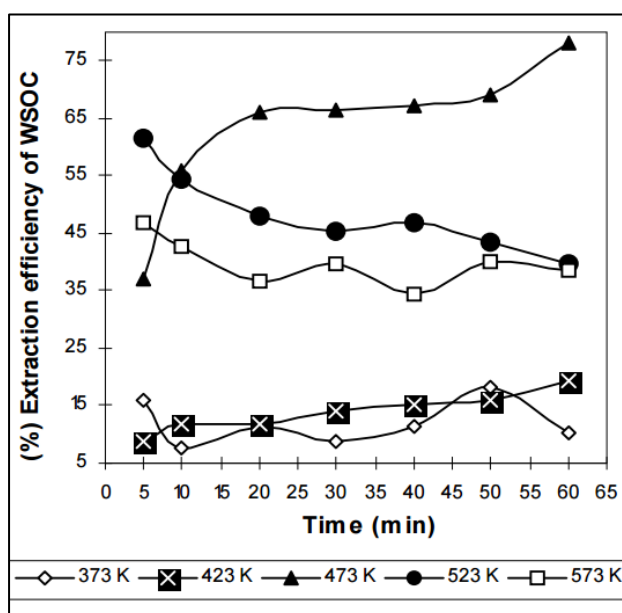


**Figure 2.16:** Extraction of nutraceuticals using Supercritical Fluid Extraction with Carbon Dioxide: the effect of extraction time on yield efficiency was only significant at low temperatures [Askin et al., 2007]

Ganoderic Acids are particularly the focus of SCFE owing to the low polarity of $CO_2$, and high-temperature water [Chen et al., 2007]. A study observed that 38% triterpenoid yield efficiency could be obtained using carbon dioxide in SCFE (with ethanol as the modifier for its affinity to triterpenoids). The study found that the concentration of ethanol was extremely influential on the yield, followed by fluid density. The authors also observed Microwave-Assisted Extraction (MAE)to be more efficient.

### 2.1.5.3.4 Microwave-Assisted Extraction (MAE)

MAE introduces microwave energy into the solvent/sample mixture, fostering dissolution of the sample into the solvent matrix. Microwave power, extraction solvent, solvent dilution, exposure time, and temperature have all been shown influential on MAE for nutraceutical extraction from various organisms [Huang et al., 2010 (c)]. Importantly, this process has proven successful for the extraction of chemotherapeutic nutraceuticals such as Taxanes and Camptothecin, essential oils, polyphenols and caffeine. MAE offers shorter extraction time and a lower solvent requirement, as energy is applied directly to the solvent molecular matrix via ionic

*Novelty processing and smart delivery of Ganoderma Lucidum spores*

conduction and dipole rotation (the alignment of the molecules with the magnetic field direction induced by MAE). The resistance of the solvent/solute system to the flow of ionic conduction causes friction and thus heat in the system to induce a gradual destruction of the plant material and release of biocompounds [Chen et al., 2007]. For example a study on the extraction of essential oils from turmeric observed that MAE could yield almost 5%, but this reduced when time exceeded 2 minutes and power exceeded 300 watts [Sahne et al., 2016].

MAE is especially effective on polar compounds like water molecules and polysaccharides as they are more rapidly heated by the microwave irradiation. In closed vessels the temperature will reach above boiling point, fostering improved extraction kinetics from higher desorption of analytes, and also increased biocompound dissolution owing to reduced surface tension and solvent viscosity [Chen et al., 2007]. Studies have found that crude polysaccharides from GL can be extracted effectively using MAE, however the yields remain low and the effects of power and time specifically remain inconclusive. It has however also been shown that Ganoderma triterpenoids were better extracted via MAE using ethanol when compared to SCFE, HWE, and UAE and a lower extraction time was required [Chen et al., 2007]. The study demonstrated that the greatest yield (5.11% total saponins and 0.97% *triterpenoid* saponins) was obtained after 5 minutes at 90°C with a solvent:solute ratio 25:1 and 9% ethanol as the solvent. This study highlighted a considerably enhanced extraction efficiency of MAE when compared to conventional solvent extraction, SCFE, and UAE. In fact, the yield from MAE was 130% and 197% higher than conventional solvent extraction and UAE, respectively, in this study. Generally, most triterpenoid extraction studies from GL using MAE have resulted in greater yields at lower extraction times than conventional methods (solvent extraction, UAE and SCFE in particular), suggesting a more scalable technique. Despite this, the disadvantages of MAE remain; principally inhomogeneous energy and the preference of polar solvents and extractants for high efficiency. The latter drawback can of course be addressed by using longer extraction times however this limits the process to a certain temperature, after which polar molecules are extracted alongside non-polar [Huang et al., 2010 (c)].

### 2.1.5.3.5 Hot Water Extraction (HWE)

Ancient Middle Eastern kings were said to have obtained valuable plant compounds by "boiling it in hot water"; a process later acknowledged as HWE [Askin et al., 2007]. This method was among the first to be used for nutraceutical extraction, and has thus provided the foundations for more sophisticated extraction techniques. It traditionally requires a minimalistic setup, and water's polarity additionally can extract valuable polar compounds like polysaccharides found in natural organisms. Furthermore, water at high temperatures has successfully yielded substances rich in antioxidants and other organic compounds that

traditionally do not dissolve in polar solvents (including sterols). Nonetheless, it is still common practice to employ less polar solvents, such as alcohols, in the extraction of organic compounds like Ganoderic Acid triterpenoids. HWE provides heat-induced kinetic energy to foster dissolution from within the plant structure into the surrounding medium via cell wall permeation (figure 2.17).
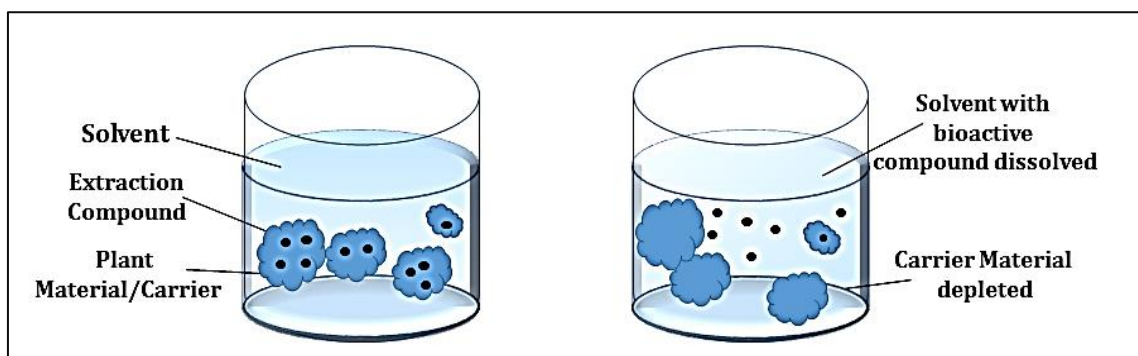


**Figure 2.17:** Schematic of Hot Water bioconstituent Extraction. Heat-induced kinetic energy causes soluble bioconstituents to be drawn out of the GL biomass and into the medium for isolation

Typically, the most influential variable is dissolution rate, driven by heat-induced kinetic energy that encourages the interaction of extraction molecules. Dissolution in the HWE system is principally affected by exposure time, solvent:solute ratio, and extraction temperature when a still bath is used. It is also common to observe interaction effects among HWE variables, on the yield of nutraceuticals simply owing to the synergy of different sources of kinetic energy [Sood et al., 2013]. For example, the effect of temperature has been shown greater when the dilution factor is low. This is explained by the greater concentration of heat energy in a smaller solvent volume. In addition, the effect of time is often interrelated with the effect of temperature [Sood et al., 2013]. These interrelations make causal conclusions between the extraction parameters and the yield less accurate unless interactions are somehow controlled. Literature primarily focuses on optimising the extraction of polysaccharides from basidiomycota, as polysaccharides have presented greater prospects for novel disease treatment using the body's own immune system. It is important to note however, that the extraction parameters that maximise polysaccharide yield will also maximise other biocompound yields, including triterpenoids, as dissolution will always enhance extraction. The only exception is the solvent used, which

*Novelty processing and smart delivery of Ganoderma Lucidum spores*

determines the selectivity of the extraction solvent through its chemical interactions with the raw material.

Although HWE remains a popular candidate for nutraceutical extraction, it maintains yields that fall below more energy-intensive methods, has a tedious processing time, and yet still poses a threat to compound degradation at high operating temperatures and long durations [Chang et al., 2006]. While the field is seeing increasing attempts at statistical optimisation, the vast array of biocompounds in Ganoderma lucidum each present their own conditions for optimal extraction. Resultantly, there is little consistency by which new developments can be shaped.

### Supporting Evidence: HWE of Polysaccharides

The extraction of polysaccharides from natural organisms via HWE has traditionally been popular owing to its simplicity, safety, and low cost. Its success in yielding potent water-soluble polysaccharides has been proven in many studies, which subsequently employ more selective evaluative techniques to avoid quantification of water-soluble impurities often dissolved. Many natural organisms have yielded valuable polysaccharides and continue to be investigated via sophisticated experimental designs like RSM [Ye et al., 2011].

Basidiomycota especially have been processed using HWE for decades, and their abundance of water-soluble polysaccharides has implicated high yields from this extraction procedure. For example, Grifola Frondosa underwent HWE under subcritical conditions, and the process was optimised statistically using RSM to achieve the variable values that would maximise Glucan yield. Extraction at 210°C, for 43.65 minutes and dilution factor 26:1 was found to be the optimal combination. Variables were found to exhibit maximum effects on yield maximisation, after which their impact was negative. Extraction time/temperature had a significant interaction effect, and temperature was concluded to be the strongest confounding variable. The authors attributed this to the additional effect of temperature on cell wall degradation. When compared to conventional 100°C HWE for 3 hours and dilution factor 20, the subcritical conditions were 2-fold more yielding [Yang et al., 2013]. Another study on the HWE of polysaccharides from both Pleurotus Ostreatus and Gonoderma lucidum observed that the Glucan yield was optimal at 180°C for both organisms, and 26 minutes and 22 minutes respectively. Pleurotus Ostreatus yielded almost 40% Glucans and Ganoderma lucidum yielded 10% Glucans, as determined by the Phenol Sulphuric Acid assay (discussed later in this review) [Smiderle et al., 2017].

A Ganoderma lucidum study sought to determine the optimal conditions for Glucan extraction using HWE using RSM optimisation, and concluded that 130°C extraction (achieved by the addition of an autoclave) for 40 minutes was the highest-yielding. After 40 minutes, the yield began to decline at all temperatures tested [Thuy et al., 2015]. Figure 2.18 shows the RSM plot

for yield. The authors of this paper concluded that the effect of temperature was positively related to Glucan yield because of the enhanced hydrolysis and therefore greater solubility. The extraction fit a second order model with high statistical significance, suggesting a confounding relationship between time, temperature and polysaccharide yield.
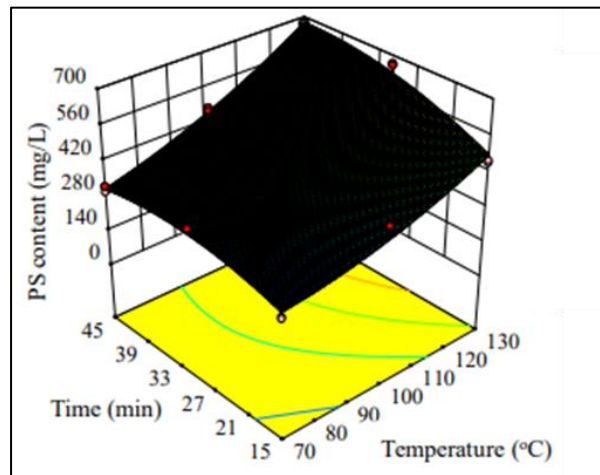


**Figure 2.18:** RSM Optimisation plot for HWE of GL glucans showing a positive effect of temperature, with the effect of time peaking at 40 minutes in parallel (a confounding relationship) [Thuy et al., 2015].

A similar study extracting crude polysaccharides form GL using HWE also observed confounding effects of ratio, temperature, and time [Kan et al., 2015] (figure 2.19). While independently, these variables indicated maximum polysaccharide yields at 30:1, 80°C and 120 minutes respectively, when the model considers all variable functioning at once, the optimal conditions were instead 35:1, 66°C, and 137 minutes.

*Novelty processing and smart delivery of Ganoderma Lucidum spores*
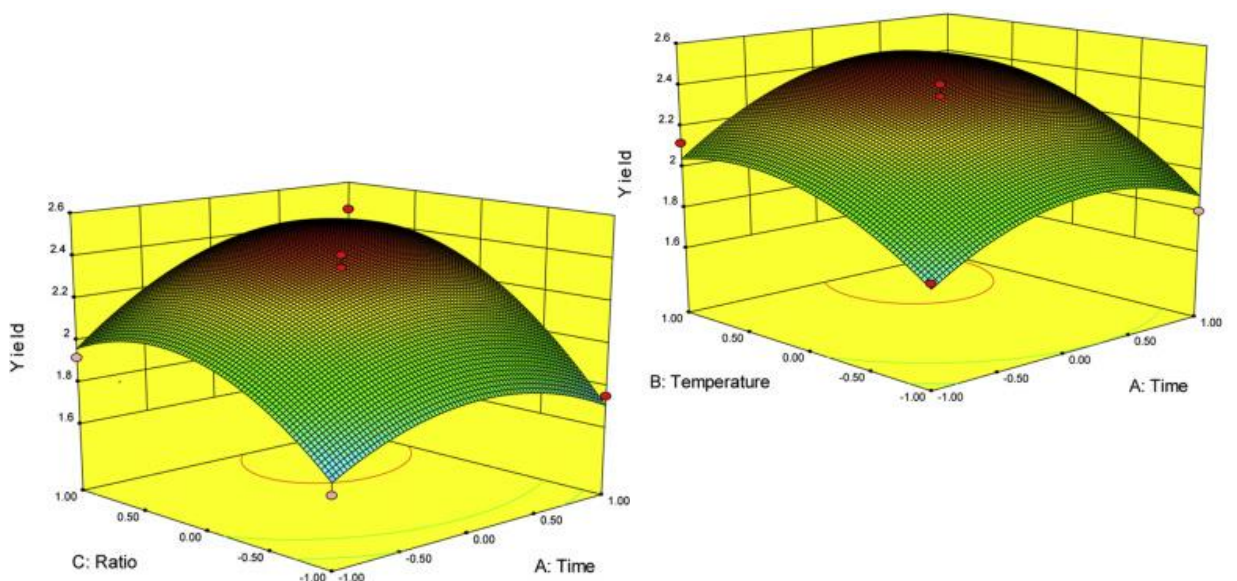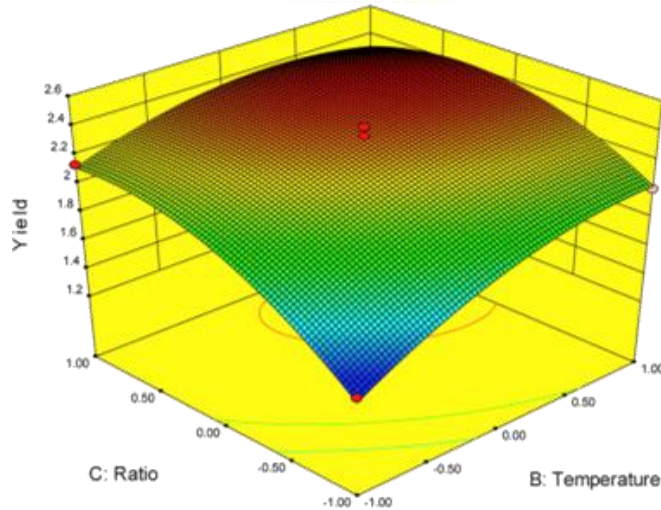
**Figure 2.19:** RSM Optimisation plots for HWE of GL polysaccharides, showing variable interaction [Kan et al., 2015]. Scale -1 → +1 represents the factor levels

Another similar study by Sood et al. was carried out on HWE GL polysaccharide extraction from GL mycelium, producing a crude polysaccharide yield of 5.7%. This study employed RSM to report that the optimal conditions were a temperature of 100°C, extraction time 3 hours, the addition of 6% sodium hydroxide, and dilution factor 20. The addition of sodium hydroxide suggested benefits of an alkaline extraction solvent. This study specified further that the mycelium was heat-treated prior *and* post-extraction using ethanol, to remove some free sugars, phenols, amino acids, and lipids. While the phenol—sulphuric acid (quantification) assay was not employed to classify the polysaccharides obtained, ammonium oxalate was used to reduce compounds prior to analysis [Sood et al., 2013]. Huang et al. also found that alkaline HWE at a similar concentration (~5%) could benefit the extraction of polysaccharides from GL (as measured by crude dry weight), when preceded by UAE and MAE treatment. RSM was employed in this study, and the achieved regression model was statistically significant. The effect of time was most significant on yield, followed by temperature and dilution factor. Recovery reached its peak 8.3% at 60.1°C, extraction time 77.3 minutes, and a dilution factor of 21. These variables each exhibited a "maximum" with respect to its effect on yield, after which it negatively affected yield [Huang et al., 2010 (b)]. These maxima are common among basidiomycota extraction [Sao Mai et al., 0215; Shang et al., 2018].

The existence of interacting and quadratic terms in GL extraction RSM models, typically suggests confounding relationships between the variables – for instance, the study found that the yield of polysaccharides dropped as extraction time increased, only when the temperature was below 60°C. The raw GL was heat-treated prior *and* post-extraction using ethanol, to remove some free

*Novelty processing and smart delivery of Ganoderma Lucidum spores*

sugars, phenols, amino acids, and lipids. Further, the extract was subject to water dialysis to further purify the compounds. At high doses, the extract from this study was shown to increase Natural Killer cell activity in the spleens removed from immunocompromised mice [Huang et al., 2010 (b)].

Crude GL yields and neutral GL yields are not definitive in the extent of purity, and can range from 0.3-90% recovery in literature. For example one study on GL extraction found that water-based HWE at 100°C for 5.5 hours and 30:1 solvent:solute dilution yielded crude polysaccharides of over 22%, however in another study just 0.35% crude polysaccharides were obtained at the same conditions [Ye et al., 2008]. The authors of the low-yielding study washed the extract 3 times with 10 volumes of ethanol to remove lipids, and sorted compounds based on a molecular weight cut-off (MWCO) to ensure that the crude yield was specific. Extracts from this study maintained good reducing powers and free radical scavenging capabilities, but this was unreported in the former study. Another study on the extraction of GL polysaccharides subjected the Fruiting Body to 130°C for 45 minutes at ratio 50:1 and yielded just 0.07% crude polysaccharides [Thuy et al., 2015]. Some studies encounter this discrepancy via variations in reporting; for example a HWE study on GL polysaccharides recovered 9% crude polysaccharides at 100°C for 8 hours, and diluted by a factor of 40. Of this, Glucan content specifically was 25.1% [Cheng et al., 2013].

The Spores of GL (GLS) are increasingly used as the source of biocompounds, as advances in sporoderm-breakage technology becomes more economical and less threatening to compound bioactivity. These entities are rich in polysaccharides (mainly D-Glucans) and triterpenoids (Ganoderic Acids). Furthermore, they have demonstrated both a higher bioactivity and yield than other fractions of the GL organism. An investigation by Nguyen et al. demonstrated that broken GLS are high-yielding of polysaccharides and phenolic compounds using HWE. The study found that 130°C for 40-45 minutes. The rate of sporoderm breakage was highest after 48 hours (instead of 24 hours) when Lactobacillus Plantarum was used as a fermenting agent. A 52.38% breakage rate was achieved. As for extraction of the biocompounds, RSM optimisation found that 130°C for 40 minutes maximised the yield of Glucan polysaccharides and phenolic compounds at 0.07% and 0.06% respectively. High antioxidant activity was observed [Cheng et al., 2013]. A similar study by Bao et al. employed broken GLS for the HWE of Glucan polysaccharides (sporoderm breakage 60-80%). A water dilution factor of 10 was applied to defatted GLS for 6 hours at boiling temperature, after which the residue was extracted again. This study further detailed steps of protein removal and introduced dialysis to limit extract molecular weight to 3000—5000 Da. The extract was ethanol-washed numerous times to finally yield 0.57% D-Glucans [Bao et al., 2002]. This study emphasised the importance of the D-Glucan structure in immunoenhancement.

*Supporting Evidence: HWE of Ganoderic Acid Triterpenoids*

The study of triterpenoids was started by Striginia, Elkin, and Elyakov (1971) and Protiva, Skorkovska, Urban, and Vystrcil (1979), focusing on Ganoderma Applanatum. Unfortunately the study of Ganoderic Acid triterpenoids has been far less frequent owing to the challenge they present to isolation and identification, and the resulting lack of references with which to verify both methodological and structural findings [Ruan et al., 2012; Ruan et al., 2014] Still, over 130 ganoderic acids and other triterpenoids have been isolated from the Ganoderma species [Aguilar-Marcelino et al., 2022]. The isomers of many triterpenoid classes are difficult to distinguish with spectroscopic techniques, and so combined setups are typically employed [Keypour et al., 2010]. Most studies have therefore veered toward GA identification rather than yield quantification, however even the composition and structure of GAs can vary between GL strains as a result of geographical environment, growth conditions and substrate [Chen et al., 1999]. In a study of Ganoderic Acid extraction, ethanol-based HWE was employed alongside spectroscopy to successfully identify 14 GA isomers from GL and another identified 11 GAs using methanol as the base for HWE, further proving their high bioavailability in rat plasma in-vivo [Adamec et al., 2009]. Apoptotic effects were observed in a study that isolated and evaluated 12 GA isomers using ethanol-based HWE and flash chromatography, and authors observed that the polarity of the GA isomers played a role in bioactive potency [Ruan et al., 2012]. While GA extraction is typically evaluated via spectroscopy in the forms in which they already exist, there are many studies that aim to extract crude GA via dry weight.

There is no more consistency in the definition of best practice with respect to GA extraction – in particular as their quantification depends mainly on observing fragmentation/cleavage patterns during spectroscopy. One study employed ethanol-based HWE to isolate GA isomers and observed that 2 hours was most efficient at 80°C and with a solvent dilution of 35:1 solvent:solute [Gao et al., 2011]. Another study however found that HWE employing 100% ethanol at 60°C for 6 hours was required for optimal GA yield of 0.2% [Ruan et al., 2014]. 7 GA isomers were further identified as Ganoderic Acids A, B, D, G, H and I with cytotoxic effects against Hep G2, HeLa and Caco-2 cells. The authors attributed the variation of inhibitory activity to discrepancies in chemical structure. Another study achieved a crude yield of 4.5% prior to fractionation via spectroscopy into 13 isomers [Chen et al., 2017]. GA extracts in another GL study employed 95% ethanol at 5:1 solvent:solute for 1.5 hours, and repeated the extraction 3 times – yielding 0.73% Ganoderic Acids. UV Spectroscopy ascertained this as Ganoderic Acid A [Lu et al., 2012]. That study further found that strains from Longquan and Dabie Mountain were most yielding of Ganoderic Acids. This reconfirms the bioconsituent variation across strains that are cultivated in different locations.

*Novelty processing and smart delivery of Ganoderma Lucidum spores*

### 2.1.5.3.6 Ultrasound-Assisted Extraction (UAE)

There are limited studies on the use of ultrasound in pharmaceutical extraction from plants, even though the results in the food industry have been promising for decades [Vinatoru et al., 1997]. UAE is in fact not the most popular choice for nutraceutical extraction owing to its cost and intense mechanical energy, however in light of the inefficiencies observed with other traditional extraction procedures like hot water extraction this technique may prove more economical by yielding more biocompounds and employing less energy and resources [Chen et al., 2014; Rocha et al., 2018]. Ultrasonic energy ruptures chemical bonds via cavitational jets exerted towards the particles of a material. The process has yielded promising results in food, plants, and industrial material, and high yields with retained bioactivities have been reported from many medicinal fungi [Chen et al., 2014].

While the variables affecting dissolution will remain true for all extraction systems, the potency of the dissolution becomes an advantage when UAE is employed for extraction of nutraceuticals. This is because UAE further introduces sonication energy and cyclic patterns (via duty cycles) to enhance mass transfer as well as provide a more efficient environment for extraction. The process exerts ultrasonic waves to form cavitation bubbles that expand and contract in the extraction medium through inducing energy jets that rupture tough materials like cell walls [Vinatoru et al., 1997]. Cavitation bubbles require ultrasonic waves to grow via the transfer of gas and vapour into the bubble, and at its critical will collapse causing the implosion-induced jet of energy [Fang et al., 2018]. The mechanism is complex however, as growing bubbles actually prove to hinder the transmission of waves and thus reduce bubble growth [Jovanović et al., 2017]. For this reason, many investigations have attempted to "pulse" ultrasound wave production to foster the growth of bubbles in shorter timeframes, between which bubbles can slightly collapse without actually imploding completely. This creates larger bubbles that produce a more intense collapse resulting in higher energy release and thus more intense cavitation effects, as shown in figure 2.20. High amplitude sound waves are also then better able to traverse the medium to create larger bubbles during each timeframe [Albu et al., 2004]. This continuous acoustic cavitation is conducive of particle interaction and enhanced dissolution through a greater mass transfer. Volatility in the medium also induces a reduced molecular weight and further implies increased water solubility.
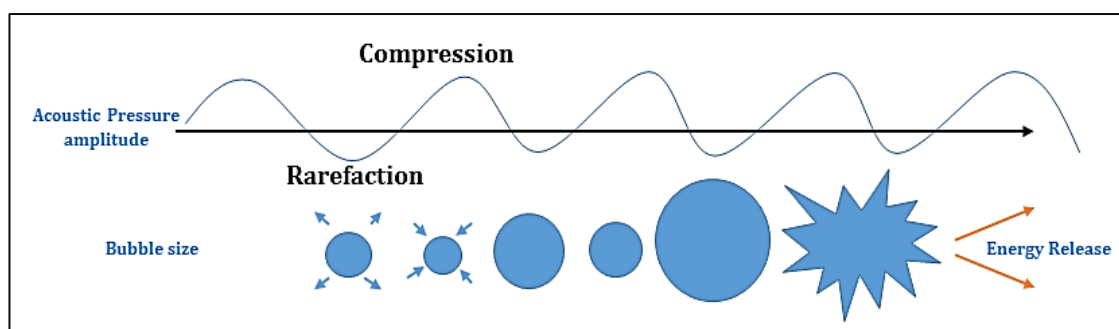
**Figure 2.20:** Schematic of UAE bioconstituent Extraction

The degradation of structure could also change compound bioactivity. Many studies on GL have in fact observed a greater bioactivity of the extracted molecules obtained from the ultrasonic process possibly as a result of the reduced molecular weight, however this association has been contradicted by studies claiming that that larger, branched structures exhibit the greatest bioactive effects [Han et al., 2014; Liu et al., 2009]. The parameters that traditionally affect HWE efficiency will of course be maintained for UAE, owing to the extraction procedure's dependence on dissolution. However, the maxima threshold that indicates degradation from kinetic energy sources (such as heat and temperature) are often reported lower. This is simply because of the added cavitational effects of UAE in the extraction medium. For example, UAE prides itself on its mechanical effects and thus may not benefit as greatly from excess solvent if the solvent:material ratio increased. This is in contrast to HWE, which is centred on high rates of diffusivity in the medium. Studies usually find that even though increased temperatures foster increased kinetic energy and thus greater particle interactions, in UAE this can increase vapour pressure and decrease of viscosity and surface tension of the solvent, proving to instead reduce cavitation effects [Fang et al., 2013]. In a study using RSM optimisation to optimised GA yield using UAE, 87% ethanol, dilution factor 28 and 300 W power for 36 minutes induced a temperature threshold of 50°C before yield efficiency declined. Simultaneous tests trialling HWE at similar conditions and 75°C resulted in less triterpenoid yield [Zhang et al., 2018].

### Supporting Evidence: UAE of GL Polysaccharides

A much shorter extraction time could recover 4.79% polysaccharides from GL in another study, along with 53.63% DPPH scavenging. This was achieved at 671 W, 48°C and 12.5 solvent:solute after just 45 minutes [Chen et al., 2014]. The yield in this study was defined as crude, as proteins and fats were not removed post-extraction. Indeed a major concern with the application of UAE to polysaccharide extraction is the potential depolymerisation in the presence

*Novelty processing and smart delivery of Ganoderma Lucidum spores*

of high pressure and temperatures; implicating potential losses in bioactivity [Wu et al., 2017]. This has resulted in many UAE extraction studies being conducted at temperatures below 30°C using intervals, and for durations below 60 minutes [Xu et al., 2013]. For example in the aforementioned study, the yield was less affected by the extraction time after 30 minutes (figure 2.21), and the antioxidant capacity (via the DPPH scavenging activity) did not benefit from additional time [Chen et al., 2014].
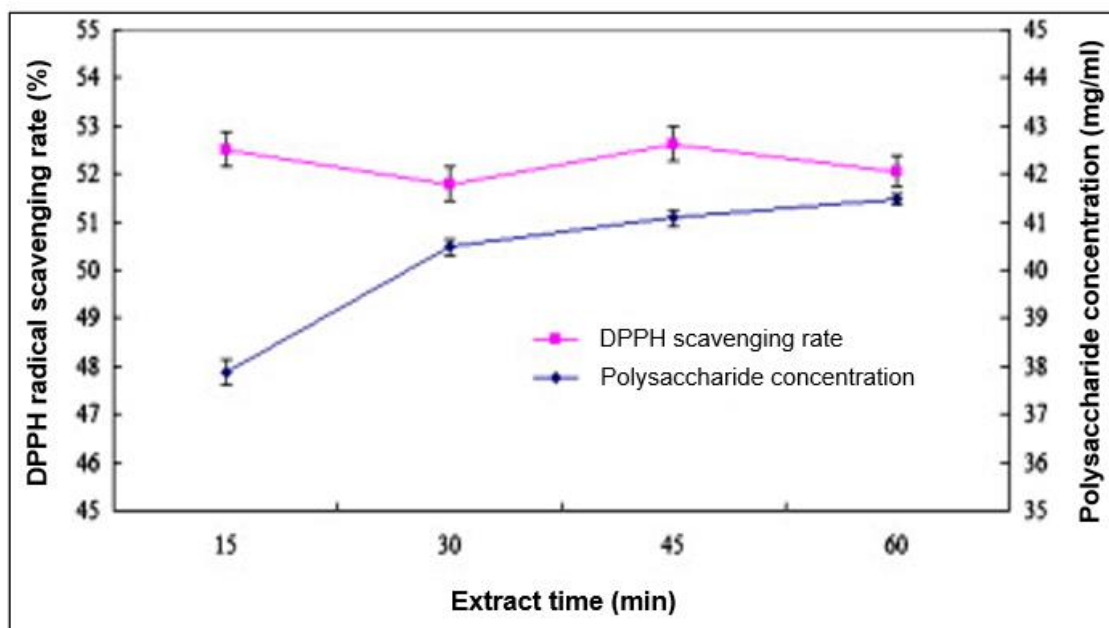


**Figure 2.21:** DPPH radical scavenging rate and polysaccharide extraction versus time in UAE. The effect of time on polysaccharide extraction is more noteworthy than the effect on DPPH scavenging [Chen et al., 2014]

While extracting polysaccharides from corn silk via UAE, yield increased with extraction time up to 20 minutes only, and the authors attributed this simply to the achieving complete extraction, and/or degradation of the biocompounds [Maran et al., 2013]. This is verified by a study by Sun and Tomkinson that reported that UAE time up to 20 minutes could actually increase molecular weight, but after this time molecular weight will decrease as a result of by breaking polysaccharide links [Sun et al., 2002].

UAE often shows dependence on extraction solvent, whereby researchers observe more impactful cavitation when using more viscous solvents, and thus greater mass transfer efficiency can be achieved. One study investigated the effect of the solvent's ethanol content on the impact UAE had on the extraction of glycoside biocompounds from Forsythia Suspensa [Fang et al.,

*Novelty processing and smart delivery of Ganoderma Lucidum spores*

2018]. The study results are shown below in figure 2.22, where the dependence on ethanol concentration can be observed, as well as the interrelation between the other parameters tested. Being a polar compound, the authors observed an increasing yield at lower ethanol concentrations however benefitted from ethanol as a small proportion. This finding was actually attributed to the different properties of the mixed solvents such as polarity, surface tension, critical molecular distance, vapour pressure and viscosity – and the resulting change in cavitational intensity [Xia et al., 2014; Chen et al., 2018; Vilkhu et al., 2008; Zhou et al., 2017]. When compared to HWE, the same solvent trends were observed, although a lower yield was observed. The study reported this a result of the intense cavitational effect that proved more significant than free diffusion in HWE.
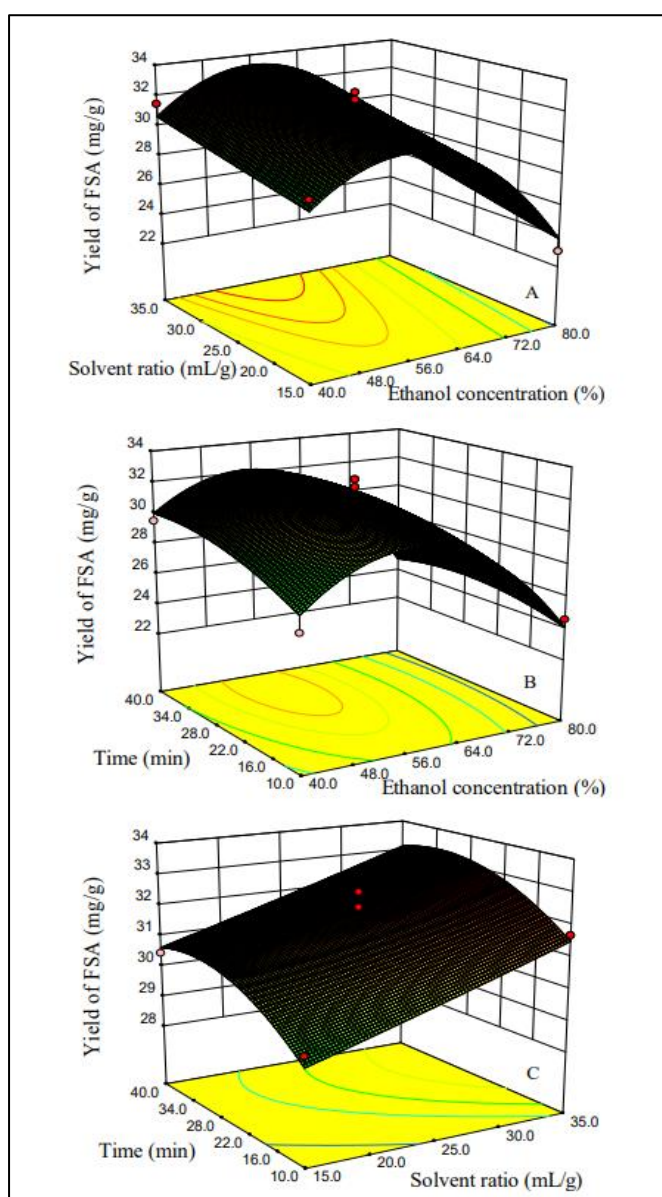


**Figure 2.22:** RSM Optimisation plot for UAE of glycosides from Forsythia Suspensa. The dependence on ethanol concentration, time, and solvent ratio is clear, as well as the interrelation between parameters. 200 W was used in the optimization [Fang et al., 2018]

*Novelty processing and smart delivery of Ganoderma Lucidum spores*

The authors concluded an optimal UAE setup could be carried out at 200W for 37 minutes, using 50% ethanol, and a solvent:solute ratio 32:1. At these conditions, the maintained temperature was 30˚C. When comparing to conventional hot water extraction at 90˚C, this optimised UAE was more yielding as a result of gains in other types of kinetic energy (mechanical) [Fang et al., 2018]. It is indeed a widespread finding that employing UAE for compound extraction has gained popularity owing to efficiency gains over traditional methods which typically achieve lower mass transfer kinetics, yet employ higher temperatures and longer extraction times [Sališová et al., 1997].

UAE of Glucans from ginseng was optimised using RSM with respect to ultrasonic power, extraction time and dilution factor. Power was observed as the most influential factor on yield, however all terms (interaction and quadratic) were significant; suggesting confounding effects of the 3 variables on yield, and a maximum effect for each variable – for example the effect of time was most influential (positively) at a lower dilution. The optimised conditions were 400 W, 71 minutes, and dilution factor 33 - yielding 8.09% Glucans. The extracts showed immunostimulating activity by up-regulating nitric oxide and specific cytokines involved in immune repsonse. Compared with HWE at 95°C for 3 hours, UAE took less time and recovered slightly more polysaccharides [Yang et al., 2014]. Similarly, in a study investigating UAE on the extraction of polysaccharides from Lycium barbarum L., authors optimised a combination of UAE and HWE with respect to temperature, time, dilution factor, and ultrasonic power using RSM. The maximum polysaccharide yield of 4.4% was observed at 100°C, extraction time 53 min, dilution factor 26, and ultrasonic power 160 W. The combinatory method was compared to HWE at 100°C for 2 h, subcritical HWE at 110°C for 1 h and 5 MPa, and UAE at 140 W and 110°C, employing dilution factor 25. The polysaccharide yield was 3.4% (HWE), 4.0% (subcritical HWE), and 3.0% (UAE). All polysaccharide extracts exhibited scavenging activities in antioxidant assays [Chao et al., 2013]. Another study on the extraction of polysaccharides from hazelnut skin reported greater extractability of the structures when more broken down. Studies were in line with previous findings [Yılmaz et al., 2016].

Medicinal fungi have been the subject of UAE extraction for many years, especially owing to the typically tough spore walls that require rupturing prior to extraction. Typically yields will decline at high temperatures in conjunction with sonication power [Ruan et al., 2012; Zheng et al., 2014]. The extraction of compounds from GL, especially when focused on spores, requires rupturing of tough cell walls; a process demanding substantial energy. However the potential for gains in both yield and time has enticed researchers into developing feasible ways of processing GL via UAE [Mason et al., 1996; Zhao et al., 2014]. The most influential factors on UAE of GL polysaccharides have been defined in existing literature as ultrasonic power, extraction time and solvent dilution.

It's limited solvent requirement, controllable temperature, and short duration introduces benefits for thermolabile compounds, however rapid increases in temperature (which are characteristic of cavitation-based kinetics) have also been shown detrimental to biomolecule yield from GL [Zhao et al., 2014; Checn et al., 2010].

The same efficiency gains have been reported when employing UAE to isolate polysaccharides from GL. An interesting study actually highlighted that even at high temperatures, UAE Ganoderma lucidum polysaccharide yield could be over 30% higher at 80℃ over 1.5 hours, at solvent:solute ratio 25:1 and subject to power 360 W, than HWE at a slightly higher temperature (90℃) for 2 hours [Sališová et al., 1997]. The extraction efficiency discrepancy between UAE of polysaccharides from GL observed that 0.06% crude GL polysaccharides could be extracted at 130 W and 30x dilution, subject to 50℃ after 60 minutes. HWE yields were less than half at the same conditions for GL [Cheung et al., 2013].

RSM was used to optimize the ultrasonic extraction parameters from GL polysaccharides in a study that observed optimal extraction at an ultrasonic power of 320W, temperature 70°C and time 34 minutes. In this study, the experimental parameters yielded 2.78%, and the extracts retained a strong oxygen radical absorbance capacity. The biomolecules that had larger structures were reported to be more potent free radical scavengers, presenting an opportunity to correlate structure with bioactivity. Furthermore, the variable showed interrelated behaviour – for example the effect of time on yield was greatest at higher power levels – in keeping with many studies [Dong et al., 2009]. Specific D-Glucan polysaccharides were yielded at 11.5% using low-power UAE for 30 minutes at 80°C, and diluted with solvent:solute 10:1 [Shi et al., 2014]. The antioxidant and immune-assays showed that the polysaccharides extracted in this study exhibited strong scavenging effects of DPPH and hydrogen oxide. The extract was also strongly stimulated proliferation of macrophages in the body's immune system by almost 170%, and the production of nitric oxide and phagocytosis.

Discrepancies in yield reporting have continued to hinder the field, as the degree of compound purity will affect the yield reported. For example, taking the example of the study just mentioned, a more recent study using RSM investigated UAE of GL using 590 W for 58 minutes at 81℃ and with dilution factor 25. This study however only reported a yield of 0.05% polysaccharides; far lower even in similar extraction conditions [Alzorqi et al., 2017]. Interestingly, this study found that ultrasonic power was not hugely significant, when evaluated in the presence of the other variables; which all exhibited maxima with respect to polysaccharide degradation. When temperature however showed a reduction after its maximum effect, the authors additionally involved the complex phenomenon described previously – high temperature may reverse the cavitational impact by increasing inter-bubble vapour pressure; thus "cushioning" cavitational

bursts. Interrelation between variables was verified by RSM. There was considerable significance assigned to the interaction between power and time. In other words, even though the impact of time on yield was positive when ultrasonic power was low, but the time impact on yield was negative when extraction power was high). This relationship between UAE time and power is a common finding in biomolecule extraction [Zhao et al., 2011]. Similarly, when temperature and power *or* time were both high, the yield reduced – another common finding in UAE systems of biomolecule extraction [Hromadkova et al., 1999]. The authors of this study compared findings to HWE using the same optimised parameters (81°C and 58 min). The yield from HWE was in fact 79% less, indicating the ability of ultrasonic power to enhance extraction rate.

Another study compared the polysaccharide extraction from GL using UAE, this time with HWE as well as Microwave-enhanced UAE (UMAE) [Huang et al., 2010 (c)]. RSM was used to optimise the parameters. In UMAE, optimal UMAE yield was obtained at ultrasonic power 50 W, microwave power 284 W, extraction time 701 seconds and water dilution factor 11.6. The corresponding yield was shown to be 115.56% higher than HWE and 27.7% higher than UAE. The greater yields of UMAE and UAE were attributed to the avoidance of excessive exposure to the heat in HWE. The combination of these particular techniques has also been shown successful in the extraction of other biomolecules from other natural organisms, primarily because the energy fed into the extraction system is greater, with diversity in temperatures and pressures presenting scope for greater extract variety [Lianfu et al., 2008].

### Supporting Evidence: UAE of GL Triterpenoids/Ganoderic Acids

As with polysaccharide extraction, UAE has shown efficiency gains over HWE when extracting GL triterpenoids. Nevertheless, the field still observes correlations between UAE parameters and yield, and to date these relationships have been well-defined with respect to GL triterpenoid yield. Ethanol-based UAE of triterpenoids and phenolic compounds from GL was optimized using RSM, and compared across UAE and HWE. Time, ethanol concentration, and temperature/ultrasonic power were varied across 5 levels. The study found that UAE was optimised at 40 min, 100.0 W, 32.5°C, dilution factor 30, and 89.5% ethanol. HWE was also investigated alongside, demonstrating optimal yield after 78.9 min, 90.0°C, dilution factor 30, and 62.5% ethanol. Overall, UAE resulted in the highest extraction yield of 4.9% crude triterpenoids [Oludemi et al., 2018]. The study reported that in UAE, there was no observed interrelation between the effects of time and solvent, nor power and solvent, however there was an interaction between exposure time and power. A study by Oludemi in 2018 used RSM optimisation and found that ethanol-based extraction (57.38%) extracted with dilution factor 70, 10.58 min extraction time, at 40°C and 500 W ultrasound power yielded 9.15% crude ethanol-soluble GL biocompounds, and both time and dilution factor were positively correlated with

yield. Comparison with conventional maceration (hot solvent extraction) revealed a higher extraction efficiency in a shorter extraction time. All extracts exhibited antioxidant and antitumour effects [Oludemi et al., 2018].

### 2.1.5.3.7 GL Extraction: Summary of Techniques

It has been highlighted throughout this section that the definition of polysaccharide and triterpenoid yield from GL has been a major cause for study discrepancy and inconsistency, hindering the development of an efficient extraction protocol. This is true for all extraction techniques, and is usually a result of discrepancies in purification, or in measurement of yield. For example a HWE temperature 95 °C for 3 h and dilution factor 12 achieved 75% crude GL polysaccharide yield, however Kan et al. demonstrated a maximum GL polysaccharide yield of 2.44% after 137 minutes at temperature 66℃, and dilution factor 35 [Kan et al., 2015]. The extracts in both studies maintained antioxidant capacity in scavenging assays. Similarly, "optimal" can vary depending on the organism, strain, and the specific combination of processing variables.

Whilst preserving the structure of the yield is crucial to maintaining its bioactivity, the foundations of traditional nutraceutical extraction has continued to build on HWE. Techniques like MAE, SCFE, and UAE certainly reduce the time and often temperature required, whilst also maintaining bioactivity. However these methods lend themselves to high costs and complexities introduced by added mechanical stress to the solute matrix [Alzorqi et al., 2017]. Typically, any extraction system is most efficient when there is an efficient dispersion of kinetic energy (i.e. enough time, enough energy, and enough surface area) to foster dissolution. A maximum however is attained once compounds begin to alter structurally, or if the system gains inefficiencies that result in less energy availability [Yılmaz et al., 2016]. This maxima however is currently not defined sufficiently for GL biomolecules.

### 2.1.5.4 Extraction Solvent

The chemical interactions involved in the extraction process render the extraction solvent a critical variable in nutraceutical extraction [Cheung et al., 2013]. More recent advances in chemical science have attributed a great deal of importance to the extraction kinetics achievable using different solvents [Sultana et al., 2009]. Water has remained popular in the extraction of biocompounds from plants owing to the polarity of sought-after compounds like polysaccharides and their complexes [Cheung et al., 2013]. The chemical properties of water are also modifiable to accommodate a variety of extraction targets; for example the polarity, viscosity and surface tension of liquid water at sub-critical temperatures can be considerably lowered

using temperature, introducing new characteristics such as changes in polarity [Askin et al., 2007]. An increasing temperature and pressure diminishes electrostatic interactions between the water molecules, and also between water molecules and surrounding ions and molecules The increased movement of water molecules then allows for dissolving less polar compounds, since the intermolecular interactions involving hydrogen bonding becomes less pronounced. This favours dispersion forces that render the water more non-polar, and thus more able to dissolve water-insoluble compounds [Plaza et al., 2015].

Water is however less selective than other solvents, and thus impurities in extraction require pre- or post-treatment washing steps. Water's high heat capacity further poses obstacles: when compared to organic solvents like ethanol, heating during extraction takes longer, and yield recovery steps (such as evaporation and concentration) are more time/energy consuming. Furthermore, an increasing understanding of plant bioactive compounds has fostered interest in non-polar compounds like some Ganoderic Acids, best extracted by organic solvents [Singh et al., 2010]. Ethanol-water mixtures are thus increasingly employed, extracting a wide range of compounds and their complexes [Askin et al., 2007]. This has revealed a capacity to target an increased spectrum of compounds, but has more recently demonstrated the ability to target various isomers/conformations of the same compound [Ha et al., 2015]. It remains common practice to employ ethanol in the extraction of increasingly popular antioxidants and Ganoderic Acids [Lu et al., 2012; Oludemi et al., 2013]. However even amidst the low selectivity and inconsistent (and low) yields from water-based extraction, the popularity of water in nutraceutical extraction lies in the safety and biocompatibility of its yield [Rodrigues et al., 2015].

The effect of HWE solvent (100% water - 80% alcohol) and temperature (20°C - 100°C) were investigated on some plant materials to measure effects on the yield of monosaccharides and oligosaccharides [Chen et al., 1993]. It was observed that during the most alcoholic extraction (80% alcohol) the process was most influenced by temperature, with maximum extraction occurring at 100°C. This is due to the higher heat capacity of alcohol, implicating a faster rate of warming. The 50:50 water:alcohol extraction process however yielded the most polysaccharides and was less influenced by the temperature changes. This can perhaps be explained by Raoult's Law, stating that ethanol-water combinations have an even lower heat capacity than the pure solvents [Lin et al., 2002]. On the contrary, water's high specific heat capacity suggests more energy is required to heat the solvent. This is attributed to water's high dipole moment due to the high charge gradient between oxygen and hydrogen, resulting in significant intermolecular attraction between the water molecules. This enhanced hydrogen bonding results in its high specific heat capacity [Plaza et al., 2015].

*Novelty processing and smart delivery of Ganoderma Lucidum spores*

### 2.1.5.5 Selecting an Extraction Process

To date, there has been no establishment of a "best method" for the extraction GL biocompounds. There has however been significant progress in establishing the parameters that are influential on yield as well as bioactivity of the obtained yield. As such, most investigations focus less on method comparison, and more on the parameter manipulation within a given extraction method that can achieve efficient yields. This is also because each method will pride itself on its own mechanisms of efficiency, which are incomparable to other techniques.

Many researchers attribute the structure to bioactivity, and thus an increasingly important outcome of the extraction method is the resulting structure of the biomolecules; something that can vary with the process employed [Min et al., 1998; You et al., 2011]. While many studies for example attribute antitumour activity to the branching structures of polysaccharides (in particular its triple helix conformation), some studies have found that biocompounds with low molecular weights are more effective. This reduction in molecular weight may even result from excessive process degradation, yet studies point to a greater bioactivity with modified (sometimes degraded) structures [Zha et al., 2009; Adachi et al., 1990].

Extraction via hot solvent extraction (using aqueous or organic solvents) poses a threat attributed to a prolonged exposure of biocompounds to high heat and temperatures, as well as harsh purification/drying chemicals that may degrade bioactive compounds and also present a threat to patient safety. Furthermore, low biocompound selectivity and poor yields have been a consistent challenge. More energy-intensive extraction techniques such as UAE, MAE and SCFE usually employ less time and solvent, and further protect the compounds from the harmful atmospheric conditions induced by excessive light and oxygen in conventional solvent extraction [Adachi et al., 1990]. These techniques have further shown an ability to maintain compound bioactivity in a variety of medicinal fungi, despite their high-energy systems. They are therefore often combined in a process chain to capitalise on the benefits of each [Huang et al., 2010 (c)].

GL currently boasts efficient extraction processes that can yield defined compounds possessing strong bioactivities, however there is little scalability of extremely high temperatures and pressures in the production of therapeutic agents. Therefore a more scalable extraction process is required, which can efficiently yield biocompounds that possess defined bioactivities. Nonetheless, polysaccharides are the most frequently reported yield from GL and its evaluation is thus more defined than that of triterpenoids.

### 2.1.5.6 Polysaccharide Yield Variation among the Physical Fractions of GL

Many studies have aimed to elucidate the chemical discrepancies between the GL physical make-up – especially the Fruiting Body (GLFB), Spores (GLS) and Mycelium (GLM) [Yue et al., 2008; Liu et al., 2002; Zhang et al., 2008]. GLFB has been shown more yielding of *phenolic compounds*, which have attracted considerable interest due to their biological properties including anti-oxidant, anti-mutagenic and anti-carcinogenic effects [Zengin et al., 2015]. These compounds possess free radical scavenging capabilities and have been observed prevalent in GL fruiting bodies in particular [Abdullah et al., 2012]. Contrastingly, GLS and GLM are usually richer in the compounds that have demonstrated tumour inhibition and immunoenhancement (*polysaccharides* and *Ganoderic Acids* in particular). Despite this classification, many studies continue to observe very potent free radical scavenging, reducing power, and lipid peroxidation inhibition from the polysaccharides and triterpenoids extracted from the spores of GL (along with their antitumour effects) [Heleno et al., 2012]. This renders extracts from the spores particularly valuable.

One study compared the extracts from the fruiting body (GLFB) and spores (GLS), observing significant tumour inhibition in-vitro from both extracts, but additionally a significant effect on splenocyte proliferation and cytokine production from spores [Yue et al., 2008]. In this study the spores displayed a D-Glucan-dominated polysaccharide composition group, contrary to the fruiting body which contained mainly Arabinans. Subsequently, broken spore extracts were verified as more potent in tumour inhibition in-vivo and in-vitro than their unbroken counterparts; a common finding in literature [Zhou et al., 2000]. Indeed the yield discrepancy between broken and unbroken spores has been debated owing to the harsh conditions required to extract from the unbroken spores, and the subsequent loss of bioactive compounds.

Tables 2.4-2.6 summarise some polysaccharide yields obtained using water-based HWE. While these tables offer an indication of the yield obtainable using varying extremities in process parameters, the attribution of GL yield to any one of these parameters is inaccurate simply as every study will employ unique experimental settings otherwise. Indeed even to date, there is little work in literature that offers a controlled comparison of the existing methods with respect to GL yield and bioactivity.

*Novelty processing and smart delivery of Ganoderma Lucidum spores*

| Yield | GL:Solvent | Temp (°C) | Extraction Time | Isolation | PS Quantification | Ref. |
|---|---|---|---|---|---|---|
| 30.70% | 1:30 | 100 | 6 | Filtration / Lyophilisation | Phenol-SA Assay | [Heleno et al., 2012] |
| 21.40% | 3:20 | 100 | 10 | Filtration | Dry wt. % | [Yue et al., 2008] |
| 16.80% | 1:10 | 100 | 3 | Filtration | Phenol-SA Assay | [Chan et al., 2005] |
| 4.10% | 1:20 | 120 | 0.67 | OD 37°C | Phenol-SA Assay | [Sone et al., 1985] |

Table 2.4: Polysaccharide extraction from GL Mycelium using HWE. OD = Oven Drying

| Yield | GL:Solvent | Temp (°C) | Extraction Time (h) | Isolation | Quantification | Ref. |
|---|---|---|---|---|---|---|
| 83% | 01:20 | 4 | 1 | Evaporation | Dry wt. % | [Dong et al., 2009] |
| 31.10% | - | 100 | 8 | VD | Dry wt. % | [Cao et al., 2006] |
| 30.07% | 03:20 | 100 | 10 | Filtration | Dry wt. % | [Yue et al., 2008] |
| 11.31% | 01:33 | 100 | 72 | Filtration/ Lyophilisation | Phenol-SA Assay | [Heleno et al., 2012] |
| 11.30% | 01:30 | 100 | 6 | Filtration/ Lyophilisation | Phenol-SA Assay | [Qin et al., 2011] |
| 9% | 01:40 | 100 | 8 | Lyophilisation | Phenol-SA Assay/HPLC | [Cheng et al., 2013] |
| 7.50% | 01:20 | 100 | - | Lyophilisation | Dry wt. % | [Herrero et al., 2006] |
| 7% | 01:20 | 120 | 0.67 | Lyophilisation | Phenol-SA Assay | [Sone et al., 1985] |
| 5.10% | 01:12 | 100 | 4 | Lyophilisation | Dry wt. % | [Cheng et al., 2013] |
| 3.40% | 01:05 | 95 | - | VD | Dry wt. % | [Cao et al., 2003] |
| 0.35% | 01:10 | 100 | 2 | FD | Dry wt. % | [Ye et al., 2008] |

Table 2.5: Polysaccharide extraction from GL Fruiting Body using HWE. VD = Vacuum Drying FD = Freeze Drying

| Yield | B/U | GL:Solvent | Temp (°C) | Extraction Time (h) | Isolation | PS Quantification | *Ref.* |
|-------|-----|------------|-----------|---------------------|-----------|-------------------|--------|
| 27.6% | U | 1:2 | 100 | 96 | VD/Lyophilisation | Phenol-SA Assay | *[Song et al., 2008]* |
| 14.5% | U | 1:33 | 100 | 72 | Filtration/ Lyophilisation | Phenol-SA Assay | *[Heleno et al., 2012]* |
| 2.98% | B | 1:50 | 75 | 6 | VD | Phenol-SA Assay | *[Fu et al., 2009]* |
| 0.94% | U | 1:50 | 75 | 6 | VD | Phenol-SA Assay | *[Fu et al., 2009]* |

**Table 2.6:** Polysaccharide extraction from GL Spores using HWE. B = Broken sporoderm, U = Unbroken sporoderm. VD = Vacuum Drying

## 2.1.5.7 Ganoderic Acids: The Importance of GL Spores

As previously discussed, there is growing importance attributed to the triterpenoic GAs in GL. These biomolecules are far less understood owing to the similarity between its various isomers – leading to significant overlap in standard analytical techniques. Their characterisation therefore typically involves advanced chemical techniques (spectroscopy in particular) in order to foster fragmentation of the isomers and ascertain the isomer [Min et al., 2000]. The gaps in knowledge about this biocompound have not only resulted in inconsistent reporting of the bioactive mechanisms that achieve its established apoptotic activities, but also in their classification. What has been established however, is the high prevalence of this invaluable triterpenoid family in GL spores [Min et al., 2000; Guo et al., 2009]. With GLS containing cytotoxic GAs, it is no wonder they have become the focus of extraction investigations. Because many investigations employ energy-intensive conditions to pre-treat spore walls and facilitate the extraction of compounds, low yields and bioactivities can result from excessive degradation [Min et al., 2001]. In addition, the extraction of triterpenoids like GAs typically benefit from less polar organic solvents that could pose a threat to patient safety; such as methanol and chloroform (or indeed water subject to very high temperatures). Indeed polar water extraction from GL spores has yielded biocompounds that exhibit limited cytotoxicity [Bao et al., 2002]. However, the spores' simultaneous high polysaccharide content in fact further increases its potential as a potent therapeutic agent possessing both cytotoxic *and* immunoenhancing capabilities [Zhang et al., 2011]. To alleviate the effects of intense pressure and chemical hydrolysis on biocompounds in spores, advances in sporoderm-breakage technology have allowed for greater breakage efficiency [Ma et al., 2011; Na et al., 2017]. By employing broken spores, superiority in both yield and bioactivity has been proven when compared to unbroken spores - even though their chemical

*Novelty processing and smart delivery of Ganoderma Lucidum spores*

compositions are often similar [Huang et al., 2006; Na et al., 2017]. For example, GLS extracts showed greater apoptotic activities in HeLa cell inhibition in-vitro when broken spore extracts were administered. This included greater cell cycle arrest, inhibited DNA synthesis, and reduced intracellular calcium in particular [Müller et al., 2006; Zhu et al., 2000].

## 2.1.6 Biomolecule Yield Quantification and Characterization

Extraction typically generates a compound-rich supernatant, and solvent precipitation subsequently purifies crude water-soluble biomolecules. Drying can quantify a physical yield, and further chemical analytical techniques can isolate and classify specific compounds and isomers. Common quantification techniques include chromatography (especially High Performance Liquid Chromatography) and ultraviolet (UV) spectroscopy. A study carried out by Dubois et al. in 1956 outlined a technique via which specific polysaccharide compounds can be detected from a pool of crude polysaccharides in the UV-Visible light spectrum. However these chemical methods have gained tremendous popularity more recently for the screening of Ganoderic Acids which are very small and difficult to distinguish [Gao et al., 2004].

### 2.1.6.1 Measuring Compound Yield

Compound yields are typically reported as a crude dry-weight percentage of initial input (equation 2.1), or more increasingly as the specific compound using a pure reference following chemical techniques like spectroscopy [Sood et al., 2013]. Indeed without chemical evaluation, the yield typically contains a variety of biocompounds such as phenolic compounds, lipids, proteins and amino acids [Heleno et al., 2010]. Thus the term "crude polysaccharides" usually describes the untreated yield obtained from GL [Zhao et al., 2010].

$$\text{Compound Yield } (\%) = \frac{\text{Dry Weight of Extract } (g)}{\text{Initial GL input } (g)} \times 100 \qquad \textbf{Eqn. 2.1}$$

Crude extracts are obtained when the extraction process is followed or preceded by purification. Purification typically includes yield "washing" with specific solvents that remove unwanted materials such as lipids, proteins, and phenolic compounds. A study would require a purification level specific to their experimental aim. For example if the aim is to isolate β-D-Glucans, purification steps would ensure that other bioactive biomolecules are minimally present.

*Novelty processing and smart delivery of Ganoderma Lucidum spores*

Examples of the crude yields typically obtained from GL include "GLPS"/"PGL" (GL *Polysaccharide*) and "GLPP/PSP" (*GL-Polysaccharide-Peptide*), which typically result from the difference in extract processing with respect to the removal of certain biocompounds. Various Ganoderic Acid isomers also result during its extraction, however because GAs are quantified using spectroscopic methods that streamline the specific isomer based on a reference characteristic, GA yield is becoming increasingly accurate [Zhong et al., 2015]. Both physical and chemical precipitation can purify GL extracts. Physical precipitation involves sedimentation of compounds based on solubility, whereas chemical precipitation capitalises on the chemical structure of the compounds, and additional requires advanced identification techniques such as chromatography and spectroscopy [Huang et al., 2010 (b)]. The discrepancies between the extraction protocol in GL studies has rendered the comparison between extracts challenging, and therefore attempts to review extraction studies are arduous and inaccurate. Common purification steps are described briefly in table 2.7.

| Organic washing | Chemical Degradation | Purification via Advanced Spectroscopy | No/Limited Purification |
|---|---|---|---|
| Organic solvents precipitate water-soluble compounds by dissolving lipids, and also facilitates extract drying. | Oxidation, reduction and hydrolysis degrade complex structures. The hydrolysis into simpler/detectable forms provides the basis for the well-known Phenol-Sulphuric Acid assay. | Compounds can be chemically classified via spectroscopic techniques such as HPLC and LCMS. | Functional biomolecules such as proteins are often bound to extracts when extracted in water owing to their hydrophilic amino acid configuration to form valuable complexes e.g. GLPS, PGL, PSP. |

**Table 2.7:** Chemical Purification of biomolecules during extraction from GL

## 2.1.6.2 Defining Compound Yield

In addition to yield *measurement*, extract yield needs to be *characterised* using more advanced chemical techniques such as spectroscopy and chromatography. It has become evident that the understanding of secondary metabolites can be invaluable to the understanding of its complex parent organisms. Methods used to investigate such intricate molecules are often based

on the detection of structurally unique characteristics such as branching conformations in GL polysaccharides; especially as these unique structural features can affect immunoenhancing and antitumour potency [Fan et al., 2014]. Many unique structures have successfully been detected using spectroscopy and NMR, which uses knowledge of the compound's behaviour in certain environments to create assumptions for its existence in the yield. This is particularly useful when defining GA yield, which could boast several valuable GA isomers that each display distinct patterns of fragmentation under spectroscopy. What is missing in literature however, is the association between the GL compound chemical structure, its bioactive potency, and the overall process scalability [Hennicke et al., 2016]. The forthcoming work aims to provide a useful association between the specific biocompound, and its candidacy for healthcare in the modern era.

### 2.1.6.2.1 Polysaccharide Analyses

Polysaccharides are undefined in shape, size, structure, and chemical composition. Polysaccharides can be defined by class, size, structural/chemical conformity and shape using biochemical analyses, as previously discussed [Sone et al., 1985; Zhao et al., 2010]. Particular interest has been fallen on the *Phenol-Sulphuric Acid (PSA) assay*, which identifies carbohydrates based on their unique conformations that absorb specific wavelengths of UV-Visible light. Figure 2.23A shows the reaction upon which this phenomenon is based. Sulphuric acid is a strong and stable acid, and is used to dehydrate hexose compounds like D-glucose to form monomer *5-hydroxymethylfurfural*, which reacts with phenol to create a purple colour as shown in the positive result in 2.23B. While the method detects most classes of carbohydrates (mono-, di-, oligo-, and polysaccharides), the absorptivity of different carbohydrates will vary.
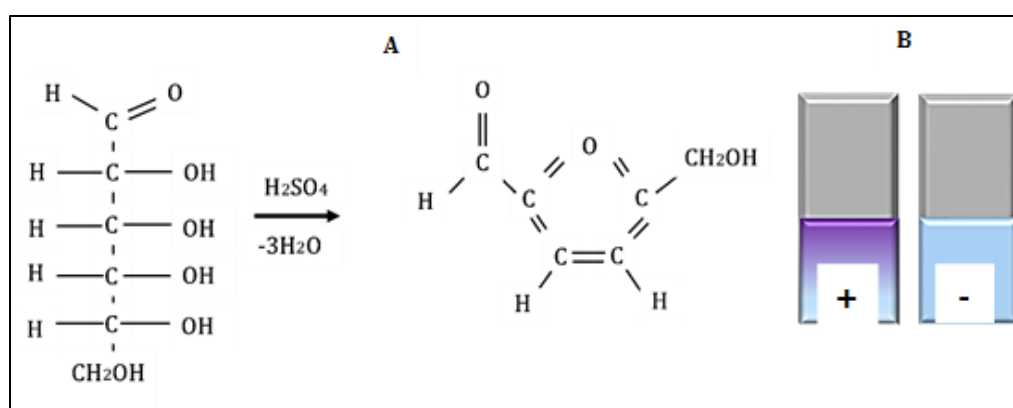


**Figure 2.23:** Phenol-Sulphuric Acid assay A) Reaction to form furfural forms of D-Glucans and B) Result of reaction

*Novelty processing and smart delivery of Ganoderma Lucidum spores*

Using UV to detect polysaccharide compounds was first reported by Dubois et al. [Dubois et al., 1956]. Complex carbohydrates could absorb UV-radiation if hydrolysed. Figure 2.24 shows the chromatogram obtained for different polysaccharide derivatives. The study developed an analytical method for detecting carbohydrates known today as the Phenol-Sulphuric Acid assay. Following hydrolysis, the monomers are detected using colour-developing compound Phenol prior to UV-Vis spectroscopy.
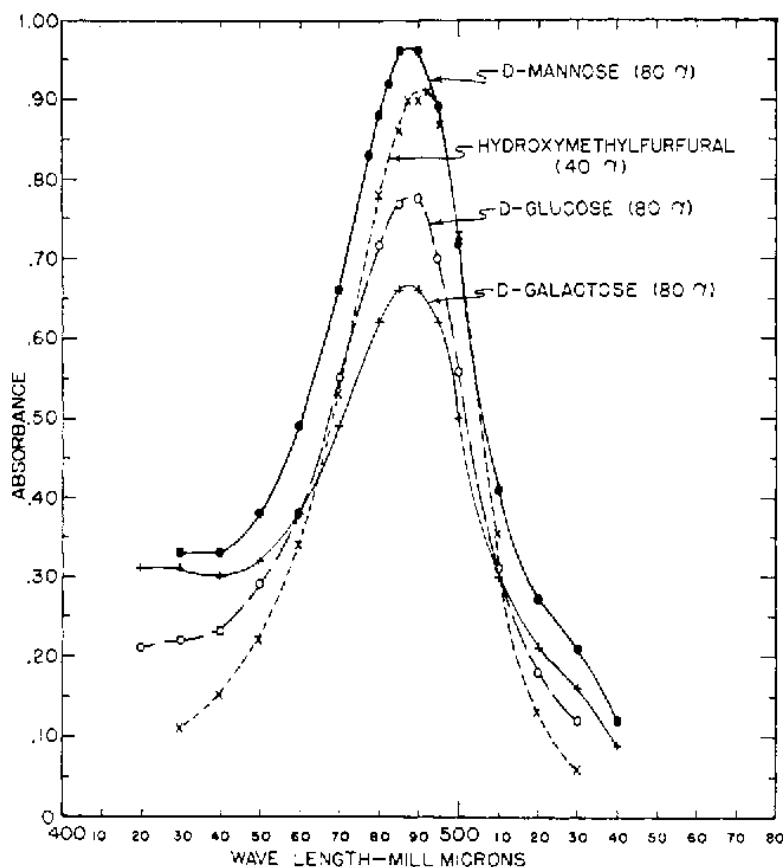


**Figure 2.24:** The absorbance peak at 485nm of various hexose monosaccharides reported by Dubois et al. [Dubois et al., 1956]

Non-selective detection is an issue that results from the wide range of D-hexose monomers absorbing UV-light at the same wavelength. D-Glucose, D-Fructose and D-Mannose are all present in GL, and therefore this method alone does not provide compound classification due to peak overlapping [Sone et al., 1985; Bao et al., 2001]. Multiple analytical methods are therefore typically employed to distinguish the compound structures, and for GL polysaccharides this has often included Gel Permeation Chromatography (GPC), Gas Liquid Chromatography (GLC), High Performance Liquid Chromatography (HPLC), and Size-Exclusion Chromatography (SEC) [Ma et

*Novelty processing and smart delivery of Ganoderma Lucidum spores*

al., 2018]. In fact chemical degradation as a means to deduce information about large polysaccharides is a common approach to yield characterisation. For example increasing amounts of information on chain conformation have been more recently identified using chemical analyses that selectively degrade the polysaccharide structures to smaller more established forms, from which structural information can be inferred. This has particularly included Smith degradation and methylation analysis [He et al., 2010]. This includes the characterisation of the triple-helix conformation, and the attribution of the spectroscopic rotations to β-linked glycosides of the D-Glucose polysaccharide [Sone et al., 1985].

Further chemical bond characteristics can be revealed by infrared-based spectroscopic techniques such as Fourier Transform (FTIR), Nuclear Magnetic Resonance (NMR) and Exchange-ion Chromatography (EIC) [Bao et al., 2001]. High-resolution microscopic techniques such as Scanning Electron Microscopy (SEM) and X-Ray Diffraction (XRD) analysis can provide a detailed structural analysis of the physical structure of extractants, through light-scattering technology [Zhao et al., 2010]. Such advanced analyses not only provide compositional insight, but also indicate the degree of homogeneity of the compounds [Bao et al., 2001]. While much of our knowledge of GL polysaccharides has been a result of spectroscopic analyses, modern findings on the toxicity of certain chemicals like phenol, and sulphuric acid has demanded the used of infrared spectroscopy owing to gains in efficiency, safety, and selectivity [Ma et al., 2018; Hell et al., 2016].

### 2.1.6.2.2 Ganoderic Acid Analyses

Ganoderic Acid isomers exhibit very little detectable differences in chemical grouping and molecular weight, and so it has proven difficult to distinguish structures that classify GA isomers. As a result, popular analytical techniques such as HPLC and UV-Vis spectroscopy often deliver inconclusive results owing to peak overlapping between compounds. Combinatory approaches have therefore been employed, whereby chromatography and spectroscopy are coupled with advanced analytical tools such as Diode Array Detection (DAD), Mass Spectrometry (MS), Electrospray Ionization (ESI), Nuclear Magnetic Resonance (NMR), and Fourier Transform Infrared (FTIR) spectroscopy. Many studies have successfully identified GA structures based on these complex spectroscopic systems, and MS in particular has shown advanced capabilities in distinguishing GA isomers from GL spores as well as fruiting bodies [Zhao et al., 2006; Zhang et al., 2018]. MS ionizes the extract and categorises the ions based on mass-to-charge ratio, in order to identify co-eluting compounds that have distinct molecular weights. Liquid-Chromatography MS (LC-MS) combines the separation capabilities of liquid chromatography with the mass analysis capabilities of mass spectrometry. In LC-MS the atoms of a material's elements are all ionized positively by the removal of electrons, and then accelerated to all have the same kinetic energy.

A magnetic field will then "deflect" the ions to a degree dependent on their weight (further if the ion is more positively charged it is more easily deflected), and thus provide insight into the size (and perhaps isotopes) of the ions. The deflected ions are then detected by the spectrometer and shown on a chromatogram against the retention time. Assuming that the ions all have a charge of 1+, the output would also include a spectrum collected in the ultraviolet light region showing the abundance of the ions of each mass/charge ratio. As the GA extract is not a single element but rather a multi-compound material containing isomeric molecules such as sterols the different m/z distinctions may well represent "fragments" of the ions which could be created after ionisation due to the lack of ion stability. The tallest peak in the spectrum (the base peak) represents the commonest fragment ion to be formed (usually summed over a specific retention time period). The height of this peak can result from either particularly high ion stability, or the prevalence of a particular ion (and its fragments) in the material.

MS is a popular analytical technique for the evaluation of GA isomers, and has been successfully coupled with LC and ESI along with other advanced techniques [Zhang et al., 2018]. Fragmentation pathways have been shown to be dominated by losses of $H_2O$ or $CO_2$; and subsequent cleavage of the rings. These losses create new ions that have distinct peaks in MS. For example one study found that a GA-A ion at m/z 515.30 created an ion at m/z 497.34 due to losing $H_2O$. The 497.34 m/z ion was further subjected to produce signals at m/z 479.32 or 453.36 by its own subsequent losses [Zhang et al., 2018]. The mass spectrum of the GA-A evaluated in this study is shown in figure 2.25, whereby a, b, c and d correspond to the rings. This concept was discussed in section 2.2.3.
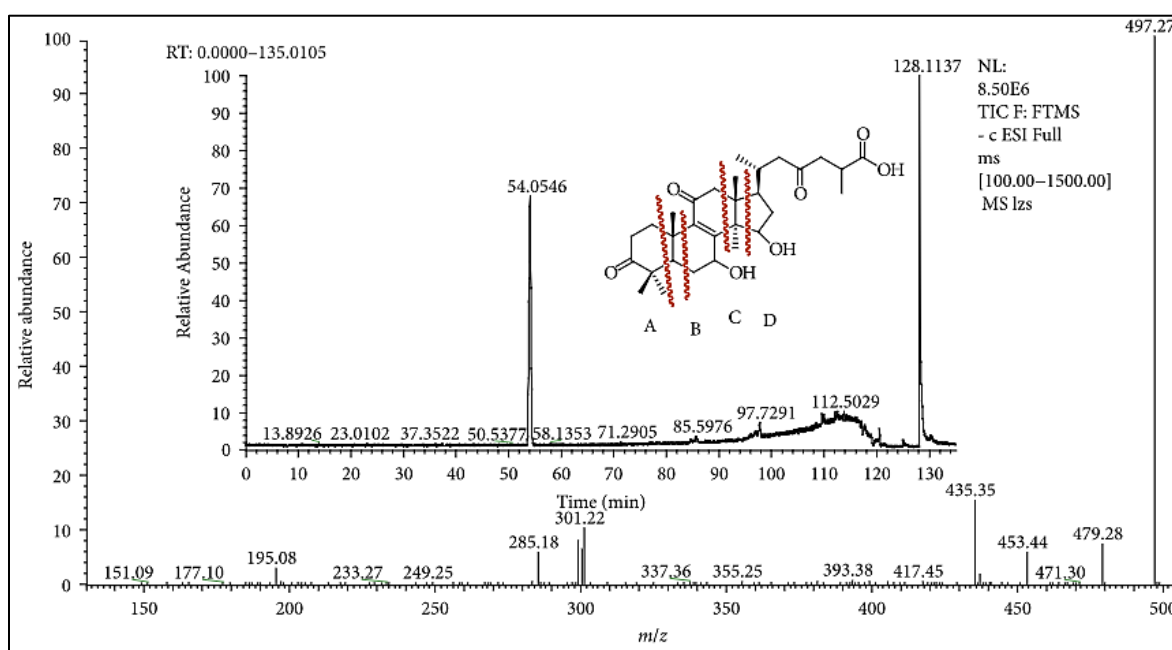


**Figure 2.25:** MS Distribution of GA-A and as reported in [Zhang et al., 2018]

*Novelty processing and smart delivery of Ganoderma Lucidum spores*

The retention time distribution can reflect a weight-dependent affinity with the mobile phase, or other distinguishable characteristics – ultimately indicating the presence certain isomers. The mass distribution (outer) shows the evaluation of GA-A via fragmentation (pathways and resulting ions) in MS. Other investigations have shown very similar mass patterns of Ganoderic Acid fragmentation, indicating the isomer variation. Studies have observed a high dependence of peak patterns on the positions of the carbonyl and hydroxyl groups, thereby providing a means for isomer distinction [Cheng et al., 2011; Cheng et al., 2012]. The mass spectrum is an invaluable evaluation in the analysis of GA samples, identifying not only the isomers themselves, but also many properties of their structures and resulting commonalities between isomers [Liu et al., 2012]. However, there still remains slight ambiguity between peaks when richer extracts are analysed. Furthermore, inconsistent reference standards make complete identification of complex samples challenging and the mass fragmentation patterns of many isomers are not fully known [Liu et al., 2012].

### 2.1.6.2.3 High-Performance Liquid Chromatography (HPLC) for GAs and Polysaccharides

HPLC is widely employed in compound analysis to chemically evaluate enigmatic materials; typically those found in nature. Individual chemical constituents in a liquid sample are released based on their biochemical nature (specifically their polar affinity with the surround eluting solvent, the *mobile* phase). The quickest release corresponds to the constituent that possesses highest solubility in the mobile phase and the release pattern forms a chromatogram of all compounds. The holding time of the biochemical in the column prior to release is known as its *retention time*. This release pattern forms a chromatogram of all compounds, facilitating advanced identification and analysis of bioactive compounds [Cai et al., 2012]. A simple schematic of HPLC is given in figure 2.26.



**Separation of individual Compounds**

Crude

Based on their affinity to the mobile phase, sample compounds will be eluted at various times (retention time) to form a unique sample spectrum reflecting the sample's composition

**Elution of each Compound**
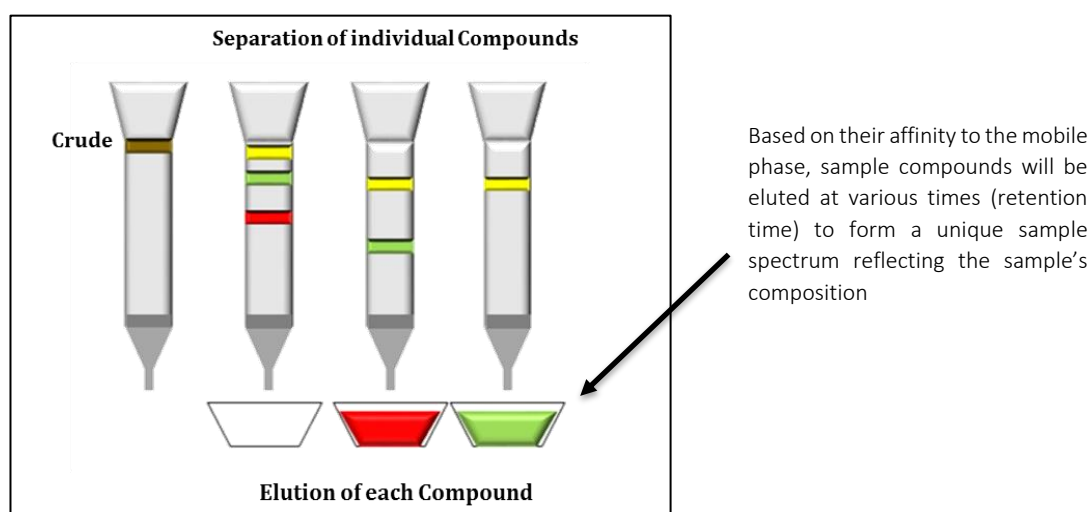
 **Figure 2.26:** Principles of HPLC: Elution of particular compounds during analysis

*Novelty processing and smart delivery of Ganoderma Lucidum spores*

Many complex natural organisms are evaluated using HPLC for quality-control as well as for advanced therapeutic analyses. Ganoderma lucidum has undergone many evaluative investigations using HPLC to characterise compounds, and also to more intricately investigate important biomolecules like Ganoderic Acids. Studies have attempted to employ HPLC in the biochemical analysis of GL and results consistently indicate a high presence of various types of triterpenoids and polysaccharides, along with amino acids, proteins, and phenolic compounds [Yang et al., 2010]. In fact most HPLC analysis topics have focused on Ganoderic Acids, owing to their growing importance in the healthcare field, but also owing to the difficulty they present in distinguishing its numerous isomer forms [Liu et al., 2012; Ha et al., 2015]. HPLC, often in tandem with mass spectroscopy, has provided an insightful tool into the evaluation of GA samples. A variety of Ganoderic Acids, Lucidenic Acids, and Ganoderiols have been isolated and identified from GL [Wang et al., 2006; Ha et al., 2015]. Without the use of further analytical techniques however (such as MS), peaks often overlap owing to similar molecular weights/chemical affinities. This is typical of natural samples containing a variety of chemically-similar structures. Resultantly, HPLC is often combined with MS to further classify the eluted compounds.

HPLC analyses has been increasingly successful in the identification of Ganoderic Acids from GL, mainly owing to the progressive growth of recorded reference standards. With respect to GL *polysaccharides*, HPLC has been investigated as a means for identification and analyses, however a compound's retention time alone cannot indicate the complex branching network of GL polysaccharides. Furthermore, the huge plethora of large and complex monosaccharide arrangements in GL polysaccharides make accurate structural identification more tedious and less accurate, using chromatography alone. Thus when HPLC is employed alone, there is often the need to simultaneously employ hydrolysing agents (Acids/enzymes) for more selective identification of monosaccharides in HPLC [Han et al., 2014].

### 2.1.6.2.4 Ultraviolet-Visible (UV-Vis) Spectroscopy for Polysaccharides and Ganoderic Acids

UV-VIS spectroscopy is one of the most widely applied yet oldest spectroscopic techniques for molecular analysis. This type of spectroscopy examines a material's light absorption behaviour in the visible and adjacent UV-Vis spectral region. When sample molecules interact with infrared light, they undergo electronic transitions to an excited state, displaying a higher energy molecular orbital. The wavelength of absorption ($\lambda$) depends on the presence of the light-absorbing groups (chromophores) in the molecule.

In a typical UV-Vis spectroscopy setup the "white" light enters the sample after being dispersed into the colours of the visible and near UV-Vis spectrum. Upon entering the sample, a fraction of the light energy will be absorbed by the molecules, and the remainder will be transmitted to the

detector (figure 2.27). Light transfer through a sample is determined by the fraction of light passing through at the specified wavelength ($\lambda$). If $I_0$ represents the intensity of the light entering and $I_1$ the transmitted light, then the transmittance, **T**, will be defined as **T = $I_1/I_0$**. Optical Density is used to describe the behaviour of the light in the sample and refers to the light absorbance of the sample and subsequent "blockage" to light transmission. It is measured by taking the inverse log of the transmittance and depends on material properties as well as the path-length [Vasser et al., 1997].
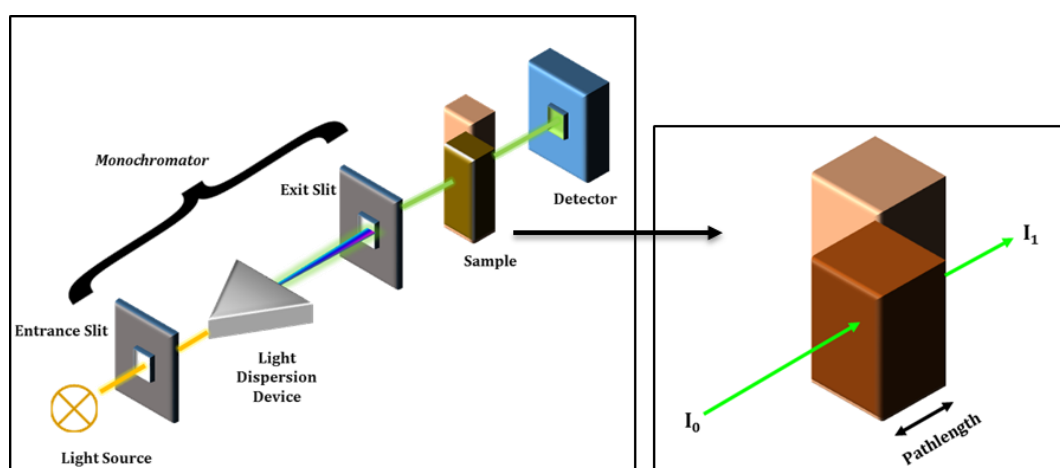


**Figure 2.27:** UV-Vis spectroscopic setup (right shows light transmittance through sample)

With evidence that particular compounds "peak" at a specific wavelength, displaying unique UV absorbance, the absolute concentration can be obtained through calibration curves of the raw compound at that wavelength. This technique is invaluable not just in the hydrolysis of structures in the previously described phenol-sulphuric acid assay, but as a tool to further enhance other spectroscopic analyses like HPLC and MS in the analysis of Ganoderic Acids, as detailed in the previous section.

## 2.1.7 Ganoderma lucidum for Healthcare: Current Outlook

Section 2.1 of the literature review has presented an insightful overview of the techniques and limitations currently present in the field of GL development. The extraction of various biomolecules (polysaccharides and triterpenoids in particular), their bioactivities, and their characterisation have created a "work-in-progress" protocol that is continuously being

enriched with respect to safety, efficiency, and process efficiency What continues to hinder the development of this organism for healthcare however, is the inconsistency resulting from a lack of references in all aspects of development: *compound extraction*, *structural evaluation*, and *bioactivity*. To date, no process has yet demonstrated a method of systematically developing the raw material into a well-defined bioactive therapy. Figure 2.28 is a schematic of the summary of steps involved in GL's development from cultivation to compound evaluation. Phase II and phase III clinical trials in Eastern Asia have been complete, with results indicating extended survival, greater quality of life, pain relief, and immunoenhancement in up to 97% of patients with cancers of the stomach, oesophagus, lung, ovary, and cervix cancer [Kidd et al., 2000].

### 2.1.7.1 Pre-/Clinical Trials

Despite the popularity of GL, it is not accurately characterised in terms of clinical efficacy and safety. According to the China National Knowledge Infrastructure, Wanfang database and PubMed 81 qualified chemical, biochemical, preclinical and clinical studies of GLPS have been documented in English and in Chinese as of 2017. Clinical trials have advanced findings of traditional in-vitro and animal-based in-vivo tests. Diseases such as cancer, diabetes, coronary heart disease (CHD), and hepatitis B are typically the most common subjects of clinical trials, and most are randomized and placebo-controlled to ensure validation of findings. Clinical trials however often highlight the subjective response of patients, disease stage and a treatment/dosage plan that requires multiple revisions and adaptation to be deemed valid across a wider human sample. Furthermore, the measures of effect in these trials can vary significantly depending on the toxicity criteria used. A good example is *Ganopoly*, a patented GL extract previously mentioned. This extract has undergone numerous clinical trials that demonstrated efficacy against heart disease, chronic hepatitis B, lung cancer and diabetes [Gao et al., 2003; Gao et al., 2004]. These trials were classified as a "fail" in a clinical setting, as results were inconsistent across biomarkers, and the drug mechanism was not defined [Zhou et al., 2005]. It is worth noting that the design of these clinical trials suffers as a result of difficulties in initially identifying GL biocompounds and their mechanisms of action. Clinical trial protocol is therefore often criticised for inconsistent findings or inconclusive bioactive relationships. This has left a critical gap in clinical trials of GL and thus no approved GL-related drugs on the market.

Platelet aggregation plays a pivotal role in disease inhibition. In 1990, a water extract of GL (mainly polysaccharides) underwent clinical trials to gauge effects on platelet aggregation in 33 patients with atherosclerotic (artery-focused) diseases. Platelet aggregation outperformed the placebo group after 2 weeks of treatment [Tao et al., 1990]. Treatment with a GL polysaccharide

extract showed hypoglycemic activity in Type II diabetes when administered for 12 weeks, also improving the symptoms of CHD patients and indicating liver protective effects in chronic hepatitis B patients [Zhou et al., 2005]. In 2016, a randomised placebo-controlled clinical trial using GLS was carried out alongside chemotherapy in patients with varying degrees of cancer. The GLS extract, containing mainly polysaccharides and triterpenoids compounds reduced the toxicity of parallel chemotherapy, and further enhance its efficacy [ClinicalTrials.gov]. The latter effect is particular interest in human studies, given the dependence on chemotherapy today.

According to the Database of Clinical Trials of the US National Library of Medicine [Clinicaltrials.gov, 2019] there are 16 ongoing clinical trials of Ganoderma drugs (various strains). Of the studies, only one has published results – highlighted below in table 2.8. This particular study employed a water-ethanol extract of GL (assumed to contain both polysaccharides and triterpenoids) alongside chemotherapy. This study was carried out on 3 patients only and the results (quality of life, alongside tumour markers were inconclusive.

| Title | Status | Conditions |
|---|---|---|
| Ganoderma Tea on Eczema Patient | Unknown status | Eczema |
| Clinical Study of Ganoderma lucidum Spore Combined With Chemotherapy | Unknown status | Carcinoma, Non-Small-Cell Lung |
| The Effect of Ganoderma on Patients With Head-and-neck Cancer | Unknown status | Head-and-neck Cancer |
| Investigating the Effects of MikeiÂ® Red Reishi Essence EX on the Immune System of Prostate Cancer Patients and Patients With Non-cancerous Conditions of the Prostate | Not yet recruiting | Prostate Cancer |
| Beta-1,3/1,6-D-Glucan Ganoderma lucidum on Ulcerative Colitis | Not yet recruiting | Ulcerative Colitis |
| Clinical Trial on Ganoderma Spore Lipids Combined With Chemo in Patients With G.I. Cancers | Unknown status | Gastrointestinal Neoplasms |
| Lingzhi for Cancer Children | Completed | Pediatric Cancers |
| Effects of Lingzhi on Disease Progression in Patients With Untreated Early Parkinson's Disease | Recruiting | Parkinson Disease |
| Efficacy and Safety of Lingzhi in Patients With Early Parkinson's Disease | Completed | Parkinson's Disease |
| Immediate or Delayed Naturopathic Medicine in Combination With Neo-Adjuvant Chemotherapy for Breast Cancer | Terminated | Quality of Life |
| Lingzhi and Sen Miao San for the Treatment of Rheumatoid Arthritis | Completed | Rheumatoid Arthritis |
| An Evaluation of Proglucamune in the Treatment of Protective Qi Insufficiency | Completed | Protective Qi Insufficiency |

*Novelty processing and smart delivery of Ganoderma Lucidum spores*

| | | |
|---|---|---|
| A Follow-up Trial of Proglucamune® in the Treatment of Protective Qi Insufficiency, a TCM Condition | Recruiting | Protective Qi Insufficiency (a Condition Term From TCM) |
| Morpho-functional Changes After Oral Supplementation of Antioxidants and Anti-inflammatory Treatment in Age-Related Macular Degeneration. | Completed | Dry AMD |
| Effect of SACCHACHITIN on Healing of a Chronic Wound | Unknown status | Wounds |
| Effects of Botanical Microglia Modulators in Gulf War Illness | Active, not recruiting | Gulf War Illness |

**Table 2.8:** Ongoing Ganoderma Lucidum Clinical Trials

Today, the fastest progress of Ganoderma drug development is the combination of Ganoderma spore lipids and chemotherapy in cancer, which is currently under phase III double-blind randomized clinical trial. This study not only evaluates medical effects on patient but also several tumour and immunity biomarkers. Taken together, Ganoderma drugs have been used as single agent or combined with other ingredients or chemotherapy drugs in clinical trials worldwide. However, the formulation of these candidate Ganoderma drugs is still complicated and requires further investigation. Such situation makes its clinical trial a challenging task for it has to be conducted under the FDA guidance on Chemistry Manufacturing and Controls (CDC) for clinical trials. Therefore, clear API of candidate drugs was needed for future clinical trials of Ganoderma.

**Figure 2.28**: GL – The Current Progress for Healthcare



*Novelty processing and smart delivery of Ganoderma Lucidum spores*
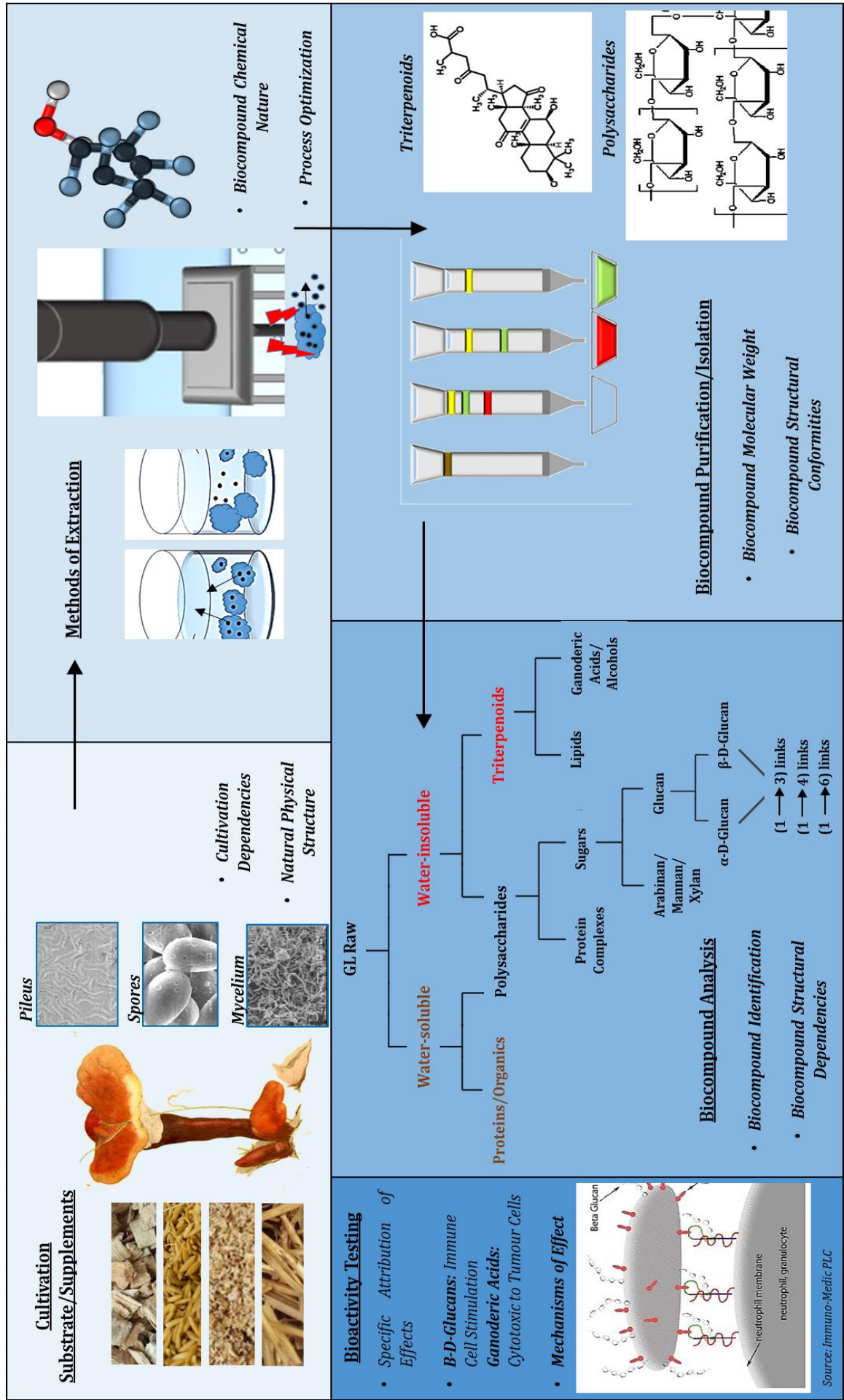
## 2.2 Creating Drug Delivery Systems

"Drug delivery" is a broad concept that covers the **delivery, protection**, and **control** of therapeutic compounds before *and* during administration [Kumari et al., 2004]. Achieving controlled temporal/spatial distribution in the physiological environment and maintaining drug plasma drug concentration has generated focus on achieving specific encapsulation and release profiles of a drug's delivery system, and the engineering of materials. In particular, this has centred studies on surface profiling, environment-responsive materials, and specific system morphologies [Nguyen et al., 2013]. Combined with the need to employ a fabrication process and materials that are biocompatible and scalable, the search for a controllable yet efficient delivery system is still a significant area of study. Figure 2.29 summarizes some of the main requirements of an efficient drug delivery system today [Mishra et al., 2011; Wan et al., 2018].



**Controlled Encapsulation/Release**
- Environment-responsive materials
- Specific morphologies
- Surface profiling

**Biocompound Protection**
- Strong and stable materials
- Flexibility to create shape/size

**Biocompatible**
- Biodegradable materials
- Small size distribution

**Scalable**
- Fabrication process/materials that are safe for patient and drug bioactivity
- Fabrication process/materials that are economically and environmentally friendly

**Figure 2.29:** Requirements of an efficient drug delivery system to achieve efficient and safe treatment

## 2.2.1 "Smart" Delivery

The world's population is undergoing an exponential rise in the incidence of diseases that require *specific* and *accurate* treatment plans. More invasive treatments like chemotherapy and radiotherapy damage local tissue and can further exhibit inefficacies owing to noncompliance

*Novelty processing and smart delivery of Ganoderma Lucidum spores*

with the treatment regime of busy lifestyles, or even as a result of the illness itself [Beyatricks et al., 2013]. Innovations in delivery have been investigated as a solution to the lack of specificity and compliance exhibited for vital treatments. Delivery systems that exhibit controllable release profiles are known as *smart delivery systems* [Alvarez-Lorenzo et al., 2014]. The controlled dosing maintains blood drug plasma by providing an alternative to multiple doses, and enhanced specificity further avoids local toxicity. However the issues that continue to hinder the development of the ideal drug delivery system include unanticipated immunological reactions, an "initial drug burst", and toxic treatment remnants [Beyatricks et al., 2013]. Figure 2.30 shows a schematic of the release profile of a controlled device compared to that of a conventional delivery device. As the polymer phase degrades (A), the drug is gradually released (B) as determined by the polymer material, drug-polymer interfacial kinetics, and delivery mechanism employed. Conventional delivery (orange) often exhibits an initial burst of drug release prior to release stagnation [Beyatricks et al., 2013; Alvarez-Lorenzo et al., 2014; Devarajan et al., 2015].
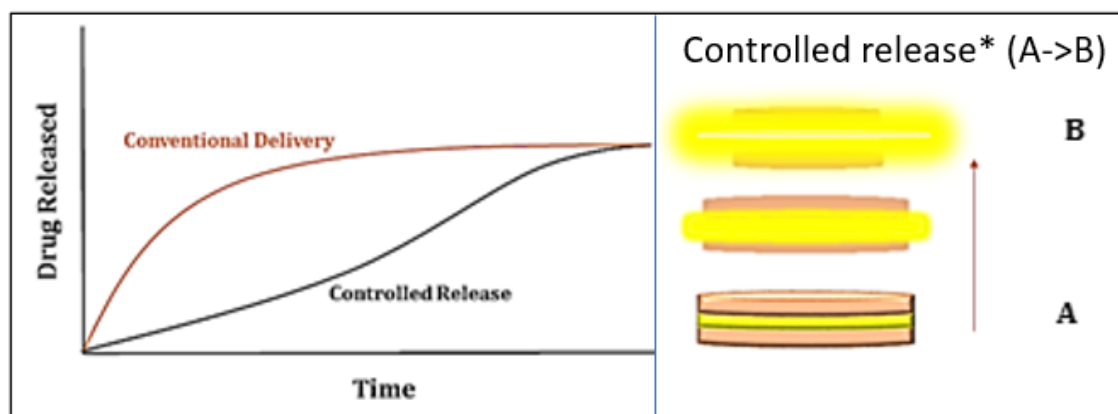


**Figure 2.30:** Release profile of controlled vs uncontrolled drug delivery. Controlled systems (black) release the treatment gradually. Point B shows the result of a controlled matrix following controlled delivery at A. *Controlled release can occur via a variety of mechanisms – this is just an example for explanatory purposes.

## 2.2.2 Factors Influencing Smart Delivery

The characterization of delivery system vehicles has become vital to the development and quality control of therapeutic agents. To attain a drug delivery system that is safe, biocompatible, and effective, the vehicles (for example particles) must demonstrate sufficient drug uptake, exhibit a controllable release profile, be accepted/retained by the target tissue to avoid premature treatment elimination, and be biocompatible and biodegradable. Literature shows that the size, shape and surface attributes are all crucial factors determining the aforementioned factors. In addition these parameters have been shown by numerous studies to

*Novelty processing and smart delivery of Ganoderma Lucidum spores*

exert strong influence on the *manufacturing* of the delivery system (including material preparation, mixing, and encapsulation) [Hlinak et al., 2006; Shekunov et al., 2007].

## 2.2.2.1 Vehicle Size

The International Council for Harmonisation of Technical Requirements for Pharmaceuticals for Human Use (ICH) offers guidelines to determine when vehicle size should be deemed important. According to their guidance, the size is to be considered when influential on treatment performance (such as dissolution, bioavailability, safety, stability) or manufacturability (such as ease of flow and compressibility) [(European Medicines Agency, 2020)]. The size of the delivery vehicles can impact degradation rate, dynamics/flowability in the bloodstream, degree of effective targeting, drug clearance, and tissue acceptance [Champion et al., 2007]. When traversing blood vessels, or other small tracts, vehicle size governs flowability and adhesion to walls. For example a study by Patil et al. reported that the adhesion of larger particles to cells was significantly lower than smaller particles – attributing this effect to reduced "slip velocity" of smaller particles under flow conditions [Shinde et al., 2001]. This was also observed by Goldman in 1967 [Goldman et al., 1967]. However, as observed by a later study in 1990, the increased contact area of larger particles can also favour adhesion [Cozens-Roberts et al., 1990]. The size of vehicles must also be small enough to avoid size-based clearance mechanisms by the immune system (particularly macrophages). Studies have reported different size thresholds to avoid this internalization, also stating that the efficiency in target cell uptake is considerably cell-dependent. Consistently however, nanoparticles have been shown as the more efficient candidate for reaching target cells and avoiding phagocytosis. For example more than one study have found the optimal size for cell uptake is around 50nm diameter (below and above which efficiency reduced) [Chithrani et al., 2006; Lu et al., 2009]. Studies have also reported that delivery particles with diameters >500 nm are at risk [May et al., 2001]. On the contrary, studies also report successful endocytosis of microparticles. Usually however, microparticles are phagocytosed in the liver or capillary beds [Tabata et al., 1990; Gratton et al., 2008].

Particle size can be controlled by manipulating the materials employed, or the experimental parameters of the fabrication method. The dependence of degradation on particle size however is a controversial area and had not yet been determined – especially given the diverse range of materials, drugs, and processes currently being explored [Dunne et al., 2000]. While larger particles have a proven lower surface area and thus limits water penetration inwards, it also increases vehicle retention as experiences reduced clearance of degradation products.

## 2.2.2.2 Vehicle Shape

While vehicle size has been heavily studied in the drug field, there are significantly less efforts dedicated towards determining the effects if vehicle *shape* on drug delivery – perhaps to do a lack of established methods for systematically and reproducible fabricating various shapes [Champion et al., 2007]. Indeed, more recent studies are revealing that vehicle shape can influence the effect of drug delivery, usually via its effect on biological processes like endocytosis, vascular dynamics, and targeting induced by attraction to disease sites [Gratton et al., 2008]. Studies also report the influence of vehicle shape on biocompatibility.

It has been reported that vehicle shape can affect the flowability of the delivery vehicles and thus the efficiency of target attainment/uniform dosing in the body, and can affect compaction and drug uptake during manufacturing [Hlinak et al., 2006]. In fact, shape will affect many of the delivery aspects affected by vehicle size – including flow velocity, solubility, and adhesion to cells - however in more *complex* ways. This is because the kinetics of spherical entities has been widely established and thus can be manipulated and controlled. Contrastingly, other abnormal entity shapes may move in ways that have not yet been observed consistently (examples in literature have included tumbling with the flow).

Indeed many of the body's physiological pathways contain tortuous trails that would benefit from more innovative and tailored shapes. Unfortunately, the effects associated with specific shapes are currently not all defined, however it is commonly observed in literature that longer, rod-like shapes with high aspect ratios (width over depth) are more quickly and effectively internalised by cells than the equal volume of a spherical particle [Gratton et al., 2008]. For example silica was observed to exert different toxicities when administered in particle vs nanowire configuration, possibly due to a greater achieved cell density [Adili et al., 2008]. Another similar study observed that micro-sized disk-like flexible shapes could infiltrate the "slit"-shaped filters in the spleen, however spherical particles cannot unless they are significantly smaller [Moghimi et al., 2001]. Shape also adds another dimension to the efficiency of a delivery system – the *curvature.* This has been shown to affect ligand adsorption and the "fit" to cell surfaces. In particular, the introduction of various extended features has been of recent focus. This is because once the delivery vehicle has adhered to the cells surface, it can easily be washed away with blood flow. Protruding curves or tails can instead increase the grip that the drug vehicles have.

As previously mentioned, phagocytosis can prevent drug delivery from attaining target sites, and is a significant challenge to effective drug delivery. While size thresholds have been established for safety during various physiological pathways, the same has not been established for carrier shape. However, studies are increasingly getting involved in defining these phenomena. When

macrophages were exposed to various polymer shapes, the authors of one study observed that the particle geometry at the attachment point specifically governed macrophage internalization [Champion et al., 2006]. The study reported that spherical particles however were more endangered from all positions of attachment. These results were independent of particle size.

Degradation to release entrapped drug molecules has been shown to a function of particle shape [Hsieh et al., 1983]. One study achieved sustained a drug release profile (termed zero-order release) using hemispherical particles – however the large particle sizes rendered the findings unsalable to applications in-vivo. Furthermore, studies show that as degradation is a function of surface area and size, shape can affect this [Dunne et al., 2000; Panyam et al., 2003].

The effect of particle shape is an area of study that needs developing across the drug delivery field. Researchers face significant challenges from phagocytosis and cell membrane adhesion, and these functions are so far enigmatically governed by distribution shape. Furthermore, the interaction between shape and size of the vehicles could prove to be a major factor influencing drug delivery.

### 2.2.2.3 Vehicle Surface Characteristics

Surface characteristics are another more recent aspect of development in drug delivery. For example, studies reported that the surface texture can govern a vehicle's retention time in the bloodstream. An important finding was the ability to prolong a vehicle's blood circulation by coating with hydrophilic polymer molecules that foster resistance of serum protein [Moghimi et al., 2001; Alexis et al., 2008]. Other studies instead focus on the adhesion to cell membranes achieved using "rougher" surfaces [Chung et al., 2003]. Importantly however, porosity of vehicles has been a particular area of progress in drug delivery. Studies consistently show the benefits in drug loading, release control, and cell targeting attributed to a porous structure [Jadhav et al., 2016]. Many of these advantages are also implicated characteristics of porosity too, like a greater surface area, and the increased possibility to add innovative features that have better affinity with the bloodstream and target cells ("active targeting"). Pores also allow drug loading post-fabrication of the vehicle, which avoids the exposure of biomolecules susceptible to degradation, like peptides and proteins. Another study observed that ibuprofen loading was not affected by introducing particle pores (size nor quantity), whereas the release was considerably slowed and thus more controllable, in keeping with other literature in the area [Gonzalez et al., 2013].

*Novelty processing and smart delivery of Ganoderma Lucidum spores*

Even though a high degree of control can be achieved using porous delivery vehicles, porosity remains challenging to measure and create accurately, therefore there is lack of reference for the direct relationship with drug delivery- especially in light of the discovery of its impactful relationship mass transport mechanisms *within* the vehicle [Klose et al., 2006].


## 2.2.2.4 Vehicle Material

Selecting the most efficient materials to deliver drugs to targeted sites in a smart way the is an ever-evolving process. This is because new materials are constantly being discovered or enhanced. A good example of this is the development of biomaterials, environment-responsive materials, and porous materials that can now be found "as needed" in nature. As naturally-derived materials become increasingly inferior in the face of highly functional synthetic imitations, the achievement of safe and effective drug delivery (via biocompatibility/biodegradability, biomolecule protection, controlled release, targeting ability, and high tissue retention) is more difficult to achieve, and remains enigmatic with respect to the relationships between the physiological environment and the material, but also newfound developments observed every day in a diseased environment.

Using polymeric encapsulation of therapeutic agents has proven considerable benefits over conventional material preparations. Studies report rigid protection prior to administration and during physiological transport, sustained release to prevent "spikes" in treatment, and tunability to control release profiles across a variety of treatment plans. *Biodegradable* polymers can have distinct degradation profiles that stabilise release of the drug owing to low water penetration of the matrix (for example with biopolymer sodium alginate). Polyester, especially Poly (lactide-co-glycolide) (PLGA), have been a particularly popular biodegradable candidate for drug carrier material as it is biocompatible, easy to processing, has considerable in-vivo stability, and can be manipulated for controlled release [Jain et al., 1998]. *Natural* polymers derived from biological systems however are also inherently biocompatible and biodegradable drug carriers, possessing low toxicity a pharmacokinetic profile that thus far has been proven efficient. The use of polysaccharides in particular (such as chitosan and sodium alginate), has been extremely promising in achieving safe and effective drug delivery, yet remains underreported [Liu et al., 2008].

For an accurate evaluation of materials for drug delivery, extensive studies are typically required to determine the effect on the material after multiple processing settings. Even though there exists an established "checklist" of desirable material properties for drug delivery, there is still a

*Novelty processing and smart delivery of Ganoderma Lucidum spores*

lack of references for non-synthetic materials (biomaterials in particular), and thus studies employing biomaterials for drug delivery have generally observed diverse findings.

Despite knowledge of the importance of physical properties of a delivery system, researchers continue to face challenges as they attempt to consider these requirements in line with both pharmacokinetics *and* the system manufacturing process. Limited progress has therefore resulted in a lack of reference methods for the characterisation of vehicles fabricated using various biomaterials, and in predicting the relationships between process variables and achieved delivery system. Table 2.9 summarises the impact of some delivery system characteristics, and their effects on aspects of drug delivery [Hlinak et al., 2006]. It is evident that particle size distribution and surface area are strongly influential on delivery system functions.

| Property | Impact Flow | Blending | Wetting | Drying | Mechanical | Dissolution | Stability |
|---|---|---|---|---|---|---|---|
| Particle size distribution | X | X | X | X | X | X | X |
| Particle shape distribution | X | | | | | | |
| True density | | | | X | X | | |
| Bulk density – poured and tapped | X | | X | | X | | |
| Pore size distribution | | | X | X | | X | |
| Surface area | X | X | X | X | X | X | X |
| Surface energy | X | X | X | | | | |
| Flow | X | | | | | | |
| Cohesiveness | X | X | | | | | |
| Internal friction | X | | | | X | | |
| Wall friction | X | | | | X | | |
| Amorphous content | | | X | | | | X |
| Elastic modulus | | | | | X | | |
| Compactibility | | | | | X | | |
| Brittleness | | | | | X | | |
| Static charge | X | X | | | | | |
| Hygroscopicity | X | | | X | | | X |

**Table 2.9:** Some effects of vehicle properties on aspects of the drug delivery system fabrication and functionality

### 2.2.3 The Challenges of Delivering GL Biocompounds

GL biocompounds, particularly when crude, are fundamentally diverse; containing compounds that possess a wide range of chemical properties like solubility. As drug concentration in blood plasma is a function of drug released from the delivery device and the solubility of the drug compounds in the bloodstream, there is an inherent low bioavailability associated with compounds such as triterpenoids (and their conjugations) [Kim et al., 2018]. The carrier properties, compound properties, and system features (shape, size) play a large role in bioavailability. Most progress in developing drug delivery systems for compounds like those in GL

*Novelty processing and smart delivery of Ganoderma Lucidum spores*

has been in the development of materials and their design, simply because new materials and new processing techniques are constantly discovered and developed. Synthetic materials can indeed can provide the answer to cheaper and more controllable delivery systems, but they introduce the risk of physiological toxicity after sustained periods of time. Biocompatible materials are therefore preferred, however they implicate higher costs and lower manipulability. As a result, a variety of avenues are being explored to enhance the feasibility and scalability of biocompatible delivery systems. Furthermore, despite the benefits of many therapeutic GL biocompounds, these treatment candidates are challenged by oxidative degradation during storage [Kivelä et al., 2012]. It restricted lifetime has indeed hindered its scale-up as a commercial therapy, and thus it is vital to find ways to protect GL biocompounds following extraction.

From the limited pool of GL encapsulation studies, those that exist primarily focus on the compounds themselves, with little regard for the value of crude forms owing to the more complex chemistry involved in their encapsulation. Furthermore they are typically encapsulated using synthetic polymers that do not offer the biocompatibility achievable with natural polymers. For example, GL polysaccharides (GLPS) were encapsulated by poly(ε-caprolactone) (PCL) to ultimately display a release sustainable over maximum 4 hours with a large (>70%) initial burst (figure 2.31). Particles were however irregularly shaped and sized, and authors reported that the GLP-PCL matrix in which GLPS were distributed across (not just core or shell) offered the most flexible treatment plan [Xing wet al., 2018].
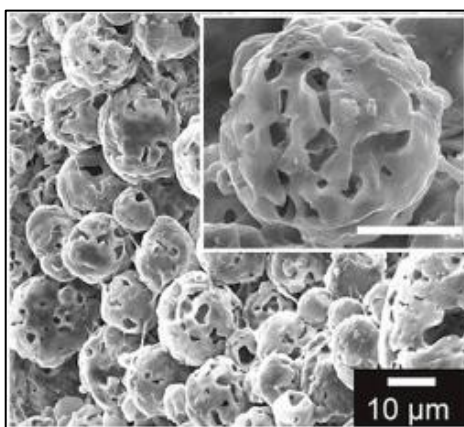


**Figure 2.31:** Scanning Electron micrograph of GLP-loaded porous PCL microparticles displaying a polydispersed particle distribution [Xing wet al., 2018]

Recent studies suggest that Ganoderic Acids could be encapsulated in a poly acrylic acid (PAA)-coated IONPs (PAA-IONPs) nanoparticle matrix, ultimately providing a combinatorial approach to cancer therapy and magnetic resonance imaging (MRI). Being entrapped within the hydrophobic

*Novelty processing and smart delivery of Ganoderma Lucidum spores*

pockets of the matrix, GA concentrations could be sustained and subsequently released to ultimately demonstrate high residence in tumour cells with no local toxicity [Zhu et al., 2007]. This study presents opportunities for further study into receptor-mediated cellular uptake of particles via vitamin attachments such as folic acid (an effective targeting agent for the folate receptor overexpressed in many tumour cells) [Radwan et al., 2011].

## 2.2.4 Naturapolyceutics

Naturapolyceutics refer to the marriage between natural polymers and pharmaceutical applications like drug delivery. Polymers in drug delivery present a promising candidate for smart delivery, principally owing to degradation and thus release control [Nair et al., 2007]. Natural polymers offer biodegradability, biocompatibility, and chemical flexibility owing to their chemical and physical diversity. Resultantly, the have been investigated for their use in controlled and safe drug delivery [Qiu et al., 2006]. Today, a variety of plant-derived polymers have successfully formulated drug delivery systems, however for optimal bioavailability the challenges of targeting and controlled release remain [Ngwuluka et al., 2014].

Carrier material plays a key role in achieving delivery systems that provide efficient, effective, and safe drug distribution to the target tissue. A material possessing physiochemical attributes that work in harmony with the body's natural environment (biocompatibility), together efficient biodegradability, avoid the risk of inflammation, and drug inefficacy. Owing to the physiochemical nature of biopolymers, they provide high-level control (temporally and spatially) and possess desirable polymer features such as strength, durability, flexibility, rendering them capable of possessing desirable structures such as porosity [Hoare et al., 2008].

## 2.2.4.1 Biopolymer Sodium Alginate ("Alginate") for Drug Delivery

Alginate is an anionic hydrophilic biopolymer from brown seaweed with Mannuronate (M) and Guluronic (G) acid residues; the arrangement of which determines the polymer's physiochemical structure. The biopolynmer has been applied to a large range of biomedical applications, including drug delivery and cell immobilisation. Its ability to form a hydrogel has rendered the polymer a popular choice for drug delivery systems that require strength, protection and controlled degradation [Hoare et al., 2008; Abbaszad et al., 2015]. Alginate displays strong ionic carboxylic interactions in its backbone in the presence of multivalent cations

*Novelty processing and smart delivery of Ganoderma Lucidum spores*

and heavy metals such as calcium ($Ca^{2+}$). Alginate's degradation is controllable through selecting certain alginate structures and release environments, and is biocompatible and cost-effective [Yao et al., 2017]. It further provides strong polymer-drug compatibility so as to prevent crystallinity of hydrophilic drugs that impede outward flow, as it is aqueously composed. For these reasons, this biopolymer is an increasingly competitive candidate for the basis of drug delivery systems [Quong et al., 1998].

## 2.2.4.2 Crosslinking Alginate for Encapsulation

Crosslinking is the process that binds the chains of a polymer to form *hydrogels*. Hydrogels have physiochemical characteristics more suitable for drug delivery than raw polymer structures; in particular high strength and flexibility. Indeed these properties render them suitable for particulate as well as scaffold –based delivery systems. Alginate can be effectively crosslinked in the presence of multivalent cations such as Calcium and Zinc, yielding "egg-box" structures, as first reported by Rees et al. [Grant et al., 1973]. This egg-box structure is dependent on the alginate composition, chain structure and molecular weight, and this behaviour renders it extremely useful in the field of drug encapsulation. Alginates with polymer chains composing more G-Acids produce high-strength gels whereas alginate with chains composed of M-Acids have higher elasticity but lower physical strength as reported by Murata et al. [Murata et al., 1993]. This study demonstrated that the larger the G-Acid regions, the slower the degradation rate.
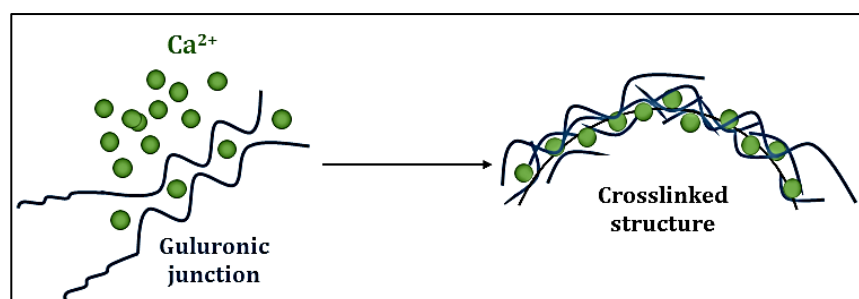


**Figure 2.32:** Calcium ion crosslinking of Alginate polymer chains. Divalent calcium crosslinks multiple polymer chains to form a 3D hydrogel structure

### *Calcium Chloride as a Crosslinking Agent*

Calcium salts ionize when immersed in an aqueous solution and thus water-soluble sources of calcium ions like calcium chloride are typically employed. Upon alginate ionization the

*Novelty processing and smart delivery of Ganoderma Lucidum spores*

positive sodium ions detach from the negative chain fragments, and calcium ions diffuse in and toward these negative regions of the alginate (figure 2.24). Because each calcium ion has two positive charges, it can "grab on" to two negative charges on different alginate molecules, crosslinking the alginate network, and resulting in more rigid collection of polymers [Chan et al., 2002].

Calcium has been shown to yield stronger and more stable structures than other multivalent cations owing to ionic nature of calcium–carboxylate bonds [Murata et al., 1993]. Calcium chloride ($Ca^{2+}$) is often employed in calcium-induced crosslinking due to its rapid solubility and non-toxicity, however its spontaneous calcium release implicates a rapid rate of crosslinking and thus high uncontrollability. Consequently, alginate structures are typically polydispersed [Murata et al., 1993]. Calcium Carbonate ($CaCO_3$) has been investigated in polymer crosslinking, as it initially requires hydrolysis to release calcium; thus leading to a slower and gradual crosslinking process. In turn, thus offers greater controllability. Weak acids are employed to release the calcium ions, and the by-product is carbon dioxide proportional to the quantity of $CaCO_3$in the system [Wang et al., 2008; Al-Musa et al., 1999]. Issues however arise in the effects of this gas on the structural integrity [Wang et al., 2008].

## 2.2.5 Polymer Drug Release Mechanisms

The basic concepts of drug release from polymer matrices typically adhere to a continual diffusion driven by polymer chain erosion, with dependence on variables such as polymer properties, matrix porosity, drug loading, drug-polymer interactions, and release environment [He et al., 2005]. Diffusion of the release solvent into the hydrogel typically leads to hydrogel swelling, inducing drug diffusion of drug outwards [Serra et al., 2009]. Upon immersion, typically the drug concentration gradient drives release, whereby water enters the polymer matrix and imitates hydrolytic polymer degradation that subsequently controls release rate. At a certain molecular weight, structural erosion of the matrix governs release, implicating the outflow of some polymer along with the drug molecules. Release tends to slow as the polymer assumes degradation [Kamaly et al., 2016].
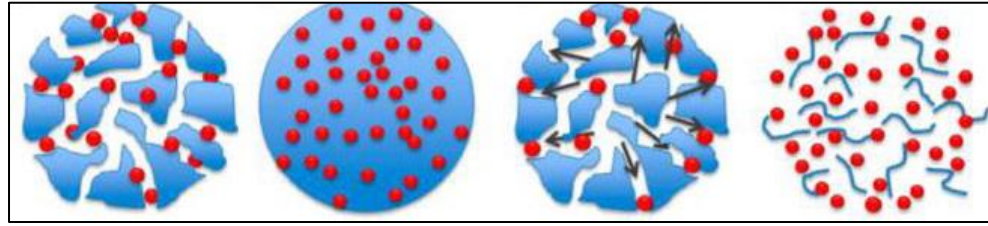
**Figure 2.33**: Drug release mechanisms from a polymer matrix. L-R: Diffusion through pores, diffusion through the matrix, osmosis and erosion [Kamaly et al., 2016]

Diffusion typically relies on the erosion of the capsule. Reservoir-diffusion involves a polymer-surrounded core, and release is determined by the drug's solubility in the polymer phase. Matrix Diffusion contain the drug dispersed arbitrarily in the polymer structure and release rate is dependent upon the polymer-drug interaction. The matrix system exhibits a decreasing release rate overtime, resulting from the decreasing surface area at the diffusion front as release progresses. The degree of crosslinking of polymer hydrogels will determine the rate of release, as the crosslinking degree controls the magnitude of matrix swelling – a driver of release from polymer hydrogels.
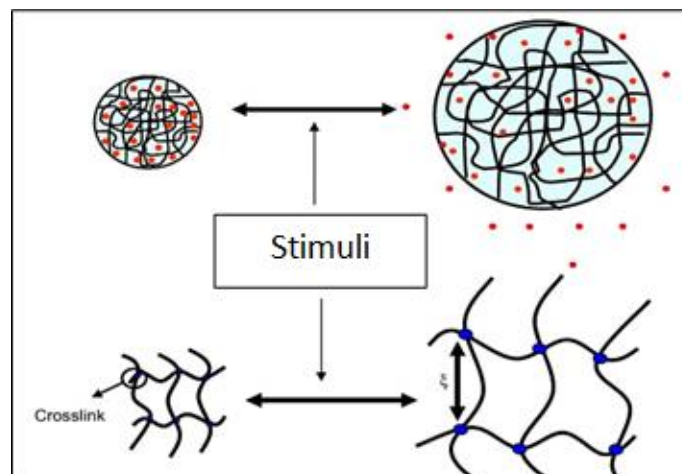


**Figure 2.34:** Schematic of physiologically responsive crosslinked polymer hydrogel. Swelling and subsequent release of the drug occurs under certain external stimuli such as pH, ionic strength and temperature [Serra et al., 2009]

*Novelty processing and smart delivery of Ganoderma Lucidum spores*

Figure 2.34 above demonstrated how a polymer hydrogel can be stimulated to swell, causing matrix expansion and outward/inward movement of particles. Stimuli typically include pH and temperature, however the degree of crosslinking (determined itself by factors such as cation strength/ratio to polymer and gelation process parameters) can also affect the behaviour of hydrogel swelling and thus release. A study in 2012 investigated drug release characteristics of calcium alginate hydrogels, when subject to various crosslinking ratios and drug sizes. Figure 2.35 reiterates that by increasing the calcium concentration, the alginate hydrogel swells less and loses less weight – leading to a lower observed drug diffusion in an MES buffer solution of pH 5.5 at 37°C for 48 h. The same relationship was found with drug size [Paradee et al., 2012].
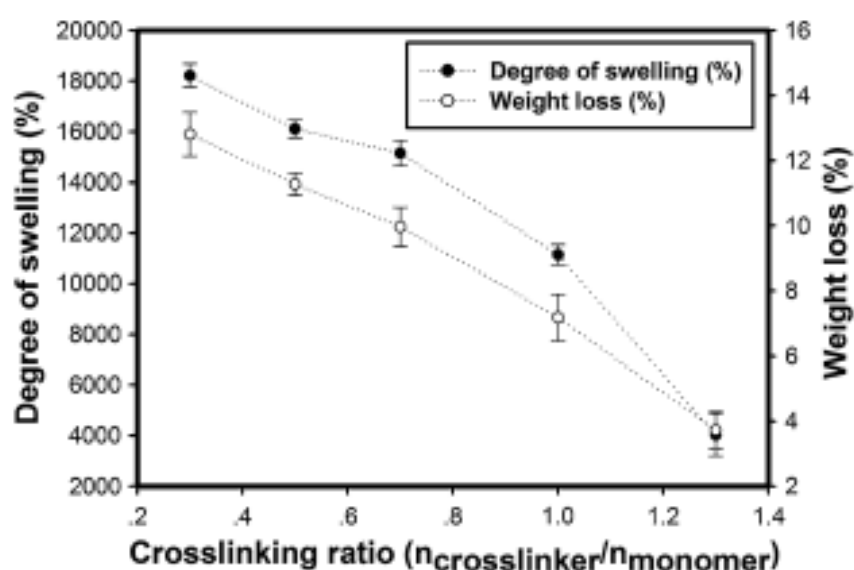


**Figure 2.35:** The degree of swelling (%) and weight loss (%) of Ca-Alg hydrogels at various crosslinking ratios [Paradee et al., 2012]

Overall, all drug release mechanisms exist as a function of similar properties, some of which are summarized in figure 2.36.

*Novelty processing and smart delivery of Ganoderma Lucidum spores*
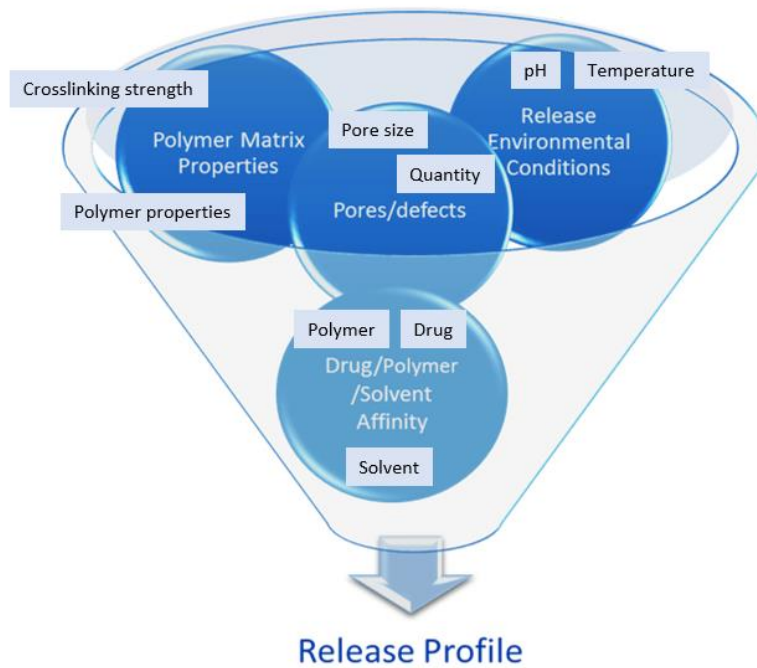
**Figure 2.36:** Determinants of drug release profile from a polymer matrix

## 2.2.5.1 "Initial Burst" of Biopolymer Drug Delivery Systems

It is common to exhibit initial bursts when employing polymer-based drug delivery systems, after which sustained release is typically observed via degradation-controlled diffusion [Achenie et al., 2017]. Despite advances in microparticulate delivery drug, the "initial burst" phenomenon can occur in the first period of administration, owing to the physiological environment into which the polymer is introduced. Typically these environments pose degradative risk owing to acidity, high temperatures, and immunological responses. An important consideration of controlled release is therefore the treatment's Minimum Toxic Level and Minimum Effective Level, shown in figure 2.37. Administration needs to ensure the drug plasma drug concentration within this range, and conventional synthetic systems can exhibit fluctuation leading to "swings" in plasma drug concentration owing to the phenomenon of bursting. Underexposure and overexposure periods therefore result [Ward et al., 2011]. In figure 2.37, the dotted lines show dosage with inconsistent drug exposure.
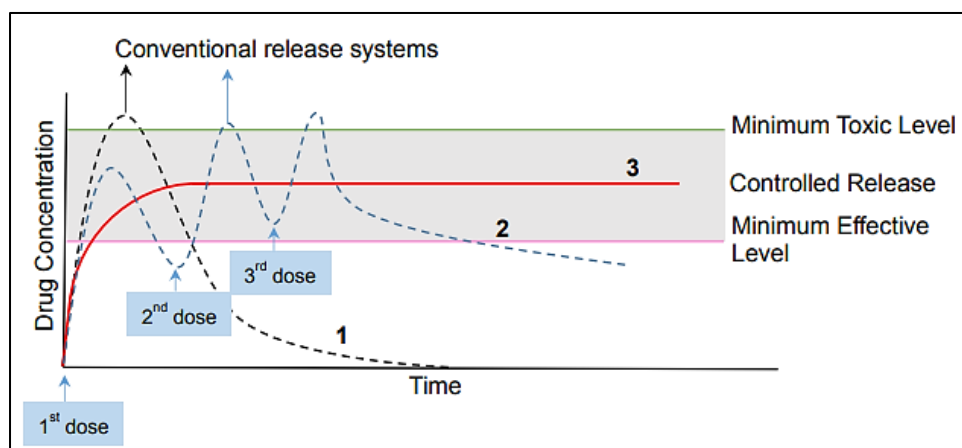
**Figure 2.37:** Drug release from conventional drug delivery systems causing inconsistent plasma blood concentrations [Ward et al., 2011]

The selection of capsule material, along with particle morphology, has been proven highly important in achieving release control and avoiding bursts [Mora-Huertas et al., 2010]. When core-shell delivery systems are not used, the drug is typically dispersed across the matrix and release rate via swelling, diffusion and erosion will be a function of time as a result of the declining concentration gradient at the polymer surface during administration.

## 2.2.5.2 Modelling Release from Biopolymer Matrices

Release models are often used to predict release profiles and thus regulate a polymer delivery system's efficacy. The models are well-defined for synthetic polymers which possess predictable characteristics and known causal relationships with process/release parameters, however these models have not been consistent for natural polymers like alginate. As a result, the field of study surrounding biopolymer-based delivery systems is underdeveloped owing to the known cost/practicality advantages of synthetic materials [Cascone et al., 1995]. Nonetheless, their biocompatibility and humble physiological clearance renders their development crucial to patient wellbeing [Agrawal et al., 2001; Sevim et al., 2017].

With mechanisms of drug release being interconnected, there is a challenge to controllably evaluate experimentally. As result, there is limited success in optimising drug release profiles without mathematical modelling. Modelling allows for the continuous development of drug

delivery systems, resulting from establishing the effects of system characteristics (morphology, surface, strength).

### 2.2.5.3 Alginate Release Models

Alginate hydrogels present the ability to control mechanical stiffness, swelling, degradation, mucoadhesive properties, and release [Shiraishi et al., 1993; Augst et al., 2006]. There is however limited modelling of alginate drug carriers in literature, stemming from limited study of their candidacy for drug delivery when not modified [Lemoine et al., 1998]. Of the studies carried out however, drug release from alginate hydrogel matrices are typically hindered by a significant initial burst that is followed by a continuous release. This is because the inherent porous and hydrophilic nature alginate rapidly drives out water-soluble drug molecules toward the hydrogel surface [Murata et al., 2007; Murata et al., 2009]. Nonetheless, relationships between release, alginate content, drug-polymer electrostatic interactions, release environment, and crosslinking density have been established across drug species for this inexpensive material [Badwan et al., 1985; Stockwell et al., 1986]. Although not consistent owing to experimental variation, it has been established that the main driving factors of alginate matrix release are crosslinking density, release environment (pH in particular), and factors affecting the vehicle morphology and surface [Chen et al., 2006; Dong et al., 2006], At many conditions, alginate matrices can exhibit zero-order release mechanisms, however there is very little confirmation of a "best fit" model for alginate-based drug delivery [Chen et al., 2006].

### 2.2.6 Microparticulate Drug Delivery

By engineering small and uniform delivery vehicles, the solubility, permeability, and stability of natural products can be enhanced [Kim et al., 2018]. Micro-sized carriers in the form of microemulsions are often developed as the process of emulsification (discussed below) is simple and quick. However greater stability and control is achievable via solid particles [Li et al., 2010]. While particle shape has been observed a key property of drug delivery control, more recent focus has shifted to the importance of particle surface ligands and other protruding characteristics/shapes that may enhance targeting ability [Cao et al., 2019]. As a result, an increasing number of studies focus on the shape of particles in addition to their size distribution. Microparticles take on a size below 1000 μm, and originally attracted attention for their level of control during drug administration. In particular, they can be fabricated in many ways, and can

meet a variety of specific therapeutic requirements (especially precise and repeatable dosing, evasion of phagocytosis, and plasma/tissue retention) [Beyatricks et al., 2013; Devarajan et al., 2015]. The effects of size were discussed previously, however importance needs to be given to the strong evidence supporting the benefits of microparticles over nanoparticles, with respect to their resemblance to existing structures in the body; viruses and serum proteins in particular – and importantly their ease of innovative design. They can be engineered to maximise acceptance into the physiological system and avoid premature uptake by the immune system [Amiji et al., 2006]. Other micro-sized forms including fibres, disks, and rods are popular for their ability to adhere to certain blood flow patterns, and to be accepted at various parts of physiological passage.

Microparticles for drug delivery are most often created by initially generating droplets that later solidify into particles. These droplets are often created using spray-drying, coacervation, emulsification, electrohydrodynamic atomization (EHDA), or some variation/combination of these [Shao et al., 2019]. While most methods have successfully been applied to alginate, the level of particle distribution controllability has been shown greatest via EHDA fabrication [Yao et al., 2017]. Spray drying is a hugely popular choice for microparticle fabrication as it is simple, low-cost, and energy efficient. In very recent studies it has successfully been used to encapsulate GL polysaccharides using polymers like maltodextrin (MD) in combination with various proteins. In a particular spray-drying study, a maximum GL polysaccharide (GLP) loading of 13.3% was achieved when particles were created using an inlet temperature of 170˚C. Microparticle shapes and sizes had depressed surface regions caused by particle shrinkage during the high temperature fluctuation causing rapid evaporation of moisture and high pressure. Unfortunately this study could not achieve a sustained release lasting more than 4 hours, in any pH tested. GLP-Maltodextrin particles without added proteins release the fastest, attaining 100% release before 3 hours (figure 2.38) [Shao et al., 2019].
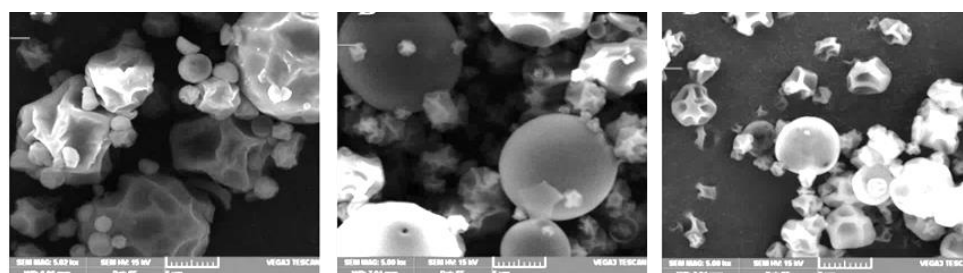


**Figure 2.38:** SEM images of microcapsules with various matrix compositions (left-right: GLP/MD microcapsules; GLP/MD-soy protein; and GLP/MD-whey protein)

*Novelty processing and smart delivery of Ganoderma Lucidum spores*

### 2.2.6.1 Microparticle fabrication via *Emulsification*

In emulsification, immiscible liquid materials create phase separation inducing small droplets. Pharmaceutical molecules are typically distributed in an aqueous polymer solution and emulsified in an organic solvent like oil to create oil-in-water (O/W) or water-in-oil (W/O) droplets (figure 2.39). The emulsion is induced and maintained using mechanical methods and surfactants, and this can be followed by gelation of the polymer matrices in a process known as crosslinking [Torchilin et al., 2001]. Much attention is given to understanding the kinetics in an emulsion system that control the droplet size, monodispersity, and stability. Advantages of emulsification to fabricate drug delivery systems include a high drug-loading capacity, small distribution size, and the ability to encapsulate and deliver hydrophobic/poorly bioavailable compounds to the body by improving their solubility [Baimark et al., 2014; Paques et al., 2014; Qu et al., 2014].
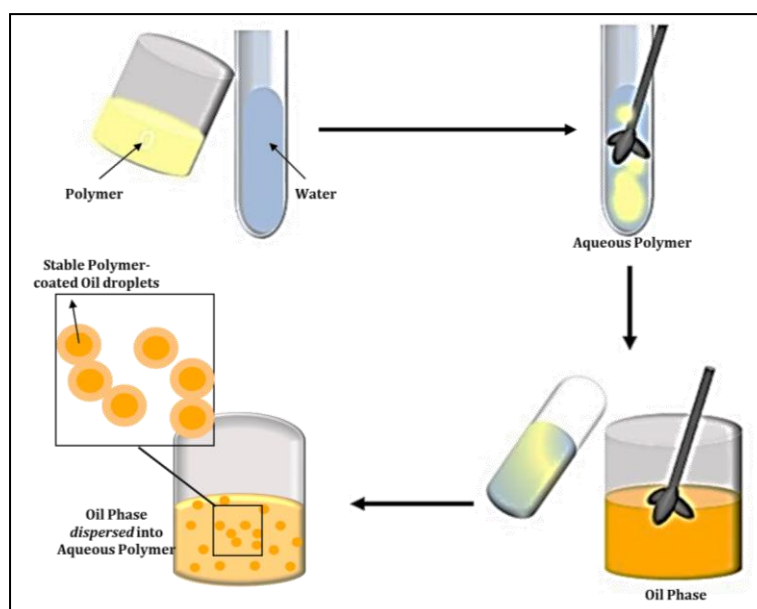


**Figure 2.39:** Emulsification to create polymer microparticles

*Surfactant properties*, *drying technique*, *organic/aqueous phase ratios*, and *polymer concentration* are among the known factors that exert influence on microparticle distribution. However, these variables confound each other's effects on yield. For example oil could create barriers to the underlying mechanisms of emulsion; including barriers to droplet interface coating and ultimately instability leading to large and deformed particles; unless counteracted by increases in surfactant [Dapčević Hadnađev et al., 2013]. The optical micrographs below are from a preliminary study, showing the droplet distribution of 1% and 3% surfactant (w/v) in an

emulsion created using a 3:1 oil:water ratio (each upper image is magnified by 10x the lower). Recently there has been a lot of focus on manipulating surface tension between the oil and water interfaces, as this is where the control over stability can be most influenced. Larger droplets, and thus particles, can often occur in stable emulsions, as these droplets disrupt less frequently [Clay et al., 2004; Weheliye et al., 2016]. There is a clear ability to control the droplet distribution, however the sensitivity of the interfacial tension to many environmental and process variables render emulsification a more variable and uncontrollable fabrication technique for delivery systems [Dahiya et al., 2016].
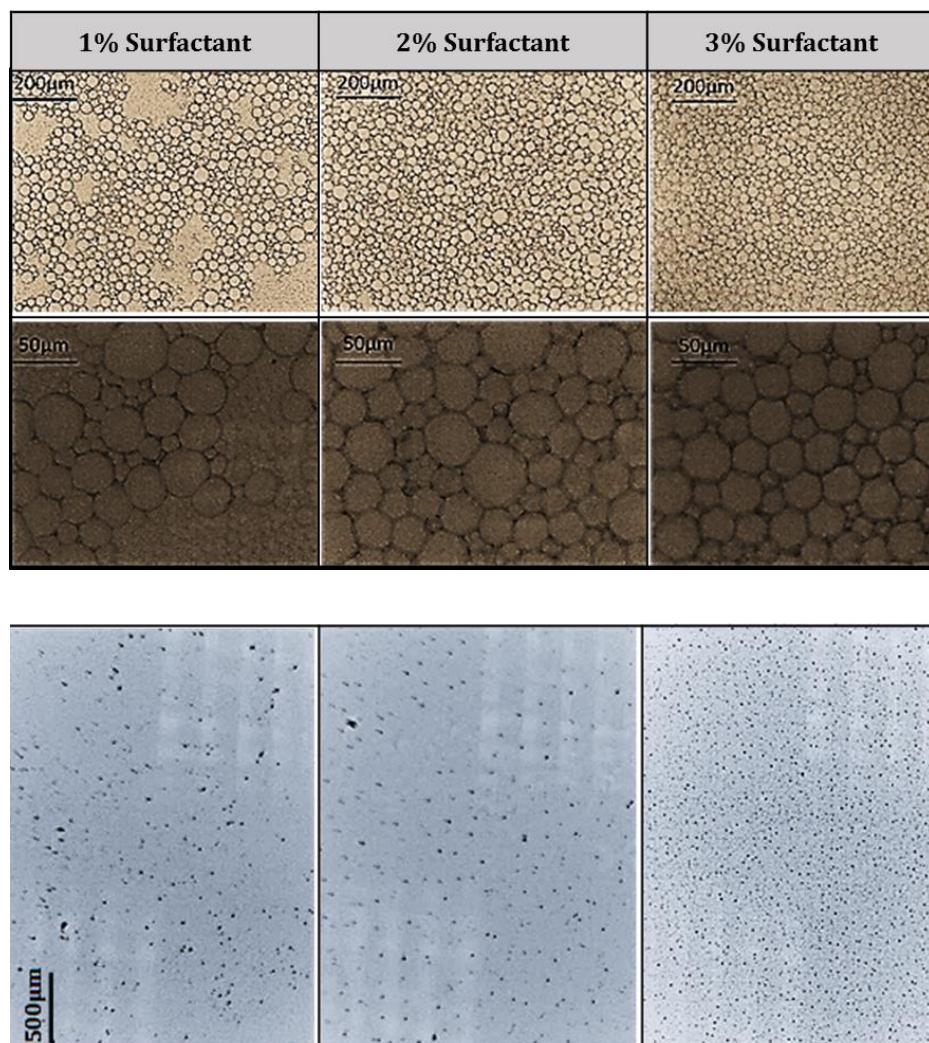


**Figure 2.40**: Oil:water emulsion after 24 hours air-drying, containing 1, 2 or 3% surfactant. Droplets were created using oil:water ratio 3:1. Greater uniformity in droplet size and shape was observed using the higher surfactant concentration

Alginate has frequently been employed in emulsification for drug delivery system fabrication, offering competitive biocompatibility, versatility and strength beneficial for drug delivery [Lupo et al., 2014; Funami et al., 2009]. Alginate particles are typically prepared by dripping aqueous

*Novelty processing and smart delivery of Ganoderma Lucidum spores*

alginate solution into a calcium chloride bath for gelation, however alginate emulsions are also often prepared via traditional oil and water emulsification followed by external gelation using a source of multivalent cations like calcium chloride. There is limited success with the emulsification of uniform alginate microparticles without exposure to degradative mechanical conditions that could encapsulated biomolecules – high shear and temperature for example, or chemical modification such as solvent exchange [Reis et al., 2006]. This is a result of alginate's viscosity and its rapid and spontaneous crosslinking behaviour when exposed to calcium chloride [Rajaonarivony et al., 1993]. A study in 2012 observed that nanoparticles averaging 50-80nm could be achieved using phase inversion temperature (PIT) emulsification, in order to capitalise on its temperature dependence (figure 2.41) [Machado et al., 2012]. The particles created using 1% (left) 1.5% (right) alginate is shown via the black arrows. This process creates a high degree of frost represented by the smaller arrows.
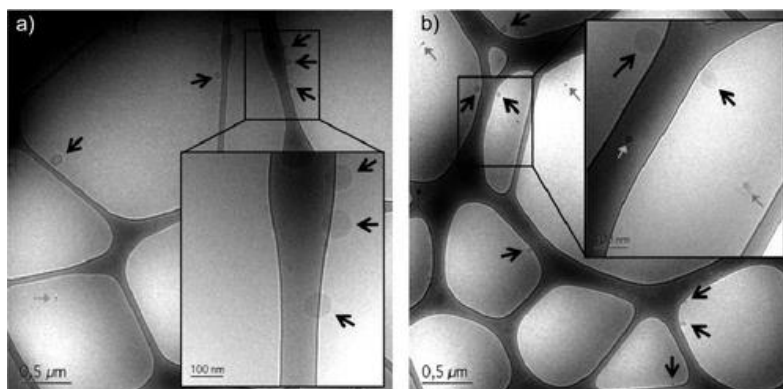


**Figure 2.41:** Cryo-TEM images of the particles prepared in nanoemulsions initially containing 1 wt % (a) or 1.5 wt % (b) alginate in the aqueous phase. The large black arrows indicate the particles [Machado et al., 2012]

To date alginate particles prepared via emulsification have typically been polydispersed with irregular surface features and a low drug-loading capacity [Heng et al., 2003; Ahmed et al., 2013]. By modifying the alginate, many of its advantages as a drug delivery material are sacrificed; in particular biocompatibility and flexibility.

Internal gelation has been employed in the fabrication of polymer particles to combat the uncontrollable spontaneous crosslinking induced by calcium chloride (as this source of calcium ions releases rapidly to instantly fix hydrogel shape and size). $CaCO_3$ is dispersed in the alginate phase prior to its emulsification after which a glacial acetic acid is added to the oil phase in order to release the calcium ions for a slow and gradual crosslinking. Using this crosslinking technique

*Novelty processing and smart delivery of Ganoderma Lucidum spores*

also leaves more space for particle growth however, explaining why literature typically sees particles larger than 100-200μm, suggesting a disadvantage compared to calcium chloride, and other methods of particular fabrication; such as EHDA. Importantly, a by-product of $CaCO_3$ crosslinking is carbon dioxide, which subsequently creates a gaseous environment within particle structures and induces porosity. This phenomenon is the root cause of the difference in particle properties when employing these sources of calcium. Indeed, porosity affects the structure's strength, flexibility, and permeability. While porosity could be useful for many biomedical demands like drug-loading, controllable release, and cell adhesion, the pore distribution should be *controlled* which is not the case here. Figure 2.42 shows an example of porosity induced by the by this carbon dioxide in a particle created using emulsification of 2% alginate.
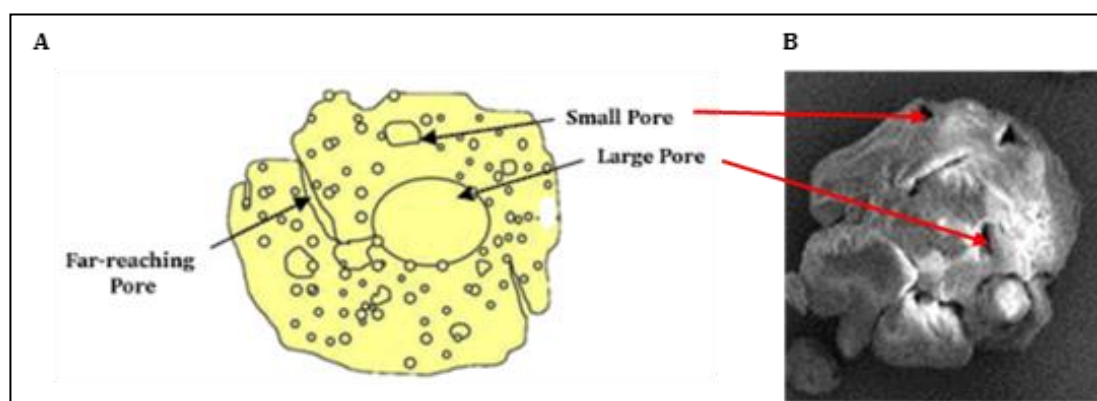


**Figure 2.42:** Effect of porosity on moisture drying-induced stress on an alginate particle after vacuum drying. A) Schematic B) Scanning electron microscopic image

## 2.2.6.2 Microparticle fabrication via *Electrohydrodynamic Atomization (EHDA)*

Fabrication of polymer microparticles by EHDA has the potential to overcome the aforementioned limitations of emulsion-based techniques and has proven capabilities in the production of reproducible loaded nano- and microparticles [Chakraborty et al., 2009]. Physicians William Gilbert and John Zeleny reported that a fluid interface could be manipulated to adopt a conical shape that can subsequently be destabilised to generate a series of droplet disruptions. "Electrospraying" was soon developed into an advanced and successful technique to create small droplets for use as microparticles for drug delivery systems [Taylor et al., 1964; Collins et al., 2008]. The droplets produced are electrically charged at the needle meniscus in the EHDA setup,

and undergo continuous coulomb fission to achieve narrow a small size and shape distributions. EHDA is effective and versatile, and its ability to attain many size requirements (from nanometres to macrometres) renders is useful for many biomedical applications [Jaworek et al., 2007; Yao et al., 2017]. Polymers employed in such an intense fabrication process are typically synthetic, prepared to withstand high electric fields; Polyethylenoxide (PEO) and Poly(lactic-co-glycolic acid) (PLGA) in particular[Stitzel et al., 2000]. However, there remains considerable interest in the use of biopolymers for EHDA.

The morphology and surface geometry of EHDA-fabricated particles have been shown directly and significantly affected by flow rate, applied voltage, polymer concentration, and collector distance in particular, however the process involves many other parameters which have been proven influential [Gao et al., 2016]. The achieved particle features have proven effects on subsequent drug release, with most recent emphasis on the effect of particle shape on controlled release.

### 2.2.6.3 Manipulating EHDA for Particle Distribution *Control*

Controllability of the shape, texture, and size distributions of structures achieved by EHDA can be achieved by varying solution properties as well as process parameters. This level of control does not only facilitate reproducibility, but also desirable release and encapsulation properties. Electrospraying small particles has been found to generate narrow size distributions, with little agglomeration when compared to larger particles [Ganan-Calvo et al., 1997]. When an electric field is applied to a droplet, the electric charge induces an electrostatic force (the Coulomb force) within the droplet. This force will challenge the existing cohesive forces holding the droplet together, succeeding to rupture the droplet into micro- and nano-sized droplets. The electric charge is induced by connecting the solution-filled nozzle to a voltage source, subsequently creating an electric field between the ejecting droplet "meniscus" and the droplet collector. The solution would be subject to electrical tension forces pushing it away from the nozzle, which is counteracted by the surface tension force minimizing the meniscus surface area. As the charge increases, the electrical force eventually surpasses the surface tension and the droplet is extruded from the nozzle, where droplet size will be inversely proportional to voltage [Stitzel et al., 2000; Bock et al., 2012]. Once the droplets pull away from the nozzle, the solvent begins to evaporate, resulting in dense, solid particles moving toward the collection plate. Studies have proven the efficacy of this method in encapsulating hydrophilic and hydrophobic drugs, proteins, antibiotics, and chemotherapeutic drugs using a variety of synthetic and natural polymers [Stitzel et al., 2000]. The generation of electrosprayed particles has been shown to be

governed principally by the strength of solution interfacial tension, solvent evaporation as droplets traverse between the needle and collection surface, and polymer diffusion during particle drying. These mechanisms are functions of voltage, solvent properties, polymer flow rate, spraying distance, and drying method.
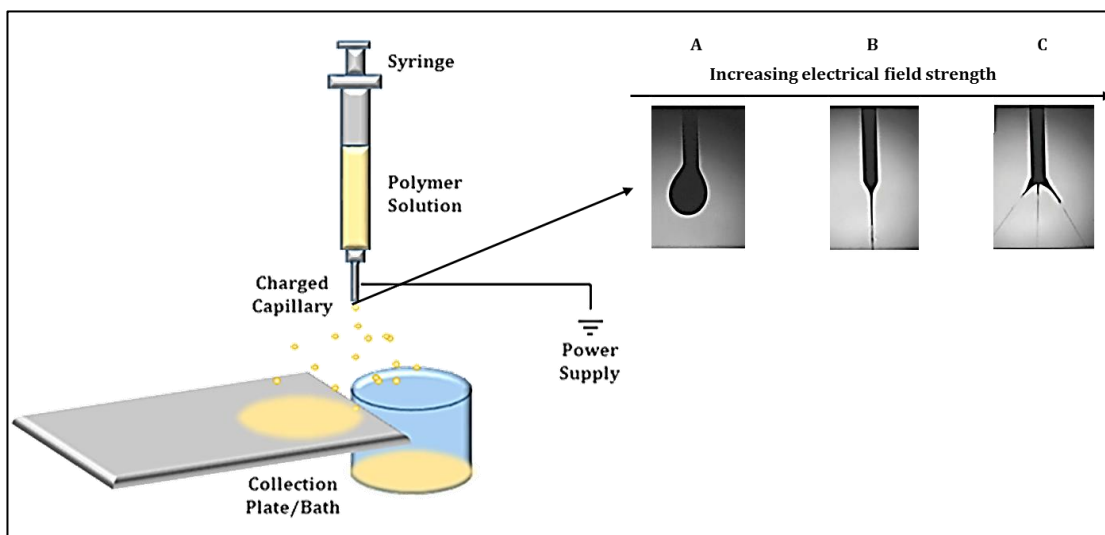


**Figure 2.43:** EHDA setup, and spraying modes typically observed during electrospraying of polymers. A) Dripping mode, B) Cone-Jet mode, C) Multi-jet mode (B and C are both variants of the Taylor cone-jet). Real images show this in practice [Keraliya et al., 2012]

There are typically three modes of droplet generation exhibited during the EHDA process (figure 2.43). Inset images B and C exemplify the cone-jet modes achievable at higher voltages; typically induced by increasing the nozzle charge. The Taylor cone-jet mode is obtained due to electrical stresses that reduce the solution flow radius, deforming the shape at the meniscus. The relationships between process variables and achieved particle features are not clear, and thus EHDA for the fabrication of particles needs to be better understood before it is applied to widespread biomolecule administration employing different biopolymers.

### 2.2.6.3.1 Effects of Voltage and Flow Rate on the EHDA Fabrication of Microparticles

EHDA has been extensively evaluated with respect to its influence on particle distribution fabrication. This includes size, uniformity, shape, and controllability. The two factors consistently observed as most critical on particle distribution are Voltage and Flow-rate.

*Effect of Applied Voltage*

The production of polymer microparticles is heavily affected by applied voltage, with greater voltage inducing greater charge density at the needle meniscus, and thus a higher frequency of successfully solution rupture into offspring particles, continuously. In essence, a higher applied voltage fosters stronger atomisation on the solution, and the meniscus at the needle will become conical – where it is most stable [Tang et al., 1994; Rasekh et al., 2015]. More frequent generation of offspring droplets of course leads to smaller droplets and thus a smaller particle generation. However the effect of voltage has been shown to plateau during EHDA (the level of which depends of other EHDA process parameters such as flow rate and polymer concentration) [Hartman et al., 1998]. Very frequent disruption however can lead to droplets attaining the Rayleigh limit before sufficient entanglement can take place – leading to deformed particle shapes that are also polydispersed [Marijnissen et al., 2009; Gomez-Estaca et al., 2012]. Voltage is a key determinant of stable jetting (usually via the cone-jet mode), where the window of variability in the face of parameter changes elsewhere will be narrowest [Hartman et al., 1998; Rasekh et al., 2015].

*Effect of Solution Flow-Rate*

The flow-rate determines how much polymer solution is extruded, and thus will govern the charge density of the droplets. With greater solution subject to a given voltage, the charge density is lower, and thus the droplet will reach the Rayleigh limit more slowly, and disrupt later. There is an ongoing less frequent droplet rupture, and thus particles are ultimately larger [Rasekh et al., 2015]. One study observed that when electrospraying alginate-curcumin, the effect of voltage was strongly affected by the flow-rate. This is essentially measuring the effect that voltage can have on a larger and larger droplets (higher and higher flow-rate) [Gomez-Estaca et al., 2012].

The process parameters of EHDA are strongly interrelated, and that will not be discussed in detail here given the plethora of combinations studies have individually employed.

## 2.2.6.3.2 Alginate Microparticles via EHDA

Alginate has successfully been processed using EHDA, for the fabrication of nano/microparticles and other shapes (fibres in particular). Many studies on the use of EHDA for drug delivery system fabrication employ *synthetic* polymers like poly(lactic-co-glycolic acid) (PLGA) owing to its biodegradability and FDA approval. Despite this, in the context of drug delivery, PLGA can degrade rapidly and can create an acidic environment during degradation [Sinha et al., 2004]. Because the use of alginate in EHDA is challenging owing to its thermolability,

often the process parameters employed are less energy-intensive (lower voltage for example), and so final particles have traditionally been polydispersed and large. Furthermore, as alginate is non-Newtonian and viscous at usual concentrations (1-3% wt%), the EHDA spraying regime will be dominated by a pulsating jet and/or dripping – implicating a larger particle distribution [Mehregan et al., 2016].

Most studies employing alginate report its dependence on mid-level voltages for a non-disperse generation of microparticles [Moghadam et al., 2010; Ahuja et al., 2011]. This for example will depend on the EHDA process parameters used in parallel. Moghadam et al. investigated the effect of the voltage on alginate nanoparticle fabrication, observing that a change of applied voltage from 4.5 to 6.5 kV would change the spray regime from dripping mode to jet mode of a viscous solution (and thus enhance the production of uniform droplets). The authors reported that 9 kV allowed the production of particles with diameters as small as 400 µm. Particles were mono-sized and spherical [Moghadam et al., 2010]. Another study investigated encapsulation of peppermint oil in alginate-pectin using EHDA. This study actually achieved near-nanometre diameters (1.58 µm), and found that increasing alginate content created a more monodispersed distribution and enhanced encapsulation efficiency increased [Koo et al., 2014]. Park et al. found that alginate particles < 150 µm could be achieved using a low alginate concentration of 0.5 wt% [Park et al., 2012]. Alginate however exhibits a wide range of size and shape distributions when processed via EHDA. For example while a study by prepared alginate microparticles using EHDA and obtained particles with diameters 70.6 µm. Another study could obtain sizes as small as 80 nm [Ghayempour et al., 2013]. These severe inconsistencies are typically attributed to the variations in EHDA process parameters as well as the variants in the alginate solution properties.

The study of EHDA-processed sodium alginate for drug delivery is increasingly exciting, especially as researchers are progressively finding ways to manipulate the biopolymer for carious applications. Unfortunately its use as a carrier for GL biocompound delivery is severely underdeveloped, not only resulting from the lack of understanding of GL biocompounds, but also owing to the inconsistency in recorded relationships between EHDA process parameters and the biocompounds and alginate itself.

## 2.2.7 EHDA for the delivery of GL Biomolecules

To date, there has limited success achieving a controlled distribution of GL-loaded microparticles for physiological administration. Furthermore, the feasibility of efficient techniques is questioned when certain thermolabile biocompounds like polysaccharides are

subject to the intense energy of the process. One study attempted to generate GLS-loaded alginate particles using EHDA, and observed that the particle size can be controlled in the EHDA process mainly by the voltage and the drying technique. The study investigated the release behaviour of the GLS-Alginate particles and observed a pH-dependent release in-vitro, and a dependence on drying method [Zhao et al., 2016]. Particles were not achievable below 400µm in diameter (figure 2.44). A rapid, size-dependent release was observed in neutral-pH conditions smaller beads released up to 50% faster than larger beads (around 2000 µm). The study also found that freeze-dried beads exhibited faster release than air/vacuum-dried beads – and thus were at greater risk of initial bursts in undesirable physiological administration of GL.
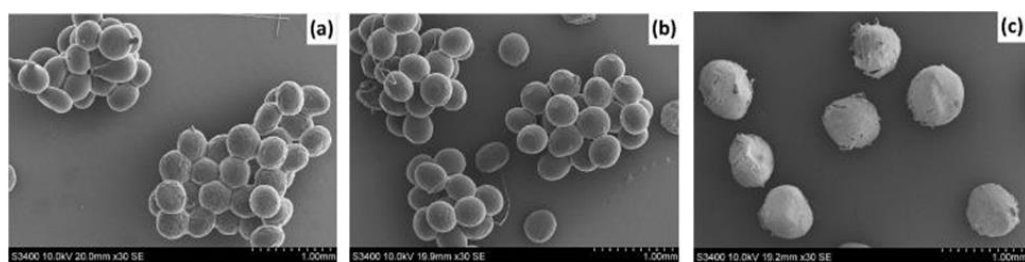


Figure 2.44: EHDA-fabricated GLS particles created at 10kV after a) air-drying b) vacuum-drying, c) freeze-drying [Zhao et al., 2016]

Another recent study was successful in encapsulating GL polysaccharides using EHDA using sodium alginate, and achieved a size distribution range of 225–355 µm [Yao et al., 2017]. The microparticles possessed a drug loading capacity of 23%, finding that 10% w/v crosslinking solution (calcium chloride) was optimal. Quickest release in-vitro was observed in pH-neutral conditions, and the effect of surface roughness (crinkled and porous) on release rate was significant. When droplet collection took place at room temperature, the resulting release rate form particles was slowest – and this actually corresponded to particles which possessed the most "tailed" structures (figure 2.45). Release rate from the alginate-GLP particles was determined as Fickian diffusion. High-temperature collection was associated with rougher surfaces, and less tailed structures - which the authors attributed to the difference in rate of solvent evaporation. This study, whilst insightful, was unable to achieve sufficiently uniform particles once GL polysaccharides were added to the alginate. Furthermore, authors could not achieve a controllable nor sustained release in stimulated intestinal conditions.

*Novelty processing and smart delivery of Ganoderma Lucidum spores*
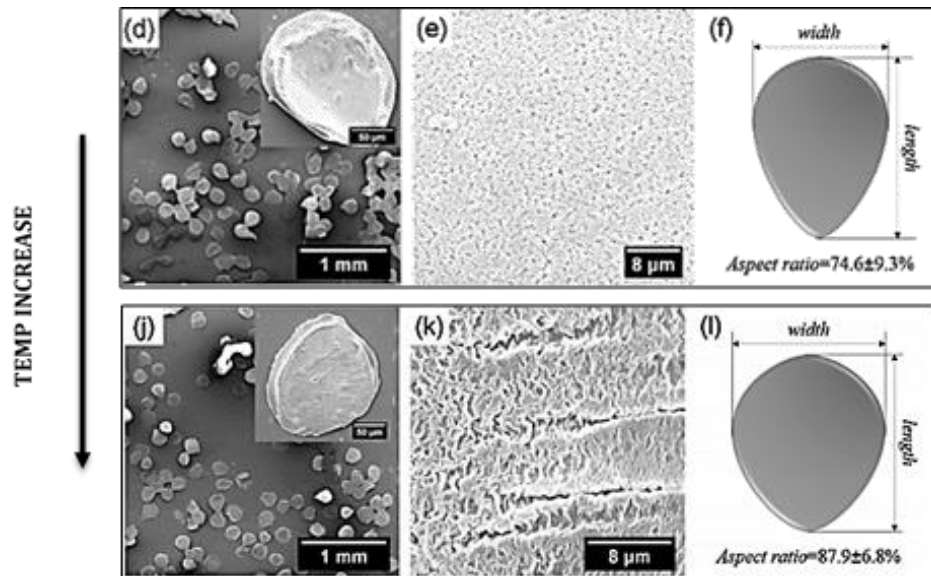
**Figure 2.45:** Impact of EHDA collection temperature on GL-A particles (25°C vs 50°C) [Yao et al., 2017]. Particles were not regularly distributed and showed a collection temperature-dependent release rate and shape

The ongoing challenges presented by the application of EHDA to GL biomolecules have been the minimum size achievable, and the lack of reported impact of process parameters. For example, studies have observed an effect of temperature collection on release rate – however this high-temperature collection exhibited both reduced tailing and a rougher surface [Yao et al., 2017]. Thus, lack of "controls" for these possible confounding variables have resulted in ambiguous relationships across the field.

## 2.2.7.1 The Importance of Polymer Concentration in EHDA Fabrication of Microparticles

Upon dissolving a polymer like alginate in water, its molecules hydrate and the solution gains viscosity. The resulting rotation around the glycosidic linkages in the Guluronic Acid-rich blocks (GG) is hindered resulting in a stiffening of the chain (and thus higher viscosity). Increasing the concentration of the alginate has been shown to affect the crosslinking process through increased binding induced by more Guluronic binding sites [Lin et al., 1969]. Many studies however have showed that increasing polymer concentration in the crosslinking process could decrease crosslinking efficiency through creating an excess pool of uncrosslinked Sodium Alginate with overall physicochemical properties that are undesirable for drug delivery (mainly rapid and uncontrollable drug phase release, known as syneresis) [Augst et al., 2006]. On the other hand, a

*Novelty processing and smart delivery of Ganoderma Lucidum spores*

small quantity of polymer restricts the amount of incorporable drug into each crosslinked entity, thus reducing economic feasibility and increasing physiological invasiveness.

Microparticle fabrication typically aims to provide inhomogeneous release profiles, both from a particle batch *and* at the particle-level. In fact a key parameter in achieving homogeneity at the particle-level is polymer entanglement determined by polymer concentration. While there have been few studies on the influence of alginate concentration in the preparation of GL microparticles specifically, studies have shown the effect of too little polymer of particle integrity during fabrication *and* during drug release [Wu et al., 2008]. Figure 2.46 a-d shows the effect of increase polymer content (PCL) from at 5%, 7.5%, 9%, and to 10% w/v respectively. The authors observed greater particle structural integrity owing to faster solvent evaporation (there is less solvent in a matrix containing more polymer) and a higher degree of polymer entanglement [Gupta et al., 2005]. Too little polymer increased the chance of a polydispersed distribution and irreproducibility as it introduces the presence of localities with high concentration gradients [Bock et al., 2011]. Increasing polymer content however was shown to increases particle size owing to added "bulk", and also by preventing the attainment of the Rayleigh limit with a disentangled structure. By employing more polymer, droplets are better entangled and Coulomb fission takes place less frequently – ultimately leading to larger particles [Almería et al., 2010].
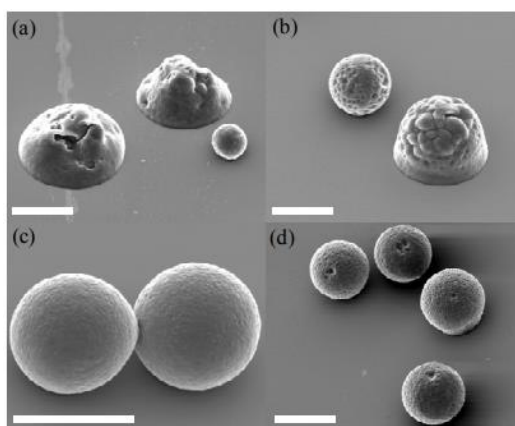


**Figure 2.46:** PCL polymer content in EHDA (a-d increasing PCL). More PCL led to stronger particles that were more spherical owing to greater polymer entanglement and faster solvent evaporation during spraying [Bock et al., 2011]

When determining polymer concentration, studies also factor in the crosslinker:polymer ratio. Indeed, too much polymer cannot be efficiently crosslinked and will lead to "weak spots", whereas too little polymer will lead to unstable release and protection during administration (and before). An alginate:calcium molar ratio between 2:1 and 4:1 has been suggested as optimal [Lin

*Novelty processing and smart delivery of Ganoderma Lucidum spores*

et al., 1969], however there are limited studies into the evaluation of the effect of *molar* ratios on polymer-drug particle fabrication.

By varying polymer content, solution conductivity is also directly affected. This is in fact an instrumental solution characteristic playing a huge part in the efficiency of droplet rupture. This parameter will determine how effective the voltage and flow-rate settings are [Rasekh et al., 2015].

## 2.2.7.2 The importance of Drying Regime on Alginate Particles

Many drying methods have been used to prepare alginate hydrogel particles, all showing a high degree of influence on the particle's physical properties [Czakkel et al., 2005]. Because alginate is particularly sensitive to extreme heat and pressure, the drying stage of its processing is an area of popular research and development. Studies have typically observed freeze-drying to be conducive to a preserved microparticle structure, however alginate typically exhibits weakness following a process like freeze-drying. Furthermore some studies record a decrease in the encapsulated drug content [Sastry et al., 1988; Rodrigo et al., 1998].

Indeed the effects of drying on final particle distributions will depend of particle strength; determined by polymer (material) type and content and crosslinking strength in particular. Owing to the mechanisms driving freeze-drying, alginate particles often develop a distinctive porous structure and avoid the shrinkage typically observed in other drying techniques. Shrinkage of alginate particles has typically been attributed to higher temperatures causing them to "fix" in an amorphous shrunken state. These outcomes subsequently have unique impacts on resulting encapsulation and release profiles. For example a study by Abubakr et al. in 2009 encapsulated vitamin B12 using 2% alginate created suing drop-wise emulsion. The particles underwent freeze/oven/vacuum-drying, revealing shrinkage and cracked surfaces of oven/vacuum-drying only owing to the higher temperatures. Freeze-dried particles were larger (around 810 µm), more porous and rough-surfaced - however exhibited no surface collapse and were most spherical [Abubakr et al., 2009]. The resulting B12 release was slowest from freeze-dried particles. Indeed these findings vary across literature owing to materials engineering and fabrication process. For example a study investigating the impact of drying method on invertase-encapsulated 1% alginate particles created using a flow-focusing microfluidics device, found that freeze-dried beads were the largest (around 900 µm); yet they were also the least spherical [Santagapita et al., 2011]. Freeze-dried invertase-alginate particles were also smoothest with smaller pores (figure 2.47).

*Novelty processing and smart delivery of Ganoderma Lucidum spores*
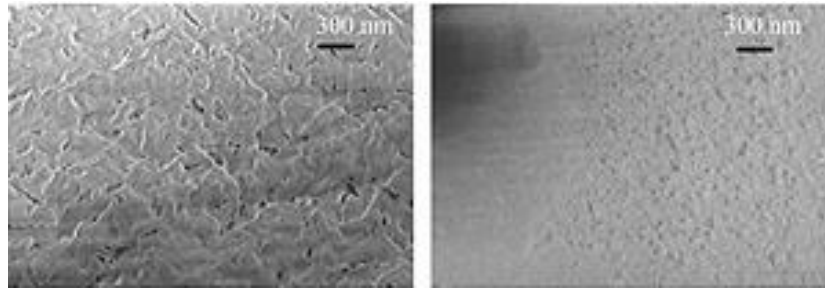
**Figure 2.47:** FEG-SEM images of vacuum-dried (VD, left) and freeze-dried (FD, right) alginate particle surface showing a smoother surface after FD [Santagapita et al., 2011]

Contradicting evidence was reported in a study by Holkem et al. in 2016 which recorded that the intensity of moisture extraction (via sublimation) in a 24h freeze-drying process caused cavities and rough surfaces in 1.5% alginate structures created using emulsification (figure 2.48) [Holkem et al., 2016]. Huang and Fu also created freeze-dried gelatine particles in a 2010 study, observing frequent cavities and wrinkles. Typically authors have attributed these features to the rapid sublimation of frozen moisture from the alginate matrix, leaving behind cavities in place of the ice crystals. The 2016 study by Holkem also indicated particle agglomerates in all the samples.
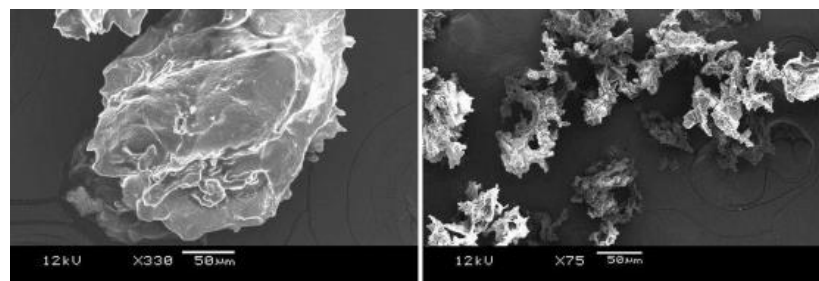


**Figure 2.48:** SEM images of FD alginate microcapsules containing Bifidobacterium BB-12 produced by emulsification/internal gelation [Holkem et al., 2016]

In order to avoid the incorporation of co-materials and chemical modification, the effect of drying on alginate particles requires further understanding. Using emulsification, oven- and vacuum-dried 2% alginate particles in a preliminary study of this project created particles that were mostly spherical and smooth. They were also smallest less polydispersed than freeze-dried particles (figure 2.49). These effects can be attributed to the absence of particle "wear" during freeze-thaw cycles in freeze-drying.

*Novelty processing and smart delivery of Ganoderma Lucidum spores*
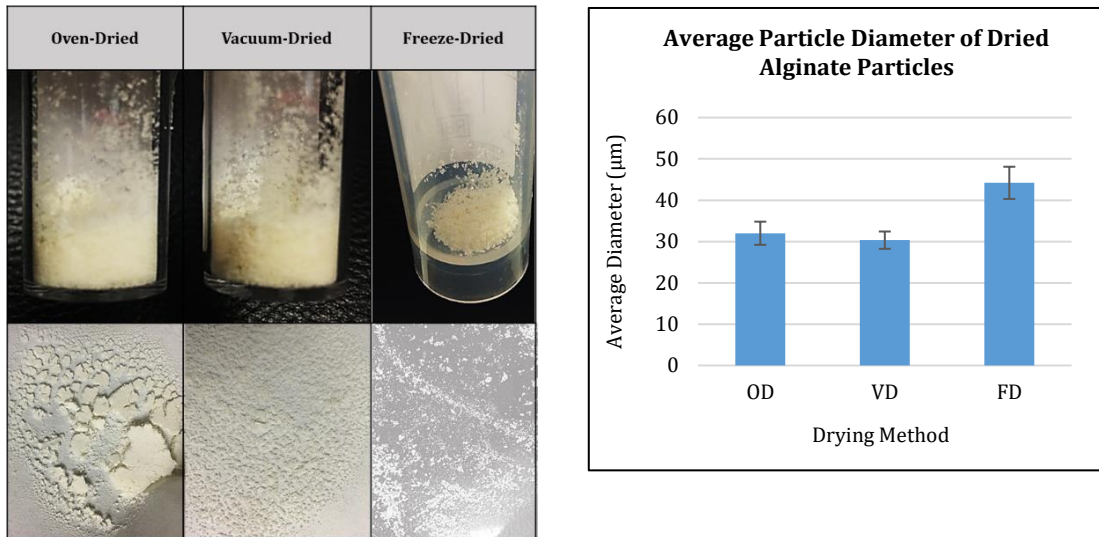
**Figure 2.49:** Dried alginate particles from emulsification and average particle size of dried alginate particles from emulsification ± SE of 30 droplets

Figure 2.50 shows the SEM micrographs of the dried particles in this preliminary study. Figure 2.51 shows a FD particle specifically, wherein the rupture/cavity appears to be a result of matrix "bursting" owing to the pressure/temperature fluctuation in the FD chamber.
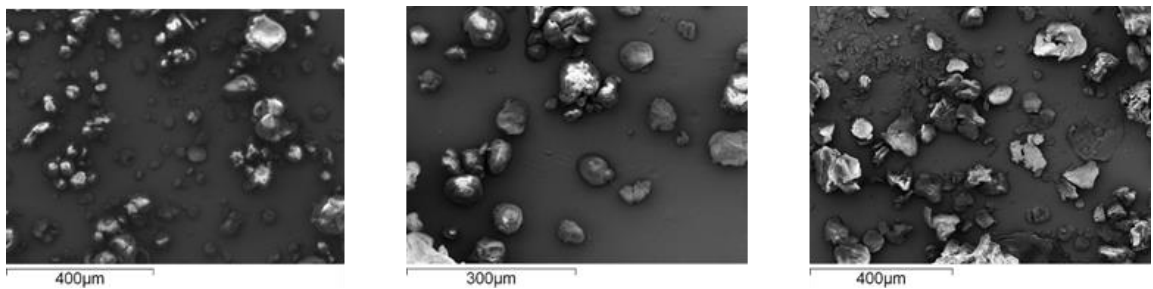


**Figure 2.50:** Dried alginate particles from emulsification following OD, VD, and FD (FEG-SEM)
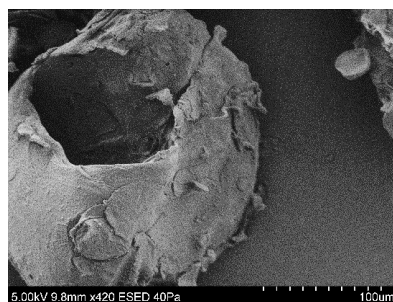


**Figure 2.51:** FEG-SEM of a freeze-dried alginate particle from figure 2.50, showing a rupture during the cyclical wear of freeze-drying

*Novelty processing and smart delivery of Ganoderma Lucidum spores*

Vacuum-drying also allows shrinking to occur, but more freely and less rapidly. The surface of freeze-dried beads appeared rougher, and the structures were more porous [Abubakr et al., 2009]. There was little difference between the size distribution of vacuum-dried and oven-dried alginate microparticles, however freeze-dried microparticles were almost 50% larger – something typically attributed to the crystallisation-induced porosity during the initial freezing process and also suggesting a reduced shrinkage from a lower temperature [Czakkel et al., 2005]. All particles were non-spherical, suggesting moisture *migration* within the pores of the alginate structure, and also the internal porosity causing surface shrinkage and expansion on the same particle [Lee et al., 2004]. When structures undergo drying, the outward migration of moisture from particles is faced by inward-migrating polymer.

## 2.2.8 Creating a Drug Delivery System for GL: Summary

Both EHDA and Emulsification have successfully been used in the creation of microparticles for drug delivery. EHDA is perceived as the superior candidate for the reproducible production of controllable biocompatible entities for GL delivery, alginate as a carrier has typically created larger diameters via EHDA as conditions need to be conducive to this thermolabile polysaccharide. Table 2.10 summarizes the main differences between the two most popular methods for GL encapsulation using alginate.

| | Emulsion | EHDA |
|---|---|---|
| Droplet Formation | Created by immiscible oil-aqueous phase, stabilised by a surfactant | Created by a polymer stream disrupted by a controlled electric field |
| Advantages for GL Encapsulation | Low-intensity processing suitable for fragile GL biomolecules and polymers<br><br>Small Diameters | High-level control and uniformity of the particle distribution |
| Primary Disadvantages | Requires large amounts of toxic chemicals traditionally<br><br>Spherical particles not typical | Intense processing conditions not suitable for many biopolymers and biomolecules<br><br>Spherical particles not typical |
| Typical Size using ~2% Alginate (no co-materials) | 50-500 µm | 300–1000 µm |
| Gelation | Crosslinking of droplets using multivalent ions (external or internal) | |

**Table 2.10:** Emulsification vs. EHDA for microparticle fabrication: Achievable attributes

*Novelty processing and smart delivery of Ganoderma Lucidum spores*

# Summary of Literature and Areas of Potential Development

The present review of literature has critically surveyed and evaluated the processes involved in the development of Ganoderma lucidum (GL) for healthcare. The current focus of literature has lent itself to the *extraction* and *identification* of valuable biocompounds from GL, however their *bioactivities* are typically explored as separate studies. There is little extensive study of the compounds' extraction as well as subsequent bioactivity. Therefore, while existing findings have certainly demonstrated remarkable progress in the field, a lack of understanding of the principally active biocompounds in GL has created limited references from which their processing and pharmacokinetic variables can be evaluated. The result is the absence of "causal" relationships that can be used to commercially develop Ganoderma lucidum for healthcare as it stands.

In parallel to the development of the biocompounds, there is growing demand for advancements in drug administration that facilitate safer and more controlled mechanisms of treatment to ultimately maximise efficacy. There has however been little progress in the development of a delivery matrix that combines controlled/effective treatment, with physiological safety and eco-friendliness. Conclusions drawn from popular fabrication methods like EHDA often fail to elucidate the roles exhibited by all *interplaying* variables, and thus this area of drug development has also resulted in inconsistent recordings and severe gaps in reference methods to extend across this diverse field of study.

The challenges faced by the development of GL treatments, combined with the need to innovate ways to safely and effectively administer its biomolecules, clarifies why this particular Traditional Chinese Medicine has remained "stuck" in development and has thus attracted attention globally.

The principal themes of this literature review are summarized below.

- The Chinese Traditional Medicine *Ganoderma lucidum* was introduced and evaluated with respect to its physiochemical composition

- A detailed evaluation of the literature surrounding certain valuable biomolecules (particularly polysaccharides and triterpenoids) is provided, with respect to their structural conformities, extractability, and proven pharmacokinetics

*Novelty processing and smart delivery of Ganoderma Lucidum spores*

- Methods of extracting these biomolecules were evaluated with respect to yield and bioactivity, and scalability in the face of process variables across various studies

- The prospect of tackling inefficient, ineffective and unsafe treatments with "smart delivery" systems is discussed; in particular with focus on *high-drug* vehicle production and alginate as an encapsulation agent

A major deficit in the development of GL has been the lack of consistent references with which to compare new findings concerning extraction, compound characteristics, and resulting bioactive effects. This has been an unavoidable consequence of variations in strain of such an immature species, but also the experimental protocol employed by various researchers and setups. Valuable biocompounds have been profiled and tested, each demonstrating unique structures and capabilities. For example, there is unanimous conformity of the potent effects exerted by GL biocompound complexes; in particular D-Glucan polysaccharides and Ganoderic Acids. However the physiochemical characteristics of these compounds are variable and thus correlations with therapeutic effects are inconsistent. When engineering a drug delivery system this review highlights substantial obstacles to the development of an alginate-based distribution in light of its conventionally low threshold for more efficient processing conditions, and resulting low-drug/high-polymer requirement. There is particularly limited work around its collaboration with GL biomolecules in the creation of a GL delivery system. Indeed the development of a delivery systems implicates evaluation of many aspects including encapsulation profile, release control/mechanism, physiological integrity, and cell uptake (governed by vehicle distribution characteristics). These are however severely undefined for alginate-based systems, let alone Alginate-GL systems.

## Research objectives

This review has detailed the progress to date in the development of GL in the field of alternative medicine as well as modern mainstream therapy. The extensive review has focused on the advances and challenges in some of the crucial stages of drug development, particularly when concerning a natural source with various inconsistencies. The overall objective of this thesis is to address the challenges and cavities that have hindered the development of Ganoderma lucidum as a healthcare candidate. This includes more targeted identification of useful biocompounds, specific detailed bioactivity assays, and exploring ways GL can effectively be

*Novelty processing and smart delivery of Ganoderma Lucidum spores*

administered. The study will therefore develop a workflow for each of these stages of development of Ganoderma lucidum. Consideration will be given to the scalability of techniques used, in particular with respect to treatment efficacy and safety. With the development of Ganoderma lucidum taking place globally with a variety of strains and processing techniques, investigators have found difficulty in collating and reporting its therapeutic value in a way that is meaningful to designing and validating new studies. The tasks required to achieve the overall objective have led to the specific objectives outlined below.

- To extract specific biocompounds, known for their bioactivity, from GL spores (GLS) using conventional methods modified to enhance efficiency with respect to biocompound yield. From reviewing literature, this implicates consideration of extraction conditions like extraction concentration (GL:Solvent), solvent type, and extraction duration. Supervised machine learning will be attempted to investigate complex parameters, particularly as they interact during extraction

- To define the cytotoxicity of the extracted compounds toward cancer cells (Human Osteosarcoma) with respect to extract formulation, dosage and exposure time

- To develop a delivery vehicle using sodium alginate as the main carrier material, which would possess characteristics that render the delivery of GLS efficient, safe and effective. This delivery vehicle would improve on existing drug delivery systems with respect to drug loading capacity, distribution uniformity, tissue adhesion (via surface traits) and controlled release in a physiological environment. This new delivery system will also enhance the bioavailability of GL compounds and control its release over a sustained period of days. It will protect GL biomolecules and negate premature metabolic breakdown

*Novelty processing and smart delivery of Ganoderma Lucidum spores*

# <u>3</u> Materials and Methods

## Introduction

This chapter details the investigative methods and materials used in this project. The literature review revealed the challenges faced in the development GLS as a source of scalable pharmaceutical compounds, revealing the typical obstacles faced by most natural organisms at their primary stage of development. Findings in literature continue to be based upon an inconsistent and undefined GLS species, resulting in a "mixed bag" of *best practice* with insufficient standards to follow when optimising its development as a commercial treatment. Subsequently, ambiguity exists among the biocompounds as they remain both chemically and bioactively uncharacterised - providing little foundation to foster further compelling research. In light of this, the foundations of the investigations presented here in Chapter 3 are based on piecing together an abstract puzzle that fuses together crucial aspects of successful drug discovery.

In this chapter, GLS is first evaluated with respect to its processability and bioactivity, so that the biocompounds can be evaluated for their candidacy as novel cancer treatments. In GLS, the proven potent biomolecules are polysaccharides (principally D-Glucans) and triterpenoids (to date, typically identified as Ganoderic Acids), which have conventionally been extracted using variants of hot-solvent or ultrasonic extraction [Hsu et al., 2001; Roselló-Soto et al., 2016]. Here, both extraction methods are assessed with respect to polysaccharide yield (GLPS). Hot water extraction is chosen to further streamline with respect to its yield of a novel complex containing both polysaccharides and Ganoderic Acid (termed PSGA), using supervised machine learning to optimise yield. The bioactivity of extracted yields is determined via an in-vitro antitumour assay. Thus, for the first time, crude GLS extracts from the established setups are compared with respect to their bioactivity. It is acknowledged that in-vitro tests do not harness the functions of the human body in-vivo, however they still provide a useful indication of drug potency with respect to the compounds tested as well as the processes used to fabricate them [Katt et al., 2016; Mengus et al., 2017].

Next, this work attempts to create a delivery vehicle to controllably deliver GLS biomolecules safely and effectively. Sodium alginate is presented as a unique delivery system candidate owing to its biocompatibility, bioavailability, and flexibility. However its integrity when subject to Electrohydrodynamic Atomisation (EHDA) processing needs considerable development owing to its established instability and resulting unpredictable/uncontrolled release profile during

physiological colonisation [Murata et al., 1993; Augst et al., 2006]. For the first time, a controllable alginate-based delivery system is attempted to encapsulate and release GLS using EHDA, without the employment of copolymers of material "aids" during processing. The simultaneous challenge of maximising drug loading capacity, especially in the face of physiological and storage environments that demand a strong polymer matrix, is addressed in this study. Consideration is given to the shape, size, and surface topology, of the delivery vehicle developed, and the GLS release is evaluated with respect to processing parameters.

**Sections 3.1 and 3.2** outline the materials and standard procedures, *and these are further detailed in each subsection of section 3.3.* **Section 3.3** provides all experimental details. **Section 3.3.1** explores conventional Hot Water Extraction (HWE) and Ultrasound-Assisted Extraction (UAE) for the extraction of crude polysaccharides (GLPS) from Ganoderma lucidum Spores. **Section 3.3.2** evaluates the extraction of a novel "complex" of GLPS and Ganoderic Acid, referred to as Polysaccharide-Ganoderic Acid (PSGA) using HWE. **Section 3.3.3** details the in-vitro culture of the crude GLPS and PSGA extracts with Human Osteosarcoma cells, to gauge the viability of cancer cells when exposed to both extracts. **Section 3.3.4** focuses on the fabrication of a safe and effective delivery and encapsulation vehicle for GLS using Electrohydrodynamic Atomisation (EHDA).

# 3.1 Materials

Section 3.1 describes all employed materials specific the forthcoming methodological setups (detailed subsequently in 3.2).

## 3.1.1 Extraction of GLS Compounds

In all investigations dried and ground GLS cultivated on wood-log were provided by the province Long Quan and had previously undergone physical grinding for sporoderm breakage. The focus of this work is *broken* spores, as preliminary investigations suggested that GL broken spores possess greater compound extractability than GL fruiting body and *unbroken* spores. Indeed many published studies attribute this to the barrier presented by chitin spore walls of unbroken samples [Su et al., 1997]. This however is still an area of controversy, as they therefore

*Novelty processing and smart delivery of Ganoderma Lucidum spores*

also require less processing to yield the biocompounds – possibly resulting in more active biocompounds [Heleno et al., 2012; Yue et al., 2008; Zhu et al., 2019]. Distilled water and 99% Absolute ethanol ($C_2H_5OH$, viscosity 1.3 cps, Sigma Aldrich UK) were used for GLS extraction. Phenol and concentrated Sulphuric Acid (≥96% and 99% respectively, Sigma Aldrich UK) were used for polysaccharide characterisation, while spectroscopy-grade methanol ($CH_3OH$, Sigma Aldrich UK) was used to characterise the Polysaccharide-Ganoderic Acid (PSGA) complex. For the calibration of D-Glucan quantification in the GPS extracts, D-(+)-Glucose ($C_6H_{12}O_6$, Sigma Aldrich UK) was used. All extraction reagents were of analytical grade.

## 3.1.2 In-vitro Cancer Inhibition

All materials employed in cell culture were obtained from Sigma Aldrich, UK. Adherent cell line Human Osteosarcoma (HOS) was cultured in Dulbecco's Modified Eagle's Medium (DMEM) containing 10% foetal calf serum (FCS), 5% of HEPES, 1% Minimal essential medium (MEM), 20 mM L-glutamines, 100 units/ml penicillin, 0.1 mg/ml streptomycin and 15% L-ascorbic acid. The medium was incubated in a humidified atmosphere with 5% $CO_2$ at 37°C before each assay. Tetrazolium dye MTT 3-(4,5-dimethylthiazol-2-yl)-2,5-diphenyltetrazolium bromide was used for to assess the viability of cells treated with the extracts in-vitro. Phosphate buffered saline (PBS, BioPerformance certified for cell culture) and dimethysulfoxide (DMSO) were employed in the viability assay.

## 3.1.3 GLS Delivery Preparation (Encapsulation)

GLS-Alginate (GLS-A) microparticles were fabricated using Electrohydrodynamic Atomisation (EHDA) to encapsulate crude GLS. The synergistic effects of GLS compounds working *together* have been shown therapeutically effective, and so a cruder extract was deemed a better candidate for health – thus, this was used as the basis of GLS-A microparticles [Zhang et al., 2003].

### GLS-A suspensions

### Sodium Alginate

Sodium Alginate ("alginate") was chosen as the biopolymer to encapsulate GLS. Alginate has a unique ability to form a biocompatible matrix for the entrapment and delivery of cells, drugs and

*Novelty processing and smart delivery of Ganoderma Lucidum spores*

proteins. Alginate is present in algae cell walls as calcium, magnesium and sodium salts of alginic acid. As calcium and magnesium salts don't dissolve in water, alginate salts are converted to sodium salt, and alginate is recovered to a hydrophilic powder available as lab-grade sodium Salt Alginic Acid.

Low-viscosity alginate derived from *Macrocystitis Pyrifera* (A2158, Sigma Aldrich UK: 8 cps for 1% w/v at room temperature) was used for all microparticle fabrication in hereafter, with a Mannuronic/Guluronic Acid ratio of 1.67 and a molecular weight of ~50,000 g/mol at 25°C in water. Alginate gelation is achieved by the exchange of the sodium ions from guluronic regions of alginate (alginic acid sodium salt) with divalent cations from multivalent cations such as calcium [Quong et al., 1998; Farrés et al., 2014]. An eggbox-like rigid structure results from gelation, and the polymer forms a strong hydrogel capable of providing protection, stability, and controlled biodegradation during physiological administration [Pillai et al., 2001; Mora-Huertas et al., 2010; Abbaszad Rafi et al., 2015; Bušić et al., 2016]. For this alginate strain, the Guluronic Acid molar fraction is 0.39. The biopolymer had a particle size of circa 250 μm while broken GLS particles were 5-6 μm. Calcium Chloride dehydrate was obtained from Sigma Aldrich. All reagents were of analytical grade.

### Crosslinking Agents for GLS-A microparticle gelation

Alginate chelates with multivalent cations to form hydrogels. Calcium Chloride (anhydrous, beads, molecular weight 110.98) was used as the source of $Ca^{2+}$ at concentration 1.5M. To generate these concentrations, solutions were stirred magnetically for at least 30 minutes.

## 3.2 Standard Procedures

3.2 provides a description of the procedures employed, using the materials in 3.1. Each procedure is further detailed in 3.3.

### 3.2.1 Physiochemical Analyses

Materials processed and created in this study are characterised to evaluate the effects and limitations of certain process techniques and conditions – namely *extraction* and

*Novelty processing and smart delivery of Ganoderma Lucidum spores*

*encapsulation*. High Performance Liquid Chromatography (HPLC) is used to characterise GLS prior to any processing. Subsequently, Scanning Electron Microscopy (SEM) and Fourier Transform Infrared Spectroscopy (FTIR) were employed in the evaluation of extraction and encapsulation techniques. The setups are described below.

### 3.2.1.1 High Performance Liquid Chromatography (HPLC)

HPLC is a chromatographic technique which separates sample constituents based on their physiochemical properties (namely polarity) by pumping a pressurized sample mixture through a column. Elution of compounds is based on their interaction with the mobile phase and a UV-Vis spectrometer detects when each bioconstituent is eluted at a specific wavelength [Coskun et al., 2016]. Thus, the resulting chromatogram reveals valuable chemical features of the sample constituents. For many years this type of "fingerprint" chromatography has been employed to monitor the quality of complex Chinese medicines, and HPLC in particular offers high precision and reproducibility [Liang et al., 2013; Jiang et al., 2010].

HPLC was employed initially to chemically **evaluate three strains of intact GLS**, prior to choosing one that would be carried forward in this project. This technique was also used to analyse the **chemical composition of the chosen GLS** (in broken form) extracted in water and ethanol in mild conditions to elucidate the bioconstituents' behaviour in different solvents prior to extraction investigations that included a solvent variable. An evaluation was also carried out on **broken and unbroken counterparts** of the chosen strain to verify the use of broken spores going forward in this project. Understanding the nature of the biocompounds before they undergo more extreme processing is valuable in judging the impact of extraction techniques on the biocompounds.

A Shimadzu HPLC system (Shimadzu Ltd., Kyoto, Japan) connected to a binary pump (LC-10ADvp), system controller (SCL-10Avp), auto-sampler (SIL-10Advp), column oven (CTO-10Asvp), and a photodiode array detector (SPD-M10Avp) were employed to analyse GL spores using an LCsolution software. GLS extracts were separated using a Phenomenex Inc. Kinetex C18 reversed-phase column (4.6 mm × 250 mm 5μm, 100Å) from Phenomenex Inc. (UK), in which the mobile phase was aqueous 0.1% acetic acid (v/v) and acetonitrile at a rate of 0.8 mL/min. The mobile phase was operated at a linear gradient and total runtime was 150 minutes. GLS extracts were filtered through 0.22 μm filters and injected into the system in 50μL aliquots and the system was maintained at 35˚C. The chromatographic peaks were measured at 254 nm. Figure 3.1 shows a schematic of the HPLC setup used to analyse the GLS samples.

*Novelty processing and smart delivery of Ganoderma Lucidum spores*
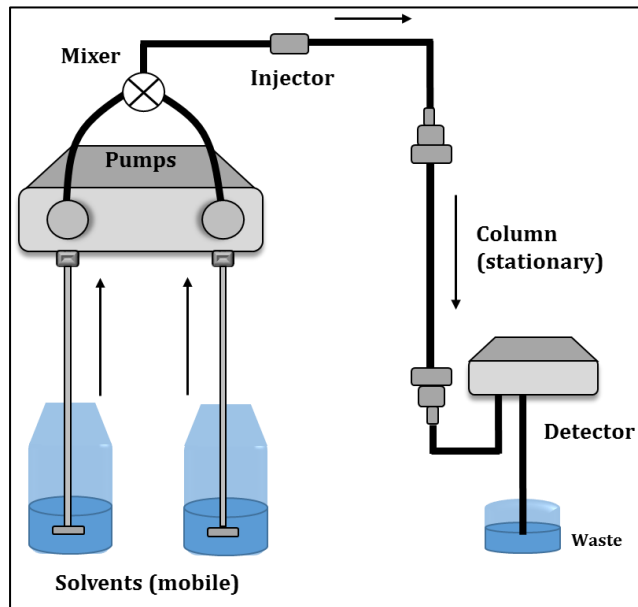
**Figure 3.1:** HLPC Setup schematic

## 3.2.1.2 Scanning Electron Microscopy (SEM)

SEM evaluates topological features of a material, delivering an evaluation of physical attributes that are useful after a material has been processed [Shaulsky et al., 2017; Costa et al., 2018]. A high-energy electron beam scans the material surface and an electron region (of a few nm) is formed. When compared to light microscopy, resolution is significantly higher owing to the considerable smaller wavelengths of electrons.

For the investigation of **GLS extracts** and **GLS-A delivery particles**, samples were fixed on a stainless steel stub using one-sided carbon tape. Electrical conduction was induced by applying an all-round 1 nm gold coating for 90 seconds (Quorum Q150R ES coating machine, Emitech UK) to avoid deposition puddles. This also improved topographical contrast for high-quality imaging and minimized sample damage from the electron beam. Beam damage is likely in hydrated specimens. As sodium alginate is hygroscopic and thus constantly able to absorb moisture from its surroundings, the examination of GLS-A via SEM introduces the risk of beam damage. This happens as the water molecules are ionized by the electrons, generating hydrogen and hydroxyl radicals that attack the organic material - a process known as radiolysis [Kitching et al., 1998]. Furthermore, polymers can accumulate charge at the surface because of traditionally high-volume resistivity. These electrons cannot be removed and could lead to undesirable contrast in the final image [Gaillard et al., 2004; Orekhov et al., 2017]. For this reason, SEM of polymers like alginate is typically carried out at 5-8kV.

### 3.2.1.2.1 SEM of GLS Extract Yields

Following HWE, the spores were physically examined via SEM to gauge the physical effects of the extraction methods on the structure of broken GLS. A high-resolution Cambridge Instruments 240 Stereoscan microscope offered intricate imaging of spores following PSGA extraction. A working distance of 7mm was maintained between the electron beam and sample, and acceleration voltage was 10kV.

### 3.2.1.2.2 SEM of GLS-A Microparticles

Following EHDA processing, the distribution and surface topography of dried GLS-A microparticles were analysed using a Hitachi S-3400N scanning electron microscope equipped with a fully eucentric stage and an electron gun with Variable Quad Bian Circuitry and a SE Accelerator Plate. A working distance of 4 mm was maintained between the electron beam and sample, and the acceleration voltage was 5kV. GLS leaching from particles was also evaluated and employed a Cambridge Instruments 240 Stereoscan microscope for more intricate imaging. In this setup a working distance of 7mm was maintained between the electron beam and sample, with an acceleration voltage of 10kV.

## 3.2.1.3 Fourier Transform Infrared Spectroscopy (FTIR)

FTIR was employed to evaluate **PSGA extracts** and **GLS-A microparticles**. FTIR spectroscopy is a powerful tool for structural analyses of biological materials containing complex and numerous biomolecules that absorb frequencies of light to reveal important chemical properties [Jackson et al., 1995; Schmitt et al., 1998]. This technique has been widely employed to analyse the chemical composition of Ganoderma lucidum and is based on established configurations of glycosidic linkages in GL Glucans and proteins. Evaluation of such intra/intermolecular bonds are of particular importance when materials have undergone physically intense processes such as high-temperature extraction or chemical interactions induced by encapsulation techniques [Ahmad et al., 2011; Choong et al., 2012]. For each measurement a Perkin Elmer Spectrum Two IR Spectrometer was employed. The sample was positioned at the centre of on the sample holder, with the detection probe fitted with a flat sapphire anvil and at a force gauge of 85 cNm (adjusted to slightly higher when smaller microparticles were analysed). A Golden Gate high-performance single reflection monolithic diamond ATR ensured high resolution. The spectra were collected over 4000-800 cm$^{-1}$ with spectral resolution 4 cm$^{-1}$ and each spectrum cumulated 64 scans. Before each spectrum was recorded, the background was corrected by scanning the unloaded diamond anvil to eliminate disturbance by water and air.

### 3.2.1.3.1 FTIR for the Examination of PSGA Extracts

FTIR was carried out on freeze-dried PSGA extracts to identify differences in structural degradation indicated by the extract's chemical composition resulting from the different extraction conditions. Biocompounds from GL have successfully been evaluated using FTIR, verifying the presence of polysaccharides and triterpenoids using specific bands of absorbance indicating their affinity to the D-Glucan and Ganoderic Acid classes, respectively [Ai-lati et al., 2017; Ma et al., 2018]. This has allowed for a more systematic understanding of causal effects attributed to certain bioconstituents of GL [Li et al., 2018].

### 3.2.1.3.2 FTIR for the Examination of GLS-A Microparticles

FTIR has also proven its potency in depicting the interaction between materials via its chemical constituents [El-Houssiny et al., 2016]. For example, a disappearance or emergence of FTIR peaks from the microparticle when compared to its individual components would indicate an interaction between GLS and alginate. FTIR was therefore also used to characterise GLS and Alginate prior to encapsulation, so that inferences could be made regarding the chemical interactions after particle fabrication. Indeed, the interactions between a drug delivery system's materials are important so that effects on delivery can be characterised. The evaluation demonstrated effects of EHDA parameters and drying on GLS-A particles.

### 3.2.1.4 Ultraviolet-Visible Spectroscopy (UV-Vis)

Chemical compounds can be detected in the UV-Vis spectrum based on their unique capacities to absorb specific wavelengths of light – indicating the presence of the specific compound(s). The detailed mechanisms behind this technique were presented in chapter 2 (specifically, 2.1.6.2.4). UV-Vis spectroscopy has been used frequently to characterise the chemical composition of GL extracts, with many studies establishing a high D-Glucan content in particular [Ai-lati et al., 2017; Li et al., 2018]. Its success however has been limited by the lack of references of biocompound structures in GLS, as well as the low selectivity of UV-Vis spectroscopy when evaluating materials with a high degree of chemical similarity between its structural conformations (as is the case with GL polysaccharides and triterpenoids) [Askin et al., 2008; Ma et al., 2018]. A calibration is typically created when quantifying a specific compound in a sample, whereby the pure target compound is used to build a graph displaying various concentrations that can later be representative of the sample's compound concentration.

*Novelty processing and smart delivery of Ganoderma Lucidum spores*

### 3.2.1.4.1 UV-Vis to Characterise GLS Extracts

As part of GLPS characterisation, the **concentration of D-Glucan polysaccharides** from HW and UA extraction were detected using a Perkin Elmer Lambda 20 UV VIS Spectrophotometer following hydrolysis. Interference was minimized through evasion of contamination and careful analyte placement to omit air. The **concentration of PSGA** from extraction was detected using a Synergy H1 Multi-mode UV microplate reader (BioTek instruments), without hydrolysis. This is because the richer and more diverse pool of compounds requires less specific hydrolysis and detection. This system contains monochromator optics that use a third-generation quadruple grating design to allow working at any excitation or emission wavelength for precise readings.

### 3.2.1.4.2 UV-Vis to Evaluate GLS Release from GLS-A Microparticles

**The release of GLS** from GLS-A microparticles was detected using a Synergy H1 Multi-mode UV microplate reader (BioTek instruments) to evaluate the release pattern of GLS in distilled water. Release of GLS from the GLS-A matrix was investigated as a measure of crosslinking strength and polymer integrity, thus indicating the efficacy and efficiency of a GLS-Alginate drug delivery system. The ability of a drug delivery system to control its release is invaluable to effective and safe treatment. Its encapsulation efficiency can be indirectly indicated by release rate [Blanco et al., 1998; Da et al., 2012]. Release rate is therefore a crucial tool in delivery system characterisation. The release environment was kept constant throughout the release investigation by replenishment after reading. This setup is detailed in section 3.3.

### 3.2.1.5 Optical Microscopy of GLS-A Microparticles

A Leica DM 1000 light microscope was employed for optical microscopy at various stages throughout the fabrication of GLS-A microparticles. This technique employs a white light to provide a basic yet intuitive visual of microparticle distribution and structure. Microparticle distributions were subsequently evaluated following EHDA, and Image-J software was used to analyse microparticle dimensions and characteristics (presented in section 3.3.4).

### 3.2.1.6 Liquid Chromatography Mass Spectrometry (LCMS) for GLS Extract Characterisation

LCMS is effective in combining information of peak detection and peak identification, in order to distinguish co-eluting compounds that have distinct molecular weights. This information can then classify compounds more accurately [De et al., 2007; Makadia et al., 2011]. In LCMS, the

atoms of a material's elements are ionized positively by the removal of electrons, and then accelerated to all have the same kinetic energy. A magnetic field will then "deflect" the ions to a degree dependent on their weight (further if the ion is more positively charged it is more easily deflected), and thus provide insight into the size (and perhaps isotopes) of the ions. The deflected ions are then detected by the spectrometer and shown on a chromatogram against the retention time [Dubbels et al., 1995]. Assuming that the ions all have a charge of 1+, the output would also include a spectrum collected in the ultraviolet light region showing the abundance of the ions of each mass/charge ratio. Negative ionization was also considered, and so this mode was also carried out. As the PSGA extract is not a single element but rather a multi-compound material containing isomeric molecules such as sterols the different m/z distinctions may well represent "fragments" of the same ion which could be created after ionisation due to the lack of ion stability [Covey et al., 1986; Kikuchi et al., 1986; Fabre et al., 2001; Moco et al., 2006]. The tallest peak in the spectrum (the base peak) represents the commonest fragment ion to be formed (usually summed over a specific retention time period). The height of this peak can result from either particularly high ion stability, or the prevalence of a particular ion (and its fragments) in the material [Kikuchi et al., 1986].

For PSGA characterisation, the difference in mass distribution resulting from the increased extraction time was sought. Freeze-dried yields of the extraction's shortest and longest time (40 minutes and 100 minutes) were subject to LCMS to evaluate the effect of HWE time on the PSGA structure. 1mg/ml PSGA concentrations were centrifuged for 15 seconds at 13,000 RPM in preparation or LCMS. LCMS was operated on a Shimadzhu Prominence UFLC System with DAD, equipped with an ESI source. The wavelengths tested were 254 and 280nm. The temperature was set to 40°C and the nebulising gas flow was set at 1.5 L/min and the drying gas flow to 15 L/min. The capillary voltage and extractor voltage were 0.75kV and 3V respectively. The molecular weight of GA (570g/mol) was analysed.

### 3.2.2 In-Vitro Cell Culture

Cell administration was carried out to verify the cancer inhibition capacity of yields obtained in the form of both GLPS and PSGA. Osteosarcoma (OS) is the most common type of primary tumour (the underlying bone is normal) that develops in the bone. Although standard chemotherapy has significantly improved long-term survival over the past few decades, the outcome for those patients with metastatic or recurrent OS remains dismally poor and, therefore, novel agents and treatment regimens are urgently required. Research has shown that this cell

line develops a resistance to conventional chemotherapeutic agents owing to the emergence of cancer stem cells (CSCs) that have progenitor properties that induce a strong resistance to treatment (and are thus accountable for the common relapse and metastasis observed in HOS patients).

In both extract administrations, a standard procedure was followed and variations were made only to dosing and cell plating volume (detailed later in section 3.3.3). Lyophilised extracts were filtered prior to administration to remove bacterial contamination using a 0.22μm EMD Millipore Millex™-GP Sterile Syringe Filter with PES Membrane. Administration took place in a 96-well plate, and the plate was incubated for 24 hours to ensure attachment prior to treatment. The cell media was changed and the culture was split to induce healthy growth, after which a visible confluence (at least 75% coverage by eye) of attached cells preceded the administration of the extracts. Confluence is shown in figure 3.2. Attachment ability of cells prior to treatment is an indication of a healthy cell population with no pre-dosage bias. In particular for an adherent cell line like HOS, cell contact on the surface attachment to the well surface is instrumental in its behaviour during culture. This is because the adhesion is what facilitates intracellular signal transduction to trigger cellular proliferation and differentiation [Barnes et al. 1984; Jang et al., 2010]. Thus, in order to ascertain the effects of drug treatment, cell attachment to the surface is crucial. Akin to the treatment stage, during the 24h inoculation it is imperative to ensure the wells are not contaminated, not over/under-cultured, have sufficient medium nutrition, and have the correct environmental gas/temperature stability.
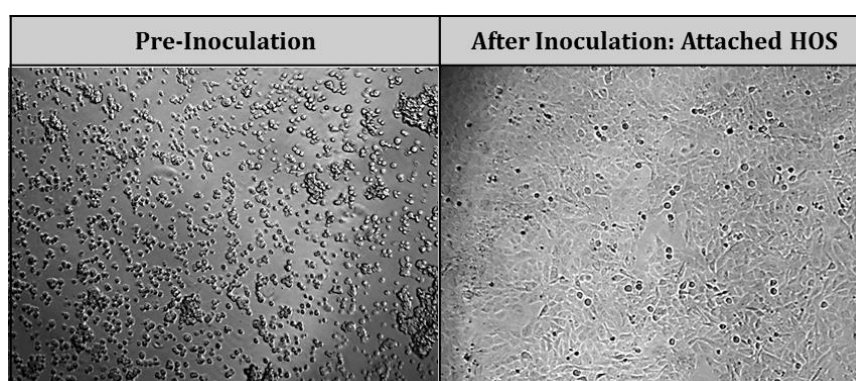


**Figure 3.2:** HOS cells before and after 24h inoculation, where confluence can be seen via attachment

### 3.2.2.1 MTT Assay for Cell Viability

The HOS proliferation was evaluated after 24 and 48 hours of G extract treatment, and was compared to a positive control of 10% ethanol and a non-treated negative control group. Cell

*Novelty processing and smart delivery of Ganoderma Lucidum spores*

viability was measured using the MTT Assay. Tetrazolium dye MTT 3-(4,5-dimethylthiazol-2-yl)-2,5-diphenyltetrazolium bromide indicated the viability assay of cells treated by the PSGA extract in-vitro. Briefly, MTT dye was dissolved in PBS and filtered, before being diluted with DMEM (acid-free) at a ratio of 1:10. After each time point, the cell media was aspirated and 100μl of MTT reagent was substituted into each well for 4 hours in incubation to determine the cellular enzyme activity. Subsequently, the MTT reagent was replaced with 100μl dimethysulfoxide (DMSO) and shaken for 5 minutes in preparation for detection. The MTT reduction by live cells generates formazan, creating a proportionately purple colour that can be read in the UV-Vis spectrum at 570nm. Eqn. 3.1 determines the percentage of treated HOS inhibition in comparison with untreated.

$$\textbf{GLS HOS Cell Viability } (\%) = \frac{\text{Treated HOS Absorbance}}{\text{Untreated HOS Absorbance}} \text{ x } 100 \qquad \textbf{Eqn. 3.1}$$

Cells were cultured for at least 24 hours until confluence prior to extract administration. All extracts were filtered prior to administration. All incubation took place at 37°C subject to 5% $CO_2$.

## 3.2.3 Solution/Material Characterisation

Solution properties were recorded during the experiments which required solution modifications as a variable. In the **extraction** of GLS biomolecules, five *water/ethanol ratios* were used to examine effects on GLPS yield composition. In **GLS encapsulation** EHDA fabrication required different *GLS-Alginate concentrations*. All solutions were prepared at room temperature.

**Solution Polarity** during GLS extraction using water/ethanol mixtures was defined using their dielectric constants from literature. While both solvents are technically polar due to their hydroxyl groups, the *ethyl group* in ethanol is non-polar, and thus ethanol can dissolve both polar *and* non-polar compounds. The effect of extraction solvent on yield composition is an insightful outcome of extraction investigations.

*Novelty processing and smart delivery of Ganoderma Lucidum spores*

**Solution Viscosity** of GLS-A solutions for GLS-A microparticles was important owing to its potential effects on the efficiency of microparticle formation and distribution via the spraying mechanisms of EHDA. Solution viscosities were indicated by the total dissolved solids, measured using a Water Quality Tester Digital Handheld TDS&EC Meter (Sourcingmap, China, 0-9990 PPM).

**Electrical Conductivity (EC)** is an important parameter defining the outcome of EHDA. As the process is based on electrical charge, a more conductive solution is influential on achieving uniform and controlled droplet distributions. Studies have reported that by employing a more conductive solvent in electrospraying, the voltage quantity flowing through the solution is higher, resulting in more rapid disruption and also more effective evaporation [Pillay et al., 2013]. The electrical conductivity of the *GLS-A solutions* was determined using a Water Quality Tester Digital Handheld TDS&EC Meter (Sourcingmap, China, 0-9990 PPM). EC in this study is therefore indicated by the dissolved solids that are ionized in the water. As ions carry the electrical current, EC is proportional to ion concentration (parts per million, PPM). Hence, the more dissolved particles of GLS in the solution the higher the EC will be. PPM will *infer the ion concentration* though total dissolved solids, hence indicating relative conductivity. Microsiemens (μS) is the unit of electrical conductivity (EC) to which PPM can be converted by dividing the PPM value by the average concentration of each ion present: 0.64 (*Lenntech Water Treatment* reports this as average). The electrode was cleaned and dried before measurements were taken, and during measurement the electrode was submerged in solution at room temperature until the recording stabilised. The mean of three consecutive PPM readings was recorded.

### 3.2.3.1 Characterising Water/Ethanol Solutions: GLS Extraction

The nature of extraction solvent can affect the chemical characteristics of yielded compounds; which can affect bioactivity [Sultana et al., 2009; Ghara et al., 2016]. As discussed in Chapter 2 water is typically used to extract neutraceuticals, and has been successful in extracting waster-soluble polar biocompounds in particular (like polysaccharides) from GLS. Organic solvents like ethanol however, are successful in extracting non-polar compounds like triterpenoids. Studies have shown that alcohol concentration is one of the most important factors in the extraction of biocompounds; in particular antioxidants [Zhang et at., 2007; Boeing et al., 2014; Waszkowiak et al., 2016]. Therefore, during GLPS extraction various water/ethanol mixtures were created and the known polarity of their mixtures is indicated in table 3.1. This was obtained from literature [Widmer et al., 1957; Snyder et al., 1974]. Although viscosity was not a variable of interest in this investigation, it was also recorded as it has been shown to impact the efficiency of ultrasonic cavitation [Vinatoru et al., 2001]. Because ethanol-water is a non-ideal

*Novelty processing and smart delivery of Ganoderma Lucidum spores*

mixture, very minor concentration changes can result in drastic modifications in solvent properties. As polysaccharides possess a polar structure, its extraction from GLS is likely to be influenced by the water/ethanol ratio [Sun et al., 2015].

| GLS Extraction | | |
|:---:|:---:|:---:|
| Water:Ethanol | Polarity Index (PI) | Viscosity *millipoise* |
| 100:0 | 9.0 | 8.94 |
| 75:25 | | 20.04 |
| 50:50 | Decreases | 23.54 |
| 25:75 | | 18.66 |
| 0:100 | 5.2 | 10.96 |

**Table 3.1:** Water/Ethanol mixtures for GLS extraction: Solution Polarity and Viscosity measured at 25°C [Snyder et al., 1974]

### 3.2.3.2 Characterising GLS-A Solutions: Electrohydrodynamic Atomization (EHDA)

GLS-Alginate (GLS-A) microparticles were fabricated to provide a platform for GLS administration that fostered high release control, non-toxicity, biodegradability, and uniformity. EHDA was investigated using different GLS-Alginate ratios to ascertain the effect of polymer concentration on microparticle fabrication, and the characterisation of these solutions is presented in table 3.2. GLS-A ratio plays an important role in EHDA fabrication of particles, in particular due to viscosity and also polymer content (and implied particle strength). To more closely analyse which effect is strongest, GLS-A particles containing 2% GLS either contained *2% alginate* or *1% alginate* (GLS:A 1-1 and 2-1 respectively). These ratios are in-keeping with many investigations assessing the impacts of drug:polymer ratios [Kılıçarslan et al., 2003]. This evaluated the effect of alginate content on the same particle. By subsequently reducing the GLS content of the low-alginate GLS-A 2-1 particle, this study investigated whether the same low-polymer effects would hold.

*Novelty processing and smart delivery of Ganoderma Lucidum spores*

| EHDA Fabrication | | | | | |
|---|---|---|---|---|---|
| GLS-Alg | GLS %w/v | Alg %w/v | PPM ± SE | Electrical Conductivity *μS/cm* | Viscosity *millipoise* |
| 1-1 | 2 | 2 | 2,018 ± 8 | 3,153 ± 12.5 | Decreases ↓ |
| 2-1 | 2 | 1 | 2,061 ± 24.5 | 3,220 ± 38.3 | |
| 1-1 | 1 | 1 | 2,063 ± 20 | 3,223 ± 31.3 | |

**Table 3.2:** EHDA fabrication mixtures for GLS-A microparticles: Solution Characterisation. SE indicates standard error of 3 PPM measurements

As a relative comparison, ethanol and distilled deionised water have an EC below 1, and thus these solutions present opportunities to enhance spraying via electrical charge capacity. A slight reduction in conductivity is observed as the solutions become less viscous (more dilute). This is likely because dilution increases ionic mobility of electrolytes in the solutions. Alginate solutions were always prepared independently to GLS solutions before being combined. This ensured that both phases were homogenous prior to encapsulation. The surface tension of the sprayed solutions in EHDA was not recorded, but indicated relatively via the solution viscosity. The physical properties of sodium alginate can vary across batches, and with the addition of GLS in particular, there is no existing record of these solutions' viscosities. As alginate is a polyelectrolyte with an existing high viscosity and conductivity, these characteristics were limiting factors in this study. Thus, a relative indication was deemed sufficient.

## 3.3 Experimental Details

Sections 3.1 and 3.2 provided details of the materials and standard procedures underlying the investigative work presented here in section 3.3 – the **extraction of GLS compounds, HOS cell culture,** and **GLS encapsulation**. The anticipated result is the development of a micro-sized delivery vehicle that exhibits controlled release of more defined crude GLS biomolecules possessing a verified inhibitory effect on human osteosarcoma proliferation.

### 3.3.1 Extracting GL Polysaccharides (GLPS)

Extraction is the first step in the recovery and identification of neutraceuticals. The yield from traditional solvent extraction is largely a function of the extraction solvents and the provision of kinetic energy via heat and/or excitement to foster mass transfer and ultimately compound solubility. Hot solvent extraction is an example of a traditional extraction procedure relying heavily on the efficiency of extraction medium (*solvent*) and time [Lee et al., 2006; Sin et al., 2006; Teo et al., 2010]. Solvent extraction (and variants of this technique) however require long extraction times and high temperatures that can thermally degrade natural products [Lee et al., 2006]. Even then, it suffers from low efficiency [Michalke et al., 2002; Hassas-Roudsari et al., Yu et al., 2015]. A development in the neutraceutical extraction field has appeared in the form of ultrasound-assisted extraction [Vinatoru et al., 1997; Mason et al., 2000; Wu et al., 2001]. Ultrasound energy has been shown to reduce extraction time, solvent requirement, and extraction temperature. This is because of its cavitational impacts that disrupt plant cell walls and facilitate inward/outward penetration [Mason et al., 1996; Wu et al., 2001]. Of course, because the efficiency of ultrasound stems from its acoustic intensity, there is often irreversible degradation to natural structures [Raso et al., 1999; Rahimi et al., 2017]. Because neutraceutical extraction is multi-dimensional with respect to influential variables however, determining the "most efficient" method is a not always relevant, nor practical. The literature review described numerous studies documenting the extraction of GLS using some traditional methods, and there is evidence supporting the efficiency of both solvent extraction and ultrasound-assisted extraction in extracting polysaccharides from GLS [Mason et al., 2000; Wu et al., 2001; Cares et al., 2010] – however it remains an area of intriguing research.

Ethanol and water provide very different extraction environments for GLS constituents and so were tested with respect to their extraction yields. Prior to extraction evaluation, HPLC was employed to characterise the chemical profiles of GLS from cultivation conditions imposed in 3 Chinese provinces - An Hui, Shan Dong or Long Quan (using either sawdust, grain, or woodlog respectively). These were termed GLS "1 – 3" respectively. The chosen strain was then profiled via HPLC, having undergone gentle room-temperature extraction in water vs ethanol so that the chemical profile could be ascertained of this particular sample before extraction processing. For all HPLC experiments, GLS were first immersed in water at 100mg/mL (1:10) at room temperature and underwent continuous rolling for 48 hours in a Thermo Denley Spiramix 10. The GLS was rolled to fineness to ensure constituents could be detected via HPLC, and to provide a better indication of the GLS chemical profiles. The supernatants from this process were centrifuged at 4000 RPM for 10 minutes (Centrifuge 5702, Eppendorf). They were injected in 50μL aliquots after being filtered through a 0.22μm filter (EMD Millipore Millex™-GP Sterile Syringe Filter with PES

*Novelty processing and smart delivery of Ganoderma Lucidum spores*

Membrane). The operating temperature was 35°C and peaks were measured at wavelength of 254 nm for unprocessed GL biocompounds [Hung et al., 2015].

In order to verify the use of broken vs intact GLS, literature was extensively surveyed (see chapter 2) to gauge the chemical differences between the two forms of spores. Broken spores are typically observed to be more yielding (in particular of D-Glucans), even after the sporoderm breakage process – likely owing to advances in breakage technology [Li et al., 2017]. Furthermore, the breakage of the spore walls has produced polysaccharide and triterpenoid yields with greater cytotoxicity toward cancer cells [Zhu et al., 2000]. Reasons could be the molecular weight of its bioconstituents that could have better bioactivity [Sliva et al., 2003; Huang et al., 2006; Xie et al., 2006; Yue et al., 2008; Guo et al., 2009; Che et al., 2017; Na et al., 2017].

In the subsequent studies, the extractability of crude GLPS is investigated using Hot Water Extraction (HWE) and Ultrasound-Assisted Extraction (UAE). The aim of this section is to evaluate these techniques with respect to their yield of GLPS, evaluating effects of **extraction solvent** and **extraction duration** and with further characterisation in the form of the extract's *D-Glucan* content. Extraction via HWE and UAE is driven by dissolution, and typically yields two fractions: a solvent-*soluble* fraction, and a solvent-*insoluble* fraction (essentially the powder of processed spores). Only the extracted fraction (solvent-soluble) is analysed for polysaccharide content, to determine the effect of extraction solvent on its ability to extract GLPS biocompounds. The solvent-insoluble processed spores are not analysed for GLPS content, but are later analysed for its bioactivity in-vitro as there are many claims in literature that these unextracted broken spores are extremely bioactive when *water*-insoluble [Sliva et al., 2003; Camargo et al., 2011]. This is because the insoluble fractions could contain bioactively valuable compounds like triterpenoic Ganoderic Acids, which are less polar and thus less likely to be dissolved in a polar extraction [Ruan et al., 2014; Wei et al., 2015]. Table 3.3 defines the process parameters for HWE and UAE. There was no solvent replenishment throughout extraction.

*Novelty processing and smart delivery of Ganoderma Lucidum spores*

| | Hot Water Extraction | Ultrasound-Assisted Extraction | Solvent-dependent temperature achieved °C | |
| --- | --- | --- | --- | --- |
| | | | HWE | UAE |
| Extract | Polysaccharides (GLPS) | Polysaccharides (GLPS) | | |
| Mechanism | **Kinetic Energy from heat** induces compound dissolution into the extraction solvent | **Mechanical Energy from bubble cavitation** induces compound dissolution into the extraction solvent | | |
| Equipment | Clifton unstirred water bath | Branson Sonifier S-250A Analog Ultrasonic Cell Disruptor / **Probe**: 1/2″ Titanium / **Translated Ultrasonic Output**: 145μm* | | |
| Temperature | 65-75°C | 57-60°C | | |
| GLS content | 2g | 2g | | |
| Vials | Closed | Closed | | |
| GLS:Solvent | 1:20 | | | |
| Extraction Duration | {40,80,120} min | {0.5,20,60} sec/cycle | | |
| Solvent Composition Ratio (W:E) | 100:0 | | 66 – 74.5 | 54.5 – 64.5 |
| | 75:25 | | 65 – 73.5 | 36.5 - 55 |
| | 50:50 | | 66.5 - 73 | 50 - 60 |
| | 25:75 | | 66.5 – 72.5 | 41 – 60.5 |
| | 0:100 | | 65.5 – 71.5 | 40.5 - 61 |

**Table 3.3:** HWE Setup vs UAE setup. Includes temperature range achievable at each solvent composition, detailed in the next section. *Ultrasonic output is measured by the peak-peak distance of the ultrasonic vibration. 145μm is the maximum for this model

*Novelty processing and smart delivery of Ganoderma Lucidum spores*

### 3.3.1.1 HWE for the Extraction GLPS

The HWE setup is illustrated in figure 3.3. A calibrated Clifton unstirred water bath was employed. A Clifton unstirred water bath was preheated to 90°C, providing kinetic energy for enhanced collision between the solvent and GLS particles. This ensured a sample temperature of 65-75°C depending on the solvent and extraction time.
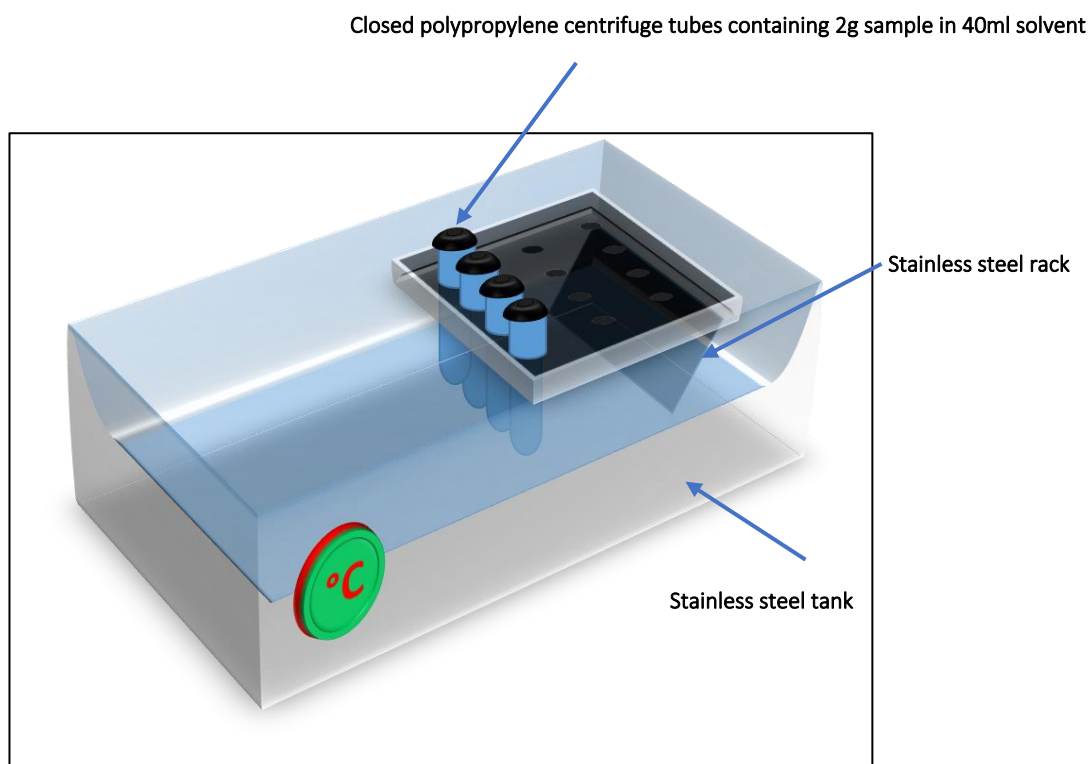


**Figure 3.3:** HWE setup for GLS extraction.

HWE efficiency is based on the rate of particle mass transfer, thus a higher temperature would increase biomolecule extraction rate as a result of increased particle kinetic energy [Chaiklahan et al., 2014]. This study employed a temperature ~70˚C as literature has frequently reported higher polysaccharide yields at this temperature, above which temperature can become detrimental to the yield as well as its structural-induced bioactivity [Benito-Román et al., 2008; Rahar et al., 2011; Lee et al., 2012; Na et al., 2017; Ma et al., 2018]. This is because the thermodynamic stability of the specific triple helix structure attributed to D-Glucan antitumour activity is formed of hydrogen bonds, which are susceptible to breakage at high temperatures [Bao et al., 2002; Femenia et al., 2003; Zeković et al., 2005; Novak et al., 2008; Benito-Román et al., 2016; Hao et al., 2018; Chang et al., 2006; Yan et al., 2014; Chen et al., 2015; Shang et al.,

2018]. While degraded structures have been shown beneficial to compound bioactivity owing to smaller molecular weights, neutraceuticals extracted at 70°C have more consistently shown greater bioactive potency when compared to those extracted at 100°C [Nambi et al., 2016; Su et al., 2017]. Furthermore, high temperatures can actually undesirably foster the extraction of small-molecule impurities that contaminate the extraction yield [Zou et al., 2015]. For example the extraction of starch has also been observed in Glucan extracts extracted at temperatures higher than this. Prior to extraction experiments, preliminary tests were carried out to determine an efficient experimental working range for HWE temperature and time and to subsequently monitor compliance of temperature during extraction (results available in chapter 4). Further preliminary single-factor studies also suggested that a solvent:GLS ratio of 20:1 was favourable to GLS extraction yield; in line with other studies [Ying et al., 2011; Wang et al., 2018; Zhu et al., 2019].

The water bath was filled to a level that completely submerged the solvent level in the vials (40ml). Heat-resistant polypropylene extraction vials containing 2g GLS and solvent were capped after being shaken to homogeneity, and placed in the preheated bath for 40, 70, or 100 minutes. Recording began 10 minutes after vial immersion, as denoted in the control tests described section 3.2.3.3. Capping ensured the extraction process maintained a stable liquid volume and pressure, favouring extraction due to increased solvent density and also increased ability to rupture complex structures [Michel et al., 2001; Yanhua et al., 2014; Sato et al.,, 2017]. Pressures vials can maintain a liquid state at a high temperature [Krieger et al., 2000; Teo et al., 2010]. Therefore even though extraction pressure has been shown to have little effect on *quantity* of yield, it may modify the type of yield obtained. The vapour pressure in the closed vial (known as the saturation pressure of the solvent) was estimated by acknowledging that when the air above a solvent surface is confined, the partial pressure exerted by its molecules increases. Very rapidly the rate at which molecules re-enter via condensation would equal to the rate at which they leave via evaporation. At this equilibrium condition the vapour pressure is at saturation point. At room temperature the vapour's saturated pressure of water is approximately 24 Torr but heating to 75°C, a 12-fold increase in pressure is achieved, resulting in ~290 Torr. Ethanol's saturation pressure starts at 60 Torr, and climbs to 665 Torr after reaching 75°C.

### 3.3.1.2 UAE for the Extraction of GLPS

Temperature tests were carried out to verify an efficient and safe experimental time range in UAE, and to monitor temperature during extraction. These tests indicated that in order to maintain a bioactively friendly temperature, total UAE time is to be limited to 120 seconds for

each 40ml sample. The importance of minimal ultrasonic exposure is in line with previous studies [Ying et al., 2011]. The recordings of temperature compliance are provided in chapter 4.

The GLS solution underwent ultrasound irradiation using a Branson Sonifier S-250A Analog Ultrasonic Cell Disruptor (Danbury, Conn., US), equipped with an ultrasonic probe (diameter 1.3 cm and ultrasonic energy 20 kHz). The probe was directly inserted into the sample vial so that the tip was fully immersed into the GLS solution. This direct sonication was employed to amplify the mechanical impact on large complex polysaccharides, enhancing their dissolution and extraction [Vinatoru et al., 2001; Mason et al., 2000; Wu et al., 2001]. Studies have shown a gain in neutraceutical yield from a higher proximity of the probe to the sample [Saleh et al., 2015]. As UAE cavitation generates heat from the energy released, thermolabile compounds are at risk of being denatured. Consequently, the ice-bath ensured that the extraction temperature was kept at a biologically safe level. It was refreshed for each sample, consistently started at 20°C, and never surpassed 26°C during extraction. UAE GLS samples were extracted in cycles of 0.5, 20, or 60 seconds and rested for 30 seconds between each cycle (the 0.5s cycle was a programme setting on the ultrasound device). The ultrasonic output was maintained at full power (200 watts) at a constant duty cycle [Zhu et al., 2019]. The setup is schematised in figure 3.4, and the variables were stated in table 3.3.
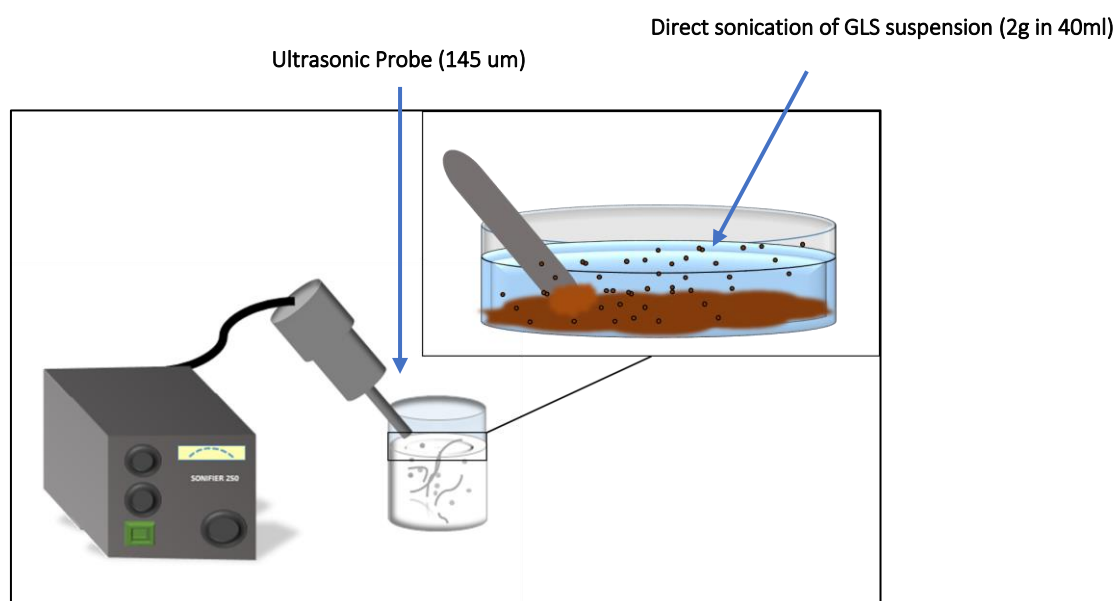


**Figure 3.4:** UAE setup for GLS extraction

### 3.3.1.3 Temperature Monitoring during GLS Extraction

The temperature regulation during a controlled extraction is important to meaningful and repeatable results. As mentioned above, the temperature was recorded for HWE and UAE.

*Novelty processing and smart delivery of Ganoderma Lucidum spores*

The temperature was recorded manually using control solvent vials prior to experimentation. This provided an indication of the compliance of extraction samples during the experimental time. In this way, any anomalous results could be connected to sample temperature.

### 3.3.1.3.1 HWE Temperature Monitoring

Capped vials containing 40ml of solvent *without* GLS were subject to planned extraction time-points, and monitored every 10 minutes. Each sample started off at 21°C, and climbed to 65°C - 66°C after 10 minutes and 74.2°C - 71.5°C after 120 minutes of immersion in a 90°C waterbath. These tests indicated also that approximately 10 minutes is required from vial immersion in the bath, to the attainment of a suitable experimental temperature range. It is assumed that once the sample reaches the maximum temperature achievable in the waterbath, its temperature and volume would not fluctuate given the static conditions in waterbath temperature and the closed vial caps [Krieger et al., 2000; Teo et al., 2008]. This test also showed sample compliance.

### 3.3.1.3.2 UAE Temperature Monitoring

To indicate the temperatures reached by the GLS samples during UAE, vials containing 40ml solvent *without* GLS (as prepared for HWE above) were employed to determine the temperatures reached at each time-point. This did not indicate and additional time to be added to extraction, as in HWE, rather it would showed sample compliance, and also allowed for inferences later on that could correlate yield with temperature. The total UAE time is 2 minutes, and it is expected that longer cycles (60 second cycles) would foster a higher temperature as it limits the sample "cool-down" during extraction. All test samples started at 21°C, and the ice bath was refreshed for each sample, consistently starting at 20°C.

### 3.3.1.4 Yield Measurement: GLPS

Crude GLPS were analysed with the same protocol for HWE and UAE extracts. There is no commercially available "crude polysaccharide" that could provide a precise calibration to quantify the crude GLPS extracted in this particular investigation. Therefore, a dry weight was taken as an indication of crude GLPS. A portion of the supernatant (35ml of the 40ml) was dried in a static oven for 48 hours at 45°C, and the ensuing concentrated extract was ethanol-precipitated to minimise the presence of water-insoluble triterpenoids and other lipids, as well as active proteins which could distort spectroscopic analysis later on (the remaining 5ml would be used to characterise for D-Glucan content of the GLPS extracts) [Choong et al., 2018]. Precipitation involved centrifugation for 10 minutes at 2500 RPM (Centrifuge 5702, Eppendorf),

after which the ethanol was decanted and the solids were frozen in preparation for freeze-drying for 72 hours in a Virtis 2.0 Advantage benchtop freeze-drier. Freezing temperatures have been shown to have insignificant effects on biocompound structure [Krieger et al., 2000; Teo et al., 2008]. Samples were pre-sealed with pierced Bemis Parafilm-M Laboratory Wrapping Film to safeguard the samples as pressure and temperature were varied across the freeze-drying cycle. Freeze-drying was carried out at 100 mTorr (approximately 1/70,000$^{th}$ of atmospheric pressure, or near-vacuum) to enhance the sublimation of the extract moisture. The chamber temperature was maintained at -5°C and the condenser at -70°C. In the absence of oxygen molecules, moisture from the sample will be extracted and drawn towards the condenser plate (*sublimation*). The powder obtained was weighed and expressed as percentage of GLS input (dry wt%, equation 3.2), representing crude polysaccharides.

$$\textbf{Crude polysaccahride Yield }(\%) = \left(\frac{\text{Weighed dry Extract (g)}}{\text{GLS input (g)}}\right) x\ 100 \qquad \textbf{Eqn. 3.2}$$

### 3.3.1.5 GLPS Characterisation via D-Glucan Content

D-Glucan content of the GLPS yield was analysed identically for HWE and UAE extracts. 5ml of the extracted supernatant were analysed via UV-Vis spectroscopy to quantify D-Glucans specifically. A chemical method of detection was required for D-Glucans because the specific class of biocompounds cannot be evaluated using a dry wt% alone. To detect D-Glucans in the UV-Vis spectrum, each GLPS supernatant underwent hydrolysis to transform complex D-Glucans to monomer D-Glucose structures that absorb a known UV wavelength. This hydrolysis process is described in the setups in section 3.2. The wavelength region absorbed by D-Glucose is 485-490nm, and thus this compound is typically associated with absorption peaks in this region [Dubois et al., 1956; Størseth et al., 2005]. At the region 485-490nm in the UV-Vis spectrum D-Glucose absorbs UV-Vis light, and this absorbing activity enables its detection at that wavelength [Dubois et al., 1956]. This wavelength is absorbable by many hexose compounds; however, it was legitimately assumed that D-Glucose is the principal hexose in GLS [Chang et al., 2004]. The spectroscopic readings are then calibrated to the prepared calibration curve to obtain D-Glucose equivalents. The phenol-sulphuric acid assay described by Dubois [Dubois et al., 1956] was used to hydrolyse the complex polysaccharides into detectable monomer forms. In this technique, 1ml of GLPS supernatant extract was incubated at 90°C for 5 minutes with 3ml of concentrated sulphuric acid (18 M) for polysaccharide hydrolysis, and subsequently 1ml of 5% Phenol was added for colour development before the sample was left to stand at room temperature. The

*Novelty processing and smart delivery of Ganoderma Lucidum spores*

absorption spectra across the UV-visible range (400-600nm) were obtained for each sample, along with the specific reading at 485.05nm (insinuating D-Glucan concentration).

### 3.3.1.5.1 D-Glucan Calibration Curve

Pure D-Glucose was used for the calibration so that the sample readings can be converted to pure D-Glucose equivalents. Using the conversion, the sample results indicated D-Glucan content in GLS. A calibration curve of pure D-Glucose was created by hydrolysing concentrations of 0 – 0.7% using the phenol-sulphuric acid assay. Using this pure calibration, the absorbance of the D-Glucose in each sample can be calibrated and thus quantified into D-Glucose equivalents (dry wt %), based on absorbance at 485nm. Using D-Glucose as an indicator of D-Glucans is a common measurement technique in the GL development field. It also facilitates the detection of many D-Glucan configurations that may exist in a sample.

Figure 3.5 outlines the extraction procedure.
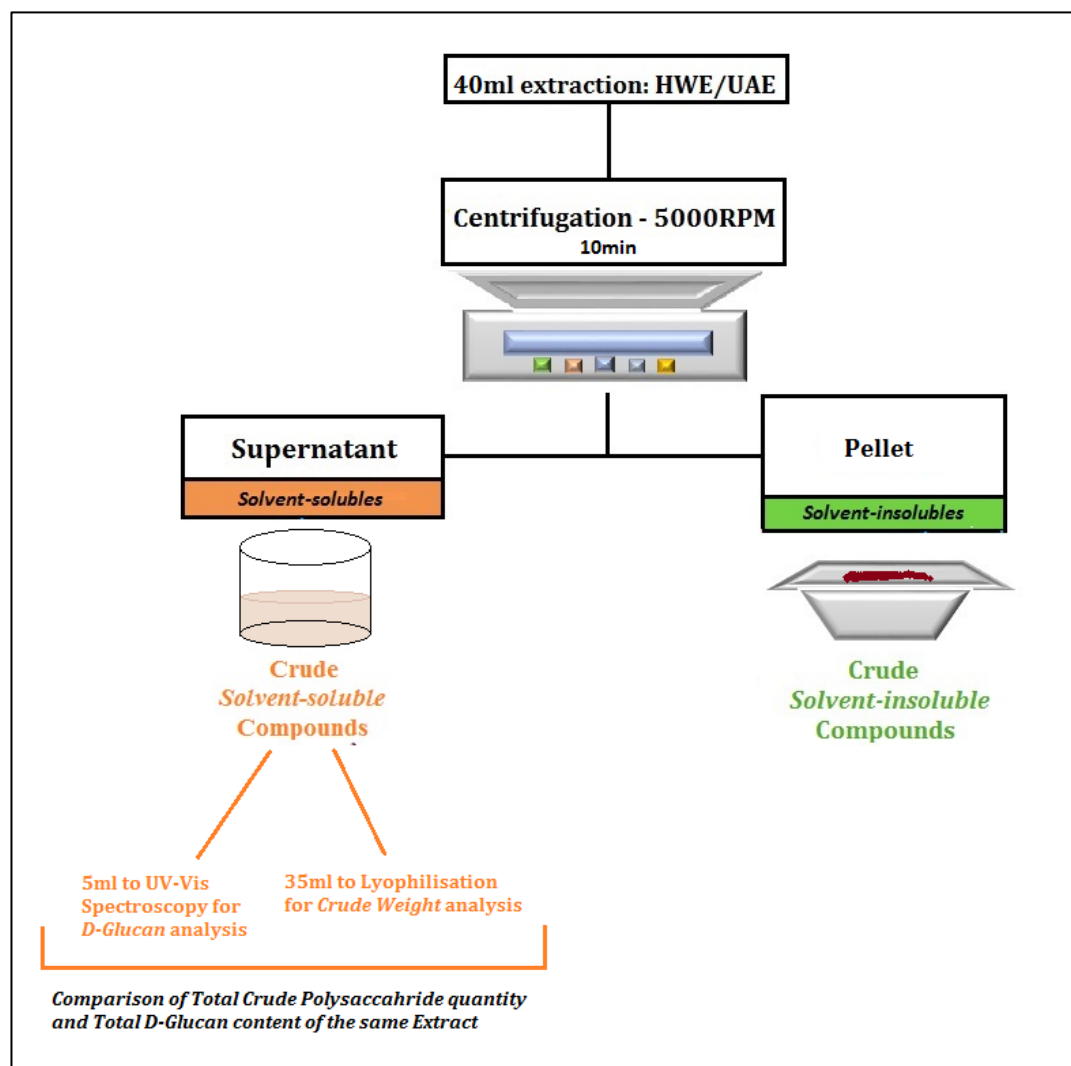


**Figure 3.5:** Extraction of crude GLPS using HWE and UAE

*Novelty processing and smart delivery of Ganoderma Lucidum spores*

### 3.3.1.6 GLPS Characterisation via Phenolic Compounds

Phenolic compounds are aromatic hydroxylated compounds that have been associated with antioxidative and anti-inflammatory effects, in particular when extracted from medicinal mushrooms like Ganoderma lucidum [Heleno et al., 2012; Sheikh et al., 2014; Oludemi et al., 2016; Sánchez et al., 2017; Oludemi et al., 2018]. These compounds, in particular flavonoids, are quickly introducing competition for synthetic antioxidants [Barros et al., 2008; Ramesh et al., 2010]. Typically extracted using organic solvents like ethanol, the absorbance of phenolic/flavonic compounds is well-documented at wavelength 400-430 nm in the UV-Vis spectrum, after undergoing phenol-sulphuric acid hydrolysis [Rawat et al., 2013; Acharya et al., 2015]. These compounds are the foundations for many commercial antioxidant supplements, and their detectability here is an interesting observation, as their extraction is typically affected by organic solvents [Boeing et al., 2014; Jacotet-Navarro et al., 2018].

### 3.3.2 Extracting a Polysaccharide-Ganoderic Acid (PSGA) Complex

Following the extraction of GLPS via HWE and UAE, section 3.3.2 now aims to use HWE to extract a novel polysaccharide-triterpenoid complex from GLS.  HWE was chosen on the basis of its simplicity, flexibility, and documented yields in literature [Miao et al., 2005; Zhang et al., 2014; Thouri et al., 2017].

**Ganoderic Acids**

Ganoderic Acids (GA) are a potent cytotoxic agent in GLS and have proven inhibitory action toward cancer growth [Wang et al., 2007; Radwan et al., 2011; Zhou et al., 2011; Ruan et al., 2012]. Whilst their anticancer effects have been documented in literature, what has not been tested is their bioactive effects when used *in conjugation* with immunoenhancing agents like GLPS – something achievable with crude extracts. The argument for a combinatory approach like this one is especially compelling in *in-vivo* conditions were there are immune responses [Suárez-Arroyo et al., 2017]. Thus, a complex of GLPS and GA as a treatment would be effective. It will be abbreviated henceforth as polysaccharide-Ganoderic Acid (**PSGA**). Furthermore, while crude complexes are the starting ground for discovering effective compounds, in the case of Chinese Traditional Medicines crude extracts have frequently been proven more effective in achieving therapeutic effects (cancer inhibition in particular) than the isolated compounds [Huie et al., 2002]. Among many reasons, this is due to the synergistic pathways opened up by each compound, and resulting enrichment of other compounds' activities [Zhu et al., 2000; Liu et al.

2002; Chen et al., 2007]. Thus, this section will investigate this conjugation as a means of comparison to GLPS.

There is very little published work defining a workflow for Ganoderic Acid extraction, let alone one defining a *complex* of polysaccharides and Ganoderic Acids. For that reason, there is little evaluation of this extract with respect to extractability or structural/bioactive characterization [Ruan et al., 2014]. To quantify this complex, this work will utilize the characteristic absorbable wavelengths of the GA compound class in the UV-Vis spectrum to simply identify the prevalence of the compounds. Of course both counterparts of this crude complex (PS and GA) are detectable at different wavelengths. Furthermore, polysaccharides typically need to be *hydrolysed* for detection at a monomer level, but Ganoderic Acids can be detected as they are [Ruan et al., 2014]. However fortunately, the UV-Vis absorbance of PS when *unhydrolysed* has been observed at the same approximate wavelength region absorbed by Ganoderic Acids – between 254-257nm [Li et al., 2005; Wang et al., 2005; Greco et al., 2014; Ruan et al., 2014; Page et al., 2016]. PSGA is assumed a scalable biomolecule for drug development owing to its possession of two valuable counterparts that could work together to achieve its effects in an in-vivo environment.

### 3.3.2.1 Optimising the Extraction PSGA using *Supervised Machine Learning* via Response Surface Methodology (RSM)

RSM, a form of supervised machine learning, is a design of experimentation that ensures experimental parameters are carried out at multiple levels, at multiple levels of other tested variables. By training the model with experimental data, RSM identifies the confounding effect of the variables and creates a model that can be used for predictive analysis of the variables' effects. A lack of knowledge of how this PSGA complex would chemically behave renders a machine learning approach most efficient to ascertain an effective extraction setup. Thus, a statistical design of experiments was employed to optimize the extraction of PSGA using HWE. Response Surface Methodology (RSM) verified the effects of two influential parameters on the yield of PSGA extracted from GLS. For the optimisation of HWE with respect to PSGA, RSM therefore provides a reliable and efficient way of determining optimal parameters for the extraction of PSGA from GL.

### RSM Experimental Design

Optimization via RSM firstly implicates a statistically designed experiment, and subsequently creates coefficient estimates in the form of a polynomial model that provides a predictive response. Finally, the model's accuracy is tested in its current setup. To create the statistical

experimental design, RSM codes the factor levels "-1" corresponding to the lowest, "1" the highest, and "0" the mid-level.   Table 3.4 outlines a 2-factor, 3-level design ($3^2$).   The corresponding factor levels are shown also.

| Extraction time ($X_1$) | Solvent:GLS ($X_2$) | $X_1$ Time (min) | $X_2$ Solvent:GLS Ratio |
|:---:|:---:|:---:|:---:|
| -1 | -1 | 40 | 20 |
| 0 | -1 | 70 | 20 |
| 1 | -1 | 100 | 20 |
| -1 | 0 | 40 | 30 |
| 0 | 0 | 70 | 30 |
| 1 | 0 | 100 | 30 |
| -1 | 1 | 40 | 40 |
| 0 | 1 | 70 | 40 |
| 1 | 1 | 100 | 40 |

**Table 3.4:** Experimental Design: RSM for GLS Extraction of PSGA from broken GLS

The experimental order run was randomized to diminish error and the effect of uncontrolled factors.

## The Optimization Model

The optimization model for biocompound yield is based on the regression coefficient estimates obtained from experimental runs. The aim of optimisation is to define the yield (Y) as a function of experimental parameters ($X_n$), simplified in eqn 3.3.

$$Y = f(X_1, X_2, X_3 \ldots X_n)$$

Eqn. 3.3

Given the dimension of effects (And their intercorrelation), an empirical model will correlate yield to the experimental parameters using a second-degree polynomial as demonstrated in eqn 3.4.

*Novelty processing and smart delivery of Ganoderma Lucidum spores*

$$Y = \beta_0 + \sum_{i=1}^{n} \beta_i X_i + \sum_{i=1}^{n} \beta_{ii} X_i^2 + \sum_{i=1}^{n} \sum_{j=i+1}^{n} \beta_{ij} X_i X_j + \varepsilon$$

Eqn. 3.4

Extraction Time ($X_1$) and Solvent:GLS ($X_2$) coefficients represent the effect of a one-unit variable change on compound yield when the other parameter are held constant. For example, when extraction time ($X_1$) increases by 1 minute, the model will show the %-increase in yield equal to the corresponding coefficient. In real experiments however, there is also a need to determine the effect of each parameter when the other parameters are *not constant* – hence the need for an interaction coefficient ($X_1$*$X_2$). The intercept term corresponds to the yield when all parameters are operating at zero.

RSM will provide a model of the PSGA yield achievable using the variables involved, and can extend over a wider range of the same variables for the prediction of experiments. The model will contain single main effects (of each parameter individually), interaction effects (the interacting effect with other variables), and quadratic effects (the interacting effect with itself). These will be explained in the context of the study in chapter 4. ANOVA (Analysis of variance) was used for significance testing and model analysis to determine the correlation between the HWE parameters and yield. The estimates of all coefficients are presented along with the statistical t-tests for each variable, indicating their model significance verified by low p-values ($<0.05$). The statistical software package JMP (SAS Institute) was used for regression analysis of experimental data, to create the response surface, and to carry out the ANOVA. The $R^2$ value signified the accuracy of the model fit.

### 3.3.2.2 Optimizing HWE for PSGA Yield: Experimental Data

As it is common to observe small Ganoderic Acids bound to polysaccharides when extracted in water, water was employed as an extraction solvent to ensure that conjugates could be obtained in the yield. In addition water is a viable candidate for Ganoderic Acid as well, especially under high-temperature conditions where water takes on non-polar characteristics [Chin et al., 2014; Che et al., 2017]. When verifying an extract's bioactive potency, ethanol traces in the sample further can positively skew anticancer effects [Tapani et al., 1996]. Thus, PSGA will be extracted and administered to cancer cells in-vitro using water-based HWE only. Crude *GLPS* will also be administered as a bioactive comparison.

The HWE was carried out to "train" the model using a faction of the required experiments. A Clifton unstirred water bath was pre-heated to 90°C, providing kinetic energy for enhanced

*Novelty processing and smart delivery of Ganoderma Lucidum spores*

collision between the water and GLS particles. From control vials in section 3.2.3.3, a sample temperature between 70-73°C was achieved in closed vials, however the PSGA extraction vials were uncapped and thus lost a small amount of heat and instead ranged from 68-72°C. Temperature recording of test vials suggested that this time 15 minutes was required for each experimental sample to attain a near-uniform experimental temperature across the extraction times (uncapped vials). Thus to all samples and their duplicates, recording began 15 minutes after sample immersion in the heated 90°C-water bath. 1g of GLS was immersed into volumes of 100% water that resulted in ratios of solvent:GLS 20:1, 30:1 and 40:1. The samples were shaken to homogeneity and placed into the water bath, which was filled to just above the level in the vials corresponding to the largest dilution (40ml). The experiment took place over 40, 70, and 100 minutes. Extraction vials were not capped so as to minimise the influence of pressure on extraction. With minimal pressure, it is anticipated that the setup will minimise the extraction of large complex polysaccharides, and instead maximise the extraction of small-molecule GA extraction that requires no structural breakdown [Michel et al., 2001; Chen et al., 2007; Tao et al., 2012; Yanhua et al., 2014; Plaza et al., 2015; Sun et al., 2016; Sato et al., 2017]. Ganoderic Acids present a much weaker intramolecular structure, however the effects of pressure during extraction are not yet known – but assumed degradative [Wang et al., 2010; Wang et al., 2011; Li et al., 2013]. The bath was covered to avoid contamination for the experimental duration.

### 3.3.2.3 PSGA Yield

Following extraction, each sample was centrifuged at 2500 RPM for 10 minutes, and its supernatant decanted and analysed to determine the PSGA content. This was either chemically via UV-Vis spectroscopy or physically via freeze-drying for 48 hours in a VirTis Sentry 2.0 Vacuum-assisted Lyophiliser at the conditions previously described. In the latter case, the supernatant was frozen in preparation for freeze-drying. Freeze drying was carried out at 100 mTorr (approximately 1/70,000[th] of atmospheric pressure) to enhance the sublimation of the yield moisture. During this time, the chamber temperature was maintained at -5°C and the condenser at -70°C. Samples were sealed with pierced Bemis Parafilm M Laboratory Wrapping Film to ensure sample safety as pressure and temperature fluctuated during freeze drying. No sample was ethanol-precipitated to ensure simple GA isomers were retained.

#### 3.3.2.3.1 PSGA Yield Quantification: Ultraviolet-Visible (UV-Vis) Spectrometry

UV-Vis detection of PSGA extracts did not involve prior hydrolysis via the phenol-sulphuric acid assay, as hydrolysis is typically only required for the detection distinct and structurally large compounds like polysaccharides which are otherwise undetectable in the UV-

*Novelty processing and smart delivery of Ganoderma Lucidum spores*

Vis spectrum. A Biotek Synergy plate reader was used to analyse 300μl of each extract and its duplicate. The extraction sample was 3x diluted to meet the system sensitivity requirements and analysed at wavelength 257nm - known for absorbance by unprocessed Ganoderic Acids, however also absorbed by unhydrolysed polysaccharides [Nishitoba et al., 1988; Li et al., 2005; Størseth et al., 2005; Wang et al., 2005; Tang et al., 2006; Greco et al., 2014; Ruan et al., 2014; Da et al., 2015; Hung et al., 2015; Page et al., 2016]. It should be noted that in a water-based extraction system, there is always a possibility of yield inflation via the extraction of other compounds like simple sugars and proteins – hence the term "crude" maintained in GLS extraction.

### 3.3.2.3.2 PSGA Calibration Curve

A raw GLS sample was scanned in the UV-Vis range to confirm that GA isomers and unhydrolysed PS could be detected without hydrolysis and the strong peak at 257nm verifies a high concentration of Ganoderic Acids and unprocessed polysaccharides at this wavelength in GLS without any hydrolysis (figure 3.6). A control of pure GLS in water (1 % w/v) was diluted to form the calibration curve depicting 0- 0.17%, from which GLS-A release could be quantified at 257nm. This calibration allowed yield conversion into an approximate PSGA concentration.
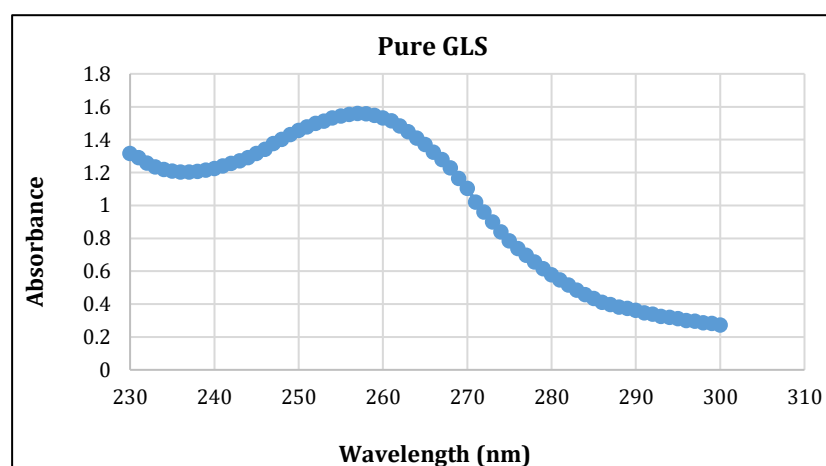


**Figure 3.6:** GA peak at 257nm in the UV-Vis spectrum, using pure GLS

As this investigation investigated the solvent ratio (i.e. GLS dilution), it was important to note that this implicated the *same GLS content* in *different solvent volumes.* Of course this introduces a confounding variable of greater extraction capacity. To control this effect when testing the effect of system volume on extraction yield, two perspectives were considered: the total *extract yield* and *extraction efficiency* – the latter controlling for greater total volume. Furthermore, while the

*Novelty processing and smart delivery of Ganoderma Lucidum spores*

total yield would indicate the benefits of one technique over another in absolute terms, the efficiency would indicate what drives extraction efficiency.

### 3.3.2.4 PSGA Structural Characterisation

The PSGA yield was chemically characterised to better understand the effects of the HWE process on the PSGA structure – something not yet established for this novel complex. Both FTIR and LCMS analyses were investigated to indicate the effect of extraction time on the extract structure. This was particularly true for the Ganoderic Acid component that is especially sensitive to heat [Chin et al., 2011; Chin et al., 2014]. The structural effect of solvent ratio was not considered to be a significant effect on structure, and so was not tested spectroscopically [Mustafa et al., 2014; Mohamad et al., 2013]. For these physiochemical analyses, the sample was centrifuged for 10 minutes at 2500 RPM and the supernatant was decanted and frozen then freeze-dried in a Virtis 2.0 Advantage benchtop Freeze Drier for 72 hours as previously described.

#### 3.3.2.4.1 Fourier-Transform Infrared (FTIR) Spectroscopy to Determine the Effect of Extraction Time on PSGA Structure

As detailed in section 3.2, FTIR is a useful tool in determining the structural change in a material. Structural change are indicated by changes in absorbance distribution of the extract's compounds, thus providing insight into the structural impact of HWE time on PSGA structures. Therefore FTIR was carried out on 2.5mg of the freeze-dried extracts using an ATR-FTIR (PerkinElmer, Spectrum Two, UK). The setup is detailed in section 3.2. The aliphatic structure is a good indicator of the damage exerted on spore structures during extraction [Chen et al., 2012]. Via FTIR, the ratio of methyl ($-CH_3$) and methylene ($-CH_2-$) groups absorbing at approximately 2956 cm$^{-1}$ and 2919 cm$^{-1}$ [Wang et al., 2012] respectively can indicate the length of aliphatic chains and thus the severity of degradation [Zampolli et al., 2014].

$$\textbf{Degree of Degradadation} = \frac{\text{Intensity at 2956 cm}}{\text{Intensity at 2919 cm}} \qquad \text{Eqn. 3.5}$$

#### 3.3.2.4.2 Liquid Chromatography-Mass Spectroscopy (LCMS) to Determine the Effect of Extraction Time on PSGA Structure

LCMS reveals prevalent molecular sizes in the sample by providing the mass distribution of a certain ion the sample. This can indicate the impact of increased exposure on the mass of GA

*Novelty processing and smart delivery of Ganoderma Lucidum spores*

molecules; indicative of structural breakdown [De Vos et al., 2007; Makadia et al., 2011; Sun et al., 2012]. Freeze-dried yields were analysed using a Shimadzhu Prominence UFLC System with DAD, equipped with an ESI source, at wavelengths 254 and 280nm and 40°C. A nebulising gas flow of 1.5 L/min was used, and the drying gas flow of 15 L/min. The capillary voltage and extractor voltage were set to 0.75 kV and 3 V, respectively. The samples obtained from 40 and 100 minute extractions were dissolved in methanol at a concentration of 1mg/ml and centrifuged for 15 seconds at 13,000 RPM. 20µl of sample was injected into the column to determine the elution pattern within 7 minutes. The molecular weight under investigation is 570g/mol, approximately that of GA. The setup is detailed in section 3.2.

SEM was also employed to evaluate the spore structures after HWE at all tested parameters, in order to determine any correlation between physical impact and the PS-GA yield obtained. A Cambridge Instruments 240 Stereoscan microscope offered more intricate imaging. The setup is described in section 3.2. A working distance of 7mm was maintained between the electron beam and sample, and the acceleration voltage was 10kV.

### 3.3.3 In-Vitro Cell Culture of GLPS and PSGA with Human Osteosarcoma

Many studies have demonstrated the efficacy of GLS extracts on tumour inhibition, however they fail to be consistent in the mechanisms behind, or the compounds responsible for, the antitumour action. This is usually because GLS biocompounds are often crude and/or thus not completely defined for a systematic casual effect. Section 3.3.2 was designed to provide two district crude HWE extracts from GLS that could be compared with respect to their bioactivity. The first extract is a crude polysaccharide extracted via HWE (GLPS) and the second extract is a crude complex of polysaccharide-Ganoderic Acid extracted via HWE (PSGA). All extractions carried out for in-vitro assays were carried out in triplicates to improve statistical validity of results and none were ethanol-washed, to avoid its positive bias on cell death.

#### Crude GLPS

Crude GLPS were obtained from HWE as described in section 3.3.1. The results of HWE indicated that the most yielding HWE was carried out at 40 and 80 minutes when solvent solution was 20:1. Thus 60 minutes of HWE was used to extract the crude GLPS administered to HOS in this investigation. As this extract would be polysaccharide-rich, both the extracts that are water-soluble and water-insoluble will be administered to verify assumptions that polysaccharides may

not be cytotoxic without certain triterpenoid counterparts (which are present in the insoluble fraction). Ethanol extraction of GLPS, while previously found to be high-yielding, was not carried out as it could introduce confounding cytotoxic biases in cell culture. For this reason also, the GLPS extracts were not ethanol-precipitated [Tapani et al, 1996]. GLPS however maintained their distinction from the PSGA extract, as they were pressurized (capped) and thus experienced a high-pressure extraction that is more conducive to large-molecule extraction [Michel et al., 2001; Yanhua et al., 2014; Sato et al., 2017]. Furthermore, by chilling the sample overnight prior to extraction, the extraction of bioactive polysaccharides is more likely – something not required for Ganoderic Acids [Hoffman 2008] - consequently, bioactive samples started at 8°C. The GLPS extraction was also much shorter, so that extract bioactivity could be maintained under the higher pressure but also because this time indicated greater extractability of crude GLPS. The temperature recording over the 60 minute GLPS extraction averaged at 75°C. From each extraction sample the pellet and supernatant were lyophilized in a VirTis Sentry 2.0 Vacuum-assisted lyophiliser that subjected samples to a zero-pressure environment at -40°C for 24 hours and 72 hours for pellets and supernatants respectively.

## Crude PSGA

The PSGA complex was obtained as per the HWE method described previously for PSGA employing the highest-yielding setup to generate the extract for this in-vitro HOS treatment. The temperature recording over the 100 minutes of PSGA extraction averaged at 70°C. The PSGA extract is expected to contain more small-molecule agents like Ganoderic Acids, which traditionally have a greater cytotoxic effect on cancer cells [Jin et al., 2015].

Table 3.5 outlines the parameters for the HWE extraction of crude GLPS and PSGA.

*Novelty processing and smart delivery of Ganoderma Lucidum spores*

| Extraction Parameter | HWE for GLPS | HWE for PSGA |
|---|---|---|
| Equipment Model | Clifton unstirred water bath | Clifton unstirred water bath |
| Solvent Composition | 100% water | 100% water |
| Vials | Closed | Open |
| Extraction Duration (min) | 60 | 100 |
| Solvent Temperature | $75 \pm 0°C$ | $70 \pm 1°C$ |
| GLS:Solvent | 1:20 | 1:20 |
| Bioactive Compounds likely present | Polysaccharides<br><br>Some proteins and lipids | GL Polysaccharides<br><br>Ganoderic Acids<br><br>PSGA complex |

**Table 3.5:** GLPS and PSGA extracts for in-vitro HOS Culture

### 3.3.3.1 In-Vitro Culture

The importance of a combinatory approach to cancer treatment was earlier highlighted. Cancer treatment in particular can benefit from this in the face of its conventional therapies such as chemotherapy and its associated local toxicity. There is therefore a need to address this opportunity in GLS development as it possesses a variety of both cytotoxic and immunoenhancing biocompounds. While GLPS is a crude extract, PSGA is therefore expected to have greater cytotoxic effects owing to its GA content [Jin et al., 2015].

In-vitro administration of the extracts to HOS cancer cells was carried out to verify extract processing variables and administration variables affecting HOS proliferation. HOS cells are easily available, with well-established documented characterization and rapid confluence rates, and can model events associated with a wide range of cancer differentiation in humans deposit through their deposition of mineralization-competent extracellular matrices [Cmoch et al., 2014]. In both cases, the cell culture procedure in section 3.2 was followed, and variations were made to dosing and incubation time. Lyophilised extracts were filtered prior to administration to remove bacterial contamination using a 0.22μm EMD Millipore Millex™-GP Sterile Syringe Filter with PES Membrane. Administration took place in a 96-well plate and extract doses were administered after the plate was pre-incubated for 24 hours to ensure cell attachment prior to treatment. All culture incubation took place at 37°C subject to 5% $CO_2$. The setup was further detailed in section

*Novelty processing and smart delivery of Ganoderma Lucidum spores*

3.2. The culture was investigated for proliferation after 24 hours and 48h without medium replenishment.

### 3.3.3.1.1 In-Vitro Administration to HOS: GLPS Extracts

Each GLPS administration was carried out in replicates of each experimental triplicate. The extract supernatant (GLPS-rich) at dosages 0.5mg, 1mg, 2.5mg, 5mg and 10mg/ml and the processed spore powder (other water-insolubles) were administered at 0.5mg, 1mg, 5mg, 10mg and 50mg/ml dosages. A positive control of 10% ethanol (a known cytotoxic agent) and a negative untreated control were both evaluated in the same well plate. The GLPS polysaccharide-rich fraction dose range was influenced by literature that typically indicates suitable test ranges below 10 mg/mL [Tong et al., 2009; Mohan et al., 2017; Guo et al., 2018; Li et al., 2018]. The dosage of cruder spore fraction was a wider range because it is assumed that this fraction would contain plant fibres and ash that do not contribute to cancer inhibition [Rawat et al., 2012; Cör et al., 2018]. Each well was cultured at a density of $10^4$/ml in a 96-well plate.

### 3.3.3.1.2 In-Vitro Administration to HOS: PSGA Extracts

Each administration of filtered lyophilised PSGA was carried in replicates. All administration replicates showed statistical similarity. The extract was administered at a dosage range higher than GLPS, in accordance with literature, at 2 – 15 mg/L alongside a positive control of 10% ethanol and a negative untreated control [Chen et al., 2010; Wang et al., 2017]. Cell density was increased from GLPS tests owing to the slightly higher dosage range; each well was cultured at a density of $1.8 \times 10^5$/ml.

### 3.3.3.2 MTT Assay to determine GLPS and PSGA bioactivity

The HOS proliferation was investigated after 24 and 48 hours and compared to a positive control of 10% ethanol and a non-treated negative control group, in both culture experiments. Cell viability was measured using the MTT Assay. Tetrazolium dye MTT 3-(4,5-dimethylthiazol-2-yl)-2,5-diphenyltetrazolium bromide indicated the viability assay of cells treated by the PSGA extract in-vitro. Briefly, MTT dye was dissolved in PBS and filtered, before being diluted with DMEM (acid-free) at a ratio of 1:10. After each time point, the cell media was aspirated and 100μl of MTT reagent was substituted into each well for 4 hours in incubation to determine the cellular enzyme activity. Subsequently, the MTT reagent was replaced with 100μl dimethysulfoxide (DMSO) and shaken for 5 minutes in preparation for detection. The mechanisms behind the MTT assay is described in section 3.2.2. Eqn. 3.6 determined the percentage of treated HOS inhibition in comparison with untreated.

$$\textbf{GLS HOS Cell Viability} \, (\%) = \frac{\text{Treated HOS MTT Absorbance}}{\text{Untreated HOS MTT Absorbance}} \; \text{x} \; 100 \qquad \text{Eqn. 3.6}$$

### 3.3.4 Encapsulation of GLS for Delivery

The development of GL to date has heavily focused on its biocompound isolation and characterisation, particularly verifying astonishing potency toward cancer inhibition. There is however very little study on the delivery of the biocompound once isolated. Inevitably, the protective sporoderm around GLS renders its breakage compulsory to isolating biomolecules. Aside from the degradative conditions exhibited by therapeutic biomolecules at this stage, the subsequent exposure to open air has been shown detrimental to the bioactivity of valuable plant-derived compounds such as Glucans, as they react with oxygen species [Champagne et al., 2007; Drosou et al., 2017]. Thus, protection of GLS biocompounds after extraction is essential to their bioactivity.

Drug delivery systems (DDS) determines the body's identification and processing of drug molecules, thus affecting the drug's biodistribution, toxicity, release profile and ultimately efficacy [Kudgus et al., 2014]. A DDS usually flaunts specific advantages for the delivery of a compound's chemical and morphological properties, typically defining a distribution that is small, uniform, and surface-enhanced [Hoffman 2008]. A traditional DDS presents undesirable side effects attributed to their "idealistic" material that withstands extremities in processing en-route to a morphologically-perfect system, but also associated with non-targeted bio-availability, uncontrolled release profiles, and a risk of long-term toxicity [Jong et al., 2008; Jahangirian et al., 2017]. There is limited progress in the field of drug delivery using materials that work in harmony with the physiological environment, yet can provide effective targeted drug delivery via stability, immune system evasion, and dosage manipulation [Soppimath et al., 2001; Lee et al., 2004; Donsì et al., 2011; Liu et al., 2011]. To date, the challenges of using biopolymers to encapsulate drug molecules remain to be the fabrication obstacles implicated by a high viscosity, and their instability in certain environments [Mehregan Nikoo et al., 2016]. The requirements of a smart delivery system and methods of achieving these are presented in chapter 2, the literature review. Another relevant angle of study is the need to maximise the *drug-loading* of a delivery system in the face of the physical characteristics required for a strong and efficient carrier– such as high polymer content.

*Novelty processing and smart delivery of Ganoderma Lucidum spores*

The aim of this experimental section is to evaluate the process parameters that could create GLS-Alginate particles that are durable, controllable (with respect to fabrication and subsequent release), without compromising drug (GLS) content.

### 3.3.4.1 Hydrogels for Drug Delivery

Hydrogels are hydrophilic polymeric networks formed by crosslinking polymer chains that can absorb large quantities of water whilst remaining stable in aqueous media. Naturally derived polymer hydrogels are biocompatible and biodegradable, fostering a desirable reaction when traversing the body [Ailincai et al., 2018; Xu et al., 2018]. Natural polymer-based hydrogels have also gained attention for their unique characteristics such as controllable porosity, and surface texture, that enhance tissue adherence, and stability in the body's natural environment [Koetting et al., 2016]. An increasingly employed example is the hydrogel made from biopolymer sodium alginate.

### 3.3.4.1.1 Hydrogel Features for Drug Delivery

Release from a hydrogel, aside from release conditions, is a function of **polymer concentration**, **porosity** (surface defects), and **crosslinking density**. These features affect the mechanism of drug diffusion out of the hydrogel matrix, including matrix swelling. Anionic polymer chains like sodium alginate respond to external stimuli such as pH and temperature [Lee et al., 2012; Koetting et al., 2016]. The vast array of variables controlling the rate of release from an alginate hydrogel increases its controllability, and thus renders this hydrogel "smart" and versatile in the drug delivery field [Wang et al., 2008; Liu et al., 2017].

Figure 3.7 shows some variables that can manipulate the release behaviour of hydrogels like alginate. When swollen, the polymer matrix expands to absorb media and subsequently release the entrapped drug. The swelling rate is determined by a variety of factors related to the matrix properties and external stimuli.
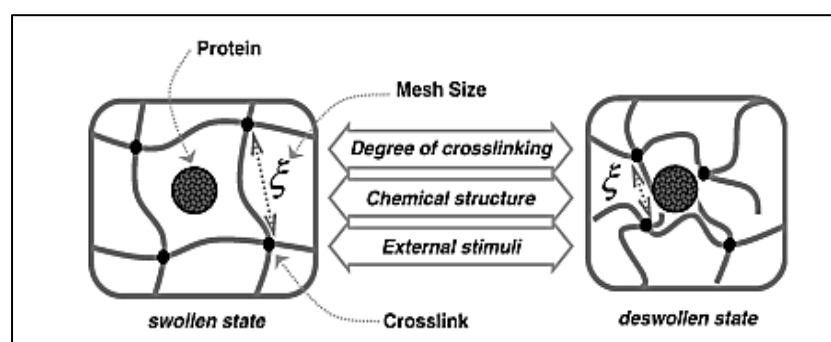


**Figure 3.7**: Schematic of hydrogel matrix in its swollen and de-swollen states [Sheikhpour et al., 2017]

*Novelty processing and smart delivery of Ganoderma Lucidum spores*

### 3.3.4.2 Microparticles for Drug Delivery

Over the past decade, particulate drug delivery has sparked considerable interest. Most notably they provide a simple route to injection directly to tissue or intravenously, provide a higher local drug concentration, create greater dosage precision, are adaptable and flexible to be used as part of a wide range of treatment regimens like inhalation, can bypass the many bio-barriers presented by the body and can also increase flowability when compared to fibres, scaffolds, and beads [Kohane et al., 2007; Gundogdu et al., 2014]. Thus, their candidacy for drug delivery is promising – particularly when positioned as a slightly more durable structure when compared to nano-sized carriers [Jamaati et al., 2014]. Being larger than nanoparticles also results in a slower release [Collnot et al., 2012]. The morphology (namely shape and size) of the microparticles has been shown influential in controlling drug release dynamics. As the drug delivery field is explored, shape in particular has been at the centre of recent drug delivery investigations owing to its undefined yet influential relationship with drug release rate.Particle shape has received limited attention in the drug delivery field, as its repeatability across studies is not straightforward and thus their investigations cannot be consistently recorded [Venkataraman et al., 2011; Jindal et al., 2017; Jeyhani et al., 2018]. More recently, the *particle surface* has been shown important in determining the safety and preservation of drug molecules/bioactivity, along with the adherence to cell tissue and release [Ahuja et al., 2009; Slütter et al., 2016]. Porosity has been a particular topic of interest by adding a new dimension of control to delivery, for example through manipulating swelling-induced release and allowing post-fabrication drug loading.

The conventional technique used to fabricate microparticles is emulsification. This technique employs two immiscible phases in order to create droplets that can later undergo ionic gelation. Electrohydrodynamic Atomisation (EHDA) however has more recently been the subject of investigation with respect to particle fabrication, owing to its capability to create smaller and more uniform particles more controllably. Nevertheless, it is built on the need for high voltage and potentially toxic solvents for its greatest efficiency. Table 3.6 details the basic principles of EHDA compared to emulsification for particle fabrication.

|  | Emulsion | EHDA |
|---|---|---|
| Droplet formation | Droplet structures created by immiscible oil-polymer phase, and stabilised by use of a surfactant | Droplet structures created by a polymer stream disrupted by controlled electric field |
| Unique Mechanisms | Crosslinking of droplets takes place from the outer shell, inwards due to the presence of calcium in the outer continuous phase. This allows "setting" of an outer boundary on each droplet, reducing coalescence | |
| Min. Size Achievable | Typically <1000 μm (1 mm) | Typically <1000 nm (1 μm) |

**Table 3.6:** Basics of Emulsification and EHDA

Emulsion-based particle generation of GLS compounds do exist and have demonstrated particle stability and bioactivity at sizes smaller than 500nm [Chen et al., 2010; Johnson et al., 2010; Radwan et al., 2011; Qu et al., 2014; Shen et al., 2016]. However emulsification as a means of creating drug delivery systems is subject to disadvantages that are not exhibited by EHDA. In particular, the resulting particle distribution is seldom uniform, without employing chemical surfactants [Buyukozturk et al., 2010; Chen et al., 2010]. The emulsification process is also characteristic of even lower drug-loading efficiency, reduced scalability, less controllability over particle size/shape profiles, and challenges in incorporating hydrophilic drugs [Nishitani Yukuyama et al., 2017]. There are also necessary steps for particle isolation involving toxic solvents, high temperature and shear stress; threatening bioactivity [Thomas et al., 2011; Torres et al., 2018]. EHDA further offers the advantage of lower particle variation and reduced agglomeration (owing to dispersible charged surfaces). In any fabrication technique however, the problem of drug loading efficiency remains, as attempts to create high-polymer durable particles takes precedence.

### 3.3.4.3 EHDA to Encapsulate GLS for Delivery

EHDA induces an electric field to foster droplet disruption, and process parameters such as voltage and solution flow-rate can be used to manipulate distributions via the achievement of specific spraying modes [Forbes et al., 2010; Wilm et al., 2011; Jeyhani et al., 2018]. This is because the generation of electrosprayed particles has been shown to be governed principally by

*Novelty processing and smart delivery of Ganoderma Lucidum spores*

the strength of solution interfacial tension, and solvent evaporation as droplets traverse between the needle and collection bath, and particle drying. These phenomena are functions of voltage, solvent, solution flow-rate, spraying distance, and drying method [Forbes et al., 2010; Wilm et al., 2011]. Once the polymer solution is extruded through the needle, the applied voltage overcomes the surface tension exhibited by the solid stream. The droplets disrupt due to electrical charge and these droplets are crosslinked into solid particles.

Previous studies have applied EHDA to synthetic polymers, however there is limited consistency in the achievable distribution using natural polymers. While natural polymers indeed present the benefit of imitating nature's chemical environment (thus offering biocompatibility) they typically possess weak mechanical properties that are too fragile to undergo efficient processing techniques [Sell et al., 2010; Soares et al 2018]. Thus, they present obstacles in their durability during extreme processing conditions, and a result are limited to micrometre-sized diameters - too large for many therapeutic applications as a result of the material's heat/pressure thresholds [Gasperini et al., 2014; Olabisi et al., 2015; Le et al., 2018]. As a result, polymer *complexes* are employed with electrospraying to enhance processability [Murata et al., 1993; Abreu et al., 2008]. For example, traditionally alginate matrices have been reinforced using a copolymer like chitosan to retard the diffusion during drug release as well as maintain particle integrity. In contrast, some studies actually employ low alginate concentrations to create nano/micro-range distributions – an issue that may prove a challenge to drug loading, particle integrity, and resulting controlled release profiles [Park et al., 2012].

GLS-Alginate microparticles will be produced with efforts for the first time being dedicated to achieving a high GLS loading in parallel to a small and uniform distribution. This method was evaluated as a technique to produce particulate forms of alginate particles in the absence of copolymers containing GLS (GLS-Alginate (GLS-A)) possessing a relatively uniform distribution with respect to size and shape in efforts to establish a treatment system that is safe, effective, and predictable, without compromising the amount of GLS that could be loaded. By observing how the particle features vary with EHDA processing parameters, this study subsequently evaluates the impact of the microparticle distribution on the release of GLS in a pH-neutral bath.

Section 3.1.3 characterised the forthcoming materials used in this part of the investigation.

### 3.3.4.3.1 GLS-A Suspension

A primary target of drug delivery is to maximise drug loading. In order to address the need to optimise the drug loading capacity, two GLS-Alginate weightings were investigated. It is expected that by changing the polymer concentration/drug content of a particle, along with its fabrication parameters, there will be a change in the distribution's morphology and release

kinetics – and thus an effect on release profile. To evaluate the effect of alginate/GLS weighting on the achievable distribution of GLS-A microparticles, three weightings were investigated: GLS-A 1-1 (containing either 1% GLS *or* 2% GLS) and 2-1 (containing 2% GLS). Water was used as the medium for alginate, as it is an effective solvent for alginate to form a homogeneous solution [Kapishon et al., 2015; Serrano-Aroca et al., 2017]. Distilled deionized water was employed to negate effects of pre-existing conductivity on EHDA spraying – either positively owing to a lower required voltage and faster evaporation, or negatively due to greater intermolecular attraction and thus "bulking" [Kwak et al., 1975]. For GLS-A 1-1 (containing 2% alginate), two solutions - 4% GLS and 4% alginate - were prepared independently in distilled water under magnetic stirring at 400 RPM for 24 hours, before being combined and stirred for a further 48 hours to create a homogeneous GLS-A suspension consisting of 2% and 2% w/v GLS and Alginate respectively. These measurements were halved for the GLS-A 1-1 containing 1% Alginate. For GLS-A 2-1 the process was consistent using 4% GLS but with 2% alginate; resulting in an alginate concentration of 1% for this solution. Thus, both suspensions contained equal amounts of GLS. Table 3.7 defines the material molar concentrations.

| Alg Concentration | GLS Concentration | GLS:A | Alg:Ca *Molar Ratio* | GG:Ca *Molar Ratio** | CaCl$_2$ (M) | Voltage Range (kV) | FR Range (µl/min) |
|---|---|---|---|---|---|---|---|
| 1% (*0.2mM*) | 2% | 2:1 | *1:750* | *1:1620* | | | |
| 1% (*0.2mM*) | 1% | 1:1 | *1:750* | *1:1620* | 1.5M | {5, 10, 15}kV | {10, 50} |
| 2% (*0.4mM*) | 2% | 1:1 | *1:375* | *1:810* | | | |

Table 3.7: EHDA solution parameters (**GG/Guluronic region is 0.39 molar fraction**) and process parameters

## 3.3.4.3.2 EHDA Processing

Preliminary studies alongside current literature observed that electrospraying 1-3% alginate is stable below 15kV (after which effect on particle diameter was not worth the instability), but at 5-6kV will create particles that were closer the millimetre range [Nedović et al., 2001; Park et al., 2012; Yao et al., 2012; Mehregan Nikoo et al., 2016; Nguyen et al., 2016]. Resultantly, the voltage range tested was 5-15kV, at a flow rate of either 10 or 50µl/min. A programmable syringe pump (Harvard PHD 4400) was used to feed the GLS-A solution into the

*Novelty processing and smart delivery of Ganoderma Lucidum spores*

capillary needle connected to a high voltage supply (Glassman Europe Ltd., Tadley, UK) at a controlled flow rate via a conducting cable. The solution flow rates and voltages (*operational parameters*) are defined below. Terumo™ syringes of 10ml volume were used to pump the GLS-A solution (VWR, UK). A stainless steel needle (ID 510μm and OD 820μm) was set in resin to ensure maximum charge insulation and rigidity and was chargeable from the voltage source (Glassman Europe Ltd., Tadley, UK) to initiate droplet disruption. A silicone rubber tubing connected the needle to the 5ml syringe pump. The tip-to-collector distance was maintained at 20cm, based on the previous finding of a "balance" between particle sphericity and small size; the former achievable at short distances, and the latter at large distances [Zhao et al., 2016]. It was also found that distances well below 20cm did not allow sufficient time for droplet formation prior to crosslinking; resulting in deformed/large final particles. Temperature during experimentation was ambient at ca. 24-26 °C with a relative humidity ca. 55%. Between every experiment, the tubing was cleaned with ethanol. Droplets were collected on a 20x20cm stainless steel scissor stand Lab Jack (VWR, UK). Figure 3.8 shows the EHDA setup and schematic.

*Novelty processing and smart delivery of Ganoderma Lucidum spores*
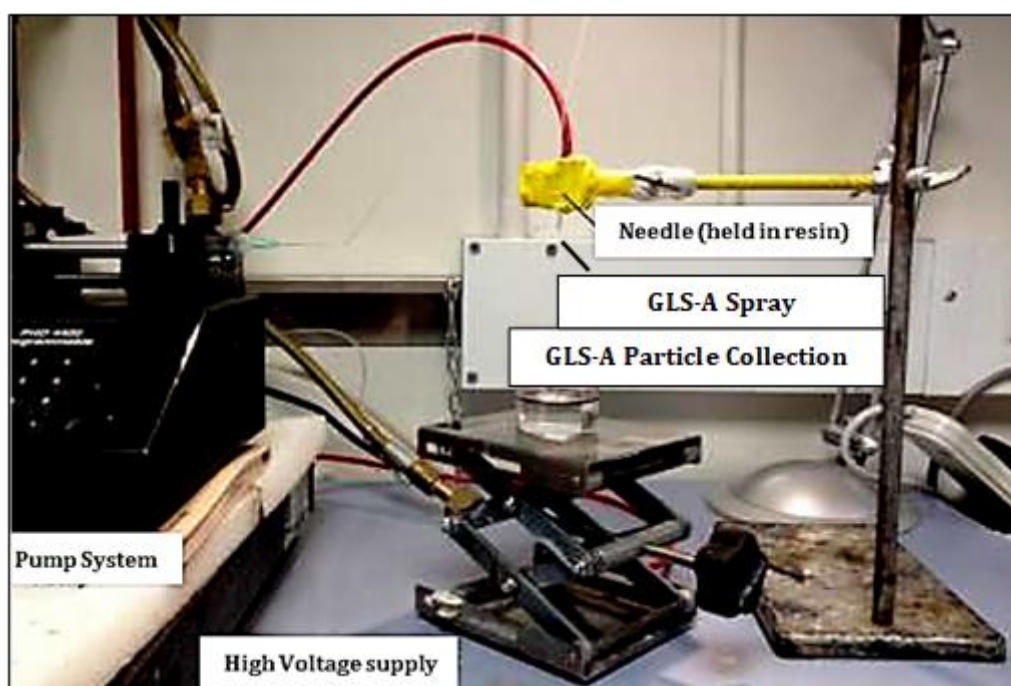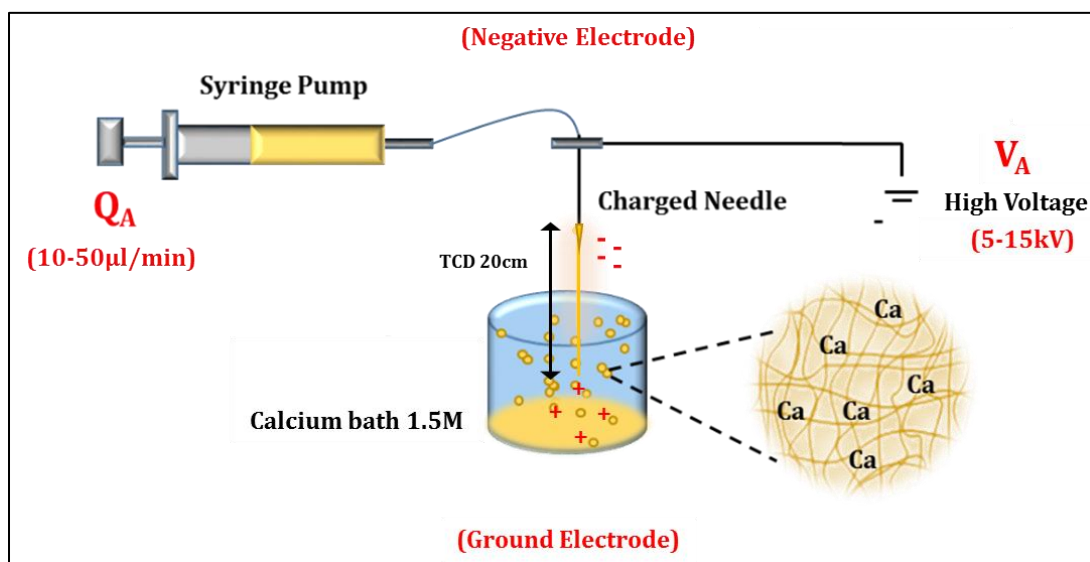
**Figure 3.8:** GLS-A microparticle fabrication using EHDA (*upper:* Setup and *lower*: Technical schematic). V and Q represent applied voltage and flow rate, respectively

### 3.3.4.3.3 Ionic Crosslinking

Alginate chains can be ionically crosslinked using multivalent cations to form a strong hydrogel resulting from bridging of Guluronic units [Russo et al., 2007]. Many multivalent cations can achieve sufficient crosslinking of alginate, however it has been shown that calcium ions can achieve smaller yet stronger hydrogel structures with greater release control during drug delivery [Kikuchi et al., 1997; Raut et al. 2013; Al-Otoum et al., 2014]. While calcium chloride is typically used as the source of calcium ions, it leads to rapid gelation due to its high aqueous solubility and can thus result in deformed particle sizes. In EHDA however, droplets are typically set in shape/size prior to crosslinking, and therefore deformation is a more significant function of the solution and spraying properties. The molar ratio between alginate chains and calcium however can influence the ionic interactions and thus the crosslinking strength and resulting integrity of the GLS-A particles [Kuo et al., 2008]. Therefore, drug encapsulation efficiency (and consequently release profile) has been shown directly and considerably affected by the concentration of calcium chloride in the crosslinking stage [Kuo et al., 2008; Mandal et al., 2010]. The $CaCl_2$ concentration was not a variable in this investigation because studies have simultaneously observed a *reduction in size and change in shape* associated with increasing calcium ion concentration during polymer crosslinking – therefore introducing a confounding effect of particle size on release profile [Saha et al., 2013]. Preliminary tests suggested that GLS-A particles created using the weightings in this study were unable to hold shape during air drying, when the calcium chloride concentration was 1M. However studies have suggested that 1.5M $CaCl_2$ is

*Novelty processing and smart delivery of Ganoderma Lucidum spores*

optimal to create strong alginate particles with controllable release profiles, and many alginate microparticle studies employing less calcium ions have in fact exhibited rapid uncontrolled drug release [Hariyadi et al., 2014]. Each batch underwent crosslinking in 1.5M Calcium Chloride. As crosslinking is external in this investigation, any excess of calcium ions would not change GLS-A solution rheology and thus would not have a confounding effect on final particle profiles [Fu et al., 2010]. This concentration was created by dissolving 16.65g Calcium Chloride in 100g water to create 1.5M Calcium Chloride via the following calculation:

$$\textbf{CaCl}_2\ \textbf{dry weight} = \frac{CaCl_2\ MW\ (110.98)\ x\ 1.5}{10\ (to\ create\ 100ml)} \qquad \text{Eqn. 3.7}$$

A 90x14 mm petri dish (VWR, UK) containing 20ml $CalCl_2$ was used for collection, as it ensured an approximate $CalCl_2$:Alginate solution ratio of 6:1 or 9:1 for GLS-A containing 2% and 1% respectively. Solution ratios above 3:1 have been found to produce particles that are strong, spherical and smooth [Rezende et al., 2007]. Preliminary trials along with literature confirmed that after 20-24 hours there is very little effect of crosslinking time on crosslinking intensity strength nor particle size, as confirmed by literature also; therefore crosslinking took place for 24 hours [Takacs et al., 2000]. After crosslinking, the calcium chloride solution was decanted and the particles were washed once with 5ml distilled water.

### 3.3.4.3.4 Particle Dehydration

Drying regime (temperature, speed and time in particular) can affect particle shrinkage as well as particle surface features - especially by inducing surface defects like porosity and cracks [Berninger et al., 2016; Gurikov et al., 2018]. This is especially the case with inherently porous materials like alginate [Santagapita et al., 2011]. Typically the intensity of these surface impacts is attributed to hydraulic pressures when moisture leaves and enters the matrix. In order to gauge the effects of drying regime on GLS-A particles, two drying regimes were applied. Air-drying only (AD) was first applied to all GLS-A particles after which some were further freeze-died (FD). Prior to drying, excess water was minimised by initial drying in open air for 120 minutes at room temperature (27.5°C) prior to its designated drying process. After each drying process, particles were stored in a desiccator until analysis.

## Particle Dehydration via Air Drying

After initial drying, GLS-A particles were transferred to a covered facility for air-drying for 48 hours at room temperature.

## Particle Dehydration via Freeze Drying

Alginate's hygroscopic nature is a cause for concern when air-drying alone is employed. This is because insufficient particle drying can lead to leaching, surface rupture, and uncontrollable release [Vaccarezza et al., 1974; Yonekura et al., 2014; Szekalska et al., 2015]. As drying conditions induce particle surface defects – namely porosity – that could influence GLS release, some GLS-A samples were additionally subject to 24 hours of freeze-drying in a Virtis 2.0 Advantage benchtop Freeze-Drier. Freeze-drying was carried out at 100 mTorr (approximately 1/70,000[th] of atmospheric pressure, or near-vacuum) on pre-frozen particles, to dry particles via the sublimation of particle moisture. During this time, the chamber temperature was maintained at -5°C and the condenser at -70°C. Partible samples were sealed with pierced Bemis Parafilm M Laboratory Wrapping Film (VWR, UK) to ensure sample safety as pressure and temperature fluctuated during freeze-drying. The process is non-invasive due to its slow rate of moisture removal, typically preserving the material's physiochemical structure. It is expected that an additional freeze-drying step will remove all trace moisture from the GLS-A particles. Table 3.8 summarises the EHDA operational parameters, including drying regime. To control confounding variables, only GLS-A particles containing 2% GLS were subject to this comparative drying investigation (GLS-A 1-1 and 2-1).

| GLS:Alg | GLS % w/v | Alginate % w/v | Flow Rate µl/min | Voltage kV | TCD cm | Drying | *Further FD* |
|---------|-----------|----------------|------------------|------------|--------|--------|--------------|
| **2:1** | 2 | 1 | 10 | 10 | 20 | Air 48h | |
| **2:1** | 2 | 1 | 10 | 15 | 20 | Air 48h | |
| **2:1** | 2 | 1 | 50 | 10 | 20 | Air 48h | *FD 24h* |
| **2:1** | 2 | 1 | 50 | 15 | 20 | Air 48h | *FD 24h* |
| **1:1** | 2 | 2 | 10 | 5 | 20 | Air 48h | |
| **1:1** | 2 | 2 | 10 | 10 | 20 | Air 48h | |
| **1:1** | 2 | 2 | 10 | 15 | 20 | Air 48h | |
| **1:1** | 2 | 2 | 50 | 5 | 20 | Air 48h | |
| **1:1** | 2 | 2 | 50 | 10 | 20 | Air 48h | *FD 24h* |

| 1:1 | 2 | 2 | 50 | 15 | 20 | Air 48h | *FD 24h* |
|-----|---|---|----|----|----|---------|----------|
| 1:1 | 1 | 2 | 10 | 10 | 20 | Air 48h | |
| 1:1 | 1 | 2 | 10 | 15 | 20 | Air 48h | |
| 1:1 | 1 | 2 | 10 | 10 | 20 | Air 48h | |
| 1:1 | 1 | 2 | 50 | 15 | 20 | Air 48h | |

**Table 3.8**: EHDA processing parameters with additionally freeze-dried samples highlighted

### 3.3.4.3.5 Particle Characterization: Particle Morphology

GLS-A beads were characterized using Optical Microscopy and Scanning Electron Microscopy to determine the physical structural attributes. To control confounding variables, only GLS-A particles containing 2% GLS were subject to these measurements (GLS-A 1-1 and 2-1).

### Optical Microscopy (OM) for Microparticle Morphology

30 microparticles were examined for distribution morphology using a Leica DM light microscope after 48 hours drying. Image-J analysis software was used to measure the microparticle dimensions. Elongation was determined via the aspect ratio using the calculation below. The dimensional analyses are schematised in figure 3.9.

$$\text{Aspect Ratio AR} = \frac{\text{Particle Width (μm)}}{\text{Particle Length (μm) } including\ tailing} \qquad \text{Eqn. 3.8}$$
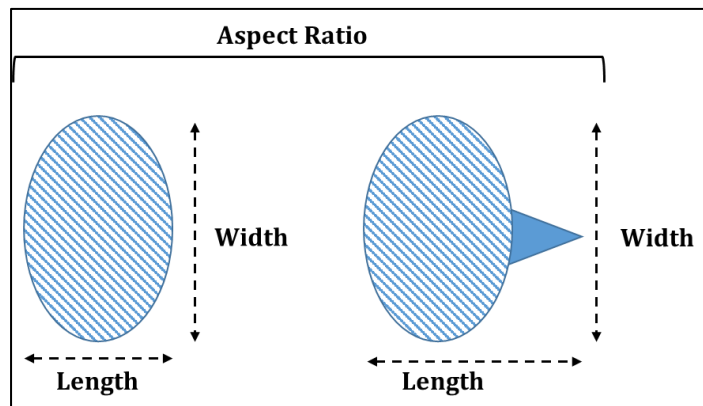


**Figure 3.9:** Measurements used in the calculation of microparticle AR

*Novelty processing and smart delivery of Ganoderma Lucidum spores*

## Scanning Electron Microscopy (SEM) for Particle Surface Analysis

Figure 3.11 on the following page shows the GLS-A microparticles prepared for SEM as described in section 3.2. SEM was employed to indicate the effects of fabrication on the alginate matrix; in particular porosity. A working distance of 4 mm was maintained between the electron beam and sample, and the acceleration voltage was 5kV to ensure GLS biomolecule protection – an accelerating voltage suggested for high-resolution SEM of biopolymers [Drummy et al., 2004; Gaillard et al., 2004]. In addition, *small particles with large pores* have become the subject of many recent investigations, with many researchers observing benefits to drug delivery and thus treatment efficacy [Wang et al., 2016]. As a result, the average pore size relative to the particle diameter measurement, referred to Surface Defect Ratio (SDR) in this study, is measured. A higher SDR would be reflective of a smaller particle with larger pores. The average of 20 pores was taken across 5 microparticles.

$$\textbf{Surface Defect Ratio SDR } (\%) = \frac{\text{Average Pore Diameter} \quad (\mu m)}{\text{Particle Width } (\mu m)} \text{ x } 100 \qquad \text{Eqn. 3.9}$$
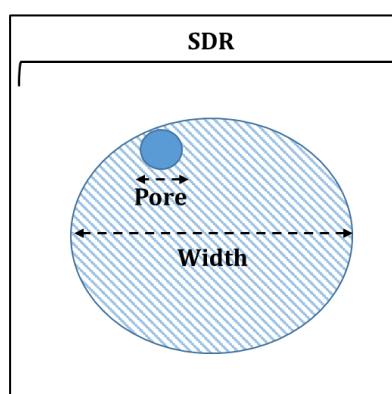


**Figure 3.10:** Measurements used in the calculation of microparticle SDR



1 nm gold-coated GLS-A particles fixed on stainless steel hubs ready for SEM

**Figure 3.11:** GLS-A microparticles prepared for SEM imaging

*Novelty processing and smart delivery of Ganoderma Lucidum spores*

GLS leaching from particles employed a Cambridge Instruments 240 Stereoscan microscope for more intricate imaging.

### 3.3.4.3.6 Microparticle Characterization: Chemical Composition and Molecular Interactions

Fourier Transform Infrared (FTIR) Spectroscopy was carried out on 2.5mg dried GLS-A microparticles as per the setup described in section 3.2. The interaction between drug delivery system materials is important so that effects on delivery can be accurately characterised. FTIR spectroscopy is a proven method of defining new chemical bonds created when materials are fused. Identifying new chemical interactions between alginate and GLS would be useful as the microparticles are characterised with respect to morphology and release profile. The technique support to GLS-Alginate interactions therefore also took place on alginate and GLS prior to encapsulation, so that inferences could be made regarding the chemical interactions after particle fabrication. To control confounding variables, only GLS-A particles containing 2% GLS were subject to these measurements (GLS-A 1-1 and 2-1).

### The Degree of "Polymerisation" (crosslinking) of GLS-A Particles

All hydrogel matrices should indicate a degree of polymerisation, having been crosslinked, compared to pure alginate. An indicated degree of hydrogel polymerisation after crosslinking can firstly be suggested by the increase in the carbonyl content (higher intensity of C=O stretching at 1740 cm$^{-1}$) [Takács et al., 2000]. Additionally, the twisting of the acrylate double bond at 806 cm$^{-1}$ is usually observed as the number of double bonds decreases with crosslinking. As polysaccharides also typically display a peak in FTIR at 760 cm$^{-1}$, which is typically unaffected after polymerisation from crosslinking, this band was chosen as a reference band against which the polymerisation peak was compared [Garcia et al., 2008]. The intensity of this ratio was used to determine the polymerisation as a result of crosslinking as shown in eqn. 3.10.

Eqn. 3.10

$$\textbf{Degree of Polymerisation } (\%) = \left(\textbf{Alginate}\left(\frac{\text{Intensity at 806 cm}}{\text{Intensity at 760 cm}}\right)\right) - \left(\textbf{GLSA}\left(\frac{\text{Intensity at 806 cm}}{\text{Intensity at 760 cm}}\right)\right)$$

### The Degree of Drying Efficacy

To indicate the effectiveness of the drying regime, dried particles were evaluated via FTIR to determine the chemical differences exhibited from the use of AD vs. AD+FD. The hydroxyl (OH) stretching of alginate at 3405 cm$^{-1}$ is indicative of water content. By taking the ratio of this peak

*Novelty processing and smart delivery of Ganoderma Lucidum spores*

to a communal steady reference peak (carbonyl, C=O at 1713 cm$^{-1}$), the degree of "effective drying" is indicated [Max et al., 2004; Santagapita et al., 2012; Castro-Cabado et al., 2016].

$$\text{Drying Effectiveness} = \frac{\text{Intensity at 1713 cm}}{\text{Intensity at 3405 cm}} \qquad \text{Eqn. 3.11}$$

### 3.3.4.3.7 Microparticle Characterization: In-vitro Release Kinetics of GLS-A Microparticles

To control confounding variables, only GLS-A particles containing 2% GLS were subject to release studies (GLS-A 1-1 and 2-1). GLS-A microparticles were evaluated for their release of GLS in distilled water. This was investigated as a measure of crosslinking strength and thus give an indication of encapsulation profile. Water was used to avoid the confounding effects of other variables introduced by various pH, polarities, and viscosities (all influential on release kinetics from a drug delivery system [Jain et al., 2014]). Furthermore, many studies have not been able to attain matrix stability using alginate in neutral medium [Tønnesen et al., 2002; Sriamornsak et al., 2007]. At a neutral pH (intestinal), alginate's carboxylic acid groups ionize, and this fosters electrostatic repulsion between its chains – ultimately inducing swelling [Segi et al., 1989; Zhao et al., 2014]. Attaining this stability would therefore indicates the polymer suitability as a drug carrier when traversing the human intestine.

0.01g GLS-A microparticles was immersed in 2ml deionized water (pH ~6.8) at room temperature. A 300µl aliquot was taken at time-points that collectively attained 2 weeks. Each bath was replenished with 300µl fresh medium after each withdrawal to maintain the system sink. Release measurements were carried out in duplicate. The release calculation prior to accumulation is shown in eqn 3.12.

$$\text{Eqn. 3.12}$$

$$\text{Release \%} = \frac{\text{Amount GLS Released (mg)}}{0.2 \text{ (mg)}} \; x \; 100$$

The cumulative release was plotted by cumulating the GLS released from the formulated dose content of GLS in 0.01g of microparticles (equating to 0.2mg GLS, or 0.01% of the 2ml release bath).

$$\text{Cumulative Release (\%)} = \frac{\text{Total \% drug released at time}^{i}}{\text{Total potential release from dose (0.01\%)}} \qquad \text{Eqn. 3.13}$$

*Novelty processing and smart delivery of Ganoderma Lucidum spores*

Release baths were shaken at 100 RPM continuously to better mimic physiological conditions during release. The recording time intervals were created based on the previous experiments, which indicated that there was *little* initial burst in the first 60 minutes. Therefore, the release was examined after 20 minutes, 60 minutes, 24 hours, 96 hours, 1 week, and finally 2 weeks and analysed in duplicates as described in section 3.2.1. The aliquots were analysed with a UV spectrometer at 257nm for GLS quantification in the release.

### Release Calibration

Knowing that 257nm was a suitable absorbance for some desired extracts in GLS, the presence of GLS in the GLS-A microparticle release was measured against a calibration curve created by executing a full scan of raw GLS at 257nm (a peak at this wavelength was previously observed in section 3.3.2, verifying its relevance). A pure 1% w/v GLS solution is diluted to form concentrations 0 - 0.05%, from which GLS-A release was quantified.

## 3.4 Statistical Validation of Experiments

Analyses of Variance (ANOVA) was essential to verify the significance of repeated experiments. Fisher's F-statistic, based on the method of least squares is used for this estimate of significance. When interpreting result significance, statistical tests are conducted with at least 90% confidence, supported by p-values. While traditionally a 95% confidence level are employed in scientific work, 90% confidence levels can be more appropriate in small sample sizes. This was the case in extraction experiments, however larger samples in GLS-A particle fabrication allowed for a higher confidence level. In the case of PSGA yield optimization via machine learning, JMP statistical software was used to create a model and output with 95% confidence. Where more replicates were possible, significance tests were most accurate. The standard error of the mean was calculated across replicates and used for error bars in the graphical representation of results. **In all experiments**, in order to confirm statistical significance of variables, the p-value was calculated between variable groups using ANOVA (F-test) to test for *differences in the means*.

**Extraction experiments** (crude GLPS and PSGA) were carried out in replicates to improve statistical validity of results.

**GLS Extract Administration** to HOS cells were carried out in multiple cell plate administrations, and in replicate experimental extracts, to ensure repeatability and validity of administration results. Cell plate administration replicates were also tested for statistical *similarity* using ANOVA (F-test).

**GLS Encapsulation** generated distributions of droplets and particles, from which numerous were analyzed for size, shape, and surface, to validate the significance of the variables and setup employed.

*Novelty processing and smart delivery of Ganoderma Lucidum spores*

# Chapter 4

# Results and Discussion

## Introduction

Chapter 4 details and discusses the results obtained from the methods described in chapter 3, in 3 sections. **Section 4.1** presents the results of the polysaccharide (GLPS) and polysaccharide-ganoderic acid complex extraction from Ganoderma lucidum Spores. **Section 4.2** outlines the antitumour results of in-vitro culture of the GLS extracts with Human Osteosarcoma cells. **Section 4.3** presents the findings obtained from evaluating the fabrication of a GLS delivery system. Together these results will indicate the current feasibility of developing valuable Ganoderma lucidum extracts for healthcare and will suggest the workflow for the creation of a structure that can deliver these compounds (and others) safely and controllably to the body.

## 4.1 Extracting GLS Polysaccharides (GLPS)

Crude Polysaccharides were extracted from GLS using HWE and UAE, evaluating the effects of the solvent's *ethanol concentration* and the *extraction time*. The crude extract, termed GLPS, contains polysaccharides along with other water-soluble biocompounds that were not specifically removed (such as proteins and fibre which were not quantified [Yeh et al., 2010]). Essentially, this yield indicated the water-soluble components after being ethanol-washed. Many studies show greater bioactive promise of cruder extracts, because many water-soluble compounds and complexes such as proteins and triterpenoids (Ganoderic Acids for example) have acclaimed bioactivities – and many in fact foster synergistic pathways [Zhu et al., 2000; Liu et al. 2002; Liao et al., 2016; Hereher et al., 2018]. It is expected that D-Glucans, a well-documented polysaccharide possessing a potent immunoenhancing effect, form a significant proportion of the chemical composition of crude polysaccharides in GLS, and so the extracts are also analysed for their D-Glucan contents [Zhu et al., 2015].

## 4.1.1 High Performance Liquid Chromatography (HPLC): GLS

### 4.1.1.1 Chemical Profile: Which of the 3 GLS strains contained the polysaccharides?

HPLC was initially employed to show the distinction between 3 GLS strains, in order to verify the strain chosen for this project's investigations. Strains were sourced from either An Hui, Shan Dong or Long Quan, cultivated on either sawdust, grain, or woodlog respectively (GLS 1 − 3 respectively). The chromatogram shows the chemical profile of the strains after gentle extraction via room-temperature milling in *water*. The HPLC mobile phase is polar. With a polar mobile phase, polar compounds like polysaccharides will be eluted first and less polar compounds like triterpenoids will be eluted later on. Being a water extract, the samples are likely to exhibit a polysaccharide-heavy spectrum. The spectra show that GLS 1 and 3 contained more polar constituents (e.g. polysaccharides) as indicated by earlier elution. GLS 2 contained very few peaks at all. This could be a result of it being a triterpenoid-rich strain (requiring a less polar organic solvent to be extracted).
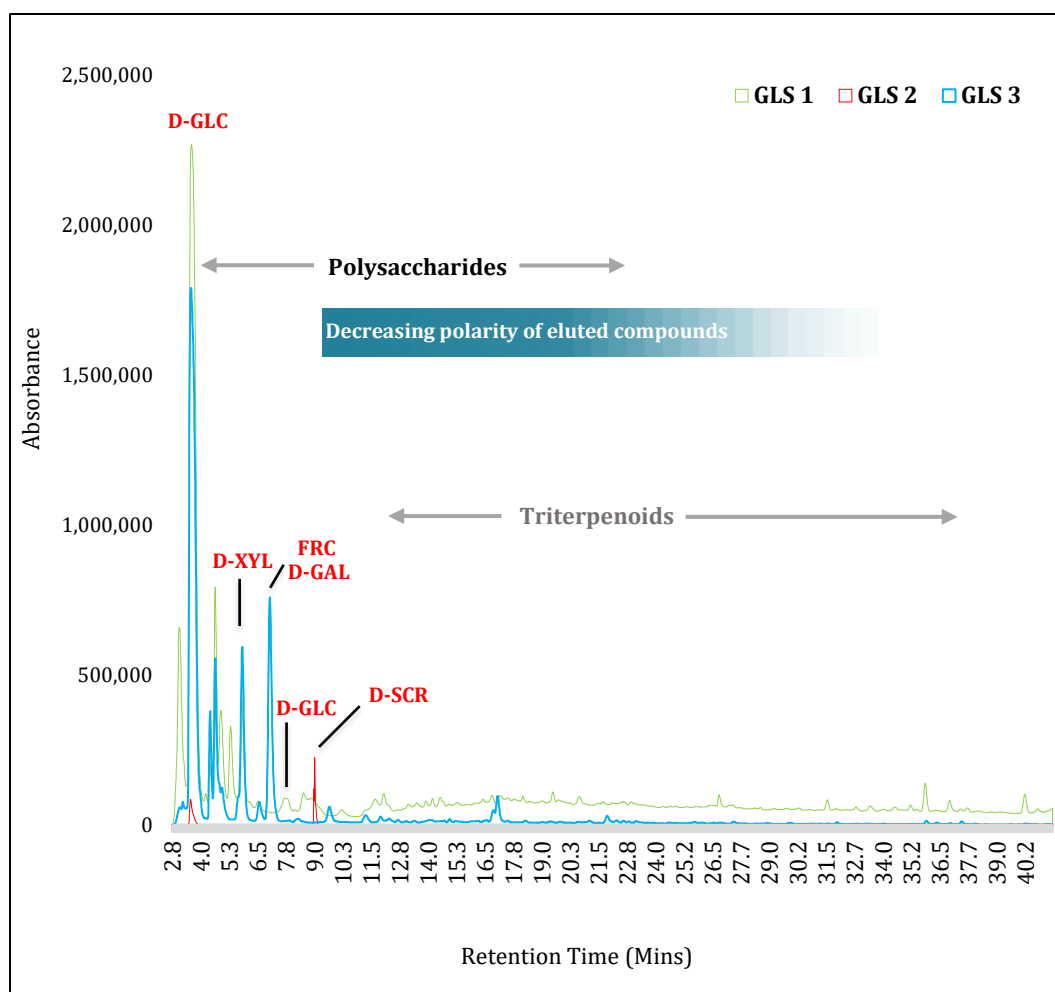


**Figure 4.1:** HPLC Spectra of water extracts of intact GLS 1/2/3 from either An Hui, Shan Dong or Long Quan respectively, cultivated on either sawdust, grain, or woodlog respectively. Wavelength 254 nm. Significant peaks labelled

*Novelty processing and smart delivery of Ganoderma Lucidum spores*

Table 4.1 shows the retention times for some of the above peaks (as recorded by HPLC), which are associated with monosaccharides in the GLS. It is important to note that due to geographical dependencies, the peak position of compounds would vary slightly across strains [Su et al., 2001]. The greater intensity of *early* peaks suggests that most strains did not yield many triterpenoids – typical of water-based samples (with the exception of some Ganoderic Acids such as B (6-7 min) in GLS 3, suggesting some water-soluble triterpenoids, or conjugates). Overall, GLS 3 appears to have a more diverse and intense monosaccharide content, in particular with respect to glucose, and therefore this strain is taken forward for this project.

| Retention Time (approx.) | Biocompound | Abbrev.* | GLS 1 | GLS 2 | GLS 3 |
|---|---|---|---|---|---|
| 4 | D-Glucose analogue | D-GLC | √ | | √ |
| 5.5 | D-Xylose | D-XYL | √ | | √ |
| 5.9 | Xylose, D-Rhamnose | XYL, D-RH | | | √ |
| 6 | D-Fructose | D-FRC | √ | | √ |
| 7 | Fructose, D-Galactose | FRC, D-GAL | √ | | √ |
| 7.5 | D-Glucose analogue | D-GLC | | | √ |
| 8 | Glucose, D-Mannose | GLC, D-MN | √ | | |
| 9 | D-Sucrose | D-SCR | √ | √ | |

**Table 4.1:** Approximate retention times of some monosaccharides that absorb in the GLS 1/2/3 strains tested [Yang et al., 2010; Sun et al., 2014]. *Abbreviations created for this work.

## 4.1.1.2 Chemical Profile: Approximating this strain's profile in water and ethanol

HPLC was then employed to define the approximate chemical composition of the *broken* form of GLS 3 in both water and ethanol prior to extraction (figure 4.2). As the aim of the forthcoming study is to evaluate the extractability of polysaccharides from broken GLS via water *and* ethanol, it is advantageous to understand the profile and rough distribution of crude compounds present in this particular strain in these solvents. Due to the high number of constituents, along with the knowledge that every strain has a slightly different chemical profile, it is challenging to identify all chemical peaks. Nonetheless, it was observed that the most significant spectral peaks occurred between 3 and 10 minutes, and between 12 and 14 minutes; regions characteristic of the elution time of monosaccharides and disaccharides, as well as some Ganoderic Acids in GLS [Chen et al., 2008; Yang et al., 2010; Zhao et al., 2014]. Table 4.2 lists some triterpenoids and monosaccharides in the two broken samples in the HPLC chromatogram.

*Novelty processing and smart delivery of Ganoderma Lucidum spores*
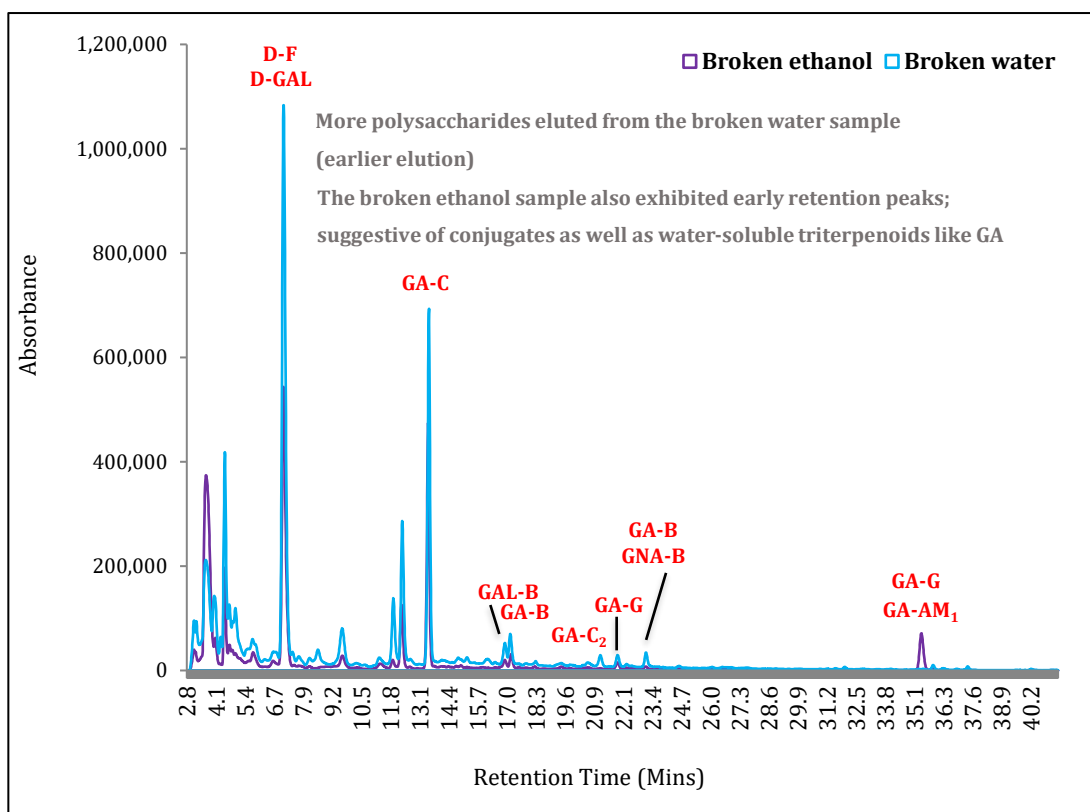
**Figure 4.2:** HPLC Spectra of water and ethanol extracts of broken from Long Quan cultivated on woodlog (GLS-3). Wavelength 254 nm. Significant peaks labelled

| Retention Time | Biocompound | Abbrev.* | Broken Water | Broken Ethanol |
|---|---|---|---|---|
| 13.8 | Ganoderic Acid C | GA-A | √ | √ |
| 16.6 | Ganolucidic acid B | GAL-B | √ | √ |
| 17.6 | Ganoderic Acid B | GA-B | √ | √ |
| 21 | Ganoderic acid $C_2$ | GA-$C_2$ | √ | |
| 22 | Ganoderic acid G | GA-G | √ | √ |
| 22.7 | Ganoderic Acid B, Ganoderenic Acid B | GA-B, GNA-B | √ | |
| 23 | Ganoderic Acid B, D-Galactose | GA-B, D-GAL | √ | |
| 35.5 | Ganoderic Acid G, Ganoderic acid $AM_1$, Glucuronic Acid | GA-G, GA-$AM_1$, GLC-A | | √ |

**Table 4.2:** Additional (approximate) retention times of some monosaccharides and triterpenoids from broken water/ethanol extracts of GLS [Wu et al., 2017; Yeung et al., 2021]. *Abbreviations created for this work.

In both extracts, polar compounds like polysaccharides are more quickly eluted into the polar mobile surrounding solvent, whereas non-polar compounds (like triterpenoids) have less affinity to the surrounding solvent and so elute later. Ethanol extracts eluted a number of triterpenoid-

*Novelty processing and smart delivery of Ganoderma Lucidum spores*

characteristic peaks later on at around 37 minutes and 120 minutes [Hsu et al., 2001; Cui et al., 2015]. Interestingly, water extracts also contained triterpenoic compounds - because some Ganoderic Acids are water-soluble, and many have also been isolated as conjugates of polysaccharides, which are water-soluble [Cao et al., 2017]. This indicates greater potential for scaling up water-based extraction.

### 4.1.1.3 GLS Form: Choosing between broken and intact GLS

In order to verify the use of broken vs intact GLS 3, literature was extensively surveyed (see chapter 2) to gauge the chemical differences between broken and unbroken (intact) spores. Broken spores are typically observed to be more yielding (in particular of D-Glucans), even after the sporoderm breakage process which has advanced via more efficient breakage technologies [Li et al., 2017]. Studies have therefore suggested a greater D-Glucan content in broken spores along with a higher biocompound cytotoxicity [Zhu et al., 2000]. Reasons include the smaller molecular weight of its bioconstituents [Sliva et al., 2003; Huang et al., 2006; Xie et al., 2006; Yue et al., 2008; Guo et al., 2009; Na et al., 2017]. The broken GLS water extract from figure 4.3 is replotted alongside the intact GLS water extract in 4.3. There is a chemical discrepancy between broken and unbroken GLS, whereby broken spores show a wider diversity of extracted compounds.
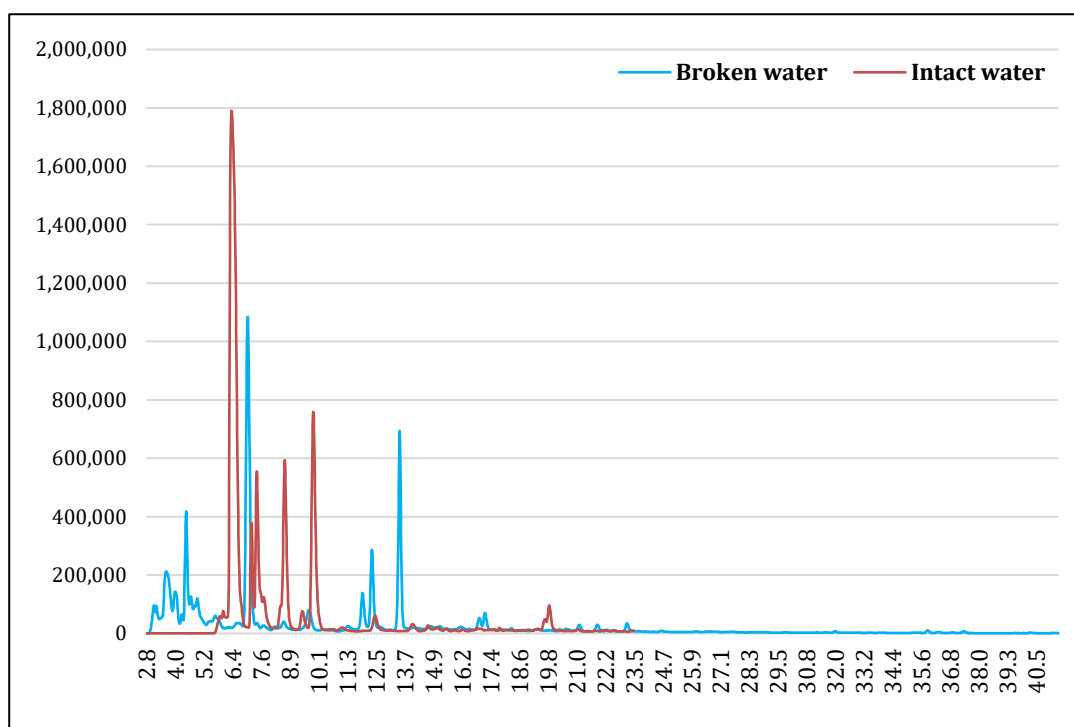


**Figure 4.3:** HPLC Spectra of water extracts of broken and intact GLS from Long Quan cultivated on woodlog. Wavelength 254 nm.

*Novelty processing and smart delivery of Ganoderma Lucidum spores*

With the inferred knowledge that:

- Both water and ethanol can effectively extract a variety of monosaccharides and triterpenoids from GLS,
- Valuable polysaccharides from GLS 3 (from Long Quan cultivated on woodlog) are most effectively extracted in water, and
- Broken spores have a greater diversity of extractable biocompounds than unbroken spores,

…the subsequent investigations will evaluate the degree of control had by extraction solvent and time on the nature of extract yield from broken GLS (Long Quan, GLS 3) extracted using HWE and UAE [Che et al., 2017; Qun et al., 2017].

## 4.1.2 Ganoderma lucidum Crude Polysaccharide (GLPS) Yield

The extraction of crude GL polysaccharides (GLPS) was attempted using both **hot water extraction** (HWE) and **ultrasound-assisted extraction** (UAE) to ascertain if extraction time and solvent polarity would influence the efficiency of the methods. The extraction methods were developed based on dissolution efficiency, which is known to be positively correlated to extraction efficiency. Following extraction, the freeze-dried supernatant was weighed as a dry-wt% of the initial 2g dry weight GLS input. A beige powder resulting from lyophilisation represented total crude polysaccharides (this includes other water-soluble compounds in the extract that were not removed such as proteins, fibres and water-soluble triterpenoids). The D-Glucan content of each GLPS was subsequently determined using the Phenol-Sulphuric Assay.

### 4.1.2.1 HWE: GLPS Yield

Temperature monitoring results are first presented (table 4.3 and figure 4.4). Subsequently, the crude GLPS yield from HWE are presented in table 4.4 as a % of initial GLS dry weight input.

**Hot Water Extraction Temperature Monitoring**

Temperature was monitored at 10-minute intervals using a solvent vial containing pure water or pure ethanol only. These tests determined the effect of HWE time on the temperatures of the

*Novelty processing and smart delivery of Ganoderma Lucidum spores*

two solvents in this study (water and ethanol), also indicating the sample compliance during the experimental time. These tests indicated that approximately 10 minutes is required from vial immersion in the bath, to attainment of the experimental temperature range for these solvents. It is assumed that once the sample reaches the maximum temperature achievable in the waterbath, its temperature and volume would not fluctuate given the static conditions in waterbath due to the closed vial caps [Teo et al., 2008]. It was demonstrated that 100% water samples could reach higher temperature than 100% ethanol after most time intervals.

| Sample | T = 0 | T = 10 | T = 120 |
|---|---|---|---|
| Pure Water | 21°C | 66 ± 0 °C | 74.5 ± 0.35 °C |
| Water 75: Ethanol 25 | 21°C | 65 ± 0.35 °C | 73.5 ± 0.35 °C |
| Water 50: Ethanol 50 | 21°C | 66.5 ± 0.35 °C | 73 ± 0 °C |
| Water 25: Ethanol 75 | 21°C | 66.5 ± 0.35 °C | 72.5 ± 0.35 °C |
| Pure Ethanol | 21°C | 65.5 ± 0.35 °C | 71.5 ± 0.35 °C |

Table 4.3: Temperature of pre-test solvent samples: HWE time-point temperature average +/- SE of 2 measurements. Time in minutes

In the inset of figure 4.4, the temperature recording from 10 minutes onwards is shown also, indicating the compliance of sample during the experimental temperature range (table 4.3).
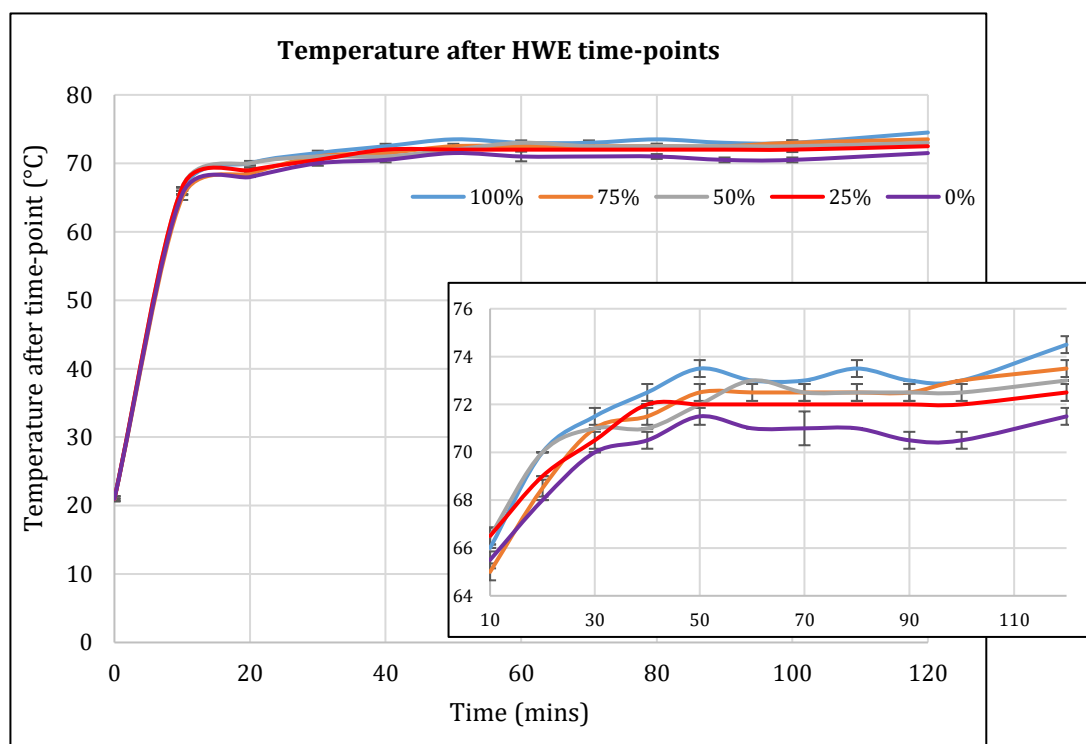


Figure 4.4: Temperature recording during HWE. Error bars represent SE of 2 measurements. Legend represents water content

*Novelty processing and smart delivery of Ganoderma Lucidum spores*

## HWE Yields of GLPS

The crude GLPS (dry weight) from HWE are presented in table 4.4 as a % of initial GLS dry weight input. Figure 4.5 plots the yield by extraction time and solvent composition.

| Water % | 40 min Crude GLPS (%) | 80 min Crude GLPS (%) | 120 min Crude GLPS (%) |
|---------|-----------------------|-----------------------|------------------------|
| 0 | 4.7 ± 0.2 | 2.6 ± 0.9 | 3.4 ± 0.5 |
| 25 | 2.9 ± 0.4 | 1.5 ± 0.6 | 4.9 ± 3.8 |
| 50 | 2.1 ± 0.5 | 1.3 ± 1.2 | 4.7 ± 0.1 |
| 75 | 6.5 ± 0.3 | 4.2 ± 0.3 | 2.1 ± 0.1 |
| 100 | 5.1 ± 0.2 | 5.9 ± 0.5 | 1.8 ± 0.1 |

**Table 4.4:** HWE crude polysaccharides as a % of initial GLS input. Crude Polysaccharides are ±SE of 2 experimental measurements
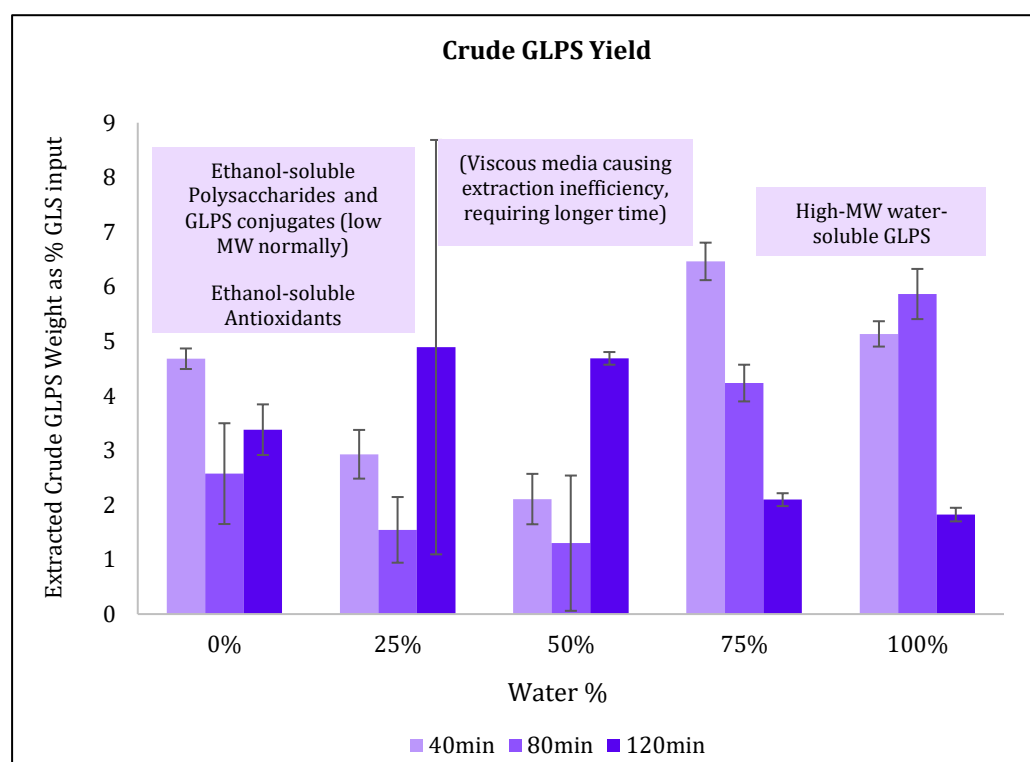


**Figure 4.5:** HWE crude GLPS yields after 40, 80 and 120m extraction with all 5 solvent concentrations. Error bars represent SE of 2 experimental measurements of crude GLPS. The effect of solvent and extraction time were both statistically significant at 90% confidence (p-value < 0.1). Prevalence of other compounds based on literature, and knowledge of the compounds' typical behaviour

*Novelty processing and smart delivery of Ganoderma Lucidum spores*

#### 4.1.2.1.1 Effect of HWE Extraction *Solvent* on Crude GLPS Extraction

Figure 4.5 shows the effects of the variable solvent on the yield of crude GLPS. All extracts were ethanol-washed, so that the determination of polysaccharides could be most accurate upon the removal of ethanol-soluble lipids and the denaturing of proteins – the latter relevant for spectroscopic analysis later on. Extraction results did not indicate a clear effect of solvent nor time on GLPS yield. Aqueous solvents were more effective at extracting crude GLPS at shorter extraction durations, yet ethanolic extracts generally favoured a longer extraction time with this difference attributed to a difference in yield composition. The most time-intensive extraction was most favourable when the extraction solvent was mixed, where the extraction is also most viscous. It is evident that the variables are likely to have confounding effects on each other whereby a longer extraction is more favourable using the high-ethanol solvents, in which the temperature was less intense owing to ethanol's lower heat capacity. Similarly, high-water extracts were favourable to GLPS yield at shorter durations. Figure 4.6 shows the average yield achieved at each solvent, across extraction times. There is a slight favour toward water-based extraction.

**Average Yield Across HWE times (by water content)**
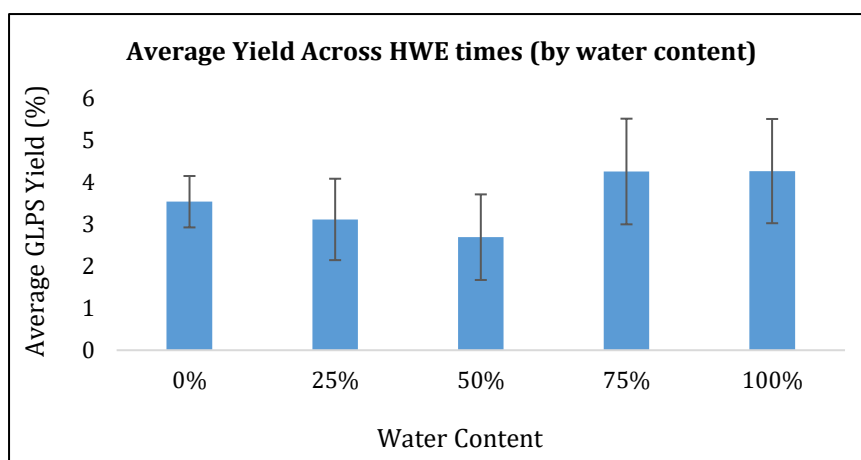
Figure 4.6: The average yield of each extraction solvent, averaged across extraction times. Error bars represent SE of groups

As a polar solvent, water extracts more polar compounds such as the sugars found in GLS (polysaccharides). Ethanol is less polar than water, and is traditionally used for the extraction of triterpenoids from food and plants. As ethanol extraction still contained comparably high crude GLPS yields, it is possible that the ethanol yield contained compounds that were conjugated to ethanol-insoluble compounds (i.e. water-soluble GLPS) – as indicated via the initial HPLC chromatograms. It is not uncommon to observe a high polysaccharide yield using ethanol [Lakshmi et al., 2003]. Indeed both solvents contain hydroxyl groups that facilitate the formation

*Novelty processing and smart delivery of Ganoderma Lucidum spores*

of hydrogen bonds and thus polysaccharide extraction [Pin et al., 2010; Razak et al., 2012]. Thus, whilst water is more effective at dissolving water-soluble compounds, ethanol can further enhance the extraction of many valuable polysaccharides and complexes [Lawther et al., 1995; Montañés et al., 2007; Hara et al., 2013].

Another important characteristic of water-ethanol mixtures is the increased viscosity of their binary mixtures. With greater viscosity (And packing density) a greater hindrance to effective particle interactions arises and thus there is a need for longer extraction to generate yield (see table 4.9). This is shown in a higher achievable yield in binary solvents when the extraction time is longest at 120 minutes. Furthermore, water-ethanol mixtures are non-ideal, rendering their molecular interactions disproportional to those of the individual solvents. The non-idealism of ethanol-water mixtures is considerable because of ethanol's non-polar hydrocarbon tail – therefore mixing them results in a dip in excess volume [Nikumbh et al., 2013]. Although slight, this resulting reduced solvent volume could negatively impact extraction efficiency if it results in lower solvent-GLS interaction [Marcus et al., 1989].

As crude polysaccharides are evaluated *physically* (not chemically) following evaporation of the extraction solvent, there is an inherent limitation in achieving selectivity. All extracts are likely to contain varying degrees of proteins as they were not specifically removed. Figure 4.7 shows the supernatant before drying, following HWE with different water-ethanol proportions. This indicates the distinction in compounds extracted by the 5 solvent compositions. While 100% water extraction produces a colloidal mixture following extraction (indicating the presence of large-molecule compounds that are not fully dissolved such as polysaccharides), increasing ethanol content generated insoluble fat globules in the extraction supernatant.
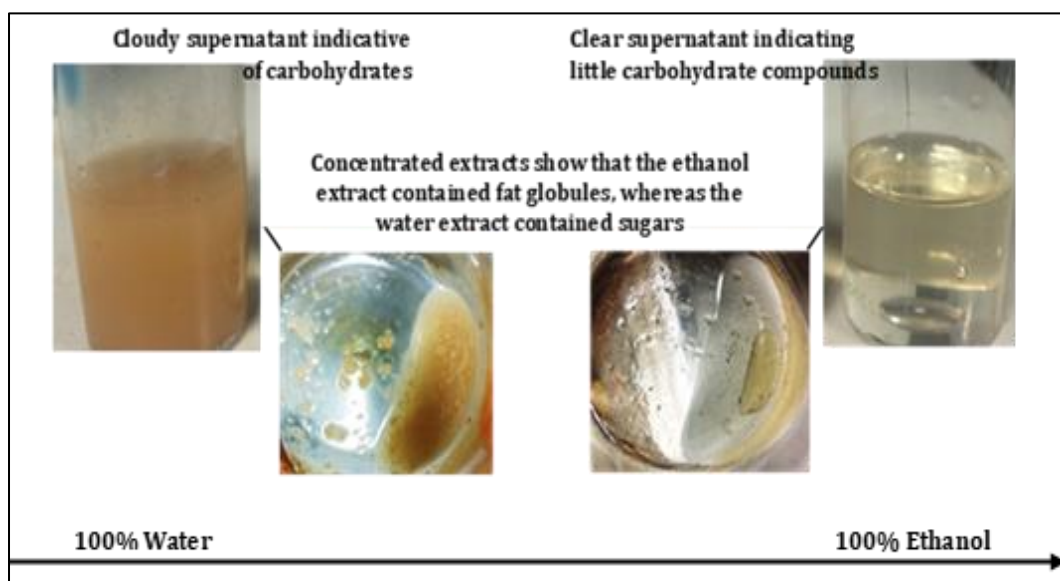


**Figure 4.7 Outset**: Supernatants after extraction 100% *Water* (left) compared to 100% *Ethanol* (right). Concentrated HWE Polysaccharides after heat-treatment, before ethanol-precipitation are shown between

*Novelty processing and smart delivery of Ganoderma Lucidum spores*

### 4.1.2.1.2 Effect of HWE Extraction *Time* on Crude GLPS Extraction

Figure 4.5 also showed the effects of the variable time on the yield of crude GLPS. Theoretically, with more time under the extraction conditions, GLS and solvent particles have increased dissolution opportunities and thus can undergo increased extraction [Sogi et al., 2010; Chan et al., 2013; Yanhua et al., 2014]. However a positive effect of time was not consistently the case in the extraction of GLPS. The most time-intensive extraction was most favourable when the extraction solvent was mixed. There was an expected confounding effect of solvent, in accordance with similar studies [Soria et al., 2014]. In the high-water extractions, greater yield was obtained using a shorter extraction. As water extracts are typically conducive of polysaccharide-rich yields, the increased time may have actually caused degradation to these typically thermolabile structures, possibly leading to a reduction in weight (or small enough to be washed out during washing) [Oliveira et al., 2012; Soria et al., 2014]. Furthermore, shorter extraction times typically yield of proteins and starch which are extractable and intact under milder conditions [Yeh et al., 2010; Usman et al., 2014; Sit et el., 2015; Zou et al., 2017; Altemimi et al., 2018; Lopez-Diago et al., 2018]. In high-ethanol extraction, GLPS yield was less conclusive as a function of time – likely because of ethanol's affinity to many conjugates in the polarity spectrum. In the average yield achieved at each time across solvents, there is a slight favour toward shorter extraction.
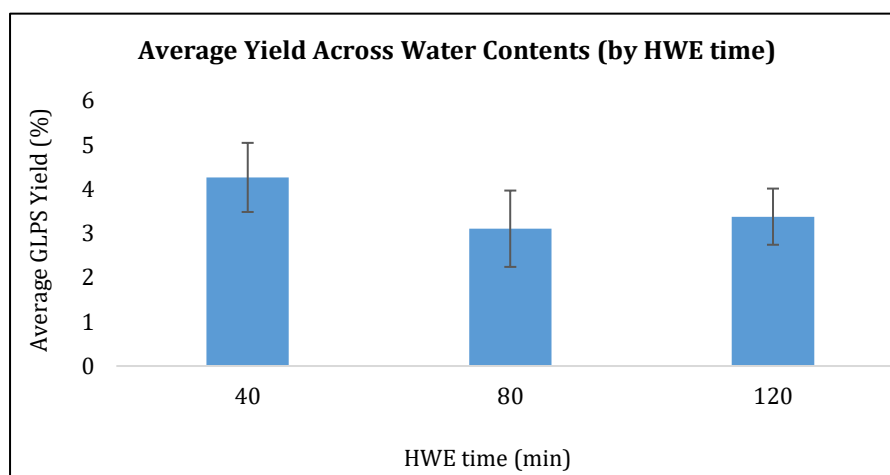


**Figure 4.8:** The average yield of each extraction time, averaged across extraction solvents. Error bars represent SE of groups

### 4.1.2.1.3 How the yield compares to recent literature

While 70˚C was chosen as the HWE temperature in this investigation, studies have used a wide range of temperatures to extract comparable polysaccharide yields, balancing extremities

*Novelty processing and smart delivery of Ganoderma Lucidum spores*

in other sources of extraction efficiency such as time. Extraction time is also diverse. As shown in table 4.5, higher temperatures have not always resulted in higher crude polysaccharide yields when surveying literature on similar studies, and the higher times have certainly not been associated with higher yields. This is a result of excessive degradation risk at higher times and temperatures – something especially true for polysaccharide structures [Chan et al., 2013]. Room-temperature extraction is increasingly common for polysaccharide isolation when *bioactivity* is under investigation – for example it was proven that lipid peroxidation was inhibited to a greater degree when administering a seaweed polysaccharide extracted at room temperature water compared to hot water [Ke et al., 2015; Ning et al., 2016; Choromanska et al., 2018; Hira et al., 2019]. Thus, this extraction study has shown the capability to extract relatively high crude polysaccharide yields from GLS despite a relatively moderate temperature and time compared to literature.

| Crude GLPS | This Study | Ruan et al., 2014 | Liu et al., 2014 | Huang et al., 2010 (b) | Cheng et al., 2013 |
|---|---|---|---|---|---|
| Yield | 6.5% | 0.37% | 1.5% | 5.1% | 8.98% |
| Extraction | HWE | HWE | HWE | HWE | HWE |
| Temperature | 70˚C | 100°C | 70˚C | 60˚C | 100°C |
| Duration | 40 min | 2 hours | 300 min | 77.3 min | 8 hours |
| Processing Chemicals* | - | - | - | Sodium hydroxide Hydrochloric Acid/Acetone-wash | - |

Table 4.5 Experimental comparison of Crude PS Yield extracted using HWE with literature. *Ethanol-washing not included

## 4.1.2.2 HWE GLPS Characterisation via D-Glucan Content

Characterisation of GLS extracts was principally via D-Glucan quantification in the extract, and was based on a chemical assay established by Dubois et al. in 1956. By evaluating its monomer form *D-Glucose,* hydrolysed using the phenol-sulphuric acid assay, D-Glucan content can be indicated in each crude GLPS sample. Absorbance was measured at the wavelength absorbed by D-Glucose monomers (~485nm), and a calibration curve allowed conversion of absorption value into D-Glucose equivalents and thus D-Glucan content. In most cases, a higher crude dry yield corresponded to a higher detected D-Glucan content. However, this was not always the case, suggesting that certain experimental conditions were more conducive to the extraction of D-Glucans.

*Novelty processing and smart delivery of Ganoderma Lucidum spores*

### 4.1.2.2.1 D-Glucose Calibration Curve

The calibration curve was prepared from pure D-Glucose at 485.05nm and is shown in figure 4.9. The subsequent sections present the corresponding results of the D-Glucan extraction.
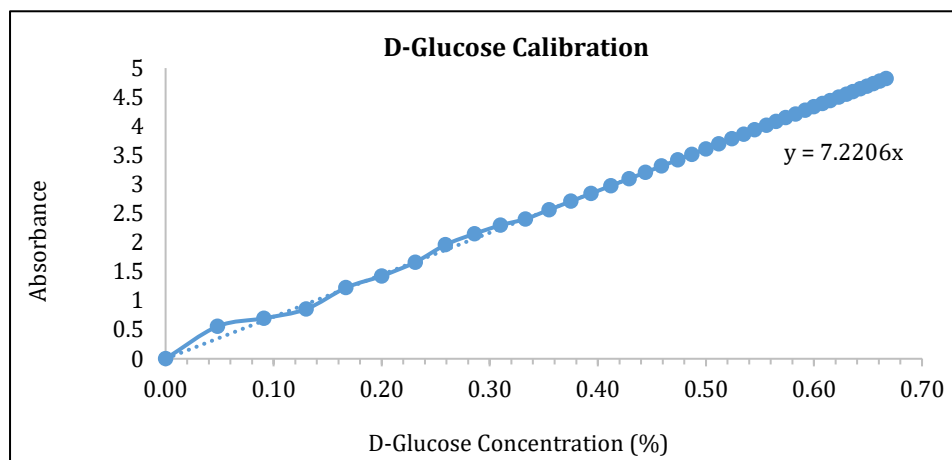


**Figure 4.9:** D-Glucose Calibration created via the 485.05 reading over D-Glucose Concentrations

The content of D-Glucans in each HWE GLPS extract is shown in figure 4.10 where the effects of HWE solvent and time are presented. The full absorbance spectra over the 400-600nm UV-Vis region at each HWE time/solvent is available upon request. Using the full spectra, peaks at 485.05nm show the absorption of D-Glucose monomers after each extraction time-point and for each solvent, from which the final yield is plotted. HWE GLPS showed a maximum D-Glucan content of 0.59% (via D-Glucose equivalents), suggesting considerable gains over existing literature.
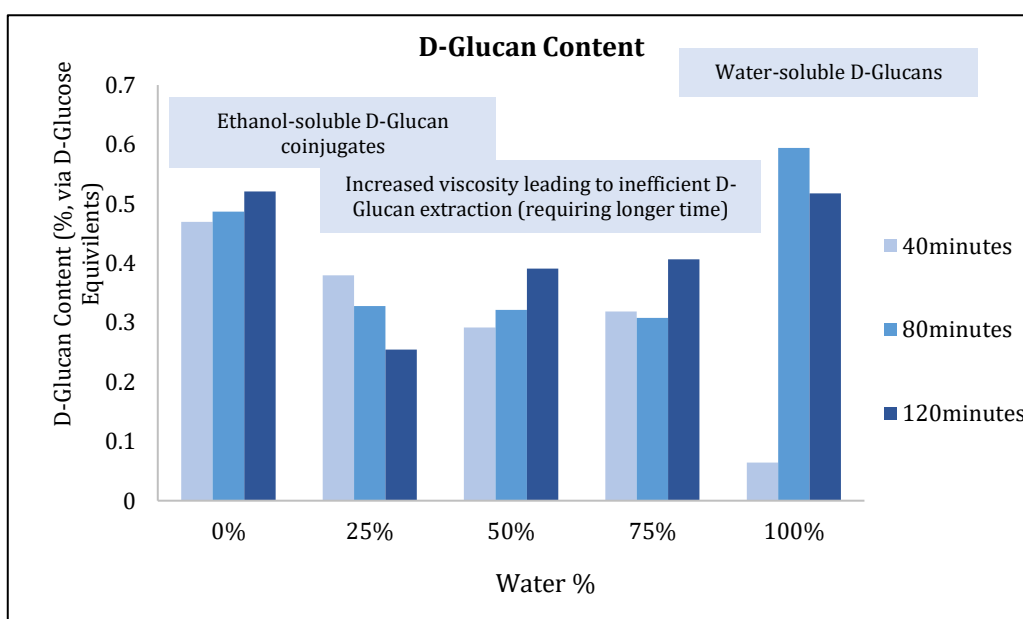


**Figure 4.10:** D-Glucose content of HWE GLPS by time (40-120 minutes) across solvent spectrum. The effect of solvent and extraction time were both statistically significant at 90% confidence (p-value < 0.1).

*Novelty processing and smart delivery of Ganoderma Lucidum spores*

### 4.1.2.2.2 Effect of HWE Extraction *Solvent* on D-Glucan Content

The results show that 100% water was the most effective extraction solvent for D-Glucan extraction, in line with the extraction of crude polysaccharides. The polar nature of pure water is more capable of extracting polar D-Glucan polysaccharides in-keeping with dissolution logic. Adsorption of water onto polar sites of the GLS biomass matrix weakens the bonds between the polysaccharides and the matrix, thus enhancing desorption [Brady et al., 1987]. Interestingly, ethanol also showed high extraction efficiency, because indeed both solvents contain hydroxyl groups that facilitate the formation of hydrogen bonds and thus polysaccharide extraction [Pin et al., 2010]. Furthermore, less polar compounds could be dissolved as "conjugates" to the polar D-Glucan structures at the experimental conditions employed [Mlyuka et al., 2016; Qun et al., 2017]. These assumptions were also previously made. The specific heat capacity of ethanol is just 2.46 Joules/gram°C, and so ethanol heats up faster given the same amount of supplied heat energy. This places ethanol extraction at an efficiency advantage over water, possessing a much higher specific heat capacity of 4.184 Joules/gram°C [Fink et al., 2014; Plaza et al., 2015]. Thus, to increase the temperature of 1g water by 1°C, more energy needs to be added – justifying the gain in yield using ethanol at the shorter extraction times. It should be noted that the triple-helix structure to which some D-Glucans in GL have been shown to conform, becomes unstable in strong ethanol concentrations. This renders resulting antitumour and antioxidant activity less effective [Gopinath et al., 2014; Liu et al., 2018].

The increase in hydrogen interactions and the dielectric constant of a binary mixture increase packing density, resulting in higher viscosity compared to the pure solvents, and a resulting lower capacity to create new bonds that foster extraction via dissolution [Resa et al., 2004; Gong et al., 2011]. Yield inefficiency resulted. Furthermore, these water-ethanol mixtures are non-ideal, rendering their molecular interactions disproportional to those of the individual solvents. For ethanol-water binary mixtures, this non-idealism is especially considerable because of ethanol's non-polar hydrocarbon tail. Mixing these solvents results in a dip in excess volume, and although small, this reduction in volume could reduce extraction efficiency if it results in lower solvent-GLS interactions [Marcus et al., 1989; Nikumbh et al., 2013].

### 4.1.2.2.3 Effect of HWE Extraction *Time* on D-Glucan Content

Typically, with more time subject to the extraction conditions, GLS and solvent particles have increased dissolution opportunities and thus can undergo increased extraction [Sogi et al., 2010; Yanhua et al., 2014]. However it was previously found that crude GLPS yield was highest at reduced HWE time, unless a binary mixture was employed – in which case shorter times were favourable. Benefits of reduced time could be explained by the degradation of some

polysaccharides at longer extraction times, and the subsequent extraction of lower-molecular weight polysaccharides at the increased duration that were washed away or had lower physical weight. In contradiction to the crude GLPS extraction, D-Glucans were most effectively extracted after *longer extraction* times. Studies have more recently shown that while low-intensity extraction favours crude polysaccharides yield, D-Glucans specifically have traditionally required longer times or higher temperatures. This is likely attributed to the triple-helix structure of D-Glucans, demanding a more intense extraction process [Liu et al., 2018]. Some nutraceutical extraction studies have observed that the extraction time has a strong positive effect on D-Glucan yield when temperature is set around 80°C and solvent:solid ratio is 20:1 – but there is a time threshold after which the yield degrades [Mustafa et al., 2011]. This *maximum* threshold would depend on the extraction solvent employed (among other things) – in this study the extraction carried out with 100% water indicates a possible maximal yield at 80 minutes; in line with many existing studies [Yanhua et al., 2014].

### 4.1.2.2.4 How the Content of D-Glucans compares to Recent Literature

Table 4.6 shows comparative literature on the extraction of D-Glucans from GL. While 70°C was chosen as the HWE temperature in this investigation, studies have used a wide range of temperatures to extract comparable D-Glucan yields, owing to variations in the HWE parameters elsewhere – a prime example being extraction time [Jing et al., 2017]. As shown in table 4.6, neither higher temperatures nor higher times have been associated with higher D-Glucan yields. Furthermore, many studies have shown better bioactive assay results using low-temperature extracts - even if this means forgoing total extraction yield [Choong et al., 2018]. This extraction study has shown the capability to extract a relatively high D-Glucan yield from GLS despite a temperature and time that are both below much of literature.

| GL D-Glucan | This Study | Bao et al., 2002 | Cui et al. 2006 | Chang et al., 2004 | Cheng et al., 2013 | Nguyen et al., 2015 |
|---|---|---|---|---|---|---|
| Yield | 0.59% | 0.15% | 10.5% | 0.4% | 2.25% | 0.067% |
| Extraction Method | HWE | HWE | HWE | HWE | HWE | HWE |
| Temperature | 70°C | 100°C | 60-65°C | 100°C | 100°C | 130°C |
| Duration | 80 min | 6-10 h | 6 h | 6 h | 8 h | 45 min |
| Processing Chemicals* | - | Trichloroacetic acid | - | Cetylpyridinium chloride, Amyloglucosidase, Protease | - | - |
| Cancer Action | - | - | - | Increased TNF-α production | - | - |

**Table 4.6:** Experimental comparison of GLS D-Glucan Yield from HWE with literature. *Ethanol-washing not included

*Novelty processing and smart delivery of Ganoderma Lucidum spores*

### 4.1.2.3 HWE GLPS Characterisation via Phenolic Compounds

The extraction of these compounds was carried out as they are established antioxidants, and have shown significant potency when extracted from GL [Jing et al., 2017; Viera et al., 2017; Choong et al., 2018]. The yield was evaluated by recording the extract absorbance in a UV range typically absorbed by these compounds, *400-430 nm*. An example spectrum from the 80 minute HWE shows the absorbance at this wavelength range. The absorbance at 402nm is subsequently shown in figure 4.11 for all HWE GLPS samples. As expected, ethanol extraction was most effective in extracting these antioxidative compounds, due to its ability to extract a broader polarity of compounds [Do et al., 2014; Sun et al., 2015; Viera et al., 2017]. Furthermore ethanol-extracted phenolic compounds have been found to exhibit greater antioxidant capacities than those extracted in water and they are typically more extractable using ethanol [Mello et al., 2010; Sun et al., 2015; Santos et al., 2016]. Water shows extraction efficiency here, however is likely to contain water-soluble compounds detected in this UV range too – proteins and some carbohydrates specifically.
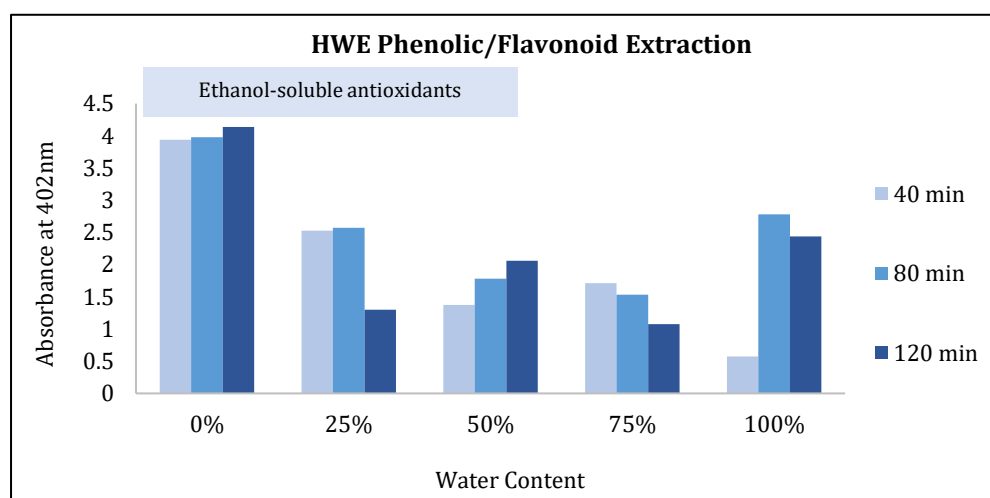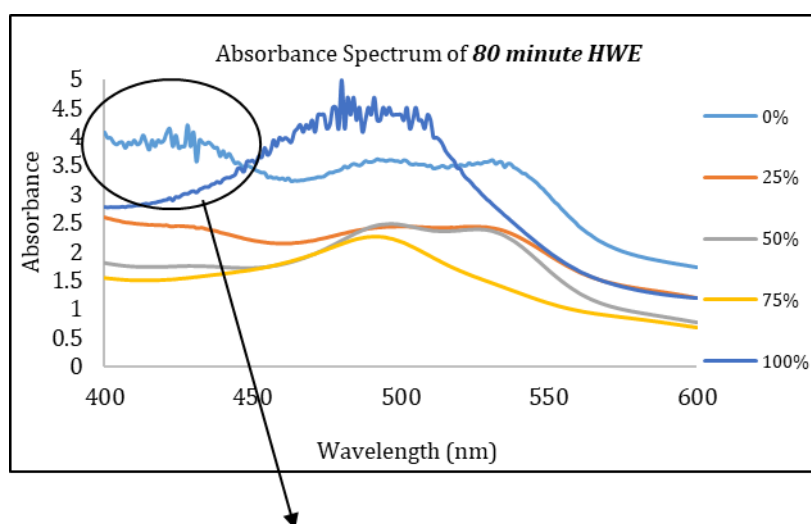


**Figure 4.11:** Ethanol-soluble compounds following HWE: *antioxidant compound extraction.*

*Novelty processing and smart delivery of Ganoderma Lucidum spores*

### 4.1.2.4 UAE: Crude Polysaccharide Yield (GLPS)

Temperature monitoring results are first presented (table 4.7 and figure 4.12). Subsequently, the UAE crude extract was analysed in the same way as HWE crude polysaccharides.

#### Ultrasound-Assisted Extraction Temperature Monitoring

Once again, dummy solvent vials were used to determine the effect of UAE cycling pattern on the temperatures using 100% water and ethanol. It was demonstrated that 100% water samples could reach the highest temperature by the end of each extraction period (55 +/- 2.4 °C), indicating an efficient extraction solvent. Yet, 100% ethanol samples could *heat up more quickly* owing to its lower heat capacity (2.46 Joules/gram°C vs water's 4.19 Joules/gram°C) [Girard, 2009]. According to the tests, the lowest temperatures would be maintained in the samples treated with ultrasound using 0.5-second cycles.

| Sample | T = 0 | 0.5sec Cycling | 20sec Cycling | 60sec Cycling |
|---|---|---|---|---|
| Pure Water | 21°C | 54.5 ± 0.5 °C | 61 ± 0 °C | 64.5 ± 0.5 °C |
| Water 75: Ethanol 25 | 21°C | 36.5 ± 0.5 °C | 53 ± 0 °C | 55 ± 0 °C |
| Water 50: Ethanol 50 | 21°C | 50 ± 0 °C | 55.5 ± 0.5 °C | 60 ± 0 °C |
| Water 25: Ethanol 75 | 21°C | 41 ± 1 °C | 53 ± 0 °C | 60.5 ± 0.5 °C |
| Pure Ethanol | 21°C | 40.5 ± 0.5 °C | 53 ± 0/5 °C | 61 ± 0 °C |

**Table 4.7:** Temperature of pre-test solvent samples: UAE time-point temperature average +/- SE of 2 measurements
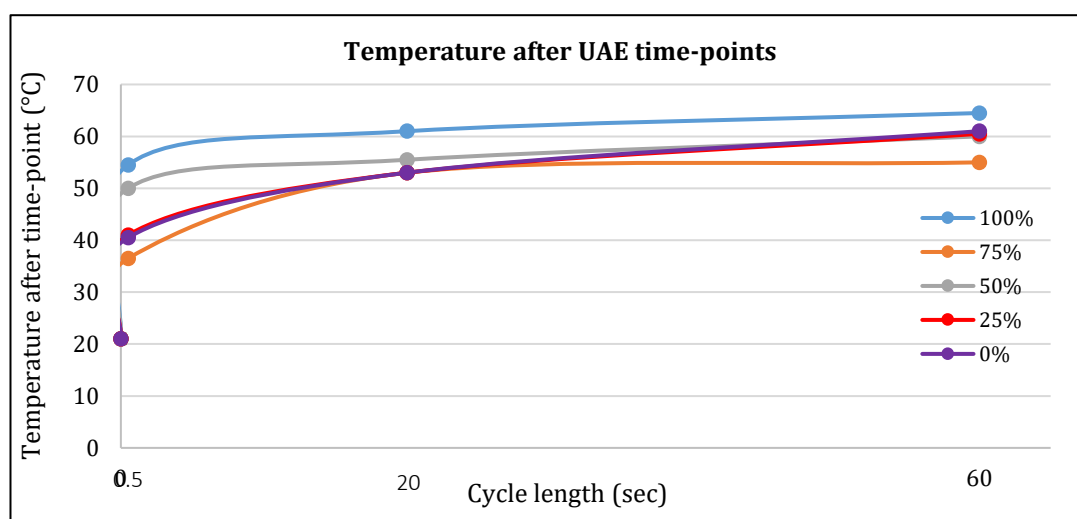


**Figure 4.12:** Temperature recording during UAE. Error bars represent SE of 2 measurements. Legend represents water content

*Novelty processing and smart delivery of Ganoderma Lucidum spores*

## UAE Yields of GLPS

The yield is presented in table 4.8. Figure 4.13 plots the yield by extraction time and solvent composition.

| Water (%) | 0.5 sec Crude GLPS (%) | 20 sec Crude GLPS (%) | 60 sec Crude GLPS (%) |
|---|---|---|---|
| 0 | 2.5 ± 0.6 | 4.1 ± 0.2 | 0.1 ± 0.1 |
| 25 | 3.1 ± 0.4 | 0.4 ± 0.1 | 5.6 ± 1.7 |
| 50 | 3.0 ± 0.4 | 1.1 ± 0.1 | 0 ± 0.0 |
| 75 | 0.6 ± 0.6 | 1.5 ± 0.5 | 6.1 ± 2.5 |
| 100 | 4.9 ± 0.1 | 1.3 ± 0.1 | 2.1 ± 0.8 |

**Table 4.8:** UAE crude polysaccharides as a % of initial GLS input. Crude Polysaccharides are ± SE of 2 experimental measurements

### 4.1.2.4.1 Effect of UAE Extraction *Solvent* on Crude GLPS Extraction

UAE extraction of GLPS showed little dependence on ethanol concentration in the extraction solvent. As was the case with HWE, extraction was efficient using ethanol as well as water, owing to polar/non-polar conjugates in the organism as well as ethanol-soluble polysaccharides in the ethanol yield. The increased viscosity and packing density of cavitation media (such as the case with binary non-ideal ethanol-water mixtures) has been reported to intensify the cavitation effects of UAE, thus enhancing extraction intensity. In principle, when greater energy is required to form bubbles, greater energy is then released upon their collapse; thus increasing extraction efficiency. However, this effect was not observed here. The increased viscosity and increased packing density of non-ideal binary ethanol-water mixtures instead hindered ultrasonic vibrations through resistance; possibly justifying lower extraction efficiency for the ethanol-water mixtures [Dutta et al., 1956; Tzanakis et al., 2017].

### 4.1.2.4.2 Effect of UAE Extraction *Time* on Crude GLPS Extraction

There was little evidence of a cycle length effect on GLPS yield via UAE. When the more viscous extraction solvents are employed (slightly the case with the ethanol-water mixtures), there is a greater need for longer extraction time to combat greater media resistance. This is because more kinetic energy is required to achieve the same cavitational effects in more viscous media [Dutta et al., 1956; Tzanakis et al., 2017]. In these samples, the longer cycle length (shown

to attain a temperature ~5°C higher than the shorter cycle lengths) was more conducive of a higher GLPS yield.
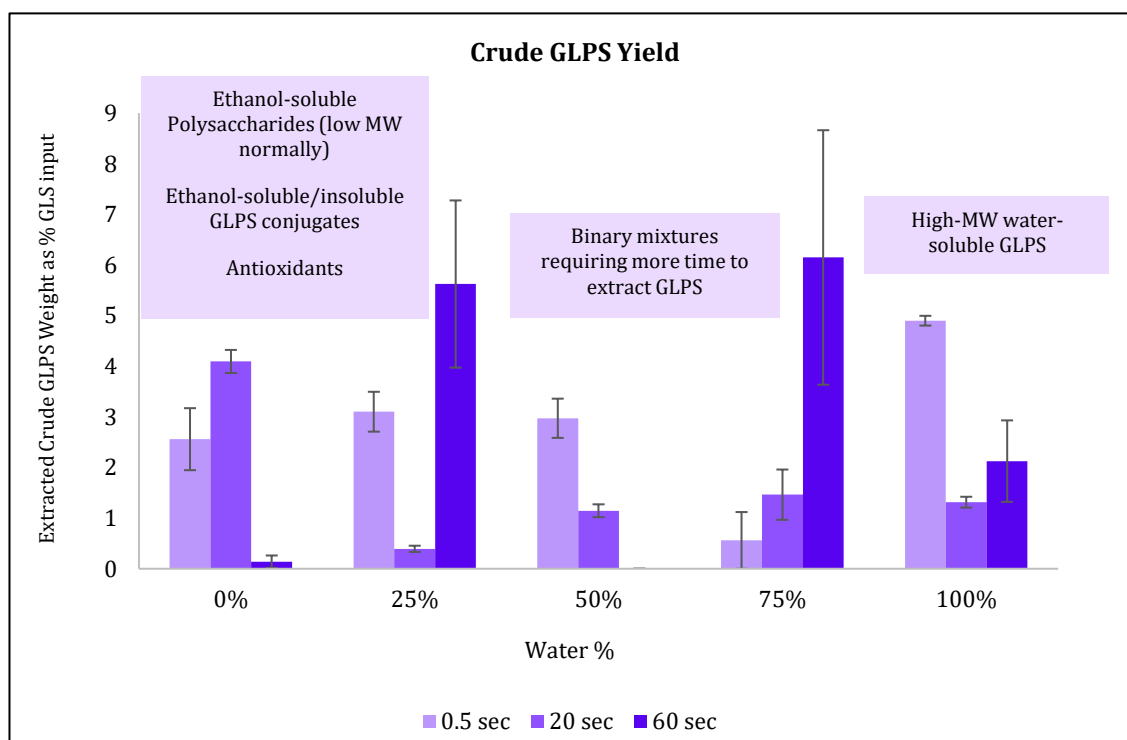


**Figure 4.13:** UAE crude GLPS as a % of initial GLS input after 0.5, 20, and 60-second cycles across all 5 solvent concentrations. Error bars represent SE of 2 experimental measurements. The effect of solvent and extraction time were both statistically significant at 90% confidence (p-value < 0.1). Prevalence of other compounds based on literature, and knowledge of the compounds' typical behaviour

In other samples, this extreme cyclic pattern could lead to molecular weight loss (and thus physical weight loss), also potential depletion during ethanol-washing [Liu et al., 2015; Chandegara et al., 2015; Tian et al., 2017]. Greater efficiency of pulsating UAE (0.5 second cycles) is in-keeping with literature and is attributed to increased permeation of cell membranes via pulsing behaviour, resulting increased diffusivity and mass transfer of the biomolecules [Ersus et al., 2010; Pan et al., 2012; Kumari et al., 2018; Sahin et al., 2018].

## 4.1.2.5 UAE GLPS Characterisation via D-Glucan Content

D-Glucan content was then evaluated in the UAE samples. The content of D-Glucans in each UAE GLPS extract is shown in figure 4.14 where the effects of solvent and time are presented. The full absorbance spectra over the 400-600nm UV-Vis region for HWE at each

extraction time/solvent is available upon request. From the full spectra, peaks at 485.05nm show the absorption of these D-Glucose monomers after each extraction time-point and for each solvent, from which the final yield below is plotted.
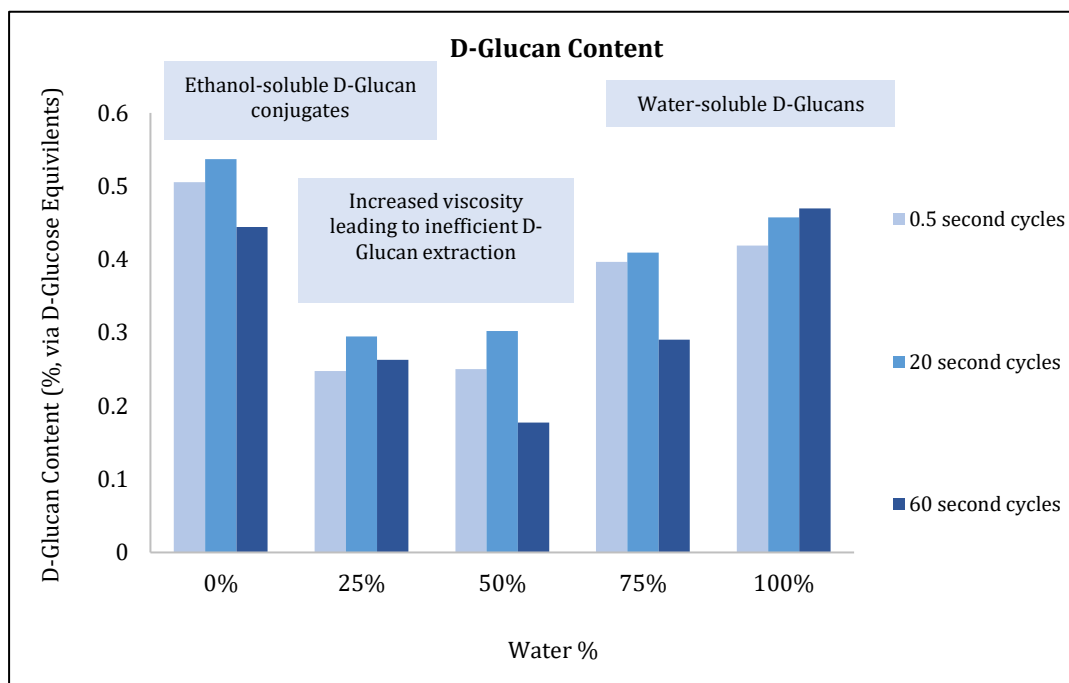


**Figure 4.14:** D-Glucose content of UAE GLPS by Cycle Time (0.5-60s per cycle) across solvent spectrum. Total sonication time: 2 minutes. The effect of solvent and extraction time were both statistically significant at 90% confidence (p-value < 0.1). UV readings were taken of one replicate once only, and thus standard errors could not be calculated

### 4.1.2.5.1 Effect of UAE Extraction *Solvent* on D-Glucan Content

In UAE, 100% water and 100% ethanol were clearly the most effective D-Glucan extraction solvents. UAE, as previously mentioned, has shown greater efficiency when using ethanol owing to greater viscosity-induced cavitational intensity [Wang et al., 2018]. This is because the increase in hydrogen interactions and dielectric constant of the binary mixtures could increase packing density, resulting in higher viscosity compared to the pure solvents [Resa et al., 2004; Gong et al., 2011]. As mentioned previously, UAE can benefit from the viscosity of a solvent undergoing ultrasonic cavitation [Tzanakis et al., 2017]. This is because greater energy is required to form bubbles, and thus greater energy is subsequently released upon their collapse; increasing extraction efficiency [Wang et al., 2018]. For ethanol-water binary mixtures, non-idealism is especially considerable because of ethanol's non-polar hydrocarbon tail. Therefore

*Novelty processing and smart delivery of Ganoderma Lucidum spores*

mixing them results in a dip in excess volume [Nikumbh et al., 2013]. Although slight, this resulting reduced solvent volume could negatively impact extraction efficiency if it results in lower solvent-GLS interaction [Marcus et al., 1989]. This, along with greater particle density in a more viscous solvent, may explain why the most viscous solvent (the binary mixtures) extracted less D-Glucans. Indeed, it may have hindered ultrasonic vibrations through greater resistance. Figure 4.15 and table 4.9 show the observed correlation between solvent viscosity and yield in this investigation.

| Water:Ethanol | Viscosity *millipoise* |
|---------------|------------------------|
| 100:0 | 8.94 |
| 75:25 | 20.04 |
| 50:50 | 23.54 |
| 25:75 | 18.66 |
| 0:100 | 10.96 |

**Table 4.9:** Viscosity of the 5 water:ethanol ratios employed in this work
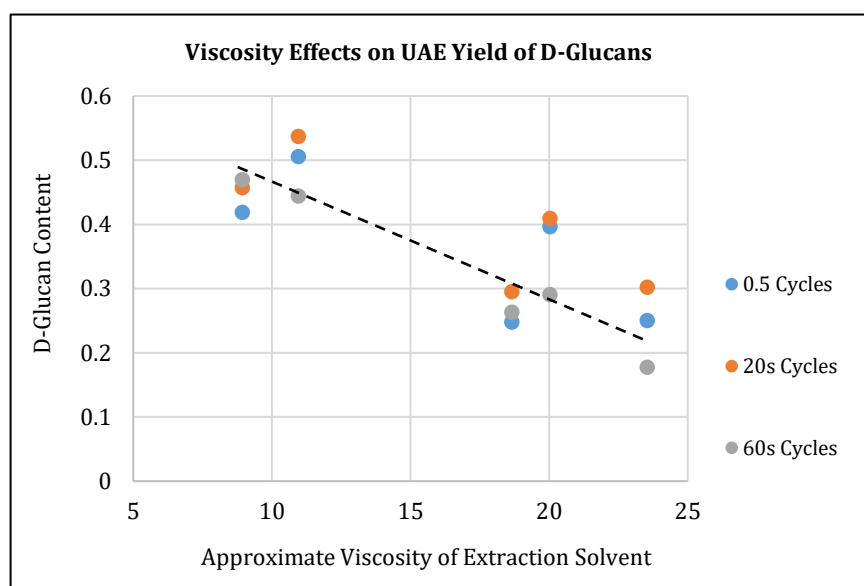


**Figure 4.15:** Viscosity correlation with D-Glucan content pf UAE GLPS samples – Viscosity appears to be negatively correlated with yield

Evidently, rather than viscosity-induced, the extraction of D-Glucan polysaccharides is likely owing to the extraction of more ethanol-soluble polysaccharides – suggesting that UAE may have kinetic advantages over HWE for the extraction of ethanol-soluble constituents of GL.

*Novelty processing and smart delivery of Ganoderma Lucidum spores*

### 4.1.2.5.2 Effect of UAE Time on D-Glucan Content

UAE employing shorter cycles was generally most yielding of D-Glucans. As previously discussed for D-Glucan extraction, the increased intensity when cycles were 0.5 seconds long with 0.5 seconds of rest, there was a slight increase in temperature caused by greater cavitation effects. This may favour extraction of D-Glucans specifically – even though it was detrimental to crude GLPS and other water-soluble compounds.

### 4.1.2.6 UAE GLPS Characterisation via Phenolic Compounds

The absorbance at 402nm is shown in figure 4.16 for UAE samples, where phenolic and flavonic compound absorbance is circled.
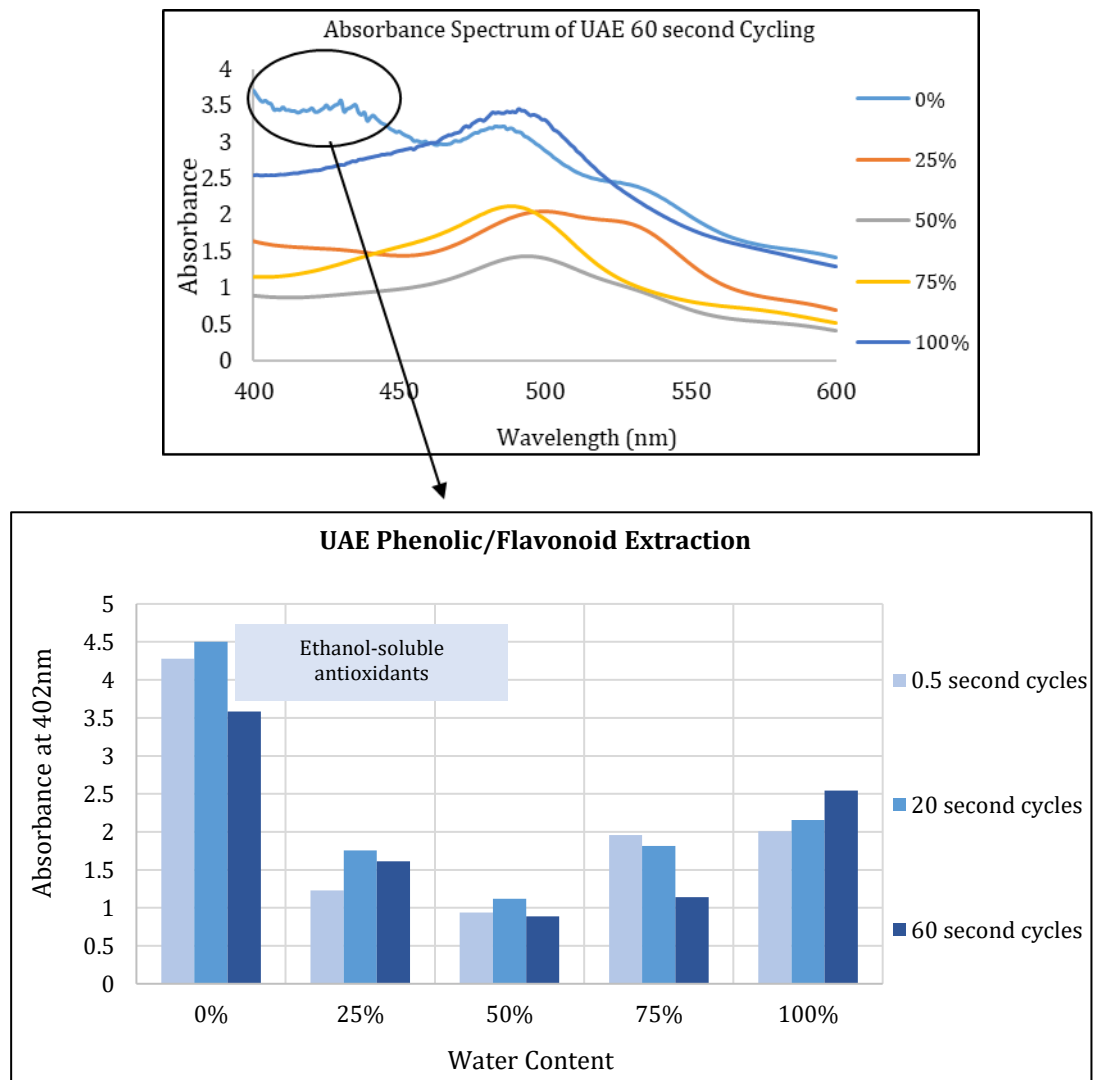


**Figure 4.16:** Ethanol-soluble compounds following UAE: *Antioxidant compound extraction.*

### 4.1.2.7 Extraction of GL Polysaccharides (PS) from GLS: Conclusions

An extraction process needs to be *scalable* with respect to resources required as well as yield efficiency. In this investigation, crude polysaccharides (GLPS) from broken GLS were extracted using both HWE and UAE, and were subject to different solvents and extraction time. Ethanol demonstrated a strong ability to also extract antioxidant compounds, typically detected as phenolic or flavonic compounds in the UV-Vis spectrum. This section observed that polysaccharides could be extracted from GLS almost comparably using the two extraction techniques. Differences in extraction quantities between the two methods can be attributed to the mechanisms exerted on the raw material – hence their physiochemical characterisation needs further study to further evaluate their effects on the biocompounds. The effects of solvent and extraction time were evaluated in each technique; however the notably significant variable was extraction solvent, whereby the investigations revealed that pure water and ethanol (not mixtures) were most effective for extracting GLPS via HWE and UAE.

## 4.1.3 Extracting a Polysaccharide-Ganoderic Acid (PSGA) Complex

PSGA was extracted using HWE optimized with supervised machine learning via Response Surface Methodology (RSM). For this investigation, HWE is optimized for the yield of smaller constituents like GA, *along with* water-soluble polysaccharides. Experimentally, this implicated an open (uncapped) extraction system that has been shown more preferential to small-molecule extraction, along with a longer extraction time [Michel et al., 2001; Mantell et al., 2003; Hilz et al., 2006; Povedano et al., 2014]. The effects of *extraction time* and *solvent dilution* were optimized with respect to PSGA yield from GLS using HWE, and a subsequent optimisation model is created using experimental results.

### 4.1.3.1 PSGA Calibration Curve to Quantify Yield

The presence of these PSGA biomolecules in GLS was confirmed by executing a full scan of raw GLS, and observing a peak at 257nm. This was then used to create a calibration curve of pure GLS to subsequently calibrate the absorbance of the PSGA samples.

As previously noted, this investigation on solvent ratio (GLS dilution) implicated the *same GLS content* in *different solvent volumes.* To avoid the confounding bias of greater extraction capacity, two perspectives were considered: the *total extract yield* and *extraction efficiency* – the latter

controlling for greater total volume. Furthermore, while the total yield would indicate the benefits of one technique over another in absolute terms, the efficiency would indicate what drives extraction efficiency.
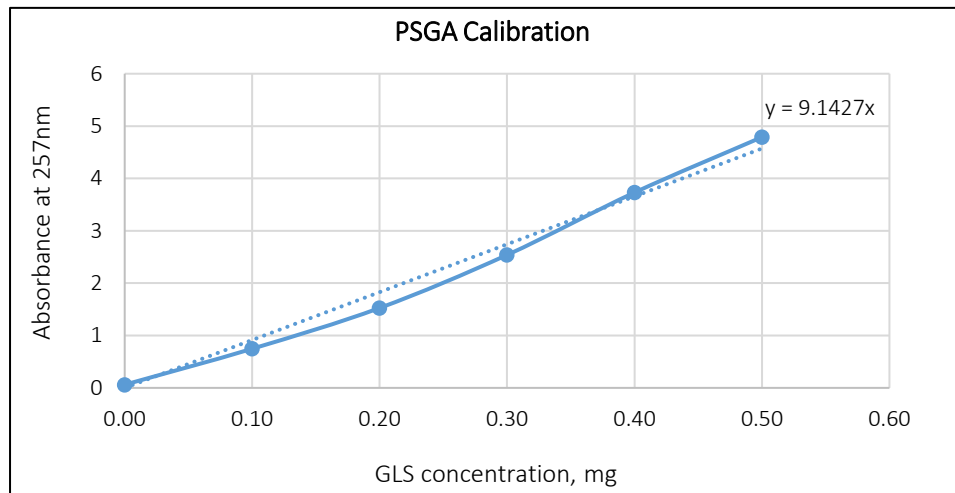


**Figure 4.17:** PSGA calibration created via the 257nm reading over GLS Concentrations

## 4.1.3.2 PSGA Extraction: Total Yield

Figure 4.18 shows the effect of solvent:GLS ratio and time on PSGA yield as a percentage of GLS input, measured using UV-Vis spectroscopy at 257nm. The highest PSGA yield is approximately 1.52%, at the highest solvent:GLS ratio (40:1) and extraction time (100 minutes).
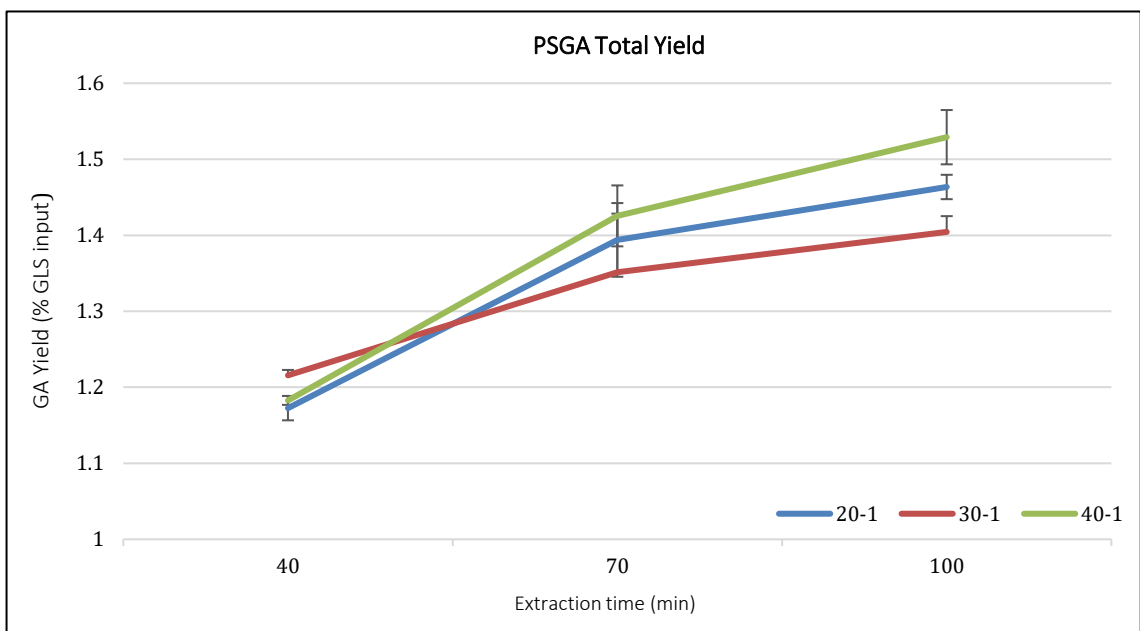


**Figure 4.18:** Effect of extraction time and solvent dilution on HWE PSGA *total yield* as a function of extraction time and ratio. Error bars represent the SE of 2 experimental replicates. Statistical tests revealed that the effect of solvent and extraction time were both statistically significant at 90% confidence (p-value < 0.1).

*Novelty processing and smart delivery of Ganoderma Lucidum spores*

The results suggest that by increasing extraction solvent volume, a slightly greater yield of PSGA can be obtained, however only when the extraction time is longer. At a reduced time, there is limited kinetic energy in the system, so a greater volume would induce less efficient dissolution as a result of molecule crowding. In addition, the energy distribution among more experiment molecules is more widespread, and thus less intense - reducing energy density during extraction [Kiarostami et al., 2014]. With increasing extraction time, more energy supplies a given solvent volume and contributes to more frequent solvent-GLS interaction. Previous studies have further demonstrated that a higher solvent:GLS can reduce system viscosity, inducing dissolution and thus extracting more polysaccharides [Chen et al., 2015; Tian et al., 2017]. In 2016 a study by Sun et al. reported a greater rate of solvent:solute interaction with a higher volume, and thus greater cell wall permeation when triterpenoids were extracted from GLS using hot solvent pressurized extraction [Sun et al., 2016]. This study also found that the yield of polysaccharides from GLS via HWE was also optimal at a solvent:solute ratio of 75:1, after which yield declined owing to dissolution inefficiencies [Vũ Kim et al., 2017].

### 4.1.3.3 PSGA Extraction: Yield Efficiency

Figure 4.19 shows the yield results with respect to extraction *efficiency*. This evaluates yield based on a volumetric cross-section (a standardised sample) of the system, in this case 20ml. This was evaluated to eliminate bias of a larger volumes of sample containing more total extract.
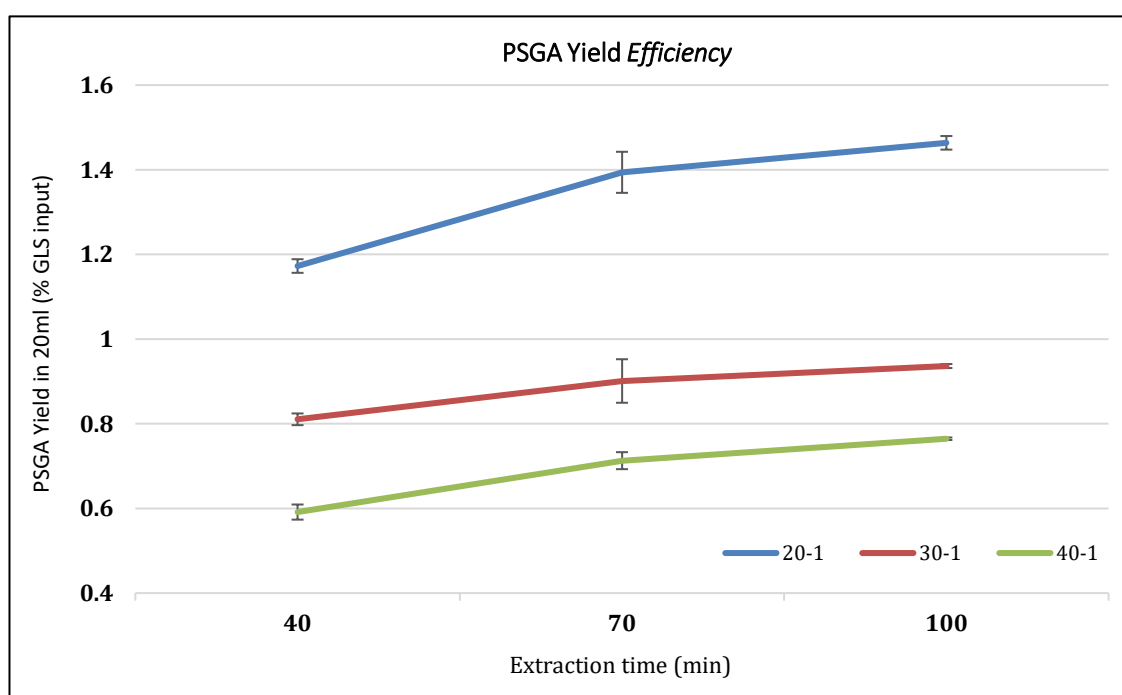


**Figure 4.19:** Effect of extraction time and solvent dilution on HWE PSGA yield *efficiency* as a function of extraction time and ratio. Error bars represent the SE of 2 experimental replicates. Statistical tests revealed that the effect of solvent and extraction time were both statistically significant at 90% confidence (p-value < 0.1).

*Novelty processing and smart delivery of Ganoderma Lucidum spores*

In this 20ml cross-section, the highest PSGA yield was achieved at the lowest solvent:GLS ratio (20:1) and highest extraction time (100 minutes). Thus, in contrast to total yield results, the efficiency results suggest that a *smaller reaction volume* is actually most efficient (per volume fraction of extraction). This is a more scalable dilution to consider for HWE of PSGA.

### 4.1.3.3.1 PSGA Yield Efficiency: Optimisation Model from Supervised Machine Learning

Using the experimental data, the optimisation model will now represent the PSGA yield *efficiency* using the current parameters, and provides a predictive response to future parameter values in the form of a polynomial function as described in chapter 3. The optimization model for this extraction is given in equation 4.1, and figure 4.20 shows the response surface plot of the extraction process. The maximum yield achieved in this experiment is circled in red. The sections below discuss the model output considering the yield efficiency results.
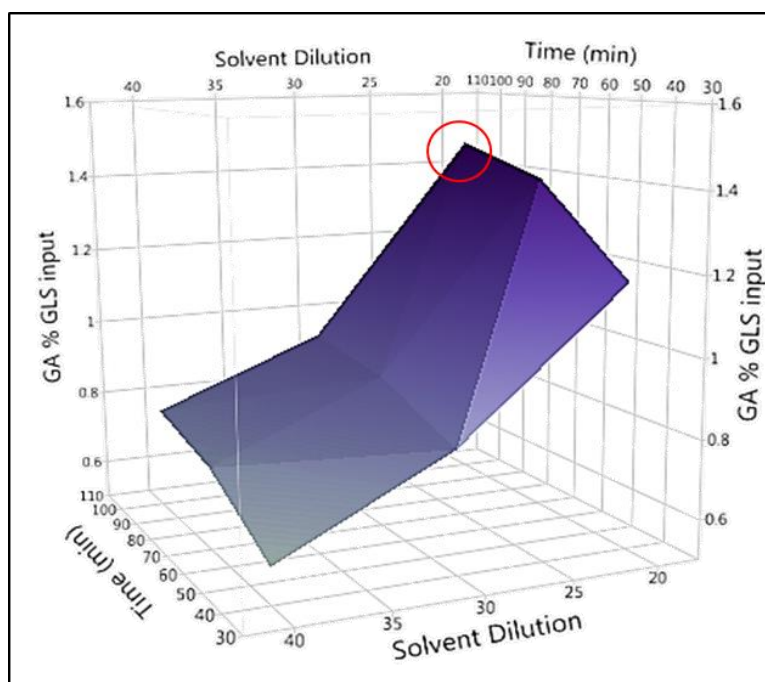


**Figure 4.20:** Effect of extraction time and solvent dilution on HWE of PSGA as a function of extraction time and ratio: Response Surface plot

The model is given in eqn 4.1, and the estimate values in table 4.10.

$$PSGA\ (\%) =$$ Eqn. 4.1

$$1.664 + 0.003\ (X_1) - 0.033\ (X_2) - 0.00005\ ((X_1-70)*(X_1-70)) + 0.001\ ((X_2-30)*(X_2-30)) - 0.00009\ ((X_1-70)*(X_2-30))$$

*Novelty processing and smart delivery of Ganoderma Lucidum spores*

Extraction Time ($X_1$) and Solvent Dilution ($X_2$) coefficients represent the effect of a one-unit change on PSGA yield when the other parameter is held constant. For example, *when extraction time increases by 1 minute, the model predicts a 0.003% increase in yield*. The interaction effect coefficient ($X_1*X_2$) represents the additional effect had by $X_1$ when $X_2$ is not held constant (and vice-versa). Coefficient estimates are presented alongside ANOVA (Analysis of variance) results which provided significance and model analysis in the correlation between the HWE parameters and PSGA yield. The estimates of all coefficients are presented along with the statistical t-tests for each variable, indicating their model significance verified by low p-values ($<0.05$).

| Parameter Estimates | | | | |
|---|---|---|---|---|
| **Term** | **Estimate** | **Std Error** | **t Ratio** | **Prob>\|t\|** |
| Intercept | 1.6644955 | 0.067912 | 24.51 | 0.0001* |
| Time (min) | 0.0032774 | 0.000537 | 6.10 | 0.0088* |
| Solvent Dilution | -0.032687 | 0.001611 | -20.29 | 0.0003* |
| (Time (min)-70)*(Time (min)-70) | -5.118e-5 | 0.000031 | -1.65 | 0.1973 |
| (Time (min)-70)*(Solvent Dilution-30) | -9.814e-5 | 6.576e-5 | -1.49 | 0.2324 |
| (Solvent Dilution-30)*(Solvent Dilution-30) | 0.0013387 | 0.000279 | 4.80 | 0.0172* |

**Table 4.10:** Effect analysis provided by Response Surface Methodology for PSGA extraction. Model terms are presented in the first column, and all are statistically significant, except the interaction terms

### 4.1.3.3.2 Significance of the PSGA Yield Efficiency: Parameters

Prior to fitting the model, two-factor ANOVA showed statistical significance of both parameters at 90% confidence level with respect to PSGA yield. Once the optimisation model was fitted, both parameters still showed significance with respect to PSGA yield, verified by its t-statistic and low p-value as shown above. Table 4.10 also showed that the *interaction effect* between the time and dilution was not statistically significant, and thus there was no confounding effect between them (i.e. the effect of time on yield was not affected by the effect of solvent, and vice-versa). If quadratic effects were significant (time*time or solvent dilution*solvent dilution), it would suggest a curvilinear relationship with yield whereby a local maximum of efficiency is suggested within the experimental range. The quadratic coefficients however were not statistically significant, indicating that the trend suggested by the experimental range holds. Nonetheless, while extraction time for example shows a positive effect on yield, excessive time might negatively affect yield and too little solvent reduce efficiency. The effect of each variable (time and dilution) is discussed below.

*Novelty processing and smart delivery of Ganoderma Lucidum spores*

## Effect of Extraction Time

Extraction time was increased from 40 minutes to 100 minutes, and a positive effect was observed on PSGA yield. Many theories support the positive correlation had between extraction time and extraction yield [Ye et al., 2011]. In particular, there is increased time to react, and thus extract [Sogi et al., 2010; Yanhua et al., 2014]. Furthermore, studies point to the advantage of increased structural degradation caused by the excessive exposure to heat and water molecules, proving to enhance dissolution into the water medium (smaller particles are more efficiently accepted into solvent structures) [Tahmouzi et al., 2014; Hosseini et al., 2017]. However studies on the extraction of nutraceuticals typically observe a maximum temperature effect, after which yield is negatively affected. At temperatures around 80°C and at the typical 20:1 solvent:material ratio, studies see the strongest effect of extraction time in the first 30-45 minutes. The *maximal* yield (after which one could typically expect a detrimental effect on yield) is not attained in this investigation. Most studies observe this time to be 1-2 hours in HWE employing similar conditions to this study. In addition, it is important to note that structural degradation has been shown to positively affect the bioactivity of GL biocompounds (in particular the polysaccharides), and this will be considered in future work [Kao et al., 2011; Lei et al., 2015].

## Effect of Extraction Dilution

The solvent:GLS dilution was increased from 20:1 to 40:1, with the dilution achieved via more solvent (rather than less GLS). Results showed that even though more total PSGA could be extracted when the system was more voluminous, the most efficient extraction was achieved at the lowest dilution factor, 20:1. The positive effect of volume on total yield is explainable by a greater concentration gradient of the particles between the cell interior and exterior, encouraging the mass transfer process. However, a smaller dilution instead increased the energy dissipation, intensifying energy density during extraction and enhancing the extraction efficiency [Kiarostami et al., 2014; Zhu et al., 2019].

### 4.1.3.3.3 Statistical Significance of the PSGA Yield Efficiency: Model Significance

As well as statistically significant individual parameters (time and solvent dilution), the model's coefficient of regression ($R^2$) was 99%, indicating that the tested parameters are strongly accountable for the PSGA yield. The Analysis of Variance (ANOVA) in table 4.11 indicates the model is significant at 95% confidence, with a model p-value <0.05.

*Novelty processing and smart delivery of Ganoderma Lucidum spores*

**Table 4.11:** Test of HWE PSGA Yield model fit: Analysis of Variance

### 4.1.3.3.4 How PSGA Yield Compares to Recent Literature

The extraction of PSGA has not yet been evaluated before, thus comparisons could not be made directly. What has been compared is the extraction of crude GLPS that has been reported by the studies to also contain Ganoderic Acids. The yields from these studies are summarised in table 4.12.

| GL GA / PS complex | This Study | Zhu et al., 2019 | Cheng et al., 2013 | Ruan et al., 2014 |
|---|---|---|---|---|
| Yield | 1.5% | 3.3% | 0.04% | 1.3% |
| Extraction Method | HWE | HWE | HWE | HWE (ethanol) |
| Temperature | 70°C | 37 °C | 100°C | 50°C |
| Duration | 100 min | 300 min | 8 hours | 6 hours |

**Table 4.12:** Experimental comparison of Crude PSGA Yield with literature, extracted using HWE

It is evident that the yield reported in this study is comparable with literature, even at the lower time employed. The effects of HWE process parameters on this complex, and on Ganoderic Acids specifically, has not been sufficiently documented in literature to make valid comparisons of yield attainable. What can be shown from the results of PSGA extraction however, is the capability of HWE to extract such a conjugate in the absence of toxic solvents.

### 4.1.3.4 PSGA Characterisation

PSGA importantly possesses two valuable counterparts that could work together to achieve its effects in an in-vivo environment: *PS immunoenhancement* and *GA cytotoxicity*. The

*Novelty processing and smart delivery of Ganoderma Lucidum spores*

PSGA yield was physically and chemically characterised to better understand the effects of the HWE process its structure. SEM was employed to determine the physical structural effects on the spores, and FTIR and LCMS were used to chemically characterise the resulting PSGA yield.

### 4.1.3.4.1 Scanning Electron Microscopy (SEM): Effect of Extraction Time and Dilution

SEM was employed to evaluate the spore structures after HWE at all tested parameters, in order to determine any correlation between physical impact and the PSGA yield obtained. Figure 4.21 summarizes the effects of the HWE variables on the GLS structure. The upper left variable setting generated the most efficient extraction (outlined in red).
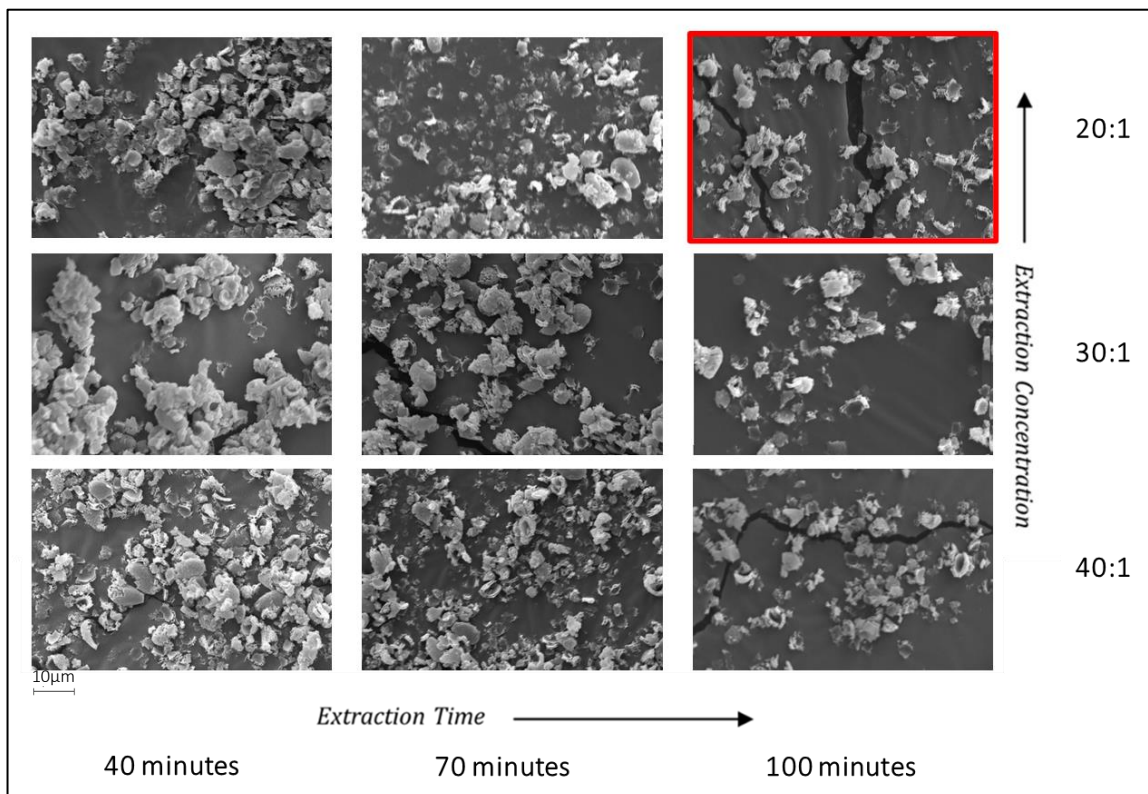


**Figure 4.21**: Effect matrix of extraction time and dilution on extraction GLS spores (denoted via efficiency)

The matrix indicates that increased extraction time is associated with greater structural damage of the GL spores – associated with a longer extraction time across all solvent dilutions. Given more time, across all dilutions, more structural damage can be done. This is indicated by increasingly smaller visible fragments in the SEM micrograph as time increases. The effect of solvent dilution is **not degradative**; rather **penetrative**. While kinetic energy from prolonged extraction time would generate increasing bond fractures, the effect of dilution was controlling penetration of the spore structures ultimately reducing spore clumping and increasing extraction efficiency with a larger surface area. Thus, at the lowest dilution (20:1) the effect of time is most prominent as

*Novelty processing and smart delivery of Ganoderma Lucidum spores*

the resulting intensity is greatest. A higher solvent dilution also fosters lower energy distribution per given extraction time [Kiarostami et al., 2014; Zhu et al., 2019].

The original unextracted spores were imaged in figure 4.22. Here, the broken GLS are larger and more uniform, indicating the effects of HWE on the spores.
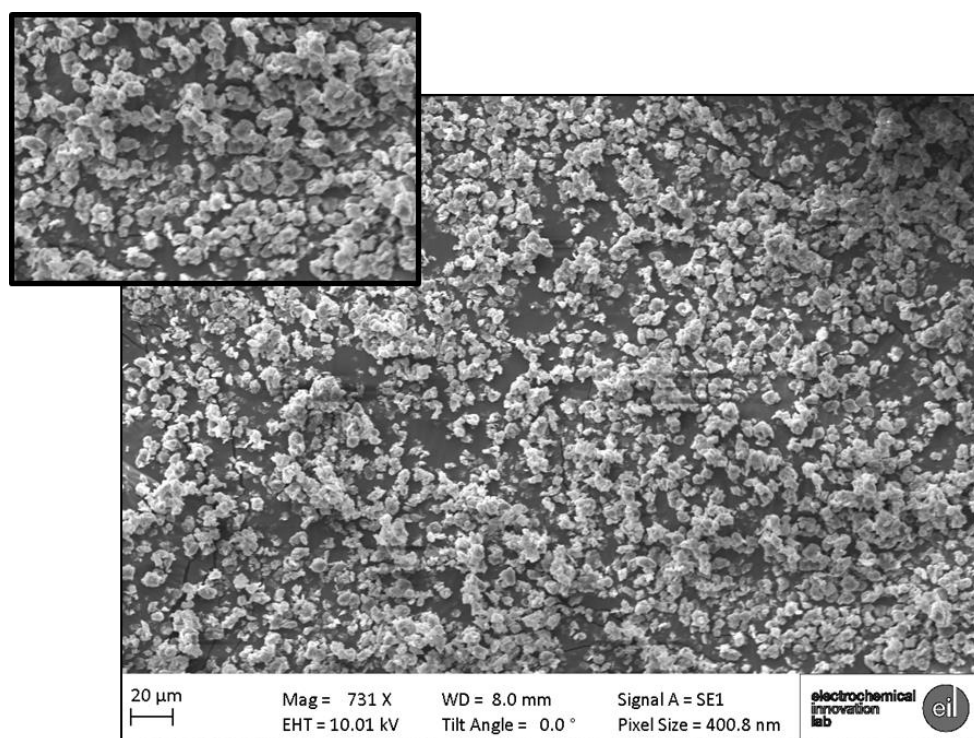


**Figure 4.22:** GLS prior to HWE, whereby the physical appearance of spores appears les scattered and fragmented

### 4.1.3.4.2 Analysing *Post-Extraction GLS* Structure: Fourier Transform Infrared (FTIR) Spectroscopy: Effect of Extraction Time and Dilution

The FTIR spectra of the spores before and after the extraction were obtained to retrieve information on chemical differences after all extraction time and dilution extremities. Figure 4.23 shows that there was no evident difference in peak position, indicating that the spores were not radically changed chemically by the process conditions. The aliphatic structure is typically a good indicator of the structural change (breakdown) exerted on spore structures during HWE [Chen et al., 2012]. This is typically analysed via FTIR, by calculating the ratio of methyl ($-CH_3$) and methylene ($-CH_2-$) groups absorbing at approximately 2956 $cm^{-1}$ and 2919 $cm^{-1}$ respectively [Wang et al., 2012]. This ratio indicated the average length of the aliphatic chains in the sample, and thus the degree of structural breakdown [Evaristi et al., 2016; Ong et al., 2017]. The results

are shown in table 4.13. The smallest ratios represent spore samples with longer aliphatic chains that suggest less intense processing impact [Gazi et al., 2005; Đorđević et al., 2012]. This is because in these samples, there is less methyl contribution and more methylene contribution indicating longer chain length and a higher molecular weight [Zampolli et al., 2014]. The longer length corresponded to the HWE taking place for the shortest time (40 minutes), suggesting a less intense effect on the sporoderm structure. Studies have indeed correlated the length of aliphatic chains in natural organisms, to the severity of its degradation [Zampolli et al., 2014].
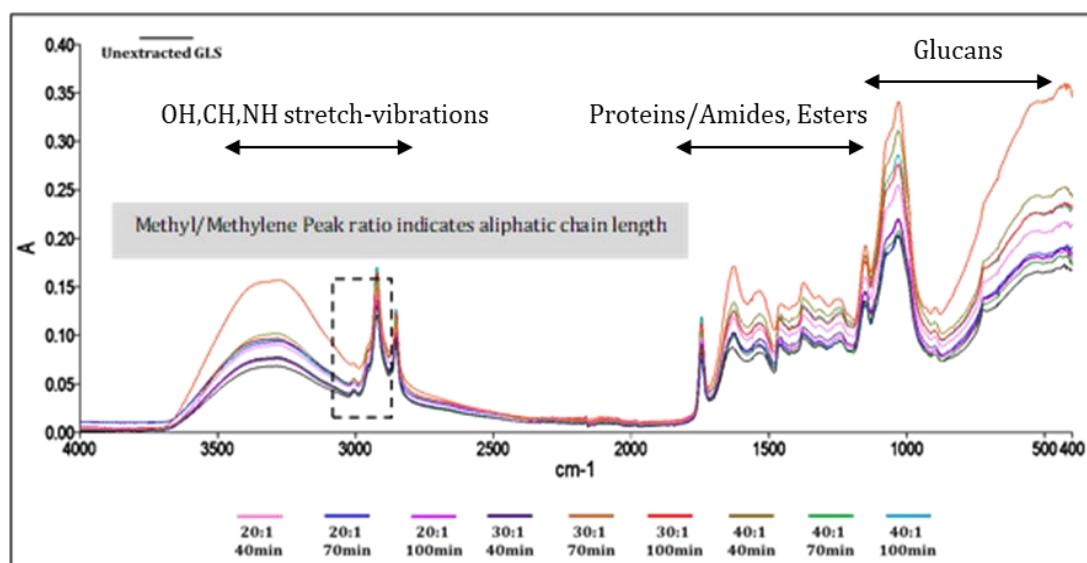


**Figure 4.23:** FTIR spectra of the GL spores after the different HWE processing conditions

| PSGA: *Extraction Time* | PSGA: *Extraction Dilution* | Methyl/Methylene Peak ratio |
|---|---|---|
| 40 | 20:1 | 0.33 |
| 40 | 30:1 | 0.31 |
| 40 | 40:1 | 0.31 |
| 70 | 20:1 | 0.40 |
| 70 | 30:1 | 0.47 |
| 70 | 40:1 | 0.33 |
| 100 | 20:1 | 0.39 |
| 100 | 30:1 | 0.37 |
| 100 | 40:1 | 0.35 |

**Table 4.13:** The increasing ratio between methyl (-CH$_3$) and methylene (-CH$_2$-) groups indicate degradative effects on aliphatic structure of spores

*Novelty processing and smart delivery of Ganoderma Lucidum spores*

### 4.1.3.4.3 Analysing *PSGA* Structure: Fourier Transform Infrared (FTIR) Spectroscopy: Effect of Extraction Time and Dilution

FTIR Spectroscopy was also carried out to compare the chemical difference in *PSGA extracts* obtained at the highest and lowest extraction time in HWE. Only time was considered to be influential on the PSGA extract structure itself, as confirmed by the SEM and FTIR results indicating that HWE extraction dilution did not have a considerable effect on structural rupture. This is because increased exposure to kinetic energy will affect the structural integrity of the extracted PSGA. Figure 4.24 shows the spectrum for the 40min and 100min extracts extracted in solvent:GLS 20:1. Overall, spectral characteristics of both extracts are similar, implying that the increased extraction time had little impact on the functional groups of the PSGA (even though the spores themselves showed differences in process impact as shown above). Peak intensities are also not largely different, suggesting a near-analogous chemical structure between the two time samples. The spectral regions important for structural characterization of GL extracts include mainly the sugar (1,200-950cm$^{-1}$) and anomeric (950-750cm$^{-1}$) regions. Neither of these indicate shifts that would suggest increased or decreased degradation [Pucetaite et al., 2012].

The broad bands between 3,405 and 2,900cm$^{-1}$ were assigned to OH, CH and NH bond stretching of triterpenes/sterols and polysaccharide groups respectively. This band width slightly decreased with increased extraction time, likely because of the loss of alcoholic groups as further decomposition occurs at the longer extraction. Dehydrogenation and deoxygenation is also more likely at higher temperatures.
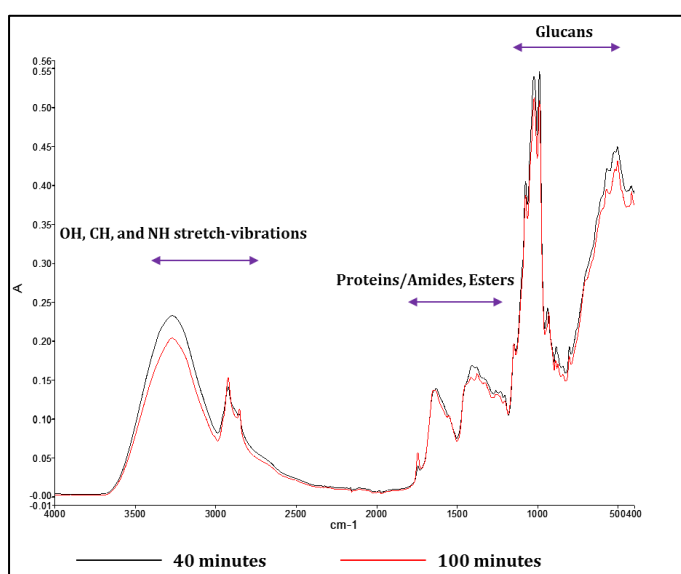


**Figure 4.24:** FTIR spectra of PSGA extract 40 minute and 100 minute extractions in Solvent:GLS 20:1

Peaks around 1,700cm$^{-1}$ correspond to unsaturated esters and protein components, as observed by Kohsuke Kino et al. (and many others) who found a novel protein *LZ-8* extracted from GL with

*Novelty processing and smart delivery of Ganoderma Lucidum spores*

mitogenic and immunomodulating activity in vivo [Kohsuke et al., 1991; Yeh et al., 2010]. Bands at 1,420 and 1,366cm$^{-1}$ arose from bending of CH$_2$, CH and OH. Intense bands in the region of 800-1,300cm$^{-1}$ correspond to CO and CC stretching and COH bending modes. The intense bands of CO and CC stretch-vibrations in glycosidic bonds dominate the lower part of this region, with characteristic GL peaks showing a sharp twin-peak [Choong et al., 2012]. Within this region, fungal (1→3)(1→6)-β-D-Glucans and (1→4)(1→6)-α-D-Glucans are typically assigned. Xu et al. for example report an isolated antitumor β-D-Glucan from the fungus Grifola Frondosa, corresponding to 890 cm$^{-1}$ in FTIR [Luo et al., 2008; Synytsya et al., 2014]. The GLS Glucan peaks in this region were greater for low extraction times, reflecting the loss of some Glucan groups [Matsunaga et al., 2014]. The strong peaks at 1385 cm$^{-1}$ indicate phenolic compounds [Sakellariadou et al., 2006].

### 4.1.3.4.4 Analysing PSGA Structure: Liquid Chromatography-Mass Spectroscopy (LCMS) to Determine the Effect of Extraction Time

Only time was considered to be influential on the PSGA extract itself, as confirmed by the SEM and FTIR results which suggested that HWE extraction dilution did not have a considerable effect on structural rupture. This is because increased exposure to kinetic energy will affect the structural integrity of the extracted PSGA. Figure 4.25 shows the LCMS spectra for the 40min and 100min extracts extracted in solvent:GLS 20:1. This indicated the effects of increased extraction time on molecular weight. This is particularly true for Ganoderic Acids which are especially sensitive to heat [Chin et al., 2011; Chin et al., 2014]. LCMS is useful in revealing the molecular size distribution in the sample, thus providing an indication of the impact of an increased exposure time on the extraction yield. The chromatograms show the retention time of the 570g/mol compounds (GA molecular weight) eluted from the samples extracted at 40m and 100m HWE respectively (at UV wavelength 254nm).

*Novelty processing and smart delivery of Ganoderma Lucidum spores*
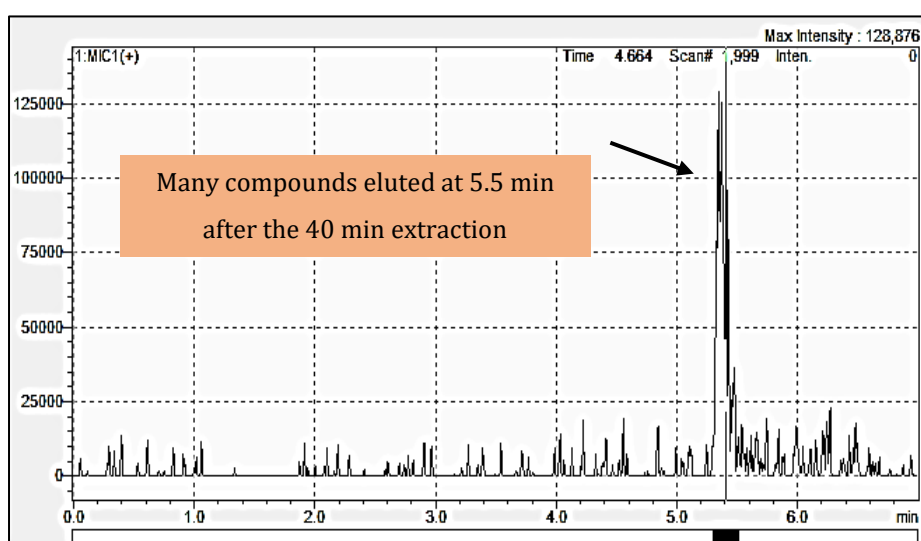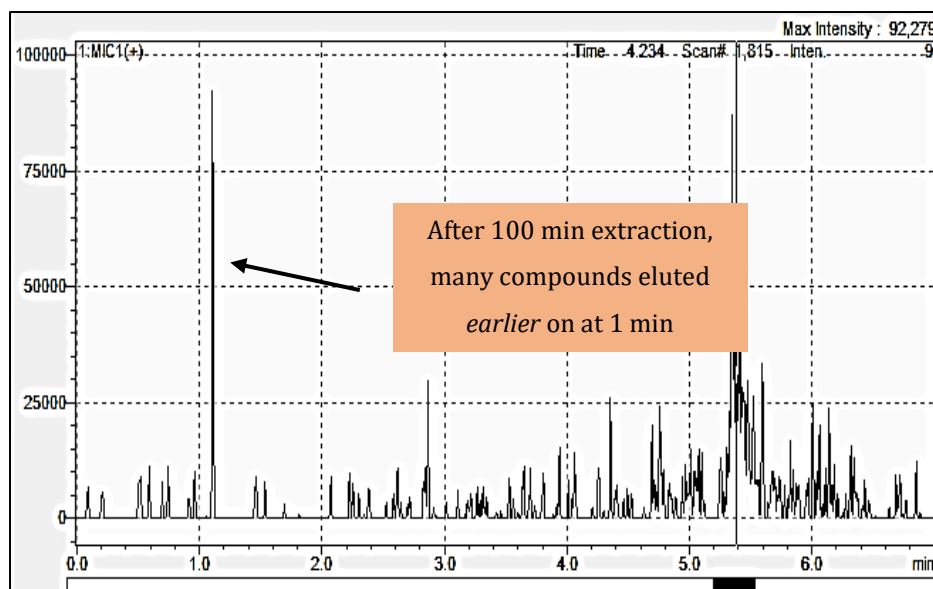
**Figure 4.25:** LCMS Spectra obtained at UV-Vis 254nm of 570 g/mol ions eluted from PSGA sample from 40 min extraction (upper) and 100 min extraction (lower) in Solvent:GLS 20:1: *Retention times.* (Vertical Axis = Intensity, Horizontal axis = Retention Time)

From the chromatograms it is evident that the elution patterns of both samples are distinct. In the shorter extraction (40 min), a greater quantity of ions is eluted later on – suggesting that more of these extract constituents have a greater affinity to the stationary phase (polar) [Pekcan et al., 2002]. On the contrary, extracts obtained from the 100-minute extraction exhibited elution much earlier as well, indicating less polar affinity. This may be an indicator of a difference in impact on particle structure using different time extremities – in particular, greater elution of non-polar compounds suggests prevalence ganoderic acid and its fragments. This further points to increased degradation using this extraction time [Krochta et al., 1987].

### 4.1.3.4.5 Elution Pattern: The m/z Distribution

The mass distributions of the 570g/mol compound extracted via 40 and 100 minutes are shown at 5.5 minutes' retention time in figure 4.26.

*Novelty processing and smart delivery of Ganoderma Lucidum spores*
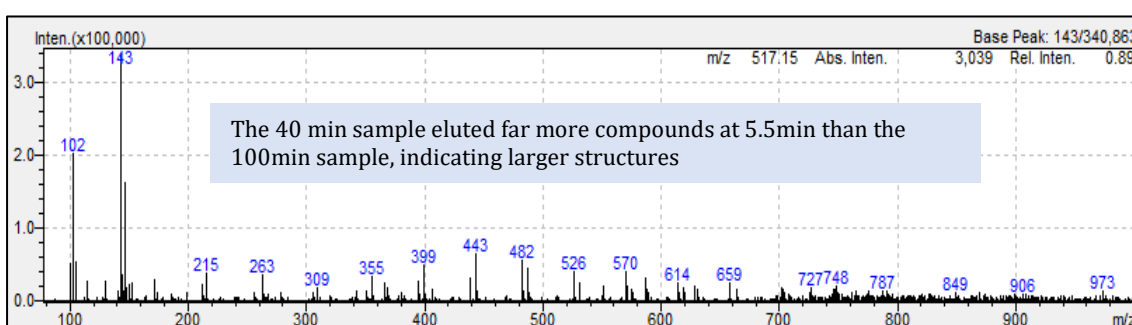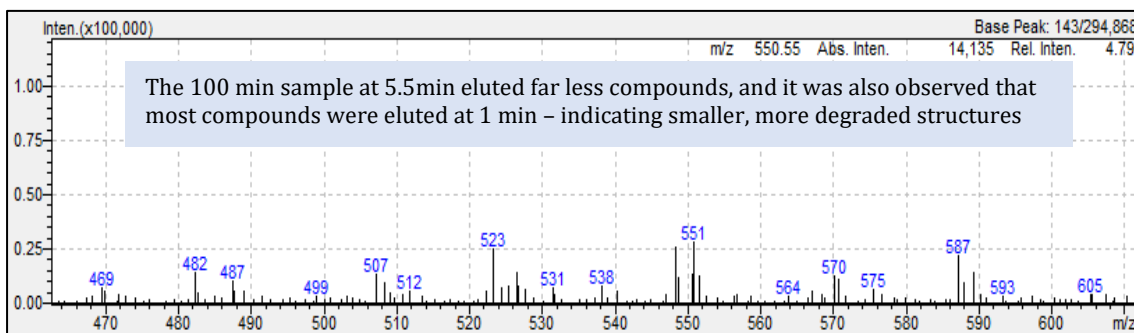
Figure 4.26: LCMS Spectra obtained at UV-Vis 254nm of 570 g/mol ions eluted from PSGA sample from 40 min extraction (upper) and 100 min extraction (lower) summed at 5.5 minutes: *Mass Ratio Distribution.* (Vertical Axis = Relative Abundance, Horizontal axis = Mass:Charge Ratio)

These spectra show the mass distribution of this particular ion, suggesting a variety of masses – and thus a variety of fragments. Even though it appears that the longer extraction time has led to a smaller variety of masses, and generally larger masses, this is due to the late retention time analysed here (5.5 min). At 1 minute retention time, the 100-minute extraction produced the mass spectrum below (for this ion) – suggesting low-mass isomers of the biocompound eluted earlier on.
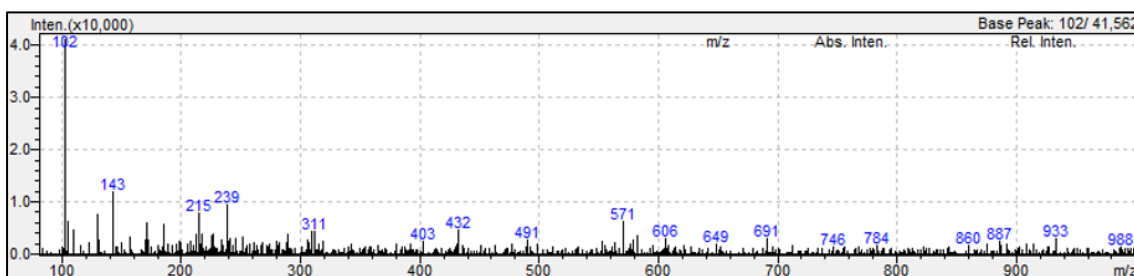


Figure 4.27: LCMS Spectra obtained at UV-Vis 254nm of 570 g/mol ions eluted from PSGA sample from 100 min extraction summed at 1 minute

It was also observed that the 100-min extract recorded most absorbance at *positive ionization*, whereas 40-min extracts were strong in *both ionization modes*. Positive ionization absorbance has been suggested to be indicative of greater metabolite degradation [Barwick et al., 2006; Yuan et al., 2012].

### 4.1.3.4.6 Pathways of Fragmentation

The fragmentation pathways of Ganoderic Acids have been studied as a means of classification of the numerous GA isomers [Yang et al., 2007]. These were observed generally via

*Novelty processing and smart delivery of Ganoderma Lucidum spores*

the mass distributions in figures 4.25 and 4.26, which indicated that the same ion (MW 570 g/mol) was present in a variety of masses and thus a variety of isomers and/or isomer fragments [Cao et al., 2017]. Typically, GA degradation is characterised by losses of $H_2O$, $CO_2$ and the acetyl/methyl groups, however, the cleavage of certain rings are also characteristic. As the PSGA sample was not purified, the GA isomers present in this complex would be difficult to characterise chemically with respect to fragmentation behaviour vs different isomers. Thus fragmentation pathways belonging to many isomers could be present. The LCMS spectra reveal very typical m/z values for GA fragments [Cao et al., 2017]. Often fragmented components of the ions insinuate lost side-chains. For example, in the mass distributions in figure 4.25, the peaks around 440 and 311 respectively show m/z transition due to the loss of mass as the carboxyl side-chain is fragmented, whereas peaks at higher or lower m/z values could indicate the losses of water or methyl groups respectively [Li et al., 2005; Yang et al., 2007; Yan et al., 2013]. The fragments typically obtained can elute faster and have a lower mass distribution (m/z) than the parent (pre-extraction). The structural impact can be indicated, but not confirmed from these investigations (without subsequent characterisation). Much work is needed to characterise this effect before PSGA can be evaluated for its medicinal potential.

### 4.1.3.5 Extraction of PSGA from GLS: Conclusions

This section demonstrated the ability to optimise the HWE approach to PSGA extraction, and thus obtained the HWE process parameters that could achieve the highest PSGA yield from GLS. Knowing the workflow that maximises extraction yield is instrumental to scaling up an extraction process, and thus this investigation creates a good foundation for future development of HWE of GLS PSGA.

## 4.2 In-Vitro Cell Culture of *GLPS* and *PSGA* with Human Osteosarcoma

GLS extracts have conventionally been tested for antitumour potential in various forms, both crude and isolated. Nonetheless, the uniqueness of every extract's biochemical compositions (resulting from experimental protocol, and strain itself) has resulted in very little *causal* mapping between compound and antitumour capacity. Section 4.3 attempts to reveal a potential compound-dependent inhibition of the GLS extracts via the administration of 2 forms of polysaccharide to HOS cells in-vitro. The first was crude GLPS obtained using HWE, and

*Novelty processing and smart delivery of Ganoderma Lucidum spores*

contained large complex crude polysaccharides – compounds typically advantageous toward a functional immune system. The second contained small-molecule Polysaccharide-Ganoderic Acid complexes (PSGA) – rich in constituents that are more cytotoxic toward cancer cells traditionally. It is expected that there will be a difference in antitumour capacity between crude GLPS and PSGA, owing to this difference in chemical composition – this may shed some light on the compounds responsible for antitumour activity. Both extracts are investigated in-vitro with respect to *dosage* and *treatment time*, and the GLPS extract was also tested with respect to the fraction of extract yield, as one would also contain triterpenoic compounds like Ganoderic acids.

## 4.2.1 In-Vitro HOS Viability: MTT Assay of Polysaccharide-Ganoderic Acid (PSGA)

For all administration, the MTT viability assay was carried out to determine the surviving tumour cells post-treatment, determined by the metabolic levels of mitochondrial enzyme *succinate dehydrogenase* from dye reduction. The reduction produces a compound detectable in the UV spectrum at 570nm proportional to cell metabolism, providing a gauge of drug efficacy. In that regard, the MTT assay is primarily a cell metabolism assay, and indicative of viability. Thus, it is ideally used in combination with other viability assays to confirm results. The average proliferation is plotted, where error bars represent the SE of experimental replicates averaged over administration replicates. The inferred proliferation of HOS following treatment is plotted as a percentage of untreated cells (*negative* control), which is indicated by the black dotted line which denoted "100% proliferation". While the MTT assay is a gold-standard in indicating cell viability, it does not on its own denote treatment cytotoxicity and thus future work should use complementary methods to confirm findings of an MTT assay. These are discussed in chapter 6.

PSGA extracts were administered in-vitro, and the MTT Assay results are presented in tables 4.14 (A and B) and plotted in figure 4.28. The HOS viability is evaluated as their percentage of the untreated cells (negative control). The dosage was in accordance with literature [Zhong et al., 2012; Jiang et al., 2018]. The PSGA extract was effective against HOS proliferation when compared to the negative control (represented by the black dotted line), showing dose-dependent inhibition after incubation. Inhibition is inferred by reduced cell metabolism.

| | A. Crude PSGA Culture with HOS: MTT Absorbance | | | | |
|---|---|---|---|---|---|
| 24h Dose (mg/ml) | 2 | 6 | 10 | 12 | 15 |
| % C – (± SE) | 45.3 ± 7.9 | 42.9 ± 2.0 | 50.4 ± 5.6 | 68.4 ± 5.9 | 71.7 ±8.1 |

*Novelty processing and smart delivery of Ganoderma Lucidum spores*

| | B. Crude PSGA Culture with HOS: MTT Absorbance | | | | |
|---|---|---|---|---|---|
| 48h Dose (mg/ml) | 2 | 6 | 10 | 12 | 15 |
| % C – (± SE) | 41.7 ± 5.2 | 57.8 ± 5.0 | 78.8 ± 7.3 | 88.2 ± 5.9 | 100.2 ± 5.6 |

**Table 4.14:** MTT Assay results of HWE PSGA after 24 and 48 hours. *Rounded to 1 d.p.*
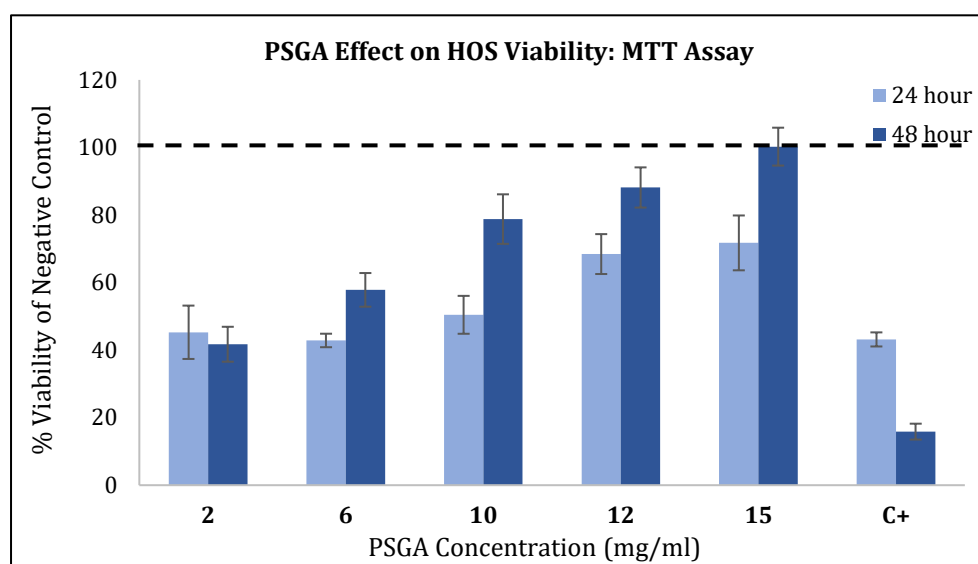


**Figure 4.28:** Effect of PSGA on HOS proliferation after 24 and 48 hours: MTT *Assay*. Error bars represent +/- SE of 8 administration replicates. Statistical tests revealed that the effect of dosage and exposure time were both statistically significant at 90% confidence (p-value < 0.1). Black dashed line represents the negative (untreated) control, of which MTT results were plotted as a percentage.

It has been shown that crude GL extracts that do not undergo high-pressure treatments contain bioactive compounds that have established antitumour effects via suppression of pro-inflammatory mediator expressions, for example the protein LZ-8 [Gross et al., 1994]. This is because they maintain valuable structures. A study in 2011 also found that the LZ-8 protein for example activated p53 and p21 expressions and demonstrated apoptosis of Lewis lung carcinoma in mice in-vivo [Wu et al., 2011; Lin et al., 2014].

## Exposure Time Effect

Incubation of HOS cells with PSGA took place at 24 and 48 hours. The MTT assay indicated that the doses were less effective after 48 hours compared to 24 hours, indicating the possibility of clonal selectivity/expansion as treatment exposure increased. This is the theory that treatment inadvertently provides selective pressure for the expansion of resistant variants. The new cells would be more resistant to treatment cytotoxicity [Ibragimova et al., 2017].

*Novelty processing and smart delivery of Ganoderma Lucidum spores*

## Concentration Effect

In this study, an increasing dose prompted less inhibition of HOS cells; yet all doses still reduced proliferation compared to the untreated negative control. This is a common finding that has been attributed to proliferation resulting from a more conducive growth space as cells die and create space [Leibovici et al., 1985; Leibovici et al., 1986; Losso et al., 2004; Sun et al., 2015; Wang et al., 2017]. Other causes of the negative relationship between dosage and HOS inhibition are discussed below.

### *Increased Inhibition at low doses: Multinucleated Giant Cells (MNGCs) and Apoptosis*

It is not uncommon to observe increased inhibitory effects of polysaccharides at low doses, however the reasons are not presented consistently in literature. Both polysaccharides and Ganoderic Acids have been shown to induce apoptosis via cell cycle arrest [Losso et al., 2004; Wang et al., 2017]. Many studies therefore report a positive correlation between crude polysaccharide or Ganoderic Acid doses, and the percentage of apoptotic cells under treatment (which indeed show as "live" in an MTT assay). A delayed treatment response is therefore often attributed to these trends when assayed via MTT, and may explain the recurrence of certain tumour cells during/following treatment. This is often reflective of sustained cell proliferation arrest (dormancy) when undergoing apoptosis [Puig et al., 2008; Mirzayans et al., 2017 (a)].

Confirming apoptosis without further cell treatment is not always possible, however it is typically indicated by morphological changes such as increased cell size with a larger nucleus (or numerous nuclei) – known as multinucleated giant cells (MNGC) [Mirzayans et al., 2018]. In addition, fringing and blebbing of the membrane and condensed chromatin while listing off of the plate could suggest MNGC formation and apoptotic behaviour. Dose dependence is shown in figure 4.30 A-E and this phenomenon is shown close up in 4.29, which shows the cells after incubation with PSGA at different doses after only 24 hours. The presence of MNGCs along with damaged cells is indicated with white arrows.
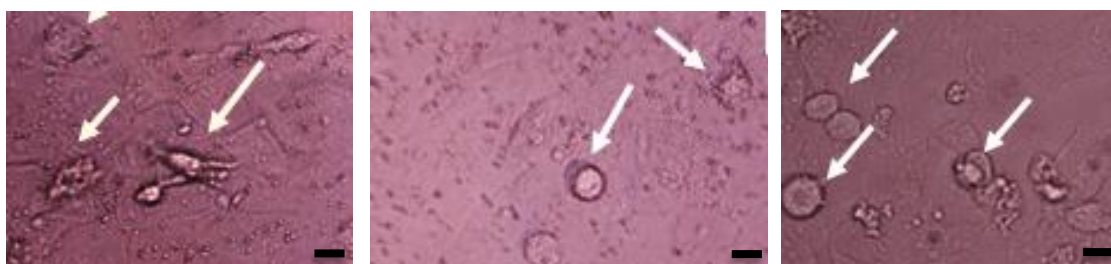


**Figure 4.29:** Optical micrographs of PSGA administration after 24 h HOS culture indicating treatment's possible apoptotic effects on HOS cells: Multinucleation and damaged cells. Scale bar represents 50µm. Doses 2mg/mL, 6mg/mL and 1mh/mL shown respectively

Multinucleation is a sign of disrupted mitosis/cytokinesis (often during apoptotic intervention), in which case cell division cannot occur and a nuclear envelope is created around random chromosomes to form an MNGC. Typically, MNGCs are formed during a recurrence of the cancer following exposure to an anticancer agent [Weihua et al., 2011; Mirzayans et al., 2018]. The finding that anticancer treatment could trigger the growth of giant cells was first recorded by Puck and Marcus when investigating the behaviour of human HeLa cancer when exposed to ionizing radiation in 1956 [Puck et al., 1956]. MNGCs usually contain an elevated nuclear content can proliferate very slowly/not at all, to the point that they could be deemed dead or alive in the MTT assay – leading to possibly skewed dosage effects. In addition, MNGCs foster the growth of offspring that are more resistant, aggressive, and metastatic, and can induce nuclear bursting, and depolyploidization – reflected by increased viability and potency of HOS at the higher doses [Solari et al., 1995; Erenpreisa et al., 2000]. The presence of MNGCs has often been shown associated with response to treatment [Losso et al., 2004; Mirzayans et al., 2016; Mirzayans et al., 2017 (a); Mirzayans et al., 2018 (b)]. Niu et al. observed that MNGC cancer cells exhibit self-renewal and undergo continuous nuclear bursting to produce more nuclei that develop enough cytoplasm to break away and attain long-term proliferation. The authors named this the "giant cell cycle." [Niu et al., 2016].

There is huge merit in diversifying the techniques used to measure cancer cell viability post-treatment, given the range of possible cell mechanisms that take place during treatment. For example the degree of MNGC formation and apoptotic behaviour can be verified via or chemically via staining techniques or immunofluorescence microscopy that evaluate plasma membrane stability and form, and the difference in cell signalling patterns via protein expressions (e.g. p53, Bax and Bcl-2) [Losso et al., 2004; Rieger et al., 2011]. Changes in media pH can also indicate varying levels of cell metabolism. These techniques will be discussed in further detail in chapter 5 (future directions).

At all treatment levels round, floating cells can also be observed, suggesting late apoptosis and death. During apoptosis cells typically retract their margins to reduce their spread area as they detach during death. By shrinking and increasing roundness more cells can flourish and PSGA efficacy will be reduced. As the dose increased, the processes above may have been initiated, reducing treatment efficacy.
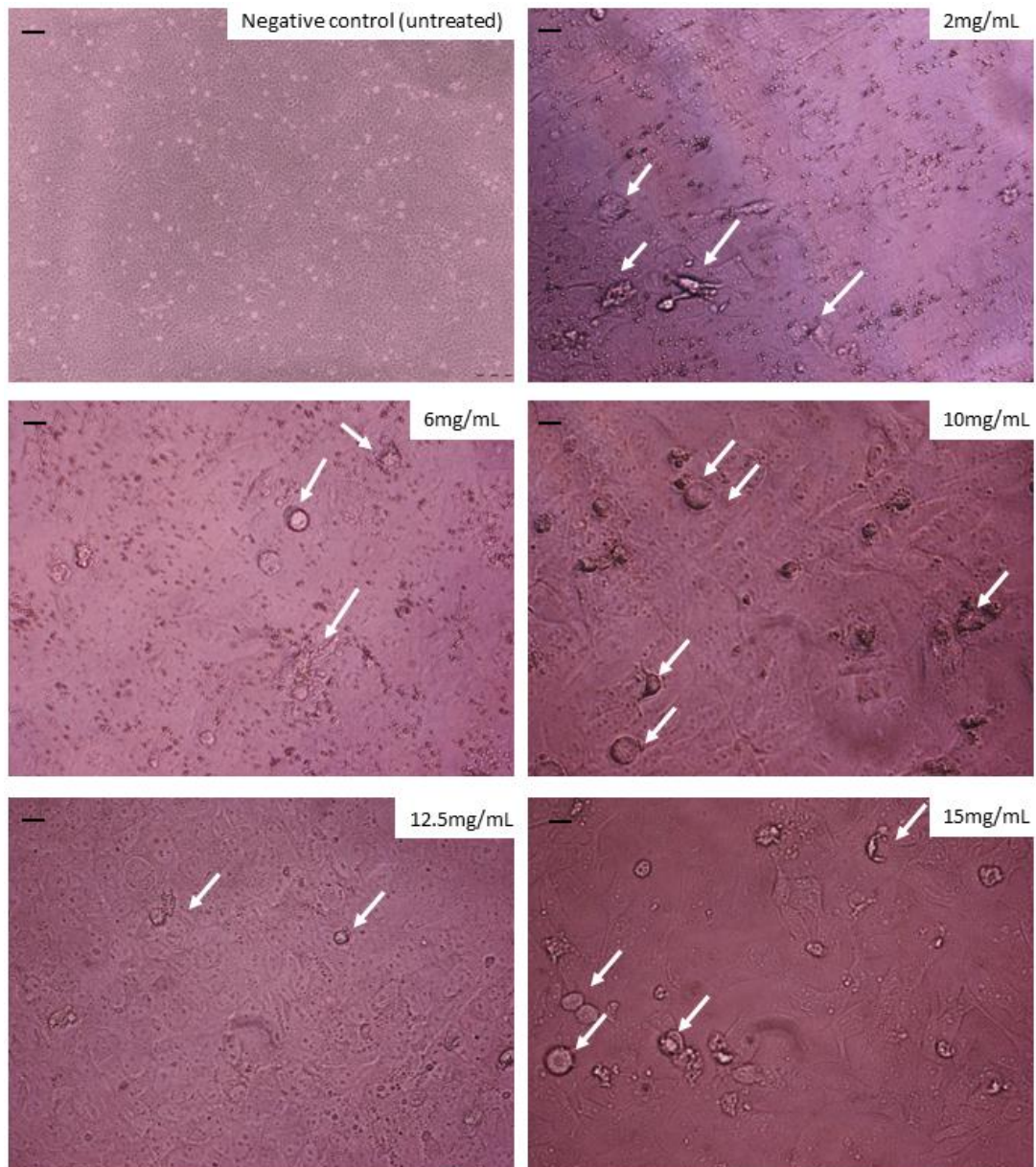
**Figure 4.30:** Optical micrographs of PSGA administration after 24 h HOS culture at tested doses. Scale bar represents 50µm. Negative control is untreated, and pictured at confluence.

### *Decreasing Inhibitory Action at high doses: Cell Resistance through PSGA acclimatisation*

Some studies observe that higher doses can foster an increasing "average resistance", inducing the development of *more resistant phenotypic variants even given the same amount of exposure time*. While higher doses technically foster a more cytotoxic environment, this could be at the cost of creating an increasingly resistant cell population during incubation; in turn creating even greater resistance as time continues – clonal expansion. This suggests the need to consider a Maximum Tolerated Dose (MTD).

## 4.2.2 In-Vitro HOS Viability: MTT Assay of GLS Crude Polysaccharides (GLPS)

The GLPS extract, as well as GLTP (the water-insoluble HWE triterpenoic compounds in the form of a "pellet" leftover from polysaccharide extraction), were administered to HOS cells in-vitro. It is an established consensus in literature that GLPS antitumour investigations carried out *in-vitro* (in the absence of a functioning immune system) typically observe no cytotoxic effect on cancer cells, however when the same treatment is carried in the presence of functional immune cells, a remarkable reduction in tumour growth could be observed. Studies therefore attribute its antitumour effects to its immunoenhancing activity. The expectation is that the GLPS extract would contain polysaccharides and the water-insoluble GLTP (pellet) would include triterpenoids like Ganoderic Acids [Camargo et al., 2011]. Water-insoluble GLTP is first presented.

## 4.2.2.1 In-Vitro HOS Viability: GLTP (Crude Triterpenoids)

Triterpenoids such as Ganoderic Acids are usually found in the water-insoluble fractions of GLS, typically known as the extraction *pellet*. The MTT assay of the HOS cells treated with GLTP is shown in figure 4.31, followed by the absolute absorbance results. Triterpenoid extracts typically exhibit cytotoxic effects on cancer cells via apoptotic pathways and sustained proliferation arrest via multinucleated cells. This can skew assays, as cancer cells remain "viable" and able to metabolise MTT initially, dependent on which phase of cell cycle arrest they are undergoing during assay [Bryant et al., 2017]. HOS cells that underwent GLTP treatment exhibited a reduction in viability after both treatment times compared to the negative control, indicating treatment efficacy. As the 24h negative control was very low (perhaps abnormal) it is possible the 24h treatment MTT assay was positively skewed. Therefore the absorbance results are also presented to gauge absolute effects of the treatments. As cancer cells typically divide continuously when not treated, low survival in the control group could be a result of cell crowding in a rapidly growing cell line like HOS, resulting in oxygen deprivation and a stationary growth state where many die out [Levayer et al., 2016].

| | Crude GLTP Culture with HOS: MTT Absorbance | | | | |
|---|---|---|---|---|---|
| 24h Dose (mg/ml) | 0.5 | 1 | 5 | 10 | 50 |
| % C - (± SE) | 74.5 ± 10.6 | 59.6 ± 3.3 | 61.0 ± 3.5 | 66.6 ± 1.4 | 73.2 ± 3.6 |

*Novelty processing and smart delivery of Ganoderma Lucidum spores*

| | Crude GLTP Culture with HOS: MTT Absorbance | | | | |
|---|---|---|---|---|---|
| 48h Dose (mg/ml) | 0.5 | 1 | 5 | 10 | 50 |
| % C - (± SE) | 90.3 ± 9.4 | 83.8 ± 4.6 | 96.7 ± 11.3 | 80.8 ± 6.6 | 77.6 ± 3.4 |

**Table 4.15:** MTT Assay results of HWE GLTP after 24 and 48 hours. *Rounded to 1 d.p.*





**Figure 4.31:** Effect of GLTP on HOS proliferation after 24 and 48 hours: *MTT Assay* and *MTT Absorbance*. Error bars represent +/- SE of 3 experimental and 2 administration replicates. Statistical tests revealed that the effect of dosage and exposure time were both statistically significant at 90% confidence (p-value < 0.1). Black dashed line represents the negative (untreated) control, of which MTT results were plotted as a percentage.

*Novelty processing and smart delivery of Ganoderma Lucidum spores*

### Exposure Time Effect

The effect of exposure time was statistically significant at 90% confidence. The *absorbance* results indicate that the 48h treatment was more effective than the 24h treatment, suggesting a powerful treatment effect with increased GLTP exposure.

### Concentration Effect

The effect of GLTP concentration was statistically significant at 90% confidence at both time points. A correlation with dosage is often difficult to observe when apoptotic agents like triterpenoids are administered to cancer cells, as increased treatment concentration can foster increasingly aggressive cell cycle arrest that could be evaluated at various points of arrest - indicating false viability [Solari et al., 1995; Erenpreisa et al., 2000].

## 4.2.2.2 In-Vitro HOS Viability: GLPS (Crude Polysaccharides)

Tables 4.16 A and B show the MTT assay results following treatment with HWE GLPS extracts.

| | Crude GLPS Culture with HOS: MTT Absorbance | | | | |
|---|---|---|---|---|---|
| 24h Dose (mg/ml) | 0.5 | 1 | 2.5 | 5 | 10 |
| % C – (± SE) | 427.2 ± 115.3 | 358.8 ± 144.9 | 493.5 ± 208.3 | 453.6 ± 127.8 | 365.3 ± 168.1 |

| | Crude GLPS Culture with HOS: MTT Absorbance | | | | |
|---|---|---|---|---|---|
| 48h Dose (mg/ml) | 0.5 | 1 | 2.5 | 5 | 10 |
| % C - (± SE) | 144.4 ± 55.0 | 119.8 ± 47.1 | 142.0 ± 6.3 | 147.3 ± 6.0 | 119.7 ± 16.4 |

**Table 4.16:** MTT Assay results of HWE GLPS after 24 and 48 hours. *Rounded to 1 d.p.*

### The MTT Assay

MTT reductions indicated that HOS cells subject to no treatment (the negative control) had less viability than those undergoing GLPS treatment, indicating that the GLPS treatment was ineffective (and even more cytotoxic) – see the black dotted line in figure 4.32 (upper). As

*Novelty processing and smart delivery of Ganoderma Lucidum spores*

discussed extensively in the literature review of this project, polysaccharides are immunoenhancing. In essence, they are antigens for immune cells, recognized by receptors such as the B-Cell receptor. This polysaccharide-receptor interaction induces signals to stimulate clonal expansion of the immune cells, and antibody generation. Resultantly, treatment may have fostered cell strains from the culture [Deters et al., 2005].

## The MTT Absorbance

When the absorbance results are *not* plotted as a percentage of the negative control however, the absorbance assay suggested something different. Figure 4.32 (lower) shows that the viability of cells was much closer to those of the negative control, especially after 48 hours of incubation. Contrastingly also, 48 hours of treatment was less effective after 48 hours. Indeed, the MTT assay above accounted for the extremely reduced viability of the 24h *untreated control*, thus the 24h treatment effects were skewed in the assay. In fact, a *reduced* 48h treatment effect makes sense in the face of increased drug resistance developed by cells with increased GLPS exposure – facilitating clonal selectivity to remain viable. This has particularly been the case when HOS cells are the subject of treatment [Burns et al., 2001]. Some studies have further observed that polysaccharide treatment may actually mask the reach of effective agents within the same treatment – in this case, within the same crude extract [Band et al., 2015]. Another possibility to be explored is that polysaccharide treatment may induce oxygen depletion in HOS cells, which has proven to enhance resistance to chemotherapeutic agents as a result of a lesser ability of oxygen to "latch onto" the free radicals generated by treatment [Sinha et al., 1990; Gu et al., 2017]. As it stands, these findings require future work.
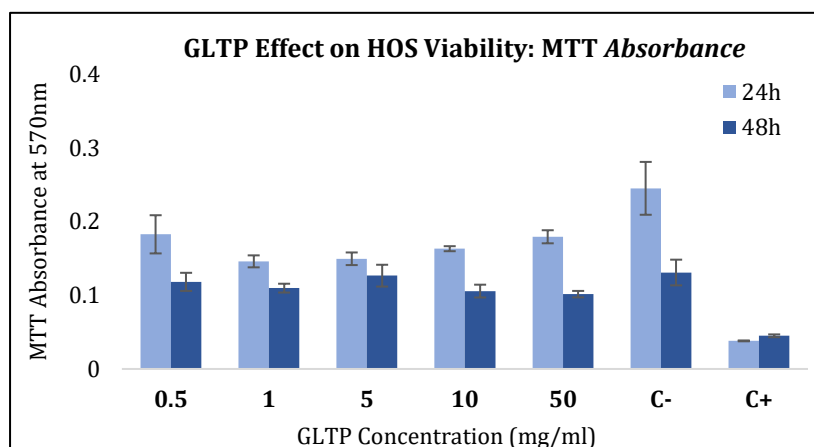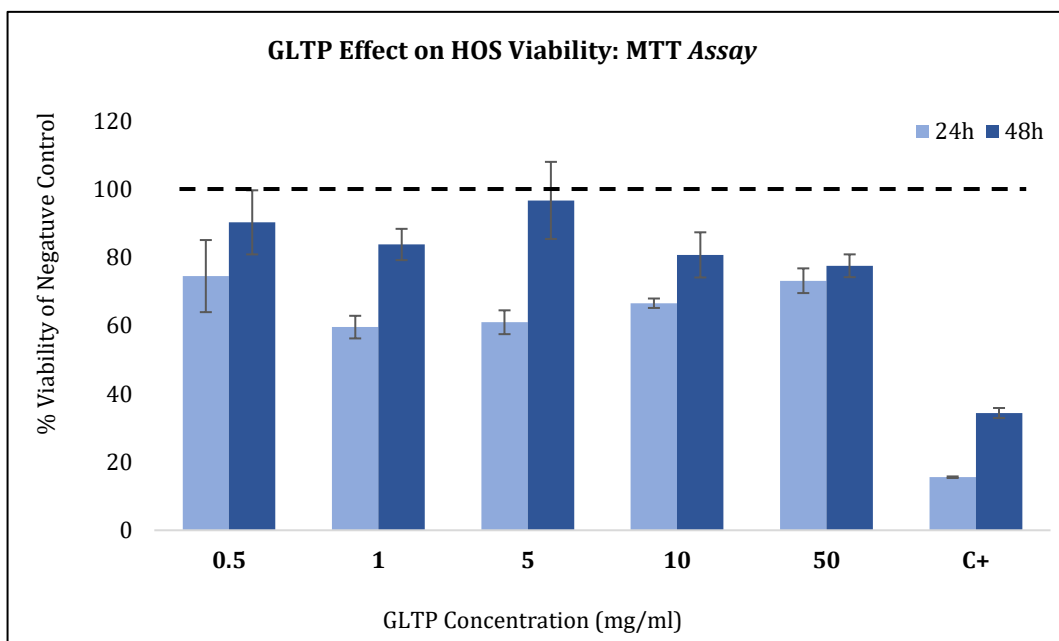
*Novelty processing and smart delivery of Ganoderma Lucidum spores*
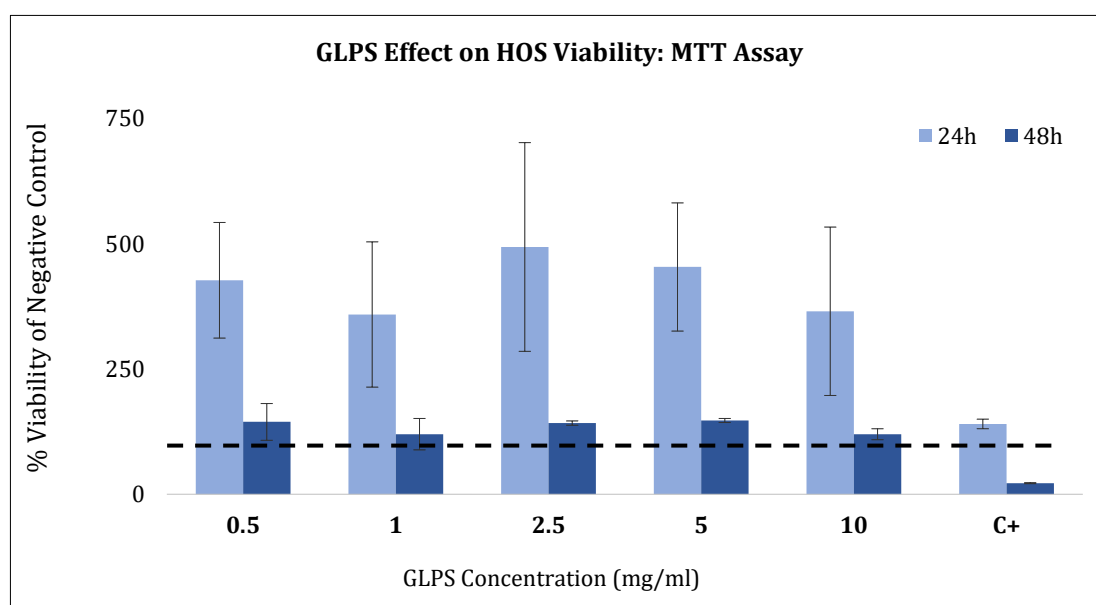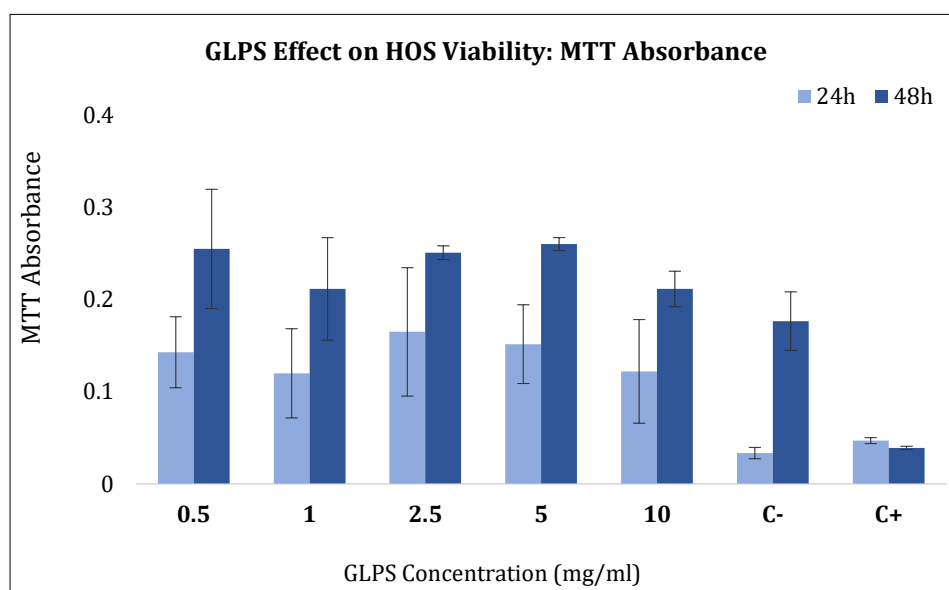
**Figure 4.32:** Effect of GLPS on HOS proliferation after 24 and 48 hours: *MTT Assay* and *MTT Absorbance*. Error bars represent +/- SE as calculated of 3 experimental and 2 administration replicates. Statistical tests revealed that the effect of dosage and exposure time were both statistically significant at 90% confidence (p-value < 0.1). Black dashed line represents the negative (untreated) control, of which MTT results were plotted as a percentage.

As the 24h negative control was very low (perhaps abnormal) it is possible the 24h treatment indicates a positively skewed result. Thus, the absorbance results are also presented to gauge absolute effects of the treatments. As cancer cells typically divide continuously when not treated, low survival in the control could be a result of cell crowding of such a rapidly-growing cell line like HOS resulting in oxygen deprivation and a stationary growth state where many may die out owing to cell crowding [Levayer et al., 2016].

## Exposure Time Effect

GLPS treatment was more impactful on HOS cell growth after 48 hours, according to the MTT *assay* results – but less impactful after 48 hours according to the *absorbance* results. The effect of exposure time was statistically significant on HOS inhibition at 90% confidence. The assay results were skewed with respect to a significantly low viability of the 24h negative control causing a higher-than-expected 24h cell viability. Thus, the absorbance results will be analysed here. An increased exposure time is often associated with less effective inhibition as part of a natural process involving the favouring of certain cells (clonal selectivity) which are suited to the current environment; either naturally present or a result of cell genetic mutation. In other words, an increasingly resistant cell population as time (and dose) continues. *Cell Resistance* is a concept that has arisen in the field of oncology and explains why many cancerous cells are able to overcome the cytotoxic effects of chemotherapeutic agents [Kansal eet al., 2000]. When tumour

*Novelty processing and smart delivery of Ganoderma Lucidum spores*

cells grow, they do so randomly and uncontrollably; often providing the foundations for growing "clones" of cell mutations. Many of these mutations are indeed equipped with an advantage against treatment. This is called "clonal selectivity" and explains why the tumour will at some point become treatment-resistant (justifying the reduced effect after 48 hours) [Gatenby et al., 2009]. When treatment is not effective, of course cells will also naturally continue to multiply until crowding results in death (which would "plateau" the positive effects on proliferation). It should also be considered that GL treatment has shown a *delayed death* response when cancer cells are treated in-vitro owing to apoptotic events that continue to show viability [Maioli et al., 2009]. Many investigators have consequently argued that certain stages of apoptotic activity do not result in cell death in the first 24 hours, thus leading to "false" cell viability results in the MTT assay – apparent viability if cells are at certain apoptotic stages.

### Concentration Effect

All GLPS concentrations failed to inhibit HOS growth to levels below the untreated group, and reasons may allude to the reasons previously described; namely, cell resistance gained from increased drug exposure. The effect of extract concentration was statistically significant at 90% confidence at both time points.

## 4.2.3 In-Vitro Culture of GLS Extracts with HOS Cells: Conclusions

In-vitro PSGA administration to HOS suggested that there is an effect of GL PSGA, as expected owing to its Ganoderic Acid content. HOS cells however were not affected by increased dose, at the range tested. The cancer cells however displayed even greater inhibition after the second tested time-point (48 hours). To evaluate whether the Maximum Tolerated Dose (MTD) was realised in this range, further tests need to be carried out at higher PSGA doses – this will be discussed din chapter 6. It was suggested that the compounds may induce apoptosis on the cell to inhibit cell growth. Alongside the alleged immunoenhancing nature of other biomolecules from the spores of Ganoderma lucidum, such as D-Glucans specifically, this cytotoxic PSGA therapy shows good promise for the development of an anticancer treatment to work alongside harsher, yet effective therapies.

In-vitro administration of the GLPS treatment did not have cytotoxic effects, and this is assumed to be a result of the absence of Ganoderic Acids in this extract (water-soluble compounds only). This inference was verified when the water-insoluble counterpart of this extract was administered to HOS cells, illustrating cytotoxicity.

*Novelty processing and smart delivery of Ganoderma Lucidum spores*

## 4.3 Encapsulation of GLS for Smarter Delivery

The exploitation of GL to date has focused on biocompound isolation and characterisation, particularly verifying potency toward inhibiting cancer. There is however very little study on the delivery of the biocompound once isolated. The need to encapsulate therapeutic compounds stems from their vulnerability to degradative physiological conditions during storage and physiological delivery, but also from the desire to control the speed at which they are released [Zhao 2014; Shao et al., 2019]. Drug delivery systems (DDS) play a large role in how the body identifies and processes drug molecules, and this therefore determines the drug's biodistribution, toxicity, release profile and efficacy [Kudgus et al., 2014]. A drug delivery system (DDS) usually flaunts specific advantages for the delivery of a compound's chemical and morphological properties, typically defining a distribution that is small, uniform, and surface-enhanced [Tiwari et al., 2012]. A traditional DDS presents undesirable side effects attributed to their "idealistic" material that withstands extremities in processing when attaining to a morphologically-perfect system, but also associated with low drug-loading, non-targeted bio-availability, uncontrolled release profiles, and a risk of long-term toxicity [Jong et al; 2008, Jahangirian et al., 2017]. There is limited progress in the field of drug delivery using materials that work in harmony with the physiological environment, as efforts typically focus on effective drug efficacy. "Smart" delivery introduces prospects of more controllable dosing and targeting using more desirable materials, rendering research into biopolymers to encapsulate pharmaceuticals particularly pressing. Biodegradable polymers offer compliance to many DDS prerequisites – ultimately presenting an opportunity to achieve biocompatibility, precise tissue targeting, controllable release, and timely clearance from the body [Tiwari et al., 2012]. To date, the challenges of using biopolymers to encapsulate drug molecules remain, owing to the obstacles to fabrication implicated by a high viscosity, and their instability in certain environments [Mazutis et al., 2015].

### The development of drug delivery *particles*

Over the past decade, smart delivery in the form of particles has sparked considerable interest. Most attractively particulate treatment provides a simple route to injection directly to tissue or intravenously, provides a higher local drug concentration, creates greater dosage precision, are adaptable and flexible to be used as part of a wide range of treatment regimens like inhalation, can overcome the bio-barriers presented by the body and can also increase flowability when compared to fibres, scaffolds, and beads [Kohane et al., 2017; Gundogdu et al., 2014]. Thus, their candidacy for drug delivery is promising – particularly when positioned as a slightly more durable structure when compared to nano-sized carriers [Jamaati et al., 2014]. Being larger than

nanoparticles also implicates a slower release [Collnot et al., 2012]. More recently, the *particle surface* has been shown important in determining the safety and preservation of drug molecules/bioactivity, along with the adherence to cell tissue and release [Gan et al., 2005; Ahuja et al., 2009; Sen Gupta et al., 2016; Slütter et al., 2016]. The ability to control these aspects of a delivery system is therefore invaluable in manipulating the treatment plan achievable. Particle shape has actually received limited attention in the drug delivery field, as its repeatability across studies is not straightforward and thus their investigations cannot be consistently recorded. In particular in the face of diseases like cancer, the physiological conditions presented in the body are less normal, with the efficacy of treatment becoming reliant upon changes to the vascular system, as well as an unusual extracellular matrix and gradient fluid pressures [Ariffin et al., 2014; Toy et al., 2014]. This renders drug delivery system engineering even more essential as "biobarriers" are overcome with features such morphology and surface topography that direct flowability, adhesion to tissue, and protection until attaining the target site [Paolino et al., 2006]. Consequently, to date, the majority of drug delivery studies focus on developing and optimising repeatable spherical particles for their ability to bypass biobarriers, their repeatability, and also their free-flowability in the bloodstream [Moghadam et al., 2008; Cooley et al., 2018]. As a result, particular interest has been directed toward the processing of polymers using powerfully mechanised systems such as Electrohydrodynamic Atomisation (EHDA) [Mehta et al., 2017]. Another crucial angle of study is the need to maximise the *drug-loading* of a delivery system in the face of the physical characteristics required for a strong and efficient carrier– such as high polymer content. This is typically evaluated via encapsulation efficiency with respect to specific fabrication techniques and material/surface features like porosity [Annabi et al., 2010]. In current DDSs based on *natural biopolymers*, there are challenges in creating a matrix that is not loaded with a **primarily polymer counterpart**, as great concern is given to particle integrity during fabrication, storage, and physiological passage particularly when concerning biopolymers [Baimark et al., 2014; Ahmed et al., 2013].

The purpose of this section of study is to establish a process that would controllably create an alginate-based matrix that would encapsulate and release GLS without compromising the GLS content of the matrix. Importance is given to the distribution *size* and *shape*, as well as surface features. The achievable release profile was subsequently evaluated and associations were made between the distribution properties and their rate of release. GLS:A ratio plays an important role in EHDA fabrication of particles, in particular due to viscosity and also polymer content (and the implicated particle strength and capacity for drug loading). To more closely analyse which effect is strongest, GLS:A particles containing the GLS matrix either contained 2% alginate *or* 1% alginate. This strategy therefore first evaluated the effect of alginate content with an identical

*Novelty processing and smart delivery of Ganoderma Lucidum spores*

drug loading, and subsequently investigated whether the polymer effects would hold in the face of a different drug loading.

## 4.3.1 EHDA to Encapsulate GLS for Delivery

Electrohydrodynamic Atomisation (EHDA) is a popular technique for the generation of small particles and fibres tailored for drug delivery [Jeyhani et al., 2018]. EHDA atomizes a liquid or polymeric solution via electrostatic forces that surpass its surface tension and foster disruption. Exposure to a high electric field causes the droplet at the capillary/needle tip to adopt a conical shape as a result of electrostatic repulsions (internal) and attractive Coulombic forces (external). Varicose instability causes subsequent rupture into smaller droplets [Nikoo et al., 2018]. EHDA is capable of exerting significant control over the resulting particle/fibre distribution as its processing parameters have consistent and measurable effects over a wide range of materials and biomaterials. Studies have already established the relationship between EHDA process parameters and the achievable size and shape of polymer particles (voltage and flow rate in particular), however employing *sodium alginate without co-polymers* in EHDA has been challenging with respect to particle stability and distribution controllability. Figure 4.33 visualises the EHDA process, from extrusion to droplet collection.
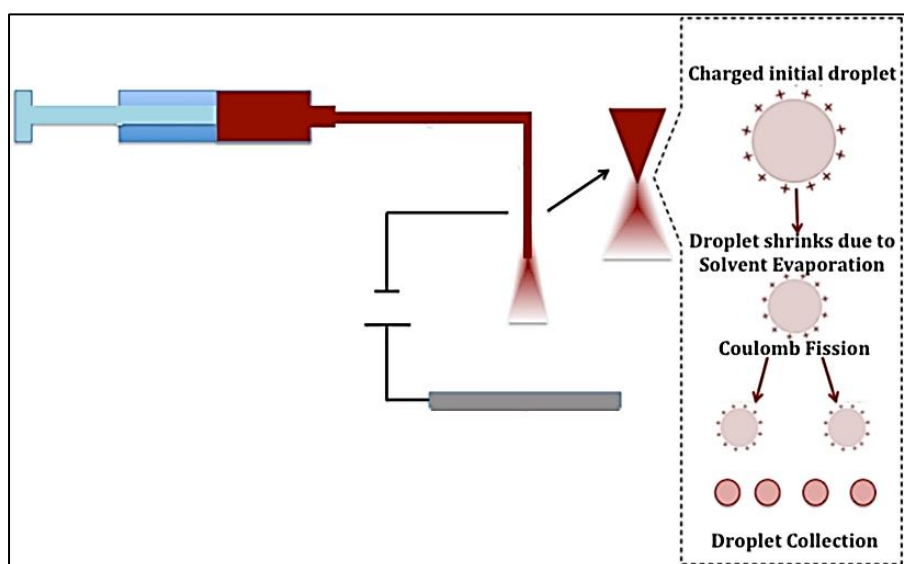


**Figure 4.33:** GLS-A solution subject to EHDA. The solution is subject to high voltage at the meniscus, before disrupting into a drip/spray as surface tension is overcome and continuous Coulomb fission occurs

The use of polyelectrolyte materials that have chain-bound electric charges like alginate, can complicate the EHDA process. This is because of the interaction between the polymer chains

*Novelty processing and smart delivery of Ganoderma Lucidum spores*

including entanglement, repulsion, and hydrogen bonding; along with the conductivity of water in the hydrogel, all of which are influenced by the EHDA electric charge [Saarai et al., 2011; Kaklamani et al., 2018; Gurikov et al., 2018]. These interactions can cause various morphological and topographical effects on the particle. The degree of chain interaction is also determined by polymer concentration, molecular weight, and solution conductivity - therefore it is inevitable that the characteristics of the final distribution will be a function of a complex product of many process parameters [Farrés et al., 2014]. To date, the study of alginate hydrogels, in particular their conductive abilities, has been very limited. Nevertheless, their study can present opportunities for increasingly effective drug delivery as well as diagnostic biosensors.

Alginate hydrogels have an interconnected pore network that typically renders controlled/sustained release challenging as compounds with a small molecular size are not easily retained. Thus traditionally, alginate matrices have been reinforced using a copolymer to retard the diffusion as well as maintain particle integrity. The aim of this investigation was to establish a workflow which could create alginate particles in the absence of copolymers, containing GLS and possessing a relatively uniform distribution with respect to size and shape in efforts to establish a treatment system that is safe, effective, and predictable, without compromising the amount of GLS that can be loaded. Unfortunately to date, alginate-only particles fabricated using EHDA have been limited to sizes that are too large for many therapeutic applications as a result of its heat/pressure thresholds, or employ very little drug to achieve desirable physical characteristics [Baimark et al., 2014; Moghadam et al., 2008; Xie et al., 2007]. In contrast, some studies actually employ low alginate concentrations to create nano/micro-range distributions – an issue that may prove a challenge to drug loading, particle integrity, and resulting controlled release profiles [Xie et al., 2007]. This section of investigation evaluates the effects of EHDA process variables (voltage, GLS:polymer ratio, and drying regime) on the final morphology and surface attributes of delivery particles. Sodium alginate is employed owing to its biocompatibility and desirable mucoadhesion properties discussed in chapter 2 [Klock et al., 1997]. Finally, the in-vitro release profile of the resulting GLS-Alginate (GLS-A) particles is studied with consideration of their distribution characteristics.

## 4.3.1.1 EHDA Spraying Regimes

Continuous droplet rupture is caused by Coulomb fission, whereby the droplets possess enough charge density (via applied voltage) to overcome its surface tension, implicating smaller and more numerous droplets. Excessive voltage however could foster spraying instability and result in deformed polydispersed distributions via "satellite" droplets [Rutkowski et al., 2018].

Droplet generation in the form of *microdripping* is therefore a desirable foundation for a small particle distribution with a high degree of uniformity [Rutkowski et al., 2018; Castillo-Orozco et al., 2017]. This concept is further elaborated in the literature review of this thesis. In this mode, single droplets are created (as in the dripping mode), but droplet diameter is smaller than the capillary diameter owing to the jet formation at the meniscus. Eventually a single droplet results from solution accumulation at the jet's tip and the jet retracts to start the cycle again [Castillo-Orozco et al., 2017]. Along with a high-enough voltage to foster rapid/frequent droplet disruption, achieving a stable multidripping mode demands a thin spraying solution to minimise the surface tension during the droplet disruption process; something more challenging to achieve using viscous alginate [Rutkowski et al., 2018; Fu et al., 2011]. Alginate has been operated in this mode using copolymers like chitosan, however even in the presence of chitosan, average particle diameters were close to 1,000 μm and particles were polydispersed [Nikoo et al., 2018]. Other studies have used pure alginate to investigate the characteristics of the spray regime when subject to various EHDA process settings. One particularly insightful study in 2018 reported very small microparticles (diameters between 1 and 5 μm) however the distribution was polydispersed with respect to shape and a high voltage of 22kV was required [Rutkowski et al., 2018]. Authors attributed the dependency of size and shape on the spraying mode achieved – the conejet mode achieved the smallest particle diameters, for example – however, this study affirmed that the alginate concentration and the spraying distance are significant influencers of droplet distribution. Ethanol was used as a part of the aqueous alginate solution, enhancing conductivity and the rate of solvent evaporation and thus fostering the modes attainable in this study [Olumee et al., 1998].

In the present investigation, the voltage range 5-15kV was chosen based on preliminary results, along with findings in literature which report electrostatic instability of alginate above 10kV during electrospraying, and limited effects on particle size at higher voltages [Nguyen et al., 2016, Mehregan Nikoo et al., 2016]. In 2015, Khorram reported that for 2wt% alginate solution, a voltage of 8kV created the smallest particle distribution [Khorram et al., 2015]. This is known as the *critical voltage*, after which droplet size is unaffected as the electrical potential can no longer overcome the solution surface tension [Mehregan Nikoo et al., 2016]. The critical voltage will vary among alginate studies owing to differences in solution viscosity, added drug, and solution flow rate. For alginate solutions typically employed in electrospraying (2-3 wt%), it is usually reported at 6-10kV [Zhao et al., 2007; Park et al., 2012; Nedović et al., 2001]. Prior to evaluating the effects of EHDA voltage on GLS-A particles in this study, it was acknowledged that the *droplet generation stage* of particle formation via EHDA is a determining factor in the final particle distribution [Xie et al., 2007]. The spraying regime therefore sets the foundation particularly for the particle morphology via its effect on droplet generation. In 2018 for example Rutkowski observed that

*Novelty processing and smart delivery of Ganoderma Lucidum spores*

spherical, cylindrical or more complex alginate particle geometries were determined by the EHDA spray-mode when varying alginate concentration and EHDA process parameters [Rutkowski et al., 2018]. The study reported that the round particles could be created using a dripping mode, however the cone-jet mode generated more polydispersed shapes (including rods) that were smaller. Processing conditions in that study confounded other effects, in particular spraying distance. Spherical particles were not achieved. Polydispersed particle distributions via the cone-jet mode of electrospraying alginate are frequently reported [Zarrabi et al., 2009].

Theoretical analyses of polymer droplets subject to an electric field have been undertaken for decades, yet the electrostatic mechanisms behind the spray characteristics are still enigmatic - largely owing to the uniqueness of polymer/drug combinations [Zhao et al., 2007]. This study intends to control certain influential variables in order to determine their effects on the achievability of desirable alginate-GLS particles. For all analyses, processing variables were evaluated with respect to their impact on the *size/shape of particles,* and particle *surface characteristics.*

## 4.3.2 EHDA to Create *High-Polymer* GLS-A 1-1 Microparticles

The transition between spraying modes has been established for many non-viscous conductive solvents like water, however it is a complex mechanism for viscous conductive materials like alginate. For alginate, the dropping mode is typically the only mode favourable of uniform particles [Mehregan Nikoo et al., 2016; Zhao et al., 2007]. GLS-A 1-1 containing 2% GLS and 2% alginate was employed in this part of the study. The alginate used was a 2wt% solution; *non-Newtonian* and *viscous* [Moghadam et al., 2009]. This has traditionally presented challenges to the cone-jet/laminar jet spraying mode, and thus a pulsating jet or dripping mode is often observed [Mehregan Nikoo et al., 2016, Moghadam et al., 2009]. In this study the spraying regime remained in the dripping mode across all voltages (subject to both flow rates). Figure 4.34 shows the achieved dripping mode for GLS-A 1-1 containing 2% GLS and 2% alginate*,* imaged at flow rate 50 μl/min. When droplets were sprayed at the lower flow rate (10 μl/min) they were smaller, owing to a higher charge density of a smaller "pumped amount". The resulting smaller droplets, possessing greater charge, in turn induced more frequent and effective disruption of the droplet surface tension [Khorram et al., 2015].

| Disruption occurs when ST is overcome and the Rayleigh limit is attained | | |
|---|---|---|
| High surface tension<br><br>Voltage insufficient to overcome surface tension and droplet grows<br><br>Final droplets are large<br><br>**Solution Accumulation** | Lower surface tension that voltage overcomes rapidly<br><br>Smaller droplets = higher charge density = more frequent disruption<br><br>**Dripping** | An increasingly narrow meniscus is attained as voltage increases and collects at the tip<br><br>Rapid attainment of the Rayleigh limit and droplets disrupt continuously into increasingly smaller droplets<br><br>**Microdripping** |
| 5kV | 10-15kV | |

**Figure 4.34:** Schematic of dripping regime observed during EHDA of GLS-A 1-1 at flow rate 50 µl/min and 5-15kV. Droplet morphology at the meniscus is described for each regime observed as a function of voltage

## 4.3.2.1 Effect of EHDA Voltage on GLS-A 1-1 Particle Size and Shape

The effect of voltage was statistically significant on both particle size and shape at both flow rates, with 95% confidence. Figures 4.35 – 4.37 show the particles created using EHDA at voltages 5, 10 and 15kV and flow rates 10 and 50µl/min after 48h air-drying, imaged using a camera, optical microscopy, and SEM, respectively.
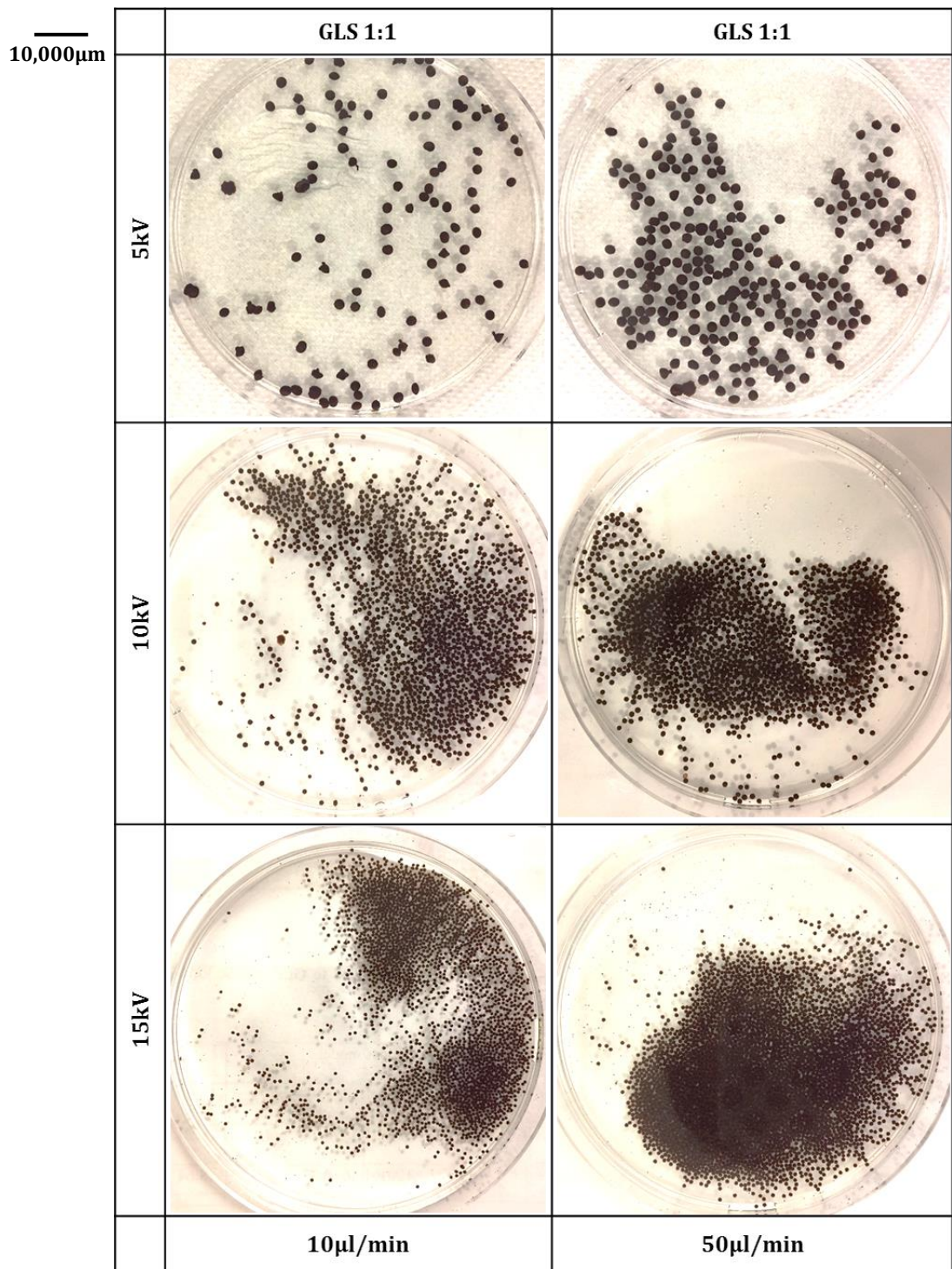
**Figure 4.35:** GLS-A 1-1 particles after 48 hours of drying. The effect of voltage is visually evident GLS-A 1-1 on particle size across both flow rates

*Novelty processing and smart delivery of Ganoderma Lucidum spores*
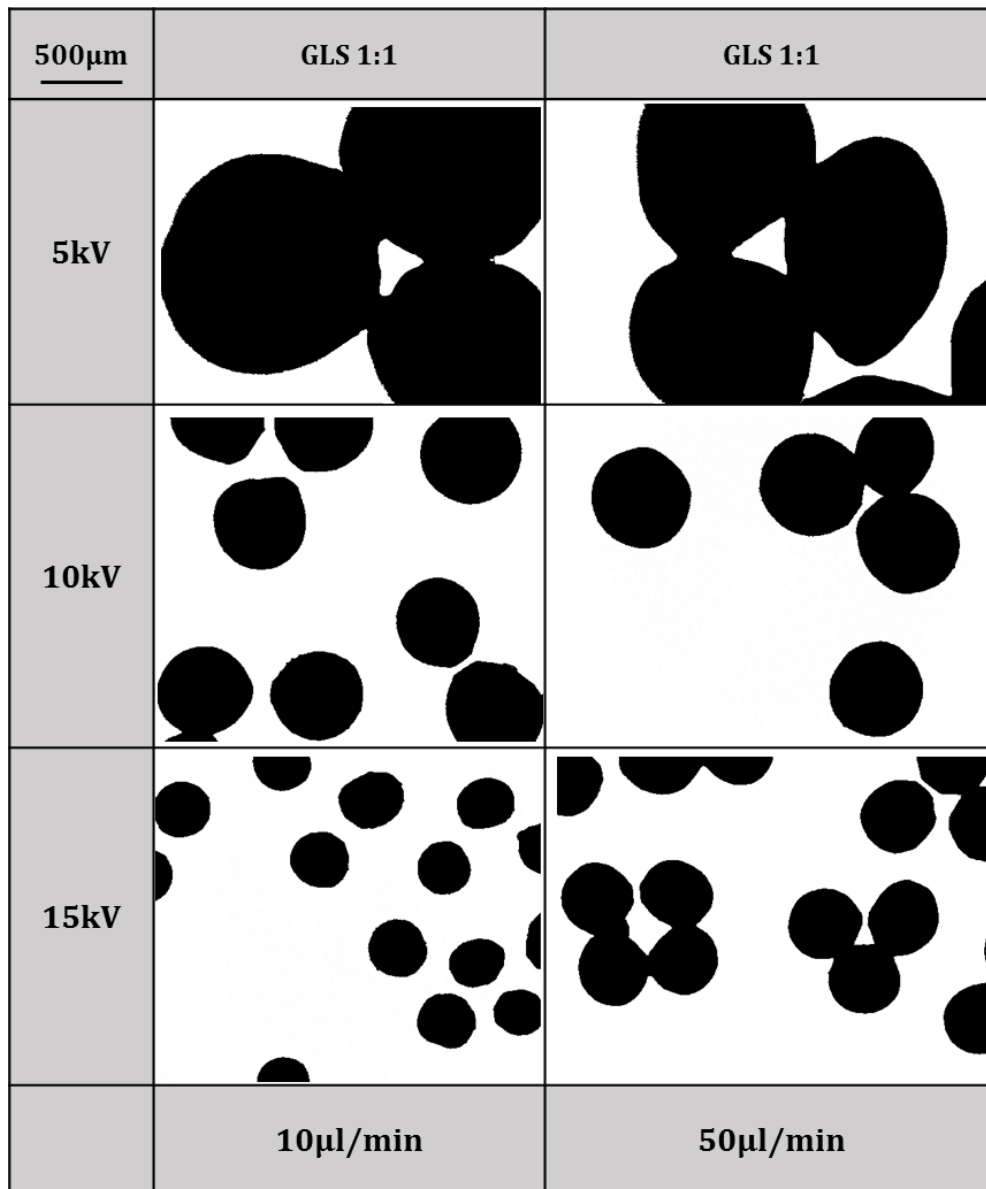
**Figure 4.36:** Optical Microscopy of GLS-A 1-1 particles air-dried for 48 hours. In this visualisation of GLS-A 1-1 particles, the effect of flow rate on particle size is most prominent at the highest tested voltage (15kV). The effect of voltage is evident on particle size

*Novelty processing and smart delivery of Ganoderma Lucidum spores*
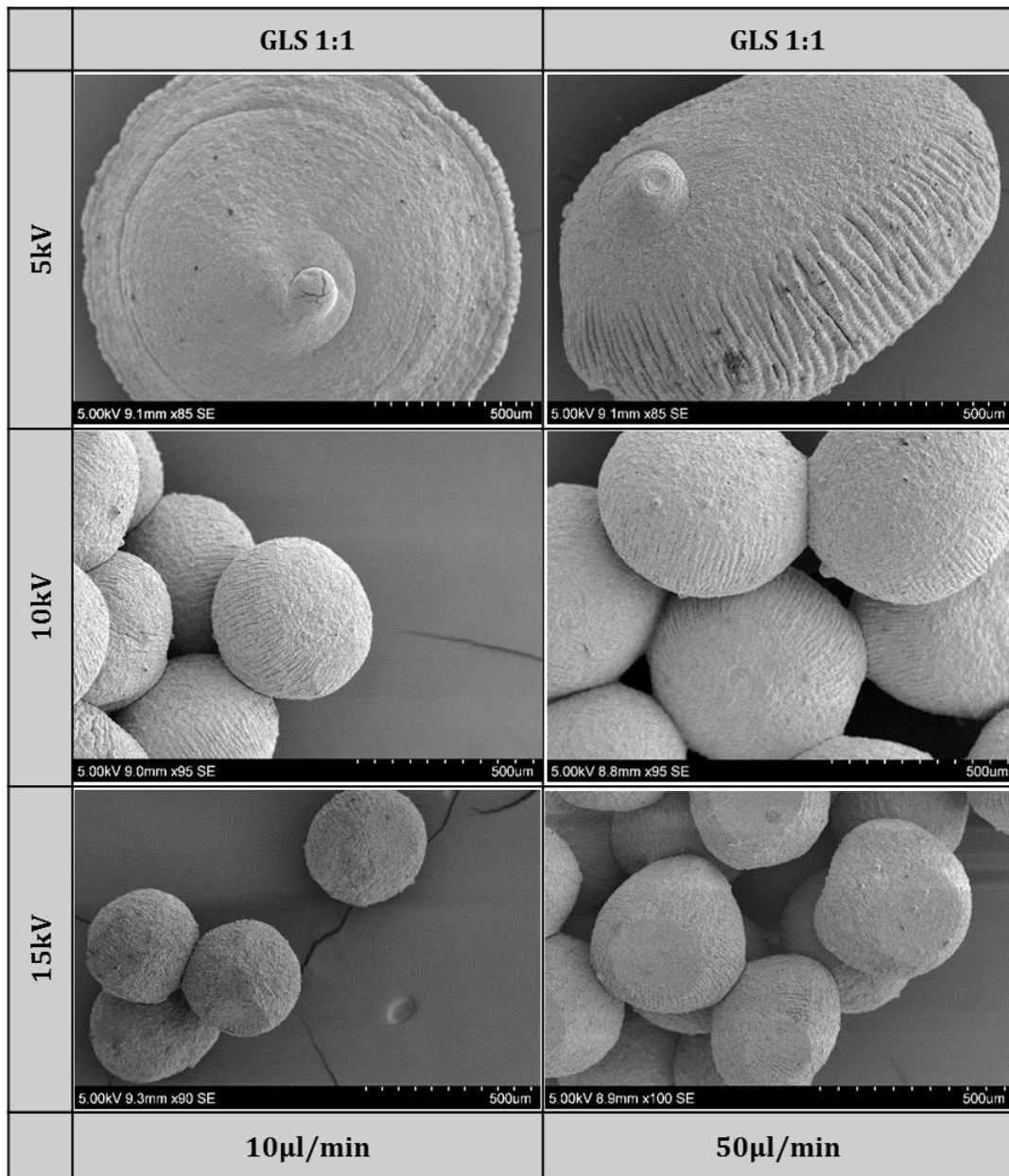
**Figure 4.37:** SEM of GLS-A 1-1 particles air-dried for 48 hours following EHDA at voltage 5 – 15kV and flow rate 10 and 50 µl/min

The effects of EHDA on particle size are governed by the rate at which droplet surface tension is overcome and its subsequent pattern of Coulomb fission. With increased applied voltage, the size of the meniscus droplet reduced owing to a higher charge density, fostering greater ability to overcome surface tension at the meniscus and continuously thereafter owing to a continuously higher droplet charge density [Wilm et al., 2011]. The law of mass conservation also suggests that the meniscus would shrink when subject to greater voltage. This resulted in a conical spindle at

*Novelty processing and smart delivery of Ganoderma Lucidum spores*

the meniscus owing to the build-up of charge density at the tip [Khorram et al., 2015]. At the highest voltage (15kV), there was an increase in the frequency of droplet disruption leading to smaller and more numerous droplets (microdripping) [Wilm et al., 2011; Moghadam et al., 2009]. Voltage therefore had a negative correlation with particle size between 5 and 15kV in this study, whereby a 74% reduction in size was achieved in samples created at the lower flow rate and a 68% reduction in size was achieved in higher flow rate samples [Khorram et al., 2015]. The rapid and frequent droplet disruption further resulted in little possibility of droplet elongation (there is less time to deform prior to fission), leading to more spherical particles – with an aspect ratio closer to 1. Figures 4.38 and 4.40 plot the effects of EHDA voltage and solution flow rate on the average particle size and shape (aspect ratio) respectively, of the GLS-A 1-1 particle distribution.
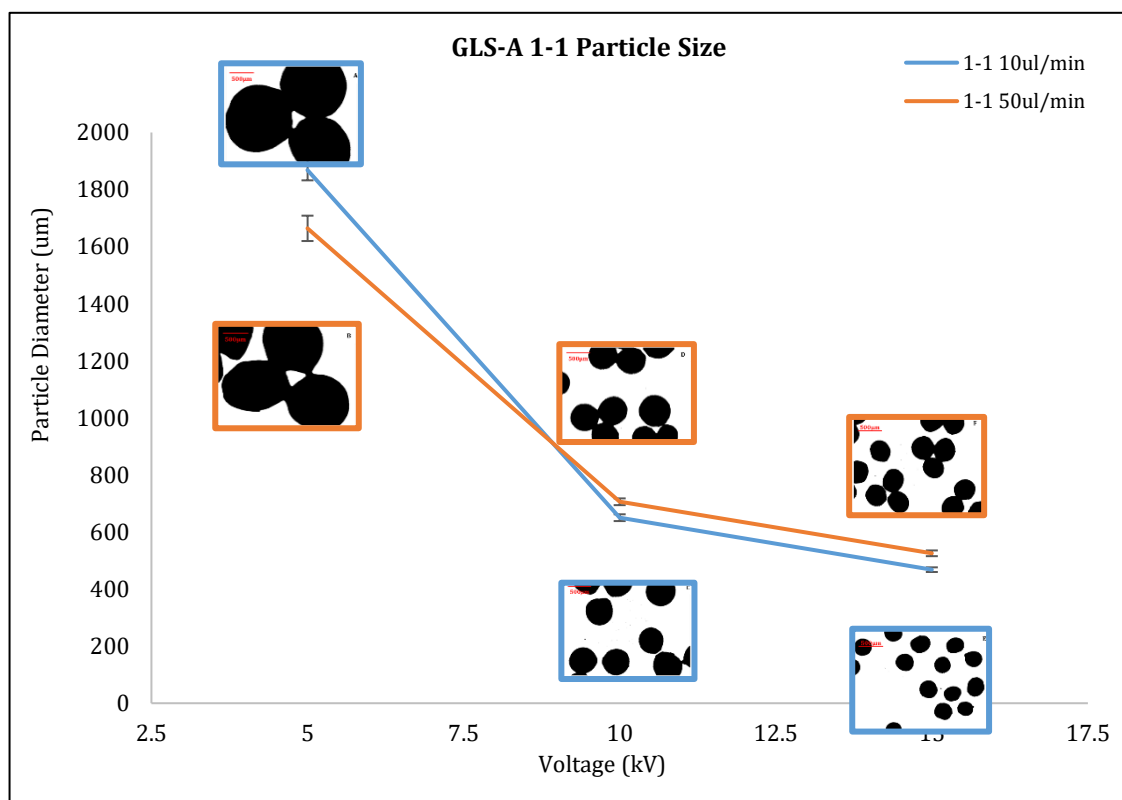


**Figure 4.38:** Voltage effect on GLS-A 1-1 particle size created at 5-15kV, at both 10 and 50µl/min. Red error bars represent the SE of 30 particles. The effects of voltage and flow rate on particle size were statistically significant at 95% confidence. *Inset images* show the corresponding optical micrographs of the particles

Furthermore, a voltage that is excessive for the polymer formulation can generate "satellite droplets" that contribute to a polydispersed distribution [Ku et al., 2002, Xie et al., 2007 (c)]. Mehregan Nikoo (2016/2018) and Khorram (2015) for instance showed that alginate particles

*Novelty processing and smart delivery of Ganoderma Lucidum spores*

were smallest and most monodispersed at 8-10kV EHDA, after which both shape and size were compromised [Mehregan Nikoo et al., 2016; Khorram et al., 2015]. Moghadam in 2008 created spherical alginate beads with a minimum achievable diameter of 578 μm using a 9 kV-induced EHDA jet, yet this particle distribution had a high standard deviation [Moghadam et al., 2008]. In the voltage range tested here, particles were most spherical at 10kV, explainable by its steady pattern of disruption when compared to the higher voltage (15kV) [Ku et al., 2002; Mehregan Nikoo et al., 2016]. By adding a ring electrode to enhance the stability and efficiency of the cone-jet spraying mode, studies have been able to generate smaller alginate microparticles maintaining a spherical shape - however not yet below 200μm [Xie et al., 2007 (c); Zeng et al., 2018].

The nature of alginate itself needs to be considered owing to the effect of its viscosity on solution spraying behaviour. Alginate's viscosity on solution spraying behaviour infers that a cone-jet spray is not easily attained, owing to its viscid and non-Newtonian behaviour that results in less efficient and continuous droplet rupture. Instability would result at the high voltages conducive to cone-jet spraying, as observed in a study by Moghadam in 2009 when processing 2% alginate via EHDA [Moghadam et al., 2009] (figure 4.39).
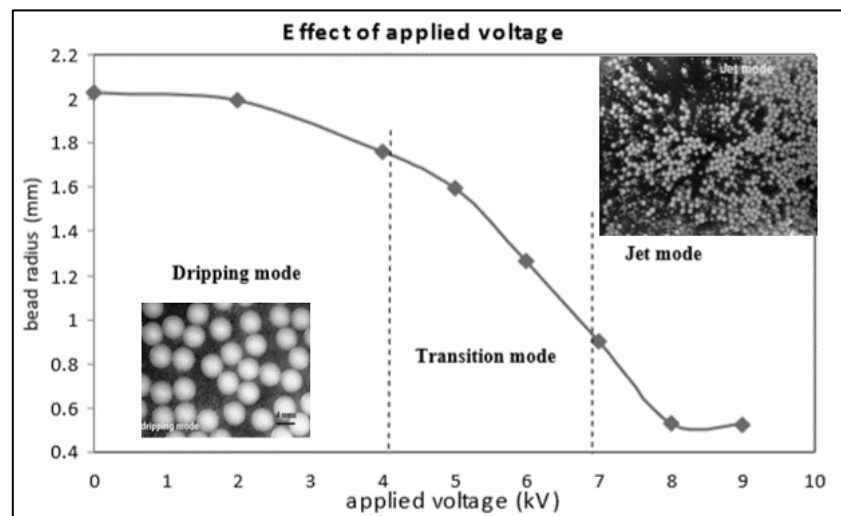


**Figure 4.39:** Achieving various spray regimes during the EHDA of 2% alginate using increasing voltage. Particles are smaller at the jet mode of spraying, however are more polydispersed

During spraying, heat/mass transfer also causes solvent evaporation from droplets, leading to particle shrinkage. This was not measured in this study. The rate of evaporation is also influenced by the electrostatic charge on the droplets, hence a more charged particle would exhibit greater shrinkage.

*Novelty processing and smart delivery of Ganoderma Lucidum spores*

The particle aspect ratio (AR) was used to gauge particle sphericity. Rapid and effective droplet disruption leaves less time for droplets to deform; resulting in more *spherical* particles as voltage increases. AR was affected by the increasing voltage only up to 10kV, due to alginate's critical voltage (figure 4.40).
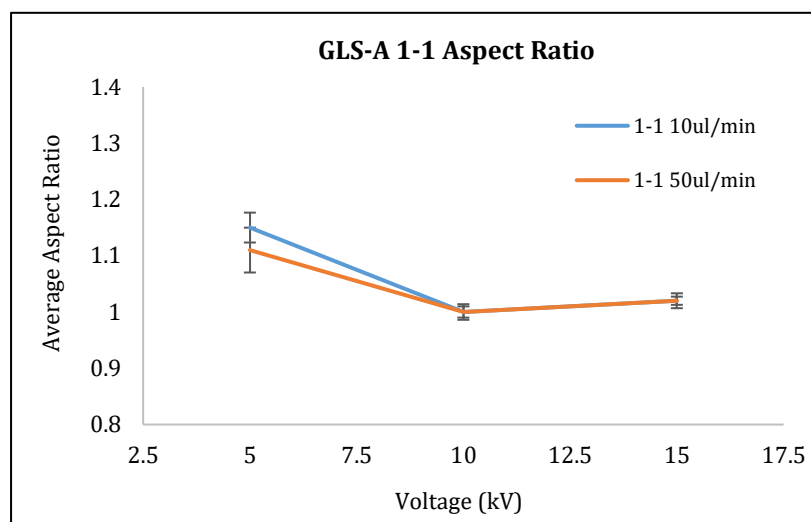


**Figure 4.40:** Voltage and flow rate effect on GLS-A 1-1 particle AR created at 5-15kV and 10-50µl/min. Error bars represent the SE of 30 particles. The effects of voltage and flow rate on aspect ratio were statistically significant at 90% confidence.

The effect of flow rate was not investigated as an experimental variable, however its effect on particle size and shape at the tested voltages was statistically significant. Generally, a higher flow rate created larger droplets because of a reduced charge density per droplet, rendering disruption less effective [Mehregan Nikoo et al., 2016; Page et al., 2007]. The resulting droplet, and its progeny, disrupted less effectively owing to less charge density, and therefore less frequently [Wilm et al., 1994]. These larger particles also undergo less evaporation than a smaller particle, resulting in less shrinkage and structural deformity [Page et al., 2007]. Thus, at a given voltage, the increase in flow rate would decrease charge density and lead to ineffective and infrequent droplet disruption and a resulting larger particle distribution [Kim et al., 2015]. Khorram in 2015 reported that at a certain flow rate (830 µl/min in that study) this relationship reversed when spraying 2wt% alginate, instead enhancing the cone-jet spray mode that was conducive of smaller particles [Khorram et al., 2015]. This phenomenon was also reported by Moghadam in 2010 [Moghadam et al., 2010]. The size discrepancy induced by flow rate was observed at the 2 higher voltages only however, suggesting that at 5kV the electrospray ionization of the GLS-A meniscus was not affected by the higher flow rate [Mehregan Nikoo et al., 2016]. Some studies have suggested that this could be attributed to the counteractive effect of the shear

*Novelty processing and smart delivery of Ganoderma Lucidum spores*

thinning behaviour of alginate at the meniscus when subject to a higher flow rate; inducing a decrease in apparent viscosity and decrease in particle size [Khorram et al., 2015; Moghadam et al., 2010]. Electrospraying is also primarily voltage-driven if the regime is stable, rendering the effect of flow parameters negligible [Ryan et al., 2014; Tang et al., 2004].

## 4.3.2.2 Effect of EHDA Voltage on GLS-A 1-1 Surface Characteristics

### 4.3.2.2.1 GLS-A Porosity and Roughness

A particle's pore size in a drug delivery system plays an instrumental role in release speed and control [Fu et al., 2011]. For example, cracked walls and pores can lead to drug leaching and drug "bursts", and imply an underlying weak structure that is prone to structural compromise during physiological passage. This can reduce treatment effect and introduce the risk of a treatment overdose or negative physiological response. Importantly, they are also inefficiently loaded. Alginate hydrogels are inherently porous, with an interconnected pore system and surface roughness that render its hydrogel form flexible and therefore controllable; desirable for tailored treatment regimens [Fu et al., 2011]. To date controllability over alginate's pore size is achievable, however it is challenging on a large scale owing to alginate's viscosity during processing and interaction with different drug compounds [Boontheekul et al., 2005; You et al., 2017]. Nonetheless, it remains one of the most widely employed biopolymers in the microencapsulation of pharmaceuticals owing to biocompatibility, hydrogel flexibility, and inexpensivity [Klock et al., 1997].

GLS-A surface analysis was evaluated by calculating the average pore diameter across the particles. In addition, a novel measurement was considered in order to gauge the pore size relative to the particle size – termed the *Surface Defect Ratio* (SDR). This is because large pores that are created on the surface of smaller particles can instigate an undesirable unstable and rapid release in the body [Pastor et al., 2015]. SEM was employed to evaluate particle surface texture features and pores were measured using Image-J, limiting measurement to "micropores" (>0.1μm). While advanced control of hydrogel porosity is achievable through microfabrication techniques such as freeze-drying, gas-foaming, and micropatterning, this work has focused on porosity as a *consequence* of the methodology employed. Ultimately, inferences can then be made on particle integrity and subsequent release profile when the polymer-drug solution is exposed to EHDA processing. Figure 4.41 plots the effect of voltage on GLS-A 1-1 average pore size. An increased voltage was associated with smaller pores – particularly where the smaller particles were concerned (those created at 10μl/min) where a pore reduction of 54% was achieved by increasing voltage from 5kV to 15kV (2.88 (± 0.3) μm to 1.32 (±0.1) μm). In all

*Novelty processing and smart delivery of Ganoderma Lucidum spores*

samples, porosity was a result of defects formed during alginate processing and drying [Dou et al., 2017].
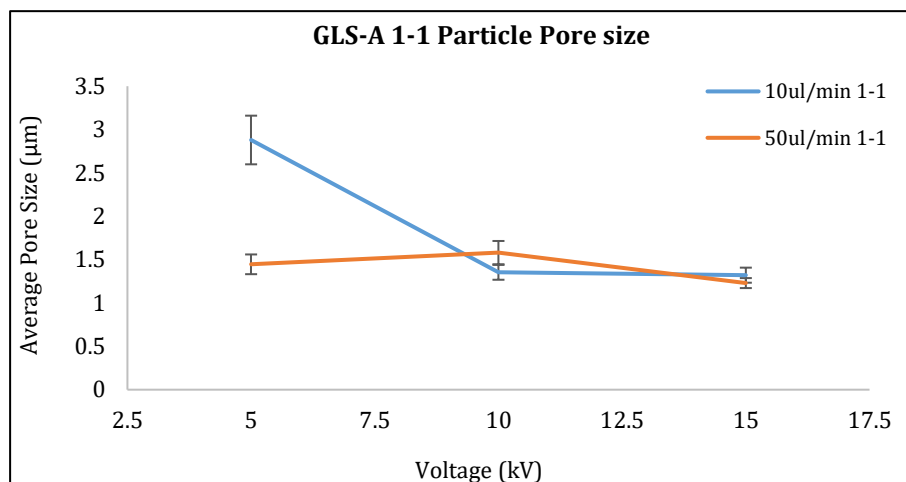


**Figure 4.41:** GLS-A 1-1 particle pore size on particles created at voltages 5-15kV and flow rate 10-50µl/min. Error bars represent SE of 5 particles, on which 20 pores were averaged. The effects of voltage and flow rate on pore size were statistically significant at 90% confidence

When the polymeric network contains charged moieties, such as the case with alginate, its conductivity during EHDA provides a rich source of electrostatic mechanisms like repulsion, chain fracture, and shrinkage – all of which can generate surface defects and ultimately result in a highly porous alginate matrix [Rutkowski et al., 2018; Du et al., 2008; Khademhosseini et al., 2006]. This led to the positive correlation between voltage and the degree of surface roughness, in particular on particles created from droplets with a higher charge density. The SEM images in figure 4.42 further demonstrate that at higher voltages particle surfaces are also more *crumpled*. Increased voltage was however associated with *smaller* pores. This could be a result of particles being correspondingly smaller at the higher voltage, thus reducing the extent of polymer chain shrinkage that would otherwise typically foster porosity and defects (a confounding effect of size on any voltage-induced porosity). Smaller droplets also exhibit an increased crosslinking density per particle. This is because each particle possesses a smaller physical size to be crosslinked and therefore an increased prevalence of crosslinkable junctions. This high crosslinking density can cause brittleness that renders the chains less flexible to movement, and thus smooth surfaces are challenging to form [Xu et al., 2014; Costa et al., 2015]. This concept is known as "chain conjunction". Any gaps between chains will likely be a source of built-up hydraulic and pneumonic pressure beneath particle surface, resulting in surface defects like wrinkling. In the drying stage,

*Novelty processing and smart delivery of Ganoderma Lucidum spores*

this could be of particular importance where entrapped water would quickly escape the particle and in the process leave behind a wrinkled structure.
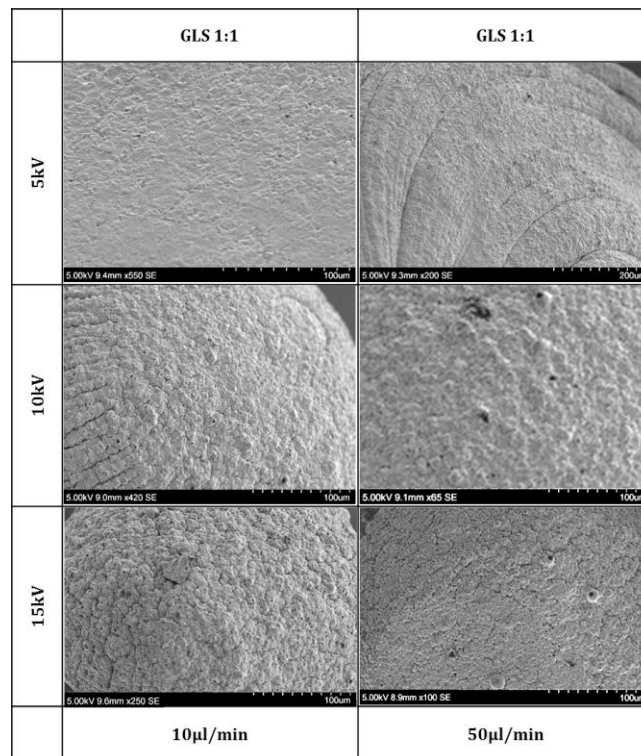


**Figure 4.42:** SEM images of surface of GLS-A 1-1 particles showing the crumpling effect of voltage on particle surface owing to increased electrostatic repulsions and activity among alginate chains

Lastly, particles that have defects from higher voltage are likely to exhibit a higher rate of water evaporation from the hydrogel network during spraying, due to a higher charge density and indirectly through its smaller size, and also during drying (due to size). Rapid water loss can cause a looser and more disordered surface. Even though particles were measurably less porous at a higher voltage, they were visibly more affected by the voltage.

Flow rate was not tested as a variable, however a higher flow rate generally correlated with a smaller average pore size. Particles created at the higher flow rate (50 µl/min) were previously associated with less charge density per particle during spraying; thus a reduced prevalence of alginate's electrostatic chain effects that could foster defects. Furthermore, crosslinking density is likely to be less extensive in these larger particles, suggesting greater flexibility of alginate chains to move around and avoid "rigid" brittle structural restrictions that could cause surface roughness and/or defects [Xu et al., 2014].

*Novelty processing and smart delivery of Ganoderma Lucidum spores*

### 4.3.2.2.2 GLS-A Porosity Relative to Size

*Small particles with large pores* have become the subject of many recent investigations, with many researchers observing benefits for drug delivery and thus treatment efficacy [Wang et al., 2016]. While the relationship between pore size and particle size was not investigated in this work, it has previously been shown that a polymer particle's porosity is associated with particle size usually as a result of increased compressibility of porous particles, leading to natural shrinkage. On the other hand, some studies have raised the notion that larger pores can be created as a result of polymer matrix expansion during drying as a result of interconnected pores [Stewart et al., 2006; Zhang et al., 2017]. The relationship between pore size and particle size is shown by the scatterplot in figure 4.43 below, measured on dried particles viewed via SEM. There is a general positive correlation between the pore size and particle size, suggesting that smaller particles typically had smaller pores, and larger particles had larger pores. It is worth pointing out that at the higher voltage, this study has observed a smaller particle size *and* smaller pores – thus, this section of study requires further controlled investigation.
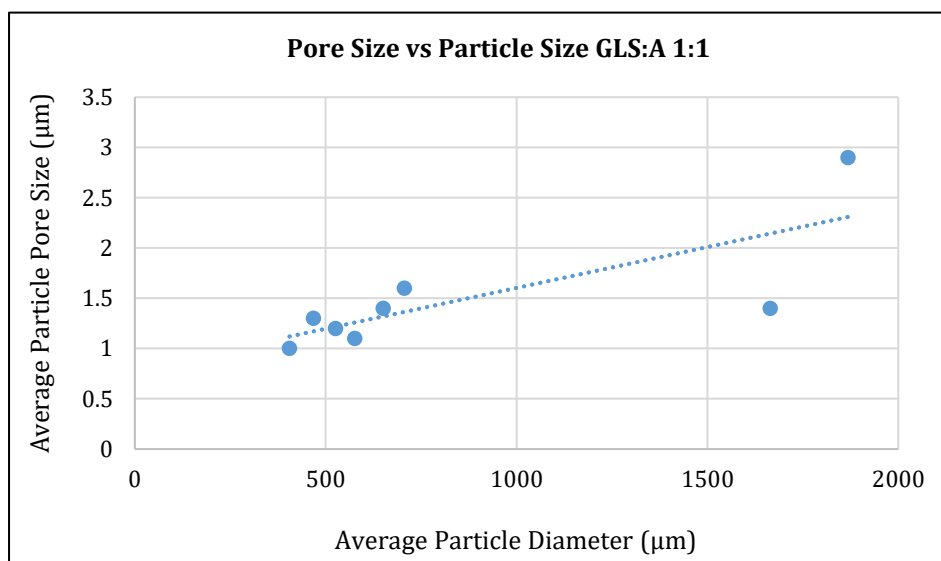


**Figure 4.43:** The relationship observed between average particle size and average pore size of GLS-A 1-1 particles (n=30 for both)

Figure 4.44 shows the GLS-A 1-1 particle porosity relative to the particle size on which it was measured (as above) however as a function of voltage. This measurement is referred to Surface Defect Ratio (SDR) in this study, and a higher SDR would be reflective of a smaller particle with larger pores. The positive correlation between the pore size and particle size however suggested

*Novelty processing and smart delivery of Ganoderma Lucidum spores*

that a small SDR is likely a result of a small pore *and* a small particle diameter (rather than the more "desirable" small particle with large pores).
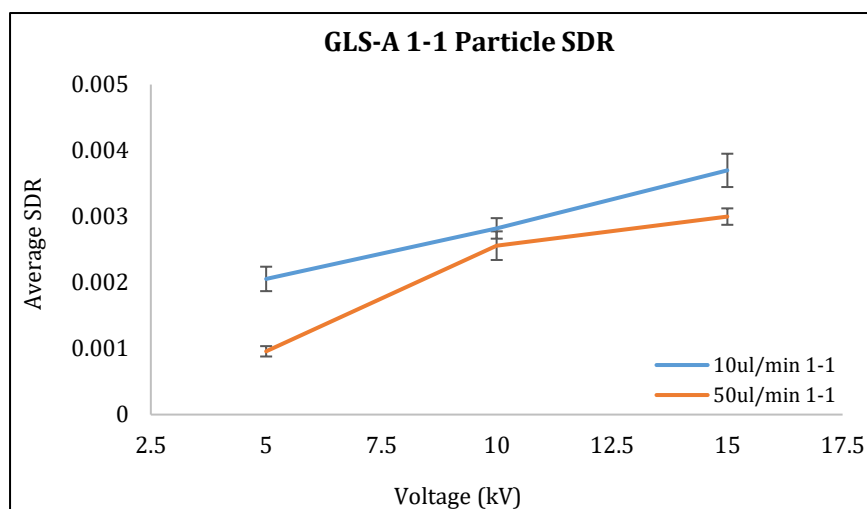


**Figure 4.44:** SDR of GLS-A 1-1 particles. Error bars represent SE of 5 particles, on which 20 pores were averaged. SDR increased with EHDA voltage

## 4.3.2.3 Effect of Drying Regime on GLS-A 1-1 Particles

Drying conditions can affect the particle's physical and chemical structure, and therefore this stage must not be considered as a just a *secondary* process [Maghsoodi et al., 2015]. Unfortunately the effect of drying on polymer particles is not comprehensively documented in literature, owing to the range of possible drying conditions and the differences in the properties of the material/drug matrix [Santagapita et al., 2011; Risbud et al., 2000; Guzman-Villanueva et al., 2013; El-Sherbiny et al., 2011]. Air-drying is typically a tedious process, and the residual water content and repetitive cycles of water absorption are a concern in further analyses; especially when drying hygroscopic materials like alginate. Studies have observed that a more rigorous process like freeze-drying, while typically more able to "completely" dry a polymer structure, introduces the possibility of ice-induced fracture as a result of the sublimation of frozen moisture. On their own, both methods can result in a stressed particle surface – whether it stems from cyclic freeze-thaw patterns, or a fluctuating air environment and inherent hygroscopicity [Bodenberger et al., 2016; Fonte et al., 2012]. To date, no study has yet combined *both* methods to negate certain disadvantages whilst capitalising on the advantages of each. Here, air-drying was intended to *remove moisture* before freeze-drying, thus reducing the formation of ice crystals during freezing and ultimately reducing the opportunity to expand, and the prevalence of surface defects [Lefsrud et al., 2008; Simoni et al., 2017; Date et al., 2010; Schwarz et al., 1997; Terada

*Novelty processing and smart delivery of Ganoderma Lucidum spores*

et al., 2012; Paradee et al., 2012; Yuan et al., 2017]. GLS-A particle morphology and surface texture were compared to GLS-A particles that were *only* air-dried (AD).

### 4.3.2.3.1 Effect of Drying Regime on GLS-A 1-1 Particle Size and Shape

Particle size and shape were measured after both drying regimes to gauge the effects of drying conditions on morphological changes. Figures 4.45 and 4.46 and table 4.17 demonstrate that the AD+FD GLS-A 1-1 particles were *smaller* than particles undergoing AD alone by 18% and 23% in samples created at 10kV and 15kV respectively. This suggests that air-drying prior to freeze-drying can reduce the size of GLS-A particles prepared using equal GLS/Alginate fractions (GLS-A 1-1 in this study) [Simoni et al., 2017].

| GLS-A 1-1 Particle Diameter | Drying Regime | 10kV | 15kV |
|---|---|---|---|
| | AD | 706.0 ± 11.9 µm | 525.4 ± 10.1 µm |
| | AD+FD | 575.6 ± 10.0 µm | 405.1 ± 10.1 µm |
| GLS-A 1-1 Aspect Ratio | Drying Regime | 10kV | 15kV |
| | AD | 1.0 ± 0.0 | 1.0 ± 0.0 |
| | AD+FD | 1.1 ± 0.0 | 1.1 ± 0.0 |

**Table 4.17:** GLS-A 1-1 particles from EHDA: Effect of drying regime on particle size and aspect ratio (± SE of 30 particle measurements). Additionally FD particles were smaller.

The size reduction from employing an additional FD step can be attributed to the removal of moisture in the initial AD stage; minimising the formation of ice crystals that typically induce surface defects during FD and resulting particle expansion [Simoni et al., 2017]. Thus with limited free water in the particle at the start of FD, the process becomes less invasive. This leaves little opportunity for alginate chains to deform or expand unevenly; creating particles that appear more compact.

*Novelty processing and smart delivery of Ganoderma Lucidum spores*
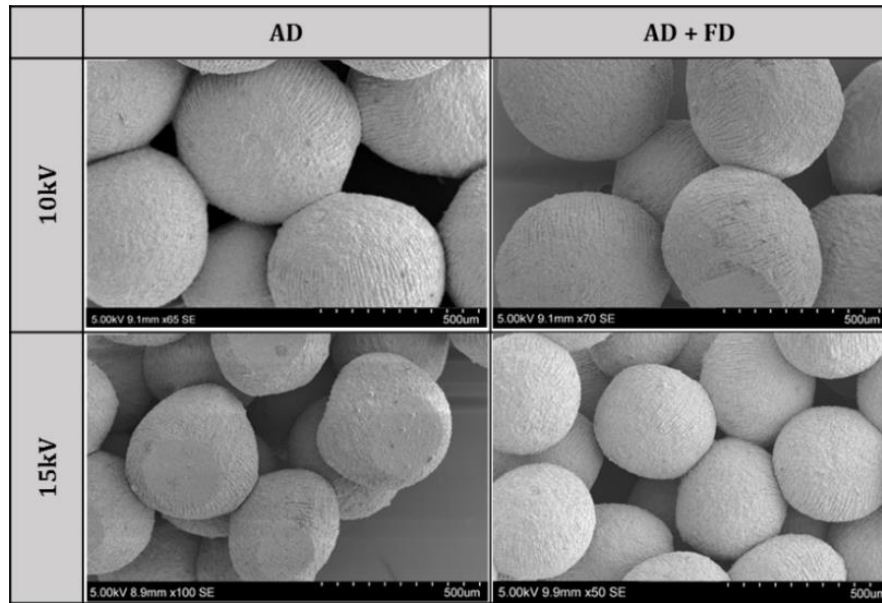
**Figure 4.45:** SEM of AD and AD+FD GLS-A 1-1 particles. The additionally FD particles were slightly smaller and had a visibly smoother surface attributed to additional drying
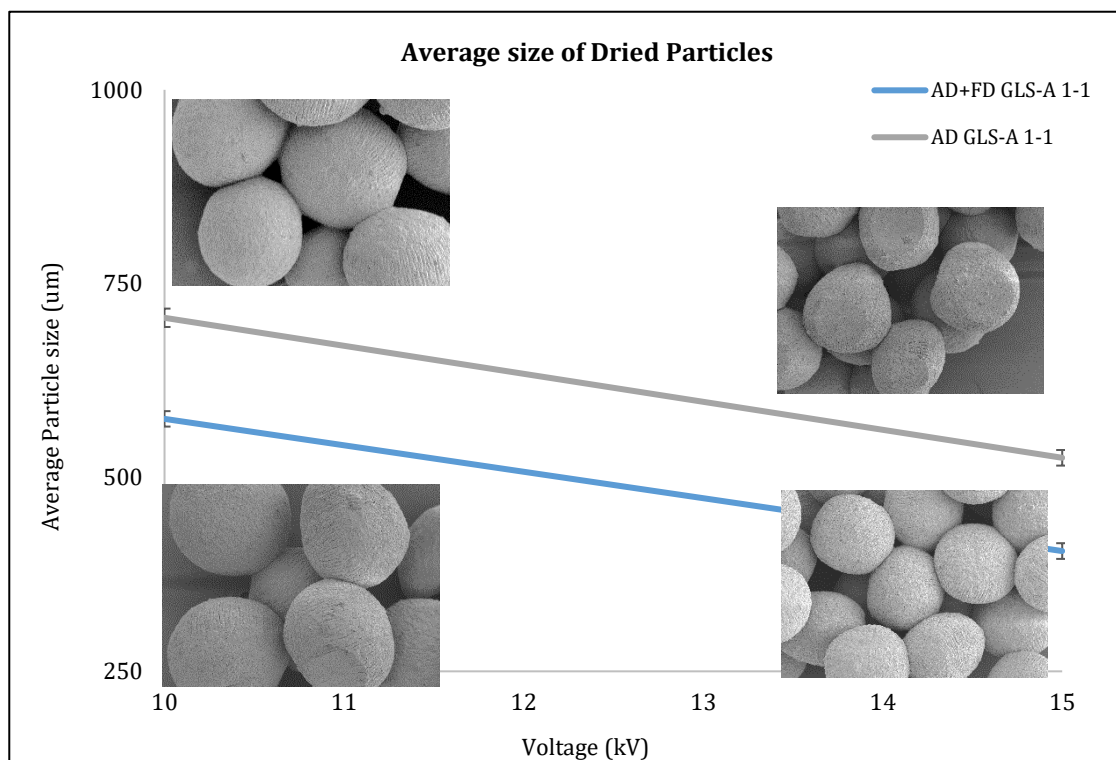


**Figure 4.46:** AD vs AD+FD GLS-A 1-1 particle size. Error bars represent the SE of 30 particle measurements. *Inset images* show the corresponding scanning electron micrographs of the created particles

*Novelty processing and smart delivery of Ganoderma Lucidum spores*

Additional FD only slightly reduced particle sphericity because the freeze-drying process requires pre-freezing; an aggressive process that can deform particle structure and surface via crystal-induced surface stress [Lefsrud et al., 2008]. This was however minimised by employing AD prior to freezing, but agglomeration can still pose a risk owing to chain movement [Date et al., 2010; Schwarz et al., 1997]. The impact of the agglomeration on the rubbery hydrogel structure usually leaves an "imprint" recognisable by the flatter side of some particles in figure 4.47 (below).

### 4.3.2.3.2 Effect of Drying Regime on GLS-A 1-1 Particle Pore Size

During the freeze-drying process, the high rate of moisture sublimation typically intensifies cavities and pores, especially in places where moisture has crystallised during initial freezing. As a result it is normal to observe the polymer surface being "pushed away" from the crystallising region, creating particle imperfections such as creases, folds and pores. In this investigation air-drying was employed prior to freezing to remove moisture beforehand, thus reducing the formation of ice crystals during freezing – reducing the average particle pore size [Terada et al., 2012; Paradee et al., 2012; Yuan et al., 2017]. A reduced average pore size could also result from the surface-tension-induced collapse of alginate chains in the chamber [Ji et al., 2017]. A study by Román Santagapita in 2012 also reported that freeze-dried alginate particles had smoother surfaces and a smaller average particle diameter [Santagapita et al., 2012]. This is supported by studies that have observed enhanced surface features following FD, so long as the particle is sufficiently crosslinked [Mehregan Nikoo et al., 2016]. This can also be a result of a resulting reduced particle shrinkage.

A smooth surface can generally also result from more stable atmospheric conditions within the FD chamber. The continuous moisture loss/gain typical of alginate's hygroscopicity during AD, along with the fluctuating humidity may lead to surface "wear" causing internal chain stress and fatigue – and without further freeze-drying, these defects remained [Shi et al., 2007; Yonekura et al., 2014; Vaccarezza et al., 1974; Szekalska et al., 2015]. The pore size of the GLS-A 1-1 particles that underwent AD and AD+FD are shown in table 4.18. Porosity of the particles created at 10kV was most affected by the additional FD, probably because at this lower voltage alginate chains were less electrically charged and less rigid/brittle; rendering them more flexible during FD and less prone to rupture [Xu et al., 2014].

| GLS-A 1-1 Pore Size | Drying Regime | 10kV | 15kV |
|---|---|---|---|
| | AD | 1.6 ± 0.1 µm | 1.2 ± 0.1 µm |
| | AD+FD | 1.1 ± 0.1 µm | 1 ± 0.1 µm |

**Table 4.18:** GLS-A 1-1 particles: Effect of drying regime on particle pore size (± SE of 20 pores across 5 particles). Pores were smaller on additionally FD particles

*Novelty processing and smart delivery of Ganoderma Lucidum spores*

The SEM images of GLS-A 1-1 particle surfaces following the two regimes, AD and AD+FD, are shown below in figure 4.47. The increased compactness and smoothness of the GLS-A particle surface after additional FD is evident.
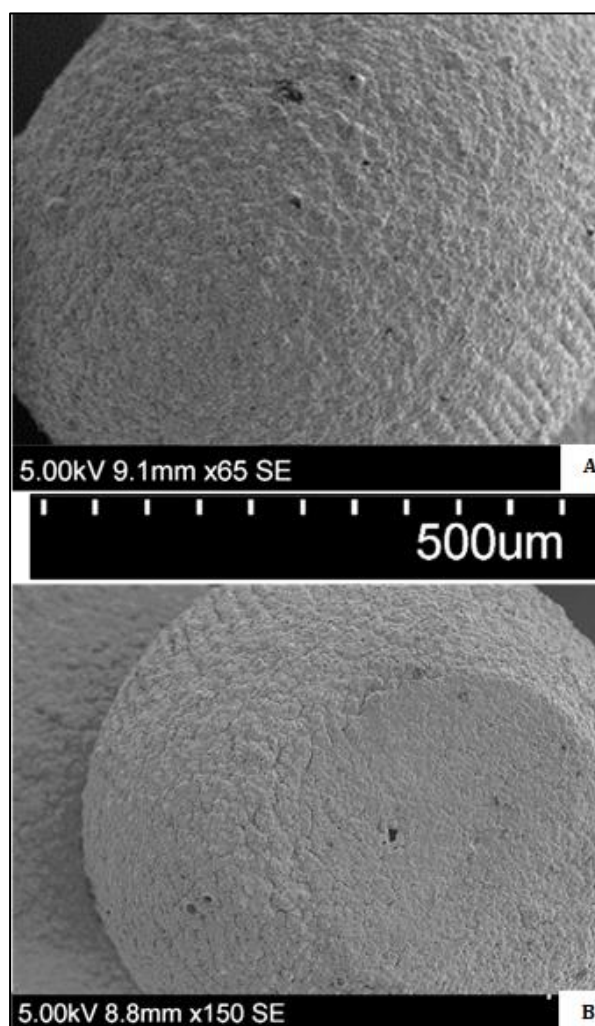


**Figure 4.47:** SEM of A) AD only B) AD+FD GLS-A 1-1 particles created at 10kV 50µl/min. The enhanced smoothness of AD+FD particles is clear

## 4.3.2.4 Chemical Composition of GLS-A 1-1 Particles

FTIR analysis was carried out on the GLS-A particles, and also raw GLS and alginate. The particles created at different EHDA process settings exhibited a similar chemical profile, indicated by similar peak positions and shapes in the FTIR analyses. This implies little chemical impact of the EHDA process parameters. Compared to non-encapsulated GLS and raw alginate powder, the GLS-A matrix possessed new peaks indicating drug-polymer interactions [Sankalia et al., 2005].

*Novelty processing and smart delivery of Ganoderma Lucidum spores*

### 4.3.2.4.1 GLS-A 1-1 Chemical Composition from different EHDA Parameters

The GLS-A particles were shown to have FTIR peak intensities attributed to both GLS and alginate (figure 4.48). This confirms the entrapment into the alginate beads at the molecular level [Sankalia et al., 2005]. There was very little difference in peak *width* and *position*, indicating that the chemical compositions in different GLS-A particles were due to an increase in the amount of the associated functional group rather than a chemical change. A change in peak strength occurs when new interactions are introduced between GLS and alginate [Zierkiewicz et al., 2011]. The spectra show the main peaks arising from pure alginate, GLS, and the crosslinked GLS-A hydrogel particles.
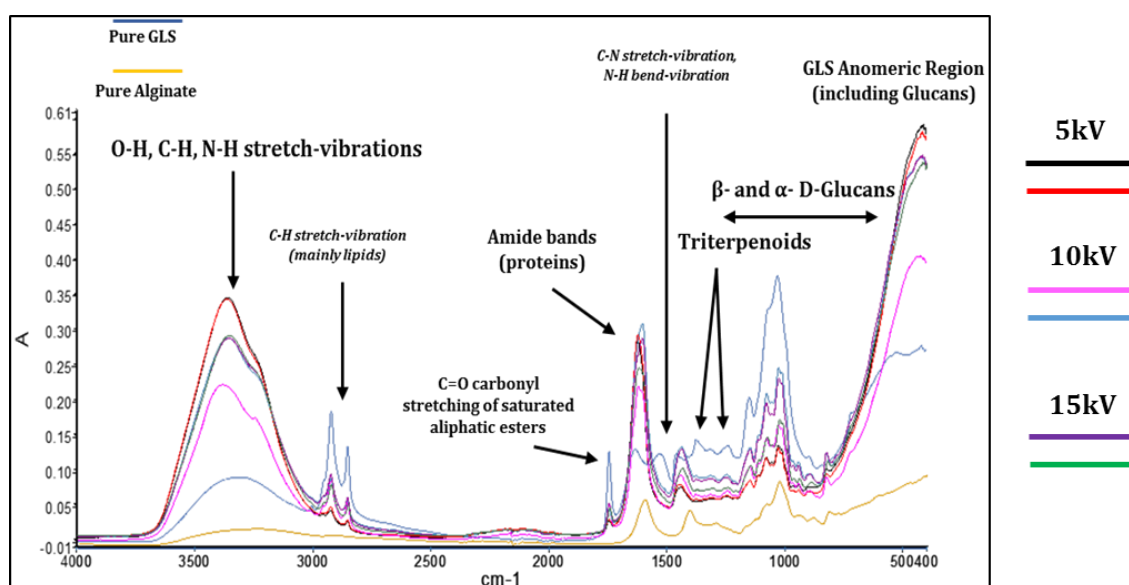


**Figure 4.48:** FTIR spectra of GLS-A particles created using EHDA at various parameters. Distinctive regions are shown, specific to alginate and GLS and their interactions

Raw alginate's characteristic peaks at wavelengths 1713 $cm^{-1}$ and 806 $cm^{-1}$ reflect the carbonyl group stretch and the acrylate double bond twist respectively. Peaks at 1408, 1296 and 1192 $cm^{-1}$ are in alginate's fingerprint region containing carboxyl and carboxylate groups [Mandal et al., 2010]. GLS-A hydrogel particles show intensities of the alginate peaks, as well as new peaks owing to interactions with GLS. A slight broadening of the spectra at 806, 1408 and 1612–1628 $cm^{-1}$ are likely a result of reductions in double bonds as crosslinked regions are formed in particles. A leftward shift of the C=O stretch vibration at 1713 $cm^{-1}$ in pure alginate, to in 1720 $cm^{-1}$ in particles

*Novelty processing and smart delivery of Ganoderma Lucidum spores*

has previously been reported for changes in the carbonyl environment of polymer hydrogels [Mandal et al., 2010].

GLS peaks are characteristic. The region of 900–400 cm$^{-1}$ indicates the polysaccharide content, particularly glucans as proven in literature [Han et al., 2008]. The peak around 890 cm$^{-1}$ has also been attributed to β-Glucan groups; still existent in all GLS-A particles. For example a study by Xu et al. reported the presence of β-D-glucans from the fruiting body of Grifola frondosa at 890 cm$^{-1}$ [Xu et al., 2006]. Glucomannan and arabinan are frequently identified at 1064 cm$^{-1}$ and 1035 cm$^{-1}$ respectively [Zhu et al., 2015]. The prominent absorption around 1150 - 1000 cm$^{-1}$ indicate both triterpenoids and polysaccharides as suggested by the C-O and C-C vibrations. More triterpenoids are observed at the prominent peaks at 1760 - 1600 cm$^{-1}$ whereby the C=O stretching vibration in carbonyl compounds typically absorb [Zhu et al., 2015]. Peaks at 1700–1500 cm$^{-1}$ are assigned to amide bands, suggesting the presence of proteins as confirmed by Kohsuke Kino in the isolation of GL protein *LZ-8* with immunomodulating activity [Kino et al., 1989]. The broad bands around 3405 cm$^{-1}$ are typically assigned to OH, CH and NH bond stretching of triterpenes/sterols and polysaccharide groups [Chen et al., 2008]. The intensity of triterpenes/sterols and polysaccharide groups is greatest for low-voltage particles, indicating that these particles (aside from being largest) may have retained the highest polysaccharide content following a less intense applied voltage, avoiding dehydrogenation and deoxygenation. The intense bands of CO and CC stretch-vibrations in glycosidic bonds dominate the region around 2900 cm$^{-1}$, and this has typically been assigned to lipids. The peak around 890 cm$^{-1}$ has also been attributed to β-Glucan groups; still existent in all GLS-A particles. Furthermore, the GLS-A rightward shifting in the asymmetrical stretching mode of COO- (around 1639 cm$^{-1}$) indicates a chemical interaction between the organic matrix and other phases encouraged by alginate's negatively charged COO- group and the positively charged Ca$^{2+}$ ions from crosslinking.

## Comparing the Degree of Polymerisation from crosslinking using the FTIR Spectrum

All hydrogel matrices indicated a degree of polymerisation, having been crosslinked, compared to pure alginate. An indicated degree of polymerisation after crosslinking can firstly be suggested by the increase in the carbonyl content (higher intensity of C=O stretching at 1740 cm$^{-1}$) [Takacs et al., 2000]. Additionally, the remaining concentration of the aliphatic C=C double bonds in the crosslinked particle relative to the total number of aromatic C=C bonds in the uncrosslinked components has also been used to gauge the degree of crosslinking. The twisting of the acrylate double bond at 806 cm$^{-1}$ is usually observed as the number of double bonds decreases with crosslinking. Polysaccharides also typically display a peak in FTIR at 760 cm$^{-1}$, which is typically unaffected after polymerisation. This band was therefore chosen as a reference band against which the degree of crosslinking/polymerisation peak was compared [Garcia et al., 2008]. The

*Novelty processing and smart delivery of Ganoderma Lucidum spores*

intensity of this ratio was used to determine the polymerisation as a result of crosslinking, and is indicated in figure 4.49 and table 4.19. The degree of polymerisation was highest for the particles created at the lowest flow rate (10 µl/min) (table 4.19).

| Voltage (kV) | Flow rate (µl/min) | 760 cm$^{-1}$ | 806 cm$^{-1}$ | Ratio | % Polymerisation (crosslinking) |
|---|---|---|---|---|---|
| 5 | 10 | 0.09 | 0.07 | 0.78 | 21.0% |
| 5 | 50 | 0.095 | 0.070 | 0.74 | 19.6% |
| 10 | 10 | 0.090 | 0.070 | 0.78 | 25.8% |
| 10 | 50 | 0.120 | 0.085 | 0.71 | 14.5% |
| 15 | 10 | 0.125 | 0.097 | 0.78 | 25.8% |
| 15 | 50 | 0.120 | 0.085 | 0.71 | 14.5% |
| Alginate | | 0.045 | 0.028 | 0.62 | - |

Table 4.19: Polymerisation (via crosslinking) of the particles using the FTIR spectral regions indicated in figure 4.48. The two peaks used to gauge the degree of crosslinking and therefore particle integrity. GLS-A particles created at the lower flow rate were consistently the most polymerised, as they were generally the smallest
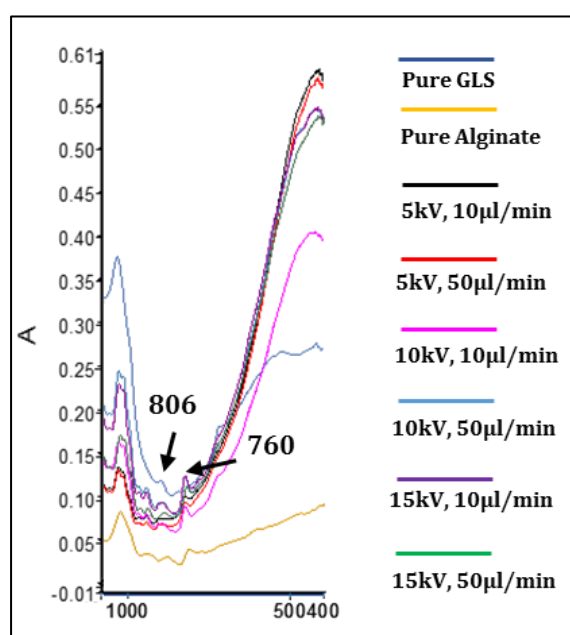


Figure 4.49: The peaks used to gauge the degree of crosslinking (polymerisation) and therefore particle integrity

The degree of polymerisation from crosslinking was highest for the particles created at the lowest flow rate (10 µl/min). These particles were also smallest, suggesting a more entangled network and a greater crosslinking density. At the higher flow rate there is also a shear-thinning effect that could foster lower solution viscosity and a less entangled network; indicating a lower degree of polymerisation potential [Khorram et al., 2015; Moghadam et al., (2009, 2010)]. The degree of alginate polymerisation after crosslinking is a useful measure of particle integrity, and may be

*Novelty processing and smart delivery of Ganoderma Lucidum spores*

reflective of certain release patterns in drug delivery. It is also an indication of a stable fabrication setup.

### 4.3.2.4.2 GLS-A 1-1 Chemical Composition from different Drying Procedures

Whilst drying can certainly affect physical characteristics, it is less likely to make chemical alterations unless the material undergoes extreme conditions during the drying process; such as very high temperature or pressure [Voo et al., 2015]. During freeze-drying, particles were subject to extremely cold temperatures and low pressure - this appeared to have only a slight chemical impact. Some studies have observed that high drying temperatures reduce the intensity of certain polysaccharide groups, and this investigation indicated depletion of polysaccharides in this regions during the freeze-drying of either GLS and/or alginate as AD-only particles flaunted greater intensity [Nep et al., 2011; Havelund et al., 2001]. Studies have however shown that breaking certain biopolymer chains via temperature/pressure extremities can lead to greater therapeutic benefits [Kelishomi et al., 2016]. Furthermore, the hydroxyl (OH) stretching of alginate at 3405 cm$^{-1}$ is indicative of water content. By taking the ratio of this peak to a communal steady reference peak (carbonyl, C=O for example at 1713 cm$^{-1}$), the result is less intense in additionally freeze-dried samples (AD+FD), suggesting a reduced water content compared to AD-only particles [Max et al., 2004; Santagapita et al., 2012; Castro-Cabado et al., 2016] (table 4.20). Smaller particles had lower ratios than the larger particles, as they are more effectively dried and so possessed less water after drying.
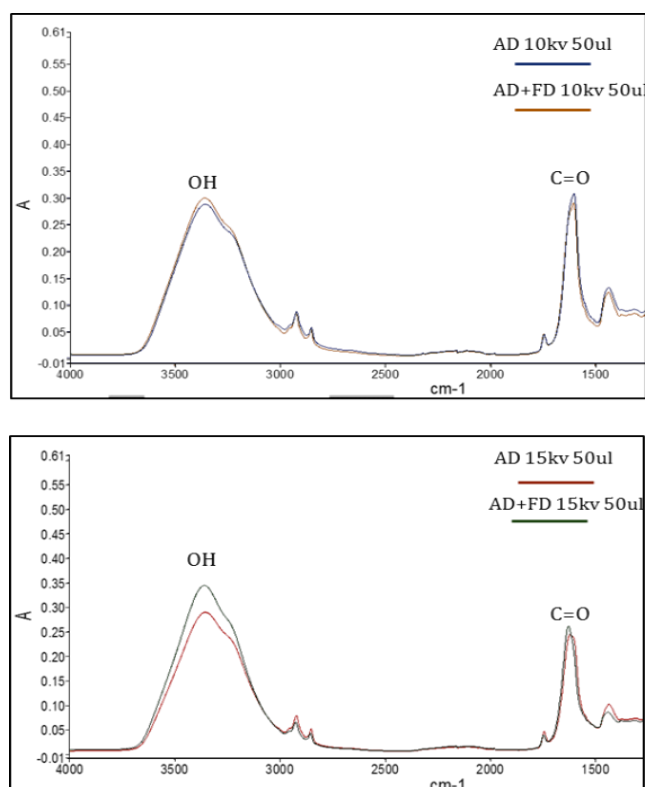


**Figure 4.50:** FTIR Scans of GLS-A 1-1 dried using AD vs AD+FD, created at EHDA 10kV and 15kV. The labelled regions are used to calculate the extent of dehydration of AD vs AD+FD particles

*Novelty processing and smart delivery of Ganoderma Lucidum spores*

| Drying | Voltage | C=O | OH | Ratio C=O / OH |
|---|---|---|---|---|
| AD | 15 | 0.245 | 0.290 | 0.84 |
| AD+FD | 15 | 0.260 | 0.345 | 0.75 |
| AD | 10 | 0.310 | 0.290 | 1.01 |
| AD+FD | 10 | 0.290 | 0.300 | 0.95 |

**Table 4.20:** Dehydration extent of the particles using the FTIR spectral regions indicated in figure 4.49. The additionally FD particles had the lowest C=O/OH ratio, suggesting a more extensive drying technique for GLS-A particles

What is to be investigated at a later stage is whether the surface physiochemistry can be controllably modified using EHDA process variables and drying conditions. Most importantly, the impact of these variables on the *pharmacology of the GLS* has to be ascertained.

## 4.3.3 EHDA to Create *High-Drug* GLS-A 2-1 Microparticles

GLS-A 2-1 particles were subsequently created to investigate whether the drug portion of each particle could be increased, *by reducing polymer content* in order to maintain a high drug dose. The effects of polymer reduction could be two-fold (and indeed they would both play a role). Firstly, a reduction in viscosity is implicated by reduced polymer content. This would theoretically foster a droplet disruption pattern that is more effective and rapid owing to reduced surface tension. Secondly however, the lack of polymer could create infrastructural issues owing to a lack of chargeable polymer but also less strong "backbone". Implications may include a reduced crosslinking density, drying-induced collapse, and a rapid uncontrollable release rate. In the GLS-A 2-1 matrix, the lack of polymer resulted in a droplet that was less charged, thus more prone to spontaneous disruption and instability at a given voltage; leading to inconsistent disruption and a resulting non-uniform size distribution with irregular shapes [Khorram et al., 2015]. As alginate is in fact electroconductive as a hydrogel, it would be the principal electrical conductor during electrospraying. A lack of alginate therefore caused droplet stretching as it slowly pulled away ineffectively from parent droplets [Mehregan Nikoo et al., 2016]. The resulting reduction in polymer infrastructure imposes further challenges to droplet stability as the solvent is evaporated during spraying [Khorram et al., 2015].

While it was reported in chapter 3 that GLS-A 2-1 was actually slightly more "electrically conductive", these values were based on *particle count*; not an accurate measure of electrical

*Novelty processing and smart delivery of Ganoderma Lucidum spores*

conductivity. Nevertheless, the relationship between alginate concentration and conductivity is still not consistent in literature and requires further study [Kaczmarek-Pawelska et al., 2017].

### 4.3.3.1 Effect of Voltage on GLS-A 2-1 Particle Size and Shape

GLS-A 2-1 particles had elongated, tailed shapes. A tailed shape is indicative of the important balance between droplet viscosity and resulting interfacial tension – both directly affected by the polymer content. GLS-A 2-1 droplet *should* exhibit rapid and efficient fission as it is less viscous than GLS 1-1 created previously. A round shape *should* form, from which solvent is easily evaporated. Elongation should theoretically only result from *increased* viscosity, which would create greater strain to disrupt (GLS-A 1-1 in this study). In turn, there would be an increased chance that the droplet attains the Rayleigh limit locked into a non-spherical shape.

Figure 4.51 shows the GLS-A 2-1 particles after 48 hours of drying following EHDA at voltages 10 and 15kV and flow rate 10 and 50 µl/min.
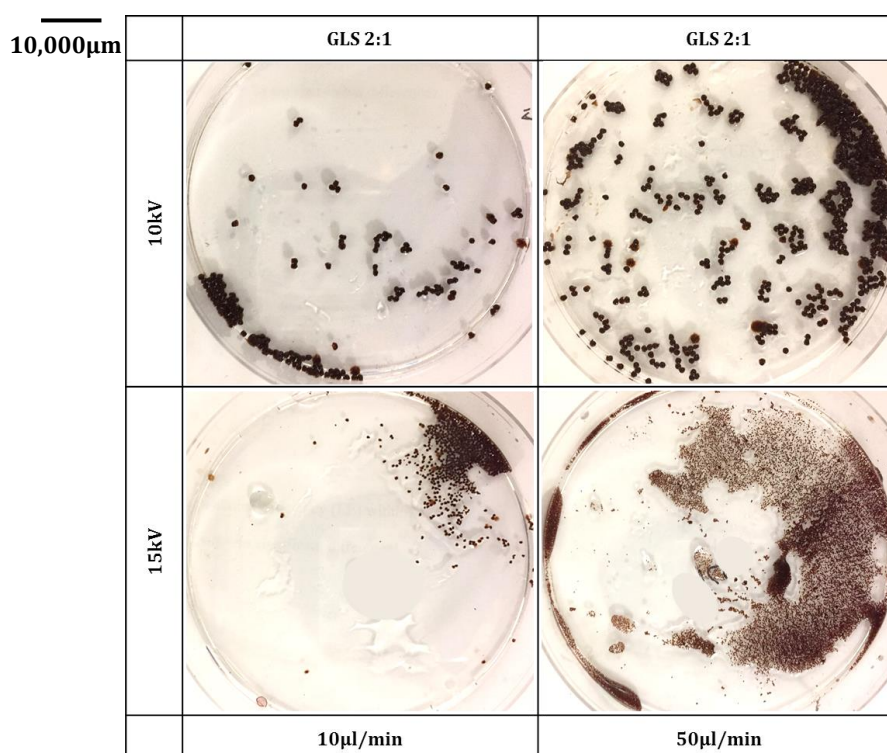


**Figure 4.51:** GLS-A 2-1 particles after 48 hours of drying. Particles were visually tailed, however were clearly affected by EHDA voltage

In this investigation, the theoretical process is interrupted (confounded) by the droplets' charge density; typically lower in droplets with less polymer (GLS-A 2-1). When the charge density is low, the Rayleigh limit is either never attained (droplets will continue to shrink owing to solvent

*Novelty processing and smart delivery of Ganoderma Lucidum spores*

evaporation), or the Rayleigh limit is delayed and droplets are deformed during evaporation [Zarrabi et al., 2009]. Thus, if low viscosity is achieved at the expense of polymer content, it is likely that the resulting charge density will be insufficient to efficiently foster the processes involved in EHDA. This would implicate challenged droplet disruption, resulting in a lack of polymer entanglement prior to disruption. This reduced disruption effectiveness induced a stretched morphology resembling tails as the droplets more slowly pulled away from its parent droplet and traversed the distance to the collection bath. Resulting droplet shapes were more likely to deform in this time. The stretching evident in the GLS-A 2-1 particles further implicates a quicker rate of evaporation due to a thinner surface and larger surface area. This further points to a prematurely locked in the deformed structure, but a smaller resulting particle. The effect of voltage on particle size is consistent with the higher-polymer GLS-A 1-1 solution. As voltage increased particle diameters became smaller owing to more efficient and frequent droplet disruption, subsequently increasing charge density per droplet and a continuous cycle of rapidly overcoming surface tension. As the viscosity of this solution is lower than GLS-A 1-1 however, the realisation of a jet spray was more realistic and thus smaller droplets resulted at each voltage. Figure 4.52 shows the optical micrograph of the corresponding particle sample after 48 hours of air drying. While GLS-A 2-1 particles were polydispersed, *tailed* particles have shown promise for drug delivery owing to an enhanced biodistribution; better targeting the tissue, safely traversing small vessels, and evading cautious immune cells [Jang et al., 2015].
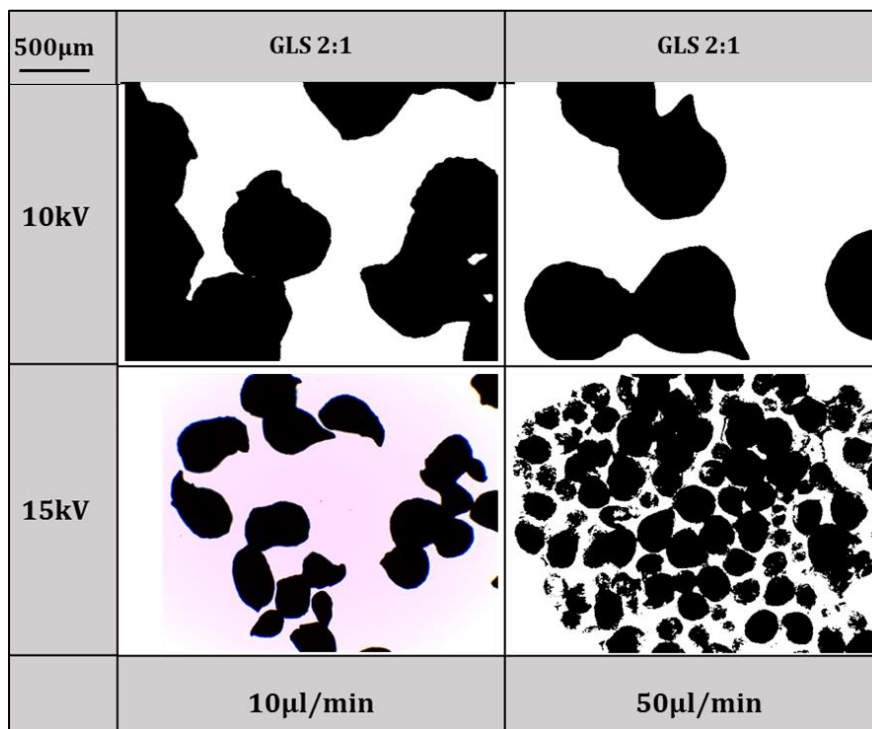


**Figure 4.52:** Optical Microscopy of GLS-A 2-1 particles air-dried for 48 hours. While the effect of voltage was consistent with GLS-A 1-1 particles, the effect of flow rate was reversed at 15kV - increasing flow rate *decreased* particle size

*Novelty processing and smart delivery of Ganoderma Lucidum spores*

The effect of solution flow rate was not tested as an experimental variable on GLS-A 2-1 particle size, but its effect was observed across the voltages. Its effect was not consistent with the effects of flow rate on GLS-A 1-1 particles. In particular, at 15kV the particles became *smaller* with an increase in flow rate (the opposite effect of the GLS-A 1-1 set-up. It is likely that the lack of chargeable polymer in GLS-A 2-1 particles led to a low charge density that created an unstable spraying regime; reducing polymer entanglement and spontaneously generating less monodispersed particles [Moghadam et al., 2009; Hao et al., 2006]. These effects would likely be amplified at a high voltage. An AR below 0.9 was maintained throughout.

Table 4.21 shows the achieved average diameter and AR of the GLS-A 2-1 particles created with 1% alginate, compared to the high-polymer GLS-A 1-1 particles created using 2% alginate.

| Particle Diameter | FR 10µl/min | | FR 50µl/min | |
|---|---|---|---|---|
| | 10kV | 15kV | 10kV | 15kV |
| GLS-A 1-1 | 650.2 ± 11.9 µm | 468.1 ± 8.1 µm | 706.0 ± 11.9 µm | 525.4 ± 10.1 µm |
| GLS-A 2-1 | 893.8 ± 30.9 µm | 416.9 ± 10.3 µm | 965.7 ± 17.2 µm | 232.1 ± 10.3 µm |
| Aspect Ratio | FR 10µl/min | | FR 50µl/min | |
| | 10kV | 15kV | 10kV | 15kV |
| GLS-A 1-1 | 1.0 ± 0.01 | 1.02 ± 0.01 | 1.0 ± 0.01 | 1.02 ± 0.01 |
| GLS-A 2-1 | 0.88 ± 0.05 | 0.71 ± 0.02 | 0.83 ± 0.02 | 0.79 ± 0.01 |

**Table 4.21:** Voltage effect on GLS-A 1-1 and 2-1 particle size and AR. SE is of 30 measurements. Particle diameters were smaller using GLS-A 2-1 only at the highest tested voltage. GLS-A 1-1 particles were consistently spherical, whereas GLS-A 2-1 particles were elongated. For GLS-A 2-1, the effects of voltage and flow rate on particle aspect ratio and size were statistically significant at 90% confidence

## 4.3.3.2 Effect of EHDA Process Parameters on GLS-A 2-1 Surface Characteristics

### 4.3.3.2.1 GLS-A Porosity and Roughness

GLS-A 2-1 particles were analysed for pore size after air-drying, to determine the effects of reduced alginate content on particle surface. Tavakol in 2013 reported that a reduced alginate content in calcium-crosslinked particles fostered cracked surfaces, attributing this to the lack of

*Novelty processing and smart delivery of Ganoderma Lucidum spores*

polymer strength as the particle undergoes processes such as drying and wetting (involving cyclic contracting/expanding chains) [Tavakol et al., 2013; Bajpai et al., 2016]. Higher alginate has also been linked to a retarded calcium penetration, resulting in *smoother surfaces* and a *less brittle structure* [Sankalia et al., 2005].

In this study low-polymer particles (1% alginate) were rougher - as expected - however particles displayed a slightly smaller average pore size than the high-polymer GLS-A 1-1 particles. High-polymer particles may have exhibited a higher crosslinking density owing to greater crosslinkable junctions. This would induce chain rigidity and brittleness that could lead to surface breakage and greater porosity [Guzman-Villanueva et al., 2013; Festag et al., 2998]. Any impact of outward hydraulic pressures during processing, evaporation, and drying, would subsequently have a more significant impact on a brittle and inflexible surface [Costa et al., 2015]. In the GLS-A 2-1 particles, a pore size reduction as voltage increased likely owing to smaller achievable particles. Table 4.22 shows the average pore size and SDR of GLS-A 2-1 low-alginate particles compared to GLS-A 1-1.

| Pore Size μm | FR 10μl/min | | FR 50μl/min | |
|---|---|---|---|---|
| | 10kV | 15kV | 10kV | 15kV |
| GLS-A 1-1 | 1.35 ± 0.09 | 1.32 ± 0.09 | 1.58 ± 0.13 | 1.23 ± 0.06 |
| GLS-A 2-1 | 1.15 ± 0.10 | 1.18 ± 0.20 | 1.14 ± 0.07 | 0.15 ± 0.03 |
| SDR | FR 10μl/min | | FR 50μl/min | |
| | 10kV | 15kV | 10kV | 15kV |
| GLS-A 1-1 | 0.003 ± 0 | 0.004 ± 0 | 0.003 ± 0 | 0.003 ± 0 |
| GLS-A 2-1 | 0.002 ± 0 | 0.003 ± 0 | 0.001 ± 0 | 0.001 ± 0 |

**Table 4.22:** Voltage and flow rate effect on GLS-A 1-1 and 2-1 pore size and SDR. Pores were generally larger on GLS-A 1-1 particles. Measurements are ± SE of 5 particles, on which 20 pores were averaged.

Figure 4.53 is the SEM image of a GLS-A 2-1, alongside a GLS-A 1-1 particle created at 10kV and 50 μl/min. Although the porosity *visually* appears greater in GLS-2-1 particles, the average measured pore size was smaller. GLS-A 2-1 exhibited stretching from an inefficient droplet disruption created a visually *less* smooth surface; a phenomenon previously discussed. This stretching is shown below.

*Novelty processing and smart delivery of Ganoderma Lucidum spores*
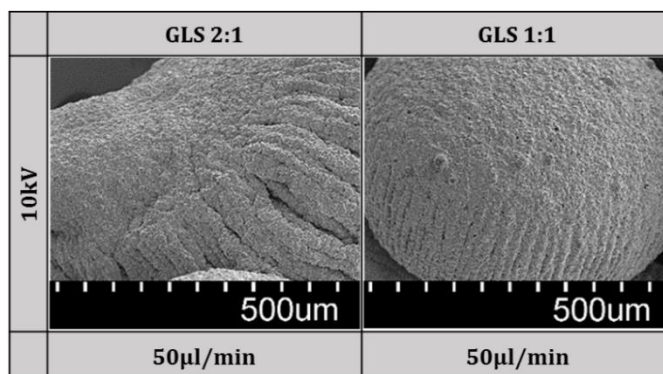
**Figure 4.53:** SEM of surfaces of a GLS-A 2-1 and 1-1 particle showing the surface differences. Stretch marks on the GLS-A 2-1 particles are indicative of the challenged droplet disruption owing to insufficient chargeable polymer

### 4.3.3.2.2 GLS-A Porosity Relative to Size

As previously discussed, small particles with large pores present benefits to drug delivery and thus treatment efficacy [Wang et al., 2016]. The relationship between pore size and particle size is shown by the scatterplot in figure 4.54 below. There is generally a positive correlation between the pore size and particle size. This suggests that smaller particles typically had smaller pores, and larger particles had larger pores. As such, a small SDR is likely a result of a small pore and a small particle diameter (rather than a "desirable" small particle with large pores). It is worth pointing out that at the higher voltage, this study previously observed a smaller particle size *and* smaller pores – thus, this section of study requires further investigation. Table 4.24 also displays the SDR values as compared to GLS-A 1-1; smaller for GLS-A 2-1 particles owing to smaller average pores.
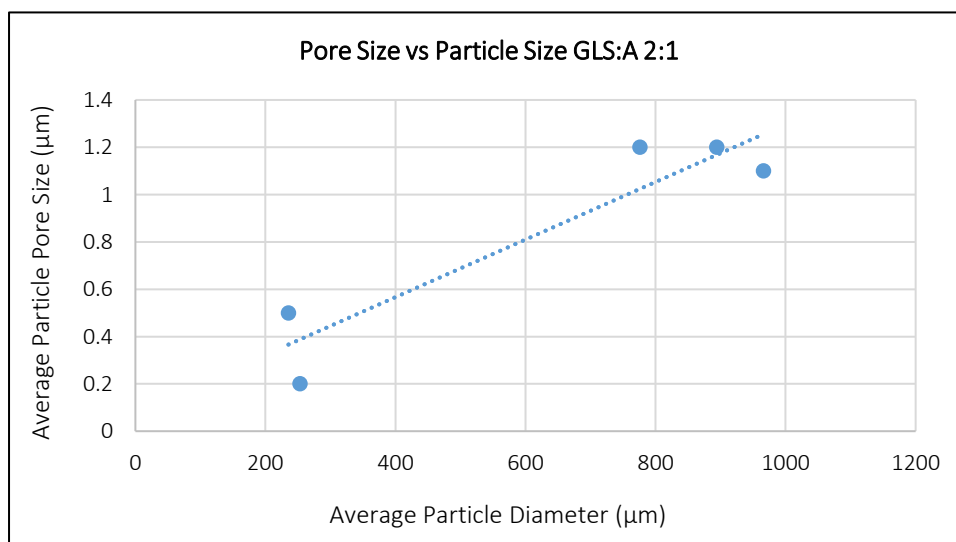


**Figure 4.54:** The relationship observed between particle size and pore size of GLS-A 2-1 particles

*Novelty processing and smart delivery of Ganoderma Lucidum spores*

## 4.3.3.4 Effect of Drying Regime on GLS-A 2-1 Particles

The impact of additional FD on GLS-A 2-1 particles was not straightforward, owing to the *confounding effect* of reduced alginate content on the integrity of GLS-A particles during drying. Reduced alginate has already indicated effects on particle size and conductivity during EHDA, and therefore many of the acquired particle characteristics following drying are "inherited" [Nguyen et al., 2016]. GLS-A 2-1 particles that were additionally freeze-dried were smaller than AD counterparts, consistent with GLS-A 1-1. This reduction was significantly greater than the reduction observed in GLS-A 1-1 particles. The size reduction from employing an additional FD step can be attributed to the removal of moisture in the initial AD stage; minimising the formation of ice crystals that typically induce surface defects during FD and resulting particle expansion [Simoni et al., 2017]. Thus with limited free water in the particle at the start of FD, the process becomes less invasive. This leaves little opportunity for alginate chains to deform or expand unevenly; creating particles that appear more compact. A lower polymer content also resulted in reduced crosslinking density that could therefore lead to greater shrinkage during drying. Previous studies have also reported that the absorption of moisture from the atmosphere decreases with reduced alginate content; thus creating greater scope to shrink [Berggren et al., 2003].

| GLS-A 2-1 Particle Diameter | Drying Regime | 10kV | 15kV |
|---|---|---|---|
| | AD | 965.7 ± 17.2 µm | 252.9 ± 6.0 µm |
| | AD+FD | 235.3 ± 26.7 µm | 775.8 ± 32.5 µm |
| GLS-A 2-1 Aspect Ratio | Drying Regime | 10kV | 15kV |
| | AD | 0.8 ± 0.0 | 0.8 ± 0.0 |
| | AD+FD | 0.8 ± 0.0 | 0.9 ± 0.1 |

**Table 4.23:** GLS-A 2-1 particles: Effect of drying regime on particle size and AR (± SE of 30 particle measurements). GLS-A 2-1 particles created at 10kV shrunk with additional FD (like GLS-A 1-1 particles), however GLS-A 2-1 particles created at 15kV grew with additional FD

The GLS-A 2-1 particles created at 15kV however did not exhibit a size reduction following additional freeze-drying. The combination of low alginate and high voltage in this particle likely

*Novelty processing and smart delivery of Ganoderma Lucidum spores*

resulted in a brittle particle surface more prone to defects that gave way to "free" GLS emigrating outwards during the extraction of moisture in drying – along with an overall weaker structure [Xu et al., 2014; Costa et al., 2015].

Table 4.24 shows the average pore size of GLS-A 2-1 particles following each drying regime. Some GLS-A 2-1 particles displayed an over 50% reduction in average pore size owing to the surface-tension-induced collapse of alginate chains during freeze-drying, and the stability of the FD chamber with respect to atmospheric moisture uptake/release. This was in-keeping with GLS-A 1-1 particles. GLS 2-1 particles however also exhibited GLS leaching onto the outer particle surface if created at the higher voltage.

| GLS-A 2-1 Pore Size | Drying Regime | 10kV | 15kV |
|---|---|---|---|
| | AD | 1.1 ±0.1 µm | 0.2 ± 0 µm |
| | AD+FD | 0.5 ± 0.1 µm | 1.2 ± 0.1 µm |

**Table 4.24:** GLS-A 2-1 particles: Effect of drying regime on pore size (± SE of 20 pores across 5 particles). GLS-A 2-1 particle pores from 10kV EHDA shrunk with additional FD (like GLS-A 1-1 particle pores), however GLS-A 2-1 particle pores created at 15kV grew with additional FD

Greater defects of the high-voltage particles in this investigation (GLS-A 2-1) led to higher water intake/nucleation during AD; fostering the growth of ice crystals during subsequent FD, and therefore a crystallisation-induced porosity [Ying et al., 2010]. The result would be larger particles and larger pores of these specific particles. Figure 4.55 shows the porous nature of the AD-only GLS-A 2-1 particles: indicating regions of potential crystallisation during freezing.
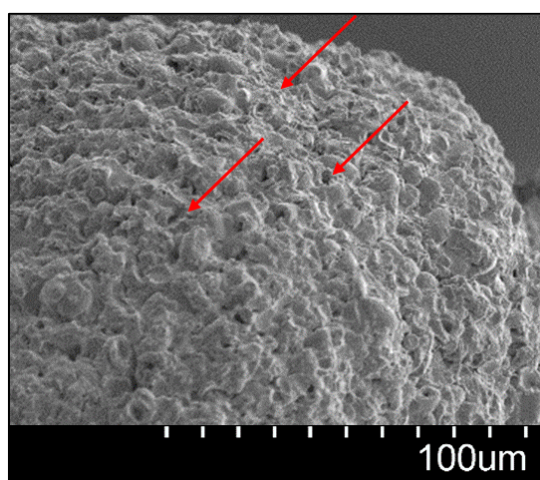


**Figure 4.55:** SEM image of GLS-A 2-1 particles created at 15kV and 50 ul/min after AD only; indicating regions of moisture settlement and subsequent potential crystallisation during additional FD

*Novelty processing and smart delivery of Ganoderma Lucidum spores*

The size of GLS-A 2-1 and 1-1 particles after additional FD is indicated by the SEM images in figure 4.56. The formation of pores in the 15kV GLS-A 2-1 particles, observed after AD (prior to FD) were conducive to an increase in particle size during additional FD.
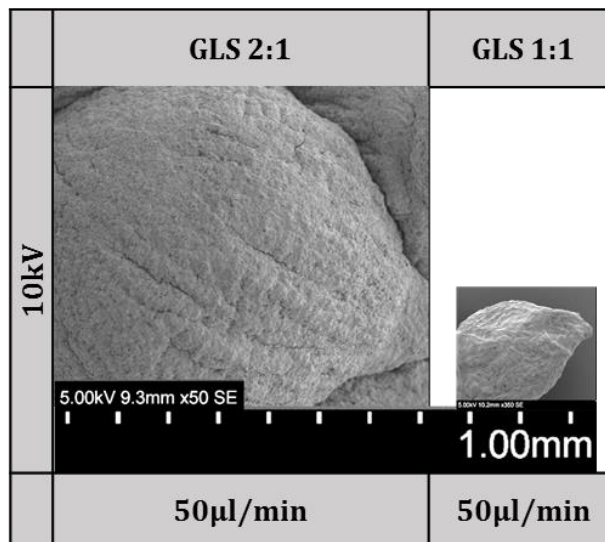


**Figure 4.56:** To scale: SEM image of GLS-A 2- 1 particles (GLS-A 1-1 inset) created at 10kV and 50ul/min after additional FD. The formation of pores in the GLS-A 2-1 particles observed after AD were conducive to an increase in particle *and* pore size during subsequent FD

GLS-A 2-1 particles, containing less alginate, exhibited a lack of structural integrity causing agglomeration during both drying regimes. Tailed and stretched particle structures resulting from the mode of droplet disruption fostered thinner polymer walls that were more conducive of agglomeration and collapse during drying. This is particularly the case as alginate is hygroscopic and would absorb/release moisture cyclically during drying [Date et al., 2010]. When freezing is employed prior to freeze-drying, the low-alginate structure is less capable of withstanding the crystal-induced stress on the particle structure - resulting in a greater chance of the agglomeration, breakage, and surface defects. This formation of ice crystals in the particle structure before and during freeze-drying can cause the GLS-A surface to be pushed away from the crystallising region, increasing the chance of particle agglomeration and collapse. Figure 4.57 shows the GLS-A 2-1 particles after both drying regimes. The particles that underwent additional FD were agglomerated and many had collapsed and broken. This highlights the advantages of having an increased polymer content. As a comparison, GLS-A 1-1 particles are shown in figure 4.58, created using the same EHDA process parameters, after both drying regimes.

*Novelty processing and smart delivery of Ganoderma Lucidum spores*
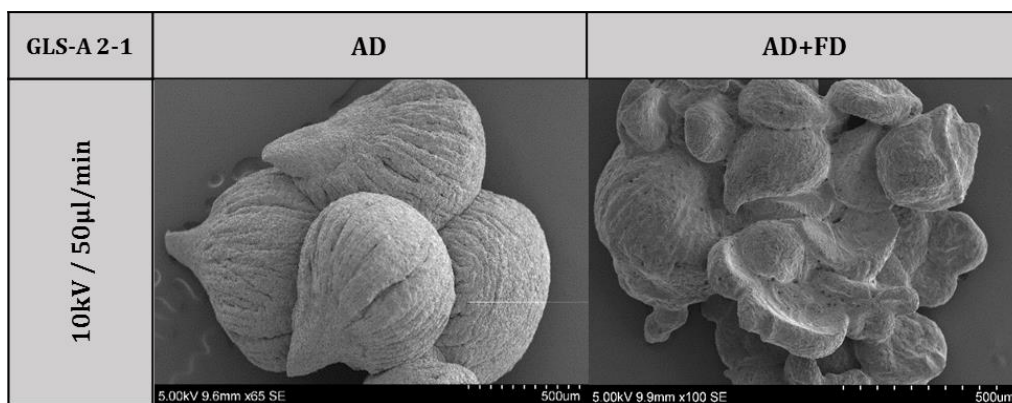
**Figure 4.57:** GLS-A 2-1 particles: Effect of drying regime on particle integrity: AD only vs. AD+FD, created at 10kv and 50ul EHDA. AD+FD GLS-A 2-1 particles had collapsed owing to insufficient polymer infrastructure
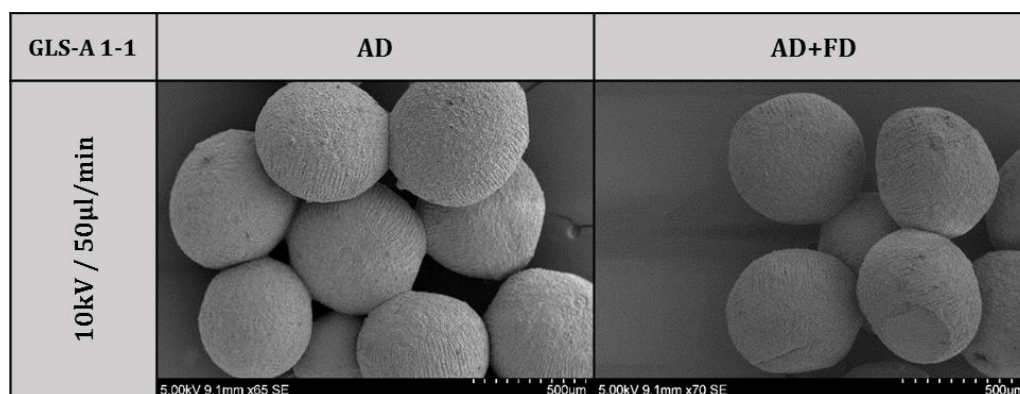


**Figure 4.58:** GLS-A 1-1 particles: Effect of drying regime on particle integrity: AD only vs. AD+FD, created at 10kv and 50ul EHDA. The particles were slightly smaller and also smoother after additional freeze drying

## 4.3.3.5 Evaluating Effects of a Reduced Alginate Content on GLS-A Particles containing 2% GLS

GLS-A particles were first created via EHDA using a GLS-A ratio of 1-1. This implied a polymer weighting already far below what has been achieved in literature, suggesting greater promise for enhanced drug loading. High polymer content has traditionally implied high strength, and alginate in particular suffers from instability when immersed in certain media typical of physiological release. For this reason, there is particular prevalence of studies centred on alginate-based drug delivery systems with low drug loading. The GLS-A 1-1 particles created and evaluated in this study not only achieved a 50-50 drug-polymer weighting, but further demonstrated high controllability over distribution characteristics *size* and *shape,* possessing a smooth surface that is atypical of this polymer when exposed to high voltage particularly. By

*Novelty processing and smart delivery of Ganoderma Lucidum spores*

reducing the polymer content (GLS-A 2-1), there were complexities introduced to the EHDA process namely as a result of a lacking chargeable polymer content and a compromised structural integrity.

### 4.3.3.5.1 Effect of Alginate Content on Particle *Size*

Table 4.25 shows the particle size achieved for each GLS-A ratio.

| Particle Diameter | GLS-A 1-1 | | GLS-A 2-1 | |
|---|---|---|---|---|
| | 10kV | 15kV | 10kV | 15kV |
| AD | 706.0 ± 11.9 µm | 525.4 ± 10.1 µm | 965.7 ± 17.2 µm | 252.9 ± 6.0 µm |
| AD+FD | 575.6 ± 10.0 µm | 405.1 ± 10.1 µm | 235.3 ± 26.7 µm | 775.8 ± 32.5 µm |

**Table 4.25:** GLS-A 1-1 and 2-1 particles: Effect of drying regime on particle size (± SE of 30 particle measurements). GLS-A 1-1 particles shrunk with additional FD, however the effect of additional drying on GLS-A 2-1 particles was less clear owing to the confounding effects of reduced polymer

Greater alginate concentration typically leads to a rise in viscosity and surface tension. An increased viscosity and surface tension would hinder droplet disruption as overcoming it with a given voltage takes longer [Moghadam et al., 2008]. Each progeny droplet will face the same greater challenge, ultimately leading to a larger final distribution. A lower spraying viscosity, implicated by the lower-polymer system (GLS-A 2-1 here) has typically been favourable to the realisation of a thinner electrospray, and thus smaller particles. GLS-A 2-1 indeed produced smaller particles. Reduced bulking and viscosity, along with retarded crosslinking, were the main drivers of the impacts on particle morphology [Li et al., 2009]. While this high-drug ratio is desirable from a theoretical point of view, encapsulating the most drug per particle, the effect of polymer on droplet disruption and structural integrity – both owing to lacking polymer - and the resulting effects on electrospray disruption, created particles that were polydispersed and structurally compromised [Moghadam et al., 2009; Festag et al., 1998; Luo et al., 2015; Speranza et al., 2001]. With greater alginate (GLS-A 1-1) the size achievable at the highest voltage was certainly not as small, however the size achievable at the lower voltage not as large – in other words the *overall effect of voltage was smaller.* An upper size limit is imposed as a high polymer content increases charge density per droplet, even in the face of bulking and viscosity (indeed, the polymer is the conductive counterpart in the particle). Studies further point to the possibility that a higher alginate concentration can foster more effective calcium penetration into the particle by *slowing crosslinking rate* at the particle surface and thus inducing more intensive and meticulous crosslinking. These studies insinuate a positive effect on particle structural integrity,

but the effect of crosslinking density on structure size is still controversial [Kuo et al., 2008]. Figure 4.59 summarises the optical micrographs of GLS-A 1-1 and GLS-A 2-1. The effect of voltage is evident across both ratios. Spherical particles were obtained uniformly across GLS-A 1-1 process parameters but GLS-A 2-1 particles were typically tailed. The effect of alginate content on particle size was statistically significant at 90% confidence.
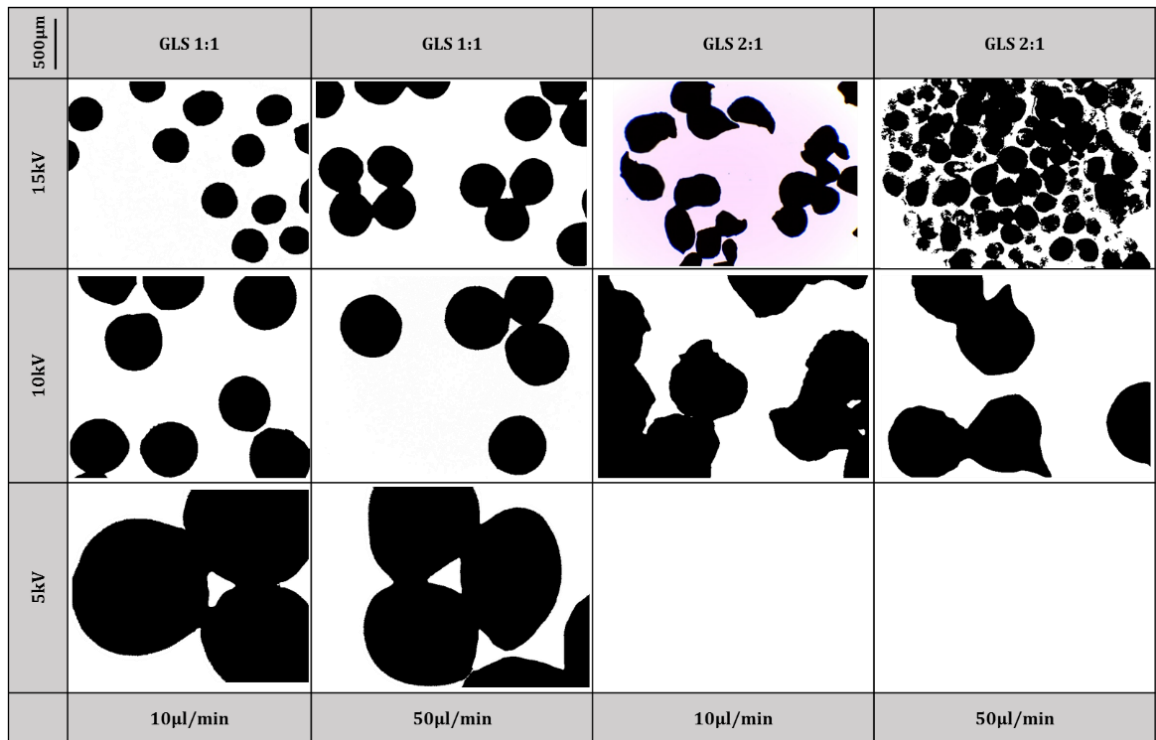


**Figure 4.59:** Optical micrographs of all GLS-A particles created at the EHDA process parameters

### 4.3.3.5.2 Effect of Alginate Content on Particle *Shape*

The effect of alginate content on particle shape (AR) was statistically significant at the voltages tested. Figure 4.60 shows GLS-A 1-1 and 2-1 particles created at 10kV and 50 μl/min, visualised by SEM. With greater polymer content comes greater polymer entanglement and thus greater particle strength prior to disruption; fostering a more rigid shape less likely to deform. The GLS-A 1-1 particles were spherical across all variables tested. The root of tailing, as with GLS-A 2-1, has not yet been investigated in the field of EHDA-processed polymers, however the mechanisms so far exhibited and described in this section support the formation of these tails in low-alginate particles.

*Novelty processing and smart delivery of Ganoderma Lucidum spores*

Particle "stretching" is a result of a lack of alginate conductivity, combined with a lack of polymer strength. The challenge to overcome the droplet surface tension during disruption arises when the particle does not have enough charge, and stretching occurs. When stretching occurs, polymer chains align and increase elasticity of the polymer structure; ultimately hindering break-up further and instead stretching (as shown by the "stretch marks" in figure 4.60). When faced in parallel with an overall reduced strength from less polymer, the result is a deformed shape owing to insufficient polymer entanglement prior to the droplet's disruption. A lower alginate concentration also undergoes less extensive calcium penetration during crosslinking; potentially leading to deformation even after the gelation stage.
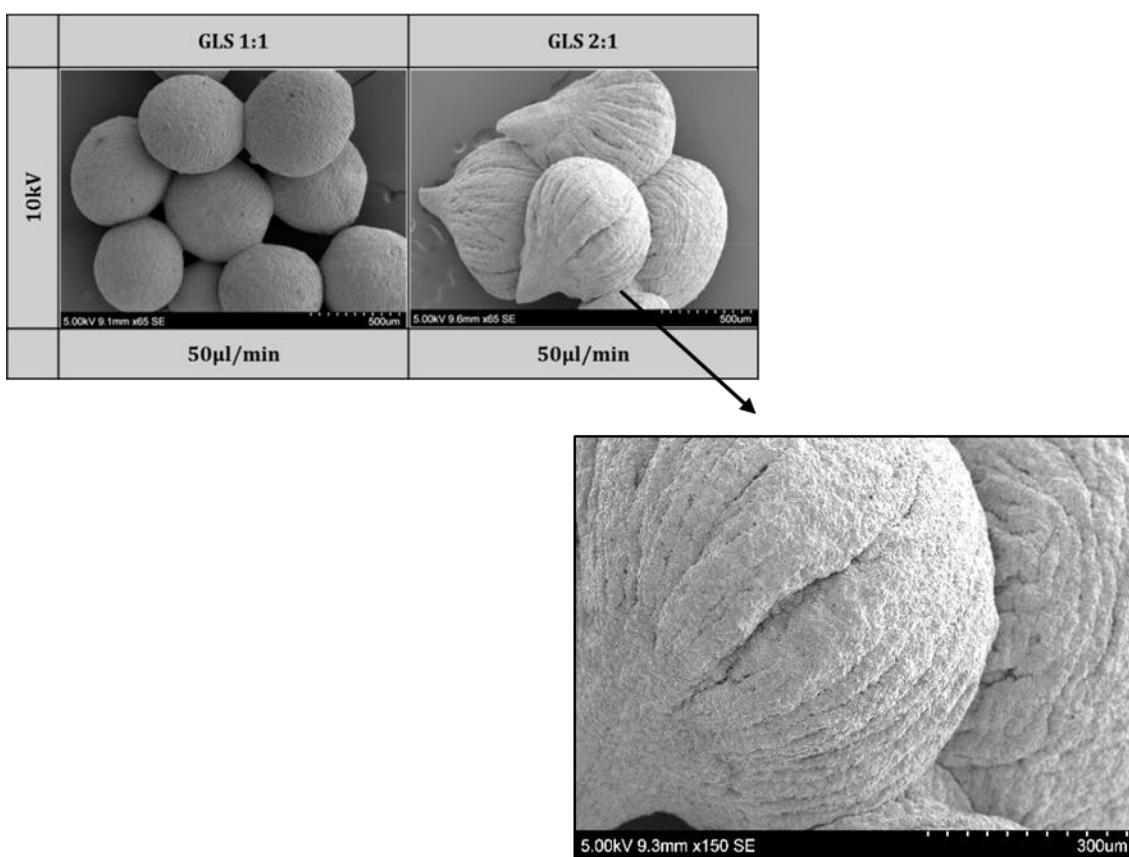


**Figure 4.60:** SEM of air-dried GLS-A particles showing the difference in particle shape between the two polymer contents GLS-A 1-1 and GLS-A 2-1. Tailed shapes resulted from insufficient chargeable polymer that resulted in reduced charge density and inefficient droplet rupture. This tailed particle shape is magnified in the lower SEM of GLS-A 2-1 air-dried particle showing stretch marks obtained during droplet break-away in electrospraying - induced by insufficient chargeable polymer

*Novelty processing and smart delivery of Ganoderma Lucidum spores*

Figure 4.61 summarizes the particle shapes obtained during the EHDA of GLS-A particles. The effect of voltage on shape is particularly observed for GLS-A 1-1 particles between 5kV and 10kV. Tailing was a feature of all GLS-A 2-1 particles.



**Figure 4.61:** Particle *shape* summary: GLS-A particle shapes containing 2% GLS created at the various tested EHDA process parameters. GLS-A 1-1 particles were spherical, with the exception of the lowest tested voltage (5kV). All GLS-A 2-1 particles exhibited tailed shapes. The mechanisms driving the voltage effect are described inset

Particle integrity was also examined – indeed, the morphology and surface attributes are not the only characteristics determining the stability of drug release from a delivery system. GLS "leaching" for example was observed to be a result of lower alginate content as it was only observed in GLS-A 2-1 particles; suggesting that particles containing less alginate had a structure more prone to breakage regardless of diameter and pore size. This is likely a result of insufficient polymer compromising the structural integrity; particularly during drying. Figure 4.62 shows a GLS-A 2-1 particle with evidence of cracking, along with phase separation (shown by the streaks on the particle) possibly indicating uncrosslinked regions [Brown et al., 1997]. Figure 4.63 further shows leaking of GLS in the form of spore fragments on the particle surface [Freiberg et al., 2004; George et al., 2006; Raemdonck et al., 2009; Nagarwal et al., 2009]. Free GLS was a result of insufficient alginate network to create a fully crosslinked structure incorporating GLS. Reasons for drug-surfacing have not yet been fully explored in the field, but are likely attributed to the surface defects allowing outward flow of entrapped drug; particularly during drying. This would ultimately

*Novelty processing and smart delivery of Ganoderma Lucidum spores*

contribute to the initial burst effect in release profiling [Corre et al., 1994; Hoffman eta l., 2008; Lu et al., 2011; Hoare et al., 2008].
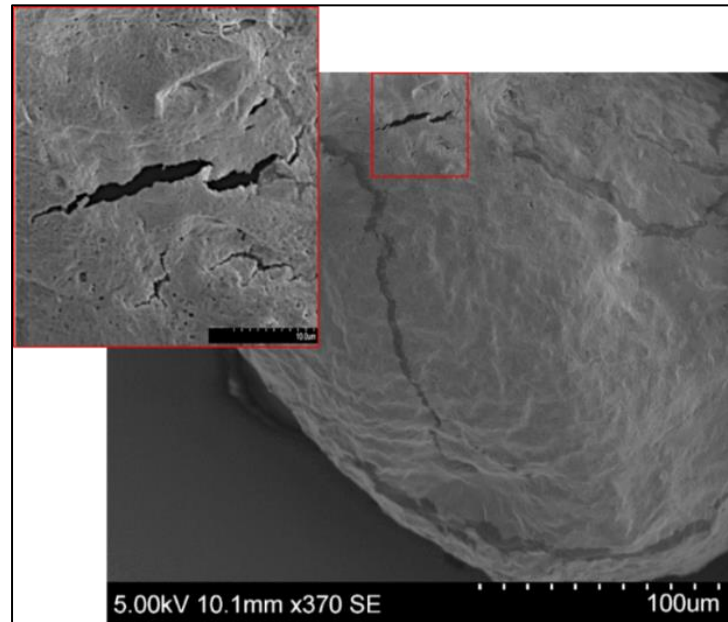


**Figure 4.62:** SEM of air-dried GLS-A 2-1 particle created at 50µl/min and 15kV showing surface defects caused by insufficient polymer infrastructure
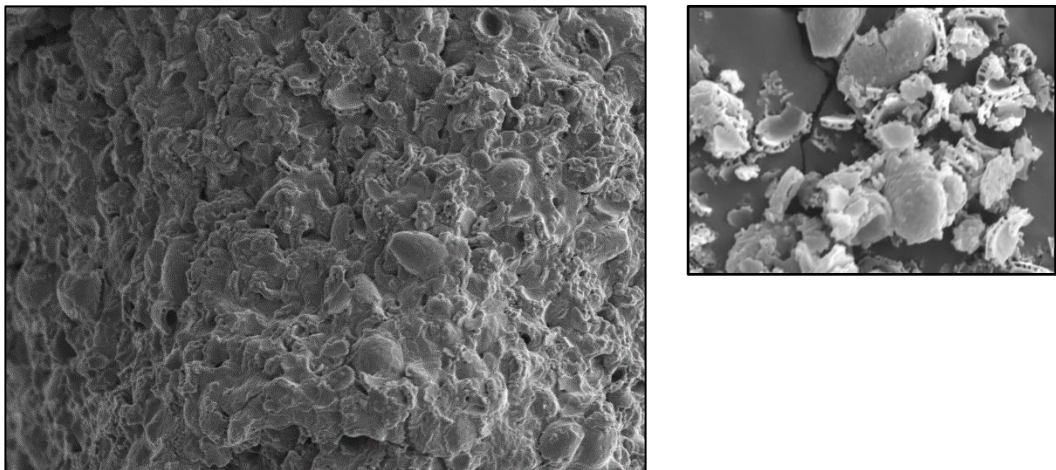


**Figure 4.63:** SEM of air-dried GLS-A 2-1 particle created at 50µl/min and 15kV showing GLS leaching. The broken GL spores imaged separately are shown as a confirmation that these surface features are indeed GL spores

*Novelty processing and smart delivery of Ganoderma Lucidum spores*

This phenomenon was only observed in the smallest GLS-A 2-1 particles, as these particles have a larger surface area-to-volume ratio and thus GLS would be nearest to the particle surface. Faster release, aside from being a result of particle size and shape, will then be a function of the leakage of the surface-associated and/or poorly entrapped GLS. Then, surface erosion and drug diffusion through the polymeric network will dominate release from these particles [Arias et al., 2004]. This is desirable for controlled drug delivery [Xu et al., 2009; Abreu et al., 2010; Buwalda et al., 2017]. An overall reduced structural integrity induced by insufficient crosslinked polymer in GLS-A 2-1 particles would also foster weakness in the face out outward pressure.

### 4.3.4 EHDA to Create *Low-Polymer* GLS-A 1-1 Microparticles

Lastly, low-alginate GLS-A particles were created (1% alginate), also containing less GLS (1%). This was investigated to gauge whether the effects of reduced polymer on particles were primarily driven by *reduced solution viscosity*, a *lack of polymer infrastructure,* or (and) insufficient *chargeability.* The relationship between the alginate content and its conductivity is not fully confirmed in literature, owing to the complexity of alginate chain conformations, and the effects of processing these chains [Kaczmarek-Pawelska et al., 2017]. GLS-A 1-1 particles were again created, however containing just 1% alginate. By also reducing GLS content to 1%, these particles exhibited the same drug:polymer ratio as the GLS-A 1-1 particles previously evaluated, however are less viscous, and are subject to a smaller GLS "burden". With less GLS than the GLS-A 2-1 solution, the charge capacity and viscosity should theoretically be more favourable to small and uniform distributions than GLS-A 2-1. With less alginate than the GLS-A 1-1 solution, the chargeability may however counteract the benefits. Figure 4.64 below shows the particles after 48 hours of air-drying. These GLS-A 1-1 particles containing 1% GLS were more uniformly shaped and sized than the same particles containing 2% GLS (GLS-A 2-1). The optical micrographs in figure 4.65 show the particle distributions.
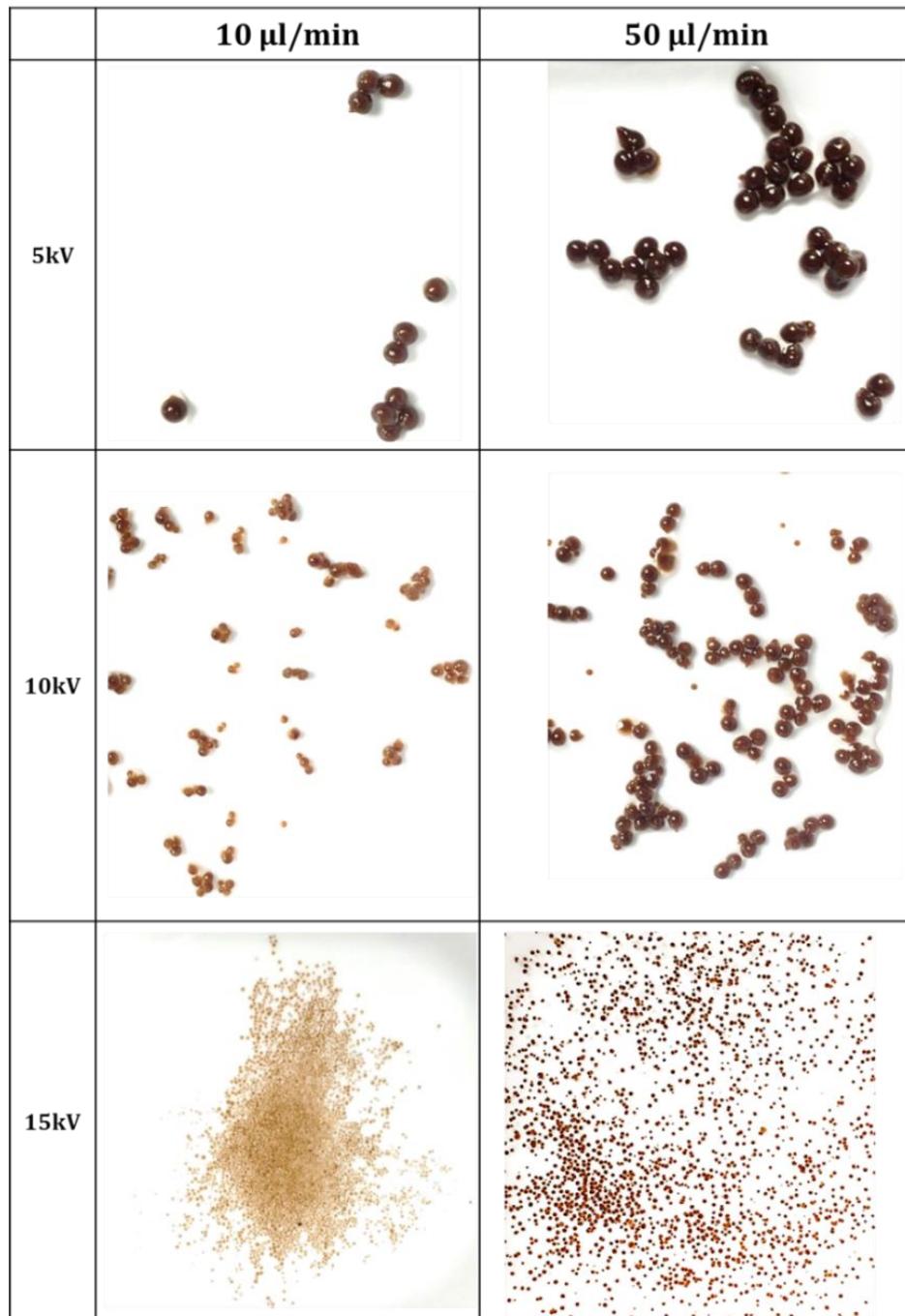
**Figure 4.64:** (1% GLS) GLS-A 1-1 particles air-dried for 48 hours. The effect of voltage is visually clear, as is the effect of flow rate on particle size

*Novelty processing and smart delivery of Ganoderma Lucidum spores*
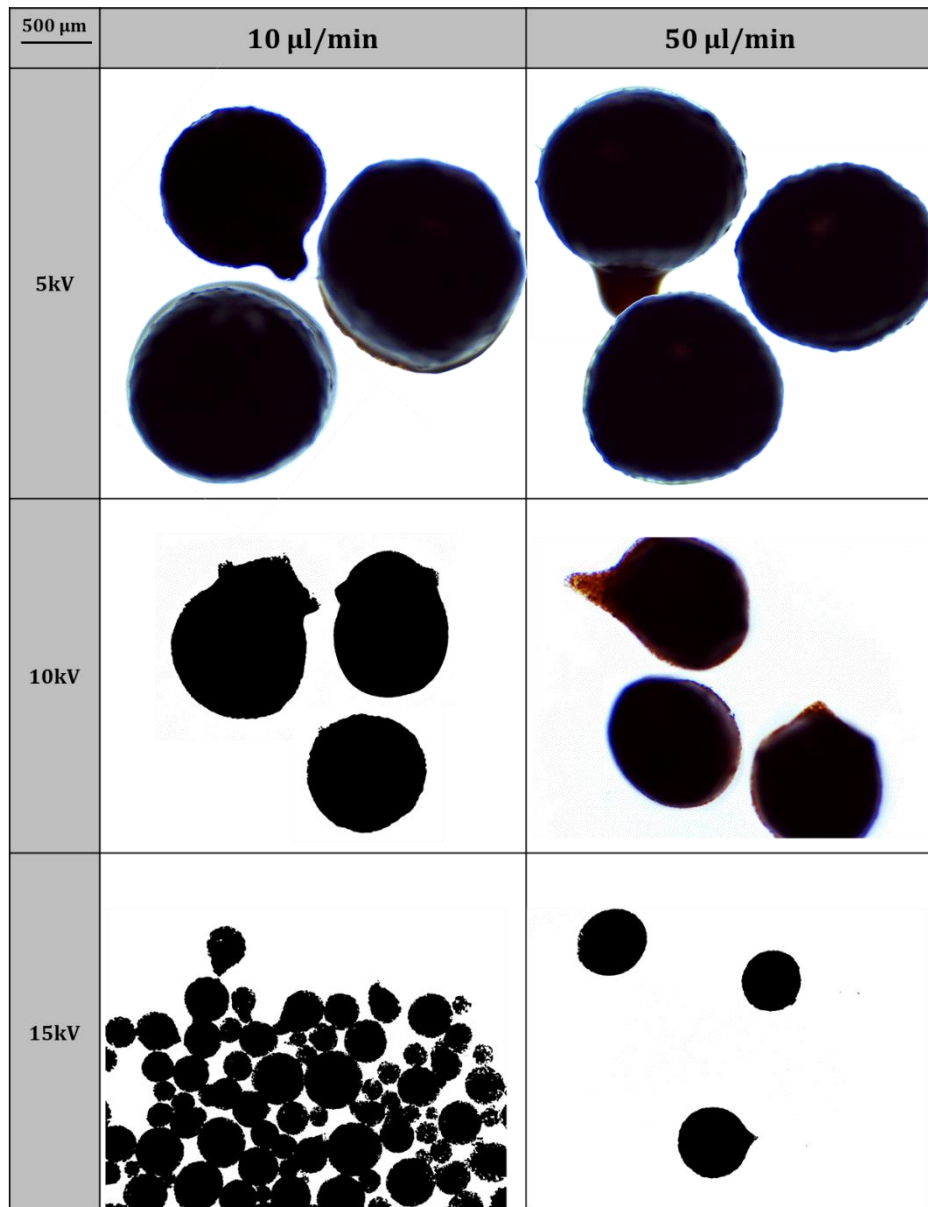
**Figure 4.65:** Optical Microscopy of (1% GLS) GLS-A 1-1 particles air-dried for 48 hours.

*Novelty processing and smart delivery of Ganoderma Lucidum spores*

The effect of voltage is shown in figure 4.66, demonstrating that voltage retains a negative correlation with particle size – as with the previous particle formulations. At the higher flow rate, particles are also larger, as previously observed. Particles maintained a smaller average size than the previous formulations, likely owing to the reduced solution viscosity.
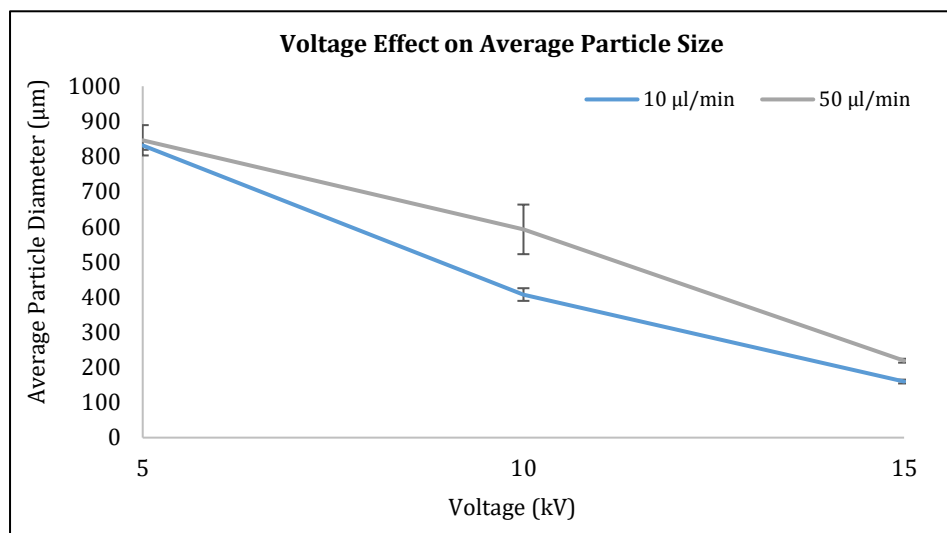


**Figure 4.66:** Effect of voltage on average particle size of (1% GLS) GLS-A 1-1 particles. Error bars represent the SE of 30 particle measurements. The effects of voltage and flow rate on particle size were statistically significant at 90% confidence

Particles maintained a near-spherical shape after air-drying, however still displayed tailing within the distribution. This can be explained using the phenomena detailed above during the evaluation of the GLS-A 2-1 particles. While the solution was less viscous, facilitating a more efficient disruptive pattern during spraying, the polymer content was clearly not sufficient to avoid tailing owing to lack of charge to foster effective disruption. This finding may indicate that the polymer content can be reduced without compromising the uniformity in particle *size*, however tailing would still be exhibited owing to a lack of ionisable polymer undergoing the established setup. These GLS-1-1 particles contained less alginate than previous GLS-A 1-1 particles, yet suffered from structural deformation and polydispersity even with the same GLS "burden".

## 4.3.5 GLS-A Particles: Which Setup?

Three GLS-A ratios were evaluated in this work: GLS-A 1-1 (containing 1%/1% OR 2%/2% GLS/A) and GLS-A 2-1 (containing 2%/1% GLS/A). Particle shape was "tailed" in particle samples

*Novelty processing and smart delivery of Ganoderma Lucidum spores*

that had more GLS than alginate (GLS-A 2-1 containing 2% GLS and 1% alginate). The particles that contained equal GLS and alginate (1%/1% OR 2%/2% GLS/A) did not exhibit low-polymer effects as these particles had sufficient polymer to maintain shape. Viscosity was however reduced in both particle distributions that contained 1% alginate, generating an EHDA spray conducive to rapid droplet disruption. There was however still an offsetting effect of reduced polymer infrastructure, causing these particles to exhibit tailing and polydispersity.
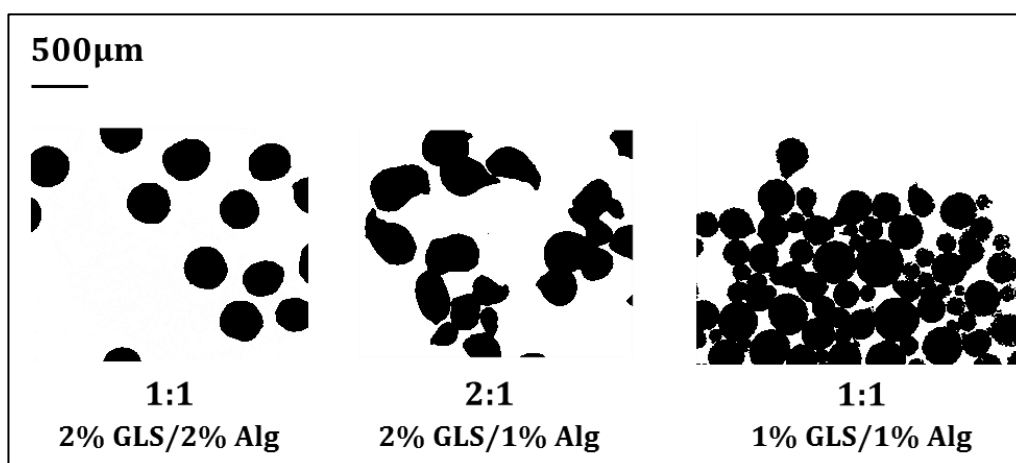


**Figure 4.67:** Three GLS-A ratios evaluated in this work: GLS-A 1-1 (containing 1%/1% OR 2%/2% GLS/A) and GLS-A 2-1 (containing 2%/1% GLS/A). The imaged particles were generated at the same EHDA process settings

## 4.3.6 In-Vitro Release from GLS-A Particles

Drug delivery from polymer hydrogels can be classified into three main mechanisms (diffusion-controlled, swelling-controlled, and erosion-controlled). Alginate-based drug delivery systems traditionally exhibit swelling *and* diffusion-controlled release. The relaxation/degradation of the polymer network at high osmotic pressure relaxes alginate chains, allowing inward is penetration of the dissolution medium and consequent swelling of the alginate matrix. Although the swelling initially creates a barrier to outward diffusivity, the drug will ultimately diffuse outward [Tønnesen et al., 2002]. When calcium ions slowly diffuse out of the hydrogel, it slowly degrades and release is therefore also driven by degradation [Tønnesen et al., 2002; Mandal et al., 2010]. As alginate hydrogels are anionic, its swelling and diffusion profiles will vary both with its hydrogel properties (specifically crosslinking density, polymer concentration, and inter-molecular interaction), and with external stimuli like pH. Together, these

factors control the behaviour of the polymer chains during release, and the speed of water inflow/drug outflow [Lin et al., 2006]. Desirably, alginate's hydrogel network swells significantly to absorb plenty water, yet its structure still remains stable due to its crosslinked polymer chains. The polymer matrix system (a variant of diffusion-controlled release) has been used to describe release from alginate matrices, however more recent developments in the field have suggested that the degree of porosity (and other surface defects) can also control the rate of drug release [Lin et al., 2006]. In this investigation, GLS is encapsulated using alginate, to form a hydrogel once crosslinked. GLS is dispersed to homogeneity in the alginate hydrogel network via magnetic stirring prior to particle fabrication. Release is evaluated as a function of particle distribution characteristics, such as size, shape, and surface attributes. The release bath was kept pH-neutral (pH 7.2), to reflect conditions in the intestinal tract – an environment not traditionally conducive of a stable release from alginate particles. This is because at this pH, electrostatic repulsions between alginic acid carboxylate anions accelerate the swelling and erosion of alginate gel as ion-exchange takes place between the gel-forming $Ca^{2+}$ ions and alginate's carboxylic acid groups ($Na^+$ ions), and the resulting electrostatic repulsions between its chains induces particle swelling and rapid and uncontrollable erosion [Mandal et al., 2009, Tomida et al., 1993]. When swelling is not significant, for example in acidic conditions, GLS release would primarily be driven by diffusion and the system would display a much slower release rate [Mazutis et al., 2015; Lee et al., 2012; Peretz et al., 2015].

So that the variable of GLS content could be controlled, the GLS-A particles containing less GLS were not evaluated with respect to their release profiled. Thus, GLS-A 2-1 and 1-1 particles containing 2% GLS were evaluated with respect to polymer content, distribution morphology, and surface characteristics.

### 4.3.6.1 GLS Calibration

The release of GLS from GLS-A particles was evaluated using UV-Vis spectroscopy. GLS in the release medium was quantified by executing a full scan of raw GLS, and recording its peak at 257nm; previously ascertained as a suitable absorbance wavelength for PSGA but also unprocessed GLS in many studies. A pure GLS solution is diluted to form concentrations between 0 - 0.05%, from which GLS release was defined using the resulting calibration (eqn 4.2).

$$\text{Absorbance of Released GLS} = 22.714 \times \text{GLS Concentration} \qquad \text{Eqn. 4.2}$$

*Novelty processing and smart delivery of Ganoderma Lucidum spores*
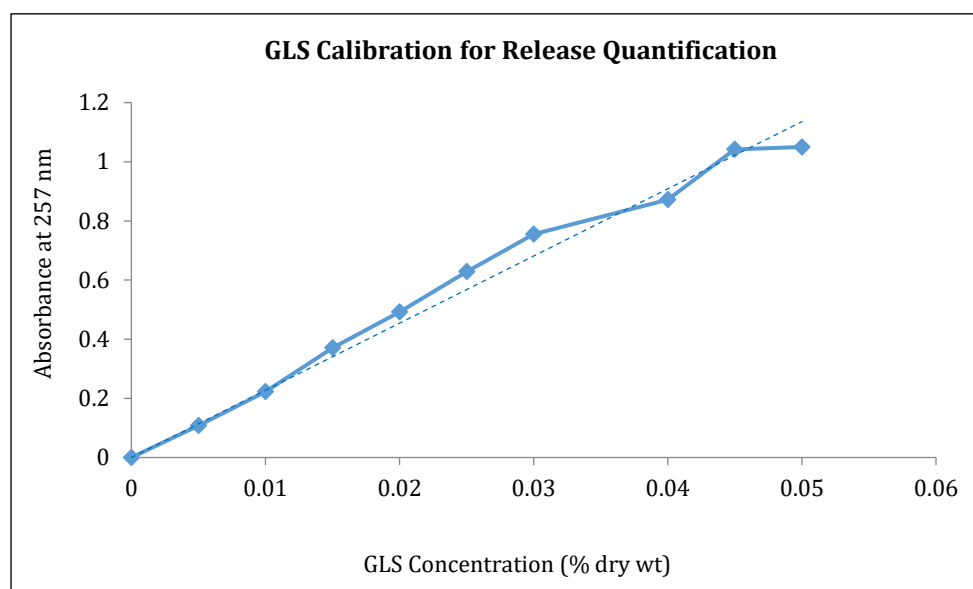
**Figure 4.68:** GLS Calibration for the determination of GLS release from GLS-A particles in-vitro

The release rate from GLS-A particles was then plotted as the percentage released from the formulated dose content of GLS (0.2mg in 0.01g particles, equating to 0.01% of the 2ml release bath).

## 4.3.6.2 GLS-A Particle Release Profile

GLS release from EHDA-generated particles was measured to determine the stability of the fabricated delivery system – a requirement of safe and effective drug delivery [Lin et al., 2006]. The release rate from a drug delivery system is also indicative of the encapsulation efficiency of the GLS-A particles. In this section, the effects of GLS-A **particle morphology**, **alginate content**, **drying regime,** and **surface features** are evaluated with respect to the GLS release from the GLS-A particles created using GLS-A ratios 1-1 and 2-1 (both containing 2% GLS). Some release patterns have been established for alginate (albeit inconsistently), however there are no published studies to date on the controlled release of GLS from GLS-Alginate microparticles created using EHDA – a promising setup owing to the therapeutic benefits of GLS and the high-level control of EHDA in the fabrication of microparticles [Berninger et al., 2016].

Particles were evaluated using the *initial GLS burst* (within the first 20 minutes) and *cumulative release across 2 weeks*. The cumulative release is plotted in figure 4.69, by sample batch (processing condition). In this investigation, the release from all GLS-A particles was steady, exhibiting a *maximum of 11% release* in the first 20 minutes and *21% release* within the first 60 minutes. Overall, a slower release was observed from GLS-A 1-1 particles (greater alginate

*Novelty processing and smart delivery of Ganoderma Lucidum spores*

content), and these particles also demonstrated the smallest initial burst in the first 20 minutes. At the end of the 2-week period, GLS-A 1-1 particles had the lowest total release. Medium saturation and a reduced concentration gradient implicated a release that slowed over time [Nanjwade et al., 2011].
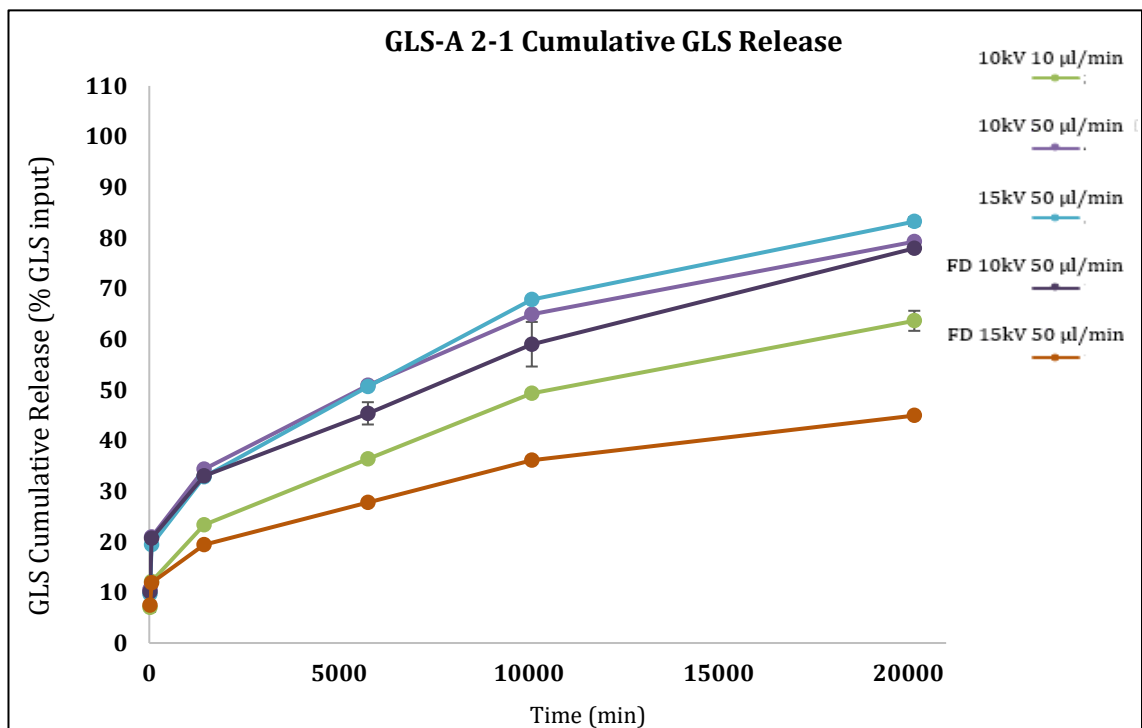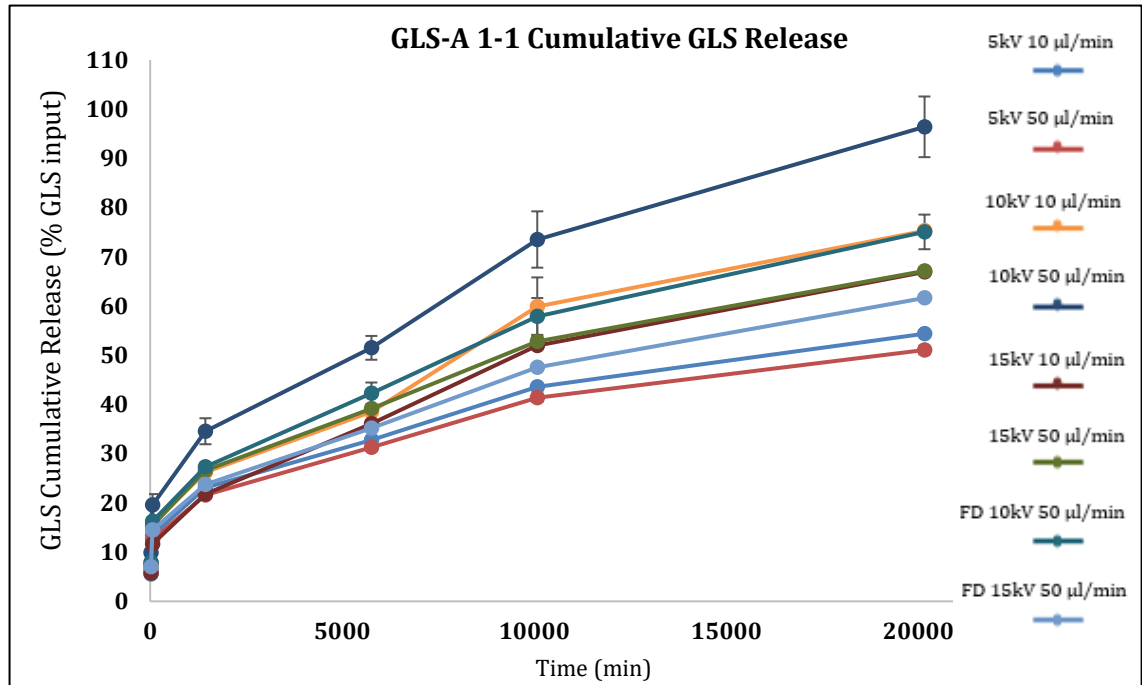


**Figure 4.69:** Cumulative release of GLS from GLS-A particles (*upper*: 1-1, *lower*: 2-1) over 2 weeks in DDI water at pH 7.2. Error bars represent the SE of two release baths

*Novelty processing and smart delivery of Ganoderma Lucidum spores*

The release from alginate matrices is closely related with the mobility of the hydrogel matrix, and the rate of water diffusion into the hydrogel matrix during swelling [Segi et al., 1989; Zhao 2014]. The rate of GLS release in the bath affected by hydrogel strength along with particle surface features like pores and cracks. A strong calcium-alginate hydrogel would delay the penetration of water into the tablet matrix and subsequently slow drug outflow. A strong matrix would be the result of greater crosslinking strength induced by increased polymer and/or calcium ions. The average release per period is given in table 4.26 for each sample.

| Voltage (kV) | Flow Rate (µl/min) | GLS-A Ratio | Drying Technique | Average Periodic Release Rate (%) |
|---|---|---|---|---|
| 10 | 50 | 1--1 | AD | 16.07 |
| 15 | 50 | 2--1 | AD | 13.87 |
| 10 | 50 | 2--1 | AD | 13.21 |
| 10 | 50 | 2--1 | FD | 12.99 |
| 10 | 10 | 1--1 | AD | 12.55 |
| 10 | 50 | 1--1 | FD | 12.51 |
| 15 | 50 | 1--1 | AD | 11.19 |
| 15 | 10 | 1--1 | AD | 11.15 |
| 10 | 10 | 2--1 | AD | 10.6 |
| 15 | 50 | 1--1 | FD | 10.27 |
| 5 | 10 | 1--1 | AD | 9.06 |
| 5 | 50 | 1--1 | AD | 8.51 |
| 15 | 50 | 2--1 | FD | 7.48 |

**Table 4.26:** GLS-A Particles average release rate calculated as the average of the release amount per time period

### 4.3.6.3 Release Kinetics: Initial Burst

The initial burst effect would be observed at the start of a treatment dosage, and is commonly observed when alginate is used as the sole encapsulation polymer [Khorram et al., 2015; Scholz et al., 2017]. In-vivo, a burst in treatment is undesirable because it may lead to dangerous level of plasma drug concentration, and further it hinders the goal of a *sustained* dosage over an extended period. The GLS-A particles in this investigation showed a very small initial burst in the first 20 minutes of media immersion, partially attributed to free GLS particles on the particle surface [Zheng et al., 2010; Ibrahim et al., 2005]. Surface-bound GLS on GLS-A particles was previously associated with particle pore size and other surface imperfections induced by insufficient polymer infrastructure and lacking charge density [Zheng et al., 2010]. The

*Novelty processing and smart delivery of Ganoderma Lucidum spores*

initial burst observed in the first 20 minutes of the study was highest for the lower-polymer GLS-A 2-1 particles - which were previously observed to contain greater stretch-induced defects and thinner polymer walls. Even though the measured pore size was smaller, the increased *quantity* of defects would be conducive to an outward flow of GLS during drying as well as increased inward penetration/outward diffusion during release; drawing GLS out to the particle surface. An example of a GLS-A 2-1 particle created at 15kV is shown in figure 4.70 below, where the spores are visible on the particle surface after air-drying (prior to the release study).



Spores evident on the surface of GLS-A 2-1 particles; indicating outward migration prior to release, and a precursor for initial burst during release
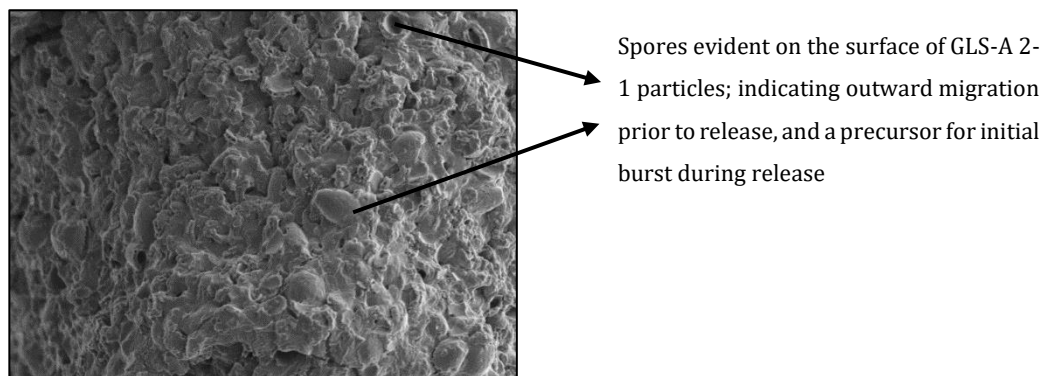
**Figure 4.70:** SEM of air-dried GLS-A 2-1 particle showing GLS leaching onto the particle surface as a result of pores and a weaker particle structure – a precursor of initial burst in release studies

## 4.3.6.4 Release Kinetics: Effect of GLS-A Particle Characteristics

The release from polymer particles is certainly a function of many variables, most of which confound each other [Dutta et al., 2016; Jaya et al., 2009]. This release study evaluated the impact that the EHDA processing variables on the GLS-A particles' release profiles. Acknowledging that processing conditions cannot be directly linked to release kinetics, the following subsections stratify particles by influential variables, such as alginate content and particle size/shape/surface characteristics.

### 4.3.6.4.1 Release Kinetics: Effect of GLS-A *Particle Composition* on Release Profile

The effect of alginate content was evaluated across particles created at one flow rate only, to control the effect of droplet volume, and without further FD to control the effects implicated by the freeze-drying process. Despite the presence of defects and pores on all GLS-A particles – owing to the nature of alginate itself - drug release was maintained across an extended period of time, without bursts. **This is due to the strong hydrogel network**, and the resulting high

*Novelty processing and smart delivery of Ganoderma Lucidum spores*

degree of entrapped GLS [Patel et al., 2016]. In this study GLS-A particles contained either 2% alginate (GLS-A 1-1) or just 1% alginate (GLS-A 2-1). GLS-A containing less alginate were faster-releasing. Less polymer leads to reduced strength and integrity of the particle, but it also triggers the effects of less chargeable polymer (particle shape deformity and stretched, thin walls in particular). Furthermore, by increasing alginate in the matrix, the increased hydrogel strength would induce less matrix swelling – thus slowing down swelling/diffusion-controlled release of GLS [Goswami et al., 2014]. Only GLS-A 1-1 particles exhibited a statistically significant relationship between morphology (size/shape) and release [Tønnesen et al., 2002]. The cumulative release as a function of GLS-A ratio (therefore alginate content) is plotted in figure 4.71 averaged across the EHDA processing settings. There is a generally faster rate of release form the GLS-A 2-1 particles, however by the end of the 2-week study the GLS-A ratio showed little impact on the overall GLS released.
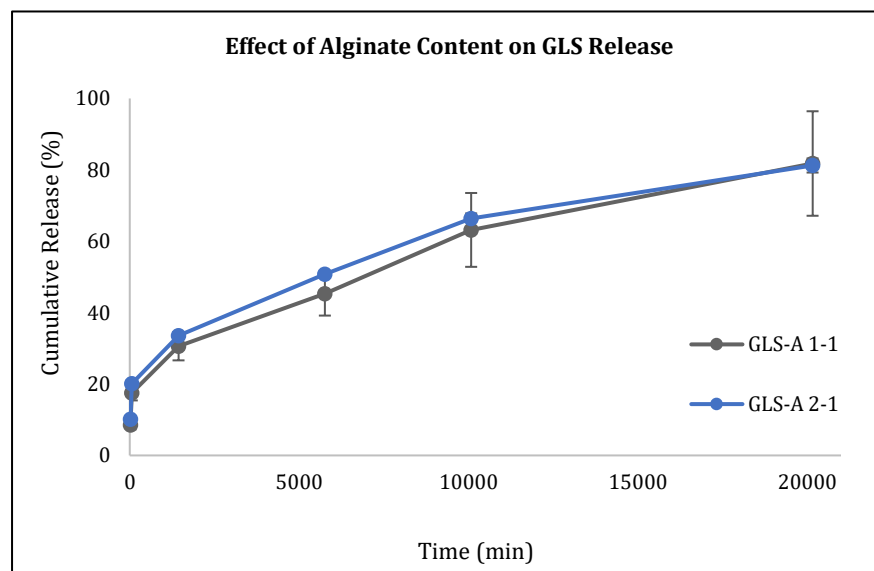


**Figure 4.71:** Effect of Alginate Content on GLS Release. Particles containing less alginate on average exhibited the fastest release rate. Error bars represent the SE of the distribution averages

The barrier to release was higher in GLS-A 1-1 particles owing to hydrogel strength [Tønnesen et al., 2002; Guzman-Villanueva et al., 2013]. This was even in the face of a measurably larger average pore size on GLS-A 1-1 particles. Slower crosslinking is typically observed at the particle surface of polymer particles with a greater polymer concentration, inducing a more intensive and meticulous crosslinking density and contributing to the release barrier [Kuo et al., 2008]. Figure 4.72 highlights defects in GLS-2-1 that would contribute to greater drug outflow. Studies have actually used alginate particle surface cracks during drug diffusion to increase release [Cruz et al., 2004]. A greater prevalence of pores in the polymer matrix could actually enhance the flexibility

*Novelty processing and smart delivery of Ganoderma Lucidum spores*

a feature already attributed to less dense crosslinking; allowing greater swelling-induced release that may have played a role in its more rapid release rate [Annabi et al., 2010; Xing et al., 2018; You et al., 2017]. The impacts of alginate content on the release rate from GLS-A particles therefore show associations to the release mechanisms governed by pores (swelling-controlled release and diffusion-controlled release), but also erosion-controlled release which is driven by polymer strength and thickness [You et al., 2017].
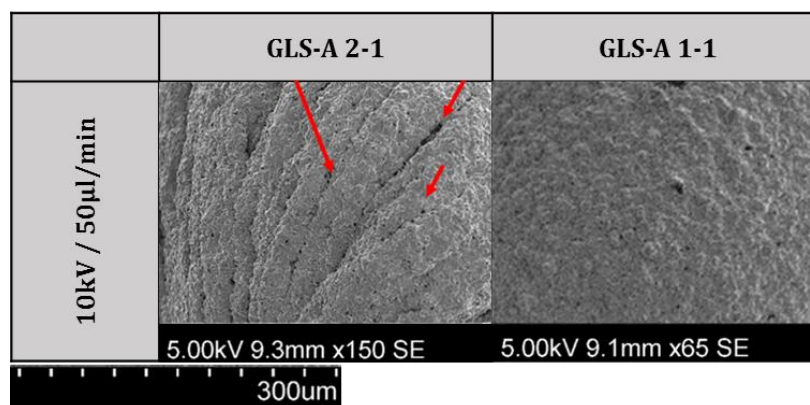


**Figure 4.72:** SEM of surfaces of GLS-A 2-1 (left) and GLS-A 1-1 (right) particles created at 10kV under 50µl/min. The stretch marks evident in GLS-A 2-1 particles are reflective of the reduced chargeable polymer content during electrospraying; challenging droplet disruption. Ultimately, large defects and thin walls remain

### 4.3.6.4.2 Release Kinetics: Effect of GLS-A *Particle Size* on Release Profile

GLS-A particles exhibited a negative correlation between size and release rate, where smaller particles generally released faster. The release is plotted by particle size in figure 4.73, for AD particles only (freeze-drying introduces confounding effects). Particle size has typically been shown influential on release kinetics, especially in swelling/diffusion-controlled mechanisms typically observed form alginate matrices [Tønnesen et al., 2002]. Altogether smaller particles have a larger distribution surface area and so provide a greater contact surface with the release medium when considering the same mass of particles. Resultantly, they are faster-releasing owing to positive impacts on the diffusion as well as swelling coefficients.

*Novelty processing and smart delivery of Ganoderma Lucidum spores*
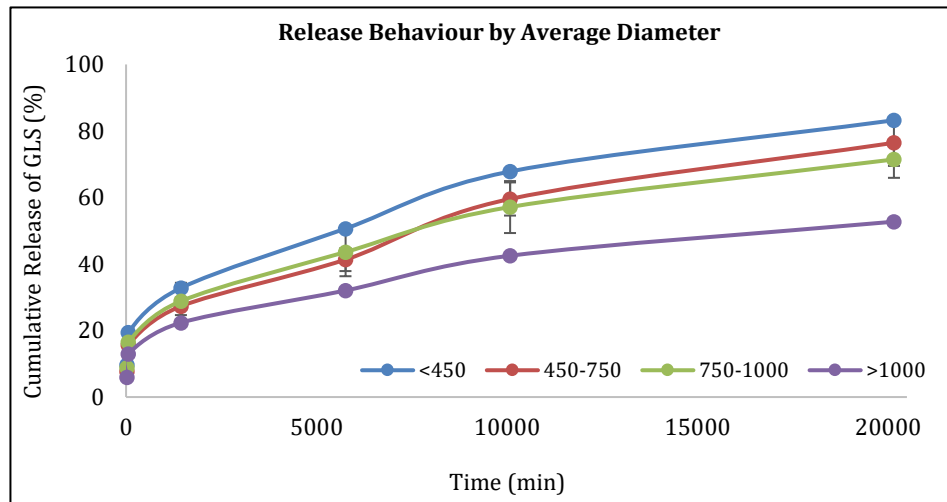
**Figure 4.73:** Release of GLS-A particles by particle diameter. As discussed, smaller particles showed the fastest release owing to the largest surface area per unit mass. Error bars represent the SE of stratified samples

### 4.3.6.4.3 Release Kinetics: Effect of GLS-A *Particle Shape* on Release Profile

The particle aspect ratio (AR) was positively correlated with GLS release, with faster release generally coming from more spherical particles (albeit these were also the particles that were freeze-dried, introducing a confounding effect). Wider particles (a larger AR) released more slowly, whereas spherical or longer particles released more rapidly. Wider particles were disc-like in shape and had a lower surface area per mass unit when compared to more spherical particles, which have a larger total surface area per volume of particles. This led to a slower release from wider particles in the release bath compared to the same mass of spherical particles or those with a "long"/" tailed" morphology. Thus, the effect of shape on release was primarily influenced by its impact on the diffusion and swelling coefficients.
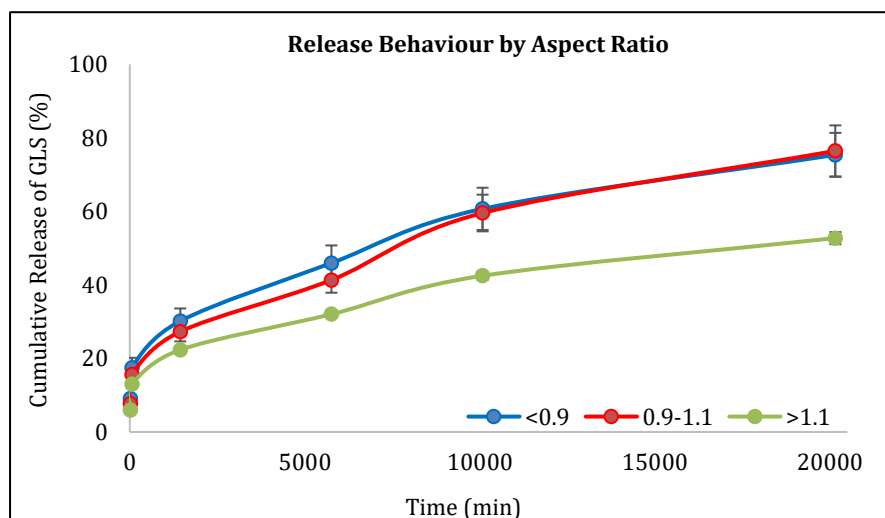


**Figure 4.74:** Release of GLS-A particles by aspect ratio. As discussed, wider particles (highest aspect ratios above 1), showed the slowest release owing to the smallest surface area per unit mass. Error bars represent the SE of stratified samples

*Novelty processing and smart delivery of Ganoderma Lucidum spores*

### 4.3.6.4.4 Release Kinetics: *Interplayed Effect* of GLS-A Particle Size and Shape on Release Profile

Particles with a higher AR were created at lower voltages, were disc-like in shape, and were also largest. Therefore, the slowed release of high-AR particles could be an effect of size as well. The influence of size is effectively eliminated when the shape (via AR) is being evaluated for one size range only. The size strata chosen was <750μm. Figure 4.75 shows the release profiles of GLS-A particles classified by AR to determine whether a higher AR did actually slow down release. The stratification shows that wider particles (AR >1) still exhibited the slowest release of GLS over 2 weeks, even though these particles were not the largest. Therefore it can be concluded that a wider particle (higher AR) will release more slowly than a longer or more spherical particle – and this is not owing to size. A reason for rapid release of longer particles is the possession of a unique tail providing additional surface area and a faster release. As well as a unique additional surface area, a tail may possess a thinner outer shell owing to the stretching. These could also be faster-degrading. This shows that the effect of AR may in fact be more instrumental on release rate than particle size. The possession of a tail arose as a consequence of inefficient coulomb fission and thus ineffective droplet disruption; fostered by insufficient polymer. However with the knowledge that they can manipulate release rate, further work is needed to determine the real implications for drug delivery.
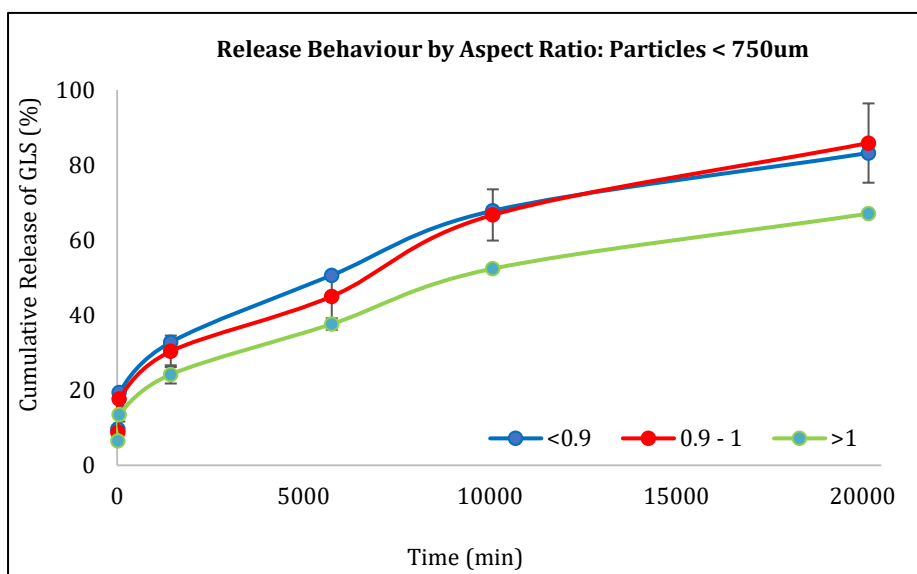


**Figure 4.75:** Release of *small* GLS-A particles by aspect ratio. The slowest release was *still* exhibited by wider particles (highest aspect ratios above 1), showing that aspect ratio was an important determinant of release speed - the particles which has the smallest surface area per unit weight. Error bars represent the SE of stratified samples

*Novelty processing and smart delivery of Ganoderma Lucidum spores*

### 4.3.6.4.5 Release Kinetics: Effect of GLS-A *Particle Drying* on Release Profile

GLS-A particles that underwent additional freeze-drying slowed the release compared to AD counterparts. Smoother and more compact surfaces were previously observed, and may justify the reduction of the diffusion-controlled component of release. A slower drug release from FD polymer matrices is actually contradictory to many studies which observe that this method of drying produces fractured or porous surfaces that induce faster (and more uncontrollable) drug release. However those studies are not evaluating FD particles have been pre-airdried as was the case in this investigation [Risbud et al., 2000; Wlosnewski et al., 2010; Guzman-Villanueva et al., 2013]. Particles that underwent additional freeze-drying for 24 hours exhibited a notably smoother surface containing less visible pores and defects. This was explained by the removal of moisture via AD that would otherwise create invasive ice crystals (and thus surface defects) during FD, FD-induced inward alginate chain collapse, and a more stable drying environment devoid of cyclic water absorption in open air [Avadi et al., 2004; Costantino et al., 2004]. As a result, the outward diffusion-controlled component of release would not have been as strong, along with reduced penetration into the alginate matrix hindering swelling-induced release [Choi et al., 2008]. Initial burst from these particles was also lower than AD counterparts. The increased rigidity of FD particles however increases the risk of surface fracture as this may inhibit expansion during the high-pressure environment of freeze-drying, leading to surface rupture due to inflexible polymer chains [Santagapita et al., 2012]. This fractured impact was *occasionally* observed in FD particles, as shown in figure 4.76. Nonetheless, this was *not* the case across the general FD particle distribution and thus had no effect on the average behaviour of FD GLS-A particle release.



**Fractures** in AD+FD particle caused by inflexible polymer chains that inhibit expansion during the high-pressure FD
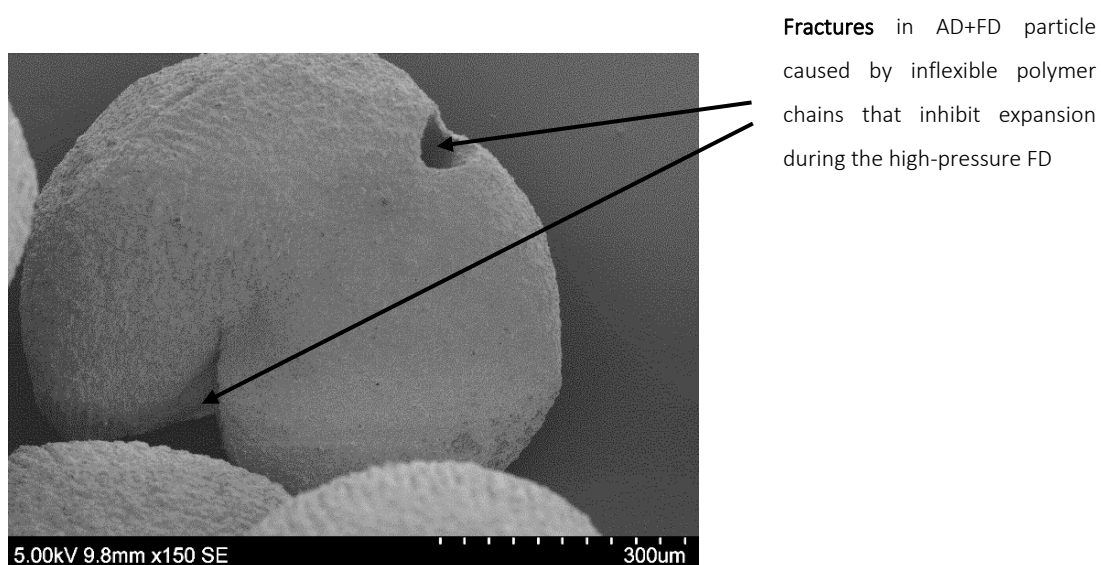
**Figure 4.76:** SEM of an example of particle fracture observed after additional FD of a GLS-A 1-1 particle created at 10kV, 50µl/min. The fracture is likely a result of a more brittle structure of a highly crosslinked particle undergoing FD

*Novelty processing and smart delivery of Ganoderma Lucidum spores*

FD has been widely proven an effective method of processing microparticles for drug delivery; both with respect to drug loading and drug release – and also with respect to chemical preservation [Yin et al., 2009]. Therefore, this work remains supportive of this technique's merits as a drying technique for GLS:Alginate microparticles.

### 4.3.6.4.6 Release Kinetics: Effect of GLS-A *Pore Size* on Release Profile

Only one quantity of alginate was stratified to evaluate the effect of pore size on cumulative release (GLS-A 1-1 particles) so that the confounding effects of alginate content on release would be negated. GLS-A particle release averaged across EHDA fabrication settings and stratified by pore size is plotted in figure 4.77 as a function of pore size. It was evident that larger pores were associated with faster release. The positive effect of pore size on release rate suggests that release is in fact primarily driven by swelling-induced and diffusion-induced mechanisms [Tønnesen et al., 2002]. Fan et al., 2013 for example reported that the release of diclofenac sodium from alginate matrices first exhibited desorption from the outer surface, after which release was dominated by pore diffusion [Fan et al., 2013].
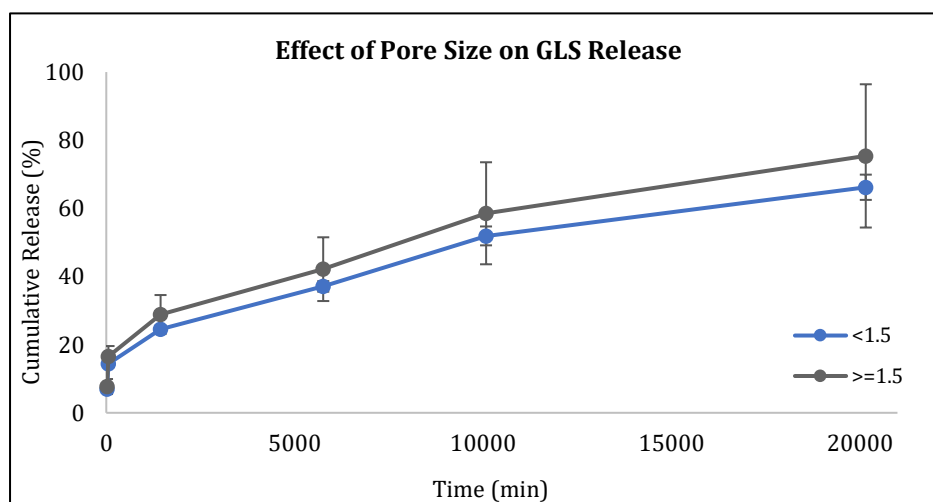


**Figure 4.77:** Effect of Pore Size on GLS Release. Particles containing large pores on average exhibited the fastest release rate. Error bars represent the SE of the pore distribution averages

### 4.3.6.4.7 Release Kinetics: Fitting a Release Model

In order to fully understand the effects of dosage, and to determine the level of controllability over a delivery system, the application of an appropriate model to the release profile is essential. Fickian diffusion occurs when there is a *faster release* of compounds *than of water entering* the hydrogel matrix (usually the case when there is a high degree of hydrogel relaxation). Conversely, a faster rate of water influx than matrix relaxation results in a slower

*Novelty processing and smart delivery of Ganoderma Lucidum spores*

release rate (non-Fickian). GLS-A particles displayed a slow and gradual release, typical of non-Fickian behaviour, suggesting a more rigid hydrogel network [Masaro et al., 1999; Park et al., 2018]. The First-Order kinetics model proposed for this GLS release is described below. This type of release has demonstrated good control over drug release from polymer hydrogels in literature; offering advantageous treatment options.

### First-Order Kinetics Model

Water-soluble drugs in porous matrices, like this GLS-A system, often exhibit a first-order release profile [Dash et al., 2010]. First-order release kinetics imply a release rate somewhat proportional to the medium drug concentration (thus, a declining nominal release rate as the release period continues) [Gouda et al., 2017]. This is typically associated with in-vivo release in the bloodstream, where first-order release would imply that the rate of release is related to the metabolism of the plasma drug content (because the body can make more enzymes available to metabolise the extra drug; thus the higher the blood plasma concentration, the faster the clearance) [Patel et al., 2016]. In this in-vitro investigation however, there is no metabolic function and thus the main influence on concentration-based kinetics would be the concentration gradient of GLS and the implied *medium saturation*. Because the release rate of GLS appeared to decrease over the 2-week study period, release profile was tested with the first-order model. Figure 4.78 shows the first-order plot of the GLS release, created by log-transforming the cumulative *remaining* amount of GLS. A log transformation of the release rate is characteristic of the first-order model. This transformation enables one to interpret the "remaining rate" in the absence of dependencies on each previous time-point (which characterises the fist-order profile). Log scales further allow visibility of small increments, thus clarifying the pattern observed between release rate and time. Theoretically, a robust first-order model would exhibit a straight negative slope – not the case here. This suggests that the release of GLS in this investigation exhibited an increasingly reduced rate of release. The deviation from a straight slope could also be attributed to the presence of water-soluble GLS *on the particle surface* from the previously discussed outward migration onto the surface – skewing the first portion of release. The corresponding $R^2$ values for a linear fit of the first-order plot are provided in table 4.27. The first-order regression coefficients are very high, suggesting a good fit of this model.

*Novelty processing and smart delivery of Ganoderma Lucidum spores*
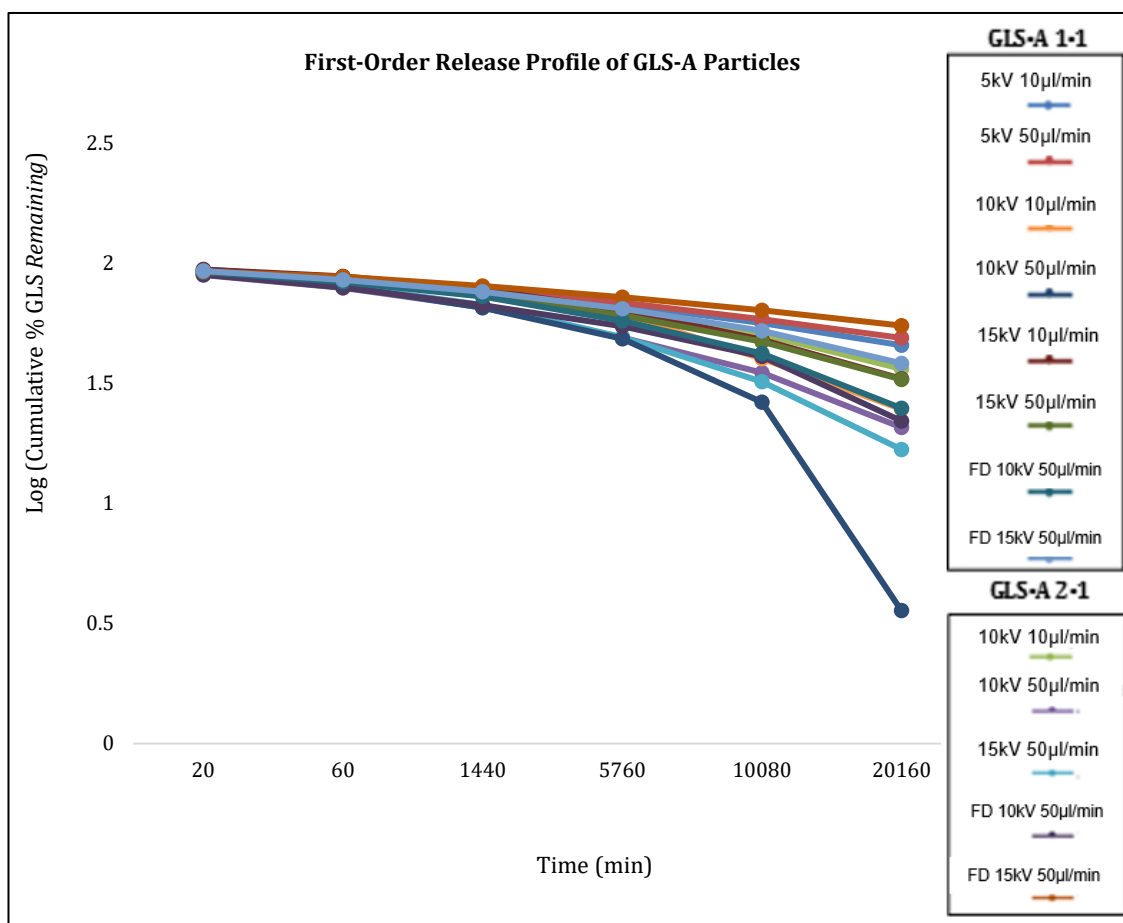
**Figure 4.78:** First-Order Release model, fit onto the release profile of GLS-A particles. The negative slope is indicative of a release rate that is somewhat proportional to the remaining drug.

| Sample | | | | | | | | | | | | |
|---|---|---|---|---|---|---|---|---|---|---|---|---|
| **kV** | 5 | 5 | 10 | 10 | 15 | 10 | 10 | 15 | 15 | 10 | 10 | 15 | 15 |
| **µl/min** | 10 | 50 | 10 | 50 | 50 | 10 | 50 | 10 | 50 | 50 | 50 | 50 | 50 |
| **GLS-A** | 1-1 | 1-1 | 2-1 | 2-1 | 2-1 | 1-1 | 1-1 | 1-1 | 1-1 | 2-1 | 1-1 | 2-1 | 1-1 |
| **Drying** | AD | AD | AD | AD | AD | AD | AD | AD | AD | AD+FD | AD+FD | AD+FD | AD+FD |
| **R²** | 0.98 | 0.98 | 0.94 | 0.95 | 0.92 | 0.9 | 0.76 | 0.93 | 0.95 | 0.91 | 0.92 | 0.98 | 0.95 |

**Table 4.27:** Regression coefficients of first–order release profile. These coefficients are near 1, suggesting these model fits the average GLS-A release profiles well

When metabolic enzymes are involved (unlike this simplistic model), first-order release avoids the build-up of drug in the body, by ensuring that the drug is eliminated as fast as it enters the

*Novelty processing and smart delivery of Ganoderma Lucidum spores*

plasma. When GLS was released in this investigation, the observed first–order kinetics appeared similar to in-vivo environments (in the presence of metabolism that could eliminate the drug concentration and foster more drug release, before reaching full capacity and slowing release) owing to medium saturation and a reduced concentration gradient [Gierszewska-Drużyńska et al., 2012; Nanjwade et al., 2011].

If instead *zero-order* kinetics governed release, the amount of drug entering the plasma would not reduce if the metabolism of it slowed down; leading to dangerous levels of drug toxicity. In a zero-order release model, GLS release is independent of the GLS concentration in the drug. In other words a constant amount of drug is eliminated per unit time. As GLS was not at the core of the particle but rather dispersed around it, there should be no increase in diffusion length for particles further in; and thus no dependence on drug remaining. The regression coefficients ($R^2$) for a zero-order linear fit corresponding to the cumulative release plot are given in table 4.28. The regression coefficients indicate that release from GLS-A particles over 2 weeks. While this not a comparison to the first-order model fit, the $R^2$ suggests that the variables do not explain the release rate as well as the first-order model.

| Sample | | | | | | | | | | | | | |
|---|---|---|---|---|---|---|---|---|---|---|---|---|---|
| kV | 5 | 5 | 10 | 10 | 15 | 10 | 10 | 15 | 15 | 10 | 10 | 15 | 15 |
| µl/min | 10 | 50 | 10 | 50 | 50 | 10 | 50 | 10 | 50 | 50 | 50 | 50 | 50 |
| GLS-A | 1-1 | 1-1 | 2-1 | 2-1 | 2-1 | 1-1 | 1-1 | 1-1 | 1-1 | 2-1 | 1-1 | 2-1 | 1-1 |
| Drying | AD | AD | AD | AD | AD | AD | AD | AD | AD | FD | FD | FD | FD |
| $R^2$ | 0.88 | 0.88 | 0.91 | 0.87 | 0.89 | 0.92 | 0.93 | 0.92 | 0.9 | 0.91 | 0.92 | 0.9 | 0.91 |

**Table 4.28:** Regression coefficients of zero–order release profile (not typically a log transformation). These are lower than those obtained when fitting the first-order model

Given the high solubility of GLS however, along with the inhomogeneity of GLS path-lengths from the release interface, zero-order release kinetics are challenged [Li et al., 2015]. Indeed it is evident from the non-linear slope of cumulative release that a zero-order release was not achieved.

In many cases, a first-order release in the bloodstream will eventually attain a zero-order release pattern as the metabolic enzymes reach full capacity (*medium saturation* or *reduced concentration gradient* in an in-vitro study like this), or as the particles themselves exhibit changes

*Novelty processing and smart delivery of Ganoderma Lucidum spores*

in structural profile (swelling capacity, chain rigidity etc.) [Malana et al., 2013; Kamble Sharad et al., 2017]. Figure 4.79 demonstrates this shift in release order. Most particles began to approach proximity to zero-order by the time GLS release reached 25% of its dose.
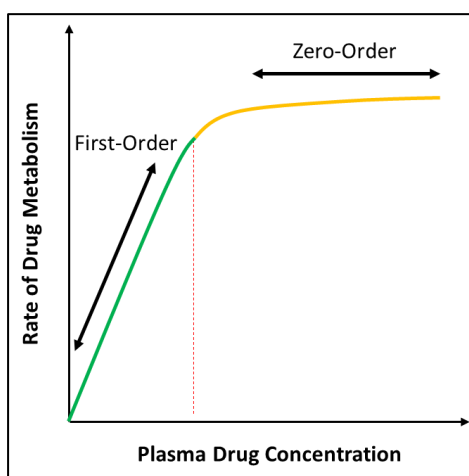


Figure 4.79: Schematic of a shift in kinetics from a first-order to zero-order model

This release investigation has revealed important phenomena in the controlled release of GLS from GLS-A microparticles. While controlled release is attainable, a comparatively small "initial burst" occurs owing to free GLS on the particle surface rather than system instability. The release rate was observed to be a function of particle morphology (size and shape); principally indicating that smaller particles were faster-releasing, along with tailed and spherically-shaped particles. Surface porosity was also observed an important driver of release from the GLS-A matrix, verifying that diffusion/swelling-controlled mechanisms of release governed the study kinetics. Erosion-controlled release was indicated to be insignificant in this study in light of the polymer content's small effect on release rate. Despite these findings, many particle characteristics are interconnected with respect to release behaviour – for example the effect of alginate may not directly show impacts on release rate, but it impacts particle size, porosity, and surface strength – which all impact release rate. Greater alginate content could not be stratified as these particles possessed little common-ground with the particles containing less alginate, Future work should focus on greater control over confounding effects.

## 4.3.7 How these GLS-A Particles Compare to Recent Studies

The comparison with existing studies is challenging when novel materials are used, such as the case with GLS (and indeed its combination with alginate). An attempt was made to compare

*Novelty processing and smart delivery of Ganoderma Lucidum spores*

recent studies with this GLS-A study so that a critical evaluation could be carried out. Two aspects are considered important with respect to comparison - *GL-loaded Polymer Matrices* and *Drug-loaded Alginate Matrices*. There is very little study of the two materials combined – indeed this marriage may be beneficial in its own right, as the tables below indicate. GLS-A 1-1 are compared here, owing to a desirable drug-loading.

### 4.3.7.1 GL-loaded Polymer Matrices

While less competitive in size, the spherical particles created in this study (those created with 50% GLS loading (equating to 2% GLS and 2% Alginate "GLS-A 1-1") contained the most drug – a competitive trait in current drug delivery formulations. Furthermore, these particles exhibited a significantly lower initial burst, and released in the most sustained fashion. This presents exciting alternatives to existing formulations. These 1-1 particles, being spherical and uniform, also present scope to enhance dosage repeatability and increase bioavailability (e.g. via greater tissue acceptance).

|  | **This Study** | Shao et al., 2019 | Zhu et al., 2019 | Yao et al., 2018 |
|---|---|---|---|---|
| Fabrication Method | EHDA 15kV | Spray Drying | EHDA 15kV | EHDA 16kV |
| GLS-Polymer Size | 468 ± 8.1 µm | 11 µm | 450 ± 100 nm | 1.21 ± 0.42 µm |
| Polymer Used | Alginate | Maltodextrin | Polyvinyl Alcohol | Zein Prolamine |
| Shape | Spherical | Irregular Particles | Fibre | Fibre |
| GL / Polymer | 50% | 33% | 20% | 14.5% |
| 60m Initial Burst ~pH 7 | 12% | 100% | 100% | ~75% |
| Achievable Release Duration | >2 weeks | 1 hour | 300 seconds | 10 hours |

**Table 4.29:** Experimental comparison of GLS encapsulation studies since 2018

While alginate is known to possess swelling-induced release, especially in neutral media, the presence of pores creates ambiguity in establishing the primary driving force of release. Indeed, by analysing the integrity of the particles after release would further indicate the role played by alginate erosion during release. More specific tests could determine the rate of swelling of the GLS-A particles via radial expansion or weight gain, to observe whether this occurs, how fast, and under which system morphological conditions. This would then allow conclusions to be drawn on the reasons behind a slowed release when compared to other polymer-encapsulated GL.

*Novelty processing and smart delivery of Ganoderma Lucidum spores*

### 4.3.7.2 Drug-loaded Alginate Matrices

Alginate matrices from literature are detailed in table 4.30 below. Once again, the particle size is not competitive when compared to alginate particles created using more alginate/less encapsulated drug. Again, it should be observed that the GLS-A particles in this study maintained a very competitive initial burst and subsequent sustained release.

| | This Study | Yao et al., 2017 | Yaacob et al., 2017 | Quinlan et al., 2017 | Nikoo et al., 2018 |
|---|---|---|---|---|---|
| Fabrication Method | EHDA 15kV | EHDA 16kV | Emulsification | Spray Drying | EHDA 8kV |
| Particle Size | 468 ± 8.1 µm | 228.3 ± 14.2 µm | 83 ± 5 µm | 3.9 µm | 765.3 ±14.5 µm |
| Particle Shape | Spherical | Tailed | Spherical | Irregular | Spherical |
| Alginate / Drug | 50% | 67% | 88% | 83% | 75% |
| 60min Initial Burst ~pH 7 | 12% | 82% | 2% | - | 98% |
| Achievable Release Duration | >2 weeks | 4 hours | >18 hours | >30 days | 7 hours |

**Table 4.30:** Experimental comparison of Alginate matrices for encapsulation studies since 2017

## 4.3.8 Encapsulation of GLS for Smarter Delivery: Conclusions

GLS-Alginate (GLS-A) microparticles were created via EHDA in order to fabricate a high-drug delivery system that was highly controlled, with a subsequent controlled release of GLS. The evaluation of EHDA as a technique for GLS-A particle fabrication indicated an ability to generate particles boasting high degrees of uniformity, with controllability over the distribution average size and shape. The importance of sufficient alginate was highlighted via structural integrity (and its effects on surface characteristics) and also conductivity during EHDA – creating a myriad of implicated effects on particle distribution, including shape and wall thickness. The ability to create specific surface features (porosity and roughness) needs further evaluation, as this study suggested its correlation with EHDA process parameters and particle release profile. The particle distribution showed a significant impact on GLS release in-vitro – in particular particle size and shape. This is crucial to the development of an effective yet safe drug delivery system for GLS and many other pharmaceutical agents. The release from GLS-A particles showed the best fit to a first-order model kinetic models, and the release mechanism is shown to be principally diffusion and swelling-controlled.

*Novelty processing and smart delivery of Ganoderma Lucidum spores*

# <u>5</u> Conclusions and Recommendations for Future Work

The increasing need to explore and evaluate alternative therapies has become urgent as traditional synthetic treatments impose greater disadvantages upon patients' standards of living. With the development of bioactive effects displayed by traditional Chinese medicine (TCM) *Ganoderma lucidum* (GL), efforts have been devoted to identifying the compounds and mechanisms responsible for this organism's potent effects on cancer inhibition and immunoenhancement in particular. An extensive literature review highlighted the current need to characterise the processes involved in its exploitation, along with the need to better understand its compound palette – crucial aspects which had not been sufficiently addressed at the time of this project's start. This project has explored avenues that engineered efficient workflows in the journey taken by GL from its natural state to a bioactive agent that would potentially provide a more effective, accessible and affordable treatment alternative for a number of illnesses today. We evaluate the process parameters affecting biocompound isolation and tumour inhibition (in-vitro). Excitingly in a new era of smarter drug delivery, this project also presented a viable mechanism for the creation of a biodegradable and biocompatible drug delivery system possessing desirable distributional features for smarter delivery. Through these concluding remarks, the contributions of this thesis to the field of GL development for healthcare are summarized. We also propose some important progressions that should result from the work presented in this thesis.

## 5.1 Conclusions

Traditional Chinese Medicines (TCM) refer to the holistic approach to diagnosis and pharmacology reported in the Chinese Materia Medica. In the western world, therapy based on TCMs is typically regarded as *complementary* or *alternative*, primarily because of its limited understanding and thus dismissal by the scientific community. In many cases, this behaviour stems from bioactive effects that are difficult to decipher and prove using modern research techniques. In particular, this refers to *Qi* (vital energy) and the balance of *yin-yang forces* apparently induced by TCMs in the body. Progress has further been hindered by a large amount

*Novelty processing and smart delivery of Ganoderma Lucidum spores*

of low-quality clinical data (with respect to study bias and methodology). Fortunately, the therapeutic promise boasted by certain TCM agents has suggested an increasingly potent candidacy for novel alternatives compared to established synthetic medicines, and therefore certain natural organism sources are achieving scientific traction around the world. Thus, we must explore the unconventional. The field of basidiomycota especially has drawn increasing interest as a source of novel drugs and drug leads.

One of the means by which the investigations into TCM contribute to the medical field is through isolating potent biochemical foundations otherwise overlooked in the development of new synthetic treatments. The understanding of these biocompounds in a consistent manner is absolutely essential for the development of TCM as a treatment, and this is still not sufficient to date, even amidst new technological advancements in chemical evaluation. Not only is there still a plethora of biocompounds waiting to be discovered and defined, but modern medicine has a significant amount to gain from the principles that underline the TCM phenomenon. This project sincerely believes that the invaluable knowledge and evidence that exists over centuries cannot be disregarded in the face of challenges to its existence in modern medical practice. The 2015 Nobel Prize awarded to the discovery of antimalarial agent Artemisinin derived from Artemisia Annua was a truly revolutionary moment for the TCM field, and continues to fuel investigations globally.

Evidence-based TCM is crucial for its development in modern medicine. However, it is important to reiterate that the work presented in this project is only a small reflection of the potential avenues of TCM development. The central problem addressed in this thesis is the welding of the factions that come together to engineer a novel therapeutic agent. The experimental studies presented here aimed to define a single extraction protocol for specific extracts, and subsequently characterise their bioactivities. Supervised machine learning was employed to optimise the extraction process. The extraction was evaluated with respect to the isolation efficiency of polysaccharides and triterpenoids, and the yields were chemically quantified and characterised. The extracts were tested for their ability to inhibit Human Osteosarcoma proliferation in-vitro when subject to various culture conditions. Finally, an alginate-based drug delivery system was developed using Electrohydrodynamic Atomisation to encapsulate GLS particles and provide a novel, controlled release profile. Below the main conclusions emerging from this work, viewed as contributions to the field, are summarised. To the best of our knowledge, the processes demonstrated in this thesis, along with their combined workflow, are for the first time evaluated and optimised. As such, this work has presented a novel experimental design that establishes specific setups which aim to critically evaluate the efficiency and scalability

*Novelty processing and smart delivery of Ganoderma Lucidum spores*

of some recognized and novel processes. The work has also established a novel bioactive complex that shows therapeutic promise in the face of osteosarcoma proliferation.

## 5.1.1 The Extraction of GL Biocompounds

The extraction from GL has been an area of controversy for decades owing to its undefined bioconstituents stemming from differences in experimental protocol and a consequent lack of reference for the chosen setup and its yield. Many claim a higher or more bioactive yield using process variables which, in other studies, show the contrary. The culprit behind these discrepancies however is not solely differences in experimental protocol, but also differences in the GL strain itself stemming from cultivation protocol. This work designed an evaluative approach to the extraction from a particular strain of GL, to ultimately define the characteristics of its yield before assessing its effects on cancer proliferation. The aim of this section of work was to determine "best practice" in the extraction of GLS biocompounds using two conventional techniques – Hot Water Extraction and Ultrasound-Assisted Extraction. They were evaluated with respect to the yield efficiency of crude polysaccharides (GLPS), quantified as a dry-weight % of the initial GLS input. The specific D-Glucan content of the crude GLPS (based on spectroscopy) provided insight into the extractability of this valuable polysaccharide compound as well. A polysaccharide-Ganoderic Acid complex was subsequently extracted, in efforts to determine and compare cytotoxic effects.

### The extraction of crude GL polysaccharides (GLPS)

o   Crude GLPS are associated with higher bioactivity than purified polysaccharides, as they contain a larger and more diverse pool of biocompounds. Without excessive processing and cleaning these compounds typically retain the original structures associated with greater bioactivity, and can provide synergistic bioactivity.

o   The extraction of crude GLPS was attempted using hot water extraction (HWE) and ultrasound-assisted extraction (UAE) to ascertain if extraction *time* and *solvent polarity* (via ethanol concentration) would influence the efficiency of either method. The extraction methods were developed based on dissolution efficiency, and it was demonstrated that pure water and pure ethanol extracted the highest GLPS yield. Whilst water is typically chosen for polar extraction as it is a polar molecule, successful ethanol extraction was a result of ethanol's capacity to dissolve certain polysaccharides, many of

*Novelty processing and smart delivery of Ganoderma Lucidum spores*

which are "joined" to ethanol-soluble non-polar compounds – such as proteins, phenolic compounds, and triterpenoids (all valuable bioactive agents). Both extraction methods showed considerable gains over similar setups in literature, each recovering over 6% GLPS even using shorter durations and lower temperatures than published studies [Kan et al., 2015; Smiderle et al., 2017]. This is particularly exciting for HWE; a traditionally low-yielding technique, yet one that is simple and cost-effective.

o Characterisation of GLS extracts was principally via D-Glucan quantification in the extract, and this was based on a chemical assay established by Dubois et al. in 1956. This method quantifies the D-Glucan content of the GLPS sample via structurally hydrolysing the polysaccharide into D-Glucose which is detectable in the UV-Vis spectrum at ~485nm. The method in fact also detects other D-Hexose compounds at this wavelength, however it is legitimately assumed that specific Glucose content is the greatest of all detected [Ahmad, 2018]. This study showed that D-Glucan content in the GLPS extracts was highest using water-based HWE and ethanol-based UAE (0.59% and 0.53% respectively) - suggesting the extraction solvent efficiency may be dependent on extraction technique (and vice versa). These results suggest marked improvements upon the yields of hexose compounds reported in similarly-designed studies, even those that employ more extreme durations, temperatures, and energy input [Alzorqi et al., 2017; Thuy et al., 2015]. The techniques in this project also yielded valuable antioxidants in the form of phenolic compounds.

### The extraction of Polysaccharide-Ganoderic Acids (PSGA)

o A novel Polysaccharide-Ganoderic Acid complex was effectively isolated using HWE, using supervised machine learning to optimise the parameter inputs. Process parameters *time* and *solvent dilution* showed statistically significant effects on extraction efficiency, with positive and negative effects on PSGA yield respectively. Response surface optimisation revealed an optimal PSGA yield of 1.46% could be achieved when GLS is subject to 100 minutes of HWE in a system dilution of 20:1 water:GLS. This suggested a longer extraction time and greater concentration were beneficial to PSGA yield.

o This yield indicates improvements upon existing studies employing hot solvent extraction of Ganoderic Acid complexes, typically reporting GA yields below 1% with similar setups but using toxic solvents [Ruan et al, 2014; Gao et al, 2011]. There was no significant interaction between the variables time and dilution. A multivariate regression model was

*Novelty processing and smart delivery of Ganoderma Lucidum spores*

generated and served as an effect predictor of any combination of time/solvent values on PSGA extraction using this method.

o Owing to the unique nature of this complex, calibrations of this extract to specific **GA** and **PS extracts** would be misleading. Instead, the PSGA extract was quantified using spectroscopy at its known absorbable wavelength.

o Scanning Electron Microscopy suggested that increased extraction time was associated with greater structural damage of the GL spores, indicated by smaller fragments in the SEM micrograph following Hot Water extraction. Indeed, this led to a more effective extraction.

o The effect of solvent dilution however was not degradative; rather *penetrative*. While kinetic energy from prolonged extraction time would generate increasing bond fractures, the effect of dilution was penetration of the spore structures ultimately reducing spore clumping and increasing extraction efficiency with a larger surface area. Thus, at the lowest dilution (20:1) the effect of time was most significant as the resulting intensity is greatest. A higher solvent dilution also fostered lower energy distribution per given extraction time. FTIR and LCMS also confirmed greatest structural damage at the higher extraction time indicated by shorter aliphatic chain length and a lower molecular weight.

## 5.1.2 Extracts' Effects on Human Osteosarcoma (HOS) Cells

The high metastatic potential of human osteosarcoma cells create challenges to achieving consistent treatment efficacy [Li et al., 2018]. Osteosarcoma is a primary solid tumour which has implicated a sustained poor outlook of patients, necessitating new treatments that can endure the high-level resistance typically exhibited by these cells during chemotherapy. HOS cells were used in this viability assay as they are traditionally a challenge for conventional chemotherapeutic drugs used today. This study introduced both GLPS and PSGA under identical culture conditions to the HOS culture for either 24 or 48 hours at increasing dosages.

o The bioactive assay of PSGA from HWE indicated inhibitory effects on human osteosarcoma cells in-vitro, attaining over 58% inhibition when compared to the negative (untreated) control. The PSGA extract could inhibit HOS after both 24 and 48 hours. Low doses and shorter incubation were most effective - suggesting concepts such as resistance (clonal selectivity) and delayed apoptosis (the latter of which was detected via

*Novelty processing and smart delivery of Ganoderma Lucidum spores*

cell fringing and blebbing following treatment). Proliferation at higher doses could also be a result of a more conducive growth space when HOS cells begin to die. These phenomena would justify why higher doses led to increased viability in the MTT assay. Triterpenoids (Ganoderic acids in particular) have shown cytotoxic effects toward osteosarcoma by apoptosis – in particular by regulating apoptosis-related genes and affecting the signalling pathways of protein expressions [Li et al., 2018; Jiang et al., 2017]. Cytotoxicity of Ganoderic Acids in this extract showed comparable cytotoxic effects to many studies – further presenting scope to utilise a polysaccharide counterpart that supports immunity during cytotoxicity [Wang et al., 1997]. This cell line continues to suffer from under-investigation owing to its fast proliferation and resistance to anti-cancer treatment.

o   The bioactive effects of GLPS were less clear. This study maintains previous assertions from literature that polysaccharides would have little cytotoxic effects; instead exerting anticancer effects via immunoenhancement (a mechanism not detectable in this cancer cell viability assay, but instead in the presence of active immune cells – a suggestion for future work). The assay showed that the effect of incubation time was negative on treatment effect, however dosage was somewhat correlated with treatment effect.

## 5.1.3 The Development of a Controllable Drug Delivery System

The need to encapsulate therapeutic compounds stems from their susceptibility to the degradative physiological and storage conditions, but also from the need to control the rate and manner in which they are released. Alginate is a biocompatible and biodegradable polymer which provides a controllable matrix for GLS delivery, effective cell adhesion, flexible processibility, and control during drug release (in the form of sustained release). Particulate drug delivery is an attractive approach mainly owing to controllability over dosage, precise and concentrated targeting, its ability to overcome bio-barriers and flowability when compared to fibres, scaffolds, and beads. Electrohydrodynamic Atomisation (EHDA) has often been optimised for its application to natural polymers like chitosan, however its performance with alginate is not yet consistent nor promising in light of this biopolymer's thermolability and thus impracticality as a stable treatment carrier (subsequently exhibiting limited control when used to deliver drugs in a physiological environment). Consequently, an EHDA-fabricated alginate delivery system has traditionally presented weaknesses without modifications like copolymer blending. Typically these modifications have implicated an alginate-based delivery system that has a **low drug loading**

**capacity** (in efforts to create a stronger polymer matrix), one that demonstrates instability in the physiological environment, or with less biocompatible properties attributed to synthetic co-polymers. Furthermore, there is very little evidence of the use of EHDA to controllably create matrices containing Ganoderma lucidum that meet certain thresholds of effective drug delivery – including morphological control, and release control. In this study, EHDA was proven an effective method to controllably synthesize uniform and spherical alginate particle distributions as carriers for a high loading of GLS as governed by the tested process variables. Importantly, the study demonstrated the ability to create a GLS carrier with a sustained GLS release profile.

## Particle fabrication: Morphology

o Three spraying modes were exhibited, defined by the voltage but also affected by flow rate. A stable jet is associated with a more uniform droplet distribution, but alginate exhibits viscid and non-Newtonian behaviour that implicates greater challenges to achieving a stable spray at voltages that are typically conducive of smaller droplets. Thus, previous studies have reported that alginate (with co-polymers) processed under a stable jet could achieve a size no smaller than 1,000 μm.

o EHDA was evaluated with respect to its voltage effect on GLS-alginate (GLS-A) particle distribution characteristics, and it was found that higher voltages could create smaller particles across 2 different flow rates. Uniform spherical particles with an average diameter of 468 (±8.1) μm could be achieved when GLS content was as high as 50%.

o Rapid and effective droplet disruption leaves less capacity for droplets to grow; resulting in smaller particles as voltage increases. By reducing alginate content, particle distributions as small as 232 (±10.3) μm were achievable using 15 kV, and although they were not as uniform nor spherical owing to a smaller alginate content, they flaunted a GLS content as high as 66%. Near-spherical particles were more achievable by increasing voltage only up to 10kV - alginate's critical voltage after which a more unstable spray is observed.

o The average particle size achieved in this study presents a competitive alternative to published studies which have only attained this range at the expense of drug loading (typically resulting in a drug loading below 25%) and/or matrix strength. Often, biocompatibility is also compromised when copolymers and proteins are used to optimise morphology and structural integrity [Brown et al., 1997; Raemdonck et al., 2009; Nagarwal et al., 2009; George et al., 2006; Feriberg et al., 2004]. The increase in voltage

*Novelty processing and smart delivery of Ganoderma Lucidum spores*

from 10-15kV demonstrated a 74% reduction in the average particle size in samples created at the lower flow rate and a 68% reduction in the higher flow rate sample.

o While sphericity has proven desirable in a drug delivery system of particles, there is less focus on developing an optimal particle shape that may more effectively traverse the body toward target tissues. Fibres, rods, and discs have been investigated but spheres have been found most effective owing to production control and flowability. This work however addresses the concern that different shapes may prove effective in adhesion or absorption to tissue - particularly when tissue is less normal. Aspect Ratio was used to gauge shape resulting from EHDA. This study was able to create competitively spherical microparticles, even when loaded with a large amount of GLS – something not yet achieved with loaded alginate [Suksamran et al., 2009; Ahuja et al., 2011; Rasekh et al., 2017]. By increasing both voltage and alginate content, this study achieved the most spherical GLS-A particles (aspect ratio nearest to 1) - an effect attributed to more effective droplet disruption and a gain in structural integrity from denser crosslinking.

o Solution parameters present a huge opportunity to influence the distribution of droplets obtained via EHDA. As well as process parameters, solution properties are dependent on drug-loading, which is usually compromised in order to achieve desirable particle distributions (uniform, and small). In this work, the GLS loading was maximised by reducing polymer counterpart of the solution. Three GLS-A ratios were evaluated in this work: GLS-A 1-1 (containing 1%/1% OR 2%/2% GLS/A) and GLS-A 2-1 (containing 2%/1% GLS/A). This study observed that by increasing the polymer content of a droplet, a larger droplet resulted, which subsequently had a lower droplet charge density, thus delaying the attainment of the Rayleigh limit during spraying. This is an outcome of greater viscosity-induced surface tension. This work found that some of these larger particles subsequently presented increased brittleness from increased crosslinking at the surface owing to more polymer junctions (also leading to pores that were up to 40% larger), but many also a displayed a strong overall structural integrity during and after spraying.

o Particle shape was "tailed" in particle samples that had more GLS than alginate; a feature attributed to insufficient polymer to maintain droplet integrity during spraying. The particles that contained equal GLS and alginate (1%/1% OR 2%/2% GLS/A) did not generally exhibit low-polymer effects as these particles had sufficient polymer to maintain shape. Viscosity was however reduced in both particle distributions that

contained 1% alginate, generating an EHDA spray conducive to rapid droplet disruption and smaller resulting particles.

## Particle fabrication: Surface topography

The surface topography of GLS-A particles was evaluated following fabrication as features like porosity and cracked walls can influence the control over drug release. In all samples, porosity was a result of defects formed during alginate processing and drying (particularly as alginate hygroscopically absorbs and release moisture cyclically). When the polymeric network contains charged moieties, such as the case with alginate, its conductivity during EHDA provides a rich source of electrostatic mechanisms like repulsion, chain fracture, and shrinkage – all of which can generate surface defects and ultimately resulted in a highly porous alginate matrix.

- o A study by Tavakol in 2013 reported that reducing alginate content in calcium-crosslinked particles fostered cracked surfaces, attributed to the lack of polymer strength during crosslinking and drying. This study observed the same effect, with smoother surfaces observed in particles containing more alginate,

- o A positive correlation was observed between voltage and surface roughness. Increased surface roughness was observed as voltage increased from 5kV to 15kV. Surface defects were more prominent in more rigid particles that had a higher crosslinking density owing to more polymer and increased electrostatic charge and where water was evaporated most (and most quickly) during spraying (smaller or less alginate-dense droplets) – hence, a pore diameter reduction of 54% could be achieved by increasing voltage, but this observation requires a further controlled study whereby voltage-induced particle size is not a factor.

## Particle drying: Morphology and surface

The effects of post-fabrication drying were evaluated by introducing a freeze-drying step to air-dried particle samples. To date, no study has yet combined both drying methods to negate certain disadvantages whilst capitalising on the advantages of each. Here, air-drying was intended to remove moisture before freeze-drying, thus reducing the formation of ice crystals during freezing and ultimately reducing the opportunity to expand, and the prevalence of surface defects. Studies have typically observed that freeze-dried particles have greater porosity and surface crumpling, something typically attributed to the moisture evaporation from cavities induced at the initial freezing stage. This study however observed a much more compact and smoother surface of particle samples which underwent freeze-drying as an additional drying step to air drying (AD + FD).

*Novelty processing and smart delivery of Ganoderma Lucidum spores*

- o Results showed that AD+FD GLS-A particles were smaller than particles undergoing only-AD particles by an average of 18% in samples created at 10kV and 23% in samples created at 15kV. This suggests that air-drying prior to freeze-drying can reduce the size of GLS-A particles. A size reduction could be a result of the previous air-drying that removed a great deal of the particle's moisture prior to freeze-drying, thus reducing cavity-induced particle expansion.

- o An average pore size reduction of 31% was also achieved in particle that underwent additional freeze-drying, with variations in the degree of effect owing to voltage-confounding effects. The effects of additional freeze-drying on particle morphology and surface require further testing that would distinguish the effects of freeze-drying *in the absence of* air-drying.

- o GLS-A 2-1 particles containing less alginate exhibited a lack of structural integrity causing agglomeration during both drying regimes.

## Particle GLS release

An important aim of this study was to develop a matrix that would exhibit a controlled release (sustained over the treatment time), yet not compromise drug-loading. For alginate, the achievable sustainable release period has been limited at just a few hours, principally owing to alginate's physiochemical properties that typically foster rapid swelling and thus *burst kinetics* in physiological conditions – posing a threat to patient health [Güncüm et al., 2018; Song, 2018; Gao et al., 2019; Bhowmik et al., 2006]. This is particularly the case in pH-neutral media where alginate chains repel each other electrostatically; and thus this behaviour is unacceptable in-vivo where this environment is inevitable. The release profiles of GLS-A particles were investigated using UV-Visible spectroscopy that detected the release of GLS in a pH-neutral bath undergoing gentle shaking over 2 weeks.

- o The release profile of the GLS-A particles created in this study showed a sustained release over a 2-week period, with only a limited "initial burst" – a maximum of 11% release in the first 20 minutes and 21% release in the first 60 minutes.

- o At the end of the 2-week period, GLS-A 1-1 particles had the lowest total release. Observing this level of integrity pf alginate particles with such a high drug loading in pH-neutral conditions has not yet been reported but is required in the pH-neutral environment of the intestinal passage during physiological delivery.

*Novelty processing and smart delivery of Ganoderma Lucidum spores*

The factors affecting release rate are highlighted below.

*Particle GLS release: Effect of particle morphology*

o In general, the study found that a slower release was observed from particles that were larger, stronger and smoother with less surface defects (those containing more alginate).

o Larger particles had the smallest surface area in a given weight of dosage and the reduced interface decreased the rate of release. The same was found for flatter particles.

o Tailed particles, an anatomy increasingly studied for new approaches to drug delivery, released fastest along with spherical particles – both possessing the largest surface area during release.

*Particle GLS release: Effect of particle polymer content*

o The release from alginate matrices was related to the mobility of the hydrogel matrix, and the rate of water diffusion into the hydrogel matrix during swelling and outward flow of GLS. This was determined by a variety of process parameters during EHDA such as voltage and polymer/drug content. Overall a slower release was observed from particles with a higher polymer content.

o The effect of increased polymer, provided that it was sufficiently crosslinked, created a stronger barrier to the inward/outward flow of water/GLS respectively. This created a much more stable and consistent release rate. Greater polymer entanglement entrapped more GLS particles, and a stronger matrix reduced swelling-induced release and at the rate of erosion. Increased brittleness from a more electrostatically-charged moieties in a high-alginate particle would also hinder the swelling movements that foster release.

o Because high-polymer particles were also larger and thus had a resulting smaller surface area per dosage, they exhibited a slower release.

*Particle GLS release: Effect of particle drying technique*

o GLS-A particles that underwent additional freeze-drying slowed the release of GLS compared to AD counterparts. These particles contained smoother and more compact surfaces, with less visible pores and defects, resulting in a reduction of diffusion-controlled component of release. Swelling-induced release was hindered as the outward

diffusion-controlled component of release was reduced, along with reduced penetration into the alginate matrix.

o The initial burst from these particles was also lower than for AD counterparts.

o A slower drug release from freeze-dried (FD) polymer matrices is actually contradictory to many studies which observe that this method of drying produces fractured or porous surfaces that induce faster (and more uncontrollable) drug release. However those studies are not evaluating FD particles have been pre-airdried as was the case in this investigation.

The interplayed effect of GLS-A particle size and shape on release profile was also investigated using stratification by size group. For example, particles with a higher AR were created at lower voltages, were disc-like in shape, and were also largest. Therefore, variables needed to be controlled to more precisely measure effect sizes. The influence of size is effectively eliminated when the shape (via AR) is being evaluated for one size range only. The size strata chosen was <750µm. The stratification shows that wider particles (AR >1) still exhibited the slowest release of GLS over 2 weeks, even though these particles were not the largest. Therefore it can be concluded that a wider particle (higher AR) will release more slowly than a longer or more spherical particle – and this is not owing to size. A reason for rapid release of longer particles is the possession of a unique tail providing additional surface area and a faster release. As well as a unique additional surface area, a tail may possess a thinner outer shell owing to the stretching. These could also more rapidly degrade. This shows that the effect of AR may in fact be more instrumental on release rate than particle size. The possession of a tail arose as a consequence of inefficient coulomb fission and thus ineffective droplet disruption; fostered by insufficient polymer. However with the knowledge that they can manipulate release rate, further work is needed to determine the implications for drug delivery.

EHDA overall presents a promising technique that could provide controllable alginate particle distributions that subsequently provide a sustained GLS release over a 2-week period. While many studies have employed alginate successfully using *emulsification* in efforts to avoid the complex polymer when using EHDA that would lead to an unstable and non-uniform drug delivery system if not fulfilled. Emulsification however has itself traditionally been associated with uncontrolled particle morphologies stemming from rapid gelation. Developments to overcome this setback have primarily focused on introducing a mechanism of more controlled/slower

crosslinking by using a calcium source that first undergoes gradual hydrolysis before becoming totally "available" for gelation. Even so however, most published work has incorporated copolymers when creating alginate matrices – in particular strong chitosan – and a large amount of diverse surfactants to ensure desirable distributions [Pasparakis et al., 2006; Shin, 2016].

## 5.2 Future Work

This thesis aimed to build some of the groundwork towards developing the spores of Ganoderma Lucidum (GLS) into a therapeutic drug. Extraction methods were explored, with respect to the yield of water-soluble crude polysaccharides, concluding that hot water extraction was the most scalable at the settings employed. In order to have a comparison during in-vitro studies, an extract rich in *both* polysaccharides and triterpenoids were extracted using HWE (and optimised using supervised machine learning). This allowed a comparison of two extracts mentioned in literature (but not yet compared adequately). There were limitations in the approach to extraction of GLS compounds, particularly the parameter range and limited replicates – both leading to low degrees of freedom. Furthermore, characterising the yield after extraction would have led to more insightful inferences when evaluating in-vitro effects of the extracts on HOS cells. The administration of GLS extracts to HOS was carried out as a function of extract nature, dosage, and incubation time. While some conclusions can be made as to why dosage had a negative correlation with cell inhibition, these inferences are purely theoretical and based on scientific logic. Further experiments and techniques would need to be carried out to verify assumptions like apoptosis, cell-crowding, and polysaccharide-induced cell death. The final stage of this project was focussed on developing a drug delivery system for the delivery of GLS that could control release rate yet employ a safe and sustainable material. Sodium alginate, while typically unstable in physiological conditions, proved to be stable for up to 2 weeks in simulated conditions, releasing GLS particles gradually with an initial burst much lower than those found even with synthetic polymers used today. The GLS-Alginate (GLS-A) particles were created using electrohydrodynamic atomisation (EHDA), and this process was evaluated with respect to applied voltage, polymer (alginate) content, and drying method. While inferences were made with good experimental evidence, particle characterisation was somewhat incomplete, limited by equipment precision and methodological approach. For example, nanopores were not measured, and porosity-linked inferences were therefore limited to micropores. Furthermore, the degree of swelling would have been a useful insight into swelling-/diffusion-controlled GLS release.

*Novelty processing and smart delivery of Ganoderma Lucidum spores*

## 5.2.1 Extraction of GLPS and PSGA

### Extraction Experimental Ranges

In all experimental analyses, particularly those with an exploratory nature, a larger experimental range is always preferred. However this is not always feasible with constraints of time and material resources. In this study, limitations in time and specialist equipment resulted in simpler extraction setups, which restricted the ability to test beyond certain thresholds of time, temperature and volume for extraction experiments.

- o Both hot water extraction and ultrasound-assisted extraction were evaluated with respect to their crude polysaccharides (GLPS) yield. The techniques were experimentally optimised using experimental ranges from literature and from preliminary tests. Solvent polarity revealed extraction dependence; however the effect of extraction duration was inconclusive in both methods. Further work should be concerned with the extension of the range of extraction durations used, to decipher the trend more completely.

- o While the effects of extraction on PSGA yield were more consistent, future work should also expand the experimental range of time and volume to increase validity of the results reported here.

### Yield Measurement Precision

The definition of GLPS in this study is described as a water-soluble extract that is not "purified" to remove other water-soluble compounds like come proteins, phenolic compounds and conjugated lipids. In many published studies, crude polysaccharides are associated with higher bioactivity for a couple of reasons – firstly because they contain potentially valuable biocompounds, and secondly because without excessive processing and cleaning these polysaccharides should retain their original large structures often associated with greater bioactivity.

- o The D-Glucan reading in this work was based on detecting chemically-similar structures to D-Glucose in the UV spectrum, Unfortunately this reading was easily conflated with other polysaccharides (other D-Hexoses) with similar structures. Thus, while it was assumed that these readings belonged to highly-prevalent D-Glucans, further work would more precisely characterise the compound in order to fully define their mechanisms of effect in future work. It does however provide an indication of the relative extraction capacity across the extraction process parameters.

*Novelty processing and smart delivery of Ganoderma Lucidum spores*

o   Further precision could be obtained via chemolytic methods or a series of more selective spectroscopic techniques, such as chromatography (gas, high performance size exclusion and high performance liquid chromatography in particular), mass spectrometry (MS), fourier transformed infrared spectrometry (FTIR), and nuclear magnetic resonance (NMR). Combining some of these techniques has been a popular approach in literature, as each approach targets distinct aspects of the material thus creating a more wholesome profile.

o   As resistance of glycosidic bonds varies depending on the specific Glucan structure (such as anomeric configuration and position), this analysis can also derive structural information. The specific structure of the D-Glucan can be evaluated using linkage analyses such as Smith degradation or methylation, which are based on the presence of certain functional groups. Physical methods like NMR can also verify configurations of anomeric carbon to determine acclaimed structures such as the α/β-D-Glucan. The structure-bioactivity relationship has indeed been a huge subject of interest, however is insufficiently defined for GL polysaccharides. For example in the study below, polysaccharides from Cordyceps Militaris were extracted and classified as two structural weight bands – CMPs-4/80 resulting from 4°C/80°C degree extractions respectively. The smaller molecular weight structures showed greater inhibition and authors also found it to contain greater glucose content (an interplay of the two may have played a role in increased bioactivity). This dependence on a complex structure is a common inference across literature.
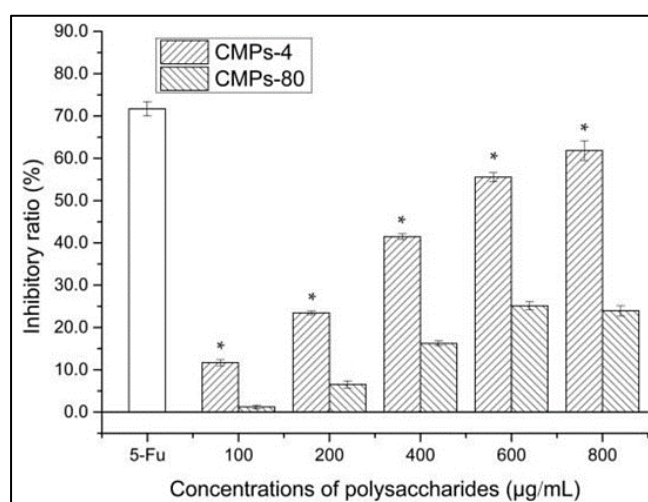


**Figure 5.1:** Effects of both polysaccharide extracts on proliferation of oesophageal cancer. CMPSs-4 refers to the smaller molecular weight extract that also contained greater glucose content [Nurmamat et al., 2018].

*Novelty processing and smart delivery of Ganoderma Lucidum spores*

o The extraction of a novel PSGA complex was carried out via hot water extraction. This technique was optimised using supervised machine learning (via statistical optimisation) and revealed process parameter trends in-line with extraction literature. Future work in this experimental study should employ a more definitive form of compound classification to detect specific compound structures. A more granular range would also allow for more precise optimisation. In this work, it was assumed that through detecting the GA-absorbed wavelength of a crude polysaccharide extract, PS-GA presence is indicated. Whilst this is indeed only an indication, it does provide a necessary angle for future direction in the extraction and development if this novel and potent complex. Indeed, should there be confirmation of this compound's structure, many correlations could be drawn between specific attributes and bioactive effects. This is something that could shed light across the field of novel drug discovery.

## 5.2.2 Extracts' Effects on Human Osteosarcoma (HOS) Cells

### Precision of Cell Mechanisms

HOS cell viability was gauged using the "gold standard" MTT Assay, which bases viability on metabolism following culture with the treatment. While this certainly provides a good indication of treatment efficacy, future work should employ further techniques to verify the *mechanisms* of treatment effect. This includes Western blotting which would distinguish the signalling of certain anti/pro-apoptotic protein expressions such as caspases, along with staining using designated assay kits such as TUNEL (terminal deoxynucleotidyl transferase dUTP nick end labeling) to detect certain chemical changes such as DNA fragmentation occurs in the final phase of apoptosis. Protein signalling may especially be useful owing to the stem cells that typically arise during HOS proliferation. Indeed, with the MTT assay only measuring cell metabolism, many cells that were in fact undergoing apoptotic would have flagged a "live" reading and thus skewed the extract's bioactivity assay.

In addition, it is necessary however to gain a widespread picture of cancer effects by administering the extract to various cancer lines, including Human Breast Cancer and Lewis Lung Carcinoma (two widely tested cancer cell lines in literature with GL extracts). Future work can then validate the assumptions made here.

*Novelty processing and smart delivery of Ganoderma Lucidum spores*

### 5.2.3 The Development of a Controllable Drug Delivery System

The release profiles of GLS-A particles were investigated using UV-Visible spectroscopy that detected the release of GLS in a pH-neutral bath undergoing gentle shaking over 2 weeks. This release was quantified using the method described for Ganoderic Acid measurement, because these compounds could be detected without hydrolysis and thus would provide an indication of GLS release in which it is prevalent. This study evaluated insightful variables in the development of a GLS-Alginate drug delivery matrix, ultimately creating a promising foundation for the development of uniformly distributed alginate-GLS particles. Nonetheless, shortcomings prevailed.

#### GLS-A Solution Characterisation

Firstly, this work acknowledges the limitations imposed by not experimentally characterising the GLS-Alginate solution used to create particles. As the investigation focused on the effects of EHDA parameters on the resulting particle distribution/release profiles, the solution properties were not originally considered variables. By not defining the solution's properties however, the efficiency of electrospraying could not accurately be associated with solution characteristics (surface tension and conductivity in particular). Solution characteristics would provide insight into the most important impacts of alginate content on particles specifically – ultimately defining impacts on release rate and thus drug delivery. Future work should build this characterisation variable into the experimental design.

#### GLS-A Particle Evaluation

Both particle size and surface were evaluated. This was important so that the effects of EHDA process parameters could be assessed, and any implication on release dynamics would be evaluated. Optical microscopy was employed to determine distribution size, and scanning electron microscopy (SEM) was used to examine the particle surfaces. Fourier transform infrared (FTIR) spectroscopy was employed as a tool to evaluate the chemical structures of the particles, indicating drug-polymer interactions in particular. The particle size and aspect ratio were measured using Image-J via the Ferret's diameter, however when tailed particles were generated, this measurement was less straightforward and was measured without the tail. Fortunately, the inclusion of the aspect ratio as a further point of analysis ensured these particles had a second morphological measurement that allowed more precise shape comparisons.

- o Pore size was limited to micrometres owing to the resolution of SEM. However, future work should employ a technology that can more accurately reflect the effects of the

*Novelty processing and smart delivery of Ganoderma Lucidum spores*

EHDA process parameters on particle pores. A pore analysis was attempted on one GLS-A particle using a Nikon CT machine (UCL Chemical Engineering, EIL) to obtain a more accurate evaluation of pores, however due to detection limitation this technique was not employed for all experimental samples. The spatial resolution of the analyser is 3 μm, unfortunately limiting detectable pore size to circa 12 μm. This particle is shown in figure 5.2.
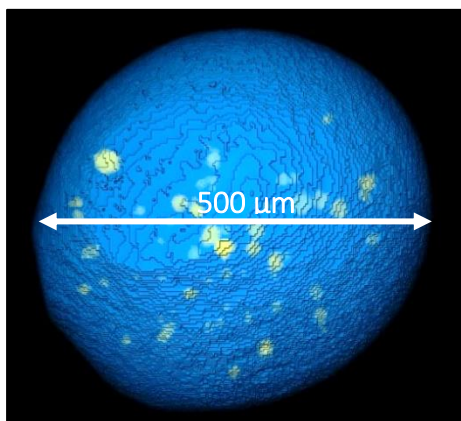


**Figure 5.2:** Nikon X-ray CT (model 225 XT) image of a GLS-A particle after oven-drying. Carried out at 224kV (top-down view)

o   During spraying, heat/mass transfer causes solvent evaporation from droplets, leading to particle shrinkage. The rate of evaporation us also influenced by the electrostatic charge on the droplets. As this was not a measured outcome, future work should include an analysis on the rate of shrinkage induced at the tested EHDA settings. This may then prove to be influential on delivery characteristics such as release rate and structural integrity.

## GLS-A Particle Drying

In this section of study, air-drying was employed to dry all particles, and an additional freeze-drying step was introduced to selected experimental samples to gauge the effects of this extra drying stage on article structure and release profiles.

o   While the results indicated that additional freeze-drying increased more compact and smooth particles, the effects were inconsistent across some experimental samples owing to the different samples' confounding effects of alginate content and voltage on the particle's ability to withstand/benefit from freeze-drying. A further controlled study is required to generate robust conclusions of the effect of freeze-drying on GLS-Alginate particle surface in the absence of air-drying and with greater control over other process variables.

*Novelty processing and smart delivery of Ganoderma Lucidum spores*

o Particle behaviour after drying (such as shrinkage) was observed, however not treated as a measured outcome. As particle shrinkage can indicate modes and effectiveness of drug delivery, this should be considered in future work.

**GLS-A Particle Release Profile and Modelling**

o While alginate is known to possess swelling-induced release, especially in neutral media, the presence of pores implicated less clarity in establishing the primary driving force of release. Indeed, analysing the integrity of the particles after release would further indicate the role played by alginate erosion during release. More specific tests could determine the rate of swelling of the GLS-A particles via radial expansion or weight gain, to observe whether this occurs, how fast, and under which system morphological conditions. One of the ways in which future studies could address this, is by repeated simulations of this release assay, which would feed into a model that would represent the release pattern accurately – one which is reflective of an established release mechanism and that allow comparisons to be made to frameworks such as the Fickian laws. The order of the release mechanisms may play a role in the release rate, and so this should be a focal point of future work.

o Release of GLS was plotted cumulatively and modelled using a first-order release model. As this was only based on one study (with replicates), an accurate model would require a number of studies to confirm its accuracy for this specific drug delivery system. Future work can focus on generating an accurate model based on repeating this investigation.

# 6 References and Bibliography

Abbaszad Rafi, A. and M. Mahkam (2015). "Preparation of magnetic pH-sensitive film with alginate base for colon specific drug delivery." International Journal of Polymeric Materials and Polymeric Biomaterials 64(4): 214-219.

AbdelAllah, N. H., et al. (2016). "Chitosan and sodium alginate combinations are alternative, efficient, and safe natural adjuvant systems for hepatitis B vaccine in mouse model." Evidence-Based Complementary and Alternative Medicine 2016.

Abdullah, N., et al. (2012). "Evaluation of selected culinary-medicinal mushrooms for antioxidant and ACE inhibitory activities." Evidence-Based Complementary and Alternative Medicine 2012.

Abreu, F. O. M. S., et al. (2008). "Influence of the composition and preparation method on the morphology and swelling behavior of alginate–chitosan hydrogels." Carbohydrate polymers 74(2): 283-289.

Abreu, F. O. M. S., et al. (2010). "Effect of the preparation method on the drug loading of alginate-chitosan microspheres." Express Polymer Letters 4(8).

Abubakr, N., et al. (2009). "Effects of drying methods on the release kinetics of vitamin B12 in calcium alginate beads." Drying Technology 27(11): 1258-1265.

Acharya, K., et al. (2015). "Pharmacognostic standardization of Ganoderma lucidum: A commercially explored medicinal mushroom." Der Pharmacia Lettre 7(7): 175-181.

Achenie, L. E. K. and N. Pavurala (2017). "Modelling of Drug Release from a Polymer Matrix System." Nov. Approaches Drug Des. Dev. 2: 1-10.

Adachi, Y., et al. (1990). "Change of biological activities of (1→ 3)-β-D-glucan from Grifola frondosa upon molecular weight reduction by heat treatment." Chemical and Pharmaceutical Bulletin 38(2): 477-481.

Adamec, J., et al. (2009). "Development of a new method for improved identification and relative quantification of unknown metabolites in complex samples: determination of a triterpenoid metabolic fingerprint for the in situ characterization of Ganoderma bioactive compounds." Journal of separation science 32(23-24): 4052-4058.

Adili, A., et al. (2008). "Differential cytotoxicity exhibited by silica nanowires and nanoparticles." Nanotoxicology 2(1): 1-8.

Agrawal, C. M. and R. B. Ray (2001). "Biodegradable polymeric scaffolds for musculoskeletal tissue engineering." Journal of Biomedical Materials Research: An Official Journal of The Society for Biomaterials, The Japanese Society for Biomaterials, and The Australian Society for Biomaterials and the Korean Society for Biomaterials 55(2): 141-150.

Aguilar-Marcelino, L., Al-Ani, L. K. T., de Freitas Soares, F. E., Braga, F. R., Padilla, A. V., & Sharma, A. (2022). Wild Mushrooms: Characteristics, Nutrition, and Processing. In Wild Mushrooms (pp. 471-492). CRC Press.

Ahmad, M. and S. Benjakul (2011). "Characteristics of gelatin from the skin of unicorn leatherjacket (Aluterus monoceros) as influenced by acid pretreatment and extraction time." Food Hydrocolloids 25(3): 381-388.

Ahmad, M. F. (2018). "Ganoderma lucidum: Persuasive biologically active constituents and their health endorsement." Biomedicine & Pharmacotherapy 107: 507-519.

Ahmed, M. M., et al. (2013). "Emulsification/internal gelation as a method for preparation of diclofenac sodium–sodium alginate microparticles." Saudi Pharmaceutical Journal 21(1): 61-69.

Ahuja, G. and K. Pathak (2009). "Porous carriers for controlled/modulated drug delivery." Indian journal of pharmaceutical sciences 71(6): 599.

Ai-lati, A., et al. (2017). "Structure and bioactivities of a polysaccharide isolated from Ganoderma lucidum in submerged fermentation." Bioengineered 8(5): 565-571.

Ailincai, D., et al. (2018). "Drug delivery systems based on biocompatible imino-chitosan hydrogels for local anticancer therapy." Drug delivery 25(1): 1080-1090.

Albu, S., et al. (2004). "Potential for the use of ultrasound in the extraction of antioxidants from Rosmarinus officinalis for the food and pharmaceutical industry." Ultrasonics sonochemistry 11(3-4): 261-265.

Alexis, F., et al. (2008). "Factors affecting the clearance and biodistribution of polymeric nanoparticles." Molecular pharmaceutics 5(4): 505-515.

Almería, B., et al. (2010). "Controlling the morphology of electrospray-generated PLGA microparticles for drug delivery." Journal of colloid and interface science 343(1): 125-133.

Al-Musa, S., et al. (1999). "Evaluation of parameters involved in preparation and release of drug loaded in crosslinked matrices of alginate." Journal of Controlled Release 57(3): 223-232.

Al-Otoum, R., et al. (2014). "Preparation of novel ionotropically crosslinked beads based on alginate-terephthalic acid composites as potential controlled release matrices." Die Pharmazie-An International Journal of Pharmaceutical Sciences 69(1): 10-18.

Altemimi, A. (2018). "Extraction and optimization of potato starch and its application as a stabilizer in yogurt manufacturing." Foods 7(2): 14.

Alvarez, V. H., et al. (2014). "Optimization of phytochemicals production from potato peel using subcritical water: Experimental and dynamic modeling." The Journal of Supercritical Fluids 90: 8-17.

Alvarez-Lorenzo, C. and A. Concheiro (2014). "Smart drug delivery systems: from fundamentals to the clinic." Chemical Communications 50(58): 7743-7765.

Alzorqi, I., et al. (2017). "Optimization of ultrasound assisted extraction (UAE) of β-D-glucan polysaccharides from Ganoderma lucidum for prospective scale-up." Resource-Efficient Technologies 3(1): 46-54.

Amiji, M. M. (2006). Nanotechnology for cancer therapy, CRC press.

André, V., et al. (2003). "Prediction of emulsion stability: facts and myth." Cosmetics and Toiletries Manufacture Worldwide 102.

Annabi, N., et al. (2010). "Controlling the porosity and microarchitecture of hydrogels for tissue engineering." Tissue Engineering Part B: Reviews 16(4): 371-383.

*Novelty processing and smart delivery of Ganoderma Lucidum spores*

Arias, J. L., et al. (2012). Multifunctional anticancer nanomedicine based on a magnetically responsive cyanoacrylate polymer. Methods in enzymology, Elsevier. 508: 61-88.

Ariffin, A. B., et al. (2014). "Releasing pressure in tumors: what do we know so far and where do we go from here? A review." Cancer research 74(10): 2655-2662.

Ashley, C. E., et al. (2011). "The targeted delivery of multicomponent cargos to cancer cells by nanoporous particle-supported lipid bilayers." Nature materials 10(5): 389.

Ruhan Askin, M. S., & Goto, M. (2008). Extraction of bioactive compounds from Ganoderma Lucidum. Department of Applied Chemistry and Biochemistry, Kumamoto University.

Askin, R., Sasaki, M., & Goto, M. (2007, November). Sub-and supercritical fluid extraction of bioactive compounds from Ganoderma lucidum. In Proc of Int Symposium on Eco Topia Science (pp. 574-57).

Augst, A. D., et al. (2006). "Alginate hydrogels as biomaterials." Macromolecular bioscience 6(8): 623-633.

Avadi, M. R., et al. (2010). "Preparation and characterization of theophylline-chitosan beads as an aapproach to colon delivery." Iranian Journal of Pharmaceutical Research: 73-80.

Awadasseid, A., et al. (2017). "Purification, characterization, and antitumor activity of a novel glucan from the fruiting bodies of Coriolus Versicolor." PloS one 12(2): e0171270.

Badwan, A. A., et al. (1985). "A sustained release drug delivery system using calcium alginate beads." Drug development and industrial pharmacy 11(2-3): 239-256.

Baimark, Y. and Y. Srisuwan (2014). "Preparation of alginate microspheres by water-in-oil emulsion method for drug delivery: Effect of Ca2+ post-cross-linking." Advanced Powder Technology 25(5): 1541-1546.

Bajpai, S. K. and N. Kirar (2016). "Swelling and drug release behavior of calcium alginate/poly (sodium acrylate) hydrogel beads." Designed Monomers and Polymers 19(1): 89-98.

Band, V. and D. Weiss (2015). "Mechanisms of antimicrobial peptide resistance in Gram-negative bacteria." Antibiotics 4(1): 18-41.

Bao, X., et al. (2001). "Structural characterization and immunomodulating activity of a complex glucan from spores of Ganoderma lucidum." Bioscience, biotechnology, and biochemistry 65(11): 2384-2391.

Bao, X., et al. (2001). "Structural and immunological studies of a major polysaccharide from spores of Ganoderma lucidum (Fr.) Karst." Carbohydrate research 332(1): 67-74.

Bao, X.-F., et al. (2002). "Purification, characterization, and modification of T lymphocyte-stimulating polysaccharide from spores of Ganoderma lucidum." Chemical and Pharmaceutical Bulletin 50(5): 623-629.

Barbieri, A., et al. (2017). "Anticancer and anti-inflammatory properties of Ganoderma lucidum extract effects on melanoma and triple-negative breast cancer treatment." Nutrients 9(3): 210.

Barnes, D. (1984). Attachment factors in cell culture. Mammalian cell culture, Springer: 195-237.

*Novelty processing and smart delivery of Ganoderma Lucidum spores*

Barrett, S. J. and W. B. Langdon (2006). Advances in the application of machine learning techniques in drug discovery, design and development. Applications of Soft Computing, Springer: 99-110.

Barros, L., et al. (2008). "Chemical composition and biological properties of Portuguese wild mushrooms: a comprehensive study." Journal of Agricultural and Food Chemistry 56(10): 3856-3862.

Barwick, V., et al. (2006). "Best practice guide for generating mass spectra." LGC Limited.

Basanta, M. F., et al. (2012). "Effect of extraction time and temperature on the characteristics of loosely bound pectins from Japanese plum." Carbohydrate polymers 89(1): 230-235.

Bastami, M. S., et al. (2007). "Hypoglycemic, insulinotrophic and cytotoxic activity of three species of Ganoderma." Malaysian Journal of Science 26(2): 41-46.

Bellary, S. A., et al. (2017). "Effects of crude oil-water emulsions at various water-cut on the performance of the centrifugal pump." International Journal of Oil, Gas and Coal Technology 16(1): 71-88.

Benayoune, M., et al. (1998). "Viscosity of water in oil emulsions." Petroleum science and technology 16(7-8): 767-784.

Benito-Román, Ó., et al. Optimization of the extraction process of beta-glucans from barley.

Benito-Román, Ó., et al. (2016). "Dissolution of (1-3),(1-4)-β-Glucans in Pressurized Hot Water: Quantitative Assessment of the Degradation and the Effective Extraction." International Journal of Carbohydrate Chemistry 2016.

Berggren, J. and G. Alderborn (2003). "Effect of polymer content and molecular weight on the morphology and heat-and moisture-induced transformations of spray-dried composite particles of amorphous lactose and poly (vinylpyrrolidone)." Pharmaceutical research 20(7): 1039-1046.

Berninger, T., et al. (2016). "The smaller, the better? The size effect of alginate beads carrying plant growth-promoting bacteria for seed coating." Journal of microencapsulation 33(2): 127-136.

Beyatricks, K. J., et al. "RECENT TRENDS IN MICROSPHERE DRUG DELIVERY SYSTEM AND ITS THERAPEUTIC APPLICATIONS–A."

Bhowmik, B. B., et al. (2006). "Preparation and in-vitro characterization of slow release testosterone nanocapsules in alginates." ACTA PHARMACEUTICA-ZAGREB- 56(4): 417.

Bishayee, A., et al. (2011). "Triterpenoids as potential agents for the chemoprevention and therapy of breast cancer." Frontiers in bioscience: a journal and virtual library 16: 980.

Blanco, D. and M. a. J. Alonso (1998). "Protein encapsulation and release from poly (lactide-co-glycolide) microspheres: effect of the protein and polymer properties and of the co-encapsulation of surfactants." European Journal of pharmaceutics and biopharmaceutics 45(3): 285-294.

Bock, N., et al. (2012). "Electrospraying of polymers with therapeutic molecules: state of the art." Progress in polymer science 37(11): 1510-1551.

Bock, N., et al. (2011). "Electrospraying, a reproducible method for production of polymeric microspheres for biomedical applications." Polymers 3(1): 131-149.

*Novelty processing and smart delivery of Ganoderma Lucidum spores*

Bodenberger, N., et al. (2016). "Evaluation of methods for pore generation and their influence on physio-chemical properties of a protein based hydrogel." Biotechnology Reports 12: 6-12.

Boeing, J. S., et al. (2014). "Evaluation of solvent effect on the extraction of phenolic compounds and antioxidant capacities from the berries: application of principal component analysis." Chemistry Central Journal 8(1): 48.

Boh, B., et al. (2007). "Ganoderma lucidum and its pharmaceutically active compounds." Biotechnology annual review 13: 265-301.

Boontheekul, T., et al. (2005). "Controlling alginate gel degradation utilizing partial oxidation and bimodal molecular weight distribution." Biomaterials 26(15): 2455-2465.

Brady, B. O., et al. (1987). "Supercritical extraction of toxic organics from soils." Industrial & engineering chemistry research 26(2): 261-268.

Brown, G. D. and S. Gordon (2001). "Immune recognition: a new receptor for β-glucans." Nature 413(6851): 36.

Brown, G. M. and J. H. Butler (1997). "New method for the characterization of domain morphology of polymer blends using ruthenium tetroxide staining and low voltage scanning electron microscopy (LVSEM)." Polymer 38(15): 3937-3945.

Bryant, J. M., et al. (2017). "Anticancer activity of Ganoderic acid DM: current status and future perspective." Journal of clinical & cellular immunology 8(6).

Burns, B. S., et al. (2001). "Selective drug resistant human osteosarcoma cell lines." Clinical Orthopaedics and Related Research (1976-2007) 383: 259-267.

Bušić, A., et al. (2016). "Application of whey protein isolates and zein for the formulation of alginate-based delivery systems encapsulating Ganoderma lucidum polyphenols." Croatian journal of food science and technology 8(2): 99-106.

Buwalda, S. J., et al. (2017). "Hydrogels for therapeutic delivery: Current developments and future directions." Biomacromolecules 18(2): 316-330.

Buyukozturk, F., et al. (2010). "Impact of emulsion-based drug delivery systems on intestinal permeability and drug release kinetics." Journal of Controlled Release 142(1): 22-30.

Cai, B., et al. (2012). High performance liquid chromatography fingerprinting technology of the commonly-used traditional Chinese medicine herbs, World Scientific.

Cai, W., et al. (2008). "Extraction, purification, and characterization of the polysaccharides from Opuntia milpa alta." Carbohydrate polymers 71(3): 403-410.

Calviño, E., et al. (2010). "Ganoderma lucidum induced apoptosis in NB4 human leukemia cells: Involvement of Akt and Erk." Journal of ethnopharmacology 128(1): 71-78.

Camargo, M. R. and R. Kaneno (2011). "Antitumor properties of Ganoderma lucidum polysaccharides and terpenoids." Annual Review of Biomedical Sciences: 1-8.

Cao, F.-R., et al. (2017). "Ganoderic acid A metabolites and their metabolic kinetics." Frontiers in pharmacology 8: 101.

Cao, J., et al. (2019). "Development of PLGA micro-and nanorods with high capacity of surface ligand conjugation for enhanced targeted delivery." Asian Journal of Pharmaceutical Sciences 14(1): 86-94.

Cao, L.-Z. and Z.-B. Lin (2003). "Regulatory effect of Ganoderma lucidum polysaccharides on cytotoxic T-lymphocytes induced by dendritic cells in vitro." Acta Pharmacologica Sinica 24(4): 321-326.

Cao, Q.-Z. and Z.-B. Lin (2004). "Antitumor and anti-angiogenic activity of Ganoderma lucidum polysaccharides peptide." Acta Pharmacologica Sinica 25: 833-838.

Cao, Q.-Z. and Z.-B. Lin (2006). "Ganoderma lucidum polysaccharides peptide inhibits the growth of vascular endothelial cell and the induction of VEGF in human lung cancer cell." Life sciences 78(13): 1457-1463.

Cao, R., et al. (2014). "Model for Rheological Behavior of Crude Oil and Alkali-Surfactant-Polymer Emulsion." The Open Fuels and Energy Science Journal 7: 55-61.

Cares, M. G., et al. (2010). "Ultrasonically assisted extraction of bioactive principles from Quillaja Saponaria Molina." Physics Procedia 3(1): 169-178.

Cascone, M. G., et al. (1995). "Blends of synthetic and natural polymers as drug delivery systems for growth hormone." Biomaterials 16(7): 569-574.

Castillo-Orozco, E., et al. (2017). "Electrospray mode transition of microdroplets with semiconductor nanoparticle suspension." Scientific reports 7(1): 5144.

Castro-Cabado, M., et al. (2016). "Thermal crosslinking of maltodextrin and citric acid. Methodology to control the polycondensation reaction under processing conditions." Polymers and Polymer Composites 24(8): 643-654.

Chaiklahan, R., et al. (2014). "Effect of extraction temperature on the diffusion coefficient of polysaccharides from Spirulina and the optimal separation method." Biotechnology and bioprocess engineering 19(2): 369-377.

Chakraborty, S., et al. (2009). "Electrohydrodynamics: a facile technique to fabricate drug delivery systems." Advanced drug delivery reviews 61(12): 1043-1054.

Champagne, C. P. and P. Fustier (2007). "Microencapsulation for the improved delivery of bioactive compounds into foods." Current opinion in biotechnology 18(2): 184-190.

Champion, J. A., et al. (2007). "Particle shape: a new design parameter for micro-and nanoscale drug delivery carriers." Journal of Controlled Release 121(1-2): 3-9.

Champion, J. A. and S. Mitragotri (2006). "Role of target geometry in phagocytosis." Proceedings of the National Academy of Sciences 103(13): 4930-4934.

Chan, G. C.-F., et al. (2009). "The effects of β-glucan on human immune and cancer cells." Journal of hematology & oncology 2(1): 25.

Chan, L. W., et al. (2002). "Cross-linking mechanisms of calcium and zinc in production of alginate microspheres." International journal of pharmaceutics 242(1-2): 255-258.

Chan, S.-Y. and W.-S. Choo (2013). "Effect of extraction conditions on the yield and chemical properties of pectin from cocoa husks." Food chemistry 141(4): 3752-3758.

Chan, W. K., et al. (2008). "Ganoderma lucidum polysaccharides can induce human monocytic leukemia cells into dendritic cells with immuno-stimulatory function." Journal of hematology & oncology 1(1): 9.

*Novelty processing and smart delivery of Ganoderma Lucidum spores*

Chan, W. K., et al. (2005). "Ganoderma lucidum mycelium and spore extracts as natural adjuvants for immunotherapy." Journal of Alternative & Complementary Medicine: Research on Paradigm, Practice, and Policy 11(6): 1047-1057.

Chandegara, V. K. (2015). "Effect of temperature on gel extraction from aloe vera leaves." Agricultural Engineering International: CIGR Journal 17(1).

Chang, C.-J., et al. (2014). "Ganoderma lucidum stimulates NK cell cytotoxicity by inducing NKG2D/NCR activation and secretion of perforin and granulysin." Innate immunity 20(3): 301-311.

Chang, S. T. and J. A. Buswell Safety, quality control and reglational aspects relating to mushroom nutriceuticals.

Chang, X. L., et al. (2006). "Effects of heat treatments on the stabilities of polysaccharides substances and barbaloin in gel juice from Aloe vera Miller." Journal of Food Engineering 75(2): 245-251.

Chang, Y.-W. and T.-J. Lu (2004). "Molecular characterization of polysaccharides in hot-water extracts of Ganoderma lucidum fruiting bodies." Journal of Food and Drug Analysis 12(1): 59-67.

Chao, Z., et al. (2013). "Ultrasound-enhanced subcritical water extraction of polysaccharides from Lycium barbarum L." Separation and Purification Technology 120: 141-147.

Che, X. Q., et al. (2017). "Ganoderma triterpenoids from aqueous extract of Ganoderma lucidum." Zhongguo Zhong yao za zhi= Zhongguo zhongyao zazhi= China journal of Chinese materia medica 42(10): 1908-1915.

Chen, B., et al. (2017). "Triterpenes and meroterpenes from Ganoderma lucidum with inhibitory activity against HMGs reductase, aldose reductase and α-glucosidase." Fitoterapia 120: 6-16.

Chen, C., et al. (2015). "Optimization for ultrasound extraction of polysaccharides from mulberry fruits with antioxidant and hyperglycemic activity in vitro." Carbohydrate polymers 130: 122-132.

Chen, D. H., et al. (1999). "Chemotaxonomy of triterpenoid pattern of HPLC of Ganoderma lucidum and Ganoderma tsugae." Journal of the Chinese Chemical Society 46(1): 47-51.

Chen, D. S. and I. Mellman (2013). "Oncology meets immunology: the cancer-immunity cycle." Immunity 39(1): 1-10.

Chen, J., et al. (2015). "Non-spherical particles for targeted drug delivery." Chemical engineering science 125: 20-24.

Chen, J., et al. (1993). "Interfacial interactions, competitive adsorption and emulsion stability." Food Structure 12(2): 1.

Chen, L. (2012). "The Innovation Research on the Extraction Technology of Ganoderma lucidum." Frontiers in pharmacology 3: 79.

Chen, L. and M. Subirade (2006). "Alginate–whey protein granular microspheres as oral delivery vehicles for bioactive compounds." Biomaterials 27(26): 4646-4654.

Chen, N.-H., et al. (2010). "Ganoderic acid T inhibits tumor invasion in vitro and in vivo through inhibition of MMP expression." Pharmacological Reports 62(1): 150-163.

*Novelty processing and smart delivery of Ganoderma Lucidum spores*

Chen, R.-Y. and D.-Q. Yu (1993). "Studies on the triterpenoid constituents of the spores from Ganoderma lucidum Karst." J Chin Pharm Sci 2: 91-96.

Chen, R.-Z., et al. (2015). "Extraction, isolation, characterization and antioxidant activity of polysaccharides from Astragalus membranaceus." Industrial Crops and Products 77: 434-443.

Chen, S. J., Lin, H. H., Huang, W. C., Tsai, P. J., Chen, W. P., Chen, D. C., & Chuang, L. T. (2017). Ling-Zhi-8 protein (LZ-8) suppresses the production of pro-inflammatory mediators in murine microglial BV-2 cells. Food and Agricultural Immunology, 28(6), 1393-1407.

Chen, S., et al. (2018). "Simultaneous optimization of the ultrasound-assisted extraction for phenolic compounds content and antioxidant activity of Lycium ruthenicum Murr. fruit using response surface methodology." Food chemistry 242: 1-8.

Chen, T.-Q., et al. (2014). "Efficient extraction technology of antioxidant crude polysaccharides from Ganoderma lucidum (Lingzhi), ultrasonic-circulating extraction integrating with superfine-pulverization." Journal of the Taiwan Institute of Chemical Engineers 45(1): 57-62.

Chen, W., et al. (2016). "Effect of particle size on drug loading and release kinetics of gefitinib-loaded PLGA microspheres." Molecular pharmaceutics 14(2): 459-467.

Chen, W., et al. (2007) (a). Synergy of Ganoderma lucidum Extract ReishiMax and Green Tea Polyphenols Tegreen in Anti-Cancer in a S180-inoculation model, Federation of American Societies for Experimental Biology.

Chen, W. C. and D. M. Hau (1995). "Effects of Ganoderma lucidum on cellular immunocompetence in γ-irradiated mice." Phytotherapy Research 9(7): 533-535.

Chen, X., et al. (2012). "Distinction of broken cellular wall Ganoderma lucidum spores and G. lucidum spores using FTIR microspectroscopy." Spectrochimica Acta Part A: Molecular and Biomolecular Spectroscopy 97: 667-672.

Chen, X., et al. (2010). "Optimization of ultrasound-assisted extraction of Lingzhi polysaccharides using response surface methodology and its inhibitory effect on cervical cancer cells." Carbohydrate polymers 80(3): 944-948.

Chen, Y., et al. (2010). "Ganoderma species discrimination by dual-mode chromatographic fingerprinting: A study on stationary phase effects in hydrophilic interaction chromatography and reduction of sample misclassification rate by additional use of reversed-phase chromatography." Journal of Chromatography A 1217(8): 1255-1265.

Chen, Y., et al. (2010). "Preparation of Ganoderma lucidum polysaccharides and triterpenes microemulsion and its anticancer effect in mice with transplant Heps tumors." Zhongguo Zhong yao za zhi= Zhongguo zhongyao zazhi= China journal of Chinese materia medica 35(20): 2679-2683.

Chen, Y., et al. (2007) (b). "Microwave-assisted extraction used for the isolation of total triterpenoid saponins from Ganoderma atrum." Journal of Food Engineering 81(1): 162-170.

Chen, Y., et al. (2008). "Purification, composition analysis and antioxidant activity of a polysaccharide from the fruiting bodies of Ganoderma atrum." Food chemistry 107(1): 231-241.

Chen, Y., et al. (2008). "Development of a chromatographic fingerprint for the chloroform extracts of Ganoderma lucidum by HPLC and LC–MS." Journal of pharmaceutical and biomedical analysis 47(3): 469-477.

*Novelty processing and smart delivery of Ganoderma Lucidum spores*

Cheng, C., et al. (2012). "Identification of metabolites of ganoderic acid D by ultra-performance liquid chromatography/quadrupole time-of-flight mass spectrometry." Drug Metabolism and Disposition 40(12): 2307-2314.

Cheng, C. R., et al. (2011). "Fragmentation pathways of oxygenated tetracyclic triterpenoids and their application in the qualitative analysis of Ganoderma lucidum by multistage tandem mass spectrometry." Rapid Communications in Mass Spectrometry 25(9): 1323-1335.

Cheng, P.-G., et al. (2013). "Polysaccharides-rich extract of Ganoderma lucidum (MA Curtis: Fr.) P. Karst accelerates wound healing in streptozotocin-induced diabetic rats." Evidence-Based Complementary and Alternative Medicine 2013.

Cheng, S. and D. Sliva (2015). "Ganoderma lucidum for cancer treatment: we are close but still not there." Integrative cancer therapies 14(3): 249-257.

Cheung, Y.-C., et al. (2013). "Kinetic models for ultrasound-assisted extraction of water-soluble components and polysaccharides from medicinal fungi." Food and bioprocess technology 6(10): 2659-2665.

Chi, B., et al. (2018). "Effects of ganoderic acid A on lipopolysaccharide-induced proinflammatory cytokine release from primary mouse microglia cultures." Experimental and therapeutic medicine 15(1): 847-853.

Chin, S. and C. Law (2014). "Maximizing the retention of ganoderic acids and water-soluble polysaccharides content of Ganoderma lucidum using two-stage dehydration method." Drying Technology 32(6): 644-656.

Chin, S. K., et al. (2011). "Effect of drying on crude ganoderic acids and water soluble polysaccharides content in Ganoderma lucidum." Int J Pharm Pharm Sci 3: 38-43.

Ching, S. H., et al. (2017). "Alginate gel particles–A review of production techniques and physical properties." Critical reviews in food science and nutrition 57(6): 1133-1152.

Chithrani, B. D., et al. (2006). "Determining the size and shape dependence of gold nanoparticle uptake into mammalian cells." Nano letters 6(4): 662-668.

Choi, J. H., et al. (2008). "Release behavior of freeze-dried alginate beads containing poly (N-isopropylacrylamide) copolymers." Journal of applied polymer science 110(1): 117-123.

Choong, Y. K., et al. (2012). "Preliminary results of determination of chemical changes on lingzhi or reishi medicinal mushroom, Ganoderma lucidum (W. Curt.: Fr.) P. Karst.(higher Basidiomycetes) carried by Shenzhou I spaceship with FTIR and 2D-IR correlation spectroscopy." International Journal of Medicinal Mushrooms 14(3).

Choong, Y.-K., et al. (2018). Extraction and Fractionation of Polysaccharides from a Selected Mushroom Species, Ganoderma lucidum: A Critical Review. Fractionation, IntechOpen.

Choromanska, A., et al. (2018). "High-and low-molecular weight oat beta-glucan reveals antitumor activity in human epithelial lung cancer." Pathology & Oncology Research 24(3): 583-592.

Chuang, J.-J., et al. (2017). "Effects of pH on the shape of alginate particles and its release behavior." International Journal of Polymer Science 2017.

Chung, T.-W., et al. (2003). "Enhancement of the growth of human endothelial cells by surface roughness at nanometer scale." Biomaterials 24(25): 4655-4661.

*Novelty processing and smart delivery of Ganoderma Lucidum spores*

Chunhua, X., et al. (2014). "Optimization of enzyme assisted extraction of polysaccharides from Ganoderma lucidum." Eng. Sci 12(1): 17.

Clay, M. A. and M. J. Miksis (2004). "Effects of surfactant on droplet spreading." Physics of Fluids 16(8): 3070-3078.

Cmoch, A., et al. (2014). "Stimulators of mineralization limit the invasive phenotype of human osteosarcoma cells by a mechanism involving impaired invadopodia formation." PloS one 9(10): e109938.

Coates, J. (2006). "Interpretation of infrared spectra, a practical approach." Encyclopedia of analytical chemistry: applications, theory and instrumentation.

Collins, R. T., et al. (2008). "Electrohydrodynamic tip streaming and emission of charged drops from liquid cones." Nature Physics 4(2): 149-154.

Collnot, E.-M., et al. (2012). "Nano-and microparticulate drug carriers for targeting of the inflamed intestinal mucosa." Journal of Controlled Release 161(2): 235-246.

Cooley, M., et al. (2018). "Influence of particle size and shape on their margination and wall-adhesion: implications in drug delivery vehicle design across nano-to-micro scale." Nanoscale 10(32): 15350-15364.

Cör, D., et al. (2018). "Antitumour, antimicrobial, antioxidant and antiacetylcholinesterase effect of Ganoderma lucidum terpenoids and polysaccharides: A review." Molecules 23(3): 649.

Coskun, O. (2016). "Separation techniques: chromatography." Northern clinics of Istanbul 3(2): 156.

Costa, A. M. S. and J. F. Mano (2015). "Highly robust hydrogels via a fast, simple and cytocompatible dual crosslinking-based process." Chemical Communications 51(86): 15673-15676.

Costa, M. J., et al. (2018). "Physicochemical properties of alginate-based films: Effect of ionic crosslinking and mannuronic and guluronic acid ratio." Food Hydrocolloids 81: 442-448.

Costantino, H. R. and M. J. Pikal (2004). Lyophilization of biopharmaceuticals, Springer Science & Business Media.

Courthaudon, J.-L., et al. (1991). "Influence of emulsifier on the competitive adsorption of whey proteins in emulsions." Food Structure 10(2): 1.

Covey, T. R., et al. (1986). "Liquid chromatography/mass spectrometry." Analytical chemistry 58(14): 1451A-1461A.

Cozens-Roberts, C., et al. (1990). "Receptor-mediated adhesion phenomena. Model studies with the Radical-Flow Detachment Assay." Biophysical Journal 58(1): 107-125.

Cruz, M. C. P., et al. (2004). "Evaluation of the diffusion coefficient for controlled release of oxytetracycline from alginate/chitosan/poly (ethylene glycol) microbeads in simulated gastrointestinal environments." Biotechnology and applied biochemistry 40(3): 243-253.

Cui, H.-Y., et al. (2014). "Comparison of conventional and ultrasound-assisted methods for extraction of nutraceutical compounds from Dendrobium candidum." CyTA-Journal of Food 12(4): 355-359.

*Novelty processing and smart delivery of Ganoderma Lucidum spores*

Cui, M.-l., et al. (2015). "Submerged fermentation production and characterization of intracellular triterpenoids from Ganoderma lucidum using HPLC-ESI-MS." Journal of Zhejiang University-SCIENCE B 16(12): 998-1010.

Cui, Z.-W., et al. (2006). "Dehydration of concentrated Ganoderma lucidum extraction by combined microwave-vacuum and conventional vacuum drying." Drying Technology 24(5): 595-599.

Czakkel, O., et al. (2005). "Influence of drying on the morphology of resorcinol–formaldehyde-based carbon gels." Microporous and Mesoporous Materials 86(1-3): 124-133.

Da, J., et al. (2015). "A reproducible analytical system based on the multi-component analysis of triterpene acids in Ganoderma lucidum." Phytochemistry 114: 146-154.

Da, J., et al. (2012). "Comparison of two officinal Chinese pharmacopoeia species of Ganoderma based on chemical research with multiple technologies and chemometrics analysis." Journal of Chromatography A 1222: 59-70.

Dahiya, P., et al. (2016). "Arrested coalescence of viscoelastic droplets: polydisperse doublets." Philosophical Transactions of the Royal Society A: Mathematical, Physical and Engineering Sciences 374(2072): 20150132.

Dapčević Hadnađev, T., et al. (2013). "Influence of oil phase concentration on droplet size distribution and stability of oil-in-water emulsions." European Journal of Lipid Science and Technology 115(3): 313-321.

Dash, S., et al. (2010). "Kinetic modeling on drug release from controlled drug delivery systems." Acta Pol Pharm 67(3): 217-223.

Date, P. V., et al. (2010). "Freeze thaw: a simple approach for prediction of optimal cryoprotectant for freeze drying." Aaps Pharmscitech 11(1): 304-313.

De Jong, W. H. and P. J. A. Borm (2008). "Drug delivery and nanoparticles: applications and hazards." International journal of nanomedicine 3(2): 133.

De Vos, R. C. H., et al. (2007). "Untargeted large-scale plant metabolomics using liquid chromatography coupled to mass spectrometry." Nature protocols 2(4): 778.

Decuzzi, P. and M. Ferrari (2006). "The adhesive strength of non-spherical particles mediated by specific interactions." Biomaterials 27(30): 5307-5314.

Dent, M., et al. (2013). "The effect of extraction solvents, temperature and time on the composition and mass fraction of polyphenols in Dalmatian wild sage (Salvia officinalis L.) extracts." Food technology and biotechnology 51(1): 84-91.

Descroix, K., et al. (2014). "β-(1→ 3)-Glucan-mannitol conjugates: scope and amazing results." Annals of translational medicine 2(2).

Deters, A. M., et al. (2005). "Kiwi fruit (Actinidia chinensis L.) polysaccharides exert stimulating effects on cell proliferation via enhanced growth factor receptors, energy production, and collagen synthesis of human keratinocytes, fibroblasts, and skin equivalents." Journal of cellular physiology 202(3): 717-722.

Devarajan, P. V. and S. Jain (2015). Targeted drug delivery: concepts and design, Springer.

Dias, D. A., et al. (2012). "A historical overview of natural products in drug discovery." Metabolites 2(2): 303-336.

*Novelty processing and smart delivery of Ganoderma Lucidum spores*

Dickinson, J. T., et al. (1990). "Mass spectroscopy study of products from exposure of cyclotrimethylene-trinitramine single crystals to KrF excimer laser radiation." Journal of Applied Physics 67(8): 3641-3651.

Do, Q. D., et al. (2014). "Effect of extraction solvent on total phenol content, total flavonoid content, and antioxidant activity of Limnophila aromatica." Journal of Food and Drug Analysis 22(3): 296-302.

Dong, Y.-h., et al. (2009). "Optimization of Ultrasonic-assisted Extraction Technology of Ganoderma lucidum Polysaccharides by Response Surface Methodology [J]." Food Science 16.

Dong, Z., et al. (2006). "Alginate/gelatin blend films and their properties for drug controlled release." Journal of Membrane Science 280(1-2): 37-44.

Donsì, F., et al. (2011). "Encapsulation of bioactive compounds in nanoemulsion-based delivery systems." Procedia Food Science 1: 1666-1671.

Đorđević, D. M., et al. (2012). "Ftir spectroscopic characterization of bituminous limestone: Maganik mountain (Montenegro)." Studia Universitatis Babes-Bolyai, Chemia 57(4).

Dou, Q., et al. (2017). "A new light triggered approach to develop a micro porous tough hydrogel." RSC advances 7(44): 27449-27453.

Drosou, C. G., et al. (2017). "Encapsulation of bioactive compounds through electrospinning/electrospraying and spray drying: A comparative assessment of food-related applications." Drying Technology 35(2): 139-162.

Drummy, L. F., et al. (2004). "Low-voltage electron microscopy of polymer and organic molecular thin films." Ultramicroscopy 99(4): 247-256.

Du, Y., et al. (2008). "Directed assembly of cell-laden microgels for fabrication of 3D tissue constructs." Proceedings of the National Academy of Sciences 105(28): 9522-9527.

Dubbels, R., et al. (1995). "Melatonin in edible plants identified by radioimmunoassay and by high performance liquid chromatography-mass spectrometry." Journal of pineal research 18(1): 28-31.

Dubois, M., et al. (1956). "Colorimetric method for determination of sugars and related substances." Analytical chemistry 28(3): 350-356.

Dunne, M., et al. (2000). "Influence of particle size and dissolution conditions on the degradation properties of polylactide-co-glycolide particles." Biomaterials 21(16): 1659-1668

Dutta, A. K., et al. (1956). "Viscosity of Liquids and Ultrasonic Studies." Nature 177(4522): 1227.

Dutta, D., et al. (2016). "Tailoring sub-micron PLGA particle release profiles via centrifugal fractioning." Journal of Biomedical Materials Research Part A 104(3): 688-696.

Eder, J. and P. L. Herrling (2015). Trends in modern drug discovery. New Approaches to Drug Discovery, Springer: 3-22.

El-Gendy, N. A. and M. H. El-Komy (2014). "Engineering Spherical Beads as an Approach to Improve the Physico-Mechanical Properties of Poorly Soluble Drugs." International Journal 1(2): 1-12.

*Novelty processing and smart delivery of Ganoderma Lucidum spores*

El-Houssiny, A. S., et al. (2016). "Drug–polymer interaction between glucosamine sulfate and alginate nanoparticles: FTIR, DSC and dielectric spectroscopy studies." Advances in Natural Sciences: Nanoscience and Nanotechnology 7(2): 025014.

Elmore, S. (2007). "Apoptosis: a review of programmed cell death." Toxicologic pathology 35(4): 495-516.

El-Sherbiny, I. M., et al. (2011). "Biodegradable pH-responsive alginate-poly (lactic-co-glycolic acid) nano/micro hydrogel matrices for oral delivery of silymarin." Carbohydrate polymers 83(3): 1345-1354.

Endo-Munoz, L., et al. (2010). "Osteosarcoma is characterised by reduced expression of markers of osteoclastogenesis and antigen presentation compared with normal bone." British journal of cancer 103(1): 73.

Erenpreisa, J. A., et al. (2000). "Release of mitotic descendants by giant cells from irradiated Burkitt's lymphoma cell lines." Cell biology international 24(9): 635-648.

Erkel, E. I. (2009). "The effect of different substrate mediums on yield of Ganoderma lucidum (Fr.) Karst." J Food Agric Environ 7: 841-844.

Ersus, S. and D. M. Barrett (2010). "Determination of membrane integrity in onion tissues treated by pulsed electric fields: use of microscopic images and ion leakage measurements." Innovative Food Science & Emerging Technologies 11(4): 598-603.

Evaristi, M. F., et al. (2016). "Increased mean aliphatic lipid chain length in left ventricular hypertrophy secondary to arterial hypertension: a cross-sectional study." Medicine 95(46).

Fabre, N., et al. (2001). "Determination of flavone, flavonol, and flavanone aglycones by negative ion liquid chromatography electrospray ion trap mass spectrometry." Journal of the American Society for Mass Spectrometry 12(6): 707-715.

Fan, L., et al. (2013). "In situ generation of sodium alginate/hydroxyapatite/halloysite nanotubes nanocomposite hydrogel beads as drug-controlled release matrices." Journal of Materials Chemistry B 1(45): 6261-6270.

Fan, Y., et al. (2014). "Characterization and antitumor activity of a polysaccharide from Sarcodia ceylonensis." Molecules 19(8): 10863-10876.

Fang, X., et al. (2018). "Optimization of ultrasonic-assisted simultaneous extraction of three active compounds from the fruits of Forsythia suspensa and comparison with conventional extraction methods." Molecules 23(9): 2115.

Farrés, I. F. and I. T. Norton (2014). "Formation kinetics and rheology of alginate fluid gels produced by in-situ calcium release." Food Hydrocolloids 40: 76-84.

Femenia, A., et al. (2003). "Effects of heat treatment and dehydration on bioactive polysaccharide acemannan and cell wall polymers from Aloe barbadensis Miller." Carbohydrate polymers 51(4): 397-405.

Feng, L., et al. (2013). "Anti-lung cancer activity through enhancement of immunomodulation and induction of cell apoptosis of total triterpenes extracted from Ganoderma luncidum (Leyss. ex Fr.) Karst." Molecules 18(8): 9966-9981.

Ferreira, I. C., Barros, L., & Abreu, R. (2009). Antioxidants in wild mushrooms. Current Medicinal Chemistry, 16(12), 1543-1560.

*Novelty processing and smart delivery of Ganoderma Lucidum spores*

Festag, R., et al. (1998). "Effects of molecular entanglements during electrospray of high molecular weight polymers." Journal of the American Society for Mass Spectrometry 9(4): 299-304.

Fink, G., et al. (2014). "Large lakes as sources and sinks of anthropogenic heat: Capacities and limits." Water Resources Research 50(9): 7285-7301.

Fonte, P., et al. (2012). "Effect of cryoprotectants on the porosity and stability of insulin-loaded PLGA nanoparticles after freeze-drying." Biomatter 2(4): 329-339.

Forbes, T. P., et al. (2010). "Electrohydrodynamics of charge separation in droplet-based ion sources with time-varying electrical and mechanical actuation." Journal of the American Society for Mass Spectrometry 21(4): 501-510.

Franz, G. and U. Feuerstein Chemical stability of some model polysaccharides, Wiley Online Library.

Freiberg, S. and X. X. Zhu (2004). "Polymer microspheres for controlled drug release." International journal of pharmaceutics 282(1-2): 1-18.

Freitas, S., et al. (2005). "Microencapsulation by solvent extraction/evaporation: reviewing the state of the art of microsphere preparation process technology." Journal of Controlled Release 102(2): 313-332.

Fu, S., et al. (2011). "Relevance of rheological properties of sodium alginate in solution to calcium alginate gel properties." Aaps Pharmscitech 12(2): 453-460.

Fu, S., et al. (2010). "Rheological evaluation of inter-grade and inter-batch variability of sodium alginate." Aaps Pharmscitech 11(4): 1662-1674.

Fu, Y.-J., et al. (2009). "Breaking the spores of the fungus Ganoderma lucidum by supercritical $CO_2$." Food chemistry 112(1): 71-76.

Fukuzawa, M., et al. (2008). "Possible involvement of long chain fatty acids in the spores of Ganoderma lucidum (Reishi Houshi) to its anti-tumor activity." Biological and Pharmaceutical Bulletin 31(10): 1933-1937.

Funami, T., et al. (2009). "Rheological properties of sodium alginate in an aqueous system during gelation in relation to supermolecular structures and $Ca^{2+}$ binding." Food Hydrocolloids 23(7): 1746-1755.

Gan, Q., et al. (2005). "Modulation of surface charge, particle size and morphological properties of chitosan–TPP nanoparticles intended for gene delivery." Colloids and Surfaces B: Biointerfaces 44(2-3): 65-73.

Ganan-Calvo, A. M., et al. (1997). "Current and droplet size in the electrospraying of liquids. Scaling laws." Journal of Aerosol Science 28(2): 249-275.

Gañán-Calvo, A. M., et al. (2013). "The minimum or natural rate of flow and droplet size ejected by Taylor cone–jets: physical symmetries and scaling laws." New Journal of Physics 15(3): 033035.

Gao, B., et al. (2019). "Methods to prepare dopamine/polydopamine modified alginate hydrogels and their special improved properties for drug delivery." European Polymer Journal 110: 192-201.

*Novelty processing and smart delivery of Ganoderma Lucidum spores*

Gao, J.-J., et al. (2004). "Quantitative determination of bitter principles in specimens of Ganoderma lucidum using high-performance liquid chromatography and its application to the evaluation of Ganoderma products." Chemical and Pharmaceutical Bulletin 52(6): 688-695.

Gao, W., et al. (2017). "Preparation, characterisation and antioxidant activities of litchi (Litchi chinensis Sonn.) polysaccharides extracted by ultra-high pressure." International journal of food science & technology 52(8): 1739-1750.

Gao, Y., et al. (2005). "Antitumor activity and underlying mechanisms of ganopoly, the refined polysaccharides extracted from Ganoderma lucidum, in mice." Immunological investigations 34(2): 171-198.

Gao, Y., et al. (2004). "A phase I/II study of Ling Zhi mushroom Ganoderma lucidum (W. Curt.: Fr.) Lloyd (Aphyllophoromycetideae) extract in patients with type II diabetes mellitus." International Journal of Medicinal Mushrooms 6(1).

Gao, Y., et al. (2011). "Study of the extraction process and in vivo inhibitory effect of ganoderma triterpenes in oral mucosa cancer." Molecules 16(7): 5315-5332.

Gao, Y., et al. (2016). "Optimising the shell thickness-to-radius ratio for the fabrication of oil-encapsulated polymeric microspheres." Chemical Engineering Journal 284: 963-971.

Gao, Y., et al. (2003). "Effects of Ganopoly®(A ganoderma lucidum polysaccharide extract) on the immune functions in Advanced-Stage cancer patients." Immunological investigations 32(3): 201-215.

Garcia, H., et al. (2008). "Characterization of dextrin hydrogels by FTIR spectroscopy and solid state NMR spectroscopy." European Polymer Journal 44(7): 2318-2329.

Gasperini, L., et al. (2014). "Natural polymers for the microencapsulation of cells." Journal of the Royal Society Interface 11(100): 20140817.

Gatenby, R. A., et al. (2009). "Adaptive therapy." Cancer research 69(11): 4894-4903.

Gavze, E. and M. Shapiro (1997). "Particles in a shear flow near a solid wall: effect of nonsphericity on forces and velocities." International Journal of Multiphase Flow 23(1): 155-182.

Gazi, E., et al. (2005). "A study of cytokinetic and motile prostate cancer cells using synchrotron-based FTIR microspectroscopic imaging." Vibrational spectroscopy 38(1-2): 193-201.

Gentile, F., et al. (2008). "The effect of shape on the margination dynamics of non-neutrally buoyant particles in two-dimensional shear flows." Journal of biomechanics 41(10): 2312-2318.

George, M. and T. E. Abraham (2006). "Polyionic hydrocolloids for the intestinal delivery of protein drugs: alginate and chitosan—a review." Journal of Controlled Release 114(1): 1-14.

Getts, D. R., et al. (2015). "Harnessing nanoparticles for immune modulation." Trends in immunology 36(7): 419-427.

Ghaghada, K. B., et al. (2005). "Folate targeting of drug carriers: a mathematical model." Journal of Controlled Release 104(1): 113-128.

Ghara, A. R. and F. E. Ghadi (2016). "Effect of Extraction Solvent/technique on the Antioxidant activity of Selected 10 herb native species south of Iran." Advances in Bioresearch 7(4).

*Novelty processing and smart delivery of Ganoderma Lucidum spores*

Ghayempour, S. and S. M. Mortazavi (2013). "Fabrication of micro–nanocapsules by a new electrospraying method using coaxial jets and examination of effective parameters on their production." Journal of Electrostatics 71(4): 717-727.

Gierszewska-Drużyńska, M. and J. Ostrowska-Czubenko (2012). "MECHANISM OF WATER DIFFUSION INTO NONCROSSLINKED AND IONICALLY CROSSLINKED CHITOSAN MEMBRANES." Progress on Chemistry and Application of Chitin and its Derivatives 17: 63-70.

Girard, J. E. and J. Girard (2013). Principles of environmental chemistry, Jones & Bartlett Publishers.

Goldman, A. J., et al. (1967). "Slow viscous motion of a sphere parallel to a plane wall—II Couette flow." Chemical engineering science 22(4): 653-660.

Golubnitschaja, O. (2009). "Paradigm Change from Curative to Predictive Medicine: Novel Strategic Trends in Europe." Croatian medical journal 50(6): 596.

Gómez-Estaca, J., et al. (2012). "Formation of zein nanoparticles by electrohydrodynamic atomization: Effect of the main processing variables and suitability for encapsulating the food coloring and active ingredient curcumin." Food Hydrocolloids 28(1): 82-91.

Gong, Y.-h., et al. (2011). "Viscosity and density measurements for six binary mixtures of water (methanol or ethanol) with an ionic liquid ([BMIM][DMP] or [EMIM][DMP]) at atmospheric pressure in the temperature range of (293.15 to 333.15) K." Journal of Chemical & Engineering Data 57(1): 33-39.

Gonzalez, G., et al. (2013). "Infuence of microstructure in drug release behavior of silica nanocapsules." Journal of drug delivery 2013.

Gopinath, A., et al. (2014). "Effect of aqueous ethanol on the triple helical structure of collagen." European Biophysics Journal 43(12): 643-652.

Goswami, S., et al. (2014). "Calcium alginate nanocarriers as possible vehicles for oral delivery of insulin." Journal of Experimental Nanoscience 9(4): 337-356.

Gouda, R., et al. (2017). "Application of mathematical models in drug release kinetics of carbidopa and levodopa ER tablets." J. Dev. Drugs 6(02).

Grant, G. T., et al. (1973). "Biological interactions between polysaccharides and divalent cations: the egg-box model." FEBS letters 32(1): 195-198.

Gratton, S. E. A., et al. (2008). "The effect of particle design on cellular internalization pathways." Proceedings of the National Academy of Sciences 105(33): 11613-11618.

Greco, M., et al. (2014). "A simple and effective method for high quality co-extraction of genomic DNA and total RNA from low biomass Ectocarpus siliculosus, the model brown alga." PloS one 9(5): e96470.

Greve, L. C., et al. (1994). "Impact of heating on carrot firmness: changes in cell wall components." Journal of Agricultural and Food Chemistry 42(12): 2900-2906.

Gross, K. C. and S. J. Wallner (1979). "Degradation of cell wall polysaccharides during tomato fruit ripening." Plant Physiology 63(1): 117-120.

Gross, M. and R. Jaenicke (1994). "Proteins under pressure: the influence of high hydrostatic pressure on structure, function and assembly of proteins and protein complexes." European Journal of Biochemistry 221(2): 617-630.

*Novelty processing and smart delivery of Ganoderma Lucidum spores*

Gu, Y. P., et al. (2017). "Inhibition of chemotherapy-induced apoptosis of testicular cells by squid ink polysaccharide." Experimental and therapeutic medicine 14(6): 5889-5895.

Güncüm, E., et al. (2018). "Development and characterization of polymeric-based nanoparticles for sustained release of amoxicillin–an antimicrobial drug." Artificial cells, nanomedicine, and biotechnology 46(sup2): 964-973.

Gundogdu, N. and M. Cetin (2014). "Chitosan-poly (lactide-co-glycolide)(CS-PLGA) nanoparticles containing metformin HCl: Preparation and in vitro evaluation." Pak J Pharm Sci 27(6): 1923-1929.

Guo, J., et al. (2018). "Ganoderma lucidum-derived polysaccharide enhances coix oil-based microemulsion on stability and lung cancer-targeted therapy." Drug delivery 25(1): 1802-1810.

Guo, L., et al. (2009). "Characterization and immunostimulatory activity of a polysaccharide from the spores of Ganoderma lucidum." International immunopharmacology 9(10): 1175-1182.

Gupta, P., et al. (2005). "Electrospinning of linear homopolymers of poly (methyl methacrylate): exploring relationships between fiber formation, viscosity, molecular weight and concentration in a good solvent." Polymer 46(13): 4799-4810.

Gurikov, P. and I. Smirnova (2018). "Non-conventional methods for gelation of alginate." Gels 4(1): 14.

Guzman-Villanueva, D., et al. (2013). "Design and in vitro evaluation of a new nano-microparticulate system for enhanced aqueous-phase solubility of curcumin." BioMed research international 2013.

Häcker, G. (2000). "The morphology of apoptosis." Cell and tissue research 301(1): 5-17.

Han, M. D., et al. (2008). "Solubilization of water-insoluble beta-glucan isolated from Ganoderma lucidum." Journal of environmental biology 29(2): 237.

Han, X.-Q., et al. (2014). "Structure elucidation and immunomodulatory activity of a beta glucan from the fruiting bodies of Ganoderma sinense." PloS one 9(7): e100380.

Hao, X., et al. (2006). "Effects of the electrospray ionization parameters on the formation and morphology of colloidal microspheres of polyacrylonitrile." Journal of applied polymer science 102(3): 2889-2893.

Hao, Z.-q., et al. (2018). "Rheological properties and gel characteristics of polysaccharides from fruit-bodies of Sparassis crispa." International journal of food properties 21(1): 2283-2295.

Hara, Y., et al. (2013). "Simple method for refining arabinan polysaccharides by alcohol extraction of the prune, Prunus domestica L." Bioscience, biotechnology, and biochemistry: 130392.

Haralampidis, K., et al. (2002). Biosynthesis of triterpenoid saponins in plants. History and Trends in Bioprocessing and Biotransformation, Springer: 31-49.

Hariyadi, D. M., et al. (2014). "Effect of cross linking agent and polymer on the characteristics of ovalbumin loaded alginate microspheres." International Journal of Pharmacy and Pharmaceutical Sciences 6(4): 470-474.

*Novelty processing and smart delivery of Ganoderma Lucidum spores*

Harnkarnsujarit, N., et al. (2016). "Impacts of freezing and molecular size on structure, mechanical properties and recrystallization of freeze-thawed polysaccharide gels." LWT-Food Science and Technology 68: 190-201.

Hartman, R. P. A. (1998). "Electrohydrodynamic atomization in the cone-jet mode. From physical modeling to powder production."

Hassas-Roudsari, M., et al. (2009). "Antioxidant capacity of bioactives extracted from canola meal by subcritical water, ethanolic and hot water extraction." Food chemistry 114(2): 717-726.

Havelund, S. (2001). Pulmonary insulin crystals, Google Patents.

He, J., et al. (2005). "Modeling of drug release from bioerodible polymer matrices." Drug delivery 12(5): 251-259.

Heleno, S. A., et al. (2012). "Fruiting body, spores and in vitro produced mycelium of Ganoderma lucidum from Northeast Portugal: A comparative study of the antioxidant potential of phenolic and polysaccharidic extracts." Food research international 46(1): 135-140.

Hell, J., et al. (2016). "A comparison between near-infrared (NIR) and mid-infrared (ATR-FTIR) spectroscopy for the multivariate determination of compositional properties in wheat bran samples." Food control 60: 365-369.

Heng, P. W. S., et al. (2003). "Formation of alginate microspheres produced using emulsification technique." Journal of microencapsulation 20(3): 401-413.

Hengartner, M. O. (2000). "The biochemistry of apoptosis." Nature 407(6805): 770.

Hennicke, F., et al. (2016). "Distinguishing commercially grown Ganoderma lucidum from Ganoderma lingzhi from Europe and East Asia on the basis of morphology, molecular phylogeny, and triterpenic acid profiles." Phytochemistry 127: 29-37.

Hereher, F., et al. (2018). "Pilot study: Tumor suppressive effect of crude polysaccharide substances extracted from some selected mushroom." Beni-Suef University journal of basic and applied sciences 7(4): 767-775.

Hilz, H., et al. (2006). "Combined enzymatic and high-pressure processing affect cell wall polysaccharides in berries." Journal of Agricultural and Food Chemistry 54(4): 1322-1328.

Hira, K., et al. (2019). "Protective effect of crude sulphated polysaccharides from Sargassum Swartzii (Turn.) C. Ag. against acetaminophen induced liver toxicity in rats." Clinical Phytoscience 5(1): 14.

Hlinak, A. J., et al. (2006). "Understanding critical material properties for solid dosage form design." Journal of Pharmaceutical Innovation 1(1): 12-17.

Ho, Y. W., et al. (2007). "Ganoderma lucidum polysaccharide peptide reduced the production of proinflammatory cytokines in activated rheumatoid synovial fibroblast." Molecular and cellular biochemistry 301(1-2): 173-179.

Hoare, T. R. and D. S. Kohane (2008). "Hydrogels in drug delivery: Progress and challenges." Polymer 49(8): 1993-2007.

Hoffman, A. S. (2008). "The origins and evolution of "controlled" drug delivery systems." Journal of Controlled Release 132(3): 153-163.

*Novelty processing and smart delivery of Ganoderma Lucidum spores*

Holkem, A. T., et al. (2016). "Development and characterization of alginate microcapsules containing Bifidobacterium BB-12 produced by emulsification/internal gelation followed by freeze drying." LWT-Food Science and Technology 71: 302-308.

Hosseini, E., et al. (2017). "Influence of temperature, pH and salts on rheological properties of bitter almond gum." Food Science and Technology 37(3): 437-443.

Hossen, S., et al. (2019). "Smart nanocarrier-based drug delivery systems for cancer therapy and toxicity studies: A review." Journal of advanced research 15: 1-18.

Hou, C. Y. (1988). "Studies on the chemical constituents of the spores from Ganoderma lucidum." Acta Bot. Sin. 30: 66-70.

Hromadkova, Z., et al. (1999). "Comparison of classical and ultrasound-assisted extraction of polysaccharides from Salvia officinalis L." Ultrasonics sonochemistry 5(4): 163-168.

Hsieh, D. S. T., et al. (1983). "Zero-order controlled-release polymer matrices for micro-and macromolecules." Journal of pharmaceutical sciences 72(1): 17-22.

Hsu, H.-Y., et al. (2004). "Extract of Reishi polysaccharides induces cytokine expression via TLR4-modulated protein kinase signaling pathways." The Journal of Immunology 173(10): 5989-5999.

Hsu, M. J., et al. (2002). "Polysaccharide purified from Ganoderma lucidum inhibits spontaneous and Fas-mediated apoptosis in human neutrophils through activation of the phosphatidylinositol 3 kinase/Akt signaling pathway." Journal of leukocyte biology 72(1): 207-216.

Hsu, R. C., et al. (2001). "The study of supercritical carbon dioxide extraction for Ganoderma lucidum." Industrial & engineering chemistry research 40(20): 4478-4481.

Huang, K. S., et al. (2014). "Synthesis of uniform core–shell gelatin–alginate microparticles as intestine-released oral delivery drug carrier." Electrophoresis 35(2-3): 330-336.

Huang, S. and X. Fu (2010) (a). "Naturally derived materials-based cell and drug delivery systems in skin regeneration." Journal of Controlled Release 142(2): 149-159.

Huang, S.-Q. et al. (2010) (b). "Optimization of alkaline extraction of polysaccharides from Ganoderma lucidum and their effect on immune function in mice." Molecules 15(5): 3694-3708.

Huang, S.-Q. and Z.-x. Ning (2010) (c). "Extraction of polysaccharide from Ganoderma lucidum and its immune enhancement activity." International journal of biological macromolecules 47(3): 336-341.

Huang, X.-l., et al. (2006). "Analysis of polysaccharide from broken cellular wall and unbroken spore of Ganoderma lucidum." Chinese Traditional and Herbal Drugs 37(6): 813.

Hughes, J. P., et al. (2011). "Principles of early drug discovery." British journal of pharmacology 162(6): 1239-1249.

Huie, C. W. (2002). "A review of modern sample-preparation techniques for the extraction and analysis of medicinal plants." Analytical and bioanalytical chemistry 373(1-2): 23-30.

Hung, T. M., et al. (2015). "An Improved HPLC-DAD Method for Quantitative Comparisons of Triterpenes in Ganoderma lucidum and Its Five Related Species Originating from Vietnam." Molecules 20(1).

*Novelty processing and smart delivery of Ganoderma Lucidum spores*

Ibragimova, M. K., Tsyganov, M. M., & Litviakov, N. V. (2017). Natural and chemotherapy-induced clonal evolution of tumors. Biochemistry (Moscow), 82(4), 413-425.

Ibrahim, M. A., et al. (2005). "Stability of insulin during the erosion of poly (lactic acid) and poly (lactic-co-glycolic acid) microspheres." Journal of Controlled Release 106(3): 241-252.

Ikekawa, T. (2001). "Beneficial effects of edible and medicinal mushrooms on health care." International Journal of Medicinal Mushrooms 3(4).

Ikekawa, T., et al. (1969). "Antitumor activity of aqueous extracts of edible mushrooms." Cancer research 29(3): 734-735.

Izadi, M., et al. Microemulsion Flow in Porous Media: Potential Impact on Productivity Loss, Society of Petroleum Engineers.

Jackson, M. and H. H. Mantsch (1995). "The use and misuse of FTIR spectroscopy in the determination of protein structure." Critical reviews in biochemistry and molecular biology 30(2): 95-120.

Jacotet-Navarro, M., et al. (2018). "What is the best ethanol-water ratio for the extraction of antioxidants from rosemary? Impact of the solvent on yield, composition, and activity of the extracts." Electrophoresis.

Jadhav, S. A., et al. (2016). "Effect of multimodal pore channels on cargo release from mesoporous silica nanoparticles." Journal of Nanomaterials 2016.

Jahangirian, H., et al. (2017). "A review of drug delivery systems based on nanotechnology and green chemistry: green nanomedicine." International journal of nanomedicine 12: 2957.

Jain, D. and D. Bar-Shalom (2014). "Alginate drug delivery systems: application in context of pharmaceutical and biomedical research." Drug development and industrial pharmacy 40(12): 1576-1584.

Jain, R., et al. (1998). "Controlled drug delivery by biodegradable poly (ester) devices: different preparative approaches." Drug development and industrial pharmacy 24(8): 703-727.

Jamaati, R., et al. (2014). "Comparison of microparticles and nanoparticles effects on the bonding of roll bonded IF steel." Transactions of the Indian Institute of Metals 67(5): 659-665.

Jang, B., et al. (2015). "Undulatory locomotion of magnetic multilink nanoswimmers." Nano letters 15(7): 4829-4833.

Jang, K., et al. (2010). "Single-cell attachment and culture method using a photochemical reaction in a closed microfluidic system." Biomicrofluidics 4(3): 032208.

Jaworek, A. (2007). "Micro-and nanoparticle production by electrospraying." Powder technology 176(1): 18-35.

Jaya, S., et al. (2009). "Effect of alginate-pectin composition on drug release characteristics of microcapsules." Journal of microencapsulation 26(2): 143-153.

Jeyhani, M., et al. (2018). "Controlled electrospray generation of nonspherical alginate microparticles." ChemPhysChem 19(16): 2113-2118.

Ji, D., et al. (2017). "Frozen "Tofu" Effect: Engineered Pores of Hydrophilic Nanoporous Materials." ACS Omega 2(8): 4838-4844.

*Novelty processing and smart delivery of Ganoderma Lucidum spores*

Ji, Z., et al. (2007). "Immunomodulation of RAW264. 7 macrophages by GLIS, a proteopolysaccharide from Ganoderma lucidum." Journal of ethnopharmacology 112(3): 445-450.

Jiang, J., et al. (2008). "Ganoderic acids suppress growth and invasive behavior of breast cancer cells by modulating AP-1 and NF-κB signaling." International journal of molecular medicine 21(5): 577-584.

Jiang, J., et al. (2004). "Ganoderma lucidum suppresses growth of breast cancer cells through the inhibition of Akt/NF-κB signaling." Nutrition and cancer 49(2): 209-216.

Jiang, J., et al. (2017). "Ginsenoside Rg3 enhances the anti-proliferative activity of erlotinib in pancreatic cancer cell lines by downregulation of EGFR/PI3K/Akt signaling pathway." Biomedicine & Pharmacotherapy 96: 619-625.

Jiang, Y., et al. (2010). "Recent analytical approaches in quality control of traditional Chinese medicines—a review." Analytica chimica acta 657(1): 9-18.

Jiang, Z., et al. (2011). "Effects of Ganoderic acid Me on inhibiting multidrug resistance and inducing apoptosis in multidrug resistant colon cancer cells." Process biochemistry 46(6): 1307-1314.

Jiang, Z.-M., et al. (2018). "Ganoderic acid A potentiates the antioxidant effect and protection of mitochondrial membranes and reduces the apoptosis rate in primary hippocampal neurons in magnesium free medium." Die Pharmazie-An International Journal of Pharmaceutical Sciences 73(2): 87-91.

Jin, Z., et al. (2015). "Pharmacokinetics and oral bioavailability of ganoderic acid A by high performance liquid chromatography-tandem mass spectrometry." International Journal Of Pharmacology 11: 27-34.

Jindal, A. B. (2017). "The effect of particle shape on cellular interaction and drug delivery applications of micro-and nanoparticles." International journal of pharmaceutics 532(1): 450-465.

Jing, C., et al. (2017). "Extraction optimization, preliminary characterization and antioxidant activities of polysaccharides from Glycine soja." International journal of biological macromolecules 103: 1207-1216.

Jinzhe, H., et al. (2010). "Analysis of structural characteristics of polysaccharide from Ganoderma lucidum." Chinese Journal of Analytical Chemistry 38(3): 372-376.

Jo, E.-K., et al. (2013). "The effects of subcritical water treatment on antioxidant activity of golden oyster mushroom." Food and bioprocess technology 6(9): 2555-2561.

Joana Gil-Chávez, G., et al. (2013). "Technologies for extraction and production of bioactive compounds to be used as nutraceuticals and food ingredients: an overview." Comprehensive Reviews in Food Science and Food Safety 12(1): 5-23.

Johansson, L. (2006). "Structural analyses of (1-> 3),(1-> 4)-β-D-glucan of oats and barley."

Johnson, B. M., et al. (2010). "Ganoderic acid DM: an alternative agent for the treatment of advanced prostate cancer." The open prostate cancer journal 3: 78.

Jovanović, A. A., et al. (2017). "Optimization of the extraction process of polyphenols from Thymus serpyllum L. herb using maceration, heat-and ultrasound-assisted techniques." Separation and Purification Technology 179: 369-380.

*Novelty processing and smart delivery of Ganoderma Lucidum spores*

Jun, T. and F. Ke-yan (1990). "Experimental and clinical studies on inhibitory effect of Ganoderma lucidum on platelet aggregation." Journal of Tongji Medical University 10(4): 240-243.

Kaczmarek-Pawelska, A., et al. (2017). "Alginate based hydrogel for tissue regeneration: optimization, antibacterial activity and mechanical properties." Journal of Achievements in Materials and Manufacturing Engineering 81(1).

Kaklamani, G., et al. (2018). "On the electrical conductivity of alginate hydrogels." Regenerative biomaterials 5(5): 293-301.

Kamaly, N., et al. (2016). "Degradable controlled-release polymers and polymeric nanoparticles: mechanisms of controlling drug release." Chemical reviews 116(4): 2602-2663.

Kamble Sharad, K. and S. Shinde Sunita (2017). "Design and Development of Fast Dissolving Tablet of Gliclazide." J Develop Drugs 6(177): 2.

Kamra, A. and A. B. Bhatt (2012). "Evaluation of antimicrobial and antioxidant activity of Ganoderma lucidum extracts against human pathogenic bacteria." International Journal of Pharmacy and Pharmaceutical Sciences 4(2): 359-362.

Kan, Y., et al. (2015). "Antioxidant activity of polysaccharide extracted from Ganoderma lucidum using response surface methodology." International journal of biological macromolecules 72: 151-157.

Kansal, A. R., et al. (2000). "Emergence of a subpopulation in a computational model of tumor growth." Journal of Theoretical Biology 207(3): 431-441.

Kao, P.-F., et al. (2011). "Structural characterization and antioxidative activity of low-molecular-weights beta-1, 3-glucan from the residue of extracted Ganoderma lucidum fruiting bodies." BioMed research international 2012.

Kapishon, V., et al. (2015). "Polymerization induced self-assembly of alginate based amphiphilic graft copolymers synthesized by single electron transfer living radical polymerization." Biomacromolecules 16(7): 2040-2048.

Katiyar, C., et al. (2012). "Drug discovery from plant sources: An integrated approach." Ayu 33(1): 10.

Katt, M. E., et al. (2016). "In vitro tumor models: advantages, disadvantages, variables, and selecting the right platform." Frontiers in bioengineering and biotechnology 4: 12.

Ke, L. Q. (2015). "Optimization of Ultrasonic Extraction of Polysaccharides from L entinus Edodes Based on Enzymatic Treatment." Journal of Food Processing and Preservation 39(3): 254-259.

Kelishomi, Z. H., et al. (2016). "Antioxidant activity of low molecular weight alginate produced by thermal treatment." Food chemistry 196: 897-902.

Keraliya, R. A., et al. (2012). "Osmotic drug delivery system as a part of modified release dosage form." ISRN pharmaceutics 2012.

Keypour, S., et al. (2010). "Separation and identification of different ganoderic acids from Ganoderma lucidum of East and West of Asia by hyphenated RP-HPLC and mass spectrometry." Food Chem 119(4): 1704-1708.

Khademhosseini, A., et al. (2006). "Micromolding of photocrosslinkable hyaluronic acid for cell encapsulation and entrapment." Journal of Biomedical Materials Research Part A: An Official

*Novelty processing and smart delivery of Ganoderma Lucidum spores*

Journal of The Society for Biomaterials, The Japanese Society for Biomaterials, and The Australian Society for Biomaterials and the Korean Society for Biomaterials 79(3): 522-532.

Khorram, M., et al. (2015). "Electrospray preparation of propranolol-loaded alginate beads: Effect of matrix reinforcement on loading and release profile." Journal of applied polymer science 132(4).

Kiarostami, V., et al. (2014). "Binary solvents dispersive liquid—liquid microextraction (BS-DLLME) method for determination of tramadol in urine using high-performance liquid chromatography." DARU Journal of Pharmaceutical Sciences 22(1): 25.

Kidd, P. M. (2000). "The use of mushroom glucans and proteoglycans in cancer treatment." Alternative medicine review 5(1): 4-27.

Kikuchi, A., et al. (1997). "Pulsed dextran release from calcium-alginate gel beads." Journal of Controlled Release 47(1): 21-29.

KikucHi, T., et al. (1986). "Constituents of the Fungus Ganoderma lucidum (FR.) KARST. II.: Structures of Ganoderic acids F, G, and H, Lucidenic acids D2 and E2, and related compounds." Chemical and Pharmaceutical Bulletin 34(10): 4018-4029.

Kılıçarslan, M. and T. Baykara (2003). "The effect of the drug/polymer ratio on the properties of the verapamil HCl loaded microspheres." International journal of pharmaceutics 252(1-2): 99-109.

Kim, H. and S. S. Kim (2015). "Development and Characterization of Saw-Tooth-Type Slit Nozzle for Electrospray." Aerosol Science and Technology 49(1): 11-15.

Kim, H., et al. (2018). "Micro-/nano-sized delivery systems of ginsenosides for improved systemic bioavailability" Journal of ginseng research 42(3): 361-369.

Kimura, Y., et al. (2002). "Antitumor and antimetastatic effects on liver of triterpenoid fractions of Ganoderma lucidum: mechanism of action and isolation of an active substance." Anticancer research 22(6A): 3309-3318.

Kino, K., et al. (1989). "Isolation and characterization of a new immunomodulatory protein, ling zhi-8 (LZ-8), from Ganoderma lucidium." Journal of Biological Chemistry 264(1): 472-478.

Kitching, S. and A. M. Donald (1998). "Beam damage of polypropylene in the environmental scanning electron microscope: an FTIR study." Journal of Microscopy 190(3): 357-365.

Kivelä, R., et al. (2012). "Oxidation of oat β-glucan in aqueous solutions during processing." Carbohydrate polymers 87(1): 589-597.

Klöck, G., et al. (1997). "Biocompatibility of mannuronic acid-rich alginates." Biomaterials 18(10): 707-713.

Klose, D., et al. (2006). "How porosity and size affect the drug release mechanisms from PLGA-based microparticles." International journal of pharmaceutics 314(2): 198-206.

Koetting, M. C., et al. (2016). "pH-responsive and enzymatically-responsive hydrogel microparticles for the oral delivery of therapeutic proteins: effects of protein size, crosslinking density, and hydrogel degradation on protein delivery." Journal of Controlled Release 221: 18-25.

Kohane, D. S. (2007). "Microparticles and nanoparticles for drug delivery." Biotechnology and Bioengineering 96(2): 203-209.

*Novelty processing and smart delivery of Ganoderma Lucidum spores*

Kohsuke, K., et al. (1991). "Immunomodulator, LZ-8, prevents antibody production in mice." International journal of immunopharmacology 13(8): 1109-1115.

Koo, S. Y., et al. (2014). "Microencapsulation of peppermint oil in an alginate–pectin matrix using a coaxial electrospray system." International journal of food science & technology 49(3): 733-739.

Krieger, M. S., et al. (2000). "Extraction of cloransulam-methyl from soil with subcritical water and supercritical $CO_2$." Journal of Chromatography A 897(1-2): 405-413.

Krishna, G., et al. (1998). "Improving Emulsification Efficacy of Lecithin by Formulation Design I: Effect of Adding a Secondary Surfactant." PDA journal of pharmaceutical science and technology 52(6): 331-336.

Krochta, J. M., et al. (1987). "Degradation of polysaccharides in alkaline solution to organic acids: Product characterization and identification." Journal of applied polymer science 33(4): 1413-1425.

Ku, B. K. and S. S. Kim (2002). "Electrospray characteristics of highly viscous liquids." Journal of Aerosol Science 33(10): 1361-1378.

Kuang, L. L., et al. (2005). "On the fabrication of microparticles using electrohydrodynamic atomization method."

Kudgus, R. A., et al. (2014). "Tuning pharmacokinetics and biodistribution of a targeted drug delivery system through incorporation of a passive targeting component." Scientific reports 4: 5669.

Kumar, M. (2000). "Nano and microparticles as controlled drug delivery devices." J. Pharm. Pharm. Sci 3(2): 234-258.

Kumar, S. and V. Mahto (2017). "Emulsification of Indian heavy crude oil using a novel surfactant for pipeline transportation." Petroleum Science 14(2): 372-382.

Kumari, A., et al. (2014). "Nanoencapsulation for drug delivery." EXCLI journal 13: 265.

Kumari, B., et al. (2018). "Recent advances on application of ultrasound and pulsed electric field technologies in the extraction of bioactives from agro-industrial by-products." Food and bioprocess technology 11(2): 223-241.

Kuo, C. K. and P. X. Ma (2008). "Maintaining dimensions and mechanical properties of ionically crosslinked alginate hydrogel scaffolds in vitro." Journal of Biomedical Materials Research Part A: An Official Journal of The Society for Biomaterials, The Japanese Society for Biomaterials, and The Australian Society for Biomaterials and the Korean Society for Biomaterials 84(4): 899-907.

Kwak, J. C. T. and R. C. Hayes (1975). "Electrical conductivity of aqueous solutions of salts of polystyrenesulfonic acid with univalent and divalent counterions." The Journal of Physical Chemistry 79(3): 265-269.

La-Beck, N. M. and A. A. Gabizon (2017). "Nanoparticle interactions with the immune system: Clinical implications for liposome-based cancer chemotherapy." Frontiers in immunology 8: 416.

Lai, G., et al. (2019). "Alcohol extracts from Ganoderma lucidum delay the progress of Alzheimer's disease by regulating DNA methylation in rodents." Frontiers in pharmacology 10: 272.

*Novelty processing and smart delivery of Ganoderma Lucidum spores*

Lakshmi, B., et al. (2003). "Antiperoxidative, anti-inflammatory, and antimutagenic activities of ethanol extract of the mycelium of Ganoderma lucidum occurring in South India." Teratogenesis, carcinogenesis, and mutagenesis 23(S1): 85-97.

Lawther, J. M., et al. (1995). "Extraction, fractionation, and characterization of structural polysaccharides from wheat straw." Journal of Agricultural and Food Chemistry 43(3): 667-675.

Le Corre, P., et al. (1994). "Preparation and characterization of bupivacaine-loaded polylactide and polylactide-co-glycolide microspheres." International journal of pharmaceutics 107(1): 41-49.

Le, M. H., et al. (2016). "The dual effect of curcumin nanoparticles encapsulated by 1-3/1-6 β-glucan from medicinal mushrooms Hericium erinaceus and Ganoderma lucidum." Advances in Natural Sciences: Nanoscience and Nanotechnology 7(4): 045019.

Le, N.-T., et al. (2018). "Mapping electrospray modes and droplet size distributions for chitosan solutions in unentangled and entangled concentration regimes." Advanced Powder Technology.

Lee, J. S., et al. (2004). "Survival of freeze-dried Lactobacillus bulgaricus KFRI 673 in chitosan-coated calcium alginate microparticles." Journal of Agricultural and Food Chemistry 52(24): 7300-7305.

Lee, K. Y. and D. J. Mooney (2012). "Alginate: properties and biomedical applications." Progress in polymer science 37(1): 106-126.

Lee, S. H., et al. (2012). "Effect of temperature, solvent concentration, and pH on the β-glucan extraction." The Korean Journal of Food And Nutrition 25(4): 871-877.

Lee, S.-Y., et al. (2009). "Shaping nano-/micro-particles for enhanced vascular interaction in laminar flows." Nanotechnology 20(49): 495101.

Lee, W. C., et al. (2006). "Optimizing conditions for hot water extraction of banana juice using response surface methodology (RSM)." Journal of Food Engineering 75(4): 473-479.

Lefsrud, M., et al. (2008). "Dry matter content and stability of carotenoids in kale and spinach during drying." HortScience 43(6): 1731-1736.

Lei, N., et al. (2015). "Effects of low molecular weight yeast β-glucan on antioxidant and immunological activities in mice." International journal of molecular sciences 16(9): 21575-21590.

Leibovici, J., et al. (1986). "Effect of tumor inhibitory and stimulatory doses of levan, alone and in combination with cyclophosphamide, on spleen and lymph nodes." International journal of immunopharmacology 8(4): 391-403.

Leibovici, J., et al. (1985). "Opposite effects on tumor growth depending on dose of an immunomodulatory polysaccharide with or without cyclophosphamide." Anticancer research 5(5): 553-558.

Lemoine, D., et al. (1998). "Preparation and characterization of alginate microspheres containing a model antigen." International journal of pharmaceutics 176(1): 9-19.

Levayer, R., et al. (2016). "Tissue crowding induces caspase-dependent competition for space." Current Biology 26(5): 670-677.

Li, B.-Z., et al. (2009). "Fabrication of starch-based microparticles by an emulsification-crosslinking method." Journal of Food Engineering 92(3): 250-254.

*Novelty processing and smart delivery of Ganoderma Lucidum spores*

Li, C., et al. (2005). "Ganoderic acid Sz, a new lanostanoid from the mushroom Ganoderma lucidum." Natural product research 19(5): 461-465.

Li, C.-H., et al. (2005). "Ganoderic acid X, a lanostanoid triterpene, inhibits topoisomerases and induces apoptosis of cancer cells." Life sciences 77(3): 252-265.

Li, J., et al. (2008). "Identification of quantitative trait loci for β-glucan concentration in barley grain." Journal of cereal science 48(3): 647-655.

Li, J., et al. (2016). "Supercritical carbon dioxide extraction of Ganoderma lucidum spore lipids." LWT-Food Science and Technology 70: 16-23.

Li, K., et al. (2017). "The ethanol extracts of sporoderm-broken spores of Ganoderma lucidum inhibit colorectal cancer in vitro and in vivo." Oncology reports 38(5): 2803-2813.

Li, L., et al. (2015). "Effect of formulation variables on in vitro release of a water-soluble drug from chitosan–sodium alginate matrix tablets." Asian Journal of Pharmaceutical Sciences 10(4): 314-321.

Li, L.-F., et al. (2018). "Comprehensive comparison of polysaccharides from Ganoderma lucidum and G. sinense: chemical, antitumor, immunomodulating and gut-microbiota modulatory properties." Scientific reports 8(1): 6172.

Li, R., et al. (2010). "Solid lipid nanoparticles as drug delivery system for water-insoluble drugs." Journal of Pharmaceutical Investigation 40(spc): 63-73.

Li, Y., et al. (2018). "Ginsenoside Rg3 suppresses proliferation and induces apoptosis in human osteosarcoma." BioMed research international 2018.

Li, Y.-B., et al. (2013). "A new ganoderic acid from Ganoderma lucidum mycelia and its stability." Fitoterapia 84: 115-122.

Li, Z., et al. (2005). "Possible mechanism underlying the antiherpetic activity of a proteoglycan isolated from the mycelia of Ganoderma lucidum in vitro." BMB Reports 38(1): 34-40.

Li, Z. and H. N. Trick (2005). "Rapid method for high-quality RNA isolation from seed endosperm containing high levels of starch." Biotechniques 38(6): 872-876.

Lianfu, Z. and L. Zelong (2008). "Optimization and comparison of ultrasound/microwave assisted extraction (UMAE) and ultrasonic assisted extraction (UAE) of lycopene from tomatoes." Ultrasonics sonochemistry 15(5): 731-737.

Liang, J., et al. (2013). "The profiling and identification of the absorbed constituents and metabolites of Paeoniae Radix Rubra decoction in rat plasma and urine by the HPLC–DAD–ESI-IT-TOF-MSn technique: A novel strategy for the systematic screening and identification of absorbed constituents and metabolites from traditional Chinese medicines." Journal of pharmaceutical and biomedical analysis 83: 108-121.

Liao, N., et al. (2016). "Protein-bound polysaccharide from corbicula fluminea inhibits cell growth in MCF-7 and MDA-MB-231 human breast cancer cells." PloS one 11(12): e0167889.

Lin, C.-C. and A. T. Metters (2006). "Hydrogels in controlled release formulations: network design and mathematical modeling." Advanced drug delivery reviews 58(12-13): 1379-1408.

Lin, H.-J., et al. (2014). "An immunomodulatory protein (Ling Zhi-8) from a Ganoderma lucidum induced acceleration of wound healing in rat liver tissues after monopolar electrosurgery." Evidence-Based Complementary and Alternative Medicine 2014.

*Novelty processing and smart delivery of Ganoderma Lucidum spores*

Lin, S.-Y., et al. (1995). "Drug-polymer interaction affecting the mechanical properties, adhesion strength and release kinetics of piroxicam-loaded Eudragit E films plasticized with different plasticizers." Journal of Controlled Release 33(3): 375-381.

Lin, T. J. and J. C. Lambrechts (1969). "Effect of initial surfactant location on emulsion phase inversion."

Lin, Y. L., et al. (2005). "Polysaccharide purified from Ganoderma lucidum induced activation and maturation of human monocyte-derived dendritic cells by the NF-κB and p38 mitogen-activated protein kinase pathways." Journal of leukocyte biology 78(2): 533-543.

Lin, Z.-B., et al. (2002). "Effects of total triterpenoids extract from Ganoderma lucidum (Curt.: Fr.) P. Karst.(Reishi Mushroom) on experimental liver injury models induced by carbon tetrachloride or D-galactosamine in mice." International Journal of Medicinal Mushrooms 4(4).

Liu, A.-j., et al. (2018). "Extraction of a novel cold-water-soluble polysaccharide from Astragalus membranaceus and its antitumor and immunological activities." Molecules 23(1): 62.

Liu, C., et al. (2015). "Anti-inflammatory effects of Ganoderma lucidum triterpenoid in human crohn's disease associated with downregulation of NF-κB signaling." Inflammatory bowel diseases 21(8): 1918-1925.

Liu, E.-H., et al. (2005). "Effect of oil on emulsion characteristics: Manipulating the interfacial domain." The Journal of Physical Chemistry B 109(27): 13332-13341.

Liu, J., et al. (2009). "Combined yeast-derived β-glucan with anti-tumor monoclonal antibody for cancer immunotherapy." Experimental and molecular pathology 86(3): 208-214.

Liu, L., et al. (2017). "pH-Responsive carriers for oral drug delivery: challenges and opportunities of current platforms." Drug delivery 24(1): 569-581.

Liu, Q., et al. (2015). "Optimized Extraction of Crude Ganoderic Acid from Ganoderma lucidum Spore and Antioxidant Effect in Vivo." Food Science 2015(24): 17.

Liu, R.-M., et al. (2012). "Cytotoxic and pro-apoptotic effects of novel ganoderic acid derivatives on human cervical cancer cells in vitro." European journal of pharmacology 681(1-3): 23-33.

Liu, R.-M. and J.-J. Zhong (2011). "Ganoderic acid Mf and S induce mitochondria mediated apoptosis in human cervical carcinoma HeLa cells." Phytomedicine 18(5): 349-355.

Liu, W., et al. (2011). "Uniform chitosan microparticles prepared by a novel spray-drying technique." International Journal of Chemical Engineering 2011.

Liu, X., Yuan, J. P., Chung, C. K., & Chen, X. J. (2002). Antitumor activity of the sporoderm-broken germinating spores of Ganoderma lucidum. Cancer letters, 182(2), 155-161.

Liu, Y., et al. (2011). "Sensitive and selective liquid chromatography–tandem mass spectrometry method for the determination of five ganoderic acids in Ganoderma lucidum and its related species." Journal of pharmaceutical and biomedical analysis 54(4): 717-721.

Liu, Y., et al. (2015). "Optimization of ultrasonic extraction of polysaccharides from Hovenia dulcis peduncles and their antioxidant potential." International journal of biological macromolecules 80: 350-357.

Liu, Y., et al. (2012). "The shape of things to come: importance of design in nanotechnology for drug delivery." Therapeutic delivery 3(2): 181-194.

*Novelty processing and smart delivery of Ganoderma Lucidum spores*

Liu, Y., et al. (2018). "Triple helix conformation of β-d-glucan from Ganoderma lucidum and effect of molecular weight on its immunostimulatory activity." International journal of biological macromolecules 114: 1064-1070.

Liu, Y., et al. (2014). "Physicochemical characterization of a high molecular weight bioactive β-D-glucan from the fruiting bodies of Ganoderma lucidum." Carbohydrate polymers 101: 968-974.

Liu, Z., et al. (2008). "Polysaccharides-based nanoparticles as drug delivery systems." Advanced drug delivery reviews 60(15): 1650-1662.

Locksley, R. M., et al. (2001). "The TNF and TNF receptor superfamilies: integrating mammalian biology." Cell 104(4): 487-501.

Lopez-Diago, L., et al. (2018). "Evaluation of the Production of Starch from Bitter Cassava (Manihot utilissima) using Different Methodologies." Chemical Engineering Transactions 65: 613-618.

Losso, J. N. and R. R. Bansode (2004). Anti-angiogenic functional food, degenerative disease and cancer. Functional Foods, Ageing and Degenerative Disease, Elsevier: 485-523.

Loyd, A. L., et al. (2018). "Identifying the "mushroom of immortality": assessing the Ganoderma species composition in commercial Reishi products." Frontiers in Microbiology 9.

Lu, F., et al. (2009). "Size effect on cell uptake in well-suspended, uniform mesoporous silica nanoparticles." Small 5(12): 1408-1413.

Lu, J., et al. (2010). "Biocompatibility, biodistribution, and drug-delivery efficiency of mesoporous silica nanoparticles for cancer therapy in animals." Small 6(16): 1794-1805.

Lu, J., et al. (2012). "Quality difference study of six varieties of Ganoderma lucidum with different origins." Frontiers in pharmacology 3: 57.

Lu, Q.-Y., et al. (2004). "Ganoderma lucidum extracts inhibit growth and induce actin polymerization in bladder cancer cells in vitro." Cancer letters 216(1): 9-20.

Lu, X.-Y., et al. (2011). Polymer nanoparticles. Progress in molecular biology and translational science, Elsevier. 104: 299-323.

Lucinda-Silva, R. M. and R. C. Evangelista (2005). "Studies on the formation of complex coacervates between chitosan and alginate during microparticles preparation." acta farmacéutica bonaerense 24(3): 366.

Luo, C. J., et al. (2015). "Preparation of polymeric nanoparticles by novel electrospray nanoprecipitation." Polymer International 64(2): 183-187.

Luo, X., et al. (2008). "Characterisation and immunostimulatory activity of an α-(1→ 6)-d-glucan from the cultured Armillariella tabescens mycelia." Food chemistry 111(2): 357-363.

Lupo, B., et al. (2014). "Preparation of alginate microspheres by emulsification/internal gelation to encapsulate cocoa polyphenols." Food Hydrocolloids 38: 56-65.

Ma, B., et al. (2011). "Triterpenoids from the spores of Ganoderma lucidum." North American journal of medical sciences 3(11): 495.

Ma, J., et al. (2007). "Breaking and characteristics of Ganoderma lucidum spores by high speed entrifugal shearing pulverizer." Journal of Wuhan University of Technology-Mater. Sci. Ed. 22(4): 617-621.

*Novelty processing and smart delivery of Ganoderma Lucidum spores*

Ma, J., et al. (2002). "New Lanostanoids from the Mushroom Ganoderma l ucidum." Journal of natural products 65(1): 72-75.

Ma, Y., et al. (2018). "Assessment of Polysaccharides from Mycelia of genus Ganoderma by Mid-Infrared and Near-Infrared Spectroscopy." Scientific reports 8(1): 10.

Machado, A. H. E., et al. (2012). "Preparation of calcium alginate nanoparticles using water-in-oil (W/O) nanoemulsions." Langmuir 28(9): 4131-4141.

Maeda, Y. Y. and G. Chihara (1971). "Lentinan, a new immuno-accelerator of cell-mediated responses." Nature 229(5287): 634-634.

Maeda, Y. Y., et al. (1971). "The mechanisms of action of anti-tumour polysaccharides. I. The effects of antilymphocyte serum on the anti-tumour activity of lentinan." International journal of cancer 8(1): 41-46.

Maghsoodi, M. and Z. Yari (2015). "Effect of drying phase on the agglomerates prepared by spherical crystallization." Iranian journal of pharmaceutical research: IJPR 14(1): 51.

Sao Mai, D., An, T. T. T., Binh, T. T., & Anh, N. D. (2015). Comparison of the effect of using cellulase, microwave and ultra-sonication on crude polysaccharides extraction from Vietnamese Lingzhi (Ganoderma lucidum). Journal of Food and Nutrition Sciences, 3(1-2), 49-53.

Maioli, E., et al. (2009). "Critical appraisal of the MTT assay in the presence of rottlerin and uncouplers." Biological procedures online 11(1): 227.

Makadia, H. K. and S. J. Siegel (2011). "Poly lactic-co-glycolic acid (PLGA) as biodegradable controlled drug delivery carrier." Polymers 3(3): 1377-1397.

Malana, M. A. and R. Zohra (2013). "The release behavior and kinetic evaluation of tramadol HCl from chemically cross linked Ter polymeric hydrogels." DARU Journal of Pharmaceutical Sciences 21(1): 10.

Mandal, B., et al. (2010). "Evaluation of the drug-polymer interaction in calcium alginate beads containing diflunisal." Die Pharmazie-An International Journal of Pharmaceutical Sciences 65(2): 106-109.

Mandal, S., et al. (2009). "Sustained release of a water-soluble drug from alginate matrix tablets prepared by wet granulation method." Aaps Pharmscitech 10(4): 1348.

Mandal, S., et al. (2010). "Development and evaluation of calcium alginate beads prepared by sequential and simultaneous methods." Brazilian journal of pharmaceutical sciences 46(4): 785-793.

Mantell, C., et al. (2003). "A screening analysis of the high-pressure extraction of anthocyanins from red grape pomace with carbon dioxide and cosolvent." Engineering in life sciences 3(1): 38-42.

Maran, J. P., et al. (2013). "Box–Behnken design based statistical modeling for ultrasound-assisted extraction of corn silk polysaccharide." Carbohydrate polymers 92(1): 604-611.

Marcus, Y. (1989). "Diluent effects in solvent extraction." Solvent Extraction and Ion Exchange 7(4): 567-575.

Marijnissen, J. C. M., et al. (2010). Medicine nanoparticle production by EHDA. Nanoparticles in medicine and environment, Springer: 39-57.

*Novelty processing and smart delivery of Ganoderma Lucidum spores*

Masaro, L. and X. X. Zhu (1999). "Physical models of diffusion for polymer solutions, gels and solids." Progress in polymer science 24(5): 731-775.

Mason, T. G. and J. Bibette (1997). "Shear rupturing of droplets in complex fluids." Langmuir 13(17): 4600-4613.

Mason, T. J. (2000). "Large scale sonochemical processing: aspiration and actuality." Ultrasonics sonochemistry 7(4): 145-149.

Mason, T. J., et al. (1996). "The uses of ultrasound in food technology." Ultrasonics sonochemistry 3(3): S253-S260.

Mathaes, R., et al. (2015). "Non-spherical micro-and nanoparticles: fabrication, characterization and drug delivery applications." Expert opinion on drug delivery 12(3): 481-492.

Matsunaga, Y., et al. (2014). "Hot compressed water extraction of polysaccharides from Ganoderma lucidum using a semibatch reactor." Asia-Pacific Journal of Chemical Engineering 9(1): 125-133.

Max, J.-J. and C. Chapados (2004). "Infrared spectroscopy of aqueous carboxylic acids: comparison between different acids and their salts." The Journal of Physical Chemistry A 108(16): 3324-3337.

May, R. C. and L. M. Machesky (2001). "Phagocytosis and the actin cytoskeleton." Journal of cell science 114(6): 1061-1077.

Mazutis, L., et al. (2015). "Microfluidic production of alginate hydrogel particles for antibody encapsulation and release." Macromolecular bioscience 15(12): 1641-1646.

McKee, J. (1988). "Holistic health and the critique of Western medicine." Social science & medicine 26(8): 775-784.

Md, S., et al. (2011). "Gastroretentive drug delivery system of acyclovir-loaded alginate mucoadhesive microspheres: formulation and evaluation." Drug delivery 18(4): 255-264.

Mehregan Nikoo, A., et al. (2016). "Controlling the morphology and material characteristics of electrospray generated calcium alginate microhydrogels." Journal of microencapsulation 33(7): 605-612.

Mello, B. C. B. S., et al. (2010). "Concentration of flavonoids and phenolic compounds in aqueous and ethanolic propolis extracts through nanofiltration." Journal of Food Engineering 96(4): 533-539.

Meng, F., et al. (2009). "Electrohydrodynamic liquid atomization of biodegradable polymer microparticles: Effect of electrohydrodynamic liquid atomization variables on microparticles." Journal of applied polymer science 113(1): 526-534.

Mengus, C., et al. (2017). "In Vitro Modeling of Tumor–Immune System Interaction." ACS Biomaterials Science & Engineering 4(2): 314-323.

Miao, Y., et al. (2005). "Advance in research on the hydrolysis of plant polysaccharide and products." Chinese Wild Plant Resources 24(2): 4-5.

Michalke, B., et al. (2002). "Effect of different extraction procedures on the yield and pattern of Se-species in bacterial samples." Analytical and bioanalytical chemistry 372(3): 444-447.

*Novelty processing and smart delivery of Ganoderma Lucidum spores*

Michel, M. and K. Autio (2001). Effects of high pressure on protein-and polysaccharide-based structures. Ultra high pressure treatments of foods, Springer: 189-214.

Min, B. S., et al. (2001). "Anticomplement activity of terpenoids from the spores of Ganoderma lucidum." Planta medica 67(09): 811-814.

Min, B.-S., et al. (2000). "Triterpenes from the spores of Ganoderma lucidum and their cytotoxicity against meth-A and LLC tumor cells." Chemical and Pharmaceutical Bulletin 48(7): 1026-1033.

Min, B.-S., et al. (1998). "Triterpenes from the spores of Ganoderma lucidum and their inhibitory activity against HIV-1 protease." Chemical and Pharmaceutical Bulletin 46(10): 1607-1612.

Mirzayans, R., et al. (2016). "The growing complexity of cancer cell response to DNA-damaging agents: caspase 3 mediates cell death or survival?" International journal of molecular sciences 17(5): 708.

Mirzayans, R., et al. (2017). "Significance of wild-type p53 signaling in suppressing apoptosis in response to chemical genotoxic agents: Impact on chemotherapy outcome." International journal of molecular sciences 18(5): 928.

Mirzayans, R., et al. (2018). "Roles of polyploid/multinucleated giant cancer cells in metastasis and disease relapse following anticancer treatment." Cancers 10(4): 118.

Mirzayans, R., et al. (2017). "Multinucleated giant cancer cells produced in response to ionizing radiation retain viability and replicate their genome." International journal of molecular sciences 18(2): 360.

Mishra, A., et al. (2011). "Translocation of HIV TAT peptide and analogues induced by multiplexed membrane and cytoskeletal interactions." Proceedings of the National Academy of Sciences 108(41): 16883-16888.

Mishra, J., et al. (2018). "Phenolic Rich Fractions from Mycelium and Fruiting Body of Ganoderma lucidum Inhibit Bacterial Pathogens Mediated by Generation of Reactive Oxygen Species and Protein Leakage and Modulate Hypoxic Stress in HEK 293 Cell Line." Advances in pharmacological sciences 2018.

Mitra, R., et al. (2009). "Back to nature-medicinal plants of Nepal point new direction to drug discovery." Asia Pacific biotech news 13(2): 50-53.

Miyazaki, T. and M. Nishijima (1981). "Studies on fungal polysaccharides. XXVII. Structural examination of a water-soluble, antitumor polysaccharide of Ganoderma lucidum." Chemical and Pharmaceutical Bulletin 29(12): 3611-3616.

Mizuno, T., et al. (1984). "Fractionation, structural features and antitumor activity of water-soluble polysaccharide from" Reishi", the fruit body of Ganoderma lucidum." Journal of the Agricultural Chemical Society of Japan (Japan).

Mlyuka, E., et al. (2016). "Characteristics of subcritical water extraction and kinetics of pentacyclic triterpenoids from dry loquat (Eriobotrya japonica) leaves." International Journal of Food Engineering 12(6): 547-555.

Moco, S., et al. (2006). "A liquid chromatography-mass spectrometry-based metabolome database for tomato." Plant Physiology 141(4): 1205-1218.

*Novelty processing and smart delivery of Ganoderma Lucidum spores*

Moghadam, H., et al. (2008). "Electro-spray of high viscous liquids for producing mono-sized spherical alginate beads." Particuology 6(4): 271-275.

Moghadam, H., et al. (2009). "Study of parameters affecting size distribution of beads produced from electro-spray of high viscous liquids." Iran. J. Chem. Eng 6(3): 83-98.

Moghadam, H., et al. (2010). "Electrospray modeling of highly viscous and non-Newtonian liquids." Journal of applied polymer science 118(3): 1288-1296.

Moghimi, S. M., et al. (2001). "Long-circulating and target-specific nanoparticles: theory to practice." Pharmacological reviews 53(2): 283-318.

Mohamad, M., et al. (2013). "Effect of extraction process parameters on the yield of bioactive compounds from the roots of Eurycoma longifolia." Jurnal Teknologi 60(1): 51-57.

Mohan, K., et al. (2017). "Anti-cancer effect of the polysaccharide extract from the Ganoderma lucidum against HeLa cell lines." Bangladesh Journal of Pharmacology 12(1): 56-57.

Montañés, F., et al. (2007). "Modeling solubilities of sugars in alcohols based on original experimental data." AIChE journal 53(9): 2411-2418.

Moradpour, H., et al. (2011). "Phase inversion in water–oil emulsions with and without gas hydrates." Energy & Fuels 25(12): 5736-5745.

Mora-Huertas, C. E., et al. (2010). "Polymer-based nanocapsules for drug delivery." International journal of pharmaceutics 385(1-2): 113-142.

Moreno-Mendieta, S., et al. (2017). "Potential of glucans as vaccine adjuvants: A review of the α-glucans case." Carbohydrate polymers 165: 103-114.

Moser, A. and M. Feuchter (2016). "Mechanical properties of composites used in high-voltage applications." Polymers 8(7): 260.

Müller, C. I., et al. (2006). "Ganoderma lucidum causes apoptosis in leukemia, lymphoma and multiple myeloma cells." Leukemia research 30(7): 841-848.

Murata, C., et al. (2016). "Extraction and isolation of ganoderic acid Σ from Ganoderma lucidum." Tetrahedron Letters 57(48): 5368-5371.

Murata, Y., et al. (2007). "The drug release profile from calcium-induced alginate gel beads coated with an alginate hydrolysate." Molecules 12(11): 2559-2566.

Murata, Y., et al. (2009). "Drug release profile from calcium-induced alginate-phosphate composite gel beads." International Journal of Polymer Science 2009.

Murata, Y., et al. (1993). "Preparation of chitosan-reinforced alginate gel beads—effects of chitosan on gel matrix erosion." International journal of pharmaceutics 96(1-3): 139-145.

Mustafa, A. and C. Turner (2011). "Pressurized liquid extraction as a green approach in food and herbal plants extraction: A review." Analytica chimica acta 703(1): 8-18.

Na, K., et al. (2017). "Anticarcinogenic effects of water extract of sporoderm-broken spores of Ganoderma lucidum on colorectal cancer in vitro and in vivo." International journal of oncology 50(5): 1541-1554.

Nagarwal, R. C., et al. (2009). "Polymeric nanoparticulate system: a potential approach for ocular drug delivery." Journal of Controlled Release 136(1): 2-13.

*Novelty processing and smart delivery of Ganoderma Lucidum spores*

Nagayasu, A., et al. (1999). "The size of liposomes: a factor which affects their targeting efficiency to tumors and therapeutic activity of liposomal antitumor drugs." Advanced drug delivery reviews 40(1-2): 75-87.

Nair, L. S. and C. T. Laurencin (2007). "Biodegradable polymers as biomaterials." Progress in polymer science 32(8-9): 762-798.

Nambi, V. E., et al. (2016). "Degradation kinetics of bioactive components, antioxidant activity, colour and textural properties of selected vegetables during blanching." Journal of food science and technology 53(7): 3073-3082.

Nandi, L. G., et al. (2013). "Properties of aqueous solutions of lentinan in the absence and presence of zwitterionic surfactants." Carbohydrate polymers 98(1): 1-7.

Nanjwade, B. K., et al. (2011). "Design and characterization of nanocrystals of lovastatin for solubility and dissolution enhancement." J Nanomedic Nanotechnol 2(2): 107.

Nedović, V. A., et al. (2001). "Electrostatic generation of alginate microbeads loaded with brewing yeast." Process biochemistry 37(1): 17-22.

Nep, E. I. and B. R. Conway (2011). "Physicochemical characterization of grewia polysaccharide gum: Effect of drying method." Carbohydrate polymers 84(1): 446-453.

Newman, D. J. and G. M. Cragg (2007). "Natural products as sources of new drugs over the last 25 years." Journal of natural products 70(3): 461-477.

Ng, T. B. (1998). "A review of research on the protein-bound polysaccharide (polysaccharopeptide, PSP) from the mushroom Coriolus versicolor (Basidiomycetes: Polyporaceae)." General Pharmacology: The Vascular System 30(1): 1-4.

Nguyen, D. N., et al. (2016). "Pharmaceutical applications of electrospraying." Journal of pharmaceutical sciences 105(9): 2601-2620.

Nguyen, M. T., & Nguyen, T. M. T. (2015). Extraction of bioactive compounds and spore powder collection from Ganoderma lucidum. Can tho University Journal of Science, (01), 53-60.

Nguyen, N.-T., et al. (2013). "Design, fabrication and characterization of drug delivery systems based on lab-on-a-chip technology." Advanced drug delivery reviews 65(11-12): 1403-1419.

Ngwuluka, N. C., et al. (2014). "Naturapolyceutics: the science of utilizing natural polymers for drug delivery." Polymers 6(5): 1312-1332.

Nhi, N. N. Y. and P. V. Hung (2012). "Nutritional composition and antioxidant capacity of several edible mushrooms grown in the Southern Vietnam."

Niazi, S. K. (2016). Specifications: Test Procedures and Acceptance Criteria for New Drug Substances and New Drug Products: Chemical Substances. Handbook of Pharmaceutical Manufacturing Formulations, CRC Press: 115-135.

Nikoo, A. M., et al. (2018). "Electrospray-assisted encapsulation of caffeine in alginate microhydrogels." International journal of biological macromolecules 116: 208-216.

Nikumbh, A. and G. Kulkarni (2013). "Density and Viscosity Study of Binary Mixtures of Ethanol-Water at Different Temperatures." Science Journal of Pure and Applied Chemistry 2013.

Ning, Y., et al. (2016). "β-glucan restores tumor-educated dendritic cell maturation to enhance antitumor immune responses." International journal of cancer 138(11): 2713-2723.

*Novelty processing and smart delivery of Ganoderma Lucidum spores*

Nishitani Yukuyama, M., et al. (2017). "Challenges and future prospects of nanoemulsion as a drug delivery system." Current pharmaceutical design 23(3): 495-508.

Nishitoba, T., et al. (1988). "Novel triterpenoids from the fungus Ganoderma lucidum." Agricultural and biological chemistry 52(2): 367-372.

Niu, N., et al. (2016). "Linking genomic reorganization to tumor initiation via the giant cell cycle." Oncogenesis 5(12): e281.

Norbury, C. J. and I. D. Hickson (2001). "Cellular responses to DNA damage." Annual review of pharmacology and toxicology 41(1): 367-401.

Novak, M. and V. Vetvicka (2008). "β-glucans, history, and the present: immunomodulatory aspects and mechanisms of action." Journal of immunotoxicology 5(1): 47-57.

Nurmamat, E., et al. (2018). "Effects of different temperatures on the chemical structure and antitumor activities of polysaccharides from cordyceps militaris." Polymers 10(4): 430.

Olabisi, R. M. (2015). "Cell microencapsulation with synthetic polymers." Journal of Biomedical Materials Research Part A 103(2): 846-859.

Oliveira, D. A., et al. (2013). "Antimicrobial activity and composition profile of grape (Vitis vinifera) pomace extracts obtained by supercritical fluids." Journal of Biotechnology 164(3): 423-432.

Oliveira, L. d. C., et al. (2012). "Effect of drying temperature on quality of β-glucan in white oat grains." Food Science and Technology 32(4): 775-783.

Oludemi, T., et al. (2018). "Extraction of triterpenoids and phenolic compounds from Ganoderma lucidum: optimization study using the response surface methodology." Food & function 9(1): 209-226.

Olumee, Z., et al. (1998). "Droplet dynamics changes in electrostatic sprays of methanol– water mixtures." The Journal of Physical Chemistry A 102(46): 9154-9160.

Ong, Z. Y., et al. (2017). "Biodegradable cationic poly (carbonates): Effect of varying side chain hydrophobicity on key aspects of gene transfection." Acta biomaterialia 54: 201-211.

Orekhov, A. S., et al. (2017). "Low-voltage scanning electron microscopy of multilayer polymer systems." Crystallography Reports 62(5): 710-715.

Otsubo, Y. and R. K. Prud'homme (1994). "Rheology of oil-in-water emulsions." Rheologica acta 33(1): 29-37.

Owens Iii, D. E. and N. A. Peppas (2006). "Opsonization, biodistribution, and pharmacokinetics of polymeric nanoparticles." International journal of pharmaceutics 307(1): 93-102.

Oyewumi, M. O., et al. (2010). "Nano-microparticles as immune adjuvants: correlating particle sizes and the resultant immune responses." Expert review of vaccines 9(9): 1095-1107.

Page, A. F. (2016). Detection and avoidance of polysaccharides in plant nucleic acid extractions.

Page, J. S., et al. (2007). "Ionization and transmission efficiency in an electrospray ionization—mass spectrometry interface." Journal of the American Society for Mass Spectrometry 18(9): 1582-1590.

Pan, Z., et al. (2012). "Continuous and pulsed ultrasound-assisted extractions of antioxidants from pomegranate peel." Ultrasonics sonochemistry 19(2): 365-372.

*Novelty processing and smart delivery of Ganoderma Lucidum spores*

Pang, X., et al. (2007). "Potential of a novel polysaccharide preparation (GLPP) from Anhui-Grown Ganoderma lucidum in tumor treatment and immunostimulation." Journal of food science 72(6): S435-S442.

Panyam, J., et al. (2003). "Polymer degradation and in vitro release of a model protein from poly (D, L-lactide-co-glycolide) nano-and microparticles." Journal of Controlled Release 92(1-2): 173-187.

Paolino, D., et al. (2006). "Drug delivery systems." Encyclopedia of medical devices and instrumentation.

Paques, J. P., et al. (2014). "Nanospheres of alginate prepared through w/o emulsification and internal gelation with nanoparticles of CaCO3." Food Hydrocolloids 40: 182-188.

Paradee, N., et al. (2012). "Effects of crosslinking ratio, model drugs, and electric field strength on electrically controlled release for alginate-based hydrogel." Journal of Materials Science: Materials in Medicine 23(4): 999-1010.

Paraskevi, T. (2012). "Quality of life outcomes in patients with breast cancer." Oncology reviews 6(1).

Park, H., et al. (2012). "Fabrication of cross-linked alginate beads using electrospraying for adenovirus delivery." International journal of pharmaceutics 427(2): 417-425.

Park, K. (2016). "Drug delivery research: the invention cycle." Molecular pharmaceutics 13(7): 2143-2147.

Park, S. Y., et al. (2018). "Physical and mechanical properties of alginate-based hydrogel film as carrier for release of acetylthiocholine." International Journal of Precision Engineering and Manufacturing 19(1): 129-135.

Pasparakis, G. and N. Bouropoulos (2006). "Swelling studies and in vitro release of verapamil from calcium alginate and calcium alginate–chitosan beads." International journal of pharmaceutics 323(1-2): 34-42.

Pastor, E. L., et al. (2015). "Pore size is a critical parameter for obtaining sustained protein release from electrochemically synthesized mesoporous silicon microparticles." PeerJ 3: e1277.

Patel, N., et al. (2016). "Development and evaluation of a calcium alginate based oral ceftriaxone sodium formulation." Progress in biomaterials 5(2): 117-133.

Patil, V. R. S., et al. (2001). "Particle diameter influences adhesion under flow." Biophysical Journal 80(4): 1733-1743.

Pekcan, Ö. and Ş. Uğur (2002). "Molecular weight effect on polymer dissolution: a steady state fluorescence study." Polymer 43(6): 1937-1941.

Peretz, S., et al. (2015). "Synthesis, characterization and adsorption properties of alginate porous beads." Polymer Bulletin 72(12): 3169-3182.

Phillipson, J. D. and L. A. Anderson (1989). "Ethnopharmacology and western medicine." Journal of ethnopharmacology 25(1): 61-72.

Pichot, R. (2012). "Stability and characterisation of emulsions in the presence of colloidal particles and surfactants."

*Novelty processing and smart delivery of Ganoderma Lucidum spores*

Pillai, O. and R. Panchagnula (2001). "Polymers in drug delivery." Current opinion in chemical biology 5(4): 447-451.

Pillay, V., et al. (2013). "A review of the effect of processing variables on the fabrication of electrospun nanofibers for drug delivery applications." Journal of Nanomaterials 2013.

Pin, K. Y., et al. (2010). "Antioxidant and anti-inflammatory activities of extracts of betel leaves (Piper betle) from solvents with different polarities." Journal of Tropical Forest Science: 448-455.

Pk, M. M. U., et al. (2019). "Optimization of extraction of antioxidant polysaccharide from Pleurotus ostreatus (Jacq.) P. Kumm and its cytotoxic activity against murine lymphoid cancer cell line." PloS one 14(1): e0209371.

Plasencia, J., et al. (2013). "Pipe flow of water-in-crude oil emulsions: Effective viscosity, inversion point and droplet size distribution." Journal of Petroleum Science and Engineering 101: 35-43.

Plaza, M., et al. (2010). "Neoformation of antioxidants in glycation model systems treated under subcritical water extraction conditions." Food research international 43(4): 1123-1129.

Plaza, M. and C. Turner (2015). "Pressurized hot water extraction of bioactives." TrAC Trends in Analytical Chemistry 71: 39-54.

Poncelet, D., et al. (1995). "Production of alginate beads by emulsification/internal gelation. II. Physicochemistry." Applied microbiology and biotechnology 43(4): 644-650.

Postow, M. A., et al. (2015). "Immune checkpoint blockade in cancer therapy." Journal of clinical oncology 33(17): 1974.

Povedano, I., et al. (2014). "Effects of high pressure on unsaturated fatty acids." High Pressure Research 34(4): 428-433.

Powell, K. C. and A. Chauhan (2014). "Interfacial tension and surface elasticity of carbon Black (CB) covered oil–water interface." Langmuir 30(41): 12287-12296.

Pucetaite, M. (2012). "Archaeological wood from the Swedish warship Vasa studied by infrared microscopy."

Puck, T. T. and P. I. Marcus (1956). "Action of x-rays on mammalian cells." Journal of Experimental Medicine 103(5): 653-666.

Puig, P. E., et al. (2008). "Tumor cells can escape DNA-damaging cisplatin through DNA endoreduplication and reversible polyploidy." Cell biology international 32(9): 1031-1043.

Qin, H.-y., et al. (2011). "Comparative study polysaccharide extraction from antler-shape ganoderma lucidum by hot-water and ultrasonic wave [J]." China Food Additives 3.

Qiu, L. Y. and Y. H. Bae (2006). "Polymer architecture and drug delivery." Pharmaceutical research 23(1): 1-30.

Qu, D., et al. (2014). "Triterpene-loaded microemulsion using Coix lacryma-jobi seed extract as oil phase for enhanced antitumor efficacy: preparation and in vivo evaluation." International journal of nanomedicine 9: 109.

Que, Z., et al. (2014). "Ganoderic acid Me induces the apoptosis of competent T cells and increases the proportion of Treg cells through enhancing the expression and activation of

indoleamine 2, 3-dioxygenase in mouse lewis lung cancer cells." International immunopharmacology 23(1): 192-204.

Quinlan, E., et al. (2017). "Controlled release of vascular endothelial growth factor from spray-dried alginate microparticles in collagen–hydroxyapatite scaffolds for promoting vascularization and bone repair." Journal of tissue engineering and regenerative medicine 11(4): 1097-1109.

Qun, Y., et al. (2017). "Ultrasonic microwave-assisted extraction of polyphenols, flavonoids, triterpenoids, and vitamin C from Clinacanthus nutans." Czech Journal of Food Sciences 35(1): 89-94.

Quong, D., et al. (1998). "External versus internal source of calcium during the gelation of alginate beads for DNA encapsulation." Biotechnology and Bioengineering 57(4): 438-446.

Radwan, F. F. Y., et al. (2011). "Apoptotic and immune restoration effects of ganoderic acids define a new prospective for complementary treatment of cancer." Journal of clinical & cellular immunology: 004.

Raemdonck, K., et al. (2009). "Advanced nanogel engineering for drug delivery." Soft Matter 5(4): 707-715.

Rahar, S., et al. (2011). "Preparation, characterization, and biological properties of β-glucans." Journal of advanced pharmaceutical technology & research 2(2): 94.

Rahimi, M., et al. (2017). "Application of high frequency ultrasound in different irradiation systems for photosynthesis pigment extraction from Chlorella microalgae." Korean Journal of Chemical Engineering 34(4): 1100-1108.

Raja, H. A., et al. (2017). "DNA barcoding for identification of consumer-relevant mushrooms: A partial solution for product certification?" Food chemistry 214: 383-392.

Rajaonarivony, M., et al. (1993). "Development of a new drug carrier made from alginate." Journal of pharmaceutical sciences 82(9): 912-917.

Ramesh, C. and M. G. Pattar (2010). "Antimicrobial properties, antioxidant activity and bioactive compounds from six wild edible mushrooms of western ghats of Karnataka, India." Pharmacognosy research 2(2): 107.

Ranganath, S. H., et al. (2009). "Hydrogel matrix entrapping PLGA-paclitaxel microspheres: drug delivery with near zero-order release and implantability advantages for malignant brain tumour chemotherapy." Pharmaceutical research 26(9): 2101-2114.

Rasekh, M., et al. (2017). "Facile preparation of drug-loaded tristearin encapsulated superparamagnetic iron oxide nanoparticles using coaxial electrospray processing." Molecular pharmaceutics 14(6): 2010-2023.

Rasekh, M., et al. (2015). "Electrohydrodynamic preparation of nanomedicines." Current topics in medicinal chemistry 15(22): 2316-2327.

Raso, J., et al. (1999). "Influence of different factors on the output power transferred into medium by ultrasound." Ultrasonics sonochemistry 5(4): 157-162.

Raut, N. S., et al. (2013). "Zinc cross-linked hydroxamated alginates for pulsed drug release." International journal of pharmaceutical investigation 3(4): 194.

*Novelty processing and smart delivery of Ganoderma Lucidum spores*

Rawat, A., et al. (2013). "Evaluation of polyphenolic contents and antioxidant activity of wildly collected Ganoderma lucidum from central Himalayan hills of India." Asian J Plant Sci Res 3(3): 85-90.

Rawat, A., et al. (2012). "Biochemical estimation of wildly collected Ganoderma lucidum from Central Himalayan Hills of India." Adv. Appl. Sci. Res 3: 3708-3713.

Razak, M. F. B., et al. (2012). "The Effect of Varying Solvent Polarity on Extraction Yield of Orthosiphon stamineus leaves." J Applied Sci 12(11): 1207-1210.

Redgwell, R. J., et al. (2002). "Effect of roasting on degradation and structural features of polysaccharides in Arabica coffee beans." Carbohydrate research 337(5): 421-431.

Reis, C. P., et al. (2006). "Review and current status of emulsion/dispersion technology using an internal gelation process for the design of alginate particles." Journal of microencapsulation 23(3): 245-257.

Resa, J. M., et al. (2004). "Influence of temperature on the volumetric properties of ethanol+ water+ 1-pentanol." J. Serb. Chem. Soc 69(12): 1073-1097.

Reshetnikov, S. V. and K.-K. Tan (2001). "Higher Basidiomycota as a source of antitumor and immunostimulating polysaccharides." International Journal of Medicinal Mushrooms 3(4).

Rezaei, S., et al. (2013). "Solvent and solvent to sample ratio as main parameters in the microwave-assisted extraction of polyphenolic compounds from apple pomace." Food science and biotechnology 22(5): 1-6.

Rezende, R., et al. Experimental characterisation of the alginate gelation process for rapid prototyping.

Rieger, A. M., et al. (2011). "Modified annexin V/propidium iodide apoptosis assay for accurate assessment of cell death." JoVE (Journal of Visualized Experiments)(50): e2597.

Risbud, M. V., et al. (2000). "pH-sensitive freeze-dried chitosan–polyvinyl pyrrolidone hydrogels as controlled release system for antibiotic delivery." Journal of Controlled Release 68(1): 23-30.

Rizvi, S. A. A. and A. M. Saleh (2018). "Applications of nanoparticle systems in drug delivery technology." Saudi Pharmaceutical Journal 26(1): 64-70.

Rocha, J. d. C. G., et al. (2018). "Optimization of ultrasound-assisted extraction of phenolic compounds from jussara (Euterpe edulis M.) and blueberry (Vaccinium myrtillus) fruits." Food Science and Technology 38(1): 45-53.

Rodrigo, F., et al. (1998). "Effect of lyophilization on the mechanical characteristics of a large particle and on the behavior of immobilized bacterial spores." Journal of food protection 61(5): 633-636.

Rodrigues, D., et al. (2015). "Impact of enzyme-and ultrasound-assisted extraction methods on biological properties of red, brown, and green seaweeds from the central west coast of Portugal." Journal of Agricultural and Food Chemistry 63(12): 3177-3188.

Roselló-Soto, E., et al. (2016). "Application of non-conventional extraction methods: toward a sustainable and green production of valuable compounds from mushrooms." Food engineering reviews 8(2): 214-234.

*Novelty processing and smart delivery of Ganoderma Lucidum spores*

Ruan, W., et al. (2014). "Extraction optimisation and isolation of triterpenoids from Ganoderma lucidum and their effect on human carcinoma cell growth." Natural product research 28(24): 2264-2272.

Ruan, W. and D. G. Popovich (2012). "Ganoderma lucidum triterpenoid extract induces apoptosis in human colon carcinoma cells (Caco-2)." Biomedicine & Preventive Nutrition 2(3): 203-209.

Russo, R., et al. (2007). "Effect of cross-linking with calcium ions on the physical properties of alginate films." Biomacromolecules 8(10): 3193-3197.

Rutkowski, S., et al. (2018). "Hydrodynamic electrospray ionization jetting of calcium alginate particles: effect of spray-mode, spraying distance and concentration." RSC advances 8(43): 24243-24249.

Ryan, C. N., et al. (2014). "The flow rate sensitivity to voltage across four electrospray modes." Applied Physics Letters 104(8): 084101.

Saarai, A., et al. (2011). "A comparative study of crosslinked sodium alginate/gelatin hydrogels for wound dressing." Recent researches in geography, geology, energy, environment and biomedicine: 384-389.

Saha, A. K. and S. D. Ray (2013). "Effect of cross-linked biodegradable polymers on sustained release of sodium diclofenac-loaded microspheres." Brazilian journal of pharmaceutical sciences 49(4): 873-888.

Şahin, S., et al. (2018). "Pulsed ultrasound-assisted extraction of natural antioxidants from mandarin (Citrus deliciosa Tenore) leaves: Experimental and modeling study." Chemical Engineering Communications 205(6): 717-726.

Sahne, F., et al. (2016). "Extraction of bioactive compound curcumin from turmeric (Curcuma longa L.) via different routes: A comparative study." Pakistan J. Biotechnol 13: 173-180.

Sakellariadou, F. (2006). "Spectroscopic studies of humic acids from subsurface sediment samples collected across the Aegean Sea." Mediterranean Marine Science 7(2): 11-18.

Saleh, I. A., et al. (2015). "Ultrasonic-assisted extraction and conventional extraction of Silymarin from Silybum marianum seeds; a comparison." RESEARCH JOURNAL OF PHARMACEUTICAL BIOLOGICAL AND CHEMICAL SCIENCES 6(2): 709-717.

Sánchez, C. (2017). "Reactive oxygen species and antioxidant properties from mushrooms." Synthetic and systems biotechnology 2(1): 13-22.

Sandoval-Rodríguez, L.-S., et al. (2014). "Rheological Behavior of Water-In-Oil Emulsions of Heavy and Extra-Heavy Live Oils: Experimental Evaluation." CT&F-Ciencia, Tecnología y Futuro 5(4): 5-22.

Sankalia, M. G., et al. (2005). "Papain entrapment in alginate beads for stability improvement and site-specific delivery: physicochemical characterization and factorial optimization using neural network modeling." Aaps Pharmscitech 6(2): E209-E222.

Sanodiya, B. S., et al. (2009). "Ganoderma lucidum: a potent pharmacological macrofungus." Current pharmaceutical biotechnology 10(8): 717-742

Santagapita, P. R., et al. (2011). "Formulation and drying of alginate beads for controlled release and stabilization of invertase." Biomacromolecules 12(9): 3147-3155.

*Novelty processing and smart delivery of Ganoderma Lucidum spores*

Santagapita, P. R., et al. (2012). "Invertase stability in alginate beads: Effect of trehalose and chitosan inclusion and of drying methods." Food research international 47(2): 321-330.

Santos, M. C. P. and É. C. B. A. Gonçalves (2016). "Effect of different extracting solvents on antioxidant activity and phenolic compounds of a fruit and vegetable residue flour." Scientia Agropecuaria 7(1): 7-14.

Sao Mai, D., et al. (2015). "Optimizing the polysaccharide extraction from the Vietnamese Lingzhi (Ganoderma lucidum) via enzymatic method." Journal of Food and Nutrition Sciences 3(1-2): 111-114.

Sargowo, D., et al. (2018). "The role of polysaccharide peptide of Ganoderma lucidum as a potent antioxidant against atherosclerosis in high risk and stable angina patients." Indian heart journal 70(5): 608-614.

Sastry, S. K., et al. (1988). "A bioindicator for verification of thermal processes for particulate foods." Journal of food science 53(5): 1528-1536.

Sato, T., et al. (2017). "Effect of temperature and pressure on the extraction of strawberry receptacles with a mixture of supercritical carbon dioxide and entrainers." The Journal of Supercritical Fluids 130: 23-29.

Schmitt, J. and H.-C. Flemming (1998). "FTIR-spectroscopy in microbial and material analysis." International Biodeterioration & Biodegradation 41(1): 1-11.

Scholz, M., et al. (2017). "In vitro chlorhexidine release from alginate based microbeads for periodontal therapy." PloS one 12(10): e0185562.

Schwarz, C. and W. Mehnert (1997). "Freeze-drying of drug-free and drug-loaded solid lipid nanoparticles (SLN)." International journal of pharmaceutics 157(2): 171-179.

Segi, N., et al. (1989). "Interaction of calcium-induced alginate gel beads with propranolol." Chemical and Pharmaceutical Bulletin 37(11): 3092-3095.

Sell, S. A., et al. (2010). "The use of natural polymers in tissue engineering: a focus on electrospun extracellular matrix analogues." Polymers 2(4): 522-553.

Sen Gupta, A. (2016). "Role of particle size, shape, and stiffness in design of intravascular drug delivery systems: insights from computations, experiments, and nature." Wiley Interdisciplinary Reviews: Nanomedicine and Nanobiotechnology 8(2): 255-270.

Sereewatthanawut, I., et al. (2008). "Extraction of protein and amino acids from deoiled rice bran by subcritical water hydrolysis." Bioresource technology 99(3): 555-561.

Serra, L., et al. (2009). "Engineering design and molecular dynamics of mucoadhesive drug delivery systems as targeting agents." European Journal of pharmaceutics and biopharmaceutics 71(3): 519-528.

Serrano-Aroca, Á., et al. (2017). "Enhancement of water diffusion and compression performance of crosslinked alginate films with a minuscule amount of graphene oxide." Scientific reports 7(1): 11684.

Sevim, K. (2017). "Modelling of Drug Release from Biodegradable Polymers."

Shang, H., et al. (2018). "Extraction condition optimization and effects of drying methods on physicochemical properties and antioxidant activities of polysaccharides from comfrey

(Symphytum officinale L.) root." International journal of biological macromolecules 112: 889-899.

Shao, P., et al. (2019). "Encapsulation efficiency and controlled release of Ganoderma lucidum polysaccharide microcapsules by spray drying using different combinations of wall materials." International journal of biological macromolecules 125: 962-969.

Sharif, S., et al. (2017). "Wild Mushrooms: A Potential Source of Nutritional and Antioxidant Attributes with Acceptable Toxicity." Preventive nutrition and food science 22(2): 124.

Shaulsky, E., et al. (2017). "Post-fabrication modification of electrospun nanofiber mats with polymer coating for membrane distillation applications." Journal of Membrane Science 530: 158-165.

Sheikh, I. A., et al. (2014). "HPLC determination of phenolics and free radical scavenging activity of ethanolic extracts of two polypore mushrooms." International Journal of Pharmacy and Pharmaceutical Sciences 6(2): 679-684.

Sheikhpour, M., et al. (2017). "Biomimetics in drug delivery systems: A critical review." Journal of Controlled Release 253: 97-109.

Shekunov, B. Y., et al. (2007). "Particle size analysis in pharmaceutics: principles, methods and applications." Pharmaceutical research 24(2): 203-227.

Shen, C.-y., et al. (2016). "Nanogel for dermal application of the triterpenoids isolated from Ganoderma lucidum (GLT) for frostbite treatment." Drug delivery 23(2): 610-618.

Shi, S. Q. and D. J. Gardner (2007). "Effect of density and polymer content on the hygroscopic thickness swelling rate of compression molded wood fiber/polymer composites." Wood and fiber science 38(3): 520-526.

Shibata, S., et al. (1968). "Antitumor studies on some extracts of Basidiomycetes." GANN Japanese Journal of Cancer Research 59(2): 159-161.

Shin, J. (2016). "Evaluation of Calcium Alginate Microparticles Prepared Using a Novel Nebulized Aerosol Mediated Interfacial Crosslinking Method."

Shiraishi, S., et al. (1993). "Controlled-release preparation of indomethacin using calcium alginate gel." Biological and Pharmaceutical Bulletin 16(11): 1164-1168.

Shu, X., et al. (2010). "Extraction, characterization and antitumor effect of the polysaccharides from star anise (Illicium verum Hook. f.)." Journal of Medicinal Plants Research 4(24): 2666-2673.

Silva, C. M., et al. (2006). "Alginate microspheres prepared by internal gelation: Development and effect on insulin stability." International journal of pharmaceutics 311(1-2): 1-10.

Simoni, R. C., et al. (2017). "Effect of drying method on mechanical, thermal and water absorption properties of enzymatically crosslinked gelatin hydrogels." Anais da Academia Brasileira de Ciências 89(1): 745-755.

Sin, H. N., et al. (2006). "Optimization of hot water extraction for sapodilla juice using response surface methodology." Journal of Food Engineering 74(3): 352-358.

Singh, N. (2010). "A comparison of both water and ethanol extracts prepared from Echinacea purpurea and Echinacea angustifolia on the response to Influenza A/PR/8/34 infection in mice."

*Novelty processing and smart delivery of Ganoderma Lucidum spores*

Singh, R. and J. W. Lillard Jr (2009). "Nanoparticle-based targeted drug delivery." Experimental and molecular pathology 86(3): 215-223.

Singh, S. N., et al. (2014). "Dipole-dipole interaction in antibody solutions: correlation with viscosity behavior at high concentration." Pharmaceutical research 31(9): 2549-2558.

Sinha, B. K. and E. G. Mimnaugh (1990). "Free radicals and anticancer drug resistance: oxygen free radicals in the mechanisms of drug cytotoxicity and resistance by certain tumors." Free Radical Biology and Medicine 8(6): 567-581.

Sinha, V. R., et al. (2004). "Poly-ϵ-caprolactone microspheres and nanospheres: an overview." International journal of pharmaceutics 278(1): 1-23.

Sit, N., et al. (2015). "Optimization of starch isolation from taro using combination of enzymes and comparison of properties of starches isolated by enzymatic and conventional methods." Journal of food science and technology 52(7): 4324-4332.

Sliva, D., et al. (2003). "Biologic activity of spores and dried powder from Ganoderma lucidum for the inhibition of highly invasive human breast and prostate cancer cells." The Journal of Alternative & Complementary Medicine 9(4): 491-497.

Slütter, B. and W. Jiskoot (2016). Sizing the optimal dimensions of a vaccine delivery system: a particulate matter, Taylor & Francis.

Smiderle, F. R., et al. (2017). "Evaluation of microwave-assisted and pressurized liquid extractions to obtain β-d-glucans from mushrooms." Carbohydrate polymers 156: 165-174.

Snyder, L. R. (1974). "Classification of the solvent properties of common liquids." Journal of Chromatography A 92(2): 223-230.

Soares, R. M. D., et al. (2018). "Electrospinning and electrospray of bio-based and natural polymers for biomaterials development." Materials Science and Engineering: C.

Sobradillo, P., et al. (2011). "P4 medicine: the future around the corner." Archivos de Bronconeumología ((English Edition)) 47(1): 35-40.

Sogi, D. S., et al. (2010). "Effect of extraction parameters on curcumin yield from turmeric." Journal of food science and technology 47(3): 300-304.

Solari, F., et al. (1995). "Multinucleated cells can continuously generate mononucleated cells in the absence of mitosis: a study of cells of the avian osteoclast lineage." Journal of cell science 108(10): 3233-3241.

Sone, Y., et al. (1985). "Structures and antitumor activities of the polysaccharides isolated from fruiting body and the growing culture of mycelium of Ganoderma lucidum." Agricultural and biological chemistry 49(9): 2641-2653.

Song, B. (2018). "Lotus leaf-inspired design of calcium alginate particles with superhigh drug encapsulation efficiency and pH responsive release." Colloids and Surfaces B: Biointerfaces 172: 464-470.

Song, Y. S., et al. (2004). "Anti-angiogenic and inhibitory activity on inducible nitric oxide production of the mushroom Ganoderma lucidum." Journal of ethnopharmacology 90(1): 17-20.

Soni, M. L., et al. (2010). "Sodium alginate microspheres for extending drug release: formulation and in vitro evaluation." International Journal of Drug Delivery 2(1).

*Novelty processing and smart delivery of Ganoderma Lucidum spores*

Sood, G., et al. (2013). "Optimization of extraction and characterization of polysaccharides from medicinal mushroom Ganoderma lucidum using response surface methodology." Journal of Medicinal Plants Research 7(31): 2323-2329.

Soppimath, K. S., et al. (2001). "Biodegradable polymeric nanoparticles as drug delivery devices." Journal of Controlled Release 70(1-2): 1-20.

Soquetta, M. B., et al. (2018). "Green technologies for the extraction of bioactive compounds in fruits and vegetables." CyTA-Journal of Food 16(1): 400-412.

Soria, A. C., et al. (2014). "Microwave-assisted extraction of polysaccharides." Polysaccharides: Bioactivity and Biotechnology: 1-18.

Sowerby, J (1797). "Coloured Figures of English Fungi or Mushrooms": Plate 134.

Speranza, A., et al. (2001). "Electro-spraying of a highly conductive and viscous liquid." Journal of Electrostatics 51: 494-501.

Squier, M. K. T. and J. J. Cohen (2000). Assays of apoptosis. Calpain Methods and Protocols, Springer: 327-337.

Sriamornsak, P., et al. (2007). "Swelling, erosion and release behavior of alginate-based matrix tablets." European Journal of pharmaceutics and biopharmaceutics 66(3): 435-450.

Sridhar, R. and S. Ramakrishna (2013). "Electrosprayed nanoparticles for drug delivery and pharmaceutical applications." Biomatter 3(3): e24281.

Stanley, G., et al. (2005). "Ganoderma lucidum suppresses angiogenesis through the inhibition of secretion of VEGF and TGF-β1 from prostate cancer cells." Biochemical and biophysical research communications 330(1): 46-52.

Stewart, M. L., et al. (2006). "A study of pore geometry effects on anisotropy in hydraulic permeability using the lattice-Boltzmann method." Advances in water resources 29(9): 1328-1340.

Stier, H., et al. (2014). "Immune-modulatory effects of dietary Yeast Beta-1, 3/1, 6-D-glucan." Nutrition journal 13(1): 38.

Stitzel, J. D., et al. Electrospraying and electrospinning of polymers for biomedical applications. Poly (lactic-co-glycolic acid) and poly (ethylene-co-vinylacetate).

Stockwell, A. F., et al. (1986). "In vitro evaluation of alginate gel systems as sustained release drug delivery systems." Journal of Controlled Release 3(1-4): 167-175.

Størseth, T. R., et al. (2005). "Structural characterization of β-D-(1→ 3)-glucans from different growth phases of the marine diatoms Chaetoceros mülleri and Thalassiosira weissflogii." Carbohydrate research 340(6): 1159-1164.

Strigina, L. I., et al. (1971). "Steroid metabolites of Ganoderma applanatum basidiomycete." Phytochemistry 10(10): 2361-2365.

Su, C.-H., et al. (2017). "Effects of different extraction temperatures on the physicochemical properties of bioactive polysaccharides from Grifola frondosa." Food chemistry 220: 400-405.

Su, C.-H., et al. (1997). "Fungal mycelia as the source of chitin and polysaccharides and their applications as skin substitutes." Biomaterials 18(17): 1169-1174.

*Novelty processing and smart delivery of Ganoderma Lucidum spores*

Su, C.-H., et al. (2001). "High-performance liquid chromatographic analysis for the characterization of triterpenoids from Ganoderma." Journal of chromatographic science 39(3): 93-100.

Suárez-Arroyo, I. J., et al. (2017). "Ganoderma spp.: a promising adjuvant treatment for breast cancer." Medicines 4(1): 15.

Sugiura, S., et al. (2004). "Preparation characteristics of water-in-oil-in-water multiple emulsions using microchannel emulsification." Journal of colloid and interface science 270(1): 221-228.

Suksamran, T., et al. (2013). "Methylated N-(4-N, N-dimethylaminocinnamyl) chitosan-coated electrospray OVA-loaded microparticles for oral vaccination." International journal of pharmaceutics 448(1): 19-27.

Suksamran, T., et al. (2009). "Biodegradable alginate microparticles developed by electrohydrodynamic spraying techniques for oral delivery of protein." Journal of microencapsulation 26(7): 563-570.

Sultana, B., et al. (2009). "Effect of extraction solvent/technique on the antioxidant activity of selected medicinal plant extracts." Molecules 14(6): 2167-2180.

Sun, C., et al. (2015). "Effect of ethanol/water solvents on phenolic profiles and antioxidant properties of Beijing propolis extracts." Evidence-Based Complementary and Alternative Medicine 2015.

Sun, H. H., et al. (2012). "Development of a rapid and confirmatory method to identify ganoderic acids in Ganoderma mushrooms." Frontiers in pharmacology 3: 85.

Sun, J., et al. (2012). "Effect of particle size on solubility, dissolution rate, and oral bioavailability: Evaluation using coenzyme Q10 as naked nanocrystals." International journal of nanomedicine 7: 5733.

Sun, L. X., et al. (2011). "Ganoderma lucidum polysaccharides antagonize the suppression on lymphocytes induced by culture supernatants of B16F10 melanoma cells." Journal of Pharmacy and Pharmacology 63(5): 725-735.

Sun, L. X., et al. (2011). "Promoting effects of Ganoderma lucidum polysaccharides on B16F10 cells to activate lymphocytes." Basic & clinical pharmacology & toxicology 108(3): 149-154.

Sun, L.-X., et al. (2012). "Enhanced MHC class I and costimulatory molecules on B16F10 cells by Ganoderma lucidum polysaccharides." Journal of drug targeting 20(7): 582-592.

Sun, P., et al. The Pressure Enhances the Extraction Yield of Total Triterpenoids from Ganoderma lucidum, EDP Sciences.

Sun, R. and J. Tomkinson (2002). "Comparative study of lignins isolated by alkali and ultrasound-assisted alkali extractions from wheat straw." Ultrasonics sonochemistry 9(2): 85-93.

Sun, S.-L., et al. (2013). "Successive alkali extraction and structural characterization of hemicelluloses from sweet sorghum stem." Carbohydrate polymers 92(2): 2224-2231.

Sun, X., et al. (2015). "Anti-tumor activity of a polysaccharide from blueberry." Molecules 20(3): 3841-3853.

Sun, X., Wang, H., Han, X., Chen, S., Zhu, S., & Dai, J. (2014). Fingerprint analysis of polysaccharides from different Ganoderma by HPLC combined with chemometrics methods. Carbohydrate polymers, 114, 432-439.

*Novelty processing and smart delivery of Ganoderma Lucidum spores*

Sun, Y., et al. (2017). "Degradation of polysaccharides from Grateloupia filicina and their antiviral activity to avian leucosis virus subgroup J." Marine drugs 15(11): 345.

Sun, Y., et al. (2017). "Gelation Behavior Study of a Resorcinol–Hexamethyleneteramine Crosslinked Polymer Gel for Water Shut-Off Treatment in Low Temperature and High Salinity Reservoirs." Energies 10(7): 913.

Synytsya, A. and M. Novak (2014). "Structural analysis of glucans." Annals of translational medicine 2(2).

Szekalska, M., et al. (2015). "Alginate microspheres obtained by the spray drying technique as mucoadhesive carriers of ranitidine." Acta Pharmaceutica 65(1): 15-27.

Tabata, Y. and Y. Ikada (1990). Phagocytosis of polymer microspheres by macrophages. New polymer materials, Springer: 107-141.

Tahmouzi, S. and M. Ghodsi (2014). "Optimum extraction of polysaccharides from motherwort leaf and its antioxidant and antimicrobial activities." Carbohydrate polymers 112: 396-403.

Takacs, E., et al. (2000). "Effect of combined gamma-irradiation and alkali treatment on cotton–cellulose." Radiation Physics and Chemistry 57(3-6): 399-403.

Tang, K. and A. Gomez (1994). "On the structure of an electrostatic spray of monodisperse droplets." Physics of Fluids 6(7): 2317-2332.

Tang, K., et al. (2004). "Charge competition and the linear dynamic range of detection in electrospray ionization mass spectrometry." Journal of the American Society for Mass Spectrometry 15(10): 1416-1423.

Tang, W., et al. (2006). "Separation of targeted ganoderic acids from Ganoderma lucidum by reversed phase liquid chromatography with ultraviolet and mass spectrometry detections." Biochemical Engineering Journal 32(3): 205-210.

Tang, W., et al. (2006). "Ganoderic acid T from Ganoderma lucidum mycelia induces mitochondria mediated apoptosis in lung cancer cells." Life sciences 80(3): 205-211.

Tao, X., et al. Optimization of Ultra-high Pressure Extraction Process of Polysaccharides from Dendrobium Candidum by Response Surface Method, Trans Tech Publ.

Taofiq, O., et al. (2016). "Anti-inflammatory potential of mushroom extracts and isolated metabolites." Trends in food science & technology 50: 193-210.

Tapani, E., et al. (1996). "Toxicity of ethanol in low concentrations: experimental evaluation in cell culture." Acta Radiologica 37(6): 923-926.

Tavakol, M., et al. (2013). "The effect of polymer and CaCl 2 concentrations on the sulfasalazine release from alginate-N, O-carboxymethyl chitosan beads." Progress in biomaterials 2(1): 10.

Taylor, G. I. (1964). "Disintegration of water drops in an electric field." Proceedings of the Royal Society of London. Series A. Mathematical and Physical Sciences 280(1382): 383-397.

Teekachunhatean, S., et al. (2012). "Pharmacokinetics of ganoderic acids A and F after oral administration of Ling Zhi preparation in healthy male volunteers." Evidence-Based Complementary and Alternative Medicine 2012.

*Novelty processing and smart delivery of Ganoderma Lucidum spores*

Teo, C. C., et al. (2008). "Evaluation of the extraction efficiency of thermally labile bioactive compounds in Gastrodia elata Blume by pressurized hot water extraction and microwave-assisted extraction." Journal of Chromatography A 1182(1): 34-40.

Teo, C. C., et al. (2010). "Pressurized hot water extraction (PHWE)." Journal of Chromatography A 1217(16): 2484-2494.

Terada, D., et al. (2012). "Transient charge-masking effect of applied voltage on electrospinning of pure chitosan nanofibers from aqueous solutions." Science and technology of advanced materials 13(1): 015003.

Thomas, C. R. and D. Geer (2011). "Effects of shear on proteins in solution." Biotechnology letters 33(3): 443-456.

Thouri, A., et al. (2017). "Effect of solvents extraction on phytochemical components and biological activities of Tunisian date seeds (var. Korkobbi and Arechti)." BMC complementary and alternative medicine 17(1): 248.

Thuy, N. M. and N. T. M. Tuyen (2015). "Extraction of bioactive compounds and spore powder collection from Ganoderma lucidum." Can Tho Uni J. Sci 1: 53-60.

Thyagarajan, A., et al. (2006). "Inhibition of oxidative stress-induced invasiveness of cancer cells by Ganoderma lucidum is mediated through the suppression of interleukin-8 secretion." International journal of molecular medicine 18(4): 657-664.

Tian, S., et al. (2017). "Optimization conditions for extracting polysaccharide from Angelica sinensis and its antioxidant activities." Journal of Food and Drug Analysis 25(4): 766-775.

Tiwari, G., et al. (2012). "Drug delivery systems: An updated review." International journal of pharmaceutical investigation 2(1): 2.

Tomida, H., et al. (1993). "Imipramine release from Ca-alginate gel beads." Chemical and Pharmaceutical Bulletin 41(8): 1475-1477.

Tong, C.-C., et al. (2009). "Cytotoxic activity induced by crude extracts of Ganoderma lucidum (W. Curt.: Fr.) P. Karst. on mouse myeloma cancer cell-line." World Journal of Microbiology and Biotechnology 25(4): 687-695.

Tønnesen, H. H. and J. Karlsen (2002). "Alginate in drug delivery systems." Drug development and industrial pharmacy 28(6): 621-630.

Torchilin, V. P. (2001). "Structure and design of polymeric surfactant-based drug delivery systems." Journal of Controlled Release 73(2-3): 137-172.

Torres, O., et al. (2018). "Emulsion Microgel Particles as High-Performance Bio-Lubricants." ACS applied materials & interfaces 10(32): 26893-26905.

Toy, R., et al. (2013). "Multimodal in vivo imaging exposes the voyage of nanoparticles in tumor microcirculation." ACS nano 7(4): 3118-3129.

Toy, R., et al. (2014). "Shaping cancer nanomedicine: the effect of particle shape on the in vivo journey of nanoparticles." Nanomedicine 9(1): 121-134.

Tzanakis, I., et al. (2017). "Characterizing the cavitation development and acoustic spectrum in various liquids." Ultrasonics sonochemistry 34: 651-662.

*Novelty processing and smart delivery of Ganoderma Lucidum spores*

Usman, M., et al. (2014). "Effects of Temperature, pH and Steeping Time on the Extraction of Starch from Pakistani Rice." Int J Scientific Engr Res: 877-892.

Vaccarezza, L. M., et al. (1974). "Kinetics of moisture movement during air drying of sugar beet root." International journal of food science & technology 9(3): 317-327.

Vander Kloet, J. and L. L. Schramm (2002). "The effect of shear and oil/water ratio on the required hydrophile-lipophile balance for emulsification." Journal of Surfactants and detergents 5(1): 19-24.

Vasser, S. P., et al. (1997). Medicinal mushrooms:'Ganoderma lucidum'(Curtis: Fr.) P. Karst: Reishi mushroom, International Centre for Cryptogamic Plants and Fungi Institute of Evolution

Veeresham, C. (2012). Natural products derived from plants as a source of drugs, Wolters Kluwer--Medknow Publications.

Venkataraman, S., et al. (2011). "The effects of polymeric nanostructure shape on drug delivery." Advanced drug delivery reviews 63(14-15): 1228-1246.

Viera, V. B., et al. (2017). "Extraction of phenolic compounds and evaluation of the antioxidant and antimicrobial capacity of red onion skin (Allium cepa L.)." International Food Research Journal 24(3).

Vilkhu, K., et al. (2008). "Applications and opportunities for ultrasound assisted extraction in the food industry—A review." Innovative Food Science & Emerging Technologies 9(2): 161-169.

Vinatoru, M. (2001). "An overview of the ultrasonically assisted extraction of bioactive principles from herbs." Ultrasonics sonochemistry 8(3): 303-313.

Vinatoru, M., et al. (1997). "The use of ultrasound for the extraction of bioactive principles from plant materials." Ultrasonics sonochemistry 4(2): 135-139.

Vladisavljevic, G. T. and R. A. Williams (2010). Recent developments in manufacturing micro-and nano-particles from emulsion droplets, CRC Press (© Taylor and Francis).

Volman, J. J., et al. (2011). "In vivo effects of dietary (1→ 3),(1→ 4)-β-d-glucans from oat on mucosal immune responses in man and mice." Scandinavian journal of gastroenterology 46(5): 603-610.

Voo, W.-P., et al. (2015). "Production of ultra-high concentration calcium alginate beads with prolonged dissolution profile." RSC advances 5(46): 36687-36695.

Vũ Kim, D. and T. Đỗ Quang (2017). "EXTRACTION OF POLYSACCHARIDES AND TANNIN FROM SOME MEDICINAL PLANTS."

Wan, Y., et al. (2018). "Aptamer-conjugated extracellular nanovesicles for targeted drug delivery." Cancer research 78(3): 798-808.

Wang, C., et al. (2008). "Alginate–calcium carbonate porous microparticle hybrid hydrogels with versatile drug loading capabilities and variable mechanical strengths." Carbohydrate polymers 71(3): 476-480.

Wang, D., et al. (2018). "Optimum Extraction, Characterization, and Antioxidant Activities of Polysaccharides from Flowers of Dendrobium devonianum." International journal of analytical chemistry 2018.

*Novelty processing and smart delivery of Ganoderma Lucidum spores*

Wang, G., et al. (2005). "A simple method for DNA extraction from sporophyte in the brown alga Laminaria japonica." Journal of Applied Phycology 17(1): 75-79.

Wang, G., et al. (2007). "Enhancement of IL-2 and IFN-γ expression and NK cells activity involved in the anti-tumor effect of ganoderic acid Me in vivo." International immunopharmacology 7(6): 864-870.

Wang, J., et al. (2017). "Breaking the sporoderm of Ganoderma lucidum spores by combining chemical reaction with physical actuation." Natural product research 31(20): 2428-2434.

Wang, J.-L., et al. (2010). "A new ganoderic acid from Ganoderma lucidum mycelia." Journal of Asian natural products research 12(8): 727-730.

Wang, J.-L., et al. (2011). "Kinetic study of 7-O-ethyl ganoderic acid O stability and its importance in the preparative isolation." Biochemical Engineering Journal 53(2): 182-186.

Wang, L., et al. (2018). "Effects of ultrasound treatment and concentration of ethanol on selectivity of phenolic extraction from apple pomace." International journal of food science & technology 53(9): 2104-2109.

Wang, P.-Y., et al. (2012). "Antitumor and immunomodulatory effects of polysaccharides from broken-spore of Ganoderma lucidum." Frontiers in pharmacology 3: 135.

Wang, Q.-S., et al. (2016). "Colon targeted oral drug delivery system based on alginate-chitosan microspheres loaded with icariin in the treatment of ulcerative colitis." International journal of pharmaceutics 515(1-2): 176-185.

Wang, S. Y., et al. (1997). "The anti-tumor effect of Ganoderma lucidum is mediated by cytokines released from activated macrophages and T lymphocytes." International journal of cancer 70(6): 699-705.

Wang, X., et al. (2012). "A study of Ganoderma lucidum spores by FTIR microspectroscopy." Spectrochimica Acta Part A: Molecular and Biomolecular Spectroscopy 91: 285-289.

Wang, X., et al. (2017). "Ganoderic acid A inhibits proliferation and invasion, and promotes apoptosis in human hepatocellular carcinoma cells." Molecular medicine reports 16(4): 3894-3900.

Wang, X.-M., et al. (2006). "Quantitative determination of six major triterpenoids in Ganoderma lucidum and related species by high performance liquid chromatography." Journal of pharmaceutical and biomedical analysis 41(3): 838-844.

Wang, Y., et al. (2016). "Small-sized and large-pore dendritic mesoporous silica nanoparticles enhance antimicrobial enzyme delivery." Journal of Materials Chemistry B 4(15): 2646-2653.

Wang, Y.-Y., et al. (2002). "Studies on the immuno-modulating and antitumor activities of Ganoderma lucidum (Reishi) polysaccharides: functional and proteomic analyses of a fucose-containing glycoprotein fraction responsible for the activities." Bioorganic & medicinal chemistry 10(4): 1057-1062.

Ward, M. A. and T. K. Georgiou (2011). "Thermoresponsive polymers for biomedical applications." Polymers 3(3): 1215-1242.

Waszkowiak, K. and A. Gliszczyńska-Świgło (2016). "Binary ethanol–water solvents affect phenolic profile and antioxidant capacity of flaxseed extracts." European Food Research and Technology 242(5): 777-786.

Weheliye, W. H., et al. (2017). "On the effect of surfactants on drop coalescence at liquid/liquid interfaces." Chemical engineering science 161: 215-227.

Wei, L., et al. (2015). "Extraction optimization of total triterpenoids from Jatropha curcas leaves using response surface methodology and evaluations of their antimicrobial and antioxidant capacities." Electronic Journal of Biotechnology 18(2): 88-95.

Weihua, Z., et al. (2011). "Formation of solid tumors by a single multinucleated cancer cell." Cancer 117(17): 4092-4099.

Widmer, P. F. (1957). "Viscosity of a Three Component System, Acetone-ethanol-water, at 25° C and 30° C."

Wilm, M. (2011). "Principles of electrospray ionization." Molecular & Cellular Proteomics 10(7): M111-009407.

Wilm, M. S. and M. Mann (1994). "Electrospray and Taylor-Cone theory, Dole's beam of macromolecules at last?" International Journal of Mass Spectrometry and Ion Processes 136(2-3): 167-180.

Wlosnewski, J. C., et al. (2010). "Effect of drying technique and disintegrant on physical properties and drug release behavior of microcrystalline cellulose-based pellets prepared by extrusion/spheronization." Chemical Engineering Research and Design 88(1): 100-108.

Who.int. 2019. Cancer [online] Available at: <https://www.who.int/healthtopics/cancer#tab=tab_1> [Accessed 7 July 2020].

Wu, C.-T., et al. (2011). "Ling Zhi-8 mediates p53-dependent growth arrest of lung cancer cells proliferation via the ribosomal protein S7-MDM2-p53 pathway." Carcinogenesis 32(12): 1890-1896.

Wu, G.-S., et al. (2012). "Ganoderic acid DM, a natural triterpenoid, induces DNA damage, G1 cell cycle arrest and apoptosis in human breast cancer cells." Fitoterapia 83(2): 408-414.

Wu, J., et al. (2001). "Ultrasound-assisted extraction of ginseng saponins from ginseng roots and cultured ginseng cells." Ultrasonics sonochemistry 8(4): 347-352.

Wu, J.-Y. (2017). "Ultrasound-Assisted Extraction of Polysaccharides from Edible and Medicinal Fungi: Major Factors and Process Kinetics." MOJ Food Processing & Technology 4(2).

Wu, L., Liang, W., Chen, W., Li, S., Cui, Y., Qi, Q., & Zhang, L. (2017). Screening and analysis of the marker components in Ganoderma lucidum by HPLC and HPLC-MSn with the aid of chemometrics. Molecules, 22(4), 584.

Wu, Y., et al. (2012). Electrospray production of nanoparticles for drug/nucleic acid delivery. The Delivery of Nanoparticles, IntechOpen.

Wu, Y., et al. (2009). "Polymeric particle formation through electrospraying at low atmospheric pressure." Journal of Biomedical Materials Research Part B: Applied Biomaterials 90(1): 381-387.

Xia, Y.-G., et al. (2014). "Optimization of simultaneous ultrasonic-assisted extraction of water-soluble and fat-soluble characteristic constituents from Forsythiae Fructus Using response surface methodology and high-performance liquid chromatography." Pharmacognosy magazine 10(39): 292.

*Novelty processing and smart delivery of Ganoderma Lucidum spores*

XiaoPing, C., et al. (2009). "Free radical scavenging of Ganoderma lucidum polysaccharides and its effect on antioxidant enzymes and immunity activities in cervical carcinoma rats." Carbohydrate polymers 77(2): 389-393.

Xie, J., et al. (2015). "Electrohydrodynamic atomization: A two-decade effort to produce and process micro-/nanoparticulate materials." Chemical engineering science 125: 32-57.

Xie, J. and C.-H. Wang (2007). "Electrospray in the dripping mode for cell microencapsulation." Journal of colloid and interface science 312(2): 247-255.

Xie, J. and C. H. Wang (2007). "Encapsulation of proteins in biodegradable polymeric microparticles using electrospray in the Taylor cone-jet mode." Biotechnology and Bioengineering 97(5): 1278-1290.

Xie, J.-H., et al. (2016). "Advances on bioactive polysaccharides from medicinal plants." Critical reviews in food science and nutrition 56(sup1): S60-S84.

Xie, Y.-Z., et al. (2006). "Ganoderma lucidum inhibits tumour cell proliferation and induces tumour cell death." Enzyme and Microbial Technology 40(1): 177-185.

Xing, L., et al. (2018). "Yeast fermentation inspired Ca-alginate hydrogel membrane: lower transparency, hierarchical pore structure and higher hydrophobicity." RSC advances 8(5): 2622-2631.

Xing, Z., et al. (2018). "Targeting oxidative stress using tri-needle electrospray engineered Ganoderma lucidum polysaccharide-loaded porous yolk-shell particles." European Journal of Pharmaceutical Sciences 125: 64-73.

Xu, C.-H., et al. (2006). "Multi-steps infrared macro-fingerprint analysis for thermal processing of Fructus viticis." Vibrational spectroscopy 41(1): 118-125.

Xu, J., et al. (2018). "Optimized microwave extraction, characterization and antioxidant capacity of biological polysaccharides from Eucommia ulmoides Oliver leaf." Scientific reports 8(1): 6561.

Xu, J., et al. (2018). "Engineering Biocompatible Hydrogels from Bicomponent Natural Nanofibers for Anticancer Drug Delivery." Journal of Agricultural and Food Chemistry 66(4): 935-942.

Xu, Q., et al. (2009). "Preparation of monodisperse biodegradable polymer microparticles using a microfluidic flow-focusing device for controlled drug delivery." Small 5(13): 1575-1581.

Xu, W.-F., et al. (2014). "Effects of internal-phase contents on porous polymers prepared by a high-internal-phase emulsion method." Journal of Polymer Research 21(9): 524.

Xu, Y. and S. Pan (2013). "Effects of various factors of ultrasonic treatment on the extraction yield of all-trans-lycopene from red grapefruit (Citrus paradise Macf.)." Ultrasonics sonochemistry 20(4): 1026-1032.

XuJie, H. and C. Wei (2008). "Optimization of extraction process of crude polysaccharides from wild edible BaChu mushroom by response surface methodology." Carbohydrate polymers 72(1): 67-74.

Yan, F., et al. (2014). "Extraction optimization of antioxidant polysaccharides from leaves of Gynura bicolor (Roxb. & Willd.) DC." Food Science and Technology 34(2): 402-407.

*Novelty processing and smart delivery of Ganoderma Lucidum spores*

Yan, Z., et al. (2013). "Fast analysis of triterpenoids in Ganoderma lucidum spores by ultra-performance liquid chromatography coupled with triple quadrupole mass spectrometry." Biomedical Chromatography 27(11): 1560-1567.

Yanaki, T., et al. (1983). "Correlation between the antitumor activity of a polysaccharide schizophyllan and its triple-helical conformation in dilute aqueous solution." Biophysical chemistry 17(4): 337-342.

Yang, L., et al. (2013). "Optimization of subcritical water extraction of polysaccharides from Grifola frondosa using response surface methodology." Pharmacognosy magazine 9(34): 120.

Yang, M., et al. (2007). "Analysis of triterpenoids in Ganoderma lucidum using liquid chromatography coupled with electrospray ionization mass spectrometry." Journal of the American Society for Mass Spectrometry 18(5): 927-939.

Yang, Q., et al. (2010). "HPLC analysis of Ganoderma lucidum polysaccharides and its effect on antioxidant enzymes activity and Bax, Bcl-2 expression." International journal of biological macromolecules 46(2): 167-172.

Yang, X.-s., et al. (2014). "Optimization of ultrasonic-assisted extraction process of polysaccharides from American ginseng and evaluation of its immunostimulating activity." Journal of Integrative Agriculture 13(12): 2807-2815.

Yanhua, W., et al. (2014). "Optimization of extraction process for polysaccharide in Salvia Miltiorrhiza Bunge using response surface methodology." The open biomedical engineering journal 8: 153.

Yao, R., et al. (2012). "Alginate and alginate/gelatin microspheres for human adipose-derived stem cell encapsulation and differentiation." Biofabrication 4(2): 025007.

Yao, Z.-C., et al. (2017). "Ganoderma lucidum polysaccharide loaded sodium alginate micro-particles prepared via electrospraying in controlled deposition environments." International journal of pharmaceutics 524(1-2): 148-158.

Yao, Z.-C., et al. (2018). "Designer fibers from 2D to 3D–Simultaneous and controlled engineering of morphology, shape and size." Chemical Engineering Journal 334: 89-98.

Ye, C.-L. and C.-J. Jiang (2011). "Optimization of extraction process of crude polysaccharides from Plantago asiatica L. by response surface methodology." Carbohydrate polymers 84(1): 495-502.

Ye, L., et al. (2008). "Structural elucidation of the polysaccharide moiety of a glycopeptide (GLPCW-II) from Ganoderma lucidum fruiting bodies." Carbohydrate research 343(4): 746-752.

Yeh, C.-H., et al. (2010). "Polysaccharides PS-G and protein LZ-8 from Reishi (Ganoderma lucidum) exhibit diverse functions in regulating murine macrophages and T lymphocytes." Journal of Agricultural and Food Chemistry 58(15): 8535-8544.

Yeung, S., Chen, Q., Yu, Y., Zhou, B., Wu, W., Li, X., ... & Wang, Z. (2021). Quality evaluation of commercial products of Ganoderma lucidum made from its fruiting body and spore. Acta Chromatographica, 34(1), 100-113.

Yılmaz, T. and Ş. Tavman (2016). "Ultrasound assisted extraction of polysaccharides from hazelnut skin." Food Science and Technology International 22(2): 112-121.

*Novelty processing and smart delivery of Ganoderma Lucidum spores*

Yin, W. and M. Z. Yates (2009). "Encapsulation and sustained release from biodegradable microcapsules made by emulsification/freeze drying and spray/freeze drying." Journal of colloid and interface science 336(1): 155-161.

Ying, D. Y., et al. (2010). "Microencapsulated Lactobacillus rhamnosus GG powders: relationship of powder physical properties to probiotic survival during storage." Journal of food science 75(9): E588-E595.

Ying, Z., et al. (2011). "Ultrasound-assisted extraction of polysaccharides from mulberry leaves." Food chemistry 127(3): 1273-1279.

Yonekura, L., et al. (2014). "Microencapsulation of Lactobacillus acidophilus NCIMB 701748 in matrices containing soluble fibre by spray drying: Technological characterization, storage stability and survival after in vitro digestion." Journal of functional foods 6: 205-214.

Yoshida, H., et al. (2012). "Preferential induction of Th17 cells in vitro and in vivo by Fucogalactan from Ganoderma lucidum (Reishi)." Biochemical and biophysical research communications 422(1): 174-180.

You, F., et al. (2017). "3D printing of porous alginate/gelatin hydrogel scaffolds and their mechanical property characterization." International Journal of Polymeric Materials and Polymeric Biomaterials 66(6): 299-306.

You, R., et al. (2011). "A comparison study between different molecular weight polysaccharides derived from Lentinus edodes and their antioxidant activities in vivo." Pharmaceutical biology 49(12): 1298-1305.

Yu, X.-m., et al. (2015). "Subcritical water extraction of antioxidant phenolic compounds from XiLan olive fruit dreg." Journal of food science and technology 52(8): 5012-5020.

Yuan, C., et al. (2017). "A novel water-based process produces eco-friendly bio-adhesive made from green cross-linked soybean soluble polysaccharide and soy protein." Carbohydrate polymers 169: 417-425.

Yuan, C., et al. (2012). "The characterization and role of leukemia cell-derived dendritic cells in immunotherapy for leukemic diseases." Intractable & rare diseases research 1(2): 53-65.

Yuan, M., et al. (2012). "A positive/negative ion–switching, targeted mass spectrometry–based metabolomics platform for bodily fluids, cells, and fresh and fixed tissue." Nature protocols 7(5): 872.

Yue, G. G. L., et al. (2008). "Comparative studies on the immunomodulatory and antitumor activities of the different parts of fruiting body of Ganoderma lucidum and Ganoderma spores." Phytotherapy Research: An International Journal Devoted to Pharmacological and Toxicological Evaluation of Natural Product Derivatives 22(10): 1282-1291.

Yuen, J. W., & Gohel, M. D. I. (2005). Anticancer effects of Ganoderma lucidum: a review of scientific evidence. Nutrition and cancer, 53(1), 11-17.

Yuen, J. W. M., et al. (2011). "The differential immunological activities of Ganoderma lucidum on human pre-cancerous uroepithelial cells." Journal of ethnopharmacology 135(3): 711-718.

Zampolli, J., et al. (2014). "Biodegradation of variable-chain-length n-alkanes in Rhodococcus opacus R7 and the involvement of an alkane hydroxylase system in the metabolism." AMB Express 4(1): 73.

*Novelty processing and smart delivery of Ganoderma Lucidum spores*

Zarrabi, A. and M. Vossoughi (2009). "Electrospray: Novel fabrication method for biodegradable polymeric nanoparticles for further applications in drug delivery systems." Roznov pod Radhostem 10: 20-22.

Zeković, D. B., et al. (2005). "Natural and modified (1→ 3)-β-D-glucans in health promotion and disease alleviation." Critical reviews in biotechnology 25(4): 205-230.

Zeng, J., et al. (2018). "Radiopaque and uniform alginate microspheres loaded with tantalum nanoparticles for real-time imaging during transcatheter arterial embolization." Theranostics 8(17): 4591.

Zeng, P., et al. (2018). "Chemical, biochemical, preclinical and clinical studies of Ganoderma lucidum polysaccharide as an approved drug for treating myopathy and other diseases in China." Journal of cellular and molecular medicine 22(7): 3278-3297.

Zengin, G., et al. (2015). "Two Ganoderma species: profiling of phenolic compounds by HPLC–DAD, antioxidant, antimicrobial and inhibitory activities on key enzymes linked to diabetes mellitus, Alzheimer's disease and skin disorders." Food & function 6(8): 2794-2802.

Zha, X.-Q., et al. (2009). "Antioxidant properties of polysaccharide fractions with different molecular mass extracted with hot-water from rice bran." Carbohydrate polymers 78(3): 570-575.

Zhang, H., et al. (2018). "Development of Global Chemical Profiling for Quality Assessment of Ganoderma Species by ChemPattern Software." Journal of analytical methods in chemistry 2018.

Zhang, H. and K. H. Row (2014). "Extraction and separation of polysaccharides from Laminaria japonica by size-exclusion chromatography." Journal of chromatographic science 53(4): 498-502.

Zhang, H.-N., et al. (2003). "In vitro and in vivo protective effect of Ganoderma lucidum polysaccharides on alloxan-induced pancreatic islets damage." Life sciences 73(18): 2307-2319.

Zhang, J., et al. (2002). "Activation of B lymphocytes by GLIS, a bioactive proteoglycan from Ganoderma lucidum." Life sciences 71(6): 623-638.

Zhang, L., et al. (2002). "Transition from triple helix to coil of lentinan in solution measured by SEC, viscometry, and 13 C NMR." Polymer journal 34(6): 443.

Zhang, L. and Y. Zhang (2011). "Structure and immunological activity of a novel polysaccharide from the spores of Ganoderma lucidum." African Journal of Biotechnology 10(53): 10923-10929.

Zhang, S. (2017). "Relationship between particle size distribution and porosity in dump leaching."

Zhang, X., et al. (2004). "Morphologies and conformation transition of lentinan in aqueous NaOH solution." Biopolymers: Original Research on Biomolecules 75(2): 187-195.

Zhang, Y., et al. (2011). "Preparation and evaluation of alginate–chitosan microspheres for oral delivery of insulin." European Journal of pharmaceutics and biopharmaceutics 77(1): 11-19.

Zhang, Z.-S., et al. (2007). "Optimization of ethanol–water extraction of lignans from flaxseed." Separation and Purification Technology 57(1): 17-24.

*Novelty processing and smart delivery of Ganoderma Lucidum spores*

Zhao, D. (2014). "Novel processing and microencapsulation of Ganoderma lucidum spores for healthcare."

Zhao, D., et al. (2014). "Investigation of Ice-Assisted Sonication on the Microstructure and Chemical Quality of Ganoderma lucidum Spores." Journal of food science 79(11): E2253-E2265.

Zhao, D., et al. (2016). "Preparation and characterization of Ganoderma lucidum spores-loaded alginate microspheres by electrospraying." Materials Science and Engineering: C 62: 835-842.

Zhao, H., et al. (2012). "Spore powder of Ganoderma lucidum improves cancer-related fatigue in breast cancer patients undergoing endocrine therapy: a pilot clinical trial." Evidence-Based Complementary and Alternative Medicine 2012.

Zhao, J., et al. (2006). "Quality evaluation of Ganoderma through simultaneous determination of nine triterpenes and sterols using pressurized liquid extraction and high performance liquid chromatography." Journal of separation science 29(17): 2609-2615.

Zhao, L., et al. (2010). "Extraction, purification, characterization and antitumor activity of polysaccharides from Ganoderma lucidum." Carbohydrate polymers 80(3): 783-789.

Zhao, Q., et al. (2011). "Optimization of ultrasonic circulating extraction of polysaccharides from Asparagus officinalis using response surface methodology." International journal of biological macromolecules 49(2): 181-187.

Zhao, Y., et al. (2007). "Preparation of calcium alginate microgel beads in an electrodispersion reactor using an internal source of calcium carbonate nanoparticles." Langmuir 23(25): 12489-12496.

Zheng, C. and W. Liang (2010). "A one-step modified method to reduce the burst initial release from PLGA microspheres." Drug delivery 17(2): 77-82.

Zheng, M. and J. Yu (2016). "The effect of particle shape and size on cellular uptake." Drug delivery and translational research 6(1): 67-72.

Zheng, S., et al. (2012). "Ganoderma lucidum polysaccharides eradicates the blocking effect of fibrinogen on NK cytotoxicity against melanoma cells." Oncology letters 3(3): 613-616.

Zheng, Y., et al. (2014). "Optimization of ultrasonic-assisted extraction and in vitro antioxidant activities of polysaccharides from Trametes orientalis." Carbohydrate polymers 111: 315-323.

Zheng, Y., Cui, J., Chen, A. H., Zong, Z. M., & Wei, X. Y. (2019). Optimization of ultrasonic-microwave assisted extraction and hepatoprotective activities of polysaccharides from Trametes orientalis. Molecules, 24(1), 147.

Zhong, D., et al. (2015). "Ganoderma lucidum polysaccharide peptide prevents renal ischemia reperfusion injury via counteracting oxidative stress." Scientific reports 5: 16910.

Zhong, J.-J., et al. (2012). "Anti-proliferation and induced mitochondria-mediated apoptosis of ganoderic acid Mk from Ganoderma lucidum mycelia in cervical cancer HeLa cells." Latin American Journal of Pharmacy 31.

Zhou, L., et al. (2011). "Ganoderic acid Me induces apoptosis through mitochondria dysfunctions in human colon carcinoma cells." Process biochemistry 46(1): 219-225.

Zhou, S., et al. (2005). "Clinical trials for medicinal mushrooms: Experience with Ganoderma lucidum (W. Curt.: Fr.) Lloyd (Lingzhi mushroom)." International Journal of Medicinal Mushrooms 7(1&2).

*Novelty processing and smart delivery of Ganoderma Lucidum spores*

Zhou, T., et al. (2017). "Ultrasound-assisted extraction and identification of natural antioxidants from the fruit of Melastoma sanguineum Sims." Molecules 22(2): 306.

Zhou, X. W., Su, K. Q., & Zhang, Y. M. (2012). Applied modern biotechnology for cultivation of Ganoderma and development of their products. Applied Microbiology and Biotechnology, 93(3), 941-963.

Zhu, F., et al. (2015). "Beta-glucans from edible and medicinal mushrooms: characteristics, physicochemical and biological activities." Journal of Food Composition and Analysis 41: 165-173.

Zhu, H. S., et al. (2000). "Effects of extracts from sporoderm-broken spores of Ganoderma lucidum on HeLa cells." Cell biology and toxicology 16(3): 201-206.

Zhu, L.-F., et al. (2019). "Engineering of Ganoderma lucidum polysaccharide loaded polyvinyl alcohol nanofibers for biopharmaceutical delivery." Journal of Drug Delivery Science and Technology 50: 208-216.

Zhu, X. and Z. Lin (2006). "Modulation of cytokines production, granzyme B and perforin in murine CIK cells by Ganoderma lucidum polysaccharides." Carbohydrate polymers 63(2): 188-197.

Zhu, X.-L., et al. (2007). "Ganoderma lucidum polysaccharides enhance the function of immunological effector cells in immunosuppressed mice." Journal of ethnopharmacology 111(2): 219-226.

Zhu, Y. and A. T. L. Tan (2015). "Discrimination of wild-grown and cultivated Ganoderma lucidum by Fourier transform infrared spectroscopy and chemometric methods."

Zierkiewicz, W., et al. (2011). "Blue shifts and unusual intensity changes in the infrared spectra of the enflurane··· acetone complexes: Spectroscopic and theoretical studies." The Journal of Physical Chemistry A 115(41): 11362-11368.

Ziping, L., Zilin, L., Shiyu, T., Qiliang, X., Haiyan, Y., & Lingli, Y. (2011). Inquiry of water-soluble polysaccharide extraction conditions from grapefruit skin. Engineering, 2011.

Zou, Y., et al. (2015). "Extraction optimization of antioxidant polysaccharides from Auricularia auricula fruiting bodies." Food Science and Technology 35(3): 428-433.

Zou, Y.-F., et al. (2017). "Purification and partial structural characterization of a complement fixating polysaccharide from Rhizomes of Ligusticum chuanxiong." Molecules 22(2): 287.

*Novelty processing and smart delivery of Ganoderma Lucidum spores*

# In loving memory of Professor Mehrdad Tamiz
## 1958 - 2022

*Your greatness will live on forever*

# 7 Appendix

With reference to preliminary work in project ***Novelty processing and smart delivery of Ganoderma lucidum spores***

**Figure A1:** Broken (upper) and unbroken (lower) spores undergoing preliminary HWE. Broken spores showed greater potential for extraction yield of PS.

| | Time: 20 | Time: 40 | Time: 60 | |
|---|---|---|---|---|
| Ratio: L 1:15 | | 8.42% | | Temperature: 40 |
| Ratio: L 1:15 | 8.52% | 6.84% | 5.22% | Temperature: 60 |
| Ratio: L 1:15 | | 8.28% | | Temperature: 80 |
| Ratio: M 1:30 | | 7.84% | | Temperature: 40 |
| Ratio: M 1:30 | 12.88% | 7.42% | 8.44% | Temperature: 60 |
| Ratio: M 1:30 | | 20.92% | | Temperature: 80 |
| Ratio: H 1:60 | | 7.52% | | Temperature: 40 |
| Ratio: H 1:60 | 14.48% | 16.84% | 16.80% | Temperature: 60 |
| Ratio: H 1:60 | | 10.80% | | Temperature: 80 |

| | Time: 20 | Time: 40 | Time: 60 | |
|---|---|---|---|---|
| Ratio: L 1:15 | | 6.88% | | Temperature: 40 |
| Ratio: L 1:15 | 8.36% | 8.92% | 10.88% | Temperature: 60 |
| Ratio: L 1:15 | | 5.20% | | Temperature: 80 |
| Ratio: M 1:30 | | 12.20% | | Temperature: 40 |
| Ratio: M 1:30 | 4.20% | 13.60% | 1.20% | Temperature: 60 |
| Ratio: M 1:30 | | 1.80% | | Temperature: 80 |
| Ratio: H 1:60 | | 10.56% | | Temperature: 40 |
| Ratio: H 1:60 | 7.84% | 8.64% | 8.56% | Temperature: 60 |
| Ratio: H 1:60 | | 10.00% | | Temperature: 80 |

**Figure A2:** UAE UV-Vis Spectra for the detection of D-Glucans, by cycle time and water % - 400-600nm

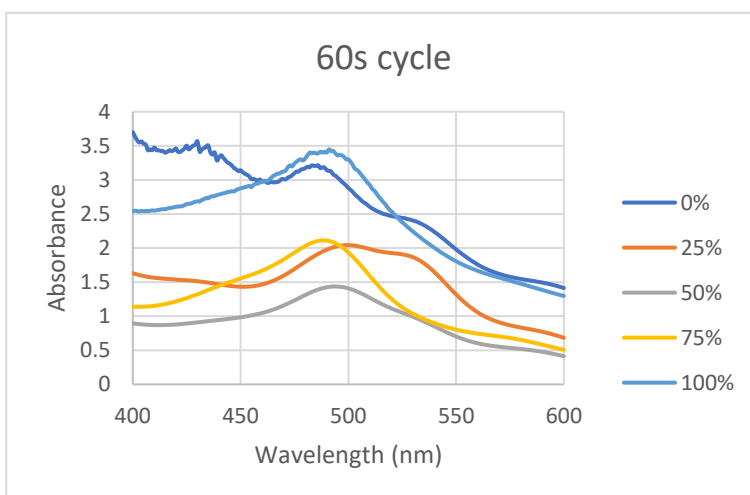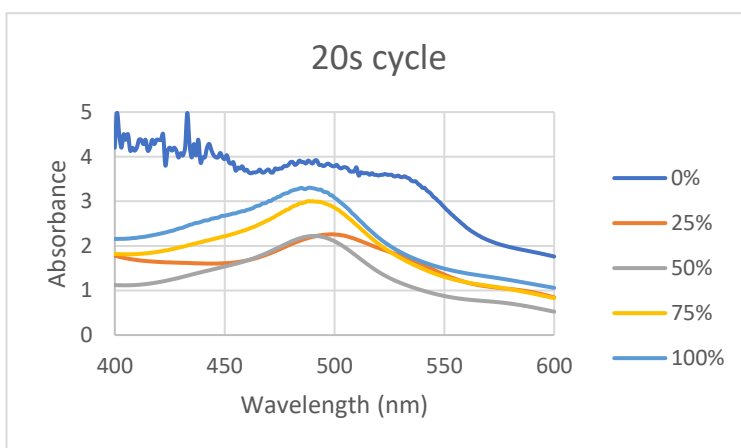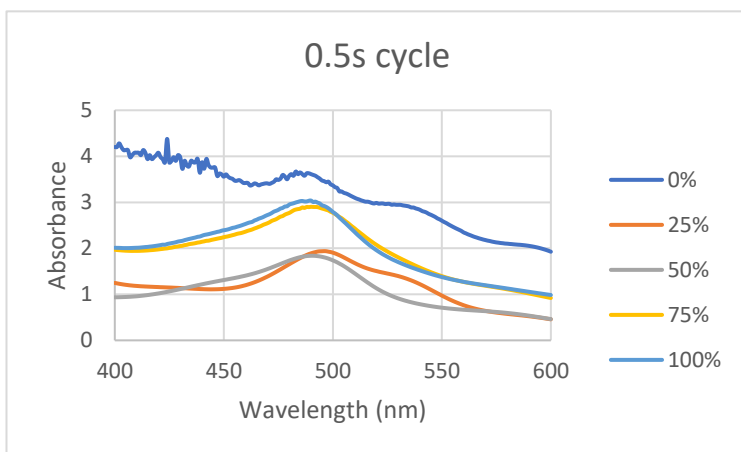*Novelty processing and smart delivery of Ganoderma Lucidum spores*

**Figure A3:** HWE UV-Vis Spectra for the detection of D-Glucans, by time and water % - 400-600nm

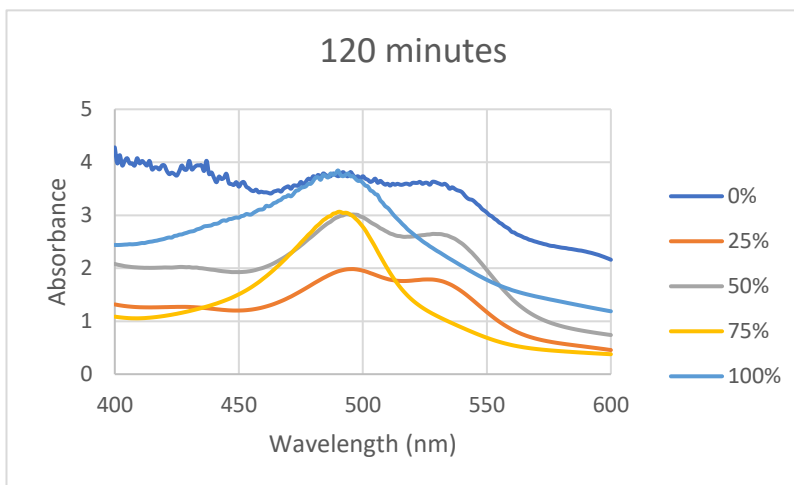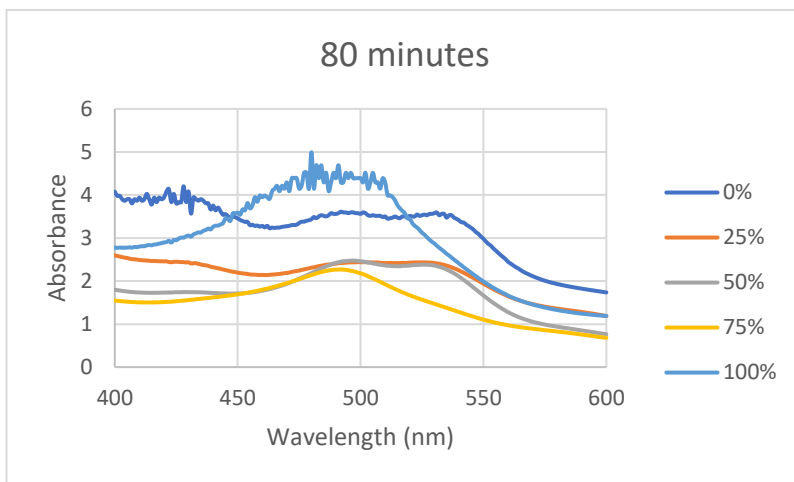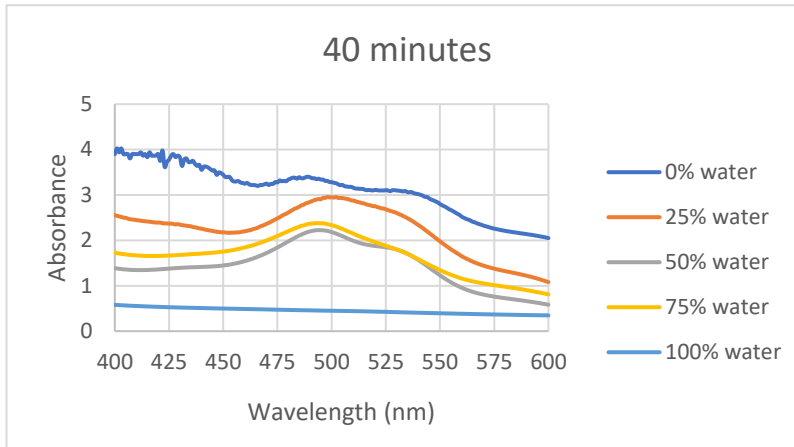*Novelty processing and smart delivery of Ganoderma Lucidum spores*

**Figure A4:** EHDA voltage range tested preliminarily on GLS-A particle diameter – 2.5kV – 20Kv at 5ul/min. Error bars represent SE
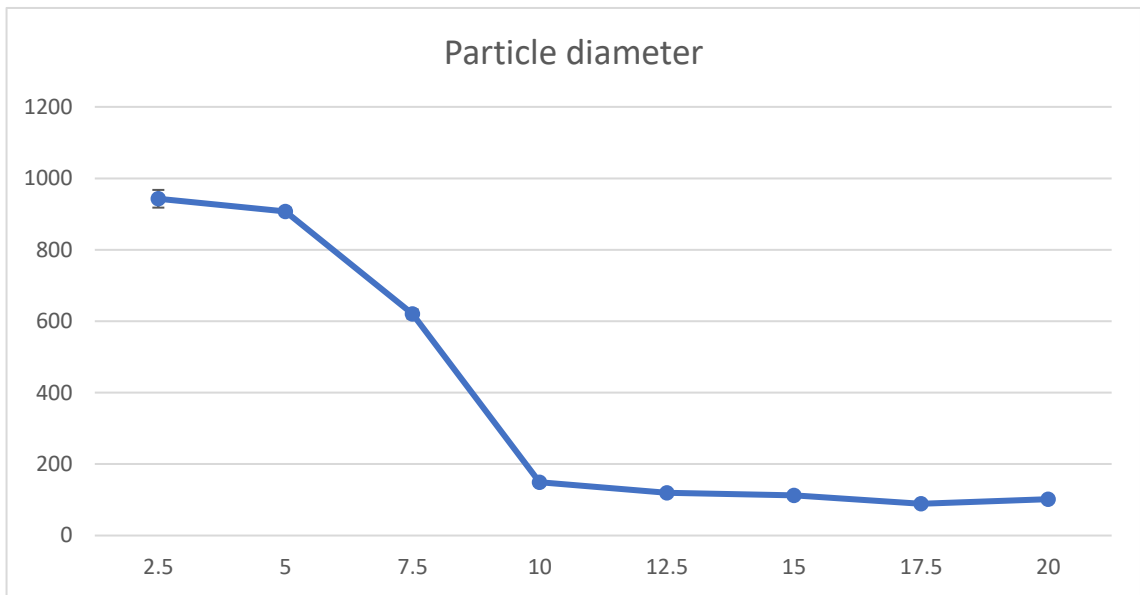


**Figure A5:** EHDA voltage range tested preliminarily on GLS-A particle aspect ratio – 2.5kV – 20kV at 5ul/min. Error bars represent SE
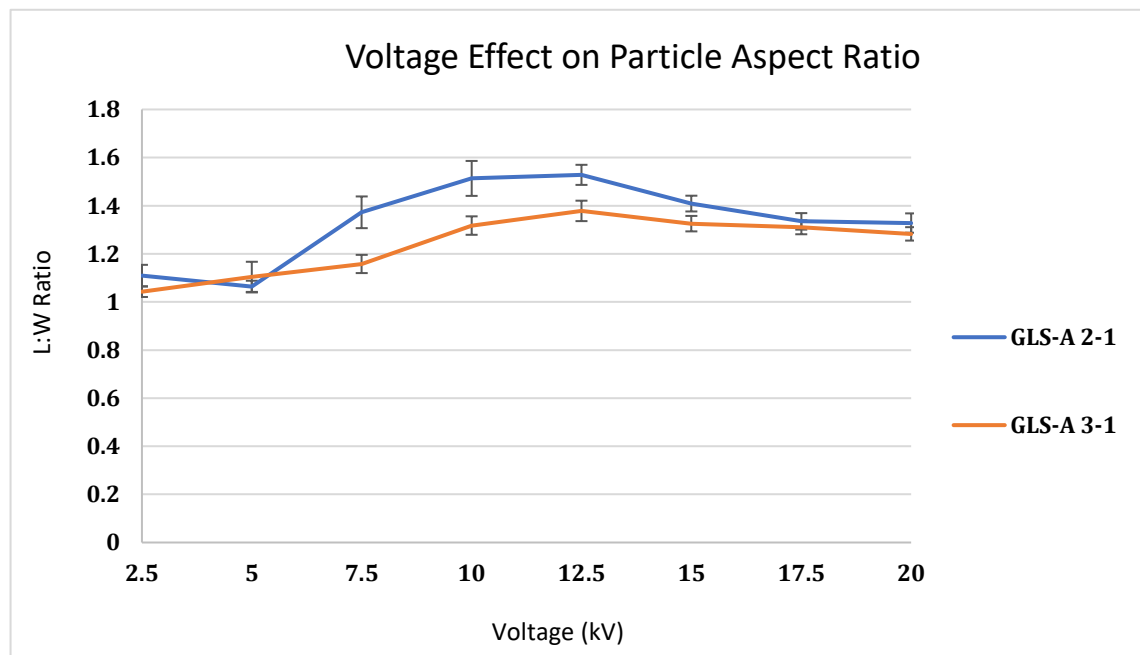
*Novelty processing and smart delivery of Ganoderma Lucidum spores*

**Figure A6:** Crosslinking GLS-A 1-1 particles with 1M CaCl$_2$ created at 5kV and 50ul/min and dried for 24h. Although still stable, agglomeration suggested that a higher calcium concentration would be more stabilising to the alginate matrix.
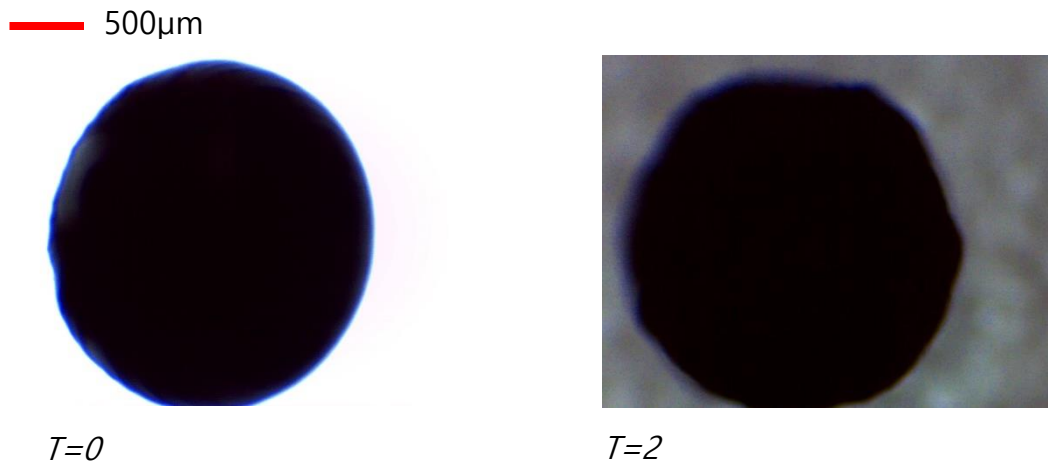
500µm



T=0                    T=2

**Figure A7:** Crosslinking GLS-A 2-1 particles with 1M CaCl$_2$ created at 10kV and 50ul/min and dried for 24h. Although still stable, agglomeration suggested that a higher calcium concentration would be more stabilising to the alginate matrix.

500µm



T=0                    T=2

**Figure A5:** Crosslinking GLS-A 2-1 particles with 1M CaCl$_2$ created at 15kV and 50ul/min and dried for 24h. Although still stable, agglomeration suggested that a higher calcium concentration would be more stabilising to the alginate matrix.
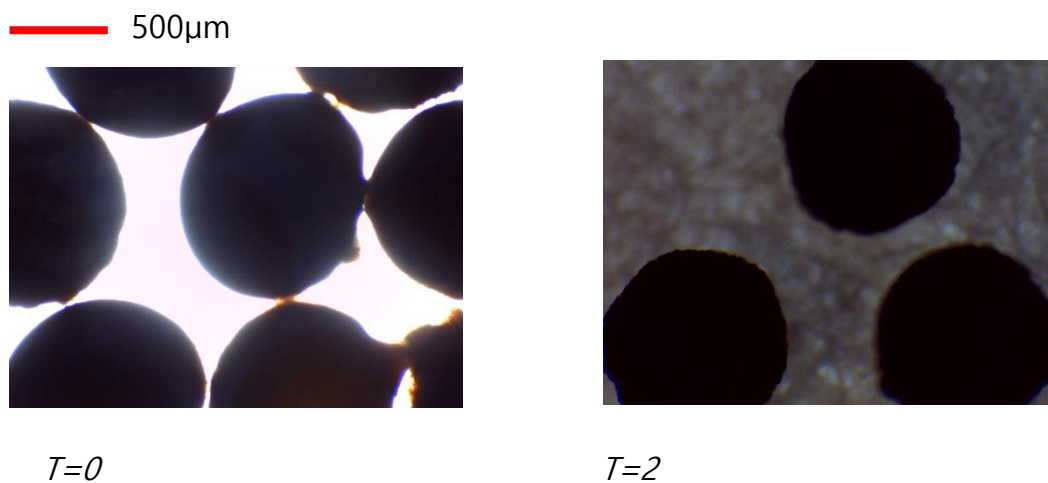
500µm



T=0                    T=2

*Novelty processing and smart delivery of Ganoderma Lucidum spores*